

# **MODERN FORMS OF DEVELOPMENT OF RESOURCE- SAVING TECHNOLOGIES FOR MINERALS MINING AND PROCESSING**

Multi-authored monograph



**MODERN FORMS OF DEVELOPMENT  
OF RESOURCE-SAVING  
TECHNOLOGIES FOR MINERALS  
MINING AND PROCESSING**

Multi-authored monograph

UNIVERSITAS Publishing  
Petroşani, 2024

UDC 622.002

<https://doi.org/10.31713/m1301>

Recommended for publication by Board of Directors of the University of Petrosani,  
Minutes № 234 as of January 17, 2024

Reviewers: **Frederick CAWOOD**, PhD in Mining Engineering, Visiting Professor:  
University of the Witwatersrand, Republic of South Africa

**Vadym SHCHOKIN**, DSc. (Engineering), Professor, Director at the Scientific-  
Research Mining Institute of Kryvyi Rih National University, Ukraine

**Mihaela TODERAS**, Professor, Ph.D.Habil.Eng., Faculty of Mines, University of  
Petroșani, Romania

Modern forms of development of resource-saving technologies for minerals mining  
and processing. The monograph is prepared and edited by Prof. Valerii Korniyenko,  
Prof. Maria Lazar and Associate Professor Serhii Chukharev – Petroșani, Romania:  
UNIVERSITAS Publishing, 2024. - 585 p.

**ISBN 978-973-741-956-9**

The monograph considers potential technological development of ore  
mining and processing industries through updating mining machines and  
technologies

The book is intended for a broad mining audience of scholars,  
practitioners, postgraduates and students.

UDC 622.002

The materials of the multi-authored monograph are in the authors'  
edition. References are obligatory in case of full or partial reproduction  
of the monograph content. All rights are reserved by the monograph  
contributors including their scientific achievements and statements.

**ISBN 978-973-741-956-9**

© Composite author, 2024





## PREFACE

Multi-authored monograph “Modern forms of development of resource-saving technologies for minerals mining and processing”, edited by Prof. Valerii KORNİYENKO and Prof. Maria LAZAR.

We are happy to present the multi-authored monograph “Modern forms of development of resource-saving technologies for minerals mining and processing”.

The monograph discusses actual and promising resource-saving technologies for exploration, development, extraction and processing of ore and non-metallic minerals. Much attention is paid to technical means and technological complexes that support these processes.

The monograph analyzes new approaches to the formation of a resource-saving model of a mining enterprise with due regard to mining safety.

In addition, the monograph analyzes principles of organizing resource-saving production, and sources of resource losses in mining. The critical analysis has enabled working out a package of measures aimed at forming a rational model of a resource-saving mining enterprise. The monograph also presents a model of a mining enterprise operating in conditions of resource saving and rational environmental management.

The monograph is intended for a wide range of scientists, specialists involved in analyzing development of mining complexes in regions, as well as master’s and doctoral students of relevant specialties of higher educational institutions.

Co-editors,

Valerii **KORNİYENKO** - Professor, DSc. (Engineering), Head of Department of Development of Deposits and Mining, National University of Water and Environmental Engineering, Ukraine

Maria **LAZAR** – Habil, Ph.D.Eng., PhD supervisor in Mines, Oil and Gas Environmental Engineering and Geology Department, Vice-Rector - Research and International Relationship, University of Petrosani, Romania



## Table of contents

Preface	3
<i>Viktor Moshynskiy, Valerii Korniyenko, Yevhenii Malanchuk.</i> Features of the application of geotechnical methods of amber extraction from sand amber-containing deposits	6
<i>Zinovii Malanchuk, Vladyslav Korniienko, Rostyslav Korniienko, Svitlana Moshchych, Oleh Proshcharuk.</i> Features and prospects of the use of Volyno-Podillia volcanic tuffs .....	19
<i>Florin Faur, Maria Lazăr, Izabela-Maria Apostu.</i> An overview of the certej mining project and assessment of the environmental implications	38
<i>Stanislav Lytvyniuk.</i> Optimization of ore deposit mining systems while changing cut-off parameters for reserves estimation .....	61
<i>Nikolaos Koukoulis, Georgios N. Anastassakis.</i> Mineral processing technologies and equipment to separate fine/ultrafine mineral values. a review	71
<i>Viktoriia Krukovska, Oleksandr Krukovskiy.</i> Simulation of coal and gas outbursts in outburst-prone zones of coal seams .....	86
<i>Victor Mutambo, Moses Mukuka.</i> Modified geomechanical dependant seismic monitoring arrangement for predicting rock bursts and failures in sesimically ctive mining blocks at mufulira mine .....	119
<i>Batma Toktosunova, Sharabidin Abdibaitov, Marsel Kozhogulov, Narmat Toktosunov, Nadira Dolomkan kyzy.</i> Extraction of useful components of ore-bearing rocks of the "Kurgak" plot of the black-shale formation of the saryjaz area .....	128
<i>Nariman Zhalgasuly, Aliya Ismailova, Nursultan Uaysuly, Madina Isagali, Orazkul Ismailova.</i> Technology for obtaining biologically active humic preparations from brown coal .....	143
<i>Artem Pavlychenko, Andrii Adamchuk, Oleksandr Shustov.</i> Technology of deep open-cast mines reclamation .....	180
<i>Ihor Fyzyk, Vitalii Zaiets, Oleksandr Vasylchuk, Myroslava Kucheruk.</i> Increase of forest plantations productivity in places of illegal amber mining of western Polissia .....	200
<i>Jerom Dankers, Jiaqi Lu, Sebastian Rother, Wiktoria Sobczyk.</i> Impact assessment of the jebel ali power and desalination plant on the environment	209
<i>Yuriy Vynnykov, Maksym Kharchenko, Oleksandr Matyash, Maryna Vovk, Marina Rybalko.</i> Utilization of overburden quaternary rocks to create soil cushions for structures .....	219
<i>Nariman Zhalgasuly, Viktor Yazikov, Tulegen Mukhanov, Uays Bektibayev, Vladimir Zabaznov.</i> Theory and practice of underground leaching of mineral resources .....	230
<i>Maria Daniela Stochitoiu, Ilie Utu.</i> Review of energy investments for strengthening resilience in energy system .....	286
<i>Ruslan Zhomyryuk.</i> Managing the localization process pollution within the influence of landfills mining production localization of pollution within the limits of influence of mining dumps .....	295

<i>Yury Kuris, Yana Vidloha.</i> The influence of biogas content on the emission of harmful impurities and the introduction of greenhouse gas emission methodology .....	330
<i>Volodymyr Panteleienko, Serhii Karpushyn, Andrii Chervonoshtan.</i> Interaction of conical monolithic thin-walled reinforced concrete shells with the soil of the foundation and their stress state under the action of static loading .....	350
<i>Oleksandr Krukovskiy, Andrii Khorolskyi, Oleksandra Ashcheulova, Volodymyr Medianyuk, Oleksandr Mamaikin.</i> Models and Methods of Operational Management in Mining Production .....	371
<i>Vasyl Kondratets, Anatolii Matsui, Oleksandr Serbul, Oles Izovita, Volodymyr Yarmolenko.</i> The scoop feeder as a means of resource saving in ball mill grinding of feed ore with classifier sands .....	387
<i>Oksana Banzak, Hehhadii Banzak, Oleg Leshchenko, Oleg Grabovsky, Antonina Gaber.</i> Development of a model of failure relationships for complex technical facility for resource-saving technologies for mining and processing of minerals .....	410
<i>Elvira Filatieva, Oleksandr Oleinichenko, Mikhail Filatiev, Inna Maksyuk, Olga Fursova.</i> Development of methods for forecasting the duration of recovery groundwater .....	430
<i>Viktoriya Mokhonko, Olena Korchuganova.</i> Storages of industrial waste are danger and secondary raw materials sources: pathways to use in the circular economy .....	445
<i>Larysa Pedchenko, Mykhailo Pedchenko, Nazar Pedchenko.</i> Justification of the choice of pneumatic structures for the formation of ground storage facilities for the gas hydrates storage .....	479
<i>Olena Fedoskina, Olena Svetkina, Kirill Ziborov. Mikola Yerisov, Valeriy Fedoskin.</i> Processing of waste sheet glass into secondary raw materials .....	502
<i>Oleksandr Shashenko, Volodymyr Shapoval, Oleksandr Skobenko, Bohdan Morkliany, Sofiia Barsukova.</i> Construction and design of buildings and structures under martial law. new challenges and ways to address them .....	515
<i>Ivan Belmas, Dmytro Kolosov, Serhii Onyshchenko, Olena Bilous, Hanna Tantsura.</i> Stress state modelling for composite tractive element with breakages of cable reinforcement and change in mechanical properties of elastomer shell .....	541
<i>Nataliia Dreshpak.</i> Ukrainian experience in implementing energy management systems in the industrial sector .....	563

## **FEATURES OF THE APPLICATION OF GEOTECHNICAL METHODS OF AMBER EXTRACTION FROM SAND AMBER-CONTAINING DEPOSITS**



**Viktor MOSHYNSKYI**

Doctor of Agricultural Sciences, Professor, Department of land management, cadastre, land monitoring and geoinformatics, National University of Water and Environmental Engineering (NUWEE), Ukraine



**Valerii KORNIYENKO**

Doctor of Engineering, Professor, Department of Mineral Deposits and Mining Engineering, National University of Water and Environmental Engineering (NUWEE), Ukraine



**Yevhenii MALANCHUK**

Doctor of Engineering, Professor, Department of automation, electrical engineering and computer-integrated technologies, National University of Water and Environmental Engineering (NUWEE), Ukraine

### **Abstract**

In the work, an analysis of scientific and technical information related to amber mining processes was carried out, which revealed that the main direction of development and improvement of amber mining technology, which is implemented by the borehole mechanical-hydraulic method with the use of water, air and vibration as the main influencing factors. A potential source of amber production can be exhausted deposits with off-balance reserves, which are man-made deposits, but this requires the development of a technological process. Due to the imperfection of the existing technologies, losses of minerals in targets and dumps significantly exceed 50%. Existing technologies for extracting amber from sandy amber-bearing deposits are highly energy-intensive, destroying rocks, and segregation requires improvement of technology and equipment to increase the efficiency of the final product extraction process and reduce energy, water, and air consumption. The proposed technological schemes do not provide for an ecological component, the possibility of reclamation of mining waste. Man-made influence requires additional research taking into account various mining and geological characteristics and host rocks and the develop-



ment of recommendations for technology and equipment taking into account the environmental component.

### **Introduction**

The main direction of development and improvement of amber extraction technology is carried out by the borehole mechanical-hydraulic method using water, air and vibration as the main influencing factors. But so far, the experience of its use is limited due to the huge difference in the mining and geological characteristics of deposits and host rocks.

Taking into account the shortcomings of the technology of amber extraction at the final stages by mechanical or hydraulic methods, when amber with a size of  $-5.0$  mm is not extracted in the process of processing the rock mass, but goes to the landfill, then the potential source of its extraction can be depleted deposits with off-balance reserves, which are artificial deposits, but this requires the development of a technological process.

Despite the well-known advantages of borehole-hydraulic mining, losses of useful components in tailings and landfills exceed 50%, so the problem of developing amber as a component of geotechnological methods of mining requires identifying the shortcomings of the existing technology and eliminating them. at a higher scientific and technical level.

In the existing technologies for the extraction of amber from sandy and sandy-clay rocks, there is no mechanism for reducing its costs.

Currently, the energy intensity of rock destruction and their segregation require the improvement of technology and equipment in order to increase the efficiency of the final product extraction process and reduce energy, water and air consumption.

The proposed technological schemes do not provide for an ecological component, the possibility of mining waste reclamation, and their man-made nature requires additional research and the development of recommendations for technology and equipment taking into account the ecological component.

Ukraine has significant reserves of amber, the deposits of which are located in conditions of various mining and geological characteristics and host rocks, which requires additional research to improve

the extraction technology, taking into account technogenic and ecological circumstances.

Therefore, in order to increase the efficiency of the process of extraction and extraction of amber, additional studies are needed to determine the dependence of the influence of factors on the process of processing amber-containing mass, the development of amber extraction methods, in order to solve the problem of improving the geotechnology of the development of amber deposits in specific conditions, which requires a significant reconstruction of the technological process taking into account mining and geological conditions, environmental requirements in a complex with technical solutions for the implementation of the proposed processes.

The purpose of the work is to study the peculiarities of the application of geotechnical methods of extraction of amber from sandy amber-bearing deposits, technology and equipment for layer-by-layer extraction of amber by a complex method, and improvement of technology and equipment to increase the extraction of amber from amber-bearing rock mass with the selection of rational parameters of the technological scheme taking into account the ecological conditions of the region.

### **1. The practice of applying geotechnological methods of amber extraction**

The conducted research aimed to determine the direction of development of systems for the development of amber-containing deposits and the equipment used for their performance. At this time, the experience of studying the processes of amber extraction, the use of equipment and the determination of regularities in the geotechnical characteristics of their interaction is insignificant. In addition, it largely depends on the mining and geological characteristics of deposits and host rocks, therefore it requires specific research and technical solutions for the perfection of technological processes and technical means. Therefore, there is a need for a systematic approach based on the principles of scientific analysis of amber hydro mining systems to identify the nature of the relationship between technological indicators in specific mining conditions and the characteristics of the equipment used.

The possibility of working out the deposit by geotechnological methods is determined by physical and geological factors.

The success of the development of deposits by geotechnological methods depends primarily on physical and geological factors.

First of all, they include the geotechnological properties of the mineral, which provide the possibility of transferring it into a mobile state. Such factors as porosity, permeability, mineralogical composition and other characteristics of the massif and fluids largely determine the economic performance indicators and must be taken into account when evaluating geotechnological methods. In a number of cases, to ensure the success of the application of geotechnological methods, it is necessary to implement technical measures that will allow to manage certain properties of minerals and rocks containing them. The study of physical and geological factors affecting the effectiveness of the application of geotechnological methods is a complex, complex problem, as it depends on many factors. Some factors have the same importance as in conventional mining methods. These are, first of all, mineral reserves, geographical and economic conditions, and the depth of occurrence. Geotechnological methods, as a rule, require less capital investment for the construction of a mining enterprise, so the scale of the deposit and the depth of mineral deposits are less important than with conventional development methods. At the same time, a number of methods can be implemented only at great depths.

Since the main factor in the use of geotechnological methods is the possibility of economically transferring a mineral into a mobile state, the study of any deposit should begin with the study of this factor, as well as those factors that ensure the spread of working agents in the subsoil and the movement of the mineral to the mining sites.

The parameters of the mining process are significantly influenced by the following physical and geological factors.

The chemical and mineralogical composition of deposits and host rocks determines the nature of their interaction with working agents (solvent, coolant, oxidizer, etc.). The most favorable is the composition of deposits that ensures selective interaction of the working agent with minerals containing a useful mineral.

Rock-forming minerals interact with the working agent without the formation of solid products, chemical reactions cause a large consumption of the mineral. The presence of minerals interacting



with the working agent can lead to serious complications (for example, clogging of the pore space).

The content of the useful component in deposits, other things being equal, determines the efficiency of the mining method.

The mechanical properties of the deposit and containing rocks in some cases determine the possibility of transferring the mineral into a mobile state (hydraulic erosion) using hydraulic fracturing. In addition, they determine the course of the process of displacement of the layer of overlying rocks.

The chemical composition of groundwater, as well as the density and viscosity associated with it, determine the speed and nature of the spread of working reagents over the deposit.

The conditions of feeding and discharge of groundwater, their connection with different horizons determine the size of leaks of working and productive agents. Most deposits are flooded. From a hydraulic point of view, they can be characterized by a closed structure, partially closed and hydraulically opened. Proximity of groundwater supply and discharge areas, as a rule, complicates the extraction process.

The porosity, texture and structure of the deposit determine the degree of availability of minerals for the working agent. The permeability of deposits for many geotechnological methods is a necessary condition for the mining process. The heterogeneity of the permeability of deposits, as a rule, complicates the mining process, since permeable areas serve as channels for the movement of working agents, and impermeable areas remain outside their scope.

It follows from the above that the range of main factors affecting the conditions of mineral extraction by geotechnological methods covers many properties of deposits.

In this regard, one of the most important tasks is to find out the degree of influence of each factor on a specific geotechnological method and to find their qualitative and quantitative assessment. And this, in turn, will provide an opportunity to establish correlations between factors and economic indicators of field development. Thus, the fundamental possibility of using geotechnological methods depends on the degree of influence of one or another natural factor on the technological regime of the extraction method.

Therefore, to support the operation of the system, it is necessary to carry out preliminary technical measures to eliminate the influence of adverse natural factors, that is, it is necessary to prepare the deposits for development.

At the same time, the following goals are pursued: improving the geotechnological properties of the mineral, increasing or decreasing the permeability of the deposit, isolating the deposit.

By geotechnological properties, minerals are divided into dispersive, soluble, combustible, extractable, and fusible. To increase the dispersion, the following can be used: dissolution with chemical reagents or microbiological methods, disruption of the natural structure by explosion or vibration, increasing the ability of minerals to form a stable aqueous mixture by adding surface-active substances (surfactants) or by the influence of bacteria. Improving the solubility of minerals can be achieved by mixing the composition of minerals. Improvements in flammability, melting, or mineral recovery can be achieved by intensification of the reactant feed process. In order to increase the permeability, mass crushing by explosion is widely used in practice. In some cases, the permeability can be increased by dissolving individual components, but for this the array must have at least a small initial permeability. Improving access to the mineral for the working agent can also be carried out by heating them in an electromagnetic field.

Much less often, artificial permeability reduction is required. Most often, it is necessary in the case of a massif that is significantly heterogeneous in structure, when the presence of karst cavities or tectonic disturbances makes it difficult to control the movement of working agents. In the presence of a connection with the surface or with other aquifers, which can be an obstacle to the ongoing processes at high temperatures and pressures, isolation of the deposit is required. Many methods of artificially reducing the permeability of rocks are known. The simplest method is based on filling voids with inert or binding materials (clay, tailings from beneficiation plants, cement mortar, lime solution, hot bitumen, various polymers, etc.).

Until now, artificial changes in the properties of rocks have been widespread mainly in the construction industry, where considerable experience has been accumulated in carrying out such activities. Now the task arises to manage the properties of rocks on a large

scale, at great depths. This is the way to further development of geotechnological methods.

The study of the influence of physical and geological factors on the conditions of application of geotechnological methods of field development allows us to formulate the requirements for deposits developed by these methods, as well as to establish the necessary degree of their study.

On this basis, it is expedient to carry out studies not only of physical extraction processes, but also of those occurring in the system elements associated with the features of the equipment, with the detection of the mechanism of formation of losses of the useful component.

## **2. Assessment of the possibility of integrated extraction of amber from sand-bearing deposits**

Today, geotechnical methods of amber extraction are developing in Ukraine, therefore there is a need to develop existing and create new technologies. There is a significant number of industrially significant amber deposits that are developed, and those that are not involved in development due to the impossibility of their exploitation by traditional methods, because they are located in difficult mining and geological conditions.

In almost all of the named deposits, amber lies in sandy or sandy-clay soils at a depth of up to 15 m. Therefore, its extraction is carried out by a mechanical method, which includes mechanical development of the soil massif by preparing the massif for the extraction of amber, opening the productive layer of the soil, excavation works, transportation of the rock from the place of development to the site of classification on the screen, where amber is separated from the rock by washing it with water on the screen, land reclamation. At the same time, sand and clay are washed away with water, and pieces of amber are selected and sent for sorting and further use.

Today, this mining method is used at the "Klesivske" and "Vilne" fields in the Rivne region. This method of extracting amber is now obsolete. Excavators with a return shovel of extraction equipment in mechanical mining systems are associated with the maximum depth of their use. At the same time, there are large operating and economic costs, and the removal of rock to the surface has a negative environmental impact on the environment.



In addition, when sorting the amber-bearing rock mass on sieves with a cell size of 5.0 mm on sieves, there are large losses of amber of a shallow fraction, because the washed rock mass together with fine amber (-5.0 mm) is waste. These dumps are man-made deposits, but they are not developed.

At this stage of technology development, hydraulic mining is the most common, where the energy of a water jet is used for destruction, erosion, disintegration, gravity transport of erosion products of amber-bearing rocks, as well as other operations in the general complex of delivering amber to the surface.

Scientists: Bulat A.F., Nadutyi V.P., Malanchuk Z.R., Lustyuk M.G., Korniyenko V.Ya., Malanchuk E.Z., Sierdobolskyi B. N., Krynytska M.V. and others [1-16].

The hydraulic method is used to wash away the productive layer of the soil with high-pressure jets. At the same time, the amber along with the containing soil is brought to the surface of the deposit by water flows.

The disadvantage of the method is: high energy costs, incomplete extraction of amber, when it is used, the structure of the soil changes, cavities are formed, which creates a significant negative man-made impact on the environment.

Two types of hydraulic production are used: borehole and underground. In the process of borehole hydraulic production (BHW), minerals at the place of occurrence are brought into a mobile state by the influence of the hydraulic mixture and its delivery to the surface through wells, which are the opening productions. When using underground hydraulic extraction (UHE), the hydraulic mixture is fed to the surface through underground mining operations.

A dispensing device is used to remove the pulp to the surface. After the formation of an undercutting gap, the hydromonitor is brought to the level of the first undercutting layer of the productive horizon. As the sloping undercut crevice deepens, the layer of the productive horizon collapses into the created space of the undercut crevice. During the operation of the hydromonitor, after connecting the undercut slot with the upper end of the casing pipes, the rise of the pulp is stopped and erosion of the collapsed soil layer begins. In the operating mode, the clay fraction together with the amber passes into the pulp, and the sand precipitates as a heavier fraction. The layer-by-

layer erosion operation is repeated until the entire productive horizon is fully developed [1].

Another method of borehole hydraulic production with a mixture of different viscosity is used.

The specified methods of well production have the following disadvantages: they require a significant amount of water; energy intensive; in the process of work, a lot of soil is brought to the surface of the well, which creates cavities at the bottom of the well; create a negative impact on the environment; do not ensure complete extraction of amber [ 1; 3-15].

Mechanical-hydraulic mining (MHM) involves bringing a mineral into a mobile state at the place of occurrence by the influence of a mechanical executive body, after which it is released with a hydraulic mixture to the surface through vertical mining operations that open the deposit.

Research carried out in the field of development and improvement of borehole hydraulic production made it possible to modernize the method of mechanical hydraulic production due to the fact that the massif, saturated with water, is activated by mechanical excitation (vibration excitation) to the formation of a solid suspension layer of such a density that a repulsive (Archimed) force occurs, which raises the amber to the surface of the deposit. To do this, rods in the form of pipes, from which water is supplied and on which vibration exciters are fixed, are immersed in the amber massif using the vibration method. At the same time, the massif is saturated with water and vibration exciters are brought into oscillating motion. Amber is freed from connections with the environment and floats to the surface. This allows you to exclude the release of mineral rock to the surface of the deposit and thereby reduce the negative man-made impact on the environment, intensify the process, increase labor productivity with a decrease in overall economic costs [16-25].

The process of rearrangement of partially liquefied sand is accompanied by a partial transfer of stresses from the soil's own weight while maintaining contacts between particles. During the entire rearrangement period, the position of particles changes - some particles lose contacts, others gain and lose again.

Thus, the particles are in an unstable position, shifting relative to each other, successively losing and gaining contacts. The number of

simultaneous contacts between particles determines the degree of destruction of the soil structure.

In contrast to the case of complete liquefaction, compaction of incompletely liquefied sand can occur simultaneously in the entire soil layer.

It is usually difficult to imagine the case of partial liquefaction of sand and the possibility of the existence of a temporarily incompletely destroyed structure, i.e. a structural mesh of sandy soil, capable of absorbing part of the stresses from external loads and grains of sand embedded in it, which do not have or have lost part of the contacts. This question is caused by the usual consideration of a static picture of the relative arrangement of sand particles. If we consider all the particles in motion and alternately lose and form contacts, then this kind of representation of the structure of partially liquefied sand does not cause complications. Over time, the number of contacts between particles increases, the soil is compacted, and when all contacts are fully combined, the liquefaction phenomenon stops.

It should be noted that the loss of contacts between particles means not only the absence of points and planes of contact of one particle with another, but also the absence of stress transmission in these contacts.

Complete liquefaction of sand can be observed even with a degree of structure destruction less than unity, but with a fairly small number of temporarily preserved contacts.

In this case, the number of contacts between particles is not enough to create a temporary structure of the soil, which perceives stresses from the external load and part of the soil's own weight.

At the last moment of time after the application of dynamic influence, the contacts are broken, and the sand goes into a completely liquefied state. The change in density, accompanied by the squeezing of water from the sand pores, depends not only on the degree of destruction of the structure, but also on the conditions of rearrangement of particles determined by the density of the sand and its stress state. As the initial density and stress state increase, the possibility of mutual displacement of soil particles decreases. Due to the fact that the self-weight of the soil significantly affects the stress state, it can be assumed that the amount of porosity depends on the depth of the location of this section of the soil.

Further development of this direction of modernization of mechanical hydraulic production with vibration excitation of the array in the well is directed to the intensification of the process due to justification and selection of the shape and spatial distribution of vibration emitters of the vibrohydraulic intensifier [1].

The main direction of development and improvement of amber extraction technology is realized by the borehole mechanical-hydraulic method using water, air and vibration as the main influencing factors.

A potential source of amber production can be exhausted deposits with off-balance reserves, which are man-made deposits, but this requires the development of a technological process.

Establishing the dependence of the influence of dominant factors on the process of extraction of amber in the process of processing amber-containing mining mass, the order of interaction and the sequence of amber mining operations in the conditions of sandy and sandy-clay deposits by the method of system analysis and the development of methods for calculating process parameters, taking into account the economic feasibility of using the proposed complex extraction method to increase the layer-by-layer extraction of amber from amber-bearing rock mass is an urgent issue today.

### **Conclusions**

In the work, an analysis of scientific and technical information related to amber mining processes was carried out, which revealed that:

1. The main direction of development and improvement of the technology of amber extraction, which is implemented by means of a borehole mechanical-hydraulic method using water, air and vibration as the main influencing factors.

2. A potential source of amber production can be exhausted deposits with off-balance reserves, which are man-made deposits, but this requires the development of a technological process.

3. Due to the imperfection of the existing technologies, losses of minerals in targets and dumps exceed 50%.

4. Existing technologies for extracting amber from sandy amber-bearing deposits are highly energy-intensive, which destroy rocks, and segregation requires improvement of technology and equipment

to increase the efficiency of the final product extraction process and reduce energy, water, and air consumption.

5. The proposed technological schemes do not provide for an ecological component, the possibility of reclamation of mining waste, while their man-made nature requires additional research taking into account various mining and geological characteristics and host rocks and the development of recommendations for technology and equipment taking into account the ecological component.

### *References*

1. Industrial technologies of amber extraction. Monograph / **A. F. Bulat, V. P. Naduty, E. Z. Malanchuk, Z. R. Malanchuk, V. Ya. Korniyenko** - Dnipro-Rivne: IGTM-NUVHP. - 2017. - 237 p.

2. **Vishnevsky O. A., Kushnir S. V. Burshtyn** of Ukraine / Institute of Geochemistry, Mineralogy and Ore Formation named after M.P. Semenenko of the National Academy of Sciences of Ukraine - Notes of the Ukrainian Mineralogical Society. – Kyiv, 2007. – P. 128–130.

3. **Krynytska M.V., Korniyenko V.Ya.** Grounding of geological conditions and technological basis of Polish amber mining / Geotechnical Mechanics: Interdiv. coll. of science works - Institute of Geotechnical Mechanics named after M.S. Polyakova National Academy of Sciences of Ukraine. - Issue 137. – Dnipro, 2018. – pp. 32–39.

4. Ukrainian amber: Mater. The first between science and practice conf. "Ukrainian Amber World". Kyiv, October 17-21, 2007 - K. - 2008. - 154 p.

5. **Maidanovych I. A., Makarenko D. E.** Geology and genesis of amber deposits of Ukrainian Polesia / K.: Nauk. Opinion. -1988. - 84 p.

6. **Korniyenko V., Naduty V., Syharev V.** Results of studies of the influence of the density and vibrational disturbance in the process of hydromechanical amber mining / Journal "Vibrations in Technology and Technologies" VNTU. – Vinnytsia, 2017. – P. 11–20.

7. **Melnychuk V.G., Krynytska M.V.** Burshtyn Polissya. Directory/ Rivne: NUVHP. - 2017. - 234 p.

8. **Naduty V.P., Korniyenko V.Ya., Sukharev V.V.** Results of research on the influence of medium density and vibrational excitation during the hydromechanical method of amber extraction / XVI International Scientific and Technical Conference "Vibrations in Engineering and Technology" October 26-27 2017 - Vinnytsia, 2017. - pp. 11–12.

9. Well hydro-mining of useful minerals: textbook / **Arens V. Zh.** and others // M.: Gornaya kniga. - 2007. - 295 p.

10. The method of well hydroproduction. A.s. 611001 USSR, MKY2 E 21 C 41/04. / **Babichev N. I., Chernei E. I., Kroitor R. V.** // No. 2180093/22-03; statement 10.10.75; published 15.06.78. - Bull. No. 22.

11. **Malanchyk Z., Korniyenko V.** Modern conditions and prospects of extraction of amber in Ukraine / Proceedings of the 1st International Academic Congress



"Fundamental and Applied Studies in the Pacific and Atlantic Oceans Countries". (Japan, Tokyo, October 25, 2014). Volume II. Tokyo University Press. – 2014. – R. 318–321.

12. **Arens V. Zh.** Well-drilled hydro-mining of solid mineral deposits. - M., Nedra. – 1980. – P. 93, 100–101.

13. **Malanchuk Z.R., Boblyakh S.R., Malanchuk E.Z.** Hydromining of minerals: [scientific. study guide higher education acc.] / National University of Water Management and Nature Management. – Rivne: NUVHP. - 2009. - 280 p.

14. **Bulat A., Naduty V., Korniyenko V.** Substantiations of technological parameters of extraction of amber in Ukraine / American Journal of Scientific and Educational Research. – No. 2 (5) (July-December). Volume II. Columbia Press. - New York. – 2014. – R. 591–597.

15. Mechanics of vibration-pneumatic ejector-type machines / **V. N. Poturaev, A. F. Bulat, A. I. Voloshyn, S. N. Ponomarenko, A. A. Voloshyn** // National Academy of Sciences of Ukraine. Institute of Geotechnical Mechanics. V.V. Vinogradov (open editor). - K.: Scientific opinion. - 2001. - 176 p.

16. Korniyenko V.Ya. Prospects and current state of amber mining in Ukraine / Bulletin of the NUVHP, Coll. scientific works. - Issue 3 (67). – Rivne, 2014. – P. 127–133.

17. Revision of areas of illegal amber mining in the Rivne region: report of the Rivne GE PDRGP "Northern Geology" [author S. Volnenko]. - K. - 2009. - 165 p.

18. **Srebrodolsky B. I.** Amber of Ukraine /Kyiv: Scientific Thought. -1980. -31 p.

19. Amber [Electronic resource]. - URL: <http://kgd.ru/news/polsha/item/52306-polskie-yantarshhiki-yantar-vosprinimaetsya-kak-cherovennyj-kamen>.

20. Special technologies of mineral extraction. **Malanchuk Z.R. Malanchuk E.Z. Korniyenko V.Ya.** Study guide - Rivne: NUVHP, 2017, p. 290

21. Modern geotechnical methods of management of the process of amber extraction. **Malanchuk E.Z., Malanchuk Z.R., Korniyenko V.Ya.** Monograph: "Innovative development of resource-saving technologies of mining of minerals" "St. Ivan Rilsky »Mining and Mining University of Geology (Sofia, Bulgaria), 2018, - 439p, 80-103 pp.

22. **Malanchuk, Z., Korniyenko, V., Malanchuk, Y., Moshynskiy, V.** Analyzing vibration effect on amber buoying up velocity. E3S Web of Conferences 123, 01018 (2019). Ukrainian School of Mining Engineering - 2019. DOI: 10.1051/e3sconf/201912301018

23. **Malanchuk, Y., Korniyenko, V., Moshynskiy, V., Soroka V., Khrystyuk, A., Malanchuk, Z.** Regularities of hydromechanical amber extraction from sandy deposits. Mining of mineral deposits. - 2019. DOI: 10.33271/mining13.01.049

24. **Z. Malanchuk, V. Moshynskiy, Y. Malanchuk, V. Korniyenko.** Physico-Mechanical and Chemical Characteristics of Amber. Non-Traditional Technologies in the Mining Industry. Trans Tech Publications Inc. Solid State Phenomena (Volume 277), 2018, pp. 80-89 doi: <https://doi.org/10.4028/www.scientific.net/SSP.277>

25. **Nadutyi, V., Korniyenko, V., Malanchuk, Z., Cholyskhina, O.** Analytical presentation of the separation of dense suspensions for the extraction of amber. E3S Web of Conferences 109, 00059 (2019). Essays of Mining Science and Practice. DOI: 10.1051/e3sconf/20191090005.

**FEATURES AND PROSPECTS OF THE USE OF  
VOLYNO-PODILLIA VOLCANIC TUFFS**



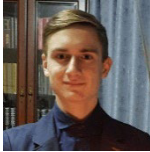
**Zinovii MALANCHUK**

Doctor of Engineering, Professor, Department of Mineral Deposits and Mining Engineering, National University of Water and Environmental Engineering (NUWEE), Ukraine



**Vladyslav KORNIENKO**

Student, National University of Water and Environmental Engineering (NUWEE), Ukraine



**Rostyslav KORNIENKO**

Student, National University of Water and Environmental Engineering (NUWEE), Ukraine



**Svitlana MOSHCHYCH**

PhD in Economics, associate professor, Department of Mineral Deposits and Mining Engineering,, National University of Water and Environmental Engineering (NUWEE), Ukraine



**Oleh PROSHCHARUK**

Postgraduate, National University of Water and Environmental Engineering (NUWEE), Ukraine

## **Abstract**

The analysis of scientific research on the physico-chemical properties of tuffs of the Volyn-Podilsky Formation confirms their suitability for wide economic use. A theoretical analysis of the suitability of zeolite-smectite tuffs for use in many branches of the economy, in particular, in animal husbandry, poultry farming, plant breeding, medicine, for the production of sorbents for various types of intoxication, was carried out.

The tuffs of the Rivne region are products of the volcanic eruption of basaltic magma. They are composed of volcanic ash and sand, cemented and subsequently recrystallized under the action of hot underground waters. Tuffs in places have completely transformed into zeolite-smectite rocks, which contain a significant amount of useful components (MgO - up to 16%, N<sub>2</sub>O - up to 7.5%, K<sub>2</sub>O - up to 7.5%) and trace elements (iron, copper, titanium, cobalt and etc.).

The mineral composition of the tuffs of the Rivne Region was determined by experimental research.

Possible ways of their use are nature protection measures, which are very relevant for the ecology of the Rivne region, as well as agriculture and the construction industry.

For the effective use of Volino-Podillia tuffs, it is necessary to develop recommendations and normative documentation for their extraction and application, which requires further research of Volino-Podillia tuffs, clarification of their reserves in the region and determination of development sites.

## **Introduction**

According to the requirements of the growth of requests and production needs, exploration and research of various, so far little-studied breeds, with the aim of their further application in various fields, is becoming relevant. Basalt quarries are being developed within the Volyn-Podilsky platform. This rock was classified as a promising mineral (agrochemical raw material) and now a more detailed study of their physical and chemical properties will open new and new opportunities for their use. Currently, tuffs are used in construction, agriculture and for the purpose of using tuffs as collection stones, that is, for nature protection purposes. In the course of the work, various types of literature were used: reference, research, and specialized scientific literature containing new data on this topic, the comparison and comparison of which gives an idea of tuffs as a rock, occurrence, and the possibilities of their wide use.

The study of new objects will provide an opportunity to diversify the areas of specialization of production, to make it more economical and cheaper.

The relevance of the work consists in collecting information on mineralogy for the systematization of the material, conducting field research at basalt quarries in the region, collecting samples of tuffogenic rocks, conducting chemical (laboratory) research with the aim of establishing their use in various branches of the economy of the Rivne region.

The object of the study is: Rafalivska basalt quarry, Berestovets quarry and Politsky quarry.

Subject of research: zeolite-smectite tuffs, minerals and rocks of basalt quarries.

Research methods: primary collection and processing of information from scientific research literature, field geological studies at basalt quarries, collection of actual material, practical studies in the mineralogical laboratory of the Shubkiv Research Station.

Purpose: to investigate the features of tufa rocks, their origin and the possibilities of use in various areas of the economy.

Main tasks:

- get to know and study tuffogenic rocks, collect collection material for laboratory research,
- to prove the value of using tufa rocks in the economy of the region.
- to find out which tuffogenic rocks can be used as a useful mineral, others as collection material.
- to present the results of laboratory studies on the influence of tufa rocks on soil fertility in the Rivne region.

### **1. General characteristics of pyroclastic rocks**

Tuffs belong to pyroclastic rocks, which are formed from solid volcanic materials - ash, volcanic sand. This volcanic material is thrown into the air during an eruption, transported by water and wind, and accumulates in areas adjacent to volcanoes [1-5].

Pyroclastic rocks have signs of both sedimentary and magmatic origin, so they are separated into a separate group. Their classification is based on a number of features, including the amount of pyroclastic material in the rock, the size of the particles, and their chemical composition.

Pyroclastic fragments, settling on the surface of the earth, form accumulations, often mixed with sedimentary rocks. If pyroclastic material is contained in an amount exceeding 90% - tuffite, from

10% to 30% - tuffogenic rock. Pyroclastic particles vary in size. Fragments with a diameter of 5 to 50 mm are called lapilli. The smallest particles, often invisible to the naked eye, are called ash (from 0.01 to 0.1 mm) and make up ash tuffs. During the deposition of ash and lapilli on low-lying areas together with sedimentary, detrital material, mixed deposits of pyroclastics with siltstone, sand and gravel particles - tuffites.

Particles from 0.1 to 5 mm are sand, forming granular tuffs. Larger fragments from 50 to 200 mm (and often larger) are called bombs, if at the time of their formation, they were completely or partially in a fragmented state as blocks, if they are represented by angular fragments of hard rocks. Rocks with a predominant content of bombs are called agglomerates, and are composed mainly of volcanic breccia blocks. With significant admixtures of ash in the latter, they are called tufobreccias.

According to their composition, pyroclastic rocks can be liparite, trachyte, andesite, basalt. Ashes and tuffs can be further divided by the content of glass, individual mineral crystals and rock particles. The formations, which mainly include glass, are called wind ashes and wind tuffs. The windclastic structure is characterized by fragments of volcanic glass of curved, sickle-shaped, and rugule-shaped shapes and is widespread mainly among finely fragmented tuffs.

Rock fragments can range in size from ash to large blocks, while single crystals or their fragments are rarely larger than coarse ash or small lapilli. Glass particles come in different sizes, but mostly they are small. During a volcanic eruption, larger and denser particles are transported to shorter distances compared to smaller and, accordingly, lighter particles and accumulate closer to the source of their formation. Lapilli containing slag or pumice of low-density precipitate together with much smaller thermal particles represented by non-porous glass and crystals. At the same size, fragments of crystals and rocks tend to fall faster and closer together than less dense fragments of glass. Thus, in the deposits of one ashfall, denser lithoclasts, crystaloclasts, will be concentrated mainly in the lower part of the layer, and glass wool - in the upper part. Therefore, a single tuff sample may not accurately reflect the magma composition. The size of the particles in individual layers of one volcanic field also depends on

the variation of the force of the eruption and the force of the wind [3, 6-10].

## **2. Features and types of tuffs, their composition**

As mentioned above, tuffs consist of fragments of igneous rocks, effusive rocks, and igneous minerals cemented by ash, rarely sedimentary material. The color of tuffs is diverse - white, gray, pink. Density 0.75-1.4 g/cm<sup>3</sup>. Porosity reaches 70%. The limit of compressive strength is from 8-10 to 70 MPa. Tuffs are poorly heat-conductive and frost-resistant, often have a pronounced layered structure. The dense, hard type of tuff is called tras, and the loose type is called puzzalan. The tuffs formed by aerial deposition have a sharply siliceous composition and are formed mainly by glassy ash and pumice lapilli. Few crystals of quartz, sanidine, sodium plagioclase, or biotite are usually scattered among the glass fragments [3-5].

A special type of basaltic tuffs are the so-called shalsteins - shale-like, always underwater basic finely fragmented tuffs, which consist of pumice-like vesicular fragments of glass. The fragments do not contain eruptive crystals - pyroxene, olivine, plagioclase or contain them in very small quantities. The presence of flat lenses of vitreous fragments oriented in parallel planes and strongly stretched and flattened is characteristic of the chalsteine structure. The more bubbles in the glass of the shards, the more easily it flattens under the pressure above the accumulated masses, and the shards are easily drawn into thin "films" that envelop the crystals, which better resist crushing, and the clusters of calcite crystals that form in the binding mass.

If shalstein contains crystals of field slag, which withstands crushing well, then a crystallastic structure is created. Porous tuff material - chloritized glass - in such rocks stretches and envelops the feldspar grains that were preserved from crushing, creating a semblance of a fluidal structure.

When ash falls through clouds saturated with moisture, very thin wet particles can collect in the form of successive layers on some fragments, forming spheroidal ash balls - accretion lapilli, the diameter of which varies from 2 to 10 mm, but often there are larger ones. They accumulate relatively close to the center of the eruption. Accumulations of accretionary lapilli are called pisolitic tuffs.

Deposits of very hot pyroclastic flows, which are also called tuffs of thermal flows, are called ignimbrite. Flows of this type move very quickly and their deposits are quickly formed at temperatures of 600-900<sup>0</sup>C. Some ignimbrites are the product of a single flow. But often they consist of many streams that moved so quickly one after the other that each previous stream did not have time to cool completely, and all the streams eventually solidified as one. In some cases, the power of some streams may not exceed 1 m, but there are those that occupy large areas reaching several hundred meters, especially if they fill the valley.

As the ignimbrite cools, it is rarely preserved as a mass of separate fragments. More often, hot particles of glass connect at the points of their collision and the entire flow is sintered. If there is no compaction of ignimbrite during binding, deformation of glass particles, initial welding is said. Such rocks often have a wind-clastic structure and are not strong enough, porous, easily broken into blocks. However, glass fragments are often deformed, more firmly welded together, and the mass is compacted. As a result, hard, relatively low-porous rocks are formed, pieces of glass are flattened while still hot, sometimes harder fragments of crystals are bent, lapillis and pumice bombs are flattened into disk-shaped lenses, which received the name fiamme. In the cross-sections, it can be seen that in most of the fiamme there are longitudinal dark veins or partitions - former pores of pumice, which were closed as a result of compaction and welding. The degree of welding is so significant that lapilli pumice tuffs turn into dense glass, almost without pores and similar to obsidian.

Volcanic rocks formed as a result of magma fragmentation, if they were subjected to rapid hardening by water, are called aquagenic tuffs or hyaloclasts, which are formed most often when lava flows into the sea or into a freshwater basin. Hyaloclasts are mainly basaltic in composition and consist mainly of glass fragments bounded by smooth fracture surfaces. Their typical fragments are pure brown basaltic glass (sideromelane) without pores, in contrast to the highly porous vitreous or cryptocrystalline fragments (tachylites) characteristic of basaltic ashes and lapilli. But since basalt glass easily reacts with water, in most aquagenic tuffs it is at least partially transformed into a yellow or brown resinous substance - palagonite. Therefore,



aquagenic tuffs can be recognized by the physical features of the glass particles. The chemical composition of palagonite is not stable, but it necessarily contains a lot of iron oxide. A palagonite tuff is formed, which, as it deepens, turns into smectite, which, in turn, turns into chlorite at a great depth. Relics of plagioclase, olivine, or pyroxene crystals are also present in many palagonite tuffs [5].

### **3. Volcanic tuffs of Volyn and their general petrographic characteristics**

Considerable deposits of smectite and zeolite-smectite volcanic tuffs have been discovered in the Rivne region, which, thanks to their valuable physical and chemical properties, are suitable for wide economic use. According to deep geological mapping, tuffs are traced under the Mesozoic-Cenozoic sediments along the western slope of the Ukrainian crystalline shield in the form of a strip 1...10 km wide at depths from 5 to 250 m. The tuffs come to the surface in basalt quarries: Berestovets, Ivanova Dolyna, Politsi, Rivne region. Tuffs are laid down in layers, forming strata with a thickness of several meters to 140 meters [4].

The following types of pyroclastic rocks of the main composition are found in Volyn:

- agglomerate tuffs and slag tufobrekcias with bombs and lapilli;
- coarse-clastic-coarse-clastic (psephytic) tuffs;
- medium clastic (psamitic) tuffs;
- fine-grained (siltstone-pelitic) tuffs;
- tuffites and sandstones.

Agglomerate tuffs and slag tufobrekcias consist of coarse pyroclastic material, among which one can distinguish volcanic debris thrown out in a solid plastic or semi-liquid state. In the group of volcanic fragments thrown out in a solid state, the homogeneity of the composition and structure is revealed, and the fragments have an angular shape. The second group is characterized by figured outlines: pear-shaped, ellipsoidal, flattened shapes with twisting elements. The composition of basalt fragments is mostly olivine-free and, much less often, olivine-bearing. They are characterized by a variety of structures - from vitrophyric, hyalopilitic to intersertal or porphyry. Ruzhyl tufobrekcias contain up to 85% of ruzhyl fragments. Their surfaces are oxidized or melted and have a micro-texture that is saturated with tonsils.

Agglomerate tuffs are cemented with ash material, as well as zeolites, chlorites and calcite. In many cases, partial sintering of fragments without significant deformation is observed. Coarse-, medium-, and fine-grained tuffs are composed of fragments of bubbly cherts, basalts, volcanic glass, and very rarely - fragments of intrusive traps and effusives of medium and acidic composition. Coarse-fragmentary tuffs contain many fragments of cherts and basalts (40...97%) and therefore they are mainly represented by lithoclastic and windoclastic varieties. Volcanic glass fragments (60...70%) predominate in medium-clastic tuffs, and sometimes the content of cinder fragments increases significantly (up to 40...50%) (Rivna focal zone). It should be noted that the accumulation of corms is observed in the cross-section of any stratum not only among medium clastic, but also fine and thin clastic tuffs. Among the fine-grained and thinly fragmented tuffs, lithovetroclastic types prevail. The size of fragments of corms and various basalts in large and medium-fine fragmental tuffs does not exceed 1...2 mm. They have an isometric shape and structural and textural features do not differ from the bombs and lapilli described above.

Important features characterizing vitreous fragments include their shape and porosity. Based on these features, it is possible to determine which of the volcanic fragments were thrown out in a plastic state. Their gas cavities are elongated in the same direction as the fragments, causing the fluid-striped microstructure. This group is characterized by pumice-like microtextures [5].

In general, most of the investigated varieties of tuffs of the Rivne region have a mixed composition of fragments with the simultaneous presence of particles thrown out in a plastic, semi-plastic, and solid state. Unchanged vitreous fragments are observed relatively rarely. Some of them contain crystallites of the type longulites and belonites, as well as microliths, fragments with weak crystallization, liquid fragments of homogeneous glass. The indices of optical refraction of glass of yellowish-brown, green and black shades vary mainly from 1.5 to 1.58. Spectral analysis revealed chromium, titanium, vanadium, cobalt, nickel, manganese, copper, tin, zinc, lead and other elements in the glass fragments, the content of which does not exceed hundredths and thousandths of a percent.

The brownish-black fragments contain ore minerals: magnetite in the form of dust; hematite, which forms secondary films in cavities, on the surface of fragments, and iron hydroxides, which displace oxidized glass. The saponified vitreous fragments have an amorphous, crytocrystalline and crystalline composition, a heterogeneous greenish-yellowish shade with variable optical refraction indices.

The mineral composition of tuff cements is diverse. The most common are analcime and other zeolites, as well as chlorites, quartz, chalcedony and iron hydroxides. White analcime forms solid masses in cement. The chemical content of analcimes and basalts, diabases and tuffs is similar in composition. Their heating curves are also similar, and dehydration takes place in a relatively narrow temperature range of 200...400<sup>0</sup>C. Next to analcime, tuffs contain thomsonite in the form of creamy-pale-yellowish granular aggregates of radially radiating and spherulite composition.

Tuffites and tuff sandstones are most widespread to the southeast from the latitude of the city of Rivne. They are characterized by admixtures of terrigenous material from 10 to 25%, rolled and semi-rolled forms of fragments of volcanic origin. Ashy material, significantly altered to complete transformation into clay products.

The content of silica, iron oxides, magnesium, calcium, and alkalis change significantly in tuffs. The amount of water and volatile components increases sharply. These deviations are due to both post-magmatic and hydrothermal changes in the rocks and the ratio of basalt debris to cement, as well as its material composition, admixtures of terrigenous material, etc. In the freshest basaltic tuff, there is a similarity of compositions with average basalt.

#### **4. Areas of use of Volyn-Podillia tuffs**

At present, many possibilities of their use in the economy are known: in the nature protection zone (reclamation of radioactive contaminated soils; purification of wastewater from NH<sub>4</sub><sup>+</sup>), agriculture (fertilizer, plant nutrition stabilizer; feed additives, bedding with further use as fertilizer), construction industry (production of bricks, roof tiles and ceramic tiles; production of expanded clay; pigments for paints and colored concrete) [6].

Tuff deposits are almost always accompanied by deposits of valuable ore metals, in particular native copper; therefore, the exploration of new tuff deposits leads to the discovery of other, more valuable minerals.

Experimental introduction of tuffs into radioactively contaminated sod-podzolic soils of the Rivne region has already shown the effectiveness of using these materials to reduce the isotope content in agricultural crops. Analcine-saponite varieties of volcanic tuffs are especially valuable in this respect. They are characterized by the highest content of zeolites (up to 40%) and smectites (up to 80%) and therefore exhibit the most sorption and cation exchange properties. An urgent problem for Ukraine and, in particular, for the Volyn-Podilskyi region, where the Rivne and Khmelnytsky NPPs are located, is the disposal of hazardous radioactive waste from the nuclear power industry. Underground disposal is defined as the most ecologically, technically and economically rational way of long-term isolation of all RW from the ecosphere.

The choice of a geological object for underground disposal is regulated by the following basic requirements regarding the economic feasibility and reliability of radioactive waste isolation: proximity of the object to sources of radioactive waste, high insulating properties of rocks and their sorption capacity in relation to radioactive isotopes, positive engineering and hydrogeological conditions of the territory cemetery Volcanic tuff layers of the Volyn series of the Lower Wend best meet these requirements.

The territory of the distribution of tuffs generally corresponds to the Volyn-Podilsky plate, which developed stably in a passive geodynamic regime for about 100 million years. The tuff bodies, undisturbed by tectonic dislocations, are tens of kilometers in area and have a thickness of up to 80-140 m.

Volcanic tuffs of Volyn-Podillia are waterproof and poorly permeable rocks. However, the possibility is not excluded that under the conditions of deep lying along the fractured zones, the pressure waters of the Gorbashiv aquifer may flow through them. In the presence of water, the primary minerals of tuffs are displaced by secondary smectites, which are capable of sorbing radionuclides and at the same time close microcracks and pores of rocks, as they occupy a larger volume than primary minerals [5].

The potential possibility of penetration through tuffs of fractured waters, despite all their conservation and sorption properties, significantly lowers the level of safety of RW burial in it. Therefore, the identification and study of such relatively dry tuff massifs in the Volyn-Podilskyi re-

gion should become an important task of future geological research and requires comprehensive engineering-geological, hydrogeological research on the subject of unconditional reliability of their insulating properties. But even now, a preliminary assessment of the insulating and sorption properties and the conditions of occurrence of the Volino-Podillia tuffs shows their high potential suitability for the burial of radioactive waste in a wide range of depths.

The positive mineralogical, physico-chemical and ecological properties of tuffs of the Volyn series, in particular their high ability to sorb radionuclides, significant specific surface area and water absorption index, low density and hardness allow considering this raw material as a useful mineral that can serve as an ameliorant of radioactively contaminated soils. At the same time, due to the high content of magnesium and lime-alkaline components, as well as the high content of a number of agronomically valuable trace elements, these rocks are potentially suitable for application to the soil as a complex natural mineral fertilizer and soil deoxidizer. Also, tuffs can be used for the production of saponite flour, which will increase the productivity of man-made and radioactively polluted soils, purify liquid food products from heavy metals and radionuclides, as a mineral admixture for livestock and poultry feed, etc.

As a result of intensive secondary processes due to pyroclastic and tuff-sedimentary rocks, deposits of kaolin, bentonite clay, alunite, mineral paints, etc. [4,5].

### **5. Research results**

An important property of tuff (Fig. 1) is that zeolite tuff has a high absorption selectivity and the ability to separate ions and molecules of various substances by size, as well as fairly high mechanical and chemical resistance. High porosity, compared to quartz sand, provides an increase in the capacity of harmful substances, therefore it has a higher ion exchange selectivity compared to a number of chemical elements, the content of which is strictly regulated. This is especially important in relation to the selectivity of radioactive elements, sorption capacity to heavy metals, phenol, ammonium nitrogen found in waste. Zeolite tuff cleans water by 30-40% better from microorganisms, from colloidal particles of mineral and organic origin. Tuffs have the ability to adsorb ammonia from the air, and therefore it is advisable to use them for deodorization of waste stor-

age areas or production areas. It was established that 1 kg of zeolite tuff can adsorb up to 100 g of ammonia [3].

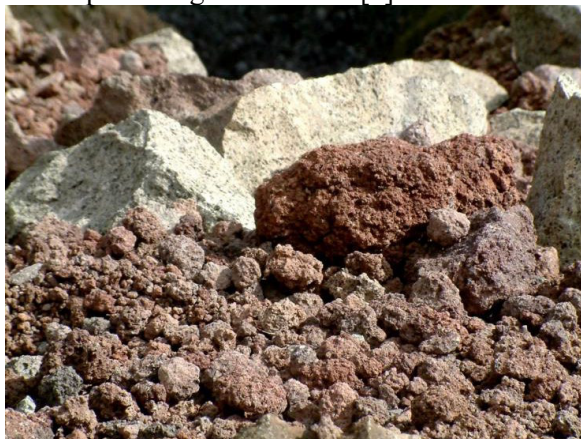


**Fig. 1.** Tuffs

Thus, the ion-exchange properties of tuff are used in the following cases:

1. To extract  $\text{NH}_4$  from municipal and technical waters. Clinoptilolite tuff is used to obtain ammonium, cesium, and phosphorus from wastewater.

2. To remove heavy metals from technical waters, in particular lead, chromium, cadmium. For cleaning acidic mine waters ( $2 < \text{pH} < 3$ ) from metals Al, Ca, Cd, Co, Si, Fe, K, Mg, Mn, Na, Ni, Pb, Zn.

3. To extract radionuclides from the wastewater of nuclear power plants, where tuff is used as a cation exchanger to capture isotopes of cesium and strontium. For example, a type of tuff, mordenite, captures up to 98% of  $\text{Cs}_{147}$ .

4. For separation and capture of gases. For example, to extract  $\text{SO}_2$ , clinoptilolite tuff is activated with a solution of hydrochloric acid and used to capture  $\text{SO}_2$  from the gases of factories that produce sulfuric acid by burning sulfides.

5. To use zeolite as a catalyst, for example, in petrochemicals. At the same time, catalytic centers can be created in zeolite without activating other components. Clinoptilolite tuff is the only zeolite in which acidic centers are not formed during acetylene hydration, which are undesirable during catalytic transformations. High rates of benzene recovery when using this tuff. The absorptive capacity of

the tufts of the Rafaliv deposit of the Rivne region compared to other deposits is shown in table 1[6].

Table 1

Absorption capacity of tufts													
Place of creation	Cation exchangeable ability	Na <sup>+</sup> g/kg	H <sup>+</sup> g/kg	NH <sub>4</sub> <sup>+</sup> g/kg	Pb <sup>+</sup> g/kg	Cs <sup>137</sup> %	Pb <sup>2+</sup> g/kg	Hg <sub>2</sub> <sup>2+</sup> g/kg	Zn <sup>2+</sup> g/kg	Sr <sup>90</sup> %	Cu <sup>2+</sup> g/kg	Co <sup>2+</sup> g/kg	Mn <sup>2+</sup> g/kg
Tendzamske (Georgia)	109	54	75	45	119	97	175	380	57	94	58	62	61
Shelves (Rivne region) обл., Україна)	118	57	79	48	162	99,5	179	420	62	97	65	60	75

6. On the basis of mineralogical analysis, it was established that the content of zeolites in the tufts of Politskyi quarry is about 43% of smectites and fine-dispersed iron materials, from 16% to 32%. X-ray structural and thermal analyzes showed that these tufts contain 65% smectites and up to 28% analcime. In the Berestovets quarry in this region, an average of 65% of smectites were found.

The presented results of the quantitative analyzes showed that according to the content of petrogenic minerals, the volcanic tufts of the Rivne region are altered and represented by zeolite-smectite rocks (Fig. 2), which have undergone significant secondary transformations and hydrothermal mineralization.



Fig. 2. Zeolite smectite tuff





**Fig. 3.** Rafalivka quarry

The conducted studies allow purposeful and effective use of tuffs. Of particular interest are the data on the average composition of trace elements in tuffs in three deposits. In the table 2 shows the average content of microelements in tuffs of three quarries of the Rivne region (Fig. 3), their correspondence to Clark values and maximum permissible concentrations (MPC) in soils.

The study of the results of these studies of trace element composition showed that tuffs cannot be regarded as basalt mining waste, but are a valuable mineral raw material that requires development and a comprehensive approach to its processing to extract useful metals and silicates.

The tuffs of the Berestovets quarry have two varieties that differ in composition. Under the basalt layer in the quarry, argillite-like siltstone tuffs with a thickness of 1-5 m lie. Deeper along the section, more granular psammite and psephyte tuffs lie. Siltstone tuffs contain an average of 65% of smectites, iron hydroxides, contain a high concentration of barium, vanadium, copper, and zirconium (see Tables 2, 3) [7].

Today, the tuffs of the Politsky deposit have been studied more fully in terms of geology and industry. Their deposits, the so-called

saponite clays, have been explored and prepared for research and industrial development. They include a high content of saponites (up to 80%) and therefore show valuable sorption and cation exchange properties. These tuffs are characterized by high magnesium content (MgO - up to 11.6%) and high content of trace elements such as copper, chromium and zinc. An important factor is the absence of such elements as arsenic, mercury, and selenium in these tuffs, which are ecologically dangerous [8-10].

Table 2

The average composition of trace elements in tuffs by quarries, %														
Elements	P	Pb	Ba	Mo	Sn	Сп	Zn	Ni	Zr	Co	Cr	V	Mп	Ti
Rafalivka quarry														
Average value	670	5	350	0,8	5	103	46	35	140	31	47	116	1240	5480
Clarks	1500	6	330	1,5	6	87	105	130	110	48	170	250	1200	8000
MPC	-	30	-	-	-	100	100	100	-	-	100	150	1500	-
Berestovts quarry														
Average value	600	6	8000	1,0	2	300	40	25	200	25	30	400	600	6000
Clarks	1500	6	330	1,5	6	87	87	130	ΠО	48	170	250	1200	8000
MPC	-	30	-	-	-	100	100	100	-	-	100	150	1500	-
Politsky quarry														
Elements	Cr	Ni	Сп	Zn	Re	Sr	Y	Pb	Th	Ba	Ge	As	-	-
Average value	150	19	75	104	32	168	23	118	3	320	2	0,1	-	-
Clarks	170	130	87	105	60	470	21	6	4	330	1,5	2	-	-
MPC	100	100	100	100	-	-	-	30	-	-	-	2	-	-

Table 3

Content of elements in tuff samples from different quarries Concentration, %

The name of the elements	Rafalivka quarry	Berestovts quarry	Politsky quarry
Aluminum	0,03	10,2	3,0
Silicon	30-32	57,2	42,0
Phosphorus	0,1	0	0,15
Sulfur	1,2	0,3	0
Potassium	1,3	2,4	4,8
Calcium	6,4-12,1	15	37,5
Titanium	2,8-4,0	1,3	0,5
Chrome	0,2	0,05	0,1
Manganese	0,070	0,12	0,07
Iron	48-50	12,8	7,0
Nickel	0,2	0,1	0,01
Copper	0,4-0,7	0,17	0,6-1,0
Zinc	0,05	1,2	0,07
Strontium	0,07-0,1	0,07	0,07

## Conclusions

1. The analysis of scientific research on the physicochemical properties of tuffs of the Volyn-Podilsky formation confirms their suitability for wide economic use. A theoretical analysis of the suitability of zeolite-smectite tuffs for use in many branches of the economy, in particular, in animal husbandry, poultry farming, plant breeding, medicine, for the production of sorbents for various types of intoxication, was carried out.

- In agriculture - as a mineral fertilizer, seed preservation, animal and bird feed additives, plant nutrition stabilizer.

- In environmental protection activities - amelioration of radioactive soil contamination, underground burial of poisonous substances, wastewater treatment.

- In construction - production of building materials (bricks, roof tiles, ceramic tiles), production of cement and expanded clay, pigment for paints and colored concrete.

- As binding materials - ore wrapping, fertilizer wrapping.

2. It has been established that the tuffs of the Rivne region are products of a volcanic eruption of basalt magma that occurred approximately 600 million years ago. They are composed of volcanic ash and sand, cemented and subsequently recrystallized under the action of hot underground waters. Therefore, the tuffs in places have completely transformed into zeolite-smectite rocks, which contain a

significant amount of useful components (MgO - up to 16%, N<sub>2</sub>O - up to 7.5%, K<sub>2</sub>O - up to 7.5%) and trace elements (iron, copper, titanium, cobalt etc).

3. The mineral composition of the tuffs of the Rivne region was determined by experimental research.

On the basis of mineralogical analysis, it was established that the content of zeolites in the tuffs of Politskyi quarry is about 43% of smectites and finely dispersed materials from 16% to 32%. X-ray structural and thermal analyzes showed that these tuffs contain 65% smectites and up to 28% analcime. On average, about 30% of smectites were found in the Rafalivskyi quarry. In the Berestovets quarry in this region, an average of 65% of smectites were found. The tuffs of the Berestovets quarry have two varieties that differ in composition. Siltstone tuffs contain an average of 65% of smectites, iron hydroxides, contain a high concentration of barium, vanadium, copper, and zirconium. Today, the tuffs of the Politsky deposit have been studied more fully in terms of geology and industry. Their deposits, the so-called saponite clays, have been explored and prepared for research and industrial development. They include a high content of saponites (up to 80%) and therefore show valuable sorption and cation exchange properties. These tuffs are characterized by high magnesium content (MgO - up to 11.6%) and high content of trace elements such as copper, chromium and zinc. An important factor is the absence of such elements as arsenic, mercury, and selenium in these tuffs, which are ecologically dangerous. During the writing of the research work, a number of laboratory and practical studies of zeolite-tufogenic rocks of the Rivne region were conducted. Prospective directions of their use in the economy of Ukraine have been determined.

4. Possible ways of their use are nature protection measures, which are very relevant for the ecology of the Rivne region, as well as agriculture and the construction industry. Together with the reclamation of radioactively contaminated soils and wastewater treat-

ment, it is economically and ecologically appropriate to directly use the Volyn-Podillia tuffs as a potential site for radioactive waste disposal. Despite their great economic importance, at present the volcanic tuffs of the Volyn series are practically not used. In the basalt quarries of the Rivne region, they are dumped in huge volumes into dumps, hindering mining operations and creating man-made "lunar" landscapes. With a new approach to the study and use of smectite and zeolite tuffs as a new type of mineral resources, prospects for their complex extraction together with basalts for further processing and multi-purpose use are opening up.

5. For the effective use of Volyn-Podillia tuffs, it is necessary to develop recommendations and regulatory documentation on their extraction and application, which requires further research of Volyn-Podillia tuffs, clarification of their reserves in the region and determination of development sites.

### *References*

1. **Z. Malanchuk, V. Zaiets, L. Tyhonchuk, S.ana Moshchych, G. Gayabazar** and Ph. Thao Dang (2021). Research of the properties of quarry tuff-stone for complex processing. E3S Web of Conferences. Volume 280 (2021) 01003, DOI:<https://doi.org/10.1051/e3sconf/202128001003>

2. **Malanchuk E.Z.** Efficiency determination of using magnetic separation during processing of basalt raw material. Coll. of science pr. Progressive technologies of coal, coalbed methane, and ores mining.– London: CRC press Balkema book.-2014.- c 71-75.

3. **Malanchuk E.Z.** Scientific justification of the technology of complex processing of metal-containing raw materials in the development of basalt deposits. autoref. thesis ... Dr. Tech. Sciences: 05.15.09. National Academy of Sciences of Ukraine, Institute of Geotechnology mechanics named after M.S. Polyakova, Dnipropetrovsk, 2015. p. 39.

4. Zeolite-smectite tuffs of the Rivne region: biological aspects of use / [**Bogdanov G. O., Mandigra M. S., Melnychuk V. G.** and others]; under the editorship MP Magpies. - Rivne: Volynski oberegy, 2005. - 184 p.

5. **Melnychuk V.G., Mateyuk V.V.** Volcanic tuffs of Volyn-Podillia as a new type of mineral resources // In the book. Problems of rational use, protection and reproduction of the natural resource potential of Ukraine. Theses add. 2nd All-Ukrainian Scientific method. conf. – Chernivtsi, Ruta, 2000. – P.133-134.

6. Protection against landscape pollution by household waste and industrial waste based on the use of natural sorbents. / **V.A. Stashuk, Z.R. Malanchuk, A.M. Rokochynskiy, M.O. Klymenko, R.V. Zhomyruk, S.Yu. Gromachenko.** / Edited by **V.A. Stashuka, Z.R. Malanchuk and A.M. Rokochinsky.** Monograph: – Kher-son: 2014. – 420 p.

7. Minerals of the Rivne region. In the book Reclamation and development of the Ukrainian Polissia. **Malanchuk Z.R., Korniyenko V.Ya., Malanchuk E.Z., Zhomyruk R.V., Ignatyuk I.Z., Malanchuk L.O., Moshchich S.Z., Solvar L.M., Tymoshchuk I .I., Romanchuk S.S., Zagurovskiy V.N.** Collective monograph / edited by Doctor of Science, Professor, Acad. NAAN Ya.M. Gadzal, Ph.D., profes-sor, member-cor. NAAS V.A. Stashuk, Ph.D., Professor A.M. Rokochinsky. – Kherson: OLDI-PLUS, 2018. – Volume 2. See 57. – 854 p. 600-617

8. Efficiency of using magnetic separation for the processing of metal-containing basalt raw materials. Topical issues of resource-saving technologies in mineral mining and processing. **Malanchuk E.Z. Malanchuk Z.R. Korniyenko V.Ya.** Multi-authored monograph. – Petroșani, Romania: UNIVERSITAS Publish-ing, 2018. – 270 p., 65-89 pp.

9. Improvement of technological parameter of the technology of production of zeolite-smectite tuffs. **Malanchuk Yevhenii, Sergey Stets, Korniyenko Valerii, Marchuk Roman.** Sustainable development of resource-saving technologies in mineral mining and processing. Multi-authored monograph. – Petroșani, Romania: UNIVERSITAS Publishing, 2019. - 400 pp., 244-265 pp.

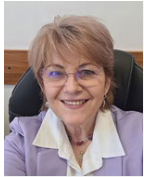
10. **Malanchuk Z. R.** Justification of the prospects for innovative development of the enterprise for the extraction of copper-containing basalts / Z. R. Malanchuk // Resource-saving technologies of raw-material base development in mineral mining and processing : multi-authored monograph. – Petroșani, Romania : UNIVERSITAS Publishing, 2020. – PP. 6-33.

## **AN OVERVIEW OF THE CERTEJ MINING PROJECT AND ASSESSMENT OF THE ENVIRONMENTAL IMPLICATIONS**



**Florin FAUR**

Doctor of Engineering Sciences, Associate Professor, Faculty of Mining, Department of Environmental Engineering and Geology, University of Petroșani, Romania



**Maria LAZĂR**

Doctor Habil of Engineering Sciences, Professor, Faculty of Mining, Department of Environmental Engineering and Geology, Vice-Rector for Scientific Research and International Relations, University of Petroșani, Romania



**Izabela-Maria APOSTU**

Doctor of Engineering Sciences, Assistant Professor, Faculty of Mining, Department of Environmental Engineering and Geology, University of Petroșani, Romania

### **Abstract**

Extractive industry, regardless of how it is performed, always leads to long-term negative effects on the environment. The environmental component that suffers the most as a result of mining activities is land, and with it the entire ecosystem in the area. The most significant destructive effects of open pit mining are produced, both by the quarry and the associated waste deposits and tailings ponds. Removing the overburden and extracting minerals from an ore deposit constitutes a destructive action, with possible repercussions on local or regional habitats and fauna. These effects can be extremely serious if they interact with natural environments of high value. The environmental implications are obvious when mining operations are performed using explosives and mechanical equipments through noise, large amounts of dust released in the atmosphere, causing major damage to vegetation and problems related to irreversible alterations of habitats, with consequences in both the project and adjacent areas. Storage of tailings from processing activities (where the mineral material is often associated with dangerous toxic substances) in ponds, may cause functional alterations or destruction of the territory in which they are located.

Given the above, based on preexisting data and field observations, the paper aims at making an inventory of the mining and processing operations and the as-



assessment of the possible consequences on the environment that may be generated by the implementation of a large-scale mining project, being taken as a case study the Certej Mining Project (exploitation and recovery of the sulphide epithermal gold-silver ore deposit quartered in the Metaliferi Mountains).

## **1. Introduction**

Quarrying affects the environment in two main ways: on one hand, through the alteration of the landscape, and on the other hand, through the brutal intervention within the natural processes and rhythms of ecosystems. All these effects have led to the emergence of a conflict of interests between the necessity of extracting raw materials and the requirements for environmental protection to such an extent that mining enterprises have begun to be perceived as "environmental destroyers" [1].

For a long period, up until about 30 years ago, priority was given to economic growth, excluding environmental protection issues. The more and more severe manifestations of environmental degradation have necessitated a change in this mindset [2].

The mining activity carried out in quarries is characterized by a significant impact on environmental components. Current quarry mining operations occupy and alter the geomorphological structure, rendering the use and recultivation of the land impossible for an extended period. Additionally, the waste dumps cover significant agricultural and forested areas, influencing adjacent lands through morphological and hydrographic changes [3].

Removing the overburden, preparation of the deposit and ore extraction constitutes destructive activities with significantly negative impacts.

Approximately 25% of the occupied areas are permanently removed from the economic circuit, being taken up by social-edilitarian constructions, communication routes, or watercourses.

The remaining 75% is temporarily removed from agricultural or forestry uses for periods ranging from a few years to dozen of years. This leads to the destruction of fertile soil and vegetation, with repercussions on the local habitat and fauna [1].

Efforts to protect the environment, through the development of non-polluting technologies in the raw material extraction sector, are hindered by the considerable financial efforts they entail. However, at the current stage of development, depending on the extraction

methods and technologies applied, solutions must be found to improve the affected environmental components, including a proactive approach in addressing the negative environmental impacts.

## 2. Location of the project

Certej mining perimeter is located according to the technical sheet, on the administrative territory of Certeju de Sus commune, Bocșa Mică village, approx. 20 km northeast of Deva city (fig. 1).

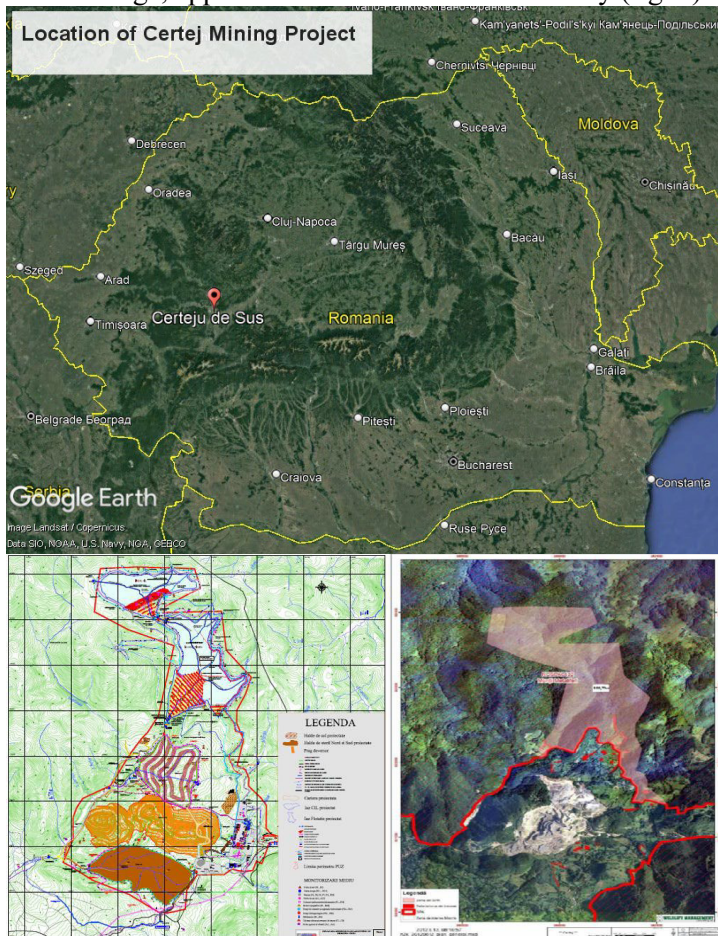


**Fig. 1.** Certej mining perimeter and it's location in relation with Natura 2000 site [4]

According to currently available data, three objectives of the project (two tailing ponds with the related dams and the andesite quarry) overlap on the Metaliferi Mountains Natura 2000 ROSPA0132 site. The footprint of the mining project overlaps on 108.7 ha, about 0.4% of the Natura 2000 site, on Macrisului Valley (fig. 1) [4].

Other reservations of national interest (Limestones from Magurile Băiței, Bholt Reservation, Magura Săcărâmbului, Măzii, Glodului and Cibului Gorges) are located at relatively small distances from the project area, between 3 and 13 km.

In 2012, an exploration drilling campaign was started, which continued until 2013 (fig. 2), estimating the reserves at 31.35 Mt for 2.1g/t Au and 11 g/t Ag [5].

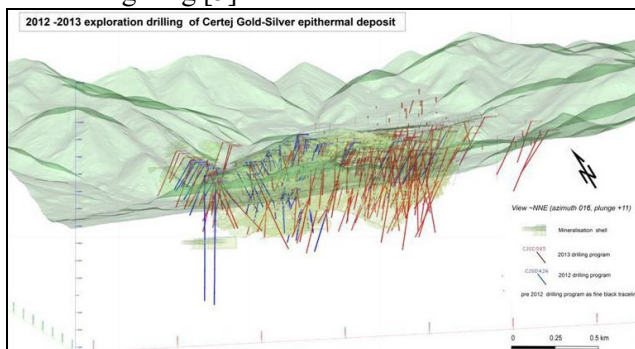


**Fig. 2.** Exploration drillings from 2012-2013 [6]

The deposit is part of the "Golden Quadrilateral" (Săcărâmb - Brad - Rosia Montana - Baia de Aries), an area which produced between 1,000 and 2,000 t Au, since pre-Roman era. Historical information about Certej deposit dates from the seventeenth century, when the mining operations were done using rudimentary methods [7].

### 3. Description of the deposit

Certej ore deposit is classified as an intermediate sulphide epithermal deposit because Au it is associated with Ag, Pb and Zn and to a lesser extent with Te and As. Mineralization footprint has a general E-W orientation and is limited between two major fault lines oriented NW-SE (east and west fault lines).

In detail the Au distribution shows a complex pattern controlled by a combination of structure. The mineralization occurs at the contact of the Baiaga breccias with the sedimentary rocks surrounding

the Hondol and Dealu Grozii andesites. Some of the higher grade mineralizations, in particular, those located in the NW-SE and NE-SW, which concentrated the mineralizing fluids around the Baiaga andesite. The mineralization is associated with disseminated pyrite (with arsenic) along with variable amounts of blende and galena. Native gold is present but confined to distal veins.

The estimation of the mineral resources for the Certej deposit was made with the help of the results obtained from the surface drilling and with the help of the samples taken from the underground exploration channels. The resource estimate was made through a 3D block model created using commercial mining planning software. The size of the block model cell was 10 m east by 10 m north by 5 m high.

Fig. 3a and b show examples of the 2 3D representations of the Certej gold-silver deposit [6].

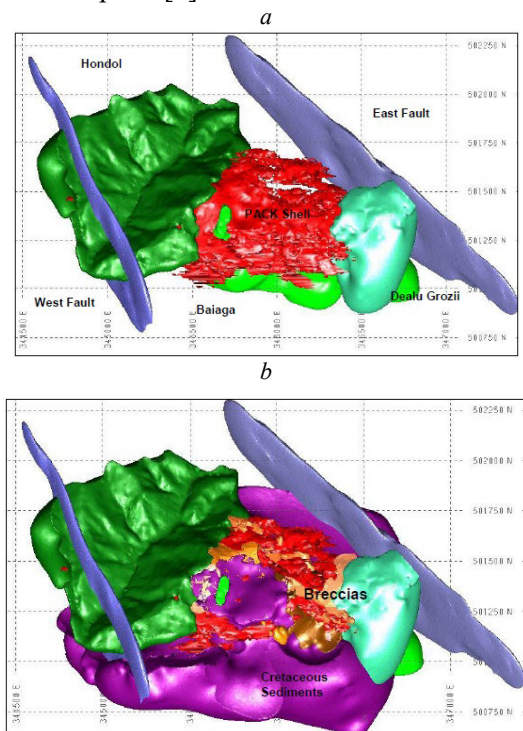


**Fig. 3.** Relationship between mineralized shell and main geologic units: *a* - Shell relative to the intrusive units; *b* - With Cretaceous sediments and breccia units superimposed [6]

The estimated mineral resources in December 2013 were based on an average content of 0.7 g/t Au. Mineral reserves are estimated at 46,984 Mt at a grade of 1.63 g/t Au and 11 g/t Ag. Fig. 4 provides additional details on the mineralization.

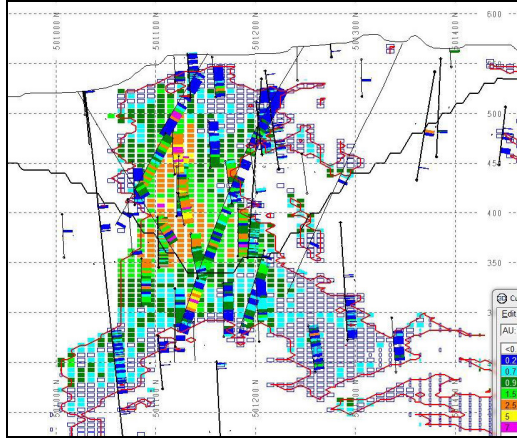


Fig. 4. N-S Cross section through the Certej mineralization [6]

Mineral reserves as reported are derived from, and are included in, mineral resources. No dilution or loss of ore has been included in the conversion of Mineral Resources to Mineral Reserves. Block model methodology was used for both determinations. Mineral reserves were estimated at an equivalent grade of 0.90 g/t Au.

#### 4. Description of the project

The project involves continuing and developing the mining activity from Certeju de Sus commune, implying exploitation and development of the existing quarry, extraction of precious metals (Au and Ag) from the ore, opening and operating the andesite quarry located on Macrisului Valley for building materials, deposition of waste rock and processing slurry, construction of dams for the two tailing ponds, construction of the processing plants, of the explosives deposit and other objectives for the economic development of the area (access roads, utility networks, etc.). In table 1 are shown the areas of land to be occupied by the project [4].

Table 1

Surfaces of land and types of uses [6]		
No	Location	Surface (ha)
Main industrial area		
1	Certej quarry	62.8
2	North waste dump	32.6
3	South waste dump	40.2
4	Processing plant	20.9
5	Access roads	6.9
6	Administrative buildings	0.2
7	Topsoil deposits	7.7
8	Protection zone (green areas)	65.3
Total main industrial area		236.8
Secondary industrial area		
9	Flotation and cyanidation tailings ponds	63.6
Total industrial area		300.5
10	Perimeter protection zone	155.7
Total area		456.2

Forecast production of processed ore is approx. 3,000,000 t/year, gold concentrate being of approximately 315,000 t/year [4, 7].

The topsoil deposit derived from the quarry will be located in the vicinity of the preparation plant and the soil from the ponds site will be deposited downstream of the flotation tailings pond. Soil deposition and the construction of the deposits will be in conformity with the conventional technology as to ensure their stability, with steps, and slopes that respect the natural angle.

The volume of soil to be removed taking into account that its thickness varies according to the location is estimated at approx. 1.408.000 m<sup>3</sup> [6].

Corresponding works to the project objectives will be achieved in four stages: construction, operation, closure and post-closure.

Mining technology is the usual one for such deposits, respectively drilling-blasting technology. The displaced material will be loaded with backhoe loaders and front loaders to large capacity dumper trucks and the ore is transported to the gyratory crusher. Crushed material (primary crushing) is then transported to the processing plant [4].

Development of Certej quarry will be carried out progressively, in 4 phases, for high efficiency (fig. 5).



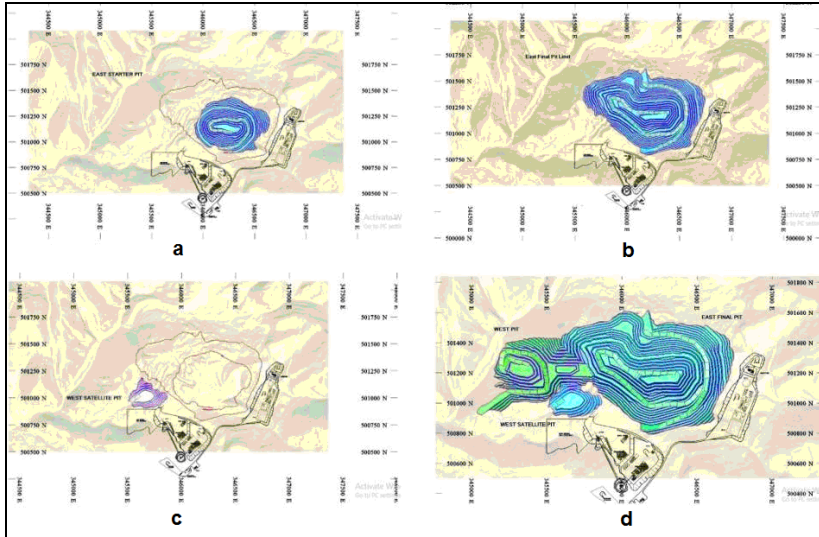


**Fig. 5.** Development of Certej quarry, *a* - Phase I, opening - East starter pit; *b* - Phase II - East expansion; *c* - Phase III - West satellite pit; *d* - Phase IV - Final quarry [6]

Waste rocks, resulted from the removal of the overburden and quarry's steps profiling works will be stored in two dumps: North and South waste dumps (fig. 6). The material will be transported and deposited using dumper trucks.

Areas with slopes exceeding  $10^\circ$  will be arranged with proper twinning steps in order to create a solid bound between the natural terrain and the waste rocks. Twinning steps are executed with reverse tilt to the foundation.

The North and South waste dumps (fig. 6) will be protected by supporting walls on a total length of 600 m, respectively 100 m. They will be executed in 5 m sections, with compaction grout between them. The foundation of the walls will be made in the bedrock. The crowning of the walls will be executed in steps of 0.5 m following the natural slope of the land. Foundations will be made of concrete [6].

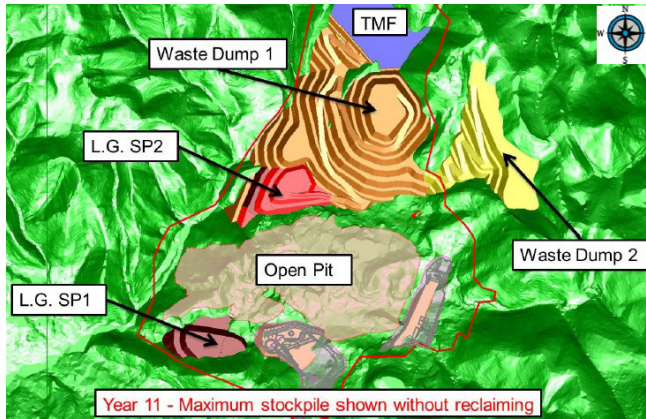


Fig. 6. Locations for waste dumps and low grade stockpiles [6]

Forecasted production of processed ore - approx. 3,000,000 t, gold concentrate - approx. 315,000 t/year (for a total period of 10 years).

For processing the quantities of ore and for obtaining the gold concentrate there are needed a range of other raw materials, hazardous or non-hazardous, whose stock and degree of dangerousness are shown in table 2.

The ore will be processed by two well-known methods: flotation and cyanidation (fig. 7). The process for preparing the gold concentrate by flotation involves the use of reactivities that are more toxic than cyanide.

Table 2

Raw materials required [5, 6]			
Name of raw materials or substances	Annual quantity in stock	Classification of raw materials or substances	
		Hazardous/ Nonhazardous (H/NH)	Dangerousness
Ammonium nitrate	3697 t/year,	NH	-
Initiating explosive - dynamite	229 t/year, stock 10 t	H	Explosive
Amyl xanthate	390 t/year; stock 20 t	NH	-
Dowfroth foam	150 t/year; stock 5 t	NH	-
Aero 3477 - collector	120 t/year; stock 10 t	NH	-
Copper Sulfate	955 t/year; stock 25 t	H	Toxic, irritant, dangerous for environment



Sodium Silicate 40%	4,120 t/year; stock 160 t	NH	-
Hydrate lime (including whitewash)	7,791 t/year; stock 219.5 t	H	Irritant
Limestone	241605 t/year; stock 250 t	NH	-
Sodium cyanide (solid and solution)	1653 t/year ; stock 276 t	H	Toxic, dangerous for environment
Active coal	35 t/year; stock 55 t	NH	-
Hydrochloric acid	898 t/year; stock 87 t	H	Corrosive
Sodium hydroxide	328 t/year; stock 27 t	H	Corrosive
Sodium metabisulphite	1909 t/year; stock 159 t	H	Toxic, irritant
Flocculants	171 t/year; stock 28 t	NH	-
Peroxide (50%)	12 t/year; stock 1 t	H	Oxidizer, Corrosive
Oxygen	183,901 t/year; stock 154 t	H	Oxidizer
Diesel fuel	5,400,000 l/an; stock 153 mc	H	Inflammable
Oils (engine oil, hydraulic oil)/lubricant	63,000 l/year	H	Irritant, toxic, dangerous for environment
LPG	240 t/year; stock 10 t	H	Inflammable
Borax	0.607 t/year	NH	-

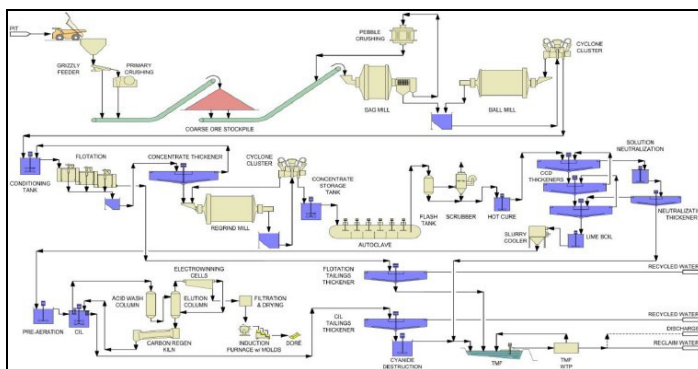
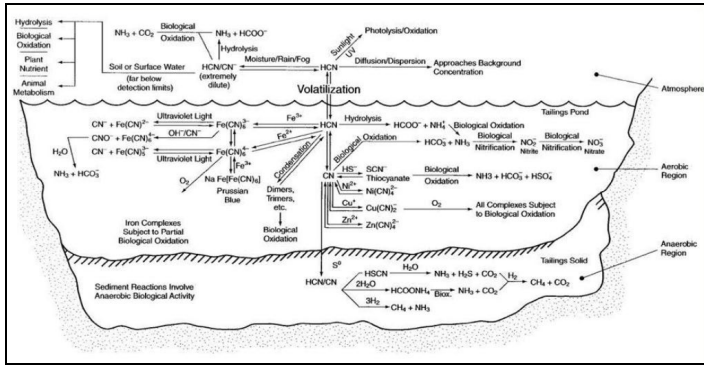


Fig. 7. Simplified process flowsheet for Certej Process Plant [6]

Cyanidation tailings contain a quantity of cyanide that is considerate harmless to humans and whose concentration will decrease naturally, cyanide decomposing under the effect of light and air into harmless compounds (fig. 8).



**Fig. 8.** The complete cycle of cyanide decomposition [4]

Tailings ponds dams (fig. 9) will be constructed of rocks (from the andezite quarry), in stages: initiation dam (starter) and successive elevations, their maximum height being 169 m for the flotation tailings pond and 70 m for cyanidation tailings pond.

Upstream slopes of the two dams are protected by three filtering layers, namely: 1.5 m filter made of crushed stone, 1.5 m filter made of fine gravel and sand, and over the fine filter a geotextile and a HDPE geomembrane for waterproofing [4].

Tailings ponds will be provided with safety dams located downstream, which will gather the exfiltration.

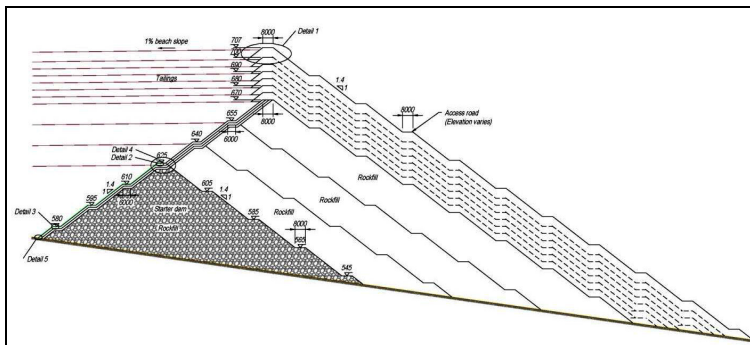


**Fig. 9.** Typical tailing pond construction details [4 - 6]

These two dams will ensure decontamination and disposal of seepage waters to a storage tank. From the storage tank the water is

pumped back into the pond, then will be brought inside the processing plant and recycled. Excess water from the flotation tailings pond will be treated and discharged into the natural watercourses; clarified water from cyanidation tailings pond is entirely recycled except for extraordinary weather events when these waters will be treated in the Detox II station [5, 6].

## **5. Environmental implications**

Certej mining perimeter is located in a severely degraded area as a result of multiple interactions, on very long-term, between environmental components and anthropogenic factors.

### **5.1. Effects of the historical pollution on the site**

Regarding the environment, the area is affected by previous mining activities and has a low value due to historical pollution: polluted water resources, fragmented habitats, degraded landscape, etc.

*Water quality* - is primarily affected by the uncontrolled discharge of wastewater resulting from the exploitation activities and minerals processing operations, acid waters with high content of pollutants, such as: copper, iron, manganese, arsenic, cadmium, nickel, lead, mercury, selenium, chromium, sulfur, dissolved salts, etc. Currently, mining activities have been abandoned since 2006, the main factor that influences and affects water quality, is the type of mineralization in the area.

Consequently, the exposure of sulphide ores to atmospheric oxygen and water, generates acid mine waters, which are collected through underground galleries and discharged untreated through various mine holes or directly into surface waters as runoff from waste dumps or other uncovered surfaces.

*Air quality* - around Certej mining area is influenced by sources located both within the industrial site and outside it and are represented by stripped areas of quarries that were exploited till 2006 and associated waste dumps, tailings ponds, surfaces exposed to wind erosion, that have become sources of air pollution with dust particles and, not least, the traffic.

*Soil quality* - around the mine site presents different forms of degradation such as: surface and deep erosion, landslides, excess moisture from rainfall and lateral leaks. Soils are polluted with heavy metals (Cd, Co, Cr, Cu, Mn, Ni, Pb, Zn), with punctual manifesta-

tions, their concentrations do not exceed the limits, and the pH indicates an acidic or moderately acidic reaction.

**Flora and fauna** - is considered one of the areas with the greatest impact on biodiversity in Romania. The mining activities from the past have led to total elimination of the open natural ecosystems. In areas where human impact has stopped for at least 50-60 years, spontaneous vegetation is present in various stages of development.

**Noise and vibrations** - because the extraction and processing operations are ceased, the associated noise and vibrations is absent. Currently, the main source of noise in the area is the traffic.

**Socioeconomic, situation and human health** - mining was the main source of employment, but with its cessation the number of jobs in the area was reduced. The agriculture and tourism are practiced at small-scale, a few months per year, but they are poorly developed.

The population is aging and there is a trend of depopulation of the village. The population shows a significant level of poverty. From a health perspective it is noted that the population has a higher incidence of chronic and acute diseases than the population in other places, one of the causes being represented by public exposure to polluted waters due to the fact that only a part of the locals have access to potable water from the public network.

## **5.2. Assessment of the environmental impact**

The highly important activity of environmental impact assessment is currently regulated in Romania, in general by Emergency Ordinance no. 195 of 2005 on environmental protection [8], and specifically by Law no. 292 of 2018 (with subsequent amendments and additions) [9], which establishes the framework procedure for environmental impact assessment [10].

Environmental Impact Assessment (EIA) - procedure of identifying and forecasting the impact on the biotic and physical environment and human health, arising from legislative activity, policy, programs, projects and operative procedures, interpretation and communication of informations regarding the impacts, but also to highlight measures to prevent, eliminate or reduce to a minimum negative impacts on the environment before they manifest [9].

Environmental impact assessment generated by any anthropogenic project is an essential step, that requires numerous analyzes, stud-

ies and researches, which should be covered regardless of the size of the project [11].

**Checklist method** - checklists are aimed at identifying and assessing the impacts of the analyzed project on environmental components by highlighting the potentially significant effects on them [12, 13].

The results for Certej mining project are synthetically presented in the form of a checklist, which identifies of positive and negative impacts and evaluates the cumulative environmental impact (table 3).

Table 3

Checklist for identification of cumulative impact [14]

Environmental components	Identification of potential negative impacts	Identification of potential positive impacts	Assessing the cumulative impact
Air	air pollution	implementation of specific management plans	negative-insignificant
Water	discharge of treated wastewater, pluvial waters	acid water treatment implementation of specific management plans	neutral
Soil	soil occupation and degradation	implementation of specific management plans	negative-significant
Flora and fauna	habitat changes and losses	establishment of compensatory ecological networks; ecological reconstruction of area; implementation of specific management plans	neutral
Landscape	changing landscape	recovery and rehabilitation of the land; implementation of specific management plans	negative
Noise and vibrations	relatively high levels of noise and vibrations	implementation of specific management plans	negative-insignificant
Socio-economic component (population, patrimony)	resettlement	improvement of living standards; implementation of specific management plans	positive significant

According to the checklist, the cumulative impact of mining project on the environment can be considered negative-negative insignificant.

nificant. The environmental component „soil” is the most affected, suffering a significant negative impact on long-term while the „socio-economic” component is characterized by a significant positive impact.

**Impact networks method** - an impact network allows the identification of direct and indirect impacts chains, primary and secondary, resulting from an action or allows determining the actions that generate a certain impact [12, 13].

In figures 10 and 11 are presented networks built to highlight the impact of primary and secondary impacts of mining activities in Certej area (if the project is implemented), both for quarrying and for gold-silver ore preparation.

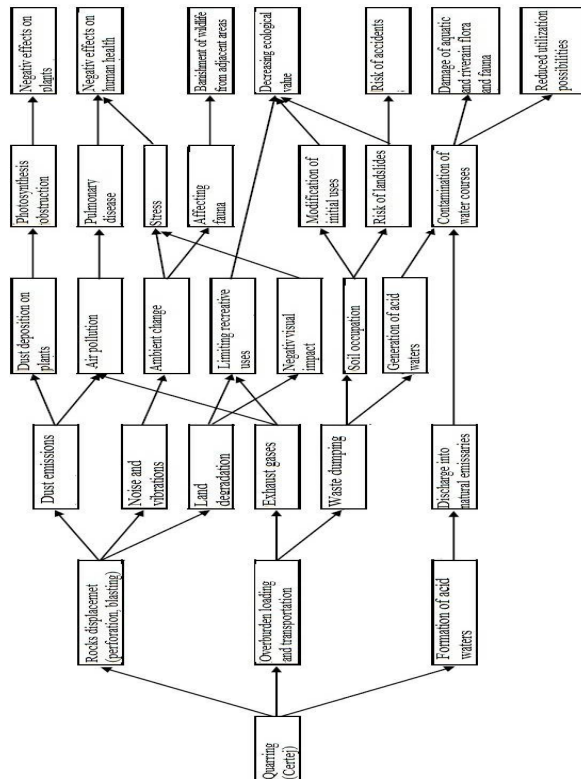


Fig. 10. Impact network for exploitation activities in Certej quarry [14]

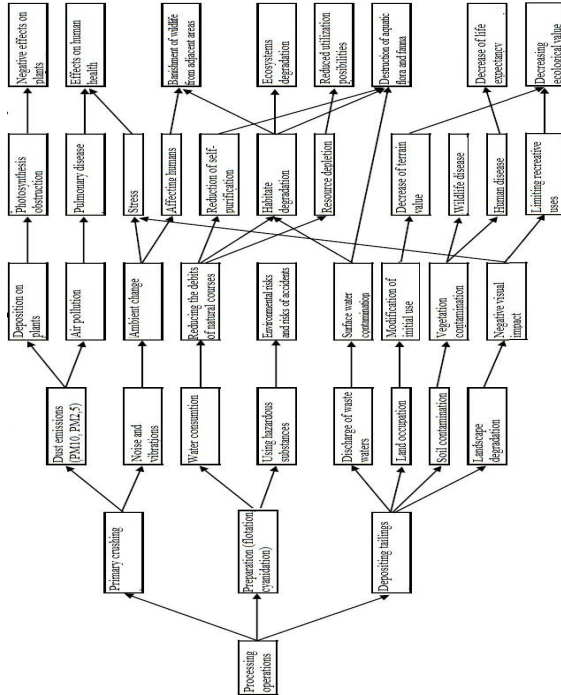


Fig. 11. Impact network for gold-silver ore processing [14]

The impact networks realized for quarrying and processing activities, emphasizes the direct and indirect environmental impacts that could be generated in case of project implementation.

**Impact matrices method** - matrices consist of double entry tables, in which on the lines are entered environmental components and factors involved, divided and grouped into categories, and on the columns are entered the elementary actions of the project. Each intersection of the matrix represents a potential impact relationship between the project actions and environmental factors [12, 15].

In this paper work it is used a matrix system which follows a logical path of analysis that leads to a summarized scheme, similar to the method of coaxial matrixes, in which the elements generating impact (causal factors) are connected to environmental components, and further to the areal typology in which the objective of the study is placed, highlighting potential environmental interactions [14, 16].

There may be assigned various causal factors to each on-site activity.

It is possible to build a matrix whose lines is a list of activities or actions considered relevant and the columns a list of possible individual causal factors.

The existence of a relationship between a relevant activity and a causal factor is emphasized by placing in the cell at the intersection of the line representing the project with the column corresponding to the causal factor.

This intersection can be marked in different ways according to the relevance of the represented relationship, and it can consider the impact as: major (3), medium (2), minimal or unimportant (1) or absent [14].

Thus, for quarrying and ore processing activities it can be build the matrix A, which is the association of the relevant actions and causal factors (table 4).

Table 4  
The association between the relevant actions and causal factors (matrix A) [14]

Matrix A	Causal factors									
Activity	Macropollutants	Micropollutants	Radioactive emissions	Noise emissions	Water consumption	Discharge of wastewater	Surface flooding	Soil occupation	Soil waterproofing	Traffic
Quarrying	3	1		3		1		3	1	3
Processing	3	3		2	3	3		3	2	2

At this point it can be individualized a possible causal relationship between the causal factors, already defined, and the various environmental components, reflected also by a matrix B (predefined) (table 5).



Table 5

The association between the list of causal factors and of environmental components

Environment components	Causal factors									
	Macropollutants	Micropollutants	Radioactive emissions	Noise emissions	Water consumption	Discharge of wastewater	Surface flooding	Soil occupation	Soil waterproofing	Traffic
Air quality	3	3								3
Microclimate	1						3		3	
Surface waters	1	1			3	3	3		3	
Groundwaters					3	3	3		3	
Fauna	3	3	3	3	2	3	3	3		3
Flora	3	3			3	2	3	3		
Ecosystems	3	3	3	2	2	3	3	3	3	3
Soil						2	3	3	3	
Lithosphere					3		3			
Noise level				3						3
Radiations			3							
Landscape	1				2	2	3	3	2	3
Risk						2				3
Mobility										3
Resources availability				3	3			2	2	

A matrix C is obtained (table 6), whose cells contain a combination of the probability contained in the corresponding cell from matrix B with the probability contained in the corresponding line from matrix A. To define associations between matrixes interactions the following rules shall be respected: 3·3→3; 2·3→3; 2·2→2; 2·1→1; 3·1→2; 1·1→1; absent·absent/1/2/3→absent.

Table 6

The intersection between matrix A and matrix B										
Matrix C	Causal factors									
Environment components	Macropollutants	Micropollutants	Radioactive emissions	Noise emissions	Water consumption	Discharge of wastewater	Surface flooding	Soil occupation	Soil waterproofing	Traffic
Air quality	3 (3)	2 (3)								3 (3)
Microclimate	2 (2)								2 (3)	
Surface waters	2 (2)	1 (2)			(3)	2 (3)			2 (3)	
Groundwaters					(3)	2 (3)			2 (3)	
Fauna	3 (3)	2 (3)		3 (3)	(3)	2 (3)		3 (3)		3 (3)
Flora	3 (3)	2 (3)			(3)	1 (3)		3 (3)		
Ecosystems	3 (3)	3 (3)		3 (2)	(3)	2 (3)		3 (3)	2 (3)	3 (3)
Soil						1 (3)		3 (3)	2 (3)	
Lithosphere					(3)					
Noise level				3 (3)						3 (3)
Radiations										
Landscape	2 (2)				(3)	1 (3)		3 (3)	1 (2)	3 (3)
Risk						2 (3)				3 (3)
Mobility										3 (3)
Resources availability				3 (3)	(3)			3 (3)	1 (2)	

It is possible to define a matrix *D* (table 7), whose columns are types of areas (where the project is located) and lines consist of environmental components. The matrix is completed with the vulnerability (certain, probable, unlikely or absent) customized for different types of areas (columns) and environmental components (lines).

Table 7

Association between environmental components and territorial areas									
Environment components	Areal types								
	Historical centers	Metropolitan areas	Urban areas	Agricultural areas	Industrial areas	Tertiary areas	Natural areas	Mountainous areas	Lake, fluvial areas
Air quality	3	3	2	2	3	2	3		
Microclimate		3		2			3		3
Surface waters		3	3	3	3	1	3	3	3
Groundwaters		3	3	3	3	1	3	3	3
Fauna				3			3	3	3
Flora			2	3			3	3	3
Ecosystems							3		3
Soil		3	3	3			3	3	3
Lithosphere							3	3	
Noise level	3	3	2		3	1	3		
Radiations		2					3		
Landscape	3		2	3			3	3	3
Risk			3		3				
Mobility		3	2			3			
Resources availability		3	2		3	2			

By combining matrix *C* and *D*, a new matrix *E* is obtained.

The cells of the matrix contain an indication on the probability of existence of an impact on the environment (table 8).

Table 8

## Environmental impact assessment generated by relevant activities (final matrix) [14]

Environment components	Causal factors										TOTAL
	Macropollutants	Micropollutants	Radioactive emissions	Noise emissions	Water consumption	Discharge of wastewater	Surface flooding	Soil occupation	Soil waterproofing	Traffic	
Air quality	3 (3)	2 (3)								3 (3)	8 (9)
Microclimate	2 (3)							2 (3)			4 (6)
Surface waters	3 (3)	2 (3)			(3)	3 (3)			3 (3)		11 (15)
Groundwaters					(3)	3 (3)			3 (3)		6 (9)
Fauna	3 (3)	3 (3)		3 (3)	(3)	3 (3)		3 (3)		3 (3)	18 (21)
Flora	3 (3)	3 (3)			(3)	2 (3)		3 (3)			11 (15)
Ecosystems	3 (3)	2 (3)		3 (3)	(3)	2 (3)		3 (3)	2 (3)	3 (3)	18 (24)
Soil						2 (3)		3 (3)	3 (3)		8 (9)
Lithosphere					(3)						(3)
Noise level				3 (3)						3 (3)	6 (6)
Radiations											
Landscape	3 (3)				(3)	2 (3)		3 (3)	2 (3)	3 (3)	13 (18)
Risk						1 (3)				3 (3)	4 (6)
Mobility										3 (3)	3 (3)
Resources availability				3 (3)	(3)				1 (2)		4 (8)
TOTAL	20 (21)	12 (15)		12 (12)	(24)	18 (24)		15 (15)	16 (20)	21 (21)	<b>114 (152)</b>

\* Values without brackets are for quarrying (in mountainous areas) and values in the brackets are for processing operations (in natural areas) (in tables 8 and 10)

For the analyzed objectives there were chosen two types of areas: mountainous areas for the quarry and natural areas for the processing activities (the two tailing ponds overlaps with a protected area).

The last line respectively column sums up the values resulting from multiple combinations of matrixes, and depending on the amounts earned in each row and column it can be appreciated which of the environmental components will be most affected and which of the specific actions of the project will generate the most severe impacts [14].

To assess the environmental impact of Certej mining project (quarrying and gold-silver ore processing), the matrix  $E$  (shown in table 8) was completed.

Analyzing the final matrix is noted that the processing of ore and tailings deposition in ponds has a potentially and significantly greater impact on the environment than the quarrying activity.

## **6. Conclusions**

Certej mining project aims to continue the exploitation and processing of Certej gold-silver ore deposit, activity that started in XVII<sup>th</sup> century and that was abandoned in the first decade of the XXI<sup>st</sup> century, this paper representing a study that aims to identify and assess the environmental impacts of the project.

There were considered the main stages of mining activity, starting from topsoil recovery, construction and development of tailing ponds, exploitation activity, waste material deposition, processing operations and sterile sludge decantation.

The accent is concentrated on the environmental impacts of mining and processing stages of the project (if implemented), being used three methods, namely: checklists, impact networks and impact matrices.

The last two methods emphasize particularly the negative impacts, while checklist identifies cumulative impacts and interactions between the effects on human and natural environment, showing that project implementation can bring a number of improvements of the existing situation.

According to the impact matrix the entire mining activity from Certej will generate a major negative impact, primarily on the following environmental components: wildlife, ecosystems and landscape. Among the specific quarrying activities, the emissions of macropollutants and traffic will generate the most significant impacts, while the processing activities have as environmental disruption causes the water consumption and discharge of wastewater.

The results obtained for Certej mining project are interpretable, however, given that current technology allows the exploitation and recovery of the gold-silver ore deposit while ensuring environmental

protection, imposing the recovery and rehabilitation of affected areas through the implementation and compliance with specific management plans for each environmental components it can be appreciated that the implementation of Certej mining project could bring major benefits on long term, for the local community and environment.

## *References*

1. **Fodor D.**, 2015, Mining and environment (in Romanian), Corvin Publishing House, Deva, Romania.
2. **Georgescu, M.**, 2022, Environmental risk management (in Romanian), Universitas Publishing House, Petrosani, Romania.
3. **Fodor D., Baican G.**, 2001, The impact of the mining industry on the environment (in Romanian), Infomin Publishing House, Deva, Romania.
4. **Hodor C., Danci O., Mancu C., Ionescu T.**, 2013, Proper assessment study for the project "Gold-silver ore mining in Certej perimeter" (in Romanian), Deva, Romania.
5. **Forward P., Liddell N., Jackson T.**, 2009, Certej Updated Definitive Feasibility Study Summary. Technical Report. National Instrument 43-101 Technical Report, February.
6. **Alexandrer R., Stephen J., Miller R., Kalanchey R.P.**, 2014, Technical Report for the Certej Project, Deva, Romania.
7. **RSG Global Consulting** (now Coffey Mining), 2007, Certej Gold Silver Project, Romania, Technical Report. National Instrument 43-101 Technical Report, November.
8. **Emergency Ordinance no. 195**, 2005, regarding environmental protection, Official Gazette, No. 1196, December 30<sup>th</sup>.
9. **Law no. 292**, 2018, regarding the assessment of the impact of certain public and private projects on the environment, Official Gazette, Part I, no. 1043, December 10<sup>th</sup>.
10. **Băbuț, G., Băbuț, C.M.**, 2012, Environmental protection legislation - course notes (in Romanian), Universitas Publishing House, Petrosani, Romania.
11. **Order No. 19**, 2010, of the Ministry of Environment and Forests (MEF), Guidelines on proper assessment of the potential effects of the plans and projects on protected natural areas of community interest (in Romanian), Bucharest, Romania.
12. **Lazăr M., Faur F.**, 2011, Identification and assessment of the anthropic impact on the environment. Project guide (in Romanian), Universitas Publishing House, Petrosani, Romania.
13. **Faur F., Brujan (Predoiu) M., Lazăr M., Apostu I.-M., Moisuc-Hojda D.**, 2023, A brief study to assess the environmental impact generated by Jiłț North open pit. Mining Revue. Vol. 29. Issue 4.
14. **Apostu I.-M., Florin Faur, Lazăr M.**. 2016. Identification and assessment of the environmental impact generated by the implementation of Certej Mining Project, Research Journal of Agricultural Science, Vol. 48, Nr. 4, pp. 254-264.
15. **Dumitrescu, I.**, 2021, Anthropogenic impact assessment methods (in Romanian), Universitas Publishing House, Petrosani, Romania.
16. **Lazăr M., Faur F.**, 2013, Identification and assessment of the risk and impact generated by Roșia Poieni quarry and Dealul Piciorului processing plant. Annals of the University of Petroșani, Mining Engineering, Vol. 14, pp. 129-143.

## **OPTIMIZATION OF ORE DEPOSIT MINING SYSTEMS WHILE CHANGING CUT-OFF PARAMETERS FOR RESERVES ESTIMATION**



**Stanislav LYTVYNIUK**

PhD in Geology, Deputy head of SCMR,  
State Commission of Ukraine on Mineral Resources  
(SCMR), Ukraine

### **Summary**

The paper defines the basic cut-off parameters for the reserves calculation of ore deposits, which affect the ore body morphometry. The optimal choice of the cut-off parameters ensures the substantiation of effective opening and extraction systems. For deposits that have been exploited for a long period, the use of irrelevant cut-off parameters may lead to the need to partially change mining systems and reduce the efficiency of economic indicators. The study determined typical cut-off parameters for iron ore deposits. The example of an underground iron ore mining deposit was analyzed, where it was necessary to partially change the mining system due to the presence of small isolated ore deposits. As an alternative option, the cut-off parameters were reevaluated, additional parameters were implemented - minimum ore reserves in isolated ore bodies and economical cut-off grade. The implementation of these parameters made it possible not to change the mining system and to improve the ore grade. The use of parameters of minimal isolated ore deposits also reduces loss and clogging of mineral compared to design solutions. According to forecast calculations, this option of mining development will provide greater indicators of economic efficiency.

### **Introduction**

Mining technical and technological solutions for the opening and extraction of ore minerals are based on the results of the balance reserves calculation within the deposit. Contouring of ore bodies and reserves calculation of ore deposits is implemented on the basis of cut-off-parameters. The list of parameters is individual for each deposit and their selection should be justified by optional calculations.

Cut-off parameters for mineral are the main tool of geological and economical modeling of mineral deposits, which contain the necessary list of limit indicators for effective development of the deposit. According to the regulatory documents cut-off parameters - a set of limit requirements for the quality and quantity of mineral raw mate-

rials in the subsoil, mining and geological, mining technical and other conditions for the deposits development, compliance with which during the calculation ensures the most complete and cost-effective extraction and use of available reserves and mineral resources (*Classification, 1997; Regulation, 2004; Regulation, 2006*).

Cut-off parameters are limit values of indicators, which are set for a sample, interval, exploratory cross section, mining ledge or calculation block on the basis of technical and economic calculations, current standards and technical conditions, technical tasks of subsoil users, experience of geological exploration work and mining operation. The cut-off parameters contain a list of limit indicators, with the use of which the most comprehensive, rational and safe use of ore deposit reserves is achieved. As a rule, not 1-2, but 4-10 limit parameters are set, which together give such an effect.

For individual cases, the same cut-off grade in deposits cause a change in the volumes of reserves in different ways, since the cut-off parameters of the mining and technical direction cause a change in the morphometry of ore deposits and act on these volumes in a complex manner.

The list of parameters of conditions for calculating reserves of an individual deposit requires geological, mining and economic justification. Geological justification includes the analysis and determination of the following characteristics: conditions of occurrence, features of the internal structure, variability of ore deposits, engineering-geological and hydrogeological conditions of development, spatial position of ore bodies, patterns of distribution of ore quality, their technological types and grades.

The mining and technical justification involves the assessment and determination of the following components:

- the choice of the method and system of deposit's opening, development, and mining system for individual ore bodies, the choice of the technological scheme of processing, the maximum level of extraction of the main and added useful components.
- determination of the production capacity and life of mine, selection of mining equipment types, means of mechanization, other design solutions,
- justification of the amount of losses and the degree of minerals impurity.



In this study, the relationship between cut-off parameters and changes in the mining system is determined for one of the domestic iron ore deposits of the Kryvyi Rih Basin, therefore, the following section provides information on the basic and additional cut-off parameters for iron ore deposits.

*Basic cut-off parameters for reserves calculating of ore deposits.*

Cut-off parameters for iron ore deposits are used at all stages of geological study and development: preliminary and temporary parameters - at the stage of exploration, constant parameters - at the stage of detailed exploration and mining operation, operational conditions - in case of significant unforeseen changes in mining and geological or economic conditions of operation.

In order to justify individual set of cut-off parameters, variable technical and economic calculations are carried out, which fix the maximum economic effect for a separate set of indicators. Indicators and cut-off parameters are characterized by significant dependencies (direct and inverse) among themselves. Thus, when the cut-off grade and the minimum capacity of ore bodies change, other geological, mining and technical-economic parameters change significantly (the reserves tonnage, their grade, the amount of capital investments, possible fluctuations in production capacity for ore extraction, etc.). Most of the cut-off parameters are determined by numerical multivariate calculations, which are aimed at identifying regular correlation between geological, technical, and economic indicators (*Instruction, 2003; Regulation, 2004*).

The object of this study is the minable and extractable reserves of iron ore deposits that are exploited. So the main attention in this section is focused on the constant parameters that are defined for the explored reserves for a long period of time. For iron ore deposits, the following cut-off parameters are most often used, which are grouped here according to the main direction of their impact:

Quality parameters of iron ores, which are adopted in domestic practice (*Instruction, 2003; Regulation, 2004; Kurylo, 2021*):

1. Economic cut-off grade for magnetic iron (for magnetite quartzite reserves), and general iron – for rich ores. The parameter is applied to counting blocks and divides balance and off-balance reserves.

2. Natural cut-off grade of magnetic iron (for reserves of magnetite quartzite), and general iron - for rich ores. The parameter for contouring ore deposits, as a rule, is applied to edge sections, edge samples, to determine the outer contours of ore bodies. The parameter is used in the absence of clear geological boundaries of the ore body.

3. Cut-off grade in the marginal cross-section - the minimum grade of the useful component in the marginal cross-section, which is included in the reserves calculation during the contouring of the deposit along the dip and extension beyond the boundaries of the mine.

4. In case of presence of multicomponents iron ores, coefficients of transition from the main metals to added components are defined.

5. Limit content of harmful impurities.

6. Conditions for selection of types and grades of iron ores for selective mining, if they have different technological properties.

7. For rich iron ores and deposits with very complex geological structure with complex patterns of useful component distribution, a minimum ore bearing coefficient can be set in the counting block.

8. Minimum thickness of ore bodies or the corresponding minimum metro-percentage.

9. The maximum permissible thickness of layers of empty rocks or substandard ores, which are included in the reserves calculation.

10. Minimum reserves of isolated ore bodies.

11. Maximum depth of reserves calculation.

12. Limit stripping ratio.

Current cut-off grade of iron associated with magnetite for domestic ferruginous quartzite deposits vary significantly from 10 to 20%. The lowest values are for Novokryvorizke, Artemivske, Petrivske, Velika Gleyuvatka deposits, average values of 14-16% are for Horyshne-Plavnynske, Lavrykivske, Yeristivske, Valyavkinske, Inguletske, Gannivske deposits. The Skelevatske Magnetitove deposit has high values of 18%. Larger values are set for objects of underground mining of ferruginous quartzites. For BIF deposits, where oxidized varieties are present in the structure of the reserves, increased values of the cut-off grade are also used precisely for them, due to the difficult processing. Thus, for the oxidized quartzites of the Valyavky deposit, the cut-off grade is 28%, for the oxidized quartzites of the Velika Gleyuvatka deposit, it is 32%.

For rich iron ores, which are mined underground, the cut-off grade is usually within 46-48%, which provide sufficiently effective mining operation (*Kurylo, 2021*).

### **Case study**

As an example of determining additional cut-off grade parameters for reserves calculating, one of the iron ore deposits of the Kryvyi Rih Basin is described below. Production is localized in the central part of the Kryvorizke deposit. In the geological structure of the deposit, the mine field includes metamorphic rocks of novokryvorizkaya, skelevatskaya, saksaganskaya, gdantsivskaya and gleyuvatska, and cenozoic deposits sediments.

The main ore-bearing stratum of the deposit is the saksagan serie, which consists of seven iron and seven shale horizons. It has the total thickness 1860 m where the most productive are the fifth and sixth iron horizons. The fifth iron horizon lies directly on the third and fourth shale horizons. The maximum depth of the horizon is 2400 m.

The majority of ore deposits belong to the fifth horizon. The content of total iron in the ores is from 45% to 70%. The thickness of the horizon is 30-90 m. In the southern part of the deposit, the horizon is cut by a diagonal fault and is observed only in the form of small remnants with a thickness of 6 to 25 m. The horizon is mainly composed of martitic quartzites with jespilites.

The sixth iron horizon is also the main ore-bearing layer. The horizon is composed of red-striped martite quartzites. The iron content in martite quartzites is from 20 to 45%. Rich martite ores are characterized by high iron content (47-70%), goethite-hematite-martite and goethite-hematite ores contain 47-60% iron. The total horizontal thickness of the horizon is 250-300 m, the dip is northwest at an angle of 50-60°.

The rich iron ores of the deposit are represented by two types according to their material composition: saksagan and ingulets. Oxidized ores of the saksagan type, confined to the fifth and sixth iron horizons, predominate. The mineral composition of saksagan type ores corresponds to the mineral composition of the host rocks and differs only in the quantitative ratio of the ore minerals that make up the framework and the wider development of the processes of superimposed epigenetic mineralization. Ores of the ingulets type have a magnetite composition.

The deposit is dominated by martite ores, which make up 38% of rich iron ores. The second place is iron-sludge-martite ores - 31%. Quartz-martite and quartz-iron-lime-martite ores make up 12%, dispersed hematite-martite - 8%, dispersed hematite ores of shale horizons - 5%. Unoxidized ores of the ingulets type - 6%.

The distribution of mineralization within iron horizons is extremely uneven and discontinuous. Ore bodies have an extremely complex morphology - they are interrupted, sometimes merge with each other, form numerous apophyses.

Taking into account the ore bodies morphology, the variability of qualitative indicators, the area of the rich iron deposit is classified as a deposit of a very complex geological structure (group 3), in accordance with the Classification of Mineral Reserves and Resources of the State Mineral Resources Fund.

The mine is developing separated sheet-like, pillar-like and nest-like ore bodies, the length of which varies from 110 to 600 m, the thickness from 8 to 25 m, and the angle of incidence is 55-72 °. Approximately 65% of ore deposits have a strength of 100-120 MPa, and 35% - 30-60 MPa. The hanging side is composed of martite quartzites with a strength of 90-130 MPa, and the lying side is composed of hematite quartzites with a strength of 70-90 MPa.

The deposit is opened by two ore-lifting shafts and two ventilation shafts. Development systems: floor-chamber, sub-floor-chamber and sub-floor collapse with ore removal by deep bore-holes.

The main system of reserve development is underground rockfall with ore hammering by deep holes into the compensation space with ore release through ducts. For this system, the project adopted the following indicators: losses - 15%; impurity - 15%, loss of quality (iron content) 3.23%. The adopted annual design capacity is 1.3 million tons.

In order to outline the ore bodies and calculate the rich iron ore reserves of the mine field, the typical cut-off parameters for rich iron ore deposits developed underground are applied:

1. The cut-off grade of total iron in the marginal sample, which is included in the reserves calculation for contouring the ore bodies by thickness, is 46%.

2. The minimum thickness of the ore body included in the reserves calculation is 4 m.

3. The maximum thickness of intra-ore layers of empty rocks and substandard ores included in the reserves calculation is 6 m.

4. The economical cut-off grade of total iron in the calculation block of balance reserves is 50%

5. The maximum depth of calculation to the horizon is 1500 m.

*Use of additional condition parameters. The minimum reserves of isolated ore bodies.*

Separated ore bodies are present within the defined deposit, the development of which is considered difficult. Mining and technical conditions are fixed here, which complicate or make their effective development impossible:

- self-rockfall of unstable quartz-carbonate rocks into the cleaning space. The chamber contains more mobile and less dense quartz-carbonate rocks with an Fe content of 5-10%. Mined ore with a content of 20-35%, even after processing on a magnetic separator, does not allow obtaining commodity products of the required quality.

- high risk of destruction of auxiliary ventilation objects. Refortification of which is not possible due to the lack of safe approaches and delivery of materials for fixing.

- areas of destruction and splits of production holes that occurred after the explosion, mechanical destruction of metal fasteners by mining pressure. In order to extract the lost stockpiles, it is necessary to go through a complex of mining works.

*Determination of minimum reserves in isolated ore bodies.* Determination of minimum reserves in isolated ore bodies was carried out in order to determine the industrial value of reserves in blocks that have particularly difficult mining and technical development conditions. The feasibility of industrial development (loss-free mining) of isolated ore bodies (sites) carried out with the formula

$$Q_{\min} = Ex_1 \times I / (P_i - Ex_2) \times L,$$

where  $Q_{\min}$  is the minimum reserves in isolated ore body with a given content of useful components in the ore;

$Ex_1$  - additional costs associated with the opening and working of the ore body

$I$  - ore impurity, %;

$P$  - the value of all useful components per 1 ton of mined ore;

$Ex_2$  - operating costs for extraction and processing to final commodity products of 1 ton of ore of the estimated (isolated) ore bodies;

$L$  - operational losses during mining, %.

The following values of technical and economic indicators were used to determine this condition parameter for reserves calculation.

$Q_{\min} = Ex_1 / (P_i - Ex_2) L$	$Q_{\min}$	9 тис т
additional costs associated with the opening and extracting of the ore body	$Ex_1$	4 000
impurity	$I$	16%
value of all ore components per 1 ton of mined ore	$P_i$	1600
operating costs for production and processing to final commercial products 1 ton of ore, evaluated (isolated) ore bodies	$Ex_2$	1150
експлуатаційні втрати operational losses	$L$	16%

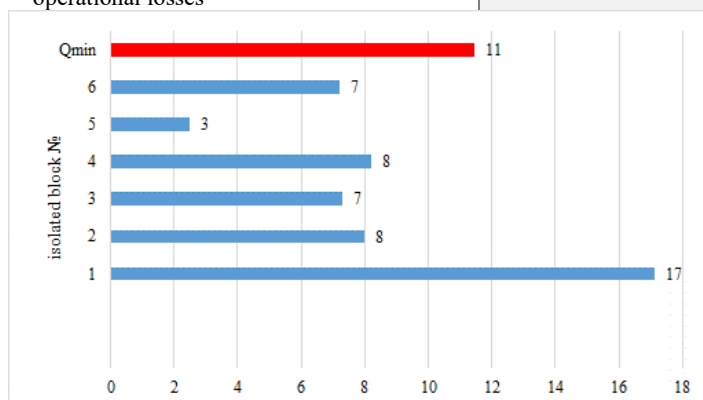


**Fig. 1.** Distribution of tonnage in isolated ore bodies and comparison with cut-off parameter

Additional costs associated with the opening and working of the ore body are determined by the average value of the specific costs of 40m<sup>3</sup>/1000t of ore for preparatory cuttings and 3 p.m. drilling wells.

Based on the results of calculations of minimum reserves in isolated ore bodies, the blocks listed in the following table do not meet the specified parameter and are not of industrial importance.

*Determination of the economical cut-off grade for blocks with complex mining and technical development conditions*

The economical cut-off grade is the content of a useful component that ensures the equality of the costs of extraction and processing of a useful mineral and the processing of commodity prod-

ucts and the value of the useful component that is extracted at the same time. This indicator determines the level of break-even mining and processing and at the same time ensures the closest connection of mining and geological, technical, technological and economic characteristics of the deposit. The economical cut-off grade is recommended to be determined based on the following ratio:

$$C_{\min} = Ex / P \cdot K_e \cdot I,$$

where  $C_{\min}$  is economical cut-off grade;

$Ex$  - full operating costs for extraction and processing of a unit mass or volume of a mineral;

$P$  - the price of a unit of mass or volume of commodity products of a mining enterprise;

$K_e$  - extraction of a useful component into commodity products from a useful mineral, part of a unit;

$I$  - mineral impurity during extraction and transportation, fraction of a unit.

The following data were used to determine the economical cut-off grade in blocks that are defined as having difficult mining and technical conditions:

$Ex$  - UAH 1200/t;

$P$  - determined individually by blocks, taking into account the Fe % content and the weighted average cost of 1% Fe - UAH 28.67;

$P$  - 16%.

$K_e$  - 0.867.

According to the results of the calculations of the minimum industrial content of the useful component, selected blocks with an iron content in the mined ore mass in the range of 20-45% are outside the limit values of  $C_{\min}$  - 62% and have no industrial value.

### **Conclusions**

Reserves of rich ores in blocks of “bottoms” and isolated ore bodies characterized by complexity of mining condition and reduced indicators of the ore’s pittance, which is accumulated instead of the bark component in species. girmichy mass. The average value of the vegetable oil in individual blocks is 18.9-54.7%, the average value is 24.52%. Such values, instead of the increase in the type of footwear stocks, are responsi-

ble for the extremely high increases in the indicators of ore detected, which are found in the range of 11.9-69.4%.

Based on the results of the breakdown of minimal reserves in isolated ore bodies, the blocks listed in the following table do not correspond to the specified parameter.

As a result, the reserves are classified as off-balance and may be excluded from the distribution circuit. This makes it possible to further adopt a mining system - subsurface deboning with ore knocking with deep drills into a compensation area with the release of ore through the chutes. The effectiveness of the change in additional conditioning parameters is also due to changes in the indicators of consumption and ore volume, and the river design volume of 1.3 million tons was adopted until then.

### *References*

1. Classification of Mineral Reserves and Resources of the State Fund of Subsoil. 1997, Official Edition of 1997, No. 19, Art. 104, Act Code 700/1997.

2. **Kurylo M.** 2021. Resource constraints in the development of iron ore deposits in the transition to quality metallurgy and renewable energy. Dissertation to achieve the scientific level of Doctor of Geological Sciences. Kiev Taras Shevchenko National University of Kyiv. 2021.

3. Regulations on the design of mining enterprises of Ukraine and the determination of mineral reserves by the degree of readiness for extraction. 2004, Official Gazette of Ukraine dated 07/23/2004, No. 27, Volume 2, p. 417, article 1807, act code 29404/2004.

4. Instruction on the Application of the Classification of Mineral Reserves and Resources of the State Fund of Subsoil to the Deposits of Construction and Facing Stone (2003). Official Edition of 21.02.2003, No. 6, Article 205, Article 261, Act Code 24374/2003.

5. Regulation on the Procedure for Development and Substantiation of Mineral Resource Conditions for Estimation of Subsoil Reserves (2006). Official Edition of February 15, 2006. No. 5, Article 137, Article 246, Act Code 35044/2006.



**MINERAL PROCESSING TECHNOLOGIES  
AND EQUIPMENT TO SEPARATE FINE/ULTRAFINE  
MINERAL VALUES. A REVIEW**



**Nikolaos KOUKOULIS**

Mechanical and Water Resources Engineering, Technological Educational Institute (TEI) of Messolonghi, currently: Researcher, National Technical Univ. of Athens (NTUA), Greece



**Georgios N. ANASTASSAKIS**

Professor, Director of Mineral Processing Laboratory, National Technical Univ. of Athens (NTUA), Greece

**Abstract**

In numerous cases of mineral processing, fine to ultrafine mineral particles are inevitably produced during the process of mineral liberation, with the percentage depending on the ore-grade. In case of low-grade ore, efficient liberation demands excessive grinding, as a necessity for efficient separation of fine-grained mineral value from gangue. Due to the peculiar properties of fine particles (physical, chemical), conventional processing methods have limited success or fail to separate the particles, especially at industrial level, because of the concomitant problems. As a result, mineral values of many commodities are lost to the tailings, e.g. phosphate, copper, tungsten, tin, sulfide minerals, iron, etc. With mining operations been shifted to the exploitation of even lower-grade ores, the problem of fine particles separation is expected to deteriorate.

The current paper deals with the innovation in equipment and processes developed to meet the problem of fine/ultrafine particles separation. Special emphasis is placed on physicochemical methods, which are mainly based on the improvement or modification of already known ones.

## 1. Introduction

Mining has been tightly bound with human history throughout centuries and highly contributed to the progress of humanity. Millennia years ago, Neanderthals used stone to make primitive tools and serve their elementary needs for living; in the relatively recent historic era, ancient Egyptians, Greeks, Romans and Incans used more sophisticated mining and processing technologies to extract and use mined materials, creating the corresponding civilizations and fabulous artifacts. Passing through the Industrial Age era that is characterized from the onset of the ability for mass production, the progress of human society has led to our modern times' demand that is characterized by bigger, faster, stronger and more products. The aforementioned clearly denote that human living, progress and civilization is based on natural resources. To see the importance of mining and related activities, let's imagine the impact of minerals on various sectors of daily use, such as building, household (appliances, cookware, decoration), transportation (cars, trains, planes, spaceships), communication (cell phones, radars, satellites), medicine (X-rays, robots, fine surgical tools), science, engineering, weaponry (although destructive), etc. What is the future trend? The staggering demand for primary raw materials will keep being even more increasing. Just consider where the advanced, and more sophisticated, technologies rely on (e.g., renewable energy equipment, sustainable energy generation, electric vehicles, just to mention some sectors of advanced engineering). What is the limit? Nobody knows, as humankind continuously sets new targets and expands its activities (e.g. into the Universe).

The aforementioned retrospect of human evolution and the emerging in the future clearly substantiate the strong dependence of human progress and economic prosperity on mineral commodities. To satisfy the continuously increasing demand in products, goods and services, there must be equal (or even higher) demand in mineral values, which leads to the extraction and processing of even larger tonnage of mineral raw materials. As the high-grade orebodies are gradually depleted, even lower-grade ones have to be extracted, followed by several problems. The major problem upon processing low-grade ore deposits is the fine particle size along with the concomitant

inefficient processing and subsequent losses of mineral values to the tailings. The increased loss along with the deposition of even larger volumes of tailings in case of low-grade deposits render extraction and mineral processing more unsustainable processes than in usual cases [1].

Mineral value losses are encountered either as rejected waste (often called “extractive waste”) because of imperfect liberation from gangue or as lost fines because of inefficient separation.

The general term “extractive waste” collectively denotes waste and tailings. They are produced in billion metric tons every year from mining and processing operations and are deposited in Extractive Waste Facilities (EWF) as waste heaps or tailing dams, depending on their particle size and prior processing. The amount of waste depends on the grade of the commodity; for high-grade commodities (e.g., coal, bauxite, iron ore) its order is some kilograms per kilogram of product while it increases to several million metric tons per ton of product for low-grade or complex ores such as gold ores [2, 3]. To obtain a view, the amount of the total extractive waste generated in EU, in the period 2004-2014, roughly ranges between 550 and 750 Mt/year [4]; the estimation for the global extractive waste is over 100 billion metric tons per year [5]. Waste can be further categorized into “mine waste”, which is of no economic value and, consequently, rejected, as well as “mineralized mine waste”, which contains some quantity of mineral value and presents future potential economic prospects [6]. Consequently, every mineralized waste could be viewed as a potential, already-mined deposit and promising for mineral value recovery, after reprocessing [7-10]. This consideration necessitates proper liberation size, application of efficient reprocessing methods, high-grade product and positive overall economic outcome. Despite the wish for relatively coarse liberation size, the separation of mineral values from gangue in fine/ultrafine particle size is often inevitable because mineralized waste is usually a low-grade deposit.

When low-grade orebodies have to be extracted, the mineral value is usually disseminated as fine particles within the mass of gangue, because of the mineralogical texture of the orebody; consequently, the material has to be ground in very small particle size to obtain liberated particles. In this case, the entire process is designed to the ideal separation of the value from gangue. In fact, severe prob-

lems, because of the very small particle size, lead to inefficient separation with conventional separation methods and equipment, as these methods fail to obtain a concentrate of high grade and recovery in value [11]. As a result, considerable part of mineral values (tin, tungsten, porphyry copper, sulfide minerals, iron ores, phosphate, etc.) is lost to the tailings [11, 12]. It is characteristic that approximately one-fifth of the world tungsten and one-half of Bolivian tin is lost as fine particles because common gravity methods fail to provide with a concentrate of increased recovery for such a fine particles size; one-third of the phosphate is discarded as slime in Florida phosphate industry, as the effort of their recovery should be uneconomic due to the excessive consumption of flotation reagents; one-tenth of iron ores explored in USA is discarded as slimes; similarly, losses for USA porphyry copper ores reach one-fifth while, even for sulfide minerals finely disseminated in the matrix, losses are so high as half of the value [12].

A lot of effort has been devoted on the role and influence of fine particles on separation methods, especially on flotation, which is the most proper method to separate particles of such a fine size [13-16]. Provided that it is important to reduce the loss of fine mineral values, the development of procedures and equipment to cope with the problem draws the attention of many workers, as the extraction of orebodies shifts to even lower grade deposits. Consequently, the improvement or modification of standard separation methods and the application of new techniques is a necessity for the processing of fine mineral particles.

The current paper reviews the progress achieved in separation methods (physical and physicochemical) and equipment to cope with the problem of fine particles separation.

## **2. Problems during fine/ultrafine particle separation**

The generation of fine particles is inevitable in many operations of mineral commodities processing. In case of low-grade ores, the mineral value is found as finely disseminated particles due to its mineralogical texture; consequently, particle liberation is achieved upon grinding of the orebody to fine particle size. Although there are differences regarding particle size characterization, fine is usually characterized a particle in the size range of  $-100\mu\text{m}+20\mu\text{m}$ , very fine of  $-20\mu\text{m}+5\mu\text{m}$ , ultrafine of  $-5\mu\text{m}+1\mu\text{m}$ , and colloid the smaller than

1 $\mu$ m [17]. Very often, particles with grain size less than 20 $\mu$ m are commonly characterized as “slimes”.

The characteristics of the ore deposits, especially the grain size of the mineral value in the ore, its dissemination in the mass of the deposit, and its association with the gangue minerals, highly determine the liberation size, the abundance of fine particles, the selection of efficient equipment, the proper separation method in some cases, and, consequently, the entire flow sheet of ore processing.

The major problems associated with the inadequate separation of fine particles are due to their following physical and chemical properties: small mass, high specific surface area, and high surface energy per unit area [11, 12, 17]. Regarding separation methods, the major problems related to these properties can be briefly summarized to the following:

- During separation with conventional gravity methods (jigging, flowing-film separation, etc.), the forces associated with water-flow dominate over those associated with gravity for fine/ultrafine particle size (less than 100  $\mu$ m). Separation becomes progressively inefficient as particle size reduces while impossible for ultrafine particles. This fact renders the major share of mineral values irrecoverable by using gravity separation through conventional equipment.

- Magnetic separation is not efficient regarding the recovery of fine/ultrafine particles (less than 100 $\mu$ m), especially when feebly magnetic particles are involved. This fact has resulted throughout the years in their deposition into tailings and, consequently, loss of considerable volumes of fine/ultrafine paramagnetic mineral values (goethite, limonite, hematite, chromite, cassiterite, etc.).

- Common electrostatic separation methods are inefficient for fine mineral particles (-75  $\mu$ m). This is mainly due to the small particle mass, influence of drag forces because of turbulence inside the chamber, as well as the difficulty of optimizing the residence time of the particles in the electric field, without affecting the other operating variables and setting parameters [18].

The problems regarding fine/ultrafine mineral flotation in conventional cells have been well substantiated [11-17]; these problems are mainly due to the small size of minerals and the concomitant effects, as well as to the hydrodynamic conditions prevailing in the cell. Flotation inefficiency for fine particles, especially for ultrafine size and

below, is related to low probability of bubble-particle collision and adhesion, large bubble size, mechanical entrainment and entrapment, slime coating, higher flotation reagent adsorption, formation of dense froths and low process kinetics.

In the previous paragraphs, the major and most common problems encountered during fine/ultrafine mineral particles processing were delineated. Given that physical properties are inherent to minerals and the possibility for their modification is not always feasible, the efforts regarding physical separation methods have been mainly focused on the development of novel equipment.

As regards physicochemical separation of fine/ultrafine particles, the efforts have been focused on the following axes (a) development of novel equipment and (b) development of novel and more sophisticated procedures. In the next section, the equipment and procedures used to cope with the problem of fine/ultrafine mineral separation are reviewed.

### **3. Separation Methods**

#### **3.1 Physical Methods**

##### *3.1.1 Gravity Separation*

As gravity circuits are much simpler than other (e.g. flotation) and mineral value (usually heavy) appears considerable density difference from gangue, the use of gravity circuits has been involved in many cases of fine/ultrafine particle separation. To efficiently treat fines and smaller particles, efforts led to innovative devices, which utilise centrifugal force to enhance the gravitational field. Centrifugal motion is usually applied along with pulsation, sluicing or oscillating motion. Such devices are the following:

Centrifugal Jigs. These devices incorporate the operating principles of jigging (pulsing action, water injection) along with centrifugal spinning motion. The ability of centrifugal jigs to highly increase the apparent gravitational field improves settling characteristics of fine particles and enhances the chance of their recovery. Separations of such fine particles as 38  $\mu\text{m}$  with small density difference have been referred [19]. Kelsey jigs, which are the well-known, have been used both to separate various heavy minerals (zircon, rutile, cassiterite, wolframite, gold, tantalum and nickel minerals, etc.) at industrial level [20-23] and to recover fine heavies from tailings [24, 25].

Mozley Multi-Gravity Separator (MGS). This machine combines centrifugal motion of an angled rotating drum with oscillating motion; it can separate particles down to  $10\mu\text{m}$ , because of the high “g” forces developed [19]. It has been employed to recover the corresponding heavy mineral from chromite, cassiterite and tungsten ores [26-28].

Knelson Concentrator utilises the combination of high centrifugal force, up to  $60\text{“g”}$ , and a back pressure force, arisen from injected water to form fluidised bed [29].

Falcon Concentrator separates through combination of centrifuge and sluicing; its operation under high “g” forces (from 50 to  $200\text{“g”}$ ) permits the concentrator to efficiently separate both coarse and very fine particles ( $15$  to  $20\ \mu\text{m}$ ) [19, 30]. This concentrator has been used to recover very fine gold particles, and tantalum ore slimes [30, 31].

Flowing-film concentrators. The following concentrators are included in this class, which holds a significant share among gravity separators for very fine particles: Bartles-Mozley Multi – deck, Bartles Cross-belt and Duplex concentrator.

Bartles-Mozley Multi - deck concentrator is a semi-continuous device, based on the combination of flowing-film phenomena on a slightly tilted deck, which is also subjected to horizontal orbital motion to develop shear between heavy and light particles’ bed. It consists of 40 fiberglass decks (tables) being arranged in two sections of 20 decks each, suspended by cables; each deck is riffled and connected by  $\frac{1}{2}$ -inch plastic formers that define the pulp channel [32]. It is used for particle size between  $100$  and  $5\mu\text{m}$ , but in case of gold and platinum separation it can reach down to  $1\mu\text{m}$  [33].

Bartles Cross-belt concentrator has been used to separate chromite and cassiterite from light gangue of  $-100+5\mu\text{m}$  size [32]. It consists of an endless belt from PVC with a central longitudinal ridge. The belt has slight slopes from the ridge out to the sides. At the same time, the belt is subjected to orbital motion, which is imparted by a rotating weight [32].

Duplex concentrator has been used to recover cassiterite, tungsten, tantalum, gold, chromite and platinum from fine ( $-100\ \mu\text{m}$ ) feed [34]. It is comprised of two decks operating under slight tilt; the decks are used alternatively to provide continuous feeding, with one deck being fed and the other being discharged from the heavy product.

### *3.1.2 Magnetic Separation*

In 1960s and 1970s, the development of Wet High-Gradient (or High-Intensity) Magnetic Separators (WHGMS or WHIMS) highly contributed in the recovery of fine weakly magnetic minerals and in the removal of color influencing contaminants from kaolin and other industrial minerals (e.g., kyanite, calcite, feldspars) in order to increase the whiteness and commercial value of the product [35-37].

With the subsequent development of high gradient superconducting magnetic separators (HGSMS) there was achieved an order of magnitude stronger field than ordinary ferromagnetic-core electromagnets and allowed industry to efficiently separate very fine weakly magnetic minerals as well as to refine kaolin [38, 39]. Further improvement of some features of the traditional Jones-type WHIMS resulted in high capacities and improved separation performances [40-43]. The innovations include: the orientation of the carousel, the utilization of 1-3 mm diameter rods as filamentary matrix, depending on feed size range and the establishment of pulsation in the separation zone through an actuated diaphragm.

### *3.1.3 Electrostatic Separation*

Research efforts on fine particle separation resulted in the development of novel separators, mainly based on tribo-electrification [18, 43-46]; the separation on various mineral commodities proved successful [18, 43-49].

## **3.2 Physicochemical Methods**

The physicochemical methods applied to cope with the problem of fine particles separation are primarily based on the combination or modification of known processes and sophisticated flotation equipment. Some of the methods are based on the principles of selective agglomeration process solely while others on the combination of selective agglomeration with another method, such as flotation or magnetic separation. The most popular methods are cited below.

### *3.2.1 Methods involving flotation*

The inefficient separation of fine particles in sub-aerating flotation cells has been known since long time ago. In this respect, flotation devices of special design have been developed and installed in flotation plants to overcome the problem, among which column cells [50-56], jet (Jameson) cells [57], "Microcell" column [58] and reflux flotation cell [59].



Also, various flotation techniques such as, dissolved air flotation [60], electro-flotation [61], oil flotation, liquid-liquid extraction [62] and carrier flotation have been developed. Thus, despite the progress at lab and industrial scale, there still exist many items to be solved, especially in the size range  $-20\ \mu\text{m}$ .

In electro-flotation, electrolytically generated fine bubbles (oxygen, hydrogen or both) are involved to efficiently float fine particles [61]. In liquid-liquid extraction and oil flotation (or emulsion flotation), oil droplets are introduced into flotation cell to collect hydrophobic particles. The droplets/particles aggregates are collected on the top of the cell as separate immiscible phase (liquid-liquid extraction) or with the aid of air-bubbles (oil flotation). The drawback of the methods seems to be the relatively high oil consumption [11]. Carrier flotation (ultraflotation or piggy-back flotation) is based on the flotation of fine particles as slime coating of coarser (carrier mineral). In industrial level, it has been applied to improve the brightness of kaolin via removing anatase impurities [63]. The major drawback of the process is high reagent and carrier mineral consumption; another drawback is the required separation of mineral value from carrier, if the mineral value is concentrated in the froth.

### *3.2.2 Methods involving hydrophobic agglomeration*

Hydrophobic agglomeration is a general term used to denote clustering of hydrophobic particles in aqueous suspension, due to hydrophobic interactions between them under intensive agitation. It is considered to be an effective and potential technique for the separation of very fine mineral particles.

Hydrophobic agglomerates present variability regarding their size, strength, structure and properties, which depend on the applied agglomeration process, the prevailing conditions and the interaction forces. The most common processes involving hydrophobic agglomeration are [1]: shear-agglomeration (or shear-flocculation), agglomerate flotation/floc-flotation, oil agglomeration (or spherical agglomeration), various magnetic carrier methods, selective agglomeration/flocculation.

In shear-agglomeration the fine hydrophobic particles are aggregated under shear field provided by intense stirring to overcome potentially existing barriers [64, 65]. The resulting hydrophobic agglomerates are not always either large or compact, unless the particles are strongly hydrophobic or reagents are added to render parti-

cles hydrophobic or reinforce hydrophobicity. The separation of agglomerates is generally achieved through screening, sedimentation, magnetic separation or froth flotation.

Agglomerate flotation (or floc-flotation) combines hydrophobic agglomeration of fine particles followed by their flotation with air-bubbles [66-68]. The size of the agglomerates must not be very large so that flocs are able to float with air bubbles.

Oil (or spherical) agglomeration is established, when large amount of non-polar oil is added [69-71]. In this case, the pores of the agglomerates are filled with non-polar oil and they appear in the form of pellets. The function of oil is to bind, through oil bridges, the particles into agglomerates that are strong enough to be separated by mechanical means (e.g., settling or screening) from the rest of the slurry.

Various sophisticated techniques of magnetic separation have been involved in the separation of fine/ultrafine mineral particles, with the following being the commonest: i) Magnetic carrier (magnetic coating) that is based on the selective coverage of feebly- or non-magnetic minerals with a very fine ferromagnetic material to artificially provide the surface of non-magnetic minerals with magnetic properties, with or without collector; this is attained by controlling the surface properties of the mineral to be covered and of the magnetic material [72]. Magnetic coat is stronger when collector is used; the combination of collector and an immiscible oil phase results in heavier magnetic coating [73, 74]. ii) Floc magnetic separation (magnetic seeding or selective co-agglomeration with ferromagnetic particles) is encountered in various forms. When hydrophobicity has been established on particles with paramagnetic properties, the inter-particle bonds are tighter, as they are subjected not only to hydrophobic attractive forces but also to magnetic attractive ones [75]. In case of non- or poorly-magnetic minerals, the incorporation of ferromagnetic particles, indifferent of size, into the hydrophobic agglomerates increases the magnetic susceptibility of agglomerates or establishes it (magnetic seeding). iii) Alternatively, if a suspension is flocculated with a high molecular weight polymer in the presence of a ferromagnetic material, then co-flocculation is obtained either due to entrapment of ferromagnetic material within the flocs or co-adsorption of polymer both on mineral and magnetic material [76].

iii) Selective wetting by ferromagnetic laden oil is achieved if naturally hydrophobic or collector-hydrophobized minerals are contacted with ferromagnetic laden oil droplets. In this case, ferromagnetic oil tends to spread over their surface rendering them selectively magnetic; hence, their separation from hydrophilic, non-magnetic particles is feasible [77].

Fine/ultrafine particles can also be selectively separated through agglomeration/flocculation by adding polymeric flocculants in the fine particle suspension.

The first step includes dispersion of the suspension using proper dispersant. Subsequently, flocculant is added to selectively agglomerate the fine particles of the target-mineral into flocs. Consequently, the target-mineral is efficiently separated from fine gangues by settling, as flocs settle faster than dispersed particles [78].

The method has been applied for the selective separation of fine synthetic mineral mixtures at lab-scale only [79], because of its sensitivity to various physicochemical and mechanical factors.

As mineral/polymer flocs are not always hydrophobic in nature, selective flocculation is not regarded as hydrophobic agglomeration method.

#### **4. Conclusions**

As high-grade orebodies are gradually depleted, mineral extraction and processing are shifted to continuously lower grade ones. This fact results in finer liberation size, inefficient separation, high losses of mineral values and high volumes of waste/tailings. To make mineral extraction and processing more sustainable, fine/ultrafine particles have to be efficiently processed.

Common separation methods fail to process fine particles, as they are scheduled to treat coarse ones. Efficient processing can be achieved through the development of innovative equipment and sophisticated processing methods. Some of them have already been applied while other have to be improved.

Among them modified flotation equipment and hydrophobic agglomeration combined with another method (flotation, settling, magnetic separation) are promising ones but they must be further improved.

#### *References*

1. **Anastassakis, G.N.** (2012). Fine/Ultrafine Mineral Particles Separation through Hydrophobic Agglomeration, Encyclopedia of Colloids and Surfaces, P. Somasundaran (Ed.), Taylor & Francis.

2. EC-JRC (2009). Reference Document on Best Available Techniques for Management of Tailings and Waste-Rock in Mining Activities. European Commission Joint Research Centre, Luxembourg.
3. IAI (2015). Bauxite Residue: Management Best Practice. International Aluminium Institute & European Aluminium Association.
4. Eurostat (2015). Waste Generation and Treatment. Publications Office of the European Union. <http://ec.europa.eu/eurostat/data/database> (accessed: January 2, 2024).
5. Rankin, W.J. (2015). Towards zero waste, AusIMM Bull., 32-37.
6. Lottermoser, B.G. (2010). Mine wastes: characterization, treatment and environmental impacts, Springer, Berlin.
7. Anastassakis, G. (2002). Design of an integrated resource management system for total resource recovery. Technical/ Economical problems and future perspectives, Proceedings TMS Fall 2002 Congress on Recycling and Waste Treatment in Mineral and Metal Processing: Technical and Economic Aspects, B. Bjorkman, C. Samuelsson, J-O Wikström (Eds.), Vol. 1, pp. 199 – 208.
8. Alcalde, J., Kelm, U., & Vergara, D. (2018). Historical assessment of metal recovery potential from old mine tailings: A study case for porphyry copper tailings, Chile. Minerals Engineering, 127, 334-338.
9. Babel, B., Penz, M., Schach, E., Boehme, S., & Rudolph, M. (2018). Re-processing of a Southern Chilean Zn Tailing by Flotation — A Case Study. Minerals, 295(8), 2-18, doi:10.3390/min8070295.
10. Leistner, T., Embrechts, M., Leissner, T., Chehreh Chelgani, S., Osbahr, I., Möckel, R., Peuker, U.A., & Rudolph, M. (2016). A study of the re-processing of fine and ultrafine cassiterite from gravity tailing residues by using various flotation techniques. Minerals Engineering, 96-97, 94-98.
11. Fuerstenau, D. W., Chander, S., & Abouzeid, A. M. (1979). The recovery of fine particles by physical separation methods. In: Beneficiation of Mineral Fines. Problems and Research Need, 1st edition, The American Institute of Mining, Metallurgical, and Petroleum Engineers Inc., Michigan, USA, 3-59, 1979.
12. Fuerstenau, D.W. (1980). Fine particle flotation, in: Fine Particles Processing, Proceedings of International Symposium Fine Particles Processing, Las Vegas, USA, Vol. 1, 669-705, 1980.
13. Gaudin, A.M., Groh, G.O. & Henderson, H.B. (1931). Effect of particle size on flotation. Technical Publications of American Institute of Mining Metallurgical Engineers, 414, 3-23.
14. Gaudin, A.M., Fuerstenau, D.W. & Miaw, H.L. (1960). Slime coatings in galena flotation. Canadian Mining and Metallurgical Bulletin, 53, 960–963.
15. Trahar, W.J. and Warren, L.J. (1976). The floatability of very fine particles – A review. International Journal of Mineral Processing, 3, 103-131.
16. Trahar, W.J. (1981). A rational interpretation of the role of particle size in flotation. International Journal of Mineral Processing, 8, 289-327.
17. Sivamohan, R. (1990). The problem of recovering very fine particles in Mineral Processing – A review. International Journal of Mineral Processing, 28 (3-4), 247.
18. Todu, E., Thompson, W.G., Whitlock, D.R., Bittner, J.D., & Vasiliauskas, A. (1996). Commercial separation of unburnt carbon from fly ash. Mining Engineering, 6, 47-50.
19. Falconer, A. (2003). Gravity separation. Old Technique/New methods, Physical Separation in Science and Engineering, 12(1), 31-48.
20. Wyslouzil, H.E. (1990). Evaluation of the Kelsey mineral jig at Rio Kemptville tin. 22<sup>nd</sup> Annual Meeting of CIM, Ottawa, 1990, Paper Number 23, 461-472.

21. **Butcher, G., & Laplante, A.** (2003). Recovery of gold carriers at Granny Smith Mine using Kelsey jigs J1800. *Advances in Gravity Separation*, SME, 2003, 155-164.
22. **Beniuk, V.G., Vadeikis, C.A., & Enraght-Moody, J.N.** (1994). Centrifugal Jigging of Gravity Concentrate and Tailing at Renison Limited. *Minerals Engineering*, 7 (5/6), 577-589.
23. **Burt, R.O., Korinek, G., Young, S.R., & Deveau C.** (1995). Ultrafine tantalum recovery strategies. *Minerals Engineering*, 8(8), 859-870.
24. **Richards, R.G., & Jones, T.A.** (2004). The recovery of fine values from tailings streams by enhanced gravity separation. Paper presented at MEI Gravity Concentration Conference, Perth, Australia, 2004.
25. **Clemente, D., Newling, P., Bothelo de Sousa, A., Le Jeune, G., Barber, S.P., & Tucker, P.** (1993). Reprocessing slimes tailings from a tungsten mine. *Minerals Engineering*, 6(8-10), 831-839.
26. **Ozkan, S.G., & Ipekoglu, B.** (2001). Concentration studies on chromite tailings by multi gravity separator. *Proceedings 17<sup>th</sup> IMCET*, 2001, 765-768.
27. **Turner, J.W.G., & Hallewell, M.P.** (1993). Process improvements of fine cassiterite recovery at Wheal Jane. *Minerals Engineering*, 6(8-10), 817-829.
28. **Traore, A., Conil, P., Houot, R., & Save, M.** (1995). An evaluation of the Mozley MGS for fine particle gravity separation, *Minerals Engineering*, 8(7), 767-778.
29. **Irwin, A.** (1982). The Knelson hydrostatic concentrator. *Min. Review*, 2(4), 41-43.
30. **Abols, J.A., & Grady, P.M.** (2006). Maximizing gravity recovery through the application of multiple gravity devices. Paper presented at MEI Gravity Concentration Conference, Perth, Australia, 2006.
31. **Deveau, C.** (2006). Improving fine particle gravity recovery through equipment behaviour modification. 38<sup>th</sup> Annual Meeting of the Canadian Mineral Processors, 2006, Ontario, Canada, 501-517.
32. **Silva, M.** (1986). Placer gold recovery methods, Department of Conservation - Division of Mines and Geology, California, Special Publication 87.
33. **Burt, R.O., & Ottley, D.J.** (1974). Fine gravity concentration using Bartles-Mozley concentrator. *International Journal Mineral Processing*, 1(4), 347-366.
34. **Pearl, M., Lewis, K., & Tucker, P.** (1991). A mathematical model of the Duplex concentrator. *Minerals Engineering*, 4(3-4), 347-354.
35. **Ciesla, A.** (2003). Practical aspects of high gradient magnetic separation using superconducting magnets. *Physicochemical Problems of Mineral Processing*, 37, 169-181.
36. **Wasmuth, H.D., & Unkelbach, K.H.** (1991). Recent developments in magnetic separation of feeble magnetic minerals. *Minerals Engineering*, 4(7-11), 825-837.
37. **Watson, J.H.P.** (1994). Status of superconducting magnetic separation in the mineral industry. *Minerals Engineering*, 7 (5-6), 737-746.
38. **Ohara, T., Kumakura, H., & Wada, H.** (2001). Magnetic separation using superconducting magnets. *Physica C: Superconductivity and its Applications*, 357-360, 1272-1280.
39. **Newns, A., & Pascoe, R.D.** (2002). Influence of path length and slurry velocity on the removal of iron from kaolin using a high gradient magnetic separator. *Minerals Engineering*, 15, 465-467.
40. **Dahe, X., Jin, C., & Shuyi, L.** (1998). New technology of pulsating high gradient magnetic separation. *International Journal of Mineral Processing*, 54(2), 111-127.

41. **da Silva M.B., & da Luz, J.A.M.** (2013). Magnetic scavenging of ultrafine hematite from itabirites. *REM: Revista Escolas de Minas*, 66(4), 499-505.
42. **Luzheng, C., Dahe, X., & Huichun, H.** (2009). Pulsating high-gradient magnetic separation of fine hematite from tailings. *Minerals and Metallurgical Processing*, 26(3), 163-168.
43. **Luzheng, C., Zhihua, Q., Shuming, W., & Songwei, H.** (2013). High-gradient magnetic separation of ultrafine particles with rod matrix. *Mineral Processing and Extractive Metallurgy Review*, 34, 340-347.
44. **Ciccu, R., Ghiani, M., Peretti, R., Serci, A., & Zucca, A.** (2000). A new electrostatic separator for fine particles. *Proceedings of the XXI International Mineral Processing Congress, Rome*, A7, 42-50.
45. **Alfano, G., Carta, M. Ciccu, R., & Del Fa, C.** (1984). Electric separation of finely divided particles in gaseous stream or in vacuo. *Conf. Record IEEE-IAS Annual Meeting, Chicago*, 955-965.
46. **Bouchillon, C.W., & Steele, W.G.** (1992). Electrostatic separation of ultrafine ground low rank coals. *Particulate Science and Technology*, 10, 73-89.
47. **Soong, Y., Link, T. A., Schoffstall, M. R., Turčániová, E., Baláž, P., Marchant, S., & Schehl, R. R.** (1998). Triboelectrostatic separation of mineral matter from Slovakian coals. *Acta Montanistica Slovaca*, 3, 393-400.
48. **Dwari, R.K., & Rao, K.A.** (2009). Fine coal preparation using novel triboelectrostatic separator. *Minerals Engineering*, 22(2), 119-127.
49. **Stencel, J. M., & Jiang, X.** (2003). *Pneumatic Transport, Triboelectric Beneficiation for the Florida Phosphate Industry*. Florida Institute of Phosphate Research, Publication No. 02-149-201.
50. **Finch, J. A., & Dobby, G.S.** (1991). Column flotation: A selected review. Part I. *International Journal of Mineral Processing*, 33(1-4), 343-354.
51. **O'Connor C.T., Mills P.J.T., & Cilliers, J.J.** (1995). Prediction of large scale column flotation cell performance using pilot plant data. *The Chem. Eng. J. and the Biochem. Eng. J.*, 59, 1-6.
52. **Espinosa-Gomez R., Johnson N.W., & Finch J.A.** (1989). Evaluation of Flotation Column Scale-Up at Mount Isa Mines Limited. *Minerals Engineering*, 2(3), 369-375.
53. **Ityokumbul, M.T., de Aquino, J.A., O' Connor, C.T., & Harris, M.C.** (2000). Fine pyrite flotation in an agitated column cell. *Int. J. Miner. Process.*, 58, 167-178.
54. **Tao D., Luttrell, G.H., & Yoon, R.H.** (2000). A parametric study of froth stability and its effect on column flotation of fine particles. *Intern. J. Miner. Process.*, 59, 25-43.
55. **Kennedy, D.L.** (2008). *Redesign of industrial column flotation circuits based on a simple residence time distribution model*. Mc Thesis, Virginia Polytechnic Inst. and State Univ.
56. **Praes, P.E., de Albuquerque, R.O., & Luz A.F.O.** (2013). Recovery of iron ore tailings by column flotation. *Journal of Minerals and Materials Characterization and Engineering*, 1, 212-216.
57. **Mohanty, M. K., & Honaker, R. Q.** (1999). Performance optimization of Jameson flotation technology for fine coal cleaning. *Minerals Engineering*, 12(4), 367 - 381.
58. **Yoon, R.H., & Luttrell, G.H.** (1994). Microcel™ column flotation scale-up and plant practice. *Proceedings 26th Annual Meeting Canadian Mineral Processing, CIM*, paper 12.
59. **Jiarui, C., Wonder, C., & Yongjun, P.** (2022). Flotation behavior in reflux flotation cell – A critical review. *Minerals Engineering*, 181, 107519.

60. **Gochin, R.J., & Solari, J.A.** (1983). Dissolved air flotation for recovery of fine cassiterite. *Transactions of the Institute of Mining and Metallurgy, Section C*, 92, C52-58.
61. **Ladesma, H., & Guzman, M.** (1988). Electroflotation of energite. In *Froth Flotation*, Castro, S.H. & Alvarez, J. (Eds.), Elsevier Science Publishers B.V., Amsterdam, 1988, 355-364.
62. **Lai, R. W. M., & Fuerstenau, D. W.** (1968). Liquid-liquid extraction of ultrafine particles. *Trans AIME*, 241, 549.
63. **Green, W.E., Duke, J.B., & Hunter, J.L.** (1961). Froth Flotation Method. US Patent 2,990,958, July 4, 1961.
64. **Song, S., & Lu, S.** (2000). Theory and application of hydrophobic flocculation technology. In *Proceedings of XXI International Mineral Processing Congress*, Massacci, P. (Ed.), Elsevier, Amsterdam, 2000; C5 31-38.
65. **Pascoe, R.D., & Wills, B.** (1994). Selective aggregation of ultrafine hematite and quartz under high shear conditions with conventional flotation collectors. *Minerals Engineering*, 7(5&6), 647-656.
66. **Pascoe, R.D., & Doherty, E.** (1997). Shear flocculation and flotation of hematite using sodium oleate. *International Journal of Mineral Processing*, 51, 269-282.
67. **Koh, P.T.L. & Warren, L.J.** (1977). Flotation of flocs of ultrafine scheelite. *Trans. AIME, Section C*, 86, 94-95.
68. **Asgari, K., Khoshdast, H., Nakhaei, F., Garmsiri, M.R., Qingqing, H., & Hassanzadeh, A.** (2023). A review on floc-flotation of fine particles: Technological aspects, mechanisms and future perspectives. *Mineral Processing and Extractive Metallurgy Review*, doi: 10.1080/08827508.2023.2236770
69. **Finkelstein, N.P.** (1979). Oil flotations - Discussion. In *Beneficiation of Mineral Fines. Problems and Research Needs, Report of Workshop*, Sterling Forest-New York, USA, August 27-29, 1978; Somasundaran, P.; Arbiter, N; The American Institute of Mining, Metallurgical, and Petroleum Engineers, Inc.: Michigan, 1979.
70. **Capes, C.E.** (1979). Wet Concentration of fine coal. Part 4: Agglomeration. In *Coal preparation*; Leonard, J.W., Ed.; 4<sup>th</sup> Edition AIME, New York, 1979; 10: 105-116.
71. **Allen, R.W., Weelock, T.D.** (1993). Effects of pH and ionic strength on kinetics of oil agglomeration of fine coal. *Minerals Engineering*, 6(1), 87-97.
72. **Parsonage, P.** (1988). Principles of mineral separation by selective magnetic coating. *International Journal of Mineral Processing*, 24, 269-293.
73. **Anastassakis, G.N.** (1999). A study on the separation of magnesite fines by magnetic carrier methods. *Colloids and Surfaces A: Physicochemical and Engineering Aspects*, 149, 585-593.
74. **Anastassakis, G.N.** (2002). Separation of fine mineral particles by selective magnetic coating. *Journal of Colloid and Interface Science*, 256(1), 114-120.
75. **Song, S., Lu, S., & Lopez-Valdivieso, A.** (2002). Magnetic separation of hematite and limonite fines as hydrophobic flocs from iron ores. *Minerals Engineering*, 15, 415-422.
76. **Iwasaki, I.** (1981). Selective Flocculation, Magnetic Separation and Flotation of Ores. US Patent 4,298, 169, November 3, 1981.
77. **Schubert, R.H.** (1980). Magnetic Separation of Particulate Mixtures. US Patent RE 30,360, August 5, 1980.
78. **Yu, S., & Attia, Y.A.** (1987). Review of selective flocculation in mineral fines. In *Flocculation in Biotechnology and Separation Systems*; Attia, Y.A., Ed.; Elsevier: Amsterdam, 1987; 601-637.
79. **Sresty, G.C., & Somasundaran, P.** (1980). Selective flocculation of synthetic mineral mixtures using modified polymers. *International Journal of Mineral Processing*, 6, 303-320.

## **SIMULATION OF COAL AND GAS OUTBURSTS IN OUTBURST-PRONE ZONES OF COAL SEAMS**



### **Viktoriia KRUKOVSKA**

Senior Researcher, Doctor of Technical Sciences, Senior Researcher in Department of Control of Dynamic Effects of Rock Pressure, M.S. Poliakov Institute of Geotechnical Mechanics of the National Academy of Sciences of Ukraine, Ukraine



### **Oleksandr KRUKOVSKYI**

Corresponding member of NAS of Ukraine, Doctor of Technical Sciences, Deputy Director of the Institute, M.S. Poliakov Institute of Geotechnical Mechanics of the National Academy of Sciences of Ukraine, Ukraine

### **Abstract**

The problem of mining safety in outburst-prone coal seams has not yet been fully studied and resolved, so research related to outbursts continues to be relevant for many coal-mining countries. The purpose of this work is to study the coupled processes of elastoplastic deformation of a coal seam, methane filtration and desorption, which occur in the outburst-prone zone of the coal seam, and to establish the regularities of their joint flow. Numerical simulation methods were used to solve this problem.

Simulation of the joint flow of geomechanical and filtration processes in the outburst-prone zone, on its border and beyond it was made. The regularities of changes in geomechanical and filtration parameters in the near-face zone of the coal seam, as well as the regularities of the influence of moisture on the outburst hazard, were established. The developed numerical model allows to identify a safe limit of moisture saturation, at which the nature of geomechanical and filtration processes in the coal seam are quasi-stationary but not dynamic for the specific geological conditions. The influence of the unloading chink on gas-dynamic processes was studied. It was shown, when using an unloading chink, a zone completely unloaded from rock pressure is formed near the mine face, in which the occurrence of cracking and destruction processes is excluded. The use of the unloading chink significantly slows down the process of fracturing, which prevents the onset of dynamic phenomena.

**Key words:** coal and gas outburst, coupled processes, elastoplastic deformation, methane filtration, mining safety, moistening, numerical simulation, unloading chink.



## **1 Introduction**

Coal and gas outbursts threaten the safety of mining operations in the coal mines and are one of the main obstacles to the intensification of underground mining and the introduction of new technologies for mining coal seams [1-4]. In the process of outburst, a large amount of gas and fractured coal mass is thrown into the roadway. Rapidly released energy can cause serious damage to mine personnel and production equipment. This problem has not yet been fully studied and resolved, so research related to outbursts continues to be relevant for many coal-mining countries [5-8], including China, Australia, the USA, Ukraine, etc.

Coal and gas outbursts occur in gas-bearing coals, which have a certain composition and physical and mechanical properties, under the influence of static and dynamic stress fields [9, 10]. Both the properties and stress state are the result of the influence of geological and technological factors [11-14].

These dynamic phenomena occur under conditions of rapidly increasing permeability, which depends on the change in stressed state of the medium and gas pressure in its pores and cracks. On the other hand, the change in gas pressure and its desorption depend on gas permeability. This two-way relationship significantly affects both gas filtration in the fractured porous medium and the occurrence and flow of coal and gas outbursts. The complex interrelation of these processes has not yet been fully studied, and the negative consequences of gas-dynamic phenomena continue to complicate mining operations in outburst-prone coal seams.

The purpose of this work is to study the coupled processes of elastoplastic deformation of a coal seam, methane filtration and desorption, which occur in the outburst-prone zone of the coal seam, and to establish the regularities of their joint flow, which will allow us to significantly approach the understanding of this very complicated phenomenon.

To achieve the goal, the following tasks were set:

- to develop a mathematical model of coupled processes of elastoplastic deformation of coal, filtration and desorption of methane in a disturbed zone near a tectonic fault;

- to study the conditions for occurrence of gas-dynamic processes in the near-face zone of a coal seam;

- to study changes in geomechanical and filtration parameters in the near-face zone of a coal seam;
- to study the impact of some technological influences (moistening and unloading of the near-face zone using unloading chink) on the occurrence and flow of outbursts.

Modern computer technologies make it possible to solve complex problems associated with mining, rock mechanics, and, in particular, with coal and gas outbursts [12, 15-18], therefore numerical simulation is the best suited to achieve the above goal.

## 2 Methods

The coupled processes of the rock massif deformation and gas filtration in a disturbed area are described by a system of equations [19-21]

$$c_g \frac{\partial u_i}{\partial t} = \sigma_{ij,j} + X_i(t) + P_i(t); \quad (1)$$

$$\frac{\partial p}{\partial t} = \frac{k_g}{2m\mu} \left( \frac{\partial^2 p^2}{\partial x^2} + \frac{\partial^2 p^2}{\partial y^2} \right) + q(t), \quad (2)$$

where  $c_g$  - the damping coefficient,  $\text{kg}/(\text{m}^3 \cdot \text{s})$ ;  $u_i$  - the displacements,  $\text{m}$ ;  $t$  - time,  $\text{s}$ ;  $\sigma_{ij,j}$  - the derivatives of the stress tensor components along horizontal axis  $x$  and vertical axis  $y$ ,  $\text{Pa}/\text{m}$ ;  $X_i(t)$  - the projections of the external forces acting on the volume unit of a solid body,  $\text{N}/\text{m}^3$ ;  $P_i(t)$  - the projections of forces due to gas pressure in the porous fractured space,  $\text{N}/\text{m}^3$ ;  $p$  - the gas pressure,  $\text{Pa}$ ;  $x, y$  - coordinates,  $\text{m}$ ;  $k_g$  - the gas permeability coefficients,  $\text{m}^2$ ;  $m$  - porosity;  $\mu$  - gas viscosity,  $\text{Pa}\cdot\text{s}$ ;  $q(t)$  - the gas release function, which models methane desorption from a coal seam,  $\text{Pa}/\text{s}$ .

In most cases, gas-dynamic phenomena occur near tectonic faults, where the coal will be ground and has an initial permeability on 10-20 m from both sides of the fault. Technological permeability  $k_{tech}$ , which depends on the components of the stress tensor [22], is superimposed on the field of initial, tectonic permeability  $k_{tect}$

$$K = k_{tech} + k_{tect}; \quad (3)$$

$$k_{tech} = \begin{cases} 0 & \text{if } Q^* < 0.4; P^* > 0.2; \\ k_{\min} & \text{if } 0.4 < Q^* < 0.6; \\ 0.64Q^{*2} - 0.36Q^* + 0.02 & \text{if } 0.6 < Q^* < 1.0; P^* > 0.1; \\ k_{\max} & \text{if } Q^* > 1.0; P^* < 0.1; \text{ in ZND;} \end{cases} \quad (4)$$

where  $K$  - absolute filtration permeability,  $m^2$ ;  $Q^* = (\sigma_1 - \sigma_3)/\gamma H$  - the parameter characterizing the diversity of the stress field components;  $P^* = \sigma_3/\gamma H$  - the parameter characterizing the unloading of rocks from the rock pressure;  $\sigma_1$ ,  $\sigma_3$  - maximum and minimum components of the principal stress tensor, Pa;  $\gamma$  - the averaged weight of the overlying mine rocks,  $N/m^3$ ;  $H$  - the mining depth, m;  $k_{min}$  - minimum permeability coefficient sufficient to start the filtration,  $m^2$ ;  $k_{max}$  - fracture permeability,  $m^2$ ; ZID - zone of inelastic deformation.

It is known that water affects the phase permeability, the amount of free gas in the crack-pore space and the methane filtration process [23, 24]. In the three-component medium "solid - gas - water" moving components (gas and water) move together in the crack-pore space of the solid with absolute filtration permeability  $K$ . On the other hand, the whole without exception the crack-pore space is filled with gas and water, with the content of  $s_g$  and  $s_w$ , respectively

$$s_g + s_w = 100\%.$$

That is, the permeability for the gas phase  $k_g$  depends on the water content

$$k_g = (1 - 0,01s_w)K. \quad (5)$$

In addition, if the gas filtration rates  $V_g = \sqrt{V_x^2 + V_y^2}$  become large, then the gas flow expands cracks in coal and gas permeability in areas with high speeds increases by a value that depends on  $V_g$

$$k_g = (1 - 0,01s_w)K + f(V_g). \quad (6)$$

The presence of water in the crack-pore space of coal reduces gas permeability and thus affects the process of gas filtration.

The initial and boundary conditions for the task are

$$\begin{aligned} \sigma_{yy}|_{t=0} &= \gamma H; & \sigma_{xx}|_{t=0} &= \lambda \gamma H; \\ u_x|_{t=0} &= 0; & u_y|_{t=0} &= 0; \\ p|_{t=0} &= p_0; \end{aligned} \quad (7)$$

$$\begin{aligned}
u_x|_{\Omega_1} &= 0; & u_y|_{\Omega_2} &= 0; \\
p|_{\Omega_1} &= p_0; & p|_{\Omega_2} &= p_0; \\
p|_{\Omega_3(t)} &= p_0; & p|_{\Omega_4} &= 0.1 \text{ MPa};
\end{aligned}
\tag{8}$$

where  $\sigma_{xx}$ ,  $\sigma_{yy}$  - components of the stress tensor, Pa;  $\lambda$  - the side thrust coefficient;  $u_x$ ,  $u_y$  - components of the displacement vector, m;  $p_0$  - the methane pressure in the virgin massif, Pa;  $\Omega_1$  - the vertical boundaries of the outer contour;  $\Omega_2$  - the horizontal boundaries of the outer contour;  $\Omega_3(t)$  - the time-varying boundary of the filtering area;  $\Omega_4$  - the internal contour (a roadway).

The conditions for the formation of the outburst cavity are the belonging of a finite element to the area of inelastic deformation caused by tensile stresses, and the fulfillment of the criterion for the filtration of methane gradient to exceed the critical value  $\text{grad } p > P_c$ , accepted here  $P_c = 2 \cdot 10^7$  Pa/m.

For the mathematical description of the process of rocks transform into a disturbed state, the Mohr-Coulomb failure theory is applied. To solve the system of equations (1)-(6) with initial and boundary conditions (7) and (8) on a certain time interval, the finite-difference method is used [25].

It is assumed that at the initial time  $t=0$  the distribution of stresses and pressure is given, and for sufficiently small values of  $\Delta t$ , we can obtain the distribution of stresses, methane pressure and its filtration rates at time point  $t+\Delta t$  by using iterative relations of the finite-difference method.

This process continues from the initial state to any current time point.

The problem is solved by the finite element method embodied in authors' computer program. Fig. 1 shows the numerical calculation scheme.

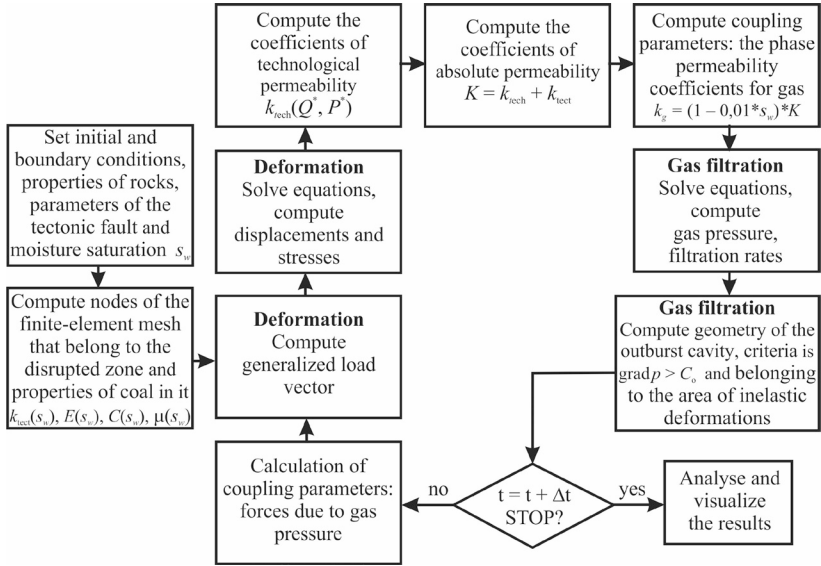


**Fig. 1.** The scheme of simulating the coupled processes of rock deformation and methane filtration, taking into account the influence of water contained in the fracture-pore space of coal

At each time iteration, in each finite element of the numerical model, the following parameters are calculated: stresses, zones of inelastic deformations, coefficients of technological permeability  $k_{tech}(Q^*, P^*)$  caused by mining operations, coefficients of absolute permeability  $K$  as the sum of  $k_{tech}$  and  $k_{rock}$ , gas permeability coefficients  $k_g$ , gas pressure and filtration rates.

The most important step in creating complex models of coupled physical processes is their detailed verification. As for this model of the gas-dynamic processes, verification of both its individual modules (deformation and methane filtration) and the entire model as a whole was performed. The developed model of gas filtration in the disturbed area was verified by comparing calculated data on gas release into the well with analytical solutions [26], on the distribution of gas pressure around the well and the change in gas pressure in the undermined coal seam with experimental data [26]. The change in stressed state of rocks was compared with data on the displacement of the roadways contour. The model of coupled geomechanical and

filtration processes was verified by comparing calculated parameters and mine data regarding the size of the outburst cavities and the amount of the burst coal [27].

### 3. Modeling of outburst-hazardous properties of coal near a tectonic fault

A significant part of coal and gas outbursts occurs near geological disturbances [9, 11, 28-31]. On flat coal seams, most of them are confined to disturbances with small amplitudes (up to 5 m), and the most dangerous are areas 10-20 meters wide on both sides of the disturbance [28]. Tectonics of coal seams is the root cause of the manifestation of such physical and mechanical properties of coal, which predetermine its outburst hazard [32].

When the layers were bent into folds and thrusts formed (Fig. 2*a*, 2*b*, 2*c*), stronger rocks moved along the most plastic and less strong coal seams. During layer-by-layer movement, the coal turned into a fine-grained aggregate consisting of fragments rotated relative to their original position and tightly pressed to each other [11].

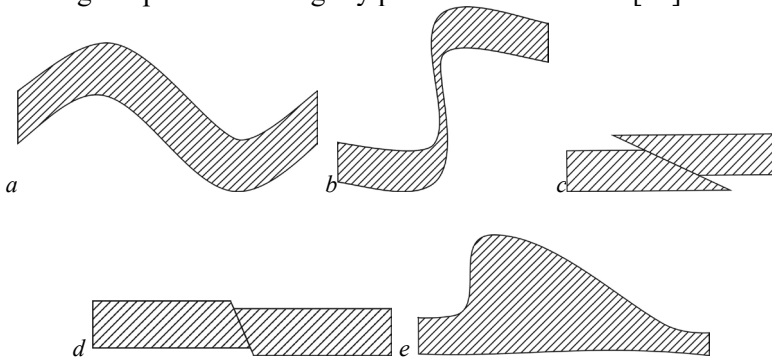


**Fig. 2.** Types of tectonic disturbances: *a* - fold; *b* - flexure; *c* - thrust; *d* - fault; *e* - swelling

Low-amplitude faults (Fig. 2*d*) arose as a result of shear and tensile stresses. After the formation of the crack zone, a larger rupture occurred in its most weakened part [33]. The formation of tectonic narrowings and swellings in the thickness of coal seams (Fig. 2*e*) is associated with the redistribution of the plastic mass of coal under the influence of tectonic stresses, as a result of layer-by-layer move-

ments in the process of folding. These are particularly dangerous areas of mine fields in terms of coal and gas outbursts.

One of the necessary conditions for mathematical modeling of coupled geomechanical and filtration processes near a tectonic disturbance is to specify the properties of coal in the disturbed zone [34], Fig. 3.



**Fig. 3.** Coal seam section with tectonic fault

In this work, it was accepted that cohesion  $C$  decreases linearly and permeability  $k_{tect}$  increases linearly from the boundary of disrupted zone to the tectonic fault; the tensile strength  $\sigma_\tau$  is approximately zero

$$C = C_0 - \frac{(C_0 - C_{\min})(x_d + l_d - x)}{l_d};$$

$$k_{tect} = \frac{k_{\max}(x_d + l_d - x)}{l_d}; \quad (9)$$

$$\sigma_\tau \approx 0; \quad \text{for } x \in [x_d; x_d + l_d].$$

where  $C_0$  - the coal cohesion in the unbroken zone, MPa;  $C_{\min}$  - the minimum cohesion value in the broken zone, MPa;  $x_d - x$  coordinate of the tectonic fault (Fig. 3), m;  $l_d$  - the length of the broken zone, m;  $\sigma_\tau$  - tensile strength, MPa.

#### **4 Flow of gas-dynamic processes in the near-face zone of a coal seam nearby tectonic faults**

For calculations it was taken, that the mine face of 3 m height is at a distance of  $L$  from the tectonic fault with a displacement amplitude of 1 m, surrounded by a ten-meter zone of disrupted coal ( $l_d=10$  m). The coal seam thickness is 1.5 m,  $H=1000$  m,  $m=10\%$ . The gas content in coal is 20 m<sup>3</sup>/t,  $p_0=8$  MPa,  $s_w=1\%$ . The host rock is argillite. Time step is 0.1 s.

If  $L>10$  m and the mine face is located outside the tectonically disturbed zone, relative methane pressure ( $p/p_0$ ) in the coal seam near the mine face decreases slowly (Fig. 4), the permeability increases

evenly here, according to the change in stress, no cavities are formed in the coal seam; all processes are quasi-stationary in nature.

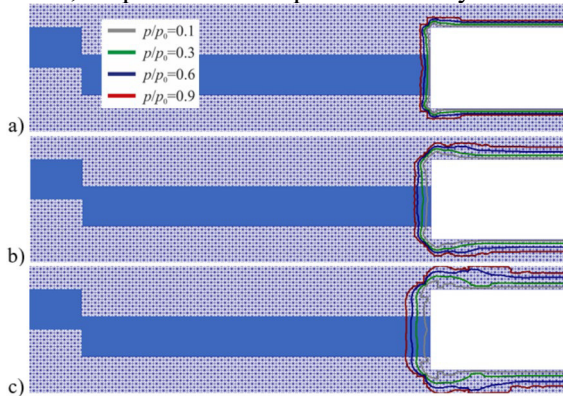


**Fig. 4.** Isobars of relative methane pressure ( $L > 10$  m) at the time points:  $a - t = 2$  s;  $b - t = 6$  s;  $c - t = 14$  s

If the distance between the fault and the mine face is  $L=10$  m, methane pressure in the near-face part of the coal seam drops quickly (Fig. 5), pressure gradients take on high values, the rate of methane filtration increases significantly and the permeability of coal increases rapidly. Coal sloughs into the roadway and a small cavity is formed in the coal seam.

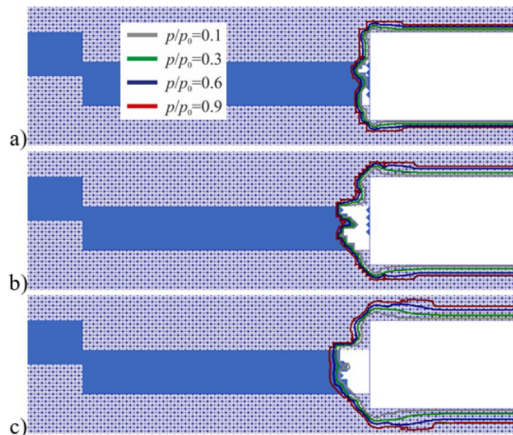


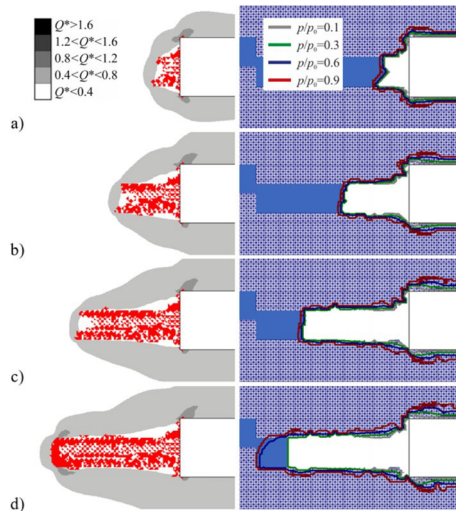
**Fig. 5.** Isobars of relative methane pressure ( $L = 10$  m) at the time points:  $a - t = 2$  s;  $b - t = 4$  s;  $c - t = 8$  s



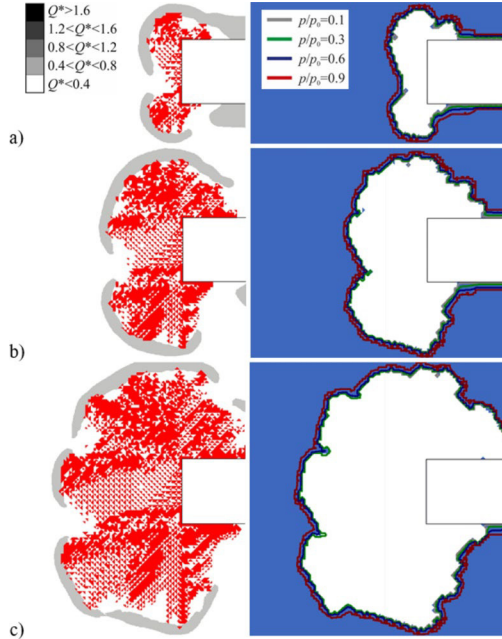
However, this process ends quickly. Deformation of the coal seam and the process of methane filtration in the disturbed zone return to a quasi-stationary regime (Fig. 5b, 5c). During the first 4 seconds, a gas-dynamic phenomenon occurs, which, due to the small volume of burst coal, should be attributed not to an outburst, but to a coal sloughing.

Fig. 6 and 7 show the results of calculating the stress field, zones of inelastic deformation and relative gas pressure in the third case, when  $L = 7.75$  m, in vertical and horizontal sections.

In the vicinity of a tectonic fault, in the zone of a disrupted coal seam, the area of increased diversity of the stress field components ( $Q^* > 0.4$ ) rapidly increases into the coal seam. The zone of inelastic deformation (this zone is shown in red) is rapidly growing from the mine face (Fig.6, left side). Methane pressure in the coal seam near the mine face quickly falls, so the relative pressure isobars are tight to the exposed surface. The pressure gradients and the methane filtration rate take very high values, the permeability of coal is growing rapidly - coal is burst and a cavity is formed in the coal seam, the length of which reaches 6.25 m under given initial and boundary conditions.



**Fig. 6.** Distributions of  $Q^*$  parameter values and inelastic deformation zones (left side), outburst cavities and isobars of relative methane pressure  $p/p_0$  (right side) in the outburst-prone zone near the fault, vertical section: a -  $t = 2$  s; b -  $t = 4$  s; c -  $t = 6$  s; d -  $t = 10$  s



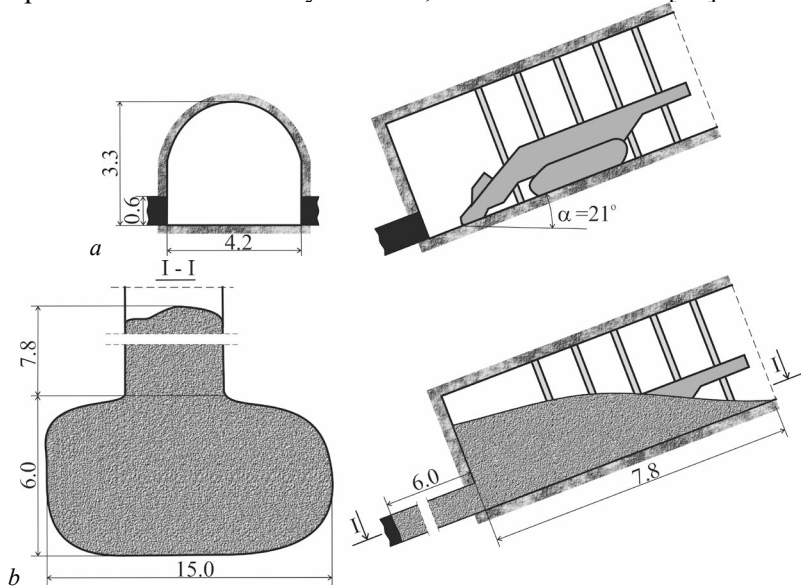
**Fig. 7.** Distributions of  $Q^*$  parameter values and zones of inelastic deformation (left side); outburst cavities and isobars of relative methane pressure (right side), horizontal section:  $a - t = 2$  s;  $b - t = 4$  s;  $c - t = 10$  s

Then the growth of the cavity stops (Fig. 6*d*), the methane filtration rates fall, the pressure of methane in the coal seam continues to slowly decrease. The disruption process and the process of methane filtration return to the quasi-stationary regime. The duration of the dynamic process is 7 s. As it can be seen from Fig. 6, the outburst cavity is located within the coal seam and it is limited from above and below by the host rocks. The vertical section of the outburst cavity has a rectangular shape, with a curved end.

In the horizontal section, the shape of the outburst cavity also almost repeats the contour of the inelastic deformation zone (Fig. 7). It has the shape of an irregular ellipse, the major axis of which is perpendicular to the axis of the roadway.

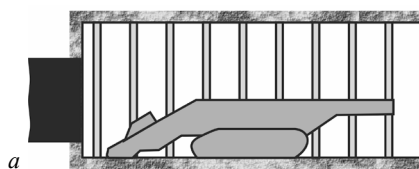
At the "Hlyboka" mine of the Production Association "Donetskuvuhillia", there was a sudden outburst in the gutter, horizon 719 m, coal seam  $h_8$ , during the removal of the rock mass (Fig. 8).

Outburst intensity was 60 tons of coal and 3000 m<sup>3</sup> of methane. The depth of the outburst cavity was 6 m, its width was 15 m [30].



**Fig. 8.** The outburst cavity dimensions, the gutter in "Hlyboka" mine [30]: *a* - before the outburst; *b* - after the outburst

At the V.R. Menzhynskyi mine Production Association "Pervomaiskvuhillia", in the southern gutter, the horizon 845 m, coal seam  $l_4$ , during coal extraction with a jackhammer, a sudden outburst occurred near the tectonic fault (Fig. 9). Outburst intensity was 70 tons of coal and 5000 m<sup>3</sup> of methane [30].



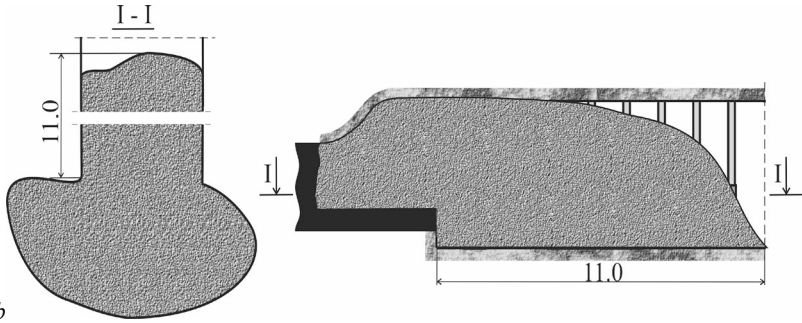


**Fig. 9.** The outburst cavity dimensions, the southern gutter in Menzhynskyi mine [30]: *a* - before the outburst; *b* - after the outburst

Thus, both calculated and actual data suggest that in the considered case the outburst cavity is located within the coal seam and it is limited from above and below by the host rocks.

The vertical section of the fracture cavity has a rectangular shape, possibly with a curved end, the horizontal section has the shape of an irregular ellipse, the major axis of which is perpendicular to the axis of the roadway [35, 36].

Comparing Fig. 6, 7 and 8, 9, we can see that, in general, the calculated shape of the outburst cavity in the near-face zone of the coal seam coincides with the actual data.

Let us consider the case when the properties of the rocks in the immediate roof of the seam, as well as the properties of coal, are weakened near a tectonic disturbance: cohesion  $C$  of argillite decreases linearly from the boundary of the disturbed zone to the tectonic disturbance, tensile strength  $\sigma_t$  is reduced by half.

The distribution of  $Q^*$  parameter values and the relative methane pressure at different time points in the vertical section along the roadway are shown in Fig.10.

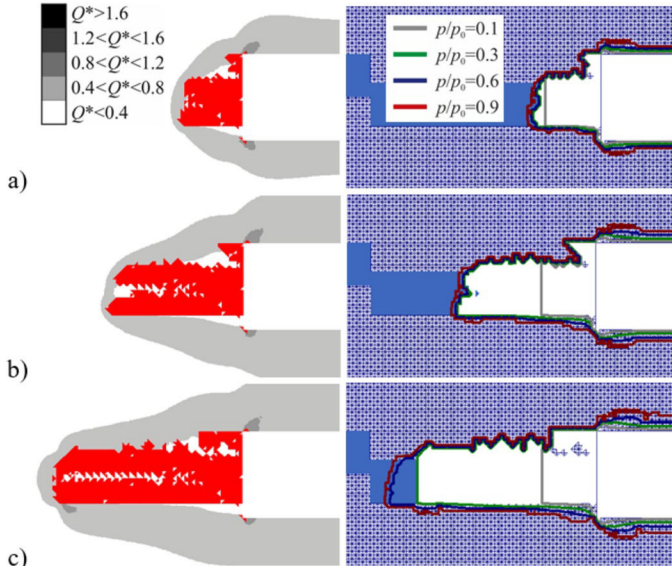


**Fig. 10.** Distributions of  $Q^*$  parameter values and inelastic deformation zones (left side), outburst cavities and isobars of relative methane pressure  $p/p_0$  (right side) when properties of the host rocks are weakened near the tectonic fault: *a* -  $t=2$  s; *b* -  $t=4$  s; *c* -  $t=6$  s

It can be seen that in this case part of the argillite above the coal seam is fractured. Near the face, the height of the cavity becomes equal to the height of the roadway. The simulation shows that if the properties of the host rock are weakened near a tectonic disturbance, then, during the outburst, it is fractured and thrown out along with coal from the growing cavity.

A similar situation was observed in the face of the transport drift of panel no. 33 near a tectonic disturbance (horizon 1012 m, coal seam  $M_8$ , Bazhanov mine, Production Association “Makeevugol”), where a sudden coal and gas outburst occurred during the stripping of the lower part of the seam by shaft-sinking set, Fig. 11. Outburst intensity was 80 tons of coal and  $600 \text{ m}^3$  of methane. The depth of the outburst cavity was 5.8 m [30].

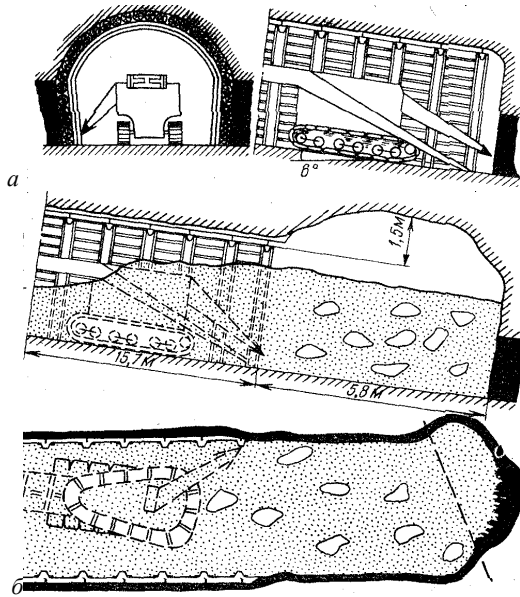


**Fig. 11.** The outburst cavity dimensions in the transport drift, Bazhanov mine [30]: *a* - before the outburst; *b* - after the outburst

When analyzing the available statistical data on outbursts that occurred in the coal mines of Donbass [30], we find that:

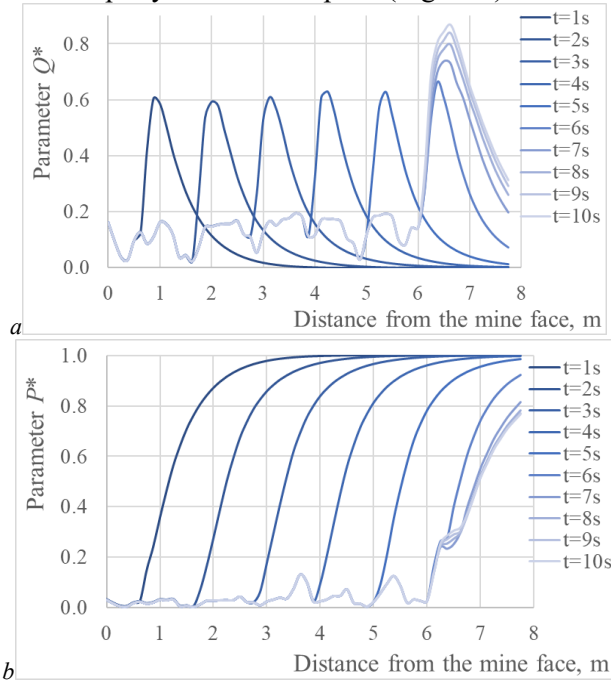
- in the vertical section outburst cavities are located within the coal seam in 75% of cases, cavities capture host rocks in 25% of cases;
- in the horizontal section, outburst cavities have the shape of an irregular oval in 58% of cases, they are determined by the position relative to the tectonic fault and are limited to the fault plane in 32% of cases.

### **5 Changes in geomechanical and filtration parameters in the near-face zone**

Graphs of changes in geomechanical and filtration parameters [37, 38] in the mine face, along the line that is perpendicular to the plane of the mine face and passes through the center of the coal seam, are shown in Fig. 12-14.

At the time interval  $t < 6$  s, the peak of  $Q^*$  parameter values, which is usually on the exposed surface, moves away from the mine face

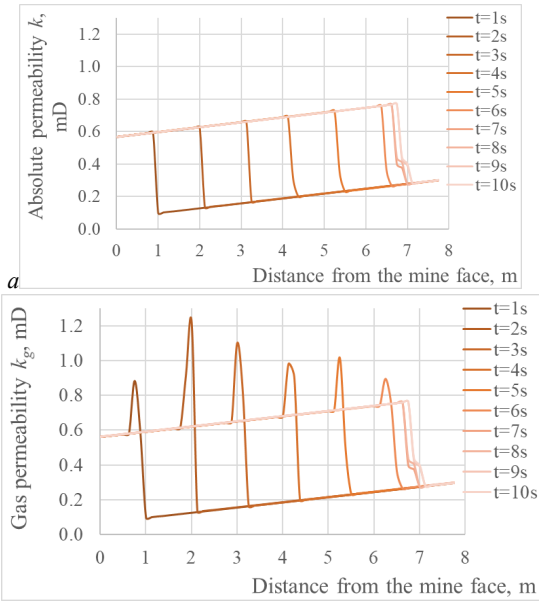
together with the newly formed surface of the outburst cavity at a speed of approximately 1 m/s for our initial and boundary conditions, Fig. 12a. Unloading of the coal seam from rock pressure (parameter  $P^*$ ) also moves rapidly at the same speed (Fig. 12b).



**Fig. 12.** Changing of geomechanical parameters over time: *a* -  $Q^*$  parameter values; *b* -  $P^*$  parameter values

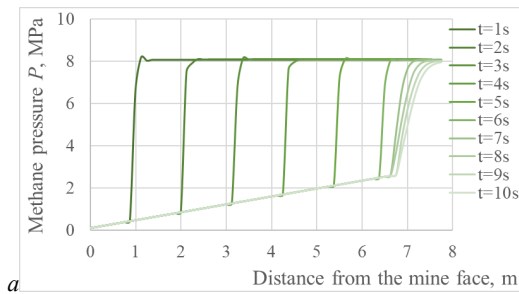
The shift of the maximum  $Q^*$  parameter values and the minimum  $P^*$  parameter values deep into the coal seam stops when  $t > 6$  s, at a distance of 6.25 m from the mine face.

Absolute permeability (Fig. 13a) in the area a few centimeters to the surface increases 6 times. Gas permeability, calculated by formulas (4)-(6), increases by the value of  $f(V_g)$  in the boundary, near-surface zone, Fig. 13b, because the gas filtration rates are very high here, Fig. 14b.



**Fig. 13.** Changing of values of permeability coefficients over time: *a* - absolute permeability; *b* - gas permeability

At the seventh second of coal and methane outburst, all processes slow down: the peak of parameter  $Q^*$  values increases, but now it does not move deep into the coal seam and reaches the mark of 6.5 m; coal permeability increases gradually; methane pressure gradually decreases in the near-surface zone and its filtration rate decrease, Fig. 14.





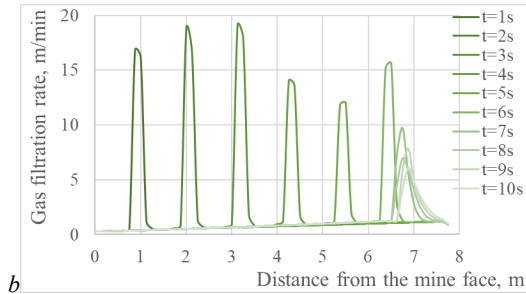


**Fig. 14.** Changing of geomechanical and filtration parameters over time,  $s_w = 1\%$   $a$  - gas pressure;  $b$  - gas filtration rate

## 6 The influence of moisture saturation on the occurrence and flow of outbursts

According to the Rules for mining operations on outburst-prone coal seams [39] coal seams wetting is used for preventing gas-dynamic processes. This method involves water injecting through long boreholes drilled within the coal seam from gateway in front of a longwall. It is well known that the presence of water in the crack-pore space of coal significantly affects the flow of gas-dynamic processes that are initiated during mining operations [40, 41].

First, moisture saturation leads to a decrease in the rock strength and bearing capacity, changes the nature of their behaviour after reaching the limiting state [42, 43]. The effect of fluids on the strength and deformation properties, on development of cracks formation process was studied in the works [43, 44]. The dependences of the effect of moistening of coal samples on their coefficient of elasticity  $E$  and Poisson's ratio  $\mu$  were established in [44, 45]. Graphs based on these data are shown in Fig. 15.

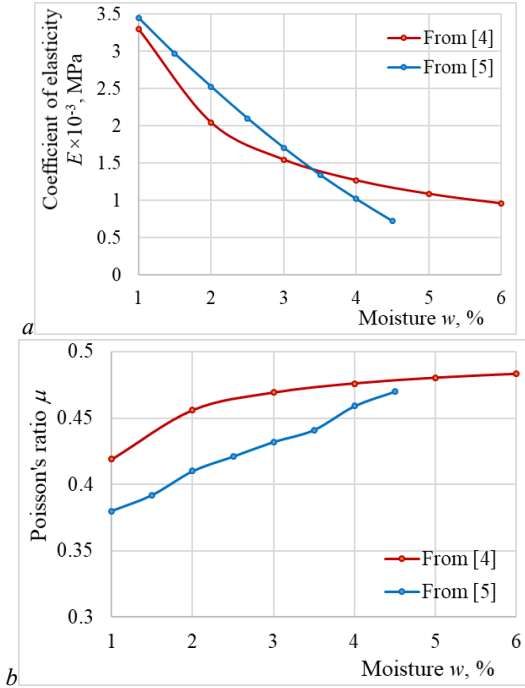


**Fig. 15.** Effect of moisture on the coal properties, according to [44, 45]: *a* - coefficient of elasticity; *b* - Poisson's ratio

With an increase in coal moisture ( $w = 0.01s_w m$ ) from 3 to 6%, the coefficients of elasticity and shear decreased by 80-85%, the Poisson's ratio increased by 20%. This indicates an increase in the plastic properties of coal, reducing its ability to accumulate energy of elastic deformation and to brittle destruction.

Second, water affects the phase permeability, the amount of free gas in the crack-pore space and the methane filtration process, formula (5). Intensity of the process of gas (methane) sorption-desorption also depends on the water content in coal. Under different conditions and at certain values of moisture, the mechanism of influence of water on the flow of sorption-desorption processes changes.

**Effect of reducing phase permeability on initiation of outbursts.** All previous calculations were performed under the con-

dition that moisture saturation was  $s_w = 1\%$ , and then  $s_w$  values in the crack-pore space of the coal seam varied in the interval  $[1\%; 100\%]$ .

Graphs of geomechanical and filtration parameters changing in the mine face, along the line passing through the center of the coal seam, for  $s_w = 30\%$  are shown in Fig. 16-18.

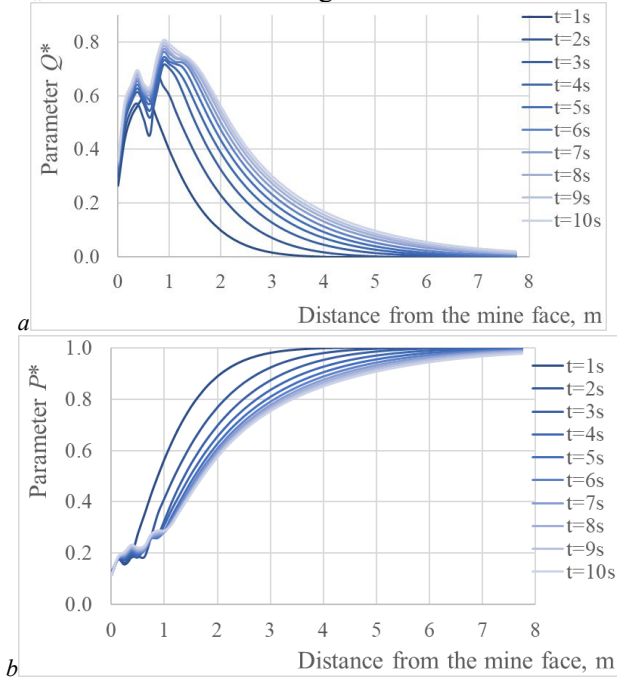


**Fig. 16.** Changing of geomechanical parameters over time,  $s_w = 30\%$ : a-  $Q^*$  parameter values; b-  $P^*$  parameter values

In the studied moments of time the peak of  $Q^*$  parameter values is at a distance of about 1 m from the mine face, Fig. 16a. Fluctuations in the  $Q^*$  and  $P^*$  parameter values near the surface of the mine face are due to influence of the zone of inelastic deformations. Unloading of the coal seam from rock pressure (Fig. 16b) and the drop in methane pressure (Fig. 18a) are slow.

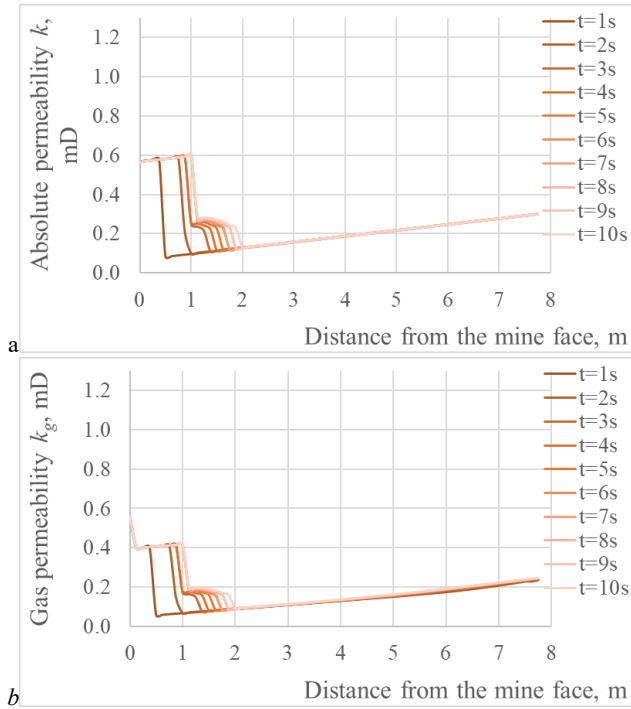


**Fig. 17.** Changing of values of permeability coefficients over time,  $s_w = 30\%$  *a*-absolute permeability; *b*-gas permeability.

Absolute permeability and gas permeability spread deep into the coal seam faster with the growth of the zone of inelastic deformations, and outside it this process also slows down, Fig. 17*a* and 17*b*. Gas permeability in this case is devoid of the nonlinear component  $f(V_g)$ , because the gas filtration rates do not exceed critical values, Fig. 17*b*. By comparing the graphs in Fig. 17*a* and 17*b*, one can see that gas permeability differs from the absolute permeability by 30% - this is the portion of the crack-pore space of coal occupied by water.

As a result of calculations it was obtained that gas-dynamic processes start in the mine face if  $s_w < 24\%$ . When this limit is exceeded, geomechanical and filtration processes in the coal seam near the mine face do not start.

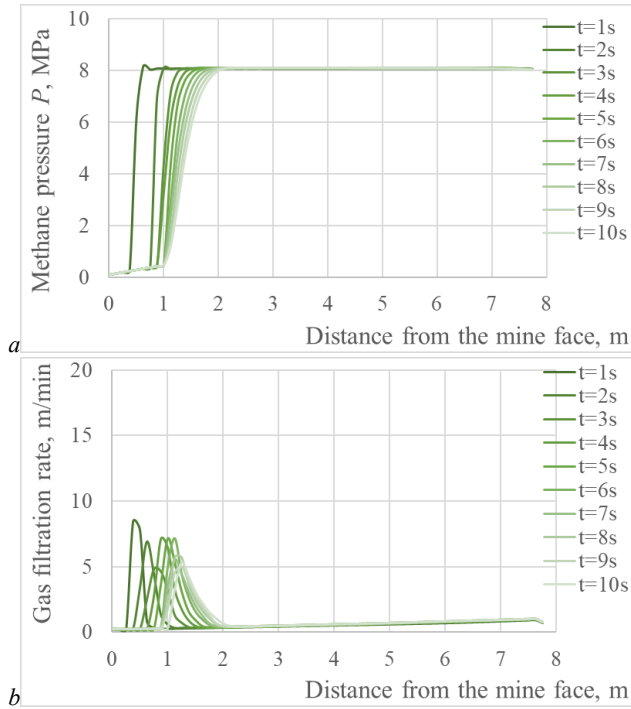


**Fig. 18.** Changing filtration parameters over time,  $s_w = 30\%$ : *a*-gas pressure; *b*- gas filtration rate

That is, for the above boundary and initial conditions, the effect of moisture on the reduction of phase permeability for methane leads to the neutralization of the outburst-hazardous properties of coal under the condition of  $s_w \geq 24\%$ . Under this condition, the flow of the studied processes occurs in a quasi-stationary mode.

**Effect of change of coal properties during moistening on initiation of gas-dynamic processes.** Based on experimental data in [44, 45], it is shown that moisture saturation affects the coefficient of elasticity of coal  $E$  and the Poisson's ratio  $\mu$ . We calculated how the studied processes occur with taking into account the change in these coal properties with increasing moisture content  $s_w$ . For the calculations,  $E$  and  $Q^*$  values were taken according to [44, 45], Fig. 15. As a result of numerical calculations with variation of  $s_w$ , it was found

that:  $Q^*$  values (parameter that characterizes different-component nature of the stress field) markedly decrease in the coal seam in front of the zone of inelastic deformations; the area of the zone of inelastic deformations in the mine face is also reduced; the growth rate of the zone of inelastic deformations (coal seam destruction) and the outburst cavity slows down [46].

If  $s_w=20\%$ ,  $E=2287$  MPa and  $\mu=0.433$ , any gas-dynamic phenomena do not occur in the mine face. The peak of parameter  $Q^*$  values is less than 1 m from the mine face. Unloading of the coal seam from rock pressure and falling methane pressure are slow. Gas permeability spreads deep into the coal seam with the growth of zone of inelastic deformations; it is devoid of nonlinear component, because the gas filtration rates do not exceed critical values. In this case, safe limit of moisture saturation decreases to  $s_w = 20\%$ , for the boundary and initial conditions accepted in this work.

Thus, the regularities of the influence of moisture on the outburst hazard of coal seams were established. The numerical model was developed that allows to identify a safe limit of moisture saturation, at which the nature of geomechanical and filtration processes in the coal seam changes from dynamic to quasi-stationary in specific geological conditions.

## **7 The influence of vertical unloading of the near-face zone of the coal seam on the occurrence of outbursts**

Unloading chinks in host rocks are used to prevent coal and gas outbursts, extrusions of coal, and rock bursts during roadways driving by shaft-sinking set on thin coal seams [39]. The unloading chink is created by pre-excavating the rock in the roof or floor of the coal seam to a depth of at least 2 m. Between the unloading chink and the coal seam, a protective rock layer with a thickness of at least 0.5 m is left. The unreduced leading of the unloading chink in the direction of roadway driving should be at least 1 m. The minimum height of the chink is 0.4 m, its maximum height is not limited [39].

For the simulation, we considered the case when the mine face is located at a distance of 8.75 m from the tectonic fault, the mining

depth is 1200 m. Other conditions remained the same as in the previous calculations.

Fig. 19 shows the simulation results. From the figures it is clear that there is a sharp decrease in methane pressure in the near-face zone of the coal seam. High values of pressure gradients and filtration rates, as well as tensile stresses on the free surface lead to the separation of plates of tectonically disturbed coal. The spalling of coal causes instantaneous exposure of a new face surface. The minimum component of the stress tensor on this surface is zero, and in the immediate vicinity of it significant compressive stresses of the bearing pressure still remain. Then the next surface layer is exposed and the whole process is repeated again.

Under these boundary and initial conditions, the duration of the gas-dynamic process is 11 s. In the first seconds, the outburst is initiated; in the interval of 2-10 s the outburst process continues, at 10-11 s this process stops. During this time, the methane pressure in the coal seam near the mine face quickly drops, the permeability of coal increases rapidly; coal is ejected and a cavity is formed in the coal seam (Fig. 19a-19e) the length of which reaches 7.75 m. Then the growth of the cavity stops (Fig. 19f) the methane pressure in the coal seam continues to slowly decrease; geomechanical and filtration processes return to a quasi-stationary regime.

Next, we simulate the flow of deformation and filtration processes if, under the same initial conditions, the roadway is driven with an unloading chink 2 m deep in the host rocks, Fig. 20.

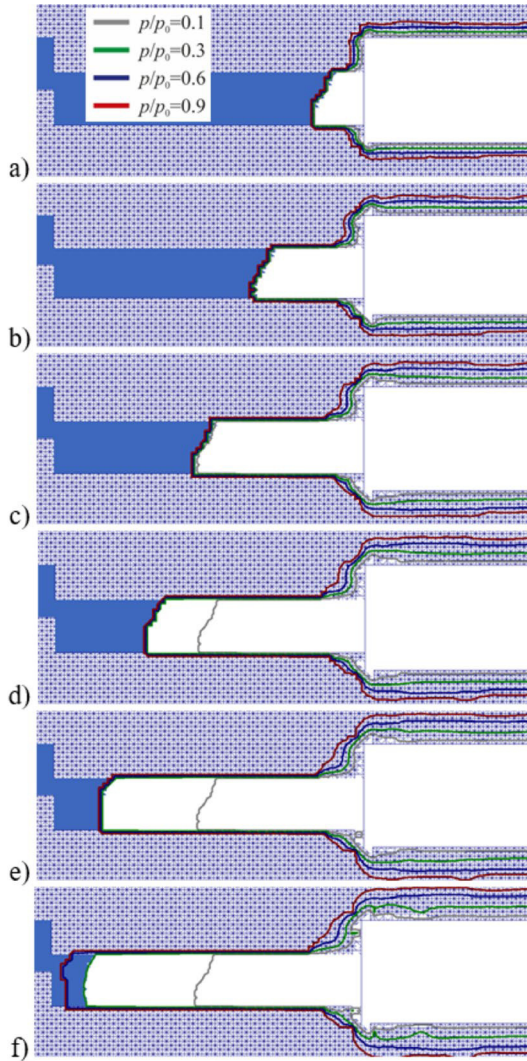


**Fig. 19.** Isobars of relative methane pressure at the time points: *a*-  $t = 2$  s; *b*-  $t = 4$  s; *c*-  $t = 6$  s; *d*-  $t = 8$  s; *e*-  $t = 10$  s; *f*-  $t = 12$  s



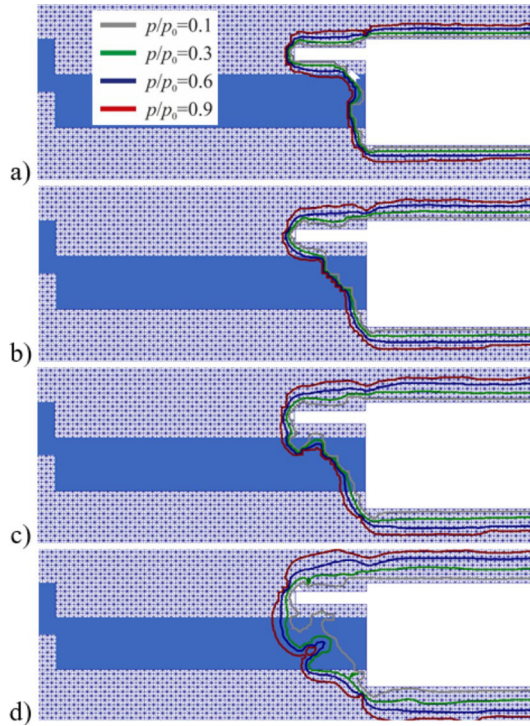


**Fig. 20.** Isobars of relative methane pressure in the roadway with the unloading chink at the time points: *a*-  $t = 2$  s; *b*-  $t = 4$  s; *c*-  $t = 6$  s; *d*-  $t = 12$  s

In this case, the coal and gas outburst does not occur, the outburst cavity is not formed. Isobars of relative methane pressure, limiting the degassed area, gradually move away from the mine face. Over the considered time period, the unloaded and degassed area extends to a depth of up to 2 m [47-49].

The unloading chink significantly changes the stress distribution in the near-face zone, Fig. 21.

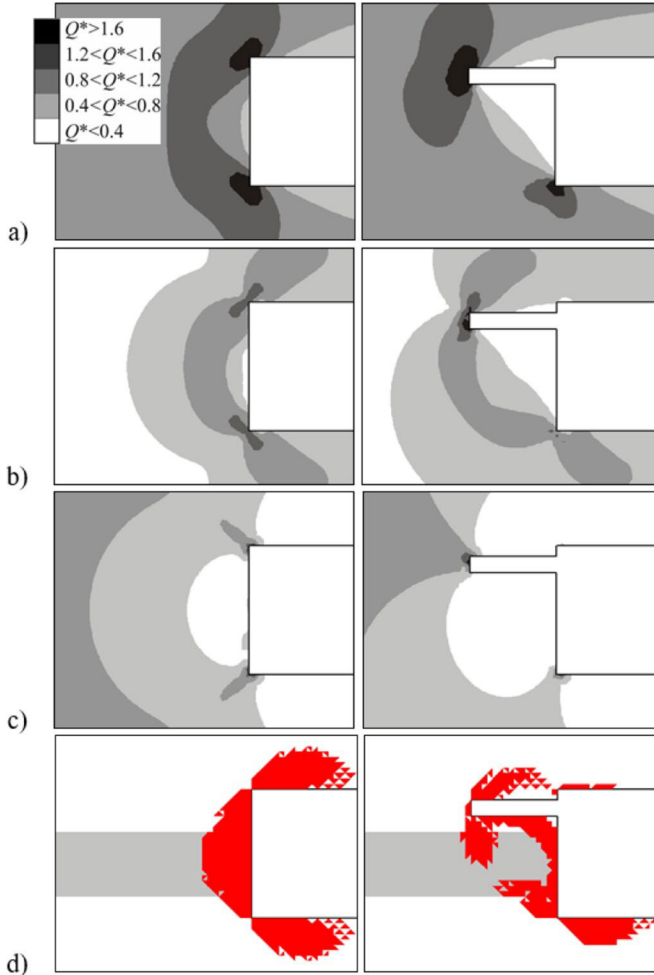


**Fig. 21.** Distributions of geomechanical parameters values in the roadway without the unloading chink (on the left side) and in the roadway with the unloading chink (on the right side): *a* -  $\sigma_1/\gamma H$ ; *b* -  $Q^*$  parameter; *c* -  $P^*$  parameter; *d* - zones of inelastic deformations

The distribution of the reduced maximum component of the principal stress tensor, which is shown in Fig. 21*a* on the right side, reveals a large zone located under the unloading chink, where  $\sigma_1/\gamma H < 0.4$ . The length of this zone is equal to the length of the un-

loading chink. In the roadway without the unloading chink (Fig. 21a, the left side), maximum stresses in the near-face zone were not lower than 0.4. On the contrary, the maximum abutment pressure was located within the two-meter near-face zone. In the presence of the unloading chink, the abutment pressure zone moves from the near-face region of the roadway to the near-face region of the unloading chink (Fig. 21b, the right side).

The spread of the zone of increased difference of the stress tensor components ( $Q^*$  parameter), in which the process of crack formation is actively occurring, deep into the coal seam slows down, and the peak of  $Q^*$  parameter values moves away from the mine face (Fig. 21b, the right side). The area of rocks unloaded from rock pressure, where  $P^* < 0.4$ , in the roadway with the unloading chink increases significantly compared to the one without the unloading chink (Fig. 21c).

Breaking of the near-face part of the coal seam begins from the face of unloading chink downward and from the lower corner of the mine face upwards. Then these zones are closed, covering the coal seam at a distance of 2 m from the mine face, which is equal to the depth of the unloading chink (Fig. 21d).

The near-face stresses in the roadway with the unloading chink are radically different from the stresses in the roadway without the unloading chink. The peak  $Q^*$  and  $\sigma_1/\gamma H$  parameters values are moved from the position of 0.75 m from the plane of mine face to the depth of unloading chink. At the same time, both the difference of the stress tensor components and the maximum stress remain at a low level and, in a long time interval, ensures deformation of the near-face zone in the elastic mode. Unloading of this zone from rock pressure occurs in two directions: in the direction of the mine face and in the direction of the unloading chink, therefore  $P^*$  parameter values for this case are the least [50].

Thus, when using an unloading chink, a zone completely unloaded from rock pressure is formed near the mine face, in which the occurrence of cracking and destruction processes is excluded.

The use of an unloading chink significantly slows down the process of fracturing, which prevents the onset of dynamic phenomena.

## 8 Conclusions

The mathematical model of the coupled processes of elastoplastic deformation of a coal seam, methane filtration and desorption, which occur in the outburst-prone zone of the coal seam, was developed to study the conditions for the occurrence and regularities of gas-dynamic phenomena flow.

The problem formulation takes into account the changes in the properties of coal near tectonic disturbances, the influence of coal moisture on phase permeability, an increase in permeability at high gas filtration rates.

Simulation of the joint flow of geomechanical and filtration processes in the outburst-prone zone, on its border and beyond it was made. It was demonstrated that when a mine face is in an undisrupted area of the coal seam, methane pressure decreases slowly, an outburst cavity does not form, all processes are quasi-stationary in nature.

At the border of the outburst zone, coal sloughs from the seam into the roadway and a small cavity is formed in the coal seam.

In the vicinity of a tectonic fault, in the zone of a disrupted coal seam, the zone of inelastic deformation grows rapidly from the mine face deep into the coal seam.

Methane pressure near the mine face quickly falls and a cavity is formed in the coal seam. Mine data confirms the correctness of the numerical calculation of the shape of the outburst cavity.

The regularities of changes in geomechanical and filtration parameters in the near-face zone of the coal seam were established. During coal and gas outburst, the peak of  $Q^*$  parameter moves away from the mine face together with the newly formed surface of the outburst cavity. Absolute permeability in the area a few centimeters to the surface increases 6 times.

When all processes slow down, the peak of  $Q^*$  parameter values increases, but now it does not move deep into the coal seam; coal permeability increases gradually; methane pressure gradually decreases in the near-surface zone and its filtration rate decrease.

The regularities of the influence of moisture on the outburst hazard of coal seams were established. The developed numerical model allows to identify a safe limit of moisture saturation, at which the nature of geomechanical and filtration processes in the coal seam

changes from dynamic to quasi-stationary in specific geological conditions.

The influence of the unloading chink on gas-dynamic processes was studied. It was shown that when using an unloading chink, a zone completely unloaded from rock pressure is formed near the mine face, in which the occurrence of cracking and destruction processes is excluded. The use of the unloading chink significantly slows down the process of fracturing, which prevents the onset of dynamic phenomena.

### *References*

1. **Shevelev, G.A.** (1989). Dynamics of coal, rock and gas outbursts. *Naukova dumka*.
2. **Liang, W.** et al. (2013). Safety technologies for the excavation of coal and gas outburst-prone coal seams in deep shafts, *International Journal of Rock Mechanics & Mining Sciences*, 57, 24–33. <https://doi.org/10.1016/j.ijrmms.2012.08.006>
3. **Ruilin, Z., & Lowndes, I.S.** (2010). The application of a coupled artificial neural network and fault tree analysis model to predict coal and gas outbursts. *International Journal of Coal Geology*, 84, 141–152. <https://doi.org/10.1016/j.coal.2010.09.004>
4. **Shu, L., Wang, K., Liu, Z., Zhao, W., Zhu, N., & Lei, Y.** (2022). A novel physical model of coal and gas outbursts mechanism: Insights into the process and initiation criterion of outbursts. *Fuel*, 323, Article 124305. <https://doi.org/10.1016/j.fuel.2022.124305>
5. **Li, H.** (2001). Major and minor structural features of a bedding shear zone along a coal seam and related gas outburst, Pingdingshan coalfield, northern China. *International Journal of Coal Geology*, 47(2), 101–113. [https://doi.org/10.1016/S0166-5162\(01\)00031-3](https://doi.org/10.1016/S0166-5162(01)00031-3)
6. **Hardgraves, A.J.** (1983). Instantaneous outbursts of coal and gas: a review. *Proceedings of the Australian Institute of Mining and Metallurgy*, 285(3), 1–37.
7. **Williams, R.J., & Weissmann, J.J.** (1995). Gas emission and outburst assessment in mixed CO<sub>2</sub> and CH<sub>4</sub> environments. *Proc. ACIRL Underground Mining Sem. Australian Coal Industry Res. Lab.*, 12.
8. **Aguado, M.B.D., & Nicieza, C.G.** (2007). Control and prevention of gas outbursts in coal mines, Riosa–Olloniego coalfield, Spain. *International Journal of Coal Geology*, 69(4), 253–266. <https://doi.org/10.1016/j.coal.2006.05.004>
9. **Zabigaylo, V.E., & Nikolin, V.I.** (1990). The influence of rock catagenesis and coal metamorphism on their outburst hazard. *Naukova dumka*.
10. **Krukovska, V.V.** (2012) Features of the process of the coal and gas outburst in the roadway face at various ways of development. *Geo-Technical Mechanics*, 102, 88–93.
11. **Zabigaylo, V.E., et al.** (1980). Geological conditions of outburst hazard in Donbass coal seams. *Naukova dumka*.

12. **Xua, T., Tanga, C.A., Yangc, T.H., Zhuc, W.C., & Liu, J.** (2006). Numerical investigation of coal and gas outbursts in underground collieries. *International Journal of Rock Mechanics & Mining Sciences*, 43(6), 905–919. <https://doi.org/10.1016/j.ijrmms.2006.01.001>
13. **Cao, Y., He, D., & Glick, D.C.** (2001). Coal and gas outbursts in footwalls of reverse faults. *International Journal of Coal Geology*, 48, 47–63. [https://doi.org/10.1016/S0166-5162\(01\)00037-4](https://doi.org/10.1016/S0166-5162(01)00037-4)
14. **Krukovskaya, V.V.** (2014). Influence of penetration depth in outburst danger zone on the gas-dynamic processes near tectonic displacement. *Geo-Technical Mechanics*, 119, 100–111.
15. **Tu, Q., Cheng, Y., Liu, Q., Guo, P., Wang, L., Li, W., & Jiang, J.** (2018). Investigation of the formation mechanism of coal spallation through the cross-coupling relations of multiple physical processes. *International Journal of Rock Mechanics and Mining Sciences*, 105, 133–144. <https://doi.org/10.1016/j.ijrmms.2018.03.022>
16. **Qin, H., Wei, J., & Li, S.** (2019). Analysis of the coal seam spalling–failure mechanism based on the seepage instability theory. *PLOS ONE*, 1–18. <https://doi.org/10.1371/journal.pone.0219735>
17. **Zhu, W.** et al. (2007). Analysis of coupled gas flow and deformation process with desorption and Klinkenberg effects in coal seams. *International Journal of Rock Mechanics & Mining Sciences*. <https://doi.org/10.1016/j.ijrmms.2006.11.008>
18. **Yankun, M., Xueqiu, H., & Zhaohua, L.** (2020). A unified model with solid-fluid transition for coal and gas outburst and FEM-LIP modeling. *Tunnelling and Underground Space Technology*, 99, Article 103349. <https://doi.org/10.1016/j.tust.2020.103349>
19. **Krukovskiy, O.P.** (2011). Modelling changes of stress-strain state of solid edge during the distance of working face of mine workings. *Problemy obchysliuvalnoi mekhaniki i mitsnosti konstruksii*, 17, 175–181.
20. **Basniev, K.S., Dmitriev, N.M., Kanevskaya, R.D., & Maksimov, V.M.** (2006). *Underground fluid mechanics*. Institute for Computer Research.
21. **Krukovskiy, O., & Krukovska, V.** (2019). Numerical simulation of the stress state of the layered gas-bearing rocks in the bottom of mine working. *E3S Web of Conferences*. International Conference Essays of Mining Science and Practice, 109, Article 00043. <https://doi.org/10.1051/e3sconf/201910900043>
22. **Krukovska, V.V.** (2015). Simulation of coupled processes that occur in coal-rock massif during mining operations. *Geo-Technical Mechanics*, 121, 48–99.
23. **Krukovska, V.V.** (2022). Numerical analysis of influence of coal seams water saturation after water injection on their outburst hazard. *Geo-Technical Mechanics*, 161, 14–27. <https://doi.org/10.15407/geotm2022.161.014>
24. **Krukovska, V.V.** (2021). Numerical analysis of influence of coal bed moisture on outburst hazard. *Science and society, patterns and trends of development: Abstracts of XVI International Scientific and Practical Conference*, 233–236. <https://doi.org/10.46299/ISG.2021.I.XVI>
25. **Zienkiewicz, O.C., & Taylor, R.L.** (2000). *The finite element method*. Butterworth-Heinemann.

26. **Krukovskaya, V.V.** (2006). Preparation method of calculation of methane filtration parameters with the account a mode of stressedly-deformed state of coal-rock mass. M.S. Poliakov Institute of Geotechnical Mechanics of the National Academy of Sciences of Ukraine.
27. **Krukovskaya, V.V.** (2013). The development of the coupled processes theory in the application to geomechanics of coal-rock massif. M.S. Poliakov Institute of Geotechnical Mechanics of the National Academy of Sciences of Ukraine.
28. **Zabigaylo, V.E., Lukinov, V.V., Pimonenko, L.I., & Sahnevich, N.V.** (1994). Tectonics and mining and geological conditions for the development of coal deposits in Donbass. *Naukova dumka*.
29. **Shepherd, J., Rixon, L.K., & Griffiths, L.** (1981). Outbursts and Geological Structures in Coal Mines: A Review. *International Journal of Rock Mechanics and Mining Sciences*, 18, 267–283.
30. Catalogue of sudden coal and gas outbursts in mines. (1989). Research Institute of Mining Geomechanics and Mine Surveying, Ukrainian Branch.
31. **Antsiferov, A.V., & Golubev, A.A.** (2006). A new approach to the problem of sudden outbursts. *Coal of Ukraine*, 5, 34–37.
32. **Baranov, V.A.** (2021). Comprehensive forecast of rock outburst hazard. Publisher Belaya E.A.
33. **Meng, ZP, Peng, SP, & Li, H.** (2001). Influence of normal faults on the physical and mechanical properties of coal and the distribution of underground pressure. *Journal of China Coal Society*, 26(6), 561–566.
34. **Krukovska, V.V., & Krukovskiy, O.P.,** (2008). Computer modelling of outburst of coal and methane process near to various tectonic displacements. *Geo-Technical Mechanics*, 80, 238–250.
35. **Krukovskiy, O.P., Krukovska, V.V., & Zhang W.** (2020). Outburst cavity formation in the working face driven along the outburst-prone coal seam. II International Conference Essays of Mining Science and Practice 2020. E3S Web of Conferences, 168, 00052. <https://doi.org/10.1051/e3sconf/202016800052>
36. **Krukovskaya, V.V.** (2015). About form of outburst cavity in mine working at roadheading by outburst coal seam. *Geo-Technical Mechanics*, 125, 216–228.
37. **Krukovskiy, A.P., & Krukovskaya, V.V.** (2015). Changing of geomechanical parameters of gas-saturated coal-rock massif under gas-dynamic phenomena. *Geo-Technical Mechanics*, 122, 57–66.
38. **Krukovska, V.V.** (2008). Change of coal permeability and parameters of the methane flow at the outburst front. *Geo-Technical Mechanics*, 78, 34–42.
39. SOU 10.1.00174088.011-2005. Rules for conducting mining operations on strata prone to gas-dynamic phenomena. (2005). Ministry of Coal Industry of Ukraine.
40. **Bulat, A.F., Skipochka, S.I., Palamarchuk, T.A., & Antsyfierov, V.A.** (2010). Methane generation in coal seams. *Lira LTD*.
41. **Bulat, A.F., Krukovska, V.V., Krukovskiy, O.P., & Zberovskiy, V.V.** (2012). Numerical simulation of hydroimpulsive impact on outburst coal seam. *Geo-Technical Mechanics*, 105, 14–25.

42. **Gu, H.** et al. (2019). The effects of water content and external incident energy on coal dynamic behavior, *International Journal of Rock Mechanics and Mining Sciences*, 123, Article 104088. <https://doi.org/10.1016/j.ijrmms.2019.104088>

43. **Makieiev, S.Iu., Pylypenko, Yu.N., Ryzhov, H.A., Andrieiev, S.Iu., & Bobro, M.T.** (2012). Study of the influence of fluids on the deformation properties of coal and rocks under different load conditions, *Suchasni resursoenerhozberihaiuchi tekhnolohii hirnychoho vyrobnytstva*, 2(10), 73–82.

44. **Petuhov, I.M., Litvin, V.A., Kucherskiy, L.V.** et al. (1969). Rock bursts and their control in the mines of the Kizel basin. Perm book publishing house.

45. **Artamonov, V.N., & Nikolaev, E.B.** (2020), Forecasting changes in dust formation by hydraulic impact during drilling and blasting in coal mines, *Proceedings of the IV scientific-practical conference Donbas 2020: science and technology for production*, 89–96.

46. **Krukovska, V.V., Krukovskyi, O.P., Kocherga, V.M., & Kostrytsia, A.O.** (2022). Solving coupled problems of geomechanics and gas filtration for mining safety ensuring. *Geo-Technical Mechanics*, 160. 106–122. <https://doi.org/10.15407/geotm2022.160.106>

47. **Krukovska, V.V., & Krukovskyi, O.P.** (2011). Primenenie razgruzochnykh polostey pri provedenii podgotovitelnykh vyirabotok po vyibrosoopasnyim plastam [The use of unloading cavities when preparatory roadways are driven on outburst-hazardous seams]. *Materials of the international conference Forum hirnykiv-2011*, 121–127.

48. **Krukovskyi, O.P., & Krukovska, V.V.** (2011). Modeling acting unloading caves by roadheading on coal seams, which dangerous by gas and coal emission. *News of Tula State University. Geosciences*, 1, 129–136.

49. **Krukovska, V.V., & Krukovskyi, O.P.** (2010). Computer simulation of the action of unloading cavities to prevent gas-dynamic phenomena in the face of preparation roadway. *Materials of the XX International Scientific School "Deformation and fracture of materials with defects and dynamic phenomena in rocks and workings"*, 172–174.

50. **Krukovska, V.V., & Krukovskyi, O.P.** (2023). Formation of the near-face stress field under the influence of natural and technological factors. *Geo-Technical Mechanics*, 165, 97–116. <https://doi.org/10.15407/geotm2023.165.097>



# **MODIFIED GEOMECHANICAL DEPENDANT SEISMIC MONITORING ARRANGEMENT FOR PREDICTING ROCK BURSTS AND FAILURES IN SEISMICALLY ACTIVE MINING BLOCKS AT MUFULIRA MINE**



**Dr. Victor MUTAMBO**

Department of Mining Engineering, University of Zambia, Great East Campus, Lusaka, Zambia  
Email: [vmutambo@unza.zm](mailto:vmutambo@unza.zm)



**Moses MUKUKA**

(MSc.), Mining Geologist, School of Mines, University of Zambia, Lusaka, Zambia

## **Abstract**

Mufulira mine is predominantly rich in copper mineralization. Due to increase in mine depth (1,557m), the mine has been experiencing rock failures and rock bursts. This has necessitated changes in mining sequences to suit the present geo-mechanical conditions such as development of de-stressing cross-cuts between 62 and 64 blocks to prevent possible rock bursts and rock falls.

This study conducted geotechnical investigations for intact rock mass to determine unconfined compressive strength (UCS), secant and tangent Young's Modulus ( $E_{Sec}$  and  $E_{Tan}$ ), secant and tangent Poisson's Ratio ( $\nu_{Sec}$  and  $\nu_{Tan}$ ), Brazilian and tri-axial compressive strength tests as well as geological field mapping to understand the Geo-mechanics mechanisms controlling rock burst prone mining blocks at Mufulira mine.

Laboratory findings have established high values of tensile strength ranging from 7 MPa to 12.1 MPa, Uniaxial Compressive Strength (UCS) ranging from 126 MPa to 226 MPa and tri-axial compressive strength ranging from 124 MPa to 466 MPa. Damage mapping conducted in the footwall drives, cross-cuts and mining drives excavations indicate that there is a changing stress loading as one move away from the retreating stope face to the east. Based on above results, an early warning monitoring system based on seismic monitoring system at Mufulira mine has been modified to suit the changing nature of geotechnical and geological parameters.

## **Introduction**

Mufulira mine comprises three ore bodies, referred to as orebody *A*, *B* and *C*. Ore body *A* is the smallest of the three and stretches hor-

izontally 300 m, orebody B is slightly larger and stretches horizontally 600 m, while orebody C is the main ore body. The ore body generally dips 45 degrees in the North East direction but at some places it flattens towards 35 degrees (Brandit, R.T., 1962). The Mufulira rock mass generally consists of a sequence of strong sedimentary formations overlying competent basement Schist and Granites, with rock strengths that range from 200 to 300 MPa.

### **Seismic monitoring at the mine**

Mufulira underground mine has been experiencing rock bursts due to seismic events during mining operations. These seismic events are accompanied by rock falls and rock busts. The failures are accelerated by geological and geotechnical structures. Rock falls/rock bursts that result from seismic events are catastrophic hazards and require an early warning system to be put in place before they occur due to the damage that accompany them (Crouch, S.L., 1976; Dubinski, J., and K. Stec 2001 & Fei, L., M. Tianhui, T. Chun'an and C. Feng 2018).

To date no detailed study has been done at the mine to develop an early warning system for predicting rock bursts that is dependent on effect of changes in geo-technical and geological environment. As a result, the seismic monitoring system has not fully addressed lapses in timely responding to ground failures.

### **Materials and Methods**

The following geo-mechanical tests were carried out: Brazilian test; Uniaxial Compressive Strength test and Tri-axial Compressive Strength test. Brazilian test was used to measure the indirect tensile strength of twenty-eight (28) NX disc rock samples.

A Digimax Compact line machine (Fig. 1) of 100 kN was used to carry out the test and pre-load was applied to all the specimens, average range was 80-90 N. Each 14 cm long NX core size sample was divided into smaller discs of 27 mm long, half the diameter of the core sample of 54 mm. Each disc was then weighed on the digital mass scale; the digital vernier caliper was used to measure both the diameter and thickness of the discs. Each disc was placed under the two platens and subjected to constant load as shown in fig. 1 C. At a given maximum load, deformation of the disc occurs as shown in fig. 1 D and results were recorded. The following formulae were used to find stress at failure;

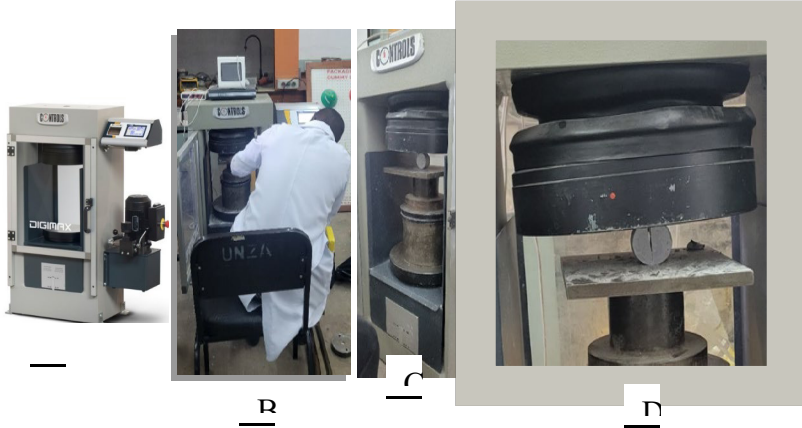


**Fig. 1.** Showing *A* Digimax Compact line machine, *B* Core disc placement between compression platens, *C* Core disc sample being subjected to constant load, *D* Core disc getting deformed

$$\sigma_1 = \frac{6P}{\pi Dt}; \sigma_2 = 0; \sigma_3 = \frac{2P}{\pi Dt}, \quad (1)$$

where  $P$  is the applied load,  $D$  is the core diameter and  $t$  the core thickness. The tensile strength,  $T_0$ , is given by the value of  $\sigma_3 = (-T_0)$  at failure. 15 drilled core samples of diameter 47 mm (NQ) size were prepared according to the International Society of Rock Mechanics (ISRM) standard. The length of each sample was 140 mm and 47mm in diameter. The length to diameter ratio was 2.97.

$$T_0 = \frac{2P}{\pi Dt}. \quad (2)$$

## Uniaxial Compressive Strength test

### Sample preparations

The cylindrical surfaces were prepared in order to be flat and smooth, levelled within 0.02 mm tolerance and made sure that no more than 0.06 degrees departure from perpendicular occurred during the laboratory testing.

### Apparatus

The apparatus (see Fig. 2) used to conduct the experiment consisted of the following: Loading Device; Platens and Strain measurement devices (electrical resistance strain gauges).

## Testing procedure

The two plates were carefully cleaned before the specimen was placed in the testing chamber. The load was continuously applied at a rate of 1.0 MPa/s and failures occurred in approximately 10 minutes. Stress and deformation data were recorded through an electronic system that has the appropriate accuracy specifications. The maximum load was recorded in Newtons within 1% accuracy and results were recorded. The following formulae were used:

The axial strain is calculated as

$$\varepsilon_a^0 = \Delta l / L_0, \quad (3)$$

where  $\varepsilon_a$  Axial strain,  $\Delta l$  Change in measured axial length and  $L_0$ : The initial length of the sample. The diametric strain is calculated as

$$\varepsilon_d^0 = \Delta_d^0 / D_0, \quad (4)$$

where  $\varepsilon_d$  Diametric strain,  $\Delta_d$  Change in diameter and  $D_0$  -the initial diameter of the sample. The compressive stress is calculated as

$$\sigma = P / A_0, \quad (5)$$

where  $\sigma$  - Compressive Stress,  $P$  - Load and  $A_0$ - the initial cross-section area of the specimen. The unconfined compressive



**Fig. 2.** Showing *A* setting up of an experiment, *B* Placing the sample on the platens of the testing chamber, connecting strain gauges to the core sample (*C*-Axial strain gauge and *D*-Radial strain gauge)

Strength was calculated for the maximum load applied:

The modulus of elasticity (Young's modulus)  $E$  which represents the ratio between axial stress and axial strain can be derived via several methods. It was calculated at stress-strain level of about 50% of the maximum load.

$$E = \Delta_{\sigma}^0 / \Delta \varepsilon_a \quad (\text{At 50\% of maximum load}) \quad (6)$$

The Poisson's ratio that represents the ratio between diametric and axial strain, was calculated as

$$n = \left( \varepsilon_d^0 / \varepsilon_a \right) \quad (7)$$

### **Tri-axial Compressive Strength test**

#### **Sample preparation**

15 drilled core samples were selected to be representative of the rock formation examined. The diameter of the samples was 47 millimeters and of 140 centimeters in length. The diameter was derived by taking measures at the top, mid and the bottom parts of the specimen with a tolerance of 0.1 millimeters. The height to diameter ratio was 2.97 within the ISRM standard of 2.0 to 3.0. The height was determined to the nearest millimeter. The ends of the samples were smoothed so that the top and bottom surfaces were flat with a tolerance of  $\pm 0.01$  mm. This ensured that the applied loads were uniformly transmitted to the sample and there was no loading eccentricity.

#### **Testing Procedure**

A cylindrical rock specimen was placed in a specifically designed cell (Hoek cell). A specially designed membrane was attached to the cell so that it remained airtight. The lateral pressure is hydrostatic and was applied through a liquid (oil) which was pumped into the membrane. A hydraulic pump or a servomotor capable of regulating pressure within 1% accuracy was utilized. The specimen was axially enclosed by steel spherical seats. To derive the vertical and circumferential deformation of the sample, strain gauges were used and results were recorded. ArcGIS software was used to digitize the geological map of the study area.

#### **Mapping of structural discontinuities**

This was conducted by plotting and analysis of data using 3D Surpac modeling, Unwedge and Rick Allmendinger Stereonet software.

### **Results and discussion**

#### **Brazilian tensile test results**

The test was done on disc shaped. In all, thirty (30) specimens of 27 mm long were obtained. The C-Quartzite had the highest average tensile strength of 11.5 MPa and Dolomite had the lowest average value of 6.2 MPa. During the test, all the rock samples showed brittle

deformation with Quartzite being harder than Dolomite as can be seen in Fig. 3 on the basis of tensile strength values.

### Uniaxial compressive strength results

The investigations of strains on rock specimens during uniaxial compression test were conducted and plotted graphically. Two components of strain in the cylindrical shape specimen, axial and radial components were studied. Strain gauges fixed on specimen surface were used in this study. Axial and radial components of strain were measured directly (see Fig. 5).

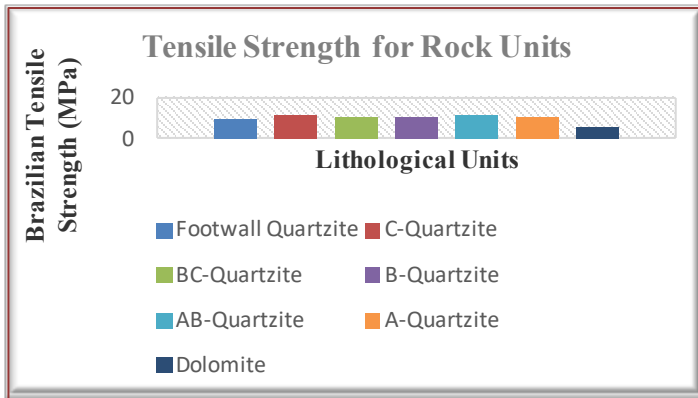


**Fig. 3.** Showing results from Brazilian Tensile Strength test, C-Quartzite with highest value & Dolomite with lowest

Strain measurement was necessary for determination of Young's modulus and Poisson's ratio. Fig. 5 shows the plotted results of one of the samples. The B-Quartzite had the highest average uniaxial compressive strength value and Dolomite had the lowest value (Fig. 4). This shows that Quartzite will require more compression load to deform than required by the Dolomite of the same rock mass size.

### Stress and Strain Curves

The typical behaviour of strain component curves of the rock samples during Uniaxial Compressive Strength tests are illustrated in fig. 5.

Axial strain (red curves) performs the lowest sensitivity and the failure can be identified in relatively short advance only.

Radial strain (blue curves) shows more nonlinear trend than axial one, thus, recognition of approaching failure is earlier.

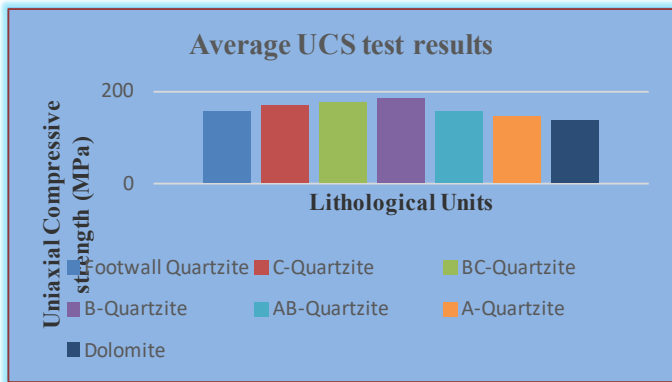


Fig. 4. Average Uniaxial Compressive Strength (UCS) for Lithological units

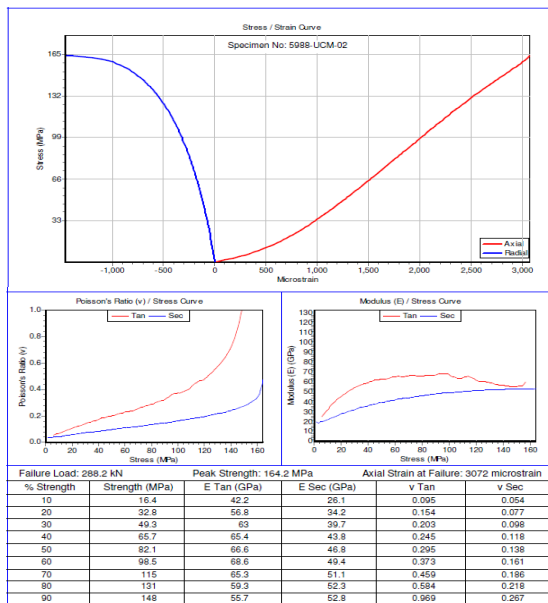


Fig. 5. showing Uniaxial Compressive Test results with elastic modulus and poisson's ratio for sample-02

Calculated Young's modulus is dependent on considered interval of axial load.

Precariousness can occur if there is not specified stress level for Young's modulus determination.

### Development of an early warning flow chart for predicting rock burst

Laboratory findings indicate that the area around the seismically active mining blocks in the deep section have high values of tensile strength ranging from 7 MPa to 12.1 MPa, uniaxial compressive strength (UCS) ranging from 126 MPa to 226 MPa and Tri-axial Compressive Strength ranging from 124 MPa to 466 MPa. Rocks with high tensile strengths undergo brittle type of deformation, hence any rock burst or rock fall will be detected to enhance safe mining. Geological and geotechnical mapping results further indicate that the rocks found in the seismically active mining blocks are highly fractured, jointed and brittle. In line with above results, a modified flow chart (Fig. 6) of Seismic Monitoring System for Predicting and Monitoring Rock Bursts and Rock Displacements was installed and tested at 1457 mL, 55P5 and 1473 ml, 67P5 closer to seismically

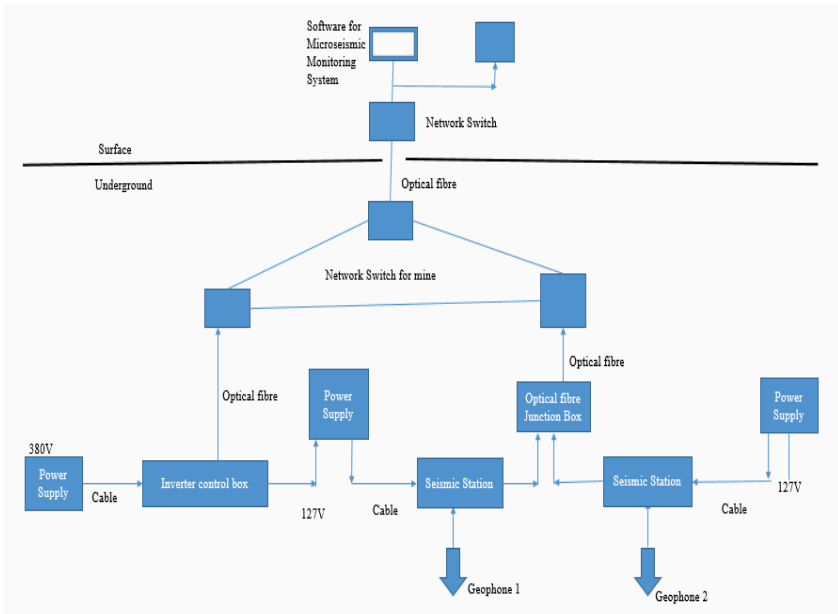


**Fig. 6.** Developed Flow Chart of Modified Seismic Monitoring System for Predicting and Monitoring Rock Bursts and Rock Displacements



## Conclusion

This study was aimed at establishing the effects of changes in geotechnical and geological parameters on the positioning of seismic monitoring system for early warning prediction of rock bursts and rock failures in seismically active mining blocks. Study findings have established high values of tensile strength from 7 MPa to 12.1 MPa, uniaxial compressive strength (UCS) from 126 MPa to 226 MPa and Tri-axial compressive strength from 124 MPa to 466 MPa.

These have the potential to induce premature failure and rock bursts.

In line with these findings, a modified Micro-seismic monitoring system at Mufulira mine deeps section was developed by installing additional geophones that take into account the changing nature of rock properties.

## References

1. Mufulira, Northern Rhodesia. Institution of mining and metallurgy. Vol. 71, 459-479.
2. **Brune, J. N.** (1968), Seismic moment, seismicity and rate of slip along major fault zones, *Journal of Geophysical Research*, 73, 777–784.
3. **Chloe A.** 2020. *Theoretical Geomechanics*. Georgia Institute of Technology.
4. **Crouch, S. L. and C. Fairhurst** (1973). *The Mechanics of Coal Mine Bumps and the Interaction between Coal Pillars, Mine Roof and Floor*, U.S.B.M. Contract report, H0101778.
5. **Crouch, S.L.** (1976). *Analysis of stress and displacements around underground excavations: an application of the displacement discontinuity method*. Tech. Rep., Department of Civil and Mineral Engineering, University of Minnesota
6. **Dubinski, J., and K. Stec** (2001), Relationship between focal mechanism parameters of mine tremors and local strata tectonics, in *Proceedings of the 5th international symposium on rock bursts and seismicity in mines*, edited by G. van Aswegen, R. J. Durrheim, and W. D. Ortlepp, pp. 113–118, South African Institute of Mining and Metallurgy.

## **EXTRACTION OF USEFUL COMPONENTS OF ORE-BEARING ROCKS OF THE "KURGAK" PLOT OF THE BLACK-SHALE FORMATION OF THE SARYJAZ AREA**



### **Batma TOKTOSUNOVA**

Doctor of Chemical Sciences, Professor of the Department "Chemistry and Chemical Technologies" Kyrgyz State Technical University named after I. Razzakov (KSTU), Kyrgyzstan, e-mail: [b.badirova@gmail.com](mailto:b.badirova@gmail.com);



### **Sharabidin ABDIBAITOV**

Candidate of technical sciences, Associate professor of the Department of UMMD Kyrgyz Mining Metallurgical Institute named after Academician U. Asanaliyev, KSTU named after I. Razzakov, Kyrgyzstan, e-mail: [abdibaitov69@bk.ru](mailto:abdibaitov69@bk.ru)



### **Marsel KOZHOGULOV**

Student of group "G-1-20" Kyrgyz Mining Metallurgical Institute named after Academician U. Asanaliyev, KSTU named after I. Razzakov, Kyrgyzstan, e-mail: [Marsel2kozhogulov@gmail.com](mailto:Marsel2kozhogulov@gmail.com);



### **Narmat TOKTOSUNOV**

Junior Researcher Kyrgyz Institute of Mineral Resources (KIMR), Kyrgyzstan



### **Nadira DOLOTKAN KYZY**

Applicant of the department of "Chemistry and chemical technologies" Kyrgyz State Technical University named after I. Razzakov (KSTU), Kyrgyzstan

## **Introduction**

The conducted scientific work is aimed at studying the acute problem in the field of ore minerals processing. The most energy-intensive and expensive process in the extraction and beneficiation of mineral raw materials is their destruction [1].

As it is known, the concept of innovative method (innovative technologies) is a novelty in the field of technology aimed at achieving new knowledge and solutions [2].

A group of authors [3] studied the effect of the degree of grinding on gold recovery using two-stage leaching. In the first stage the ore was subjected to bio-oxidation (active associations of acidophilic bacteria), while in the second stage gold recovery was carried out.

In the article "Evaluation of the granulometric composition of the crushed product obtained by crushing "in layer"" [4] describes the granulometric characteristics and evaluates the correspondence of the obtained parameters of the crushed product obtained as a result of industrial tests of the crusher operating "in a layer", according to the equations of Rosin-Rammler and Godin-Andreev.

Purpose of work: studying the possibility of maximum extraction of useful components from ore-bearing rocks of black shale formation of Sarydjaz area.

The relevance of scientific research is to create new highly effective methods of extracting useful components in maximum quantity from ore-bearing minerals of Saryjaz.

The choice of this research direction is determined by the need to solve the following problems:

Complexity of studying solid mineral deposits, ensuring high profitability of the modern mineral resource base of the Kyrgyz Republic, taking into account the environmental problems of the country arising from the processing of mining ores

Object of study: minerals of black shale formation of Saryjaz area.

Subject of the study: physical, physicochemical and structural characteristics of mineral samples.

To achieve the goal the following tasks were solved:

Preparatory works were carried out: sampling of rock ore samples, crushing, screening, separation.

Carrying out physical and chemical analyses of initial samples.

Determination of suitability of the proposed new method of crushing for ore minerals of black shale formation of Sarydjaz area.

Analysis, processing and generalization of the experimental data obtained.

## Experimental section

### 1. Objects and methods of research

**The object of the study is the ore-bearing rock** of the black shale formation of the Saryjaz ploshad from the site "Kurgak", located above sea level 3500 meters.

For the study the samples were prepared using the following methods: crushing, screening, fractionation and magnetic separation.

Brought samples of large-sized pieces of ore-bearing rocks of black shale formation from the site "Kurgak" first crushed on a ball mill (1.5-2.0 mm), then on a non-stand crushing plant (with a 3-phase electric motor 3000 rpm 2 kW, at a pressure of 30-60 atm/cm<sup>2</sup>), it consists of a cylindrical cup and a lid made of ceramic products, so that when crushing does not occur dust emission into the environment cup tightly closed with a lid. The crushing of the loaded sample in the amount of 20 grams is prolonged for 30-60 min.

The prepared crushed samples for spectral analysis are presented below

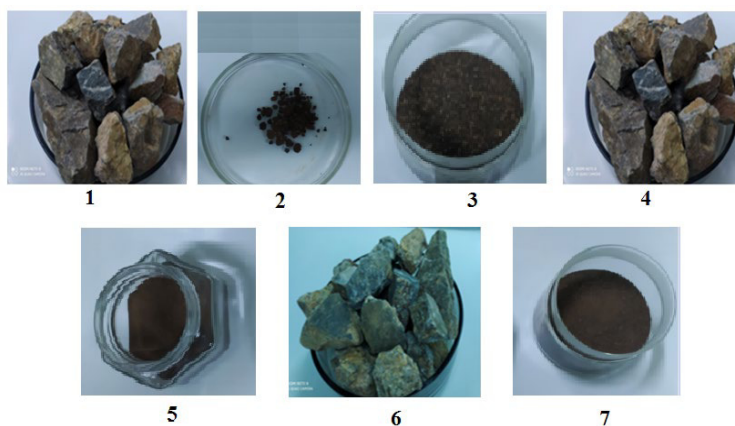


**Fig. 1.** Prepared for analysis of different fractions of samples:  
1,4,6 - pieces of initial samples (PI (S-AS)); 2-TCF (the coarsest fraction);  
3-CF (coarse fraction); 5-FF (fine fraction); 6-TSF (the smallest fraction)

The chemical composition of the initial sample and crushed fractions of the black shale formation from the locality "Kurgak" of Saryjaz area is presented in Tables 1 and 2.

Table 1

Chemical composition of the initial sample of black shale formation from the area of "Kurghak" of Saryjaz area

Образцы	Mn	Ni	Co	Ti	V	Cr	Mo	W	Zr	Nb
	10-2	10-3	10-3	10-1	10-2	10-3	10-3	10-2	10-2	10-3
PI (S-AS)	5	20	< 0.3	3	0,5	30	0,9	0,9	5	< 1.2
PI (S-AS)	In	Cu	Pb	Ag	Sb	Bi	As	Zn	Cd	Sn
	10-3	10-3	10-3	10-4	10-2	10-3	10-2	10-2	10-2	10-3
	< 0.5	300	20	9	0,3	0,3	3	2	< 0.3	20
PI (S-AS)	Ge	Ga	Yb	Y	La	P	Be	Sr	Ba	Li
	10-3	10-3	10-3	10-3	10-2	10-1	10-4	10-2	10-2	10-3
	< 0.12	1,5	0.4	3	< 1.2	< 2	< 2	2	< 2	< 3
PI (S-AS)	Th	U	Au	Sc	Породообразующие элементы в %					
	10-2	10-1	10-3	10-3	SiO2	(S-AS)	10-2	10-1	10-3	10-3
	Pd< 1.2	< 0.5	< 0.5	< 2	>50		Pd< 1.2	< 0.5	< 0.5	< 2

Table 2

Results of spectral analysis of different fractions of the black shale formation of the Saryjaz area of the Kurghak locality

Samples	Mn	Ni	Co	Ti	V
1	10-2	10-3	10-3	10-1	10-2
PI (S-AS)	5	20	< 0.3	3	0.5
TCF(S-AS)	90	12	0.5	20	< 0.3
GF(S-AS)	50	12	0.5	4	< 0.3
CF (S-AS)	30	3	0.3	3	< 0.3
FF (S-AS)	50	0.5	0.4	15	< 0.3
MMF(S-AS)	70	9	0.4	9	< 0.3
TSF (S-AS)	30	1.5	0.3	7	< 0.3
Samples	Cr	Mo	W	Zr	Nb

1	10-3	10-3	10-2	10-2	10-3	
PI (S-AS)	30	0,9	0,9	5	< 1.2	
TCF(S-AS)	15	0.7	>100	7	<1.2	
GF(S-AS)	15	0.5	>100	1.5	<1.2	
CF (S-AS)	5	0.3	30	1.2	<1.2	
FF (S-AS)	1.2	0.7	>100	7	<1.2	
MMF(S-AS)	15	0.5	>100	15	<1.2	
TSF (S-AS)	15	0.5	>100	15	<1.2	
Samples	In	Cu	Pb	Ag	Sb	
2	10-3	10-3	10-3	10-4	10-2	
PI (S-AS)	< 0.5	300	20	9	0,3	
TCF (S-AS)	<0.5	300	120	1.5	>100	
GF(S-AS)	<0.5	200	120	1.5	30	
CF (S-AS)	<0.5	300	50	0.4	20	
FF (S-AS)	<0.5	200	120	1.5	>100	
MMF(S-AS)	<0.5	120	120	1.5	>100	
TSF (S-AS)	<0.5	150	120	1.2	>100	
Samples	Bi	As	Zn	Cd	Sn	
2	10-3	10-2	10-2	10-2	10-3	
PI (S-AS)	0,3	3	2	< 0.3	20	
TCF (S-AS)	100	12	1.5	<0.3	>1000	
GF(S-AS)	70	15	1.2	<0.3	>1000	
CF (S-AS)	12	15	1.5	<0.3	>1000	
FF (S-AS)	50	15	1.5	<0.3	>1000	
MMF(S-AS)	50	12	1.5	<0.3	>1000	
Samples	Ge	Ga	Yb	Y	La	P
3	10-3	10-3	10-3	10-3	10-2	10-1
PI (S-AS)	< 0.12	1,5	0.4	3	< 1.2	< 2
TCF (S-AS)	<0.12	0.4	0.3	3	<1.2	<2
GF (S-AS)	<0.12	0.3	0.3	3	<1.2	<2
CF (S-AS)	<0.12	0.4	0.4	4	<1.2	<2
FF (S-AS)	<0.12	0.4	0.3	3	<1.2	<2
MMF (S-AS)	<0.12	0.4	0.3	3	<1.2	<2
TSF (S-AS)	<0.12	0.3	0.4	4	<1.2	<2
Samples	Be	Sr	Ba	Li	Ta	
3	10-4	10-2	10-2	10-3	10-1	
PI (S-AS)	< 2	2	< 2	< 3	< 1.2	
TCF (S-	<2	5	2	<3	<1.2	

AS)					
GF (S-AS)	<2	2	2	<3	<1.2
CF (S-AS)	<2	2	3	<3	<1.2
FF (S-AS)	<2	3	3	<3	<1.2
MMF (S-AS)	<2	3	3	<3	<1.2
TSF (S-AS)	<2	3	2	<3	<1.2

Samples	Be	Sr	Ba	Li
3	10-4	10-2	10-2	10-3
PI (S-AS)	< 2	2	< 2	< 3
TCF (S-AS)	<2	5	2	<3
GF (S-AS)	<2	2	2	<3
CF (S-AS)	<2	2	3	<3
FF (S-AS)	<2	3	3	<3
MMF (S-AS)	<2	3	3	<3
TSF (S-AS)	<2	3	2	<3

Samples	Rock-forming elements in %						
4	SiO <sub>2</sub>	Al <sub>2</sub> O <sub>3</sub>	MgO	Fe <sub>2</sub> O <sub>3</sub>	CaO	Na <sub>2</sub> O	K <sub>2</sub> O
PI (S-AS)	>50	12	1.2	>12	1.2	1.5	0.4
TCF (S-AS)	50	12	1.5	9	3	0.4	1.5
GF(S-AS)	40	1.5	0.9	>12	1.2	0.4	2
CF (S-AS)	50	12	2	9	4	0.9	0.3
FF (S-AS)	40	9	0.9	>12	2	0.4	1.5
MMF(S-AS)	40	9	0.9	>12	2	0.4	1.5
	40	12	1.5	7	4	0.9	1.2

As can be seen from the table there is an increase in the quantitative content of a number of elements Mn, Ti, W, Pb, Sb, Sn, Au, Zr, Co, Bi, As, especially Mn from 5-90 g/t, W from 0.9->100, Pb from 20-120, Sb from 0.3->100, Sn from 20->1000 and Au from <0.5-5 g/t.

At the same time, the amount of some elements remains unchanged as in the original sample V, Nb, In, Cd, Th, U, Sc, Ge, Y, La, Ta, and some have a slight decrease (Cr, Ga, Ag, Zn).

The microstructure of the initial (PI) and fragmented particles (CF, TSF) and their local composition were studied by means of scanning electron microscope (SEM)

Microstructure of initial samples (PI)

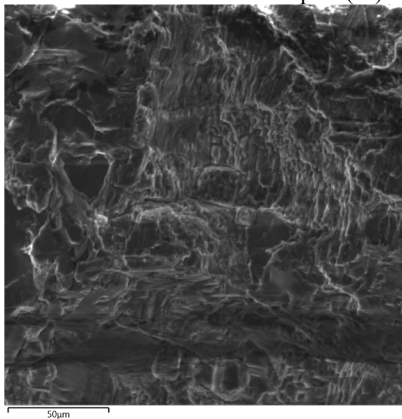


**Fig. 2.** Image of PI 3, St. 1 (surface area 200 μm)

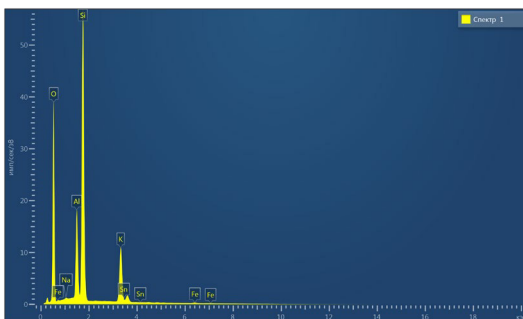


**Fig. 3.** Spectrum of PI 3, st.1

Table 3

Result type	Elemental composition of PI 3, st.1 Weight %
Spectrum name	Spectrum 1
O	58.82
Na	0.15
Al	7.42
Si	25.05
K	7.96
Fe	0.28
Sn	0.31
Summa	100.00



Statistics	O	Na	Al	Si	K	Fe	Sn
Max	58.82	0.15	7.42	25.05	7.96	0.28	0.31
Min	58.82	0.15	7.42	25.05	7.96	0.28	0.31
averaging	58.82	0.15	7.42	25.05	7.96	0.28	0.31
Standard deviation	0.00	0.00	0.00	0.00	0.00	0.00	0.00

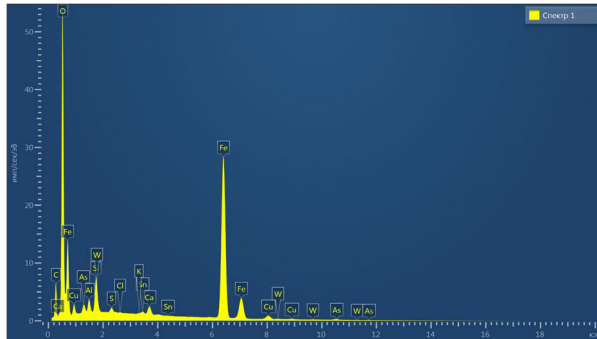


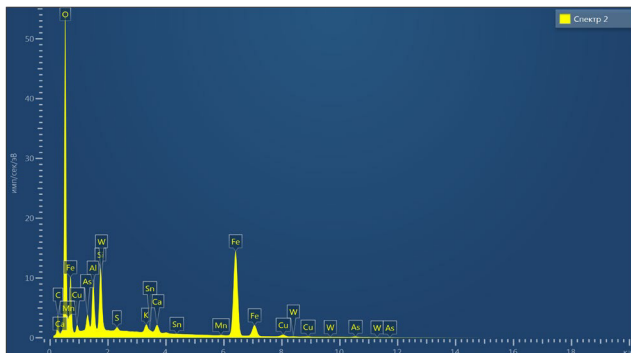
Fig. 4. Spectrum of GBF 2, st. 1

Table 4

Elemental composition of CF 2, st. 1

Result type	Weight %
Spectrum name	Spectrum 1
C	14.37
O	40.27
Al	0.86
Si	1.80
S	0.28
Cl	0.05
K	0.09
Ca	0.57
Fe	37.80
Cu	1.53
As	1.12
Sn	0.59
W	0.67
sum	100.00

Statistics	C	O	Al	Si	S	Cl	K	Ca	Fe	Cu	As	Sn	W
Max	14.37	40.27	0.86	1.80	0.28	0.05	0.09	0.57	37.80	1.53	1.12	0.59	0.67
Min	14.37	40.27	0.86	1.80	0.28	0.05	0.09	0.57	37.80	1.53	1.12	0.59	0.67
averaging	14.37	40.27	0.86	1.80	0.28	0.05	0.09	0.57	37.80	1.53	1.12	0.59	0.67
Standard deviation	0.00	0.00	0.00	0.00	0.00	0.00	0.00	0.00	0.00	0.00	0.00	0.00	0.00



**Fig. 5.** Spectrum of CF 2, st. 2

Table 5

Elemental composition of CF 2, st.2

Result type	Weight %
Spectrum name	Spectrum 2
C	10.81
O	50.28
Al	3.62
Si	4.17
S	0.24
K	0.74
Ca	0.70
Mn	0.10
Fe	24.73
Cu	1.05
As	2.36
Sn	0.66
W	0.54
sum	100.00

Microstructure of the smallest fraction (TSF)

Statistics	C	O	Al	Si	S	K	Ca	Mn	Fe	Cu
Max	10.81	50.28	3.62	4.17	0.24	0.74	0.70	0.10	24.73	1.05
Min	10.81	50.28	3.62	4.17	0.24	0.74	0.70	0.10	24.73	1.05
averaging	10.81	50.28	3.62	4.17	0.24	0.74	0.70	0.10	24.73	1.05
Standard deviation	0.00	0.00	0.00	0.00	0.00	0.00	0.00	0.00	0.00	0.00

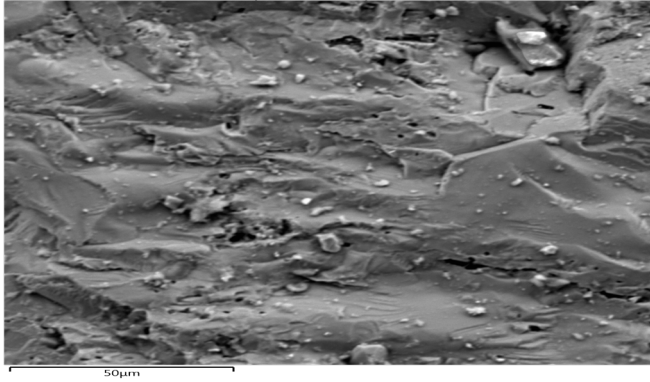


**Fig. 6.** Image of TSF 1, st.1. (surface of main particles zone 150 µm)

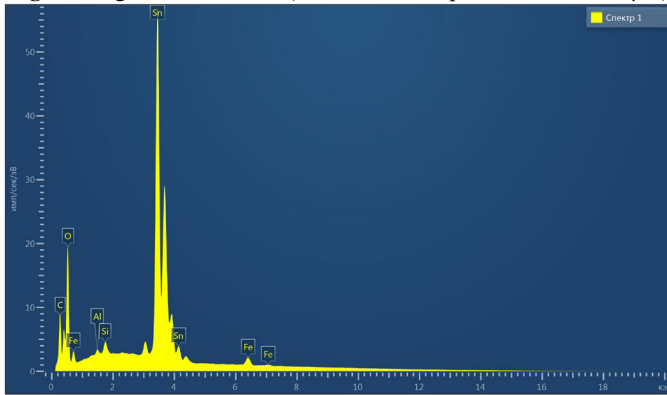


**Fig. 7.** Spectrum of THF 1, st. 1

Table 6

Elemental composition of the THF 1, st. 1.

Result type	Weight%							
Spectrum name	spectrum 1							
C	6.57							
O	33.03							
Al	0.26	Statistics	C	O	Al	Si	Fe	Sn
Si	0.46	Max	6.57	33.03	0.26	0.46	1.49	58.19
Fe	1.49	Min	6.57	33.03	0.26	0.46	1.49	58.19
Sn	58.19	averaging	6.57	33.03	0.26	0.46	1.49	58.19
sum	100.00	Standard deviation	0.00	0.00	0.00	0.00	0.00	0.00

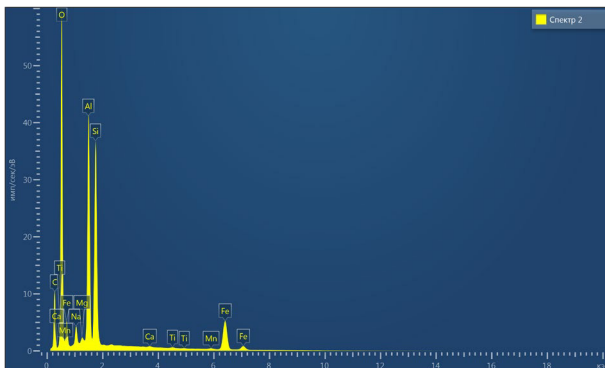


**Fig. 8.** Spectrum of THF 1, st..2

Table 7

Elemental composition of THF 1, st 2

Result type	Weight %									
Spectrum name	spectrum 2									
C										21.84
O										50.86
Na										1.36
Mg										0.21
Al										10.01
Si										9.23
Ca										0.06
Ti										0.09
Mn										0.13
Fe										6.21
sum										100.00
Statistics	C	O	Na	Mg	Al	Si	Ca	Ti	Mn	Fe
Max	21.84	50.86	1.36	0.21	10.01	9.23	0.06	0.09	0.13	6.21
Min	21.84	50.86	1.36	0.21	10.01	9.23	0.06	0.09	0.13	6.21
averaging	21.84	50.86	1.36	0.21	10.01	9.23	0.06	0.09	0.13	6.21
Standard deviation	0.00	0.00	0.00	0.00	0.00	0.00	0.00	0.00	0.00	0.00

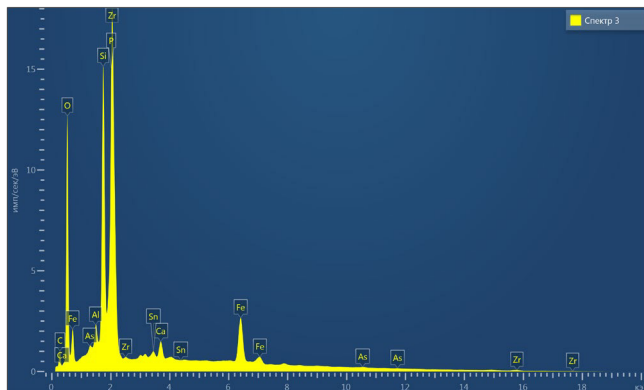


**Fig. 9.** Spectrum of THF 3, st.3

Table 8

Elemental composition THF 3, st.3

Result type	Weight %									
Spectrum name	Spectrum 3									
C	7.59									
O	43.15									
Al	0.81									
Si	9.52									
P	1.42									
Ca	1.04									
Fe	7.91									
As	0.38									
Zr	27.15									
Sn	1.05									
sum	100.00									
Statistics	C	O	Al	Si	P	Ca	Fe	As	Zr	Sn
Max	7.59	43.15	0.81	9.52	1.42	1.04	7.91	0.38	27.15	1.05
Min	7.59	43.15	0.81	9.52	1.42	1.04	7.91	0.38	27.15	1.05
averaging	7.59	43.15	0.81	9.52	1.42	1.04	7.91	0.38	27.15	1.05
Standard deviation	0.00	0.00	0.00	0.00	0.00	0.00	0.00	0.00	0.00	0.00

When studying the spectra and elemental composition of the initial samples of PI 3 in both sites 1 and 2, an overestimation of Si and O followed by Al, K, C, Fe is observed;

In CF 2 sample in both sites 1 and 2 also observed overestimation of O and Fe followed by elements for study 1 - C, Si, Cu, As, Al, W, Sn, Ca for study 2 - Si, Al, As, Cu, Ca, Sn, W;

All the THF samples overestimated the amount of oxygen (O) except THF 1, study 1 - Sn, O, C, Si, Al, Fe; SMF 1, study 2 - O, C, Al, Si, Fe, Na, Mg, Mn, Ti; THF 3, study 3 - O, Zr, Si, Fe, C, P, Sn, Ca, Al, As.

Images of initial sample (PI) particles are presented below in Fig. 10, 11:

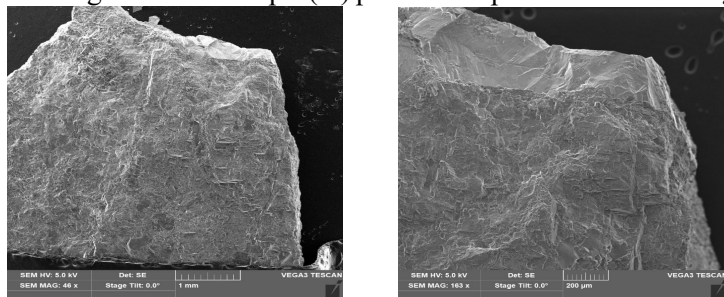


**Fig. 10.** Morphological structure of large particles of PI 5×5 mm

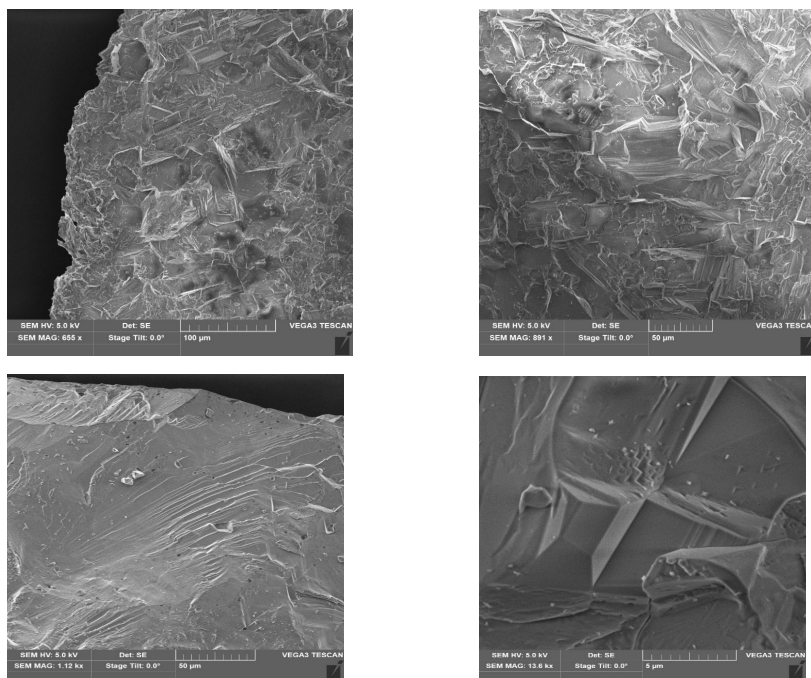


**Fig. 11.** Image of the surface of large particles of PI 5×5 mm

Thus, when studying the morphological structure of the material of large particles containing ore of 5X5 mm size, large fracture, step structure and quasi-skid facets are observed on the surface of the material.

Next, we present images of the coarse fraction (CF) with an indication of their size established through SEM, Fig. 12.

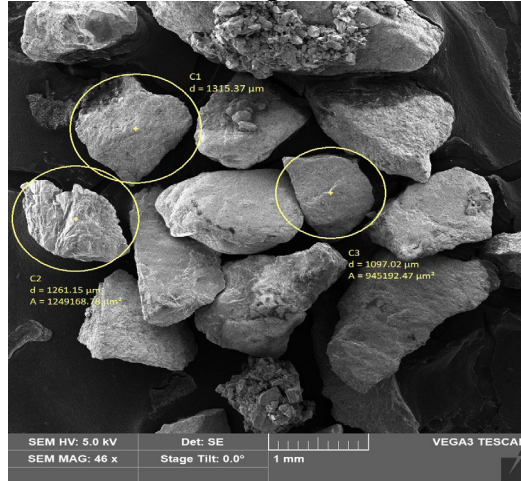


**Fig. 12.** CF sample (powdered  $\emptyset$  particles 1-1.5  $\mu\text{m}$ )

The studied CF material is a coarse powder of oval shape, particle diameter size = from 1mm to 1.5 mm, there are inclusions of particles of the same material of about 50 microns.

According to morphology the surface of particles represents: stone-like structure, brittle and quasi-brittle fracture.

Further the sizes of the smallest fractions (THF) were determined by SEM, which are presented in the following images, Fig. 13-14.

The studied THF material is a powder with crystalline particles, which the average value of the diameter of the main particles was 167,7  $\mu\text{m}$ , the cross-sectional area of the crystalline particles from 879, 65  $\mu\text{m}^2$  to 2664.51  $\mu\text{m}^2$ .

The morphological structure of the surface of basic particles is stone-like structure, quasi brittle fracture, and the surface of crystalline particles: flat with small chips at an angle, presumably a single crystal or polycrystal.

In publications of scientists in the field of geology and mining, "black shales" are considered as a new promising and unconventional source of noble and rare-metal raw materials.

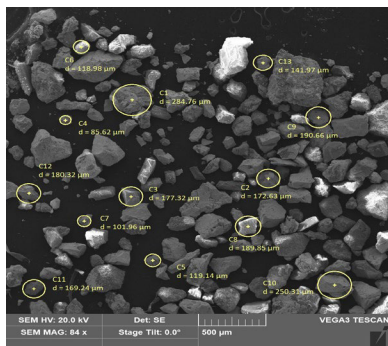


**Fig. 13.** diameter of the main particles THF (av.) ( $\text{Ø}$  167,7  $\mu\text{m}$ )

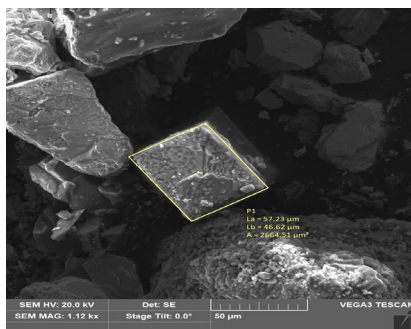


**Fig. 14.** Powder with crystalline THF particles ( $\text{Ø}$  167.7  $\mu\text{m}$ )

## Conclusion

1. Ore-bearing rock of the Kurghak section of the Saryjaz area has the highest openness in relation to the non-standard crushing plant;

2. There is an increase in the quantitative content of a number of elements - Mn, Ti, W, Pb, Sb, Sn, Au, Zr, Co, Bi, As, especially Mn from 5-90 g/t, W from 0.9->100, Pb from 20-120, Sb from 0.3->100, Sn from 20>1000 and Au from <0.5-5 g/t ;

## References

1. **Portnov V.S., Yurov V.M., Tursunbaeva A.K.** et al. Issues of optimization of the process of crushing of refractory ores. *Fundamental Research*. №9, 2012.

2. Source: Innovative technologies. Modern innovative technologies. - <https://kstu.kg/innovative-technologies/>.

In our country innovation activity is supported in every possible way, this is confirmed by the Law "On innovation activity" adopted in the Kyrgyz Republic on November 26, 1999, № 128.

Law "On innovation activity" from November 26, 1999 № 128.

3. **Kanaev A.T., Baimyrzaev, K.M., Semenchenko G.V.** and others. Influence of the degree of grinding of ore of Bolshevik deposit on the gold recovery. 2017.



## TECHNOLOGY FOR OBTAINING BIOLOGICALLY ACTIVE HUMIC PREPARATIONS FROM BROWN COAL



### **Nariman ZHALGASULY**

Head of the Department "Ecology and Safety of Mining" Institute of Mining. D.A. Kunaev, Ph.D., prof. , academician of the International Academy "Ecology", (Almaty, Kazakhstan), av. Abay, 191, phone: 3765364. (<https://orcid.org/0000-0001-7550-9782>)



### **Aliya ISMAILOVA**

The head of the laboratory "Physico-chemical methods of processing of mineral raw materials" of the Mining Institute.D.A. Kunaev, Ph., Almaty city. Abay av., 191, (<https://orcid.org/0000-0001-5705-3363>)



### **Nursultan UAYSULY**

master, researcher at the laboratories "Physical and chemical methods of processing of mineral raw materials", Institute of Mining after D.A. Kunaeva, Senior Researcher, (Almaty, Kazakhstan)



### **Madina ISAGALI**

master, National center of science and technology evaluation (NCSTE), Head of the Secretariat (Almaty, Kazakhstan)



### **Orazkul ISMAILOVA**

Senior Lecturer, Doctoral Student, Kazakh National Pedagogical University named after. Abay, (Almaty, Kazakhstan)

### **Annotation**

The Republic of Kazakhstan belongs to the desert zone, and the steppe belt to the third reclamation zone with regimes and methods of irrigation characteristic of each of them. Desert soils are intensively used for the cultivation of zoned agricultural varieties. Large agricultural areas are degraded due to soil salinity. The consequences of the dried-up bottom of the Aral Sea and toxic emissions from rockets from the Baikonur Cosmodrome negatively affect agricultural yields. An example is the use of piedmont sloping proluvial-alluvial plains where winter and spring wheat crops are located. Grain crops are cultivated mainly in unsecured rainfed areas with an annual rainfall of 200-250 mm, in the zone of semi-sufficient rainfed areas (400 mm) and only about 10% - in irrigated agriculture

Since the water resources of the arid regions of the south and south-east of Kazakhstan are close to exhaustion, it is obvious that the most promising measure for further increasing the production of grain and other agricultural products compared to their current level is the use of special agro-reclamation techniques on the fields on a humic basis, increasing the environmental plant resistance.

The purpose of this work is to develop a technology for producing a plant growth stimulant drug from Kazakhstani brown coals with a low degree of metamorphism and to experimentally confirm its effectiveness in increasing the yield of cultivated plants on low-productive soils. The results of testing a sample of the drug and agricultural practices on various types of low-productive soils are presented.

The biotesting method was used to determine the concentrations of aqueous solutions of a humic preparation for treating agricultural seeds, technological parameters for preparing seeds for sowing (duration of treatment with a humic preparation, seed storage, drying), and to determine the optimal conditions for sowing seeds into the soil (humidity, temperature, salinity, etc.).

Laboratory experiments were carried out according to the method of B.P. Stroganov; the seeds of rice, wheat, barley, soybeans, sorghum and corn were studied, which were germinated in a thermostat in fivefold repetition on highly saline and non-saline soil substrates in accordance with the requirements of GOST (GOST 10250-80, GOST 12038-84).

In conclusion, it can be noted that the effectiveness of the preparation from coal increases the yield of grain crops, which reaches 24.2 - 42.1%, rice 76.2 - 78.6%, and soybeans - 34.8%. on low-productive soils with a salinity level of 0.8 - 2.2%.

### **Introduction**

Kazakhstan has significant reserves of brown coal, which is a raw material for processing to produce various plant growth stimulants. Despite the presence in the Republic of large brown coal deposits and a sufficiently developed infrastructure for the production of such products, their production has not been established. Therefore, the development and industrial implementation of technology for producing modified humic preparations from natural hydrocarbon raw materials is an urgent task, and the creation of production of such

products helps expand the export potential of the Republic and import substitution. At the same time, not only economic problems are solved, but also social problems such as creating additional jobs, developing regional infrastructure, and increasing the well-being of the population.

Extensive irrigation development of soils in the desert and foothill desert-steppe zones of Kazakhstan without sufficient scientific justification led to the tragedy of the Aral Sea, the Ili-Balkhash problem, irrational use of water resources, their almost complete exhaustion, soil degradation, in particular progressive secondary salinization, waterlogging and desertification landscapes, contamination of soils and drainage waters with pesticides and salts of heavy metals, reduction in the profitability of agricultural production.

The problem of “waste” land and unpromising villages has emerged. In the Kzylorda and Almaty regions alone, more than 30 thousand hectares of rice lands due to intense secondary salinization turned into salt deserts, covered with rare bushes of salt-tolerant halophytes. Lands saturated with destructive salt turn into meager pastures and a source of aerosol bitter-salty dust, which is carried by air masses for thousands of kilometers, poisoning all living things.

In connection with the current situation, ecologists, soil scientists, land reclamation specialists and other specialists of the republic were faced with the difficult task of developing environmentally friendly, water- and resource-saving agricultural technologies that would make it possible to do without preliminary leaching of saline soils with the corresponding consumption of scarce irrigation water and combine the reclamation period with the operational period. .

To solve these complex mutually exclusive problems, fundamentally new scientific and theoretical developments and methodological approaches are required.

A novelty is the technology for obtaining plant growth stimulants from Kazakhstani brown coals with a low degree of metamorphism, increasing the yield of agricultural crops on highly saline soils.

Currently, about 400 coal basins, deposits and large coal occurrences have been explored in Kazakhstan with a reserve of about 34 billion tons (9th place in the world) and production of over 100 million tons per year (6th place in the world) and the question rational use of these coals is always relevant.

The purpose of this work is to study, develop and test agro-reclamation techniques aimed at increasing the environmental sustainability of cultivated plants in low-productive soils based on the rational use of physiologically active sodium humate in combination with other methods of complex and differentiated agricultural technology.

Since 2018, in the laboratory of physical and chemical processes of processing mineral raw materials of the Institute of Mining named after D.A. Kunaev is developing a technology for producing physiologically active sodium humate from brown coal, enriched with macro-, microelements and wormwood extract, which increases the environmental resistance of agricultural crops to extreme environmental factors.

The results of tests of an experimental sample of the drug obtained using the developed technology and agricultural practices on various types of low-productive soils in the arid zones of the republic are presented. The biotesting method was used to determine the optimal concentrations of aqueous solutions of a humic preparation for treating agricultural seeds, the optimal technological parameters for preparing seeds for sowing (duration of treatment with a humic preparation, seed storage, etc.); the optimal conditions for sowing seeds into the soil (substrate humidity, temperature, salinity) were determined. This will reduce fluctuations in crop yields from year to year due to fluctuations in atmospheric precipitation, as well as unfavorable soil and reclamation conditions caused by progressive salt accumulation with low natural drainage of landscapes.

### **1 Development of a new technology for producing humic preparation**

Mining and processing enterprises pollute the atmosphere with various emissions. Dust-like pollution received from various sources is transported by air currents from one layer of the atmosphere to another (from the troposphere to the stratosphere). The average residence time of non-settling dust (light) is about 2 years in the stratosphere, 1-4 months in the upper troposphere and 6-10 days in the lower troposphere. In the process of anthropogenic impact on nature, the area of pastures and arable land is constantly decreasing.

The purpose of the research is to eliminate the negative consequences of mining operations by carrying out reclamation measures

while restoring biological balance. Reducing dust emissions from and tailings of processing plants is achieved through biotechnical reclamation. Biotechnical reclamation involves sowing seeds and shrubs on tailings and waste rock dumps using physiologically active drugs - plant growth stimulants obtained from coal deposits in Kazakhstan.

Currently, the following measures for the protection of land during the development of minerals and their processing at processing plants and metallurgical plants are known and applied both in the Republic of Kazakhstan and in neighboring and foreign countries:

- prevention and reduction of the area of disturbed and contaminated lands. rational placement of industrial sites and other various structures;
- improvement of mining technology, including dumping,
- disposal of waste generated during the production process, elimination of soil pollution, etc.;
- restoration of the landscape - returning to it the properties and functions it had lost;
- transforming the landscape by giving it new functions for the purpose of rational use and environmental protection.

Land reclamation is usually carried out in two stages: technical and biological. During technical reclamation, land is prepared for its intended use (agricultural, forestry, water management, fisheries, recreational, construction and other uses of restored lands). Technical reclamation includes terracing and formation of slopes, transportation and application of fertile rocks to reclaimed lands, radical reclamation of roads, special hydraulic structures, etc.

Biological reclamation includes a set of agrotechnical and phytomeliorative measures to restore the fertility of disturbed lands. The main measures for biological reclamation include the application of increased doses of organic and mineral fertilizers and sowing of perennial crops.

All biotechnological methods for reclamation of disturbed and contaminated lands can be divided into methods with the application of a new soil cover (layer), consisting of fertile loams and/or glauconitic sand, as a potassium fertilizer, and without their application. Applying new soil cover is expensive, labor-intensive, and technically challenging.

In practice, four types of biotechnological methods are used in the world: reclamation without applying a new soil cover. The first method includes restoring the fertility of disturbed and weeded lands through nitrogen-phosphorus-potassium fertilizers and sowing pioneer plants. The average period of generation of a stable fertile soil layer with this method is that large doses of mineral fertilizers (700-1200 kg/ha) are introduced into disturbed and contaminated soils, and high-yielding plants are used as pioneer plants. The duration of soil formation with this method is 8-10 years.

The third direction of restoring the fertility of disturbed and weeded lands is carried out by inoculation (introduction) of active soil microflora into the soil surface with a period of restoration of land fertility within 3-5 years. And finally, with the fourth method, stabilization and restoration of soil fertility over 4-6 years is carried out by adding a bioactive drug to the soil in an amount of 5-50 g/ha.

All these methods and directions have their advantages and disadvantages in different soil and climatic conditions, as is known in Kazakhstan, the arid zone and arid climate predominate. The main disadvantage of all of these methods is the need to use energy costs to add various ingredients (mineral fertilizers, microflora, bioactive preparations) to the soil. Other disadvantages of these methods are the relatively long period of soil restoration. The third group of disadvantages includes the low efficiency of methods when used in clogged, saline and toxic soils, as well as in extreme conditions - drought, lack of snow.

The method we propose is the most economical and efficient in terms of labor, material and financial resources.

Institute of Mining named after. YES. Kunaev developed a technology for producing humic preparations from brown coal. A representative batch of the resulting drug was tested as a growth stimulant for various crops in the extreme conditions of the Republic of Kazakhstan, which was studied in laboratory conditions and tested at a pilot industrial site.

According to Professor L.A. Khristeva (Ukraine) [1] the physiological effect of humates is more effective when there are adverse external influences on plants or their habitat (excess or lack of moisture, light, heat, nutrients).

The arid climate, scarcity of water resources and the significant participation of saline soils in the structure of the soil cover of Kazakhstan are a serious obstacle to increasing the productivity of land using classical methods.

From the analysis of known methods it follows that at present, none of the technologies for producing humates has been brought to industrial production due to objective reasons. The basic requirements for the feedstock have not been worked out, the L:T ratio, the concentration of the alkali solution, the fractional composition of the feedstock and the duration of its treatment with alkali, temperature conditions, etc. have not been determined.

We have studied a number of lignite deposits in Kazakhstan with satisfactory characteristics, especially in terms of the content of humus components. Among the numerous raw material objects, the Oy-Karagayskoye and Kiyaktinskoye deposits were selected. The yield of humates is respectively 15-30%, 65-69%. The diversity of the feedstock is explained by the fact that coals not only from different deposits differ in composition, but also within the same deposit there is a significant variation in indicators.

Basically, the new technology for producing humates involves the following operations: mechanical cleaning of the feedstock from foreign inclusions, crushing the feedstock to the required fraction with simultaneous drying. Treatment of the resulting mass with an alkaline solution with a concentration of 1 to 10%, for 2-10 hours and a L:S ratio of 5 to 10, at a temperature of 60-800C, filtration with washing, drying, grinding, sifting.

The use of humic stimulants in agriculture opens up wide opportunities for increasing the yield of grains, vegetables, fruits and berries, melons and industrial crops.

The action of humic preparations is especially effective in the initial period of plant development and during the period of greatest tension in biochemical processes, as well as when the external conditions of plant growth deviate from the norm due to drought and frost, excess nitrogen in the soil, etc.

## **2 New technologies for increasing the fertility of saline soils**

### **2.1 Literature review**

Saline soils are an essential component of territories. The presence in them of high concentrations of specific mineral substances,

accumulated in the conditions of effluent water in the active part of the root layer, causes extremely unfavorable conditions for cultivated plants and constitutes a characteristic feature of their low natural fertility [2]

According to academician V.M. Borovsky [3], saline soils in Kazakhstan occupy 111550.1 thousand hectares, or 41% of all soils in the Republic.

In accordance with the climatic characteristics of soil zones, their number is steadily increasing in the direction from north to south. Thus, in the forest-steppe zone they occupy 29-30, steppe - 37, dry-steppe - 40-51, desert-steppe and desert - 46-55, and foothill desert-steppe - 5% of the area of zonal soils.

With such a wide distribution of soils of the saline series in the zonal aspect, the ratio between solonchaks and solonchets in the steppe zones is on average 1:50, in desert zones - about 1:3.

It is known that when the content of water-soluble salts in the root layer of soil is up to 0.4-0.8%, most cultivated plants develop poorly and produce a reduced yield, and when the salt content is more than 1.2-1.5%, the plants do not produce agricultural products. Therefore, on such soils a set of special reclamation techniques is usually used to ensure the effective reproduction of the fertility of the reclaimed lands.

Fertility is an integral qualitative property of any soil, expressed by a complex functional dependence on the elements and life support conditions of plants, reflecting the interaction of a complex of soil formation factors. In the process of natural soil formation, various levels of natural soil fertility are formed, measured by the levels of biological productivity of phytocenoses. Different plant species react specifically and ambiguously to deviations of soil fertility components from optimal to extreme values. This determines the cyclical nature of soil formation with evolutionary variability and the leading role of the biological factor, thanks to the adaptive reactions of plant communities to new environmental conditions.

The vegetation cover of saline soils is sparse and poor in species composition. The sparse grass stand is dominated by salt-tolerant plants, which in the process of evolution have developed mechanisms for maintaining ionic homeostasis, as a result of which the level of accumulation of ballast salt ions and their ratio when life sup-



port conditions change are maintained within physiological norms [4].

According to A.A. Shakhov, the adaptive evolution of halophytic plants to high concentrations of salts in soil solutions is a consequence of the physiological restructuring of plants in generations with the creation of a halo-resistant type of metabolism in the offspring. This ultimately determines the characteristics of the development of halophytes and their active ecological and biological reactions to soil salinity conditions, due to which and a change in heredity, soil salinity from a negative factor becomes a positive one, ensuring high salt tolerance of plants and their ability to regulate metabolism in the presence of the amount required by the plant in the substrate absorption of ions by the root system, their transport, metabolization of used mineral elements from the body [4].

During individual development, profound qualitative changes occur in halophytic plants to conditions of varying salinity, but the difference in the influence of types of soil salinity, which is significant for most glycophytes, is smoothed out.

Cultivated plants grown on non-saline soils have a relatively limited ability to adapt to salinity and do not have the characteristic morphological and anatomical features characteristic of halophytes, since the conditions of their existence in the process of long evolution were not favorable for the emergence of this property [5]. Deviations of environmental conditions to extreme values under the influence of natural factors and negative anthropogenic influences lead to a sharp decrease in yield, loss and death of agricultural crops. According to G.V. Udovenko and E.A. Goncharova [6-7], extreme factors of different nature (salinity, drought, etc.) have the same effect on the structure of the yield of cultivated plants. Therefore, in recent years, agriculture has dictated the need to study, develop and implement in the fields effective methods of targeted anthropogenic impact on both low-productive soil and the plant itself, which contributes to the reproduction of its artificial fertility, which materializes in the harvest of zoned varieties of cultivated plants, creating effective soil fertility.

The problem of increasing the productivity of agrocenoses and soil fertility is based on the well-known laws of agro-soil science formulated by V.R. Williams, as well as the use of the biological

characteristics of those crops that are supposed to be grown on reclaimed lands.

The level of increase in soil fertility depends on its initial state and the interconnected system of factors that regulate the expanded reproduction of fertility and exclude the occurrence of undesirable consequences of economic activity on the natural environment when carrying out various types of reclamation, which are divided by content by V.V. Egorov [9] into two groups. The author includes in the first group all types of reclamation that improve only the condition of soils, and the second - reclamation that not only transforms low-productive soils, but simultaneously contributes to changing the state of one or more soil-forming factors.

Gypsum is considered one of the well-known effective chemical ameliorants. Over the past time, a wealth of experience has been accumulated in the reclamation of solonetz soils with gypsum under rainfed and irrigated farming conditions [10]. An analysis of the literature shows that, depending on regional conditions, the use of gypsum has a positive effect on the improvement of solonetzic soils of neutral salinity and is noticeably reduced during the reclamation of alkaline soils. The best results in rainfed conditions are achieved by combining the use of gypsum with physical and biological methods of reclamation. The average duration of the reclamation period varies within a fairly wide range of 5-7 years or more.

Irrigated agriculture differs from rainfed agriculture in the more intensive use of agricultural land. It makes significant changes to the natural soil-forming process and the structure of the soil cover [11].

Irrigation has a multifaceted effect on soils, causing changes in the mineral part of the soil, the structure, quantity and composition of humus, morphological structure, microbiological, biochemical and nutritional regimes, water-physical properties [12], and in general on the ecological environment. The nature and speed of changes are determined by the soil and climatic characteristics of the region, the culture of irrigated agriculture, the level of zonal agricultural technology and the land reclamation methods used. To increase the fertility of alkaline solonetz soils under irrigation conditions, it is important to properly use irrigation water and organize the necessary system of agrotechnical, hydraulic and other measures, taking into

account the dynamics of soil processes. Otherwise, irrigation can quickly lead not to soil cultivation, but to secondary salinization.

Along with gypsum, other calcium salts are increasingly being used, which in their effect are often superior to the classic ameliorant. Thus, the development of soda-sulfite solonchaks in the Voronezh region revealed the exceptional reclamation value of chalk [25], and the saline soils of the Kuban revealed the positive effect of fluff lime, the effectiveness of which increased with the joint application of fourfold doses of ammonium sulfate [13].

Among local raw materials, industrial waste is used to improve solonchak soils, in particular, cement dust, gypsum waste from a tartaric acid production plant, alabaster, synthetic gypsum, calcium metasilicate, soot, calcium chloride, defecate and phosphogypsum [14].

Due to low reclamation efficiency, many of these substances are not justified or are of local importance. The most widely used are calcium chloride and phosphogypsum.

Some studies show that the use of sulfur-containing calcium substances (especially gypsum) is not always effective [15], and on saline soils of rice plantations it is even negative, as it is associated with the process of sulfate reduction. Most calcium salts are either very poorly soluble, or contain various toxic elements, or do not effectively regulate the alkaline reaction of the environment. Therefore, in some regions of the former Soviet Union, methods of activating calcium-containing substances with acidic chemical reagents are widely practiced [33,34]. By their nature, acidic reagents are divided into acids (sulfuric, sulfurous, hydrochloric, nitric, etc.) and salt hydrates ( $\text{FeSO}_4 \times 7\text{H}_2\text{O}$ ,  $\text{Fe}_2(\text{SO}_4)_3$ ,  $(\text{NH}_4)_2\text{SO}_4$ , etc.).

The use of acidic chemical reagents for the reclamation of alkaline solonchak soils began in Kazakhstan relatively recently and in the initial period was associated mainly with sulfuric acid and iron sulfate. Large-scale pilot production work on the use of sulfuric acid and iron sulfate for the development of lands with soda salinity was carried out by the Research Institute of Soil Science and Agrochemistry of Armenia [16].

The experience of Armenian researchers in the use of acidic chemical reagents was a prerequisite for their widespread use in other regions with saline soils [17].

From the laboratory and field experiments with acidic chemical reagents described in the literature, it is impossible to draw clear conclusions regarding the most appropriate form of a particular ameliorant, since their choice may be influenced by local factors.

According to T.N. Voinova and R.Sh. Turdiev [18], the introduction of iron sulfate into takyrl-like alkaline soils of the Akdala massif not only increased the removal of salts from the meter layer, but also had a stimulating effect on the growth and development of rice in ontogenesis. However, the use of various concentrations of sulfuric acid for the reclamation of these soils, despite a significant improvement in their water-physical and chemical properties, caused inhibition of plant growth in the tillering phase. By the end of the growing season, the height of the rice was 30-40 cm and no harvest was obtained. The authors associate this phenomenon with the process of sulfate reduction.

The most important indicator of the potential fertility of cultivated soil is organic matter. The additional use of various types of organic and mineral fertilizers serves as a kind of reserve of nutrients necessary for agricultural crops, is an energy and nutritional source for the life of microorganisms, an additional source of carbon dioxide for plants, a radical means of improving water-physical, chemical properties and targeted regulation of effective soil fertility. The effectiveness of fertilizers increases provided that differentiated agricultural technology is followed, which allows for the most rational use of irrigation water and protects the soil from secondary salinization against the background of various drainage systems. Of the organic fertilizers in crop production, the most promising are manure, straw and various types of composts. The fertilizing and ameliorating value of manure has been known for a long time and enjoys universal recognition both in Kazakhstan and abroad. However, its reserves in most regions are limited and do not satisfy the ever-increasing demand of crop production. Therefore, along with manure, in many soil-climatic zones, crushed straw is increasingly used as a fertilizing and reclamation fertilizer - as a new form of providing low-productive soils with organic matter and increasing agricultural yields [42]. According to V.D. Pannikov and V.G. Mineev [19], when harvesting grain crops using combine harvesters with straw collectors, the cost of straw harvesting is approximately twice as

high as the cost of grain harvesting. Due to overloaded equipment and lack of labor, straw harvesting is delayed for a long period, which makes it difficult to carry out timely and high-quality autumn tillage. Therefore, leaving straw in the field is an important organizational and economic measure that speeds up and reduces the cost of harvesting.

On black and chestnut soils of rice fields, autumn surface (0-6, 0-10 cm) plowing of straw is preferable at least 1-1.5 months before sowing cultivated plants, which contributes to less accumulation of toxic compounds formed during decomposition in the arable layer straw. On soils depleted of organic matter in the south of Kazakhstan, spring surface incorporation of straw at a dose of 6.5 t/ha with a production dose of mineral fertilizers is most effective [46]. The ameliorative and fertilizing effect of straw on alkaline saline soils is enhanced when it is used together with chemical ameliorants (gypsum, polyacrylonitriles K-4, K-9), polyphosphate fertilizers, zinc and nickel salts and preliminary inoculation with cultures of lactic acid bacteria [20].

The unfavorable agrophysical properties of alkaline solonchic soils are due to the presence of an illuvial horizon enriched with peptized highly dispersed particles. When dry, this horizon becomes compacted and breaks up with cracks into blocky, columnar or nutty sections, and when moistened, it floats and turns into a continuous sticky, smearing mass, which sharply reduces the water permeability of soils and is one of the reasons for the long-term preservation of their negative properties, which are difficult to improve by leaching using high-volume calcium-containing substances, acidic chemicals, reagents, as well as waste from industrial and agricultural production and requiring special structure-forming preparations.

A significant role in structuring and increasing the effective fertility of saline soils belongs to polymers and surfactants.

V.P. Batyuk [21] subdivides all polymers used for soil structure formation into three types: horse polymers (salts of acrylic and methacrylic acid, sulfo derivatives of polystyrene); nonionic polymers (polyvinyl alcohol); copolymers of acrylonitrile, acrylamide, vinyl acetate, raspberry anhydride with acrylic, methacrylic malic acids.

Over the past 30 years, systematic experiments have been carried out to determine the effectiveness of reclamation of saline soils with

various polymer substances in various soil and climatic conditions. The most widely used in reclamation practice are industrially developed and economically available preparations made from hydrolyzed polyacrylonitrile (K-4, K-9) and polyacrylamide (PAA), which have structure-forming ability and are good nitrogen fertilizers [22]. In field and laboratory studies N.D. Gradoboeva, R.P. Alekseeva, L.V. Berezina, carried out on non-irrigated solonetzic soils of the Omsk region, it was found that the effect of adding polyacrylamide is more significant on low-sodium solonetz and extremely weak on polysodium solonetz. According to R.P. Aleseyeva [23], the reason for the unequal action of PAA lies in the different microaggregation of low- and high-sodium solonetzes and the ability of the polymer to impart good water resistance only to existing aggregates.

According to V.A. Vinogradov [24], the effectiveness of polymers on saline soils is associated with the establishment of their doses and methods of application. Under irrigation conditions, the action of polymer substances is more effective. Moreover, preparations that provide high water resistance of the structure, as a rule, also provide the greatest filtration capacity of soils, and this creates favorable conditions for rational leaching of saline soils [25].

Analyzing the available data on the effect of polymer substances on desalinization and desalinization of soils, it can be stated that the use of polymers improves the physicochemical properties of low-productive soils and contributes to the maximum reduction of the reclamation period at relatively low costs, since the rate of their consumption per unit area is insignificant, the effectiveness of polymers depends on the soil and climatic conditions of the region, and also on the dose and method of introducing their composition.

Polymer surfactants can be structure formers, nutrition sources, plant growth stimulants or regulators of water-salt regime, physicochemical properties of saline soils, and each of them has a specific function.

Employees of the Department of Chemistry of Macromolecular Compounds of the Kazakh National University. Al-Farabi developed methods for the synthesis of new soluble polymeric substances (polyampholytes, RPA) - which simultaneously serve as an acidic chemical reagent, a humic-like organo-mineral fertilizer, a structure former, a regulator of alkali processes in soil and irrigation water, a

growth stimulant and a means for increasing the salt tolerance of rice seeds [26]. Due to the high cost of this drug, its production was discontinued at the stage of vegetation and field experiments.

Thus, to date, a large amount of experimental material has been accumulated in Kazakhstan and abroad on the reclamation of saline soils using classical methods. However, recommendations for obtaining the maximum yield of any crop, compiled on the basis of numerous experiments on the studied massifs, are usually far from optimal for other developed areas with different climatic and reclamation conditions. This explains the organization of a large number of experimental stations and research institutes that are developing optimal reclamation methods for the development and exploitation of saline soils in various regions.

The high cost and long-term development of reclamation recommendations are due to the empirical approach to solving the problems of reclamation of each isolated massif. At the same time, necessary environmental protection measures are often violated. For example, to flush saline soils and maintain design reclamation conditions in developed areas, a large amount (from 5 to 40 thousand m<sup>3</sup> per 1 ha) of fresh water is consumed. Drainage salt water is usually discharged into river beds or onto territories adjacent to developed areas, turning them into “dead” ecological zones in a few years.

Reclamation resuscitation of such zones against the background of drainage systems necessitates an ever-increasing increase in water consumption for flushing, which leads to negative environmental consequences in large areas of the delta plains of southern Kazakhstan, which received comprehensive coverage in the works of V.M. Borovsky [27] and M. A. Orlova [28].

Indicative in this regard are the large-scale reclamation activities in the desert zone of Kazakhstan, which over the past 40 years have led to the Aral environmental tragedy and the Ili-Balkhash problem.

It should be emphasized that on the soils of the saline range of the arid zone of Kazakhstan, the amount of crop yield depends on many factors, but primarily on the degree and chemistry of soil salinity, alkalinity of soil solutions, meteorological conditions of individual years, the effectiveness of reclamation measures, the quality of seeds and the level of agricultural technology, as well as the environmental sustainability of the plants themselves.

Thanks to many years of experimental research by A.A. Shakhov, B.P. Stroganov, L.A. Boyko, G.V. Udovenko, M. Ya. Shkolnika [29] and others. By now, the physiological basis that determines the salt tolerance of many agricultural crops in a wide range of soil salinity is well known, which served as a theoretical basis for the development of diagnostic methods and special agricultural techniques for increasing plant resistance to unfavorable conditions. environmental factors of great practical importance in the development of saline lands.

Therefore, over the past 70 years, along with the search for effective traditional reclamation methods for increasing the fertility of saline soils, agronomic practices are increasingly being introduced into agronomic practices for actively influencing the physiological processes occurring in cultivated plants in extreme environmental conditions, using electrophysical factors , salt solutions , microelements, extracts of halophytic plants, as well as environmentally friendly, physiologically active sodium humates obtained from brown coal [30]. Due to the low energy intensity of technological processes and the high return on material and labor costs, the widespread introduction of these agricultural practices is relevant under certain soil reclamation conditions, as it is associated with a sharp reduction in the overall energy intensity and cost of agricultural products.

To increase the effective fertility of saline soils in various regions of Kazakhstan, the most promising is the use in crop production of special physiologically active humic preparations enriched with macro-, microelements and extracts of wild plants.

The direction proposed by T.A. Kukharenko, L.L. Khristeva, I.I. Yarchuk and others: [31] provides for the widespread use of humic fertilizers obtained from coal to increase the productivity of agricultural crops. Humic fertilizers are generally considered to be those fertilizers that contain water-soluble humic acids (humophos, humcophos, sodium, ammonium, potassium humates, etc.). The most widely used in agriculture are humates, which are a product of the interaction of brown coal with an aqueous solution of alkali (KOH, NH<sub>4</sub>OH, NaOH).

Numerous studies conducted in laboratories in Ukraine, Belarus, Czechoslovakia, Hungary, Kazakhstan, Kyrgyzstan, Italy) have shown that water-soluble salts of humic acids have high bioactivity.



They enhance the supply of nutrients to plants, activate soil microflora, the synthesis of proteins, carbohydrates, increase the resistance of plants to low and high temperatures, to the action of increased doses of mineral fertilizers and pesticides, activate plant growth, help increase yield and improve its quality.

In addition, it is known to use sodium humate as a biologically active feed additive for cattle, pigs and poultry in order to increase weight gain and enhance the general non-specific resistance of the body .

Research by Professor I. Yarchuk [32], who studied the effectiveness of humates, showed that the yield of corn on sandy soils in the south of Ukraine increased by 30.3%, while the application of organomineral fertilizers in the form of a mixture: peat + superphosphate + ammonium sulfate led to an increase in yield by only 23.5%. Corn plants fertilized with humophos were almost twice as heavy as the control plants and contained more nutrients valuable for silage. In addition, the use of humophos reduced the gap between the flowering of male and female flowers, which created optimal conditions for more complete pollination. Humophos increases wheat yield on chestnut soils in southern Ukraine by 35%.

Summarizing the results of experimental tests, G.V. Kukharevsky concludes that 1 ton of humophos is equivalent in efficiency to 6-8 tons of humus or 10 tons of peat mixed with mineral fertilizers.

The positive effect of nitrogen and sodium humate, used in liquid form during vegetation irrigation, as well as when applying 1 liter of a 0.001% aqueous solution under potatoes at the time of planting, accelerates the emergence of seedlings and increases the yield by 8%. Adding the same amount of sodium humate to the budding phase increased the yield by 15%. And the addition of sodium humate both during planting and during the flowering period resulted in a 48% increase in yield.

Agrobiological studies of various humates have shown that sodium and ammonium humates have the most effective effect. Less effective are humates of potassium, calcium, and iron.

Analysis of the results obtained allows us to conclude that humates are easily soluble in water, form highly dispersed and true solutions, ensure high digestibility by plants and, as a result, have a

strong stimulating effect, but not all types of plants respond unambiguously to these preparations.

According to L.L. Khristeva et al. [33], potatoes, tomatoes and sugar beets give the highest yield increases, and wheat, winter and spring, barley, oats, millet, corn, rice, wheatgrass, alfalfa react somewhat worse; peas and beans give a slight increase in yield, while sunflower, pumpkin and a number of cotton varieties do not respond to the presence of humates.

The widespread use of brown and oxidized coals mixed with organic and mineral fertilizers in a number of European countries, as well as in Ukraine and Belarus, has shown their promise [69,72-75,80,90].

The advantage of this fertilizer compared to humates is that not only humic acids are used, but also residual organic matter and mineral components rich in micro- and macroelements. In addition, having a high adsorption capacity, brown coals attract individual scattered soil particles, improving its structure.

The combined application of these coals with mineral fertilizers protects soils from diversion erosion, ensures better growth and development of plants and, ultimately, increases the yield and its quality.

In world practice, the results of these studies are used quite widely. Thus, in Czechoslovakia, carbon dioxide is fruitfully used - a mixture of fossil coals (brown, lignites, etc.) with mineral fertilizers, and in Germany - brown coal waste with slurry.

Biominerals fertilizers are a mixture of brown coal with various bottom sediments, inoculated with special soil bacteria grown on waste water from sugar production.

Bacteria contribute to the development of the process, deamination (formation of an assimilable form of nitrogen) and the production of compounds necessary for plant growth, etc.). The use of these fertilizers is based on their properties to form soil sorbents - organomineral colloids that serve as absorbers of elements necessary for plants. The use of these fertilizers helps to increase the yield of cultivated plants and improve the quality of agricultural products. Studies on the production of composts and organomineral mixtures from oxidized brown coals and manure have shown that when these components are mixed in various ratios, the content of components

vital for plants, namely nitrogen, phosphorus, and potassium, increases [34].

The results obtained indicate that, under conditions of microbiological life, brown coals absorb ammonia nitrogen compounds, as a result, the quality of manure is significantly improved and the effectiveness of its impact on the yield of grain potatoes, flax, sugar beets and oats increases. This composting technique increases the efficiency of not only manure, but also mineral fertilizers.

Brown coals formed in Meso-Cenozoic swamps are based on humic acids, similar to the organic matter of modern peats, as well as macro- and microelements: calcium, magnesium, iron, aluminum, sulfur, phosphorus, manganese, copper, molybdenum, vanadium, nickel, scandium, beryllium, etc.).

Analysis of the composition of fossil fuels shows that they contain trace elements in large quantities compared to soils.

Studies on the effect of brown coals on plant growth when added to the soil in their natural state have shown an increase in the height and weight of plants, grain yield and the amount of chlorophyll in the leaves [35].

During the experiments, brown coals from the Alexandria deposit of Ukraine were used, containing total nitrogen - 0.53 -1.15%; phosphorus slots - 0.39; K<sub>2</sub>O - 0.67%; traces of Mg, Na and trace elements.

No less convincing results were obtained when testing sugar beet crops. If mineral fertilizers alone increased the sugar beet yield by 10.5 c/ha, the amount of sugar by 2.9 c/ha, then when adding 20-30 kg/ha of brown coal, the yield increased by 20.5-56.1 c/ha. ha, sugar content - by 0.2-1.0% and the amount of sugar by 5-6 c/ha.

In the Donbass, waste from coal preparation plants, containing 6-17% organic matter, was used as organic fertilizer in doses of 10,15,20 t/ha on eroded chernozems. The increase in grain yield ranged from 1 to 5.2 c/ha.

In addition, there was an increase in the activity of the humification process in the arable layer. In slightly acidic chernozems formed on loess-like loams, with the addition of these wastes, the content of humic acids increased almost 1.5 times.

Float tailings from coke production were also used as organic fertilizers on sandy loam chernozem at a dose of 5 t/ha, which showed a positive effect on increasing productivity.

Along with brown coals, L.A. Khristeva [36] tested shale at a dose of 2-4 t/ha, which showed positive results.

From the above data it follows that raw-milled oxidized coals in their natural form and in a mixture with various substances effectively increase yield and product quality, improve humus content and soil structure.

The physiological effect of humates, according to L.A. Khristeva [37], is more effective when there are adverse external influences on plants or their habitat (excess or lack of moisture, light, heat, nutrients).

Increased resistance of plants in the presence of humates to high doses of mineral fertilizers, as well as when they are exposed to increased doses of radiation and pesticides, has been revealed. According to the author, humic preparations relieve allelopathic tension of substrates or soil fatigue. The action of humic preparations is especially effective during the initial period of plant development under extreme environmental conditions.

## **2.2 Marketing research**

An analysis of patent and scientific and technical literature has shown that currently in many countries of the world, namely in the USA, Canada, Germany, Great Britain, Japan, Italy, Spain, India, Bulgaria, Russia, Belarus, Ukraine, Uzbekistan, Turkmenistan, work is underway on the creation of technology for the industrial production of humic preparations from brown coals and their use. At the moment, in a number of countries there are pilot industrial installations with a small capacity of up to tens of tons per year, and the use of humates has not yet expanded beyond experimental stations and individual farms. In Kazakhstan, research on the development of technology for the production of humic preparations is in its infancy.

According to static data, in the gross agricultural output of Kazakhstan, agriculture accounts for 47.3%, and livestock farming accounts for 52.7%; the total sown area of agricultural crops is 25991.4 thousand hectares.

68.4% of the total area is occupied by grain crops (including 60.7% by wheat), 0.6% by industrial crops, 1% by potatoes and vegetables and melons, and 30% by forage crops.

When using a humic preparation as a growth stimulator for agricultural plants, both pre-sowing seed treatment and 2-fold treatment of plants during the growing season are carried out.

In addition, when treating mineral fertilizers (nitrogen, phosphorus and potassium) with humic preparations, it is possible to reduce the consumption rates of these fertilizers

Thus, the estimated need of Kazakhstan for the production of humic preparations for growing only wheat, corn for green mass, raw cotton, potatoes and vegetables is about 3000 tons (in terms of dry powder). More accurate data will be obtained after 2-3 years of testing a humic preparation obtained from brown coals of the Kiyakty deposit in various climatic zones of Kazakhstan on different agricultural crops [38].

The need to use humic fertilizers is dictated by the following factors:

1. The high cost of industrial mineral fertilizers - 180-200 US dollars per 1 ton, which is unaffordable for economically weak rural producers.

2. A sharp decrease in the volume of fertilizer applied to fields;

3. Depletion of land, reduction in productivity;

4. Deterioration of the economic situation of rural producers;

5. At a consumption rate of 8-10 centners of industrial mineral fertilizers per 1 hectare of sown area, the costs are 12-13 thousand tenge; at a consumption rate of humic fertilizers of 5 t/1 ha, the costs are 3-4 thousand tenge, i.e. 3-4 times less, and industrial fertilizers only improve plant nutrition, and humic fertilizers increase the humus content in the soil;

6. No special capital storage facilities are required for storing humic fertilizers and preparations. They are non-toxic, do not cake and do not deteriorate when stored in open areas.

Until recently, this drug was imported in small quantities from neighboring Uzbekistan; there were small pilot plants in the Turkestan, Pavlodar and Almaty regions. However, due to disorganization and poor work among agricultural producers and agricultural authorities, the use of humates has not been established.

### 2.3 Economic efficiency of using humic preparations

The technology for producing humic preparations is characterized by low energy and material consumption. Therefore, the cost of producing a unit of product is relatively small, but it is consumed in small doses. Consequently, transport costs are insignificant.

All this predetermines the low cost of work associated with its production, application and use over large areas. Approximate calculations show that when treated with humate, 345.5 thousand hectares (seeds treated with the drug are recalculated per area based on the seeding rate). The costs of this work will amount to 41.9 million tenge, and the increase in production from the action of the drug will be received by 1.52 billion tenge, i.e., the net profit will be 1.48 billion tenge. All this will certainly affect the economy of rural producers.

The Republic of Kazakhstan has quite significant reserves of B3 brown coal, the largest of which are the following deposits: Alakol - 7.6 million tons; Maikuben - 104.6 million tons; Oy-Karagay - 8.0 million tons; Kiyakty - 130 million tons.

The integrated use of these reserves opens up wide opportunities for providing both the republic and neighboring countries with highly effective fertilizers and physiologically active preparations that increase the productivity of plants on saline soils [39-40].

As a result of the work performed, the effectiveness of the drug obtained using the developed technology on low-productive soils with a salinity level of 0.8-2.2% was established. At the same time, the increase in the yield of grain crops reached 24.2-42.1%, rice 76.2-78.6%, and soybeans - 34.8% (see Table 1).

Table 1

Optimal concentrations of aqueous solutions of humic preparation			
Culture	Variety, hybrid	Sodium humate, %	
Rice	Sunny, Солнечный, Kuban 3, Ushtobinsk	1,0-3,5	2,5-3,0
Wheat	Saratovsk 29, Karlygash Kazakhstan10	1,0-2,5	2,0-2,5
Barley	Chernogovsk 5	0,5-3,5	2,5-3,0
Soybeans	Arna	0,005-0,05	0,02-0,04
Sorghum	Eureka	1,0-2,0	1,0-1,5
Corn	Venichnoe 623	0,6-1,5	0,6-1,0

Humic compounds are part of brown coals and are substances of non-synthetic origin, non-toxic to humans and the ecosystem as a whole, which is a positive aspect of their use for various needs.

To solve pressing problems of modern industry and agriculture, new types of composite materials are needed. These materials include modified humic preparations. The complexity of the structure and the presence of different functional groups, amino acids, polysaccharides, etc. in the composition of humus determine their functions such as accumulative, transport, regulatory, protective, physiological, etc [41-42].

Humate-containing compounds have unique properties, which allows expanding their areas of application:

- The country's electrical industry needs humic composite materials, which are used as extenders and corrosion inhibitors for batteries. For these purposes, domestic enterprises use expensive and toxic products imported from abroad: BNF tanning agent, boric acid,  $\lambda$ -hydroxynaphthoic acid. This leads to high costs for their acquisition, transportation, etc.;

- in the metallurgical industry, modified humic compounds are used to increase the strength of pellets and reduce granulation time. They can also act as biologically active substances, sorbents of heavy metals, radioactive elements and toxic organic compounds, i.e. they can incorporate some pesticides, hydrocarbons. These compositions are also used for the purification of natural and wastewater, for the reclamation of degraded and contaminated soils.

#### **2.4 Experience in biological remediation of tailings dumps**

Over 55 billion tons of waste from mining enterprises are stored in Kazakhstan, which pollutes the atmosphere with various toxic gases and dust. The average residence time of non-settling dust (light) is about 2 years. Coal mining enterprises and coal preparation plants emit up to 2 million tons of dust into the atmosphere per year.

All this indicates the need to develop a strategy for ensuring the environmental safety of subsoil development, increasing the efficiency of use and reproduction of georesource potential. The solution to this problem lies in the creation of effective synthesized technologies for the extraction and processing of coal, the development of a systematic approach for specific conditions, and the study of an individ-

ual object from the perspective of a more general system of which it is a part.

Analyzing the results of laboratory studies, it can be assumed that the tested agricultural techniques can become the basis for a new technology of biological reclamation by growing green mass on the surface of tailings to reduce dust formation [43-44].

It is almost impossible to completely eliminate dust in all tailings dumps with modern mining technology, but it is possible and necessary to reduce the dust content in mine air to such limits that the possibility of occupational diseases can be reduced.

The fact is that mine dust is heterogeneous in mineralogical composition, since the products of grinding various rocks, especially quartz minerals, enter the air. Also most dangerous in relation to silicosis is the content of free silicon dioxide in dust. The higher this content, the more dangerous the mine dust. Quartz is a widespread mineral in the earth's crust, representing an essential component of many igneous and metamorphic rocks - granites, porphyries, hornfels, gneisses, etc., forming an independent rock - quartzite, which is often found in the form of veins in igneous rocks and constitutes the main mass of sandstones. Almost all mines in Kazakhstan have high levels of silicon dioxide.

The amount of silicon dioxide in rocks and in the air, as a rule, is not the same. For example, in the rocks of the Maslosko-zavodskaya formation the SiO<sub>2</sub> content averaged 70%, and in dust 54%; The Zhezdinsky mine has SiO<sub>2</sub> in rocks of 30%, in dust 30%; East Korumadsky mine - 78% in rocks, 70% in dust.

Mine dust usually has a complex mineralogical composition. So, for example, according to chemical analysis, the rocks that make up the Maslosko-Zavodskaya suite contain: SiO<sub>2</sub> -48-73%, Al<sub>2</sub>O<sub>3</sub> -3.2-25.1%, FeO -2.7-4.1%, MgO - 0.3-9.6%, CaO -0.2-4.6%, K<sub>2</sub>O -0.5-6%. The average particle diameter for three groups of observations was determined to be 0.72-0.75 μm.

In accordance with the considered strategy for rational environmental management, an option was chosen based on the targeted impact on the biocenosis of the technogenic landscape, namely waste storage facilities for processing asbestos-containing and manganese-containing tailings with the aim of forming a biologically active en-



vironment using biotechnological, agrotechnical and chemical methods.

The results of the research made it possible to determine the optimal modes for preparing seeds of wild plants for experimental tests.

The objects of research were the tailing dump of JSC "Kostanay Minerals", located in the city of Zhitikara, Kostanay region, the tailings dump of the Zhezdinsky processing plant, which is located in the Ulytau district of the Ulytau region (Kazakhstan).

These wastes occupy large areas, for example, the experimental site located on the territory of the Zhezdinsky enrichment plant is 25 hectares. From an economic point of view, a technology for dust removal using green spaces using adaptogen drugs has been proposed [45-46].

To carry out experimental tests on dust suppression, seeds of wormwood Zhungarskaya, Kellera, wormwood white earth and wheatgrass varieties Sharapat were used. The chemical composition of pollen and wheatgrass is given in Table 2.

Table 2

Content of basic nutrients in plants											
Plant	Season	N	P	K	Ca	N:P:K	protein	fat	sugar	fiber	ash
Wormwood Belozemel'naya	Весна	1,8 5	0,1 7	2,2 0	0,6 3		11,56	4,4 0	6,00	13,4 0	5,10
	Лето	1,5 1	0,1 2	1,3 0	0,8 0		9,14	3,4 0	6,20	23,4 0	4,70
	В сред- нем	1,6 8	0,1 4	1,7 5	0,7 1	12:1: 12	10,35	3,9 0	6,10	18,4 0	4,90
Wormwood Zhungarskaya	Весна	1,7 8	0,1 9	1,5 5	0,7 2		11,2	7,6 0	3,80	17,2 0	10,6 0
	Лето	1,4 8	0,1 5	1,3 7	0,8 5		9,25	8,5 0	3,80	22,0	10,1 0
	В сред- нем	1,6 3	0,1 7	1,4 6	0,7 8	9:1:8	10,18	8,0 5	3,80	19,6 0	1,35
Zhitnyak	Весна	1,0 5	0,1 8	1,2 0	0,1 8		6,56	2,2 0	11,2 0	23,4 0	5,40
	Лето	0,7 8	0,1 6	1,5 2	0,1 6		4,94	2,4 0	12,5 0	27,4 0	5,50
	В сред- нем	0,9 1	0,1 7	1,3 6	0,1 7	5:1:8	5,75	2,3 0	11,8 5	25,4 0	5,45

The technology for planting green mass on dusty surfaces is as follows: seeds of wild plants growing around the tailings pond, selected for testing, were soaked in 0.1; 0.2; 0.3; 0.4; 0.5; 0.6; 0.7; 0.8 and 0.9% aqueous solutions of humic preparation for 60 minutes. After the processing time of the test seeds had expired, they were removed from the working solutions and dried at a temperature of 20-40°C to an air-dry state. The treated seed material was sown in 0.5 L test beakers without drainage with the studied phytotoxic enrichment tail. The substrate humidity was maintained at 65-70% of its total moisture capacity. Exposure of the experiment - 15 days.

According to the research results, it is clear that among the tested wormwood species, the most promising for the biological reclamation of phytotoxic enrichment tailings is white earth wormwood. The effectiveness of working solutions for wormwood seeds increases in the concentration range of 0.3-0.7%, and when they increase, it noticeably decreases. Lower concentrations of the humic preparation do not have a significant effect on the sowing quality of seeds and are not effective enough in increasing the salt tolerance of plants.

Tailings samples from the surface of the tailings dump were taken from a depth of 20 cm, and similarly samples were taken from the surface and from a depth of 20 cm of adjacent natural soil. The samples were subjected to chemical and granulometric analysis. The results of the analysis are shown in Table 3.

Table 3

Results of analysis of samples from the tailings dump											
Sample name	Granulometer. composition, %			Chemical composition, %							
	0+2	- 2+10	- 10+15	SiO <sub>2</sub>	Fe <sub>2</sub> O <sub>3</sub>	Al <sub>2</sub> O <sub>3</sub>	MgO	CaO	FeO	K <sub>2</sub> O Na <sub>2</sub> O	Heavy metals
Tails from the surface	5	10	5	37,0	1,9	0,8	39,1	1,09	0,9	0,32	0,3
From a depth of 20 cm	85	10	5	40,9	5,4	1,4	41,6	1,6	2,7	0,3	0,32

As can be seen from the results given in the tables, the tailings material is represented by SiO<sub>2</sub> - 37.0-40.9%, MgO - 39.1-41.6% in the form of fine material of class O+2, accounting for 85%.

The content of ammonium, iron, calcium does not exceed 1.6-5.45%, and heavy metals (manganese, chromium, nickel, cobalt) reaches 0.3-0.32%.

Analysis of soils adjacent to the tailings dump showed that the content of heavy metals varies widely and differs from the depth of sampling (in the surface layer (5 cm) or at a depth of 20 cm). The highest level of pollution is observed on the border of the sanitary protection zone (C33) to the west of the asbestos quarry and for most pollutants their content on the soil surface exceeds the content in the soil, except for copper and vanadium, for which they are almost the same.

A high level of pollution is also observed on the soil surface at a distance of 300 m from the tailings dump, where the concentration of nickel is 5.7 times higher than the maximum permissible concentration, copper - 2.3, chromium - 2.3.

The high biotesting ability of barley for the phytotoxicity of the studied breed made it possible to determine the most promising methods for its detoxification. The greatest stimulating effect on seed germination and germination was observed in the presence of drecato in an amount from 10 to 30% of the mass of the main enrichment substrate; the results of the experiment are shown in Table 4.

Table 4  
Promising methods for detoxification of rock from the tailings dump of Kostanay Minerals OJSC

Option	Seed germination, %	Average plant height on the 17th day, cm	Signs of inhibition of plant growth and development
1. Breed + humic preparation at a dose of 5% by weight of the breed	20	1,8	Complete death in the 1st leaf phase
2. Breed + defect – 10% of the mass of the breed	44	6,8	Complete death in the 2nd leaf phase
3. Breed + defect – 20% of the mass of the breed	64	7,8	Complete death in the phase of 2-3 leaves
4. Breed + defect – 30% of the mass of the breed	80	6,3	Complete death in the phase of 2-3 leaves

As can be seen from the test results, the most promising detoxi-  
cant is defecate. Taking into account the fact that the Republic:

Kazakhstan has 8 sugar factories, and waste is generated in quite  
large quantities, and taking into account the dumps that have been  
equipped since the 1940-1950s when these factories began operating,  
we can focus on the huge quantities of this waste, estimated in mil-  
lions of tons.

The study, development and testing of agro-reclamation methods  
for pre-sowing treatment of seeds of wild plants were carried out  
through laboratory, field, stationary and production experiments.

All this indicates the need to develop a strategy for ensuring the  
environmental safety of subsoil development, increasing the efficien-  
cy of use and reproduction of georesource potential. The solution to  
this problem is facilitated by the creation of effective technologies  
for coal mining and processing.

Laboratory studies were carried out on the substrate of the tailings  
of the Zhezdinsky processing plant using seeds of plants growing in  
this region - black wormwood, wheatgrass, parsnip, alabote, etc. The  
seeds were soaked in aqueous solutions of a humic preparation with  
a concentration of 0.1÷0.9% for 60 minutes, then dried at a tempera-  
ture of 20÷40°C to an air-dry state for 2÷3 hours and sown in pre-  
pared sand in the tailings substrate. During the observation, it was  
found that among the tested plants, the most promising for the bio-  
logical reclamation of enrichment tailings are wormwood, wheat-  
grass and alabote (Table 5).

Table 5

Effect of pre-sowing treatment on seed germination

Plant variety	Seed germination, %	Average
Wormwood – control	24	3
Processed wormwood	90	4
Zhitnyak - control	16	-
Processed wheatgrass	34	14
Alabota - control	26	5
Alabbota processed	91	6

The experimental testing scheme included the following condi-  
tions: soil preparation, i.e. cultural and technical photography; seed-  
ing rate for wormwood at the rate of 4 kg/ha, for wheatgrass - 15  
kg/ha; seeding depth of wheatgrass is 2-3 cm, wormwood – without

seeding; method of sowing wormwood and wheatgrass in rows with a row spacing of 15 cm. Based on the results of laboratory studies, the consumption rate of wormwood and alabote seeds was established, which is 4 kg/ha. The observation results showed that in control plots sown with wormwood seeds not treated with the drug, germination was 18÷21%, and in experimental plots using the drug - 87%.

The drug obtained using the developed technology will be competitive in the domestic and foreign markets due to its low price, environmental friendliness, availability and effectiveness. In addition, when obtaining a humic preparation, cheap local raw materials and available reagents are used, and it is produced using standard equipment. The possibilities for export and import substitution of this drug are high, because the Republic is currently purchasing similar products abroad. Establishing production using technology, which was developed on the basis of the presented research, will not only replace analogues imported to Kazakhstan, but also export the humic preparation, since imported analogues are inferior in properties and price. The technology for its production and implementation in production is aimed at increasing the complexity of the use of Kazakhstan's raw materials [47].

And so the scientific significance of the work being carried out lies in the development of the concept of biotechnical reclamation of man-made objects using biologically active preparations-humates, ensuring the growth of plants in extreme conditions, and the applied significance is in the development of technologies for growing vegetation on man-made formations in conditions of high salinity and aridity.

Patent and licensing search conducted for the period 2018-2023. showed the prospects of the developed area, since the proposed technology will allow the reclamation of man-made formations within 2-3 years. Sowing seeds treated with physiologically active humic preparations and introducing a surface layer of man-made formations promotes the growth of herbaceous plants characteristic of a given region.

Known technologies make it possible to reclaim technogenic formations only within 4-12 years, even with the introduction of ac-

tive soil microflora into the soil surface. It should be noted that these technologies require significant capital investment.

As a biotest culture, we used barley seeds of the Arna variety, which were germinated in a thermostat in triplicate on the test substrates in accordance with the requirements of GOST (GOST 12038-66, GOST 12040-66).

The humidity of the substrates was maintained by weight in the morning and evening at a level of 90% of their lowest moisture capacity. Exposure of the experiment - 19 days.

One of the main reasons for the decrease in the amounts of HMs transferred from soil to plants is their participation in complexation reactions with HA, leading to the formation of stable chelate compounds, which are then fixed on the surface of bentonite clays due to adsorption. On the other hand, the fixation of HM ions is due to the ability of clay minerals to ion exchange due to the presence, along with a positive charge, of a large negative charge on their surface.

Since bentonite clay and soil humic acids have cation exchange centers and a total amount of large negative charge, the positively charged particles of HM ions are adsorbed more firmly and, accordingly, due to such accumulation in the soil environment, the translocation process into plants is sharply reduced.

By comparing the experimental data obtained by introducing bentonite clay and its mixture with HA into the soil system, the independence of the process of cadmium translocation into plants from the presence of HA was established. The amount of cadmium in plants was almost the same both in the presence of HA and without it, which can be explained by the absence of chemical interaction between cadmium and humic acid with the formation of complex compounds [48].

The addition of bentonite and its mixture with humic acid has a different quantitative effect on the supply of the studied elements, for lead and cadmium, where the effect is higher than for zinc. Under the same conditions, the supply of Pb to tomatoes is reduced by 78-83%, Zn by 30-45%, Cd by 80-86%; in clover, respectively, P - by 85-97%, Zn - by 23-48%, Cd - by 97-98%.

The research results indicate that bentonite clay used as an ameliorant and its mixture with HA have a great influence on the mobili-

ty of lead and cadmium than zinc, which is obviously explained by differences in the chemical properties of these elements.

Thus, the introduction of bentonite clays, as well as their mixtures with humic acids and other organic substances, into soils contaminated with lead, cadmium and zinc makes it possible to eliminate the undesirable effects of heavy metals on cultivated plants and obtain environmentally friendly products.

Experimental studies also confirmed that the most effective method for improving the hygienic quality of plant products and restoring the productive properties of soils contaminated with heavy metals adjacent to agricultural roads is clay-sorption detoxification.

The main factors regulating the behavior of heavy metals in the soil-plant system include the reaction of the environment and redox conditions, the granulometric, mineralogical and chemical composition of the mineral part of the soil, the group composition of humic substances and the biological characteristics of plants and the specifics of their cultivation.

An alternative to existing soil restoration methods. This is especially important for mountainous areas poor in vegetation, as this improves the landscape.

Vegetation reduces the spread of heavy metals due to wind erosion, stormwater runoff, and infiltration. The grown plants can be processed using conventional methods or placed in small volumes.

In this regard, the experience of foreign countries whose soil conditions and climate are similar to Kazakhstan is interesting.

Results from field studies on metal-bearing tailings from lead and zinc mines located in semi-arid and saline areas of Central Iraq showed that while the average concentrations of lead, zinc and cadmium in soils were 4431, 4920 and 37 mg/kg, respectively, the concentrations in plant samples were relatively high. Thus, *Chenopodium album* L., growing under natural conditions, accumulated lead up to 557 mg/kg in dry stems. Planted *Atriplex leucoceada* contained the highest amounts of zinc and cadmium - 3165 14 mg/kg dry stems, respectively.

The possibility of using genetic engineering to dramatically increase the amount of arsenic extracted from soil is currently being explored.

A team of US researchers has developed the first transgenic system for removing arsenic from soil by growing genetically modified plants on it. Transgenic plants extract arsenic from the soil and accumulate it in the leaves in a form that is easier to remove and destroy.

### **Conclusion**

Low-productive saline-alkaline soils of the arid zone of Kazakhstan create extremely unfavorable conditions for the growth, development and yield of cultivated plants, which is a serious obstacle to their intensive use in agricultural production.

Reclamation of such soils using classical methods, in conditions of acute shortage of irrigation water, poor natural drainage of territories, and the absence of special drainage systems, is not effective enough and is accompanied by significant difficulties arising from the progressive secondary salinization of soils and deterioration of environmental conditions. In this regard, there is a need for widespread use in plant growing of physiologically active drugs with multifunctional properties that increase the environmental resistance of cultivated plants to extreme environmental factors. The solution to this problem requires not only purely scientific interest, but also life itself, since with the transition to market relations, the growth of land productivity in the republic largely depends on the effectiveness of the agricultural technologies used. The use of agro-reclamation methods in crop production to increase the environmental resistance of plants to salinity and other unfavorable environmental factors ensures the sustainability of agricultural production and allows minimizing its dependence on natural and climatic conditions.

For the harsh soil and climatic conditions of Kazakhstan, the most promising is an environmentally friendly, physiologically active humic preparation from brown coals, enriched with macro- and microelements and wormwood extract.

The balance of the ingredient composition in this preparation in relation to the low-productive soils of the desert zone of Kazakhstan suggests its widespread use in the cultivation of agricultural crops and in other soil-climatic zones with more favorable hydrothermal conditions.

Kazakhstan has significant reserves of brown coal, which is the raw material for obtaining these materials. However, despite the



presence of large brown coal deposits in the Republic and a sufficiently developed infrastructure for the production of such products, their production has not been established. Therefore, the development and industrial implementation of technology for producing modified humic preparations from natural hydrocarbon raw materials is an urgent task, and the creation and production of such materials contributes to expanding the export potential of the Republic and import substitution. At the same time, not only economic problems are solved, but also social problems, which consist in creating additional work, developing the infrastructure of the regions, increasing the well-being of the population, etc.

The effectiveness and feasibility of investing in the proposed work is ensured by reducing dust, restoring the biological balance of the region by fixing dusty particles of man-made objects with vegetation, the formation of biota, moderating the climate of the region, reducing the morbidity of the population and budget expenses for treating the population.

### **Conclusions.**

1. As a result of research carried out in 2018, the following work was completed: a cartogram of the Kiyaktinsky coal mine was compiled, showing the spatial location of brown coal varieties suitable for obtaining humic preparations;

2. An optimal technology for producing experimental humic preparations enriched with macro- and microelements and wormwood extracts has been developed;

3. The resulting preparation was analyzed by gel chromatography and thermography, and it was found that the preparation is represented by sodium humates and consists of aromatic compounds and various functional groups;

4. The maximum effect of salt tolerance was obtained in variants with pre-sowing seed treatment, %: wheat 1.0-2.5%, barley - 0.5-3.0%, rice - 1.0-3.0%, soybean -0.005 -0.04% solution of the drug. In this case, the optimal time regimes for pre-sowing seed treatment are 30-120, 30-240, 30-120, 5-10 minutes, respectively.

5. Increases germination energy and seed germination; promotes enhanced growth of roots and above-ground parts of plants; improves the mineral nutrition of plants on irrigated soils in the arid

zone of Kazakhstan by an average of 25-30%; accelerates the ripening of grains, legumes, fodder, oilseeds, industrial, melons, fruits and berries, vegetable crops in open and protected ground, as well as potatoes for 7-12 days; reduces the nitrate content in agricultural products by 25-40% and the negative effect of pesticides applied to the soil; contribute to an increase in the size of inflorescences; increases the yield of agricultural plants by an average of 25-30%.

The article was prepared within the framework of grant funding for scientific and (or) scientific and technical projects "Technology for obtaining an adaptogen drug based on humates from coal and extracts of wild plants to create a sustainable vegetation cover on man-made objects 2022-2024 y. (AP14871298)

### *References*

1. **Stroganov B.P.** (1962). Fiziologicheskie osnovy soleustoichivosti rastenii. - M., 1962, 325 s.
- 2 **Shakhov A.A.** (1956). Soleustoichivost' rastenii.- M.; -1956.- 552 s.
3. **Borovskii V.M.** (1982). Formirovanie zasolennykh pochv i galogeokhimicheskie provintsii Kazakhstana - Alma-Ata, 1982. -S. 107-109.
4. **Boiko L.A.** (1981). Solevoi obmen rastenii.- Perm', 1981, 80 s. v5.
5. **Stroganov B.P.** (1967). Soleustoichivost' rastenii. Fiziologiya sel'skokhozyaistvennykh rastenii. Izd-vo MGU, 1967, t.3, 325 s.
6. **Boiko L.A.** (1969).Fiziologiya kornevoi sistemy rastenii v usloviyakh zasoleniya.-L., 1969.-94 s.
7. **Udovenko G.V.** (1977). Solestoichivost' kul'urnykh rastenii.- L., 1977.- 64 s.
8. **Udovenko G.V., Goncharova E.A.**(1982). Vliyanie ekstremal'nykh uslovii sredy na strukturu urozhaya sel'skokhozyaistvennykh rastenii. -L.; 1982.- 137 s.
9. **Kuznetsov M.S.** (1986). Pochvovedenie i problemy produktivnosti agrotsenozov. Problemy pochvovedeniya i agrokhimii.- M., 1986, 24 s.
10. **Egorov V.V.** Melioratsiya zemel' kak ekologicheskaya problema.(1986). Problemy pochvovedeniya i agrokhimii. M., 1986, 107 s.
11. **Mozheiko A.M.** Khimicheskaya melioratsiya sodovykh solontsov yuzhnoi chasti srednego pridnestrov'ya pri pomoshchi gipsovaniya i vneseniya khloristogo kal'tsiya.(1971). / Materialy Mezhdunarodnogo simpoziuma po melioratsii pochv sodovogo zasoleniya. Erevan, 1971, S. 381-385.

12. Kovda V.A., Minashina N.G., Penman N.L., Kanonova M.M. (1966). Vliyanie orosheniya i drenazha na zasolnyye pochvy. / Mezhdunarodnoe rukovodstvo po orosheniyu i drenazhu zasolennykh pochv. M., 1966, 148 s.
13. **Gorbunov N.I.** (1978). Minerologiya i fizicheskaya khimiya pochv. M., 1978, 150 s.
14. **Parashenko V.N.** (1978). Rost i produktivnost' risa pri sovместnom vnese-nii izvesti, azotnykh i fosfornykh udobrenii / Nauch. tr. Kubanskogo SKhI, 1978, vyp. 162 (190), -C. 41-43.
15. **Nekol'chenko L. N.** (1977). Kharakteristika i ispol'zovanie promyshlennykh otkhodov fosfogipsa i ila v sel'skom khozyaistve. / Nauch, tr. Stavropol'skogo ordena Trudovogo Krasnogo Znameni SKhI, 1977, t. 3, vyp.40, S. 21-25.
16. **Panov N.P., Aznobekov T.A., Kokurina 3.I., Folina M.N.** (1972). Opyt osvoeniya stapnykh chernozemnykh lugovo-stanykh solonchakovykh solontsov Pavlodar-skogo Priirtysh'ya. / Melioratsiya solontsov, M., 1972, S. 255-270.
17. **Piruzyan S.S.** (1971). Rezul'taty kislovaniya sodovykh solontsov-solonchakov s pred-varitel'noi i bez predvaritel'noi promyvki. / Materialy Mezhdunarodnogo simpoziuma po melioratsii pochv sodovogo zasoleniya. Erevan, 1971., S.105-108.
18. **Kharchenko A.M., Rybal'chenko E.E., Shilina R.A.** (1973). K voprosu melioratsii so-dovo-zasolennykh pochv kislovaniem v Checheno-Ingushskoi ASSR. /Sbornik nauch. tr. Yuzhn. proekt.-izysk. i NII «zhgiprovodkhoz», 1973, vyp. 14,4.2.- C. 54-59.
19. **Voinova T.N., Turdiev R.Sh.** (1976). Rezul'taty opytov po melioratsii shchelochnykh pochv sodovo-sul'fatnogo zasoleniya sul'fatom zheleza na Akdalinskom massive orosheniya. // Byul. pochv. in-ta VASKhNIL, 1976, vyp. 14, S. 33-37.
20. **Pannikov V.D, Minesv V.** (1977). Pochva, klimat, udobrenie i urozhai.- M., 1977,
21. **Nelidov S.N., Mamutov Zh.U., Mamonov A.G.** (1983). Sposoby usileniya meliori-ruyushchego deistviya solomy na shchelochnykh pochvakh pod risom. / Inf. Listok Kaz NIINTI, 1983, Mo 85, seriya 21.03, 6 s.
22. **Batyuk V.P.** (1978). Primenenie polimerov i poverkhnostno-aktivnykh veshchestv v pochvakh. M., 1978, 154 s.
23. **Gradoboev N.D., Alekseeva R.P.**(1973). Vliyanie obmennopogloshchennogo natriya na ostrukturivanie solontsov poliakrilamidom./Nauch. tr. Omskogo SKhI, 1973, t. 104, S. 31-33.
24. **Alekseeva R.P.** (1974). Puti povysheniya effektivnosti poliakrilamida na mnogo-natrievom solontse. / Nauch. tr. Omskogo SKhI, 1974, t. 125, S. 43-48.

25. **Vinogradov V.A.** (1979). Konditsionirovanie solontsovykh pochv putem primeneniya polimernykh preparatov. / Melioratsiya solontsov v usloviyakh orosheniya Nizhnego Povolzh'ya, Volgograd, 1979, S. 101-112.
26. **Mosolova A.I., Utkaeva V.F.** (1976). Primenenie polimernykh materialov dlya povysheniya fil'tratsionnoi sposobnosti pochvogrunтов. // Vest. MGU. Ser. biol., pochvovedenie, 1976, N 6, S. 109-115.
27. **Mamonov A.G., Mamutov Zh.U., Ergozhin E.E.** (1985). Primenenie rastvorimyykh poliamfolitov pri osvoenii sil'nozasolennykh solontsevatykh pochv pod risoseyanie. / Povyshenie produktivnosti pochv risovykh polei. Almata, Nauka, 1985, C. 53-70.
28. **Borovskii V.M.** (1989). Genezis i melioratsiya pochv Kazakhstana, Alma-Ata, 1989, 208 s.
29. **Orlova M.A.** (1983). Rol' zolovogo faktora v solevom rezhimme territorii. Alma-Ata, 1983, 227s.
30. **Shkol'nik M.Ya.** (1950). Znachenie mikroelementov v Zhizni rastenii i v zemledelii. M.- L., 1950, 238 s.
31. **Khristeva L. A. Reutov V.A.** i dr.(1984). Fiziologicheskii, aktivnyi preparat gumat natriya i ego primeneniye pod razlichnyye sel'skokhozyaistvennyye kul'tury s tsel'yu povysheniya ikh urozhainosti. Metodicheskie rekomendatsii. Dneprpetrovsk, 1984, 20 s.
32. **Boby' L.F.** (1982). Vliyaniye gumusovykh veshchestv na protsessy fotosinteza // Trudy Mezhdunar. Simpoz. IV i II komis. MTO. Minsk, 1982, S. 159-163.
33. **Yarchuk I.I.** (1957). Guminovyye udobreniya. / Sb. Teoriya i praktika ikh primeneniya. ch. 1-3, Izd. KhGU, 1957-1968.
34. **Khristeva L.A.** (1951). Rol' guminovykh kislot v pitanii rastenii i guminovyykhe o udobreniya. / Trudy pochvennogo instituta, M., 1951, t.38, S. 108.
35. **Roda V.V., Ryzhkov O.G.** (1994). Guminovyye preparaty iz burykh uglei mestorozhdenii Rossii. // Khim. tverd. topliva, 1994, N° 6, S.43.
36. **Avgushevich I V., Karavaev N.M.** (1969). Metod ionoobmennogo titrovaniya guminovykh kislot. // Khimiya tv. topliva, 1969, Le 2, S. 12-19.
37. **Khristeva L.A., Bulgakova M.P.** i dr. (1982). Fiziologicheskii aktivnyye veshchestva gumusovoi prirody kak faktor adaptatsii sel'skokhozyaistvennykh rastenii k gerbetsidam. / Tr. Mezhdun. simpoz. IV i II Komis. MTO. Minsk, 1982, S. 106-110.
38. **Khristeva L.A.** (1968). O prirode deistviya fiziologicheskiiaktivnykh form gumino-vykh kislot i drugikh stimulyatorov rosta rastenii. / Guminovyye udobreniya. Teoriya i praktika ikh primeneniya. Kiev, Urozhai, 1968, g.3, S. 13-27.39. A.A. Ismailova, A. T. Kanayev, N. Zhalgassuly, Magaoya Asjan, A.G. Mamonov. (2018). Известия национальной академии наук Республики Казахстан «Серия

геологии технических наук» Technology of saline land reclamation by brown coal products..-Алматы.-С.120-128., 2018.

40. **Estemesov Z.A., Kogut A.V., Ismailova A.A., Darmenkulova A.B.** (2020). Chemical and mineralogical characteristics of technogenic raw materials of mining enterprises of Kazakhstan. 20th International Scientific Multidisciplinary Conference on Earth and Planetary Sciences SGEM2020 Conference Period: Congress Center "Maritim Paradise Blue", Albenia Resort & Spa. -16 August, 2020 – 25 August, 2020

41. **Zhalgasuly N., Kogut A.V., Estemesov Z.A., Ismailova A.A., Shaltabaeva S.T.** (2021). Development of technologies for recycling and biotechnical recovery of ash slags waste. News of the NAS RK. "Geology and Engineering Science Series". ISSN 2224-5278, Volume 6, Number 450 (2021), 64-70.

42. **Nariman Zhalgasuly, Zatkali Estemesov, Kylyshbai Bissenov, Panabek Tanzharikov, Alexandr Kogut1 and Aliya Ismailova** (2021). Use of bottom ash waste of a thermal power plant for producing a construction binder. ARPN Journal of Engineering and Applied Sciences S ISSN November 2021| Vol. 16 No. 22

43. **N. Zhalgasuly, A.A. Asanov, S.V. Efremova, U.A. Bektibayev, A.A. Ismailova** (2023). The significance of modern brown coal processing technologies for the development of agricultural production and public heat power. Известия НАН РК. Геология и технические науки, ISSN 2224-5278, Volume 6 (462).- 2023, Pp. 89-100.

44. **A.A. Ismailova, A. T. Kanayev, N. Zhalgassuly, Magaoya Asjan** (2018). Studying the technology and methods of increasing the yield of cultivated plants on strongly saline soils//Ecology, nvironment and conservation. Vol. 24 (4) : 2018.- P. 1666-1670.

45. **N. Zhalassuly, A.A. Ismailova** (2019). The energy capacity of an aqueous solution of the drug-stimulator of plant growth//Reports of the National academy of Sciences of the Republic of Kazakhstan/Volume 4, Number 326 (2019). – P. 5-9

46. **Bisenov K.A., Zhalgasuly N., Tanzharykov P.A., Kogut A.V., Ismailova A.A.** (2021). Tekhnologiya pererabotki otkhodov predpriyatii Kazakhstana. Izd-vo «Tumar»-2021g. -344 s.

47. **Galits V.I., Mamonov A.G., Zhalgasuly N.** i dr.(2001). Biotekhnologicheskaya rekul'tivatsiya tekhnogennykh territorii Kazakhstana //Materialy mezhdun. Nauchno-prakt. konf. «Inzhenernaya nauka na rubezhe XXI veka». - Almaty, 2001. -S. 206-207.

48. **Zhalgasuly N., Galits V.I., Pak V.V.** i dr.(2000). Kompleksnaya pererabotka ugol'nykh mestorozhdenii Kazakhstana. TsAGS // Gornoe delo v Kazakhstane. Sostoyanie i perspektivy. - Almaty: RIO VAK RK, 2000. - S. 171-173.

## TECHNOLOGY OF DEEP OPEN-CAST MINES RECLAMATION



### Artem PAVLYCHENKO

Doctor of Technical Sciences, Professor, First Vice-  
rector, Dnipro University of Technology, Ukraine



### Andrii ADAMCHUK

Candidate of Engineering Sciences, Associate  
Professor of the Department of Surface Mining,  
Dnipro University of Technology, Ukraine



### Oleksandr SHUSTOV

Candidate of Engineering Sciences, Associate  
Professor of the Department of Surface Mining,  
Dnipro University of Technology, Ukraine

#### Abstract

The subject of the study is the surface mining the mineral  
of deep occurrence and further reclamation of disturbed land.

The purpose of the work is the scientific and practical task of the study is to justify a new technology of flooded open-cast mines reclamation, taking into account depth of mine, its flooding level and the physical and mechanical properties of rocks.

The calculations were performed in manual and automatic search mode for the most stressed sliding surface on several calculated sliding surfaces. The formula for calculating the value of the distance from the safety embankment to the axis of movement of the excavator is obtained using the cosine theorem and a number of trigonometric identities.

New technology is based on the phenomenon of when water flooding of the slope reaches the critical value at the level of 0,19 from the total height of the tier slope, there is an increase in stability and a decrease in the width of the prism of a possible landslide by increasing the influence of water retaining forces in the open pit space.

**Key words:** internal dump, single-tier dump, physical and mechanical properties of rocks, dragline excavator, safety factor.

### Introduction

Currently, one of the most important problems of the iron ore surface mining with an increasing depth of an open pit more than 500 m, due to the depletion of the capacity of existing dumps of the overburden rocks, is the formation of new external dumps [1–10]. For their construction, additional lands, which can reach 100 hectares and more, are involved in land allotments and should be located near open pits [11-20]. In the direct proximity of other mining companies and residential buildings, it is virtually impossible to obtain a permit to place a dump near an open pit that is being operated [21-26].

In the Open Pit No 2-bis of the PJSC “ArcelorMittal Kryvyi Rih” this problem was solved by storing the overburden rocks in the open pit space of the Open Pit No 1 belonging to the former mining and processing plant “Novokryvyi Rih GOK” by forming a single-tier internal dump with the excavator installed on the ground surface near the upper edge of the open pit side.

However, with the development of dumping works during the installation of the excavator on the dumped massif deformation processes began: the upper platform of the dump – the formation of cracks and fissures (Fig. 1) and there was a threat of landslide of rock mass into the mined-out space. Thus, determining the safe distance for installation of mining equipment from the upper edge of the formed single-tier dump is the relevant task.



**Fig. 1.** Scheme of forming cracks on the northern side of the Open Pit No 1 of the Mining and Processing Plant “Novokryvyi Rih GOK”(formation of terraces)

## Methodology

Calculations of the stability of the slopes of the dumps were made by algebraic summation of forces using the method of slices in Rocscience Slide software. The calculation of the width of the prism of the possible landslide ( $a$ , m) and the guaranteed landslide ( $a_1$ , m) of the formed one-tier dump relates to finding the curved sliding surface.

For this, a cross-section of a one-tier dump with the necessary parameters is constructed. The location of the square is determined, in which the centers of the radii of the curved sliding surfaces are located. Next, the program finds the safety factor on curved surfaces according to all center points and radii. After that, it is necessary to determine the distance from the crest of the dump to the farthest point of intersection of the curved surface  $SF=1.2$  and  $SF=1$  with the surface.

Taking into account the previous experience of similar calculations, the following physical and mechanical properties of the soil massif were taken: unit weight -  $20.6 \text{ kN/m}^3$ , cohesion -  $44 \text{ kPa}$ , internal friction angle -  $21^\circ$ . Rocks are dumped in a dump in the underwater part: unit weight -  $20.0 \text{ kN/m}^3$ , cohesion -  $22 \text{ kPa}$ , internal friction angle -  $18^\circ$ . We accept the angle of the natural slope of the massif of soil  $35^\circ$  (fig. 3).

For the simulation of single-tier dumps of overburden rocks, their height was taken from 100 m to 500 m with a step of 50 m, dumping height from 0 m to 40 m with a step of 50 m, the following physical and mechanical properties of the material: unit weight -  $18,83 \text{ kN/m}^3$ , cohesion -  $20 \text{ kN/m}^2$ , internal friction angle - 30 degrees (fig. 4).

The "Slide" software complex was used to compare the indicators of rock stability. The essence of the Slide software is that it builds the section of the calculated array, determines the location of the square in which the centers of radiuses of curved sliding surfaces are placed, then the program finds coefficients by the curved surfaces according to all points of centers and radiuses and points to the smallest indicator. Therefore, to determine the stability near the equipment, the operator must manually determine the coefficient there. The horizontal scale (X) corresponds to the distances between the points of slopes and sites on the respective horizons. The vertical



scale (Y) corresponds to the height position of respective horizons and surfaces of the open pit and the dump (Fig. 2).

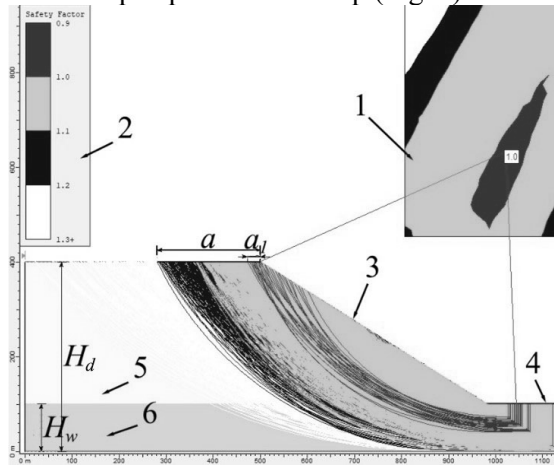


**Fig. 2** Example of calculation of parameters of the prism of a possible landslide in the Slide software. 1 - square of the centers of radiuses of the curved sliding surfaces; 2 - panel with the legend of the safety factors; 3 - slope of a single-tier dump; 4 - water surface; 5 - overburden rocks, not flooded with water; 6 - overburden rocks flooded with water;  $a$  - the width of the prism of a possible landslide, m when  $SF=1.2$ ;  $a_1$  - the width of the prism of a possible landslide, m when  $SF=1.0$ ;  $H_d$  - the height of the dump,  $H_w$  - the height of the flooded part of the dump

### Calculation of stability parameter

The results of processing the parameters obtained during the calculations of the width of the prism of the possible landslide the data charts were obtained, the functions of which are mainly polynomials of the third degree, which exist only in the first coordinate angle (fig. 3-4).

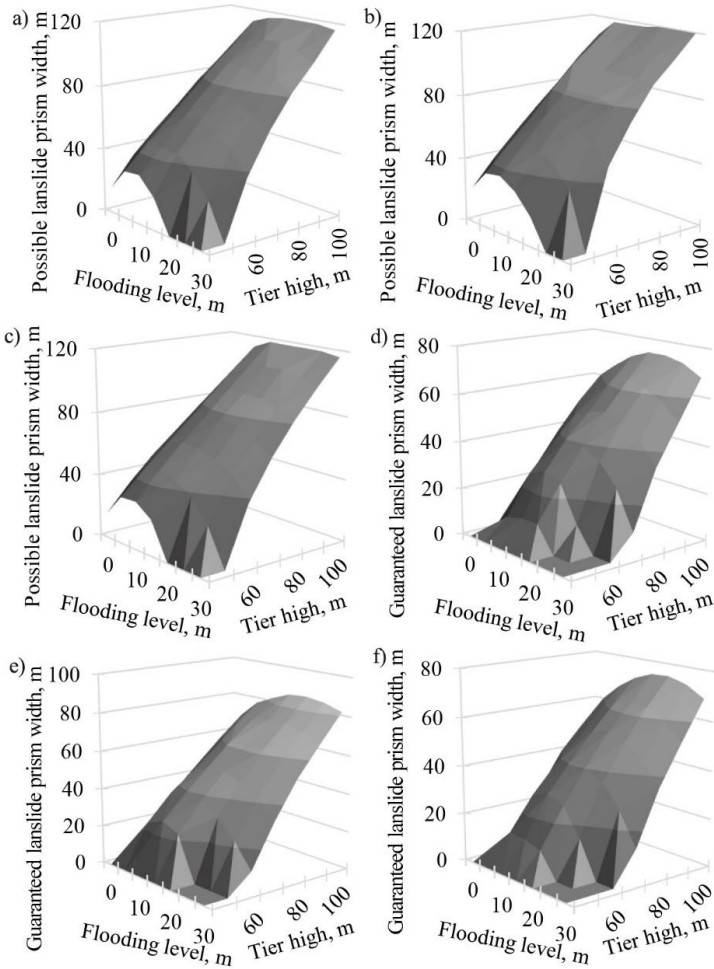


**Fig. 3.** Chart of the dependence of the width of the prism of a possible landslide ( $SF=1.2$ , *a-c*) and guaranteed ( $SF=1.0$ , *d-f*) on the height of dump tier and the thickness of the flooded part of the soil slope

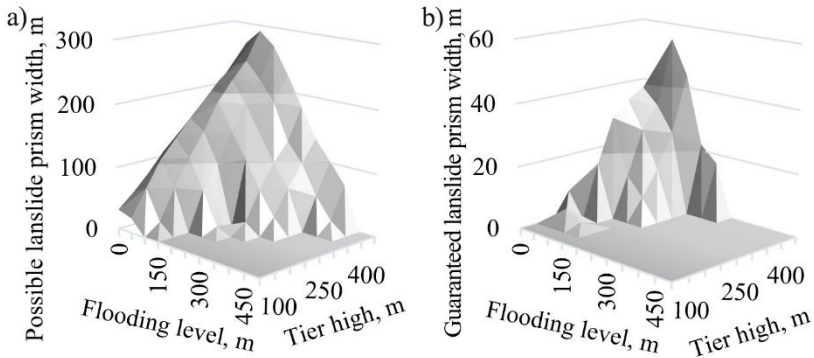


**Fig. 4.** Chart of the dependence of the width of the prism of a possible landslide ( $SF=1.2$ , a) and guaranteed ( $SF=1.0$ , b) on the height of dump tier and the thickness of the flooded part of the overburden rock slope

Analysis of fig. 3, 4 for the extremum showed that for rocks with physical and mechanical properties typical for the overburden rocks of dumps of the iron ore open pits of the Kryvbas the greatest value is the distance from the upper edge to the sliding surface for the safety factor  $SF=1.2$ , and hence the slope in the single-tier dump has the least stable state when it is flooding to  $H_w=0.19H_o$ , with an average deviation of the calculation data of parameters of the prism of a possible landslide of 2.71%, the maximal deviation - 7.24%, and the minimal deviation - 0.09%.

The chart in the fig. 4 shows that the non-flooded tier of the open pit has a parameter of the width of the prism of a possible landslide depending on the height of the tier.

Then, when it is flooded with water, the physical and mechanical properties of the tier base change, and the stability of the slope begins to decrease, and the width of the prism of a possible landslide increases.

After reaching the critical point of flooding the slope with water to  $H_w=0.19H_o$  the stability increases and the width of the prism of a possible landslide decreases due to the increased influence of the retaining forces of water weight in the internal open pit space.

The slope acquires the greatest stability at its maximal flooding by water.

### **Technology of deep open-cast mines reclamation**

During the development of mineral deposits, especially in the open method, overburden rock dumps are formed. Since the stockpiled material is loose, the dump is deformed during its construction due to compaction. The compaction of the dump occurs most intensively in the massif of the freshly poured backfill due to the filling of air cavities under the influence of the weight of the deposited rocks. Therefore, the formation of a dump is carried out with the installation of mining equipment outside the prism of possible displacement, the width of which depends on the physical and mechanical properties of the overburden rocks deposited in the dump, its height and level of flooding. The worst conditions are observed when the slope is flooded by 20–30% of its height [27]. A further increase in the level of inundation of the slope by means of natural water inflow will help to increase its stability due to the effect of the weight of water on the slope of the dump.

There is a known method of forming internal dumps in the produced space of spent deep quarries, which includes the transportation of overburden rocks from the mine to the place of formation of the dump in the produced space from the day surface of the quarry in one tier to its full depth. This method simplifies the organization of dump operations and ensures minimum costs for the transportation of overburden rocks [28].

The disadvantage of this method is that the possibility of its application is limited by the depth of the mine and the properties of the overburden rocks deposited in the intra-quarry space. If the stable height of the dump layer is equal to the depth of the mine, then it can be filled with one ledge, if it is less – not.

The closest to the proposed method is the method of internal dump formation with the formation of supporting prisms in the bottom of the dump, which includes the formation of an internal dump and the formation of an overburden by bulldozers from rocks delivered by motor vehicles, ahead of the development of the dump layer. This method makes it possible to slightly increase the stability of the backfill massif [29].

The disadvantage of this method is the need to transport overburden rocks from the day surface to the bottom of the pit by dump trucks to form a supporting prism, which increases the costs of overburden transportation and necessitates the need to drain water from

the internal pit space. In addition, the formation of a waste layer on the side of the spent quarry can partially block the transport berms, which significantly limits the application of the method.

The basis of the invention is the task of improving the method of reclamation of deep quarries, in which, by introducing new technological operations, the possibility of full use of the original conditions of the intra-pit space of spent quarries, regardless of their depth, is achieved in full in conditions of constant water inflow with the provision of a rational distance transportation of overburden rocks under stable and safe parameters of the internal dump in the continuous process of its formation and, due to this, increasing the efficiency of the technology while simplifying and reducing costs.

The task is solved by the fact that in the known method of reclamation of deep pits, which includes the formation of a waste layer by a dragline excavator in the produced space of a deep pit with natural water inflow to fill the internal pit space with overburden rocks and water when the dragline excavator is installed outside prisms of possible displacement, according to the invention, pre-determine the height of the layer of the internal dump of overburden rocks based on their physical and mechanical properties, the value of the width of the prism of possible displacement and the specified water level, form the dump layer with a dragline excavator, and when the water level of the specified mark is reached, form the next tier, adjusting the height of the dump while maintaining the specified width of the prism of a possible shift [30].

Fig. 5 shows the reclamation scheme of deep open-cast mines. In fig. *a* shows the mine in its finished contours; in fig. *b* – the beginning of the formation of the pioneer dump; in fig. *c* – the beginning of dragline operation on the formed pioneer dump; in fig. *d* – formation of the next dump tier by a dragline; in fig. *e* – the combination of two tiers with the formation of the next one; in fig. *f* – work of the dragline on the next tier; in fig. *g* – creating the possibility of forming a dump tier from the day surface; fig. *h* – the formation of a dump tier from the day surface.

The method of reclamation of deep open-cast mines is implemented as follows. The height of the layer of the internal dump of overburden rocks is pre-set based on their physical and mechanical

properties, the value of the width of the prism of possible displacement and the given water level (see fig. 3, 4).

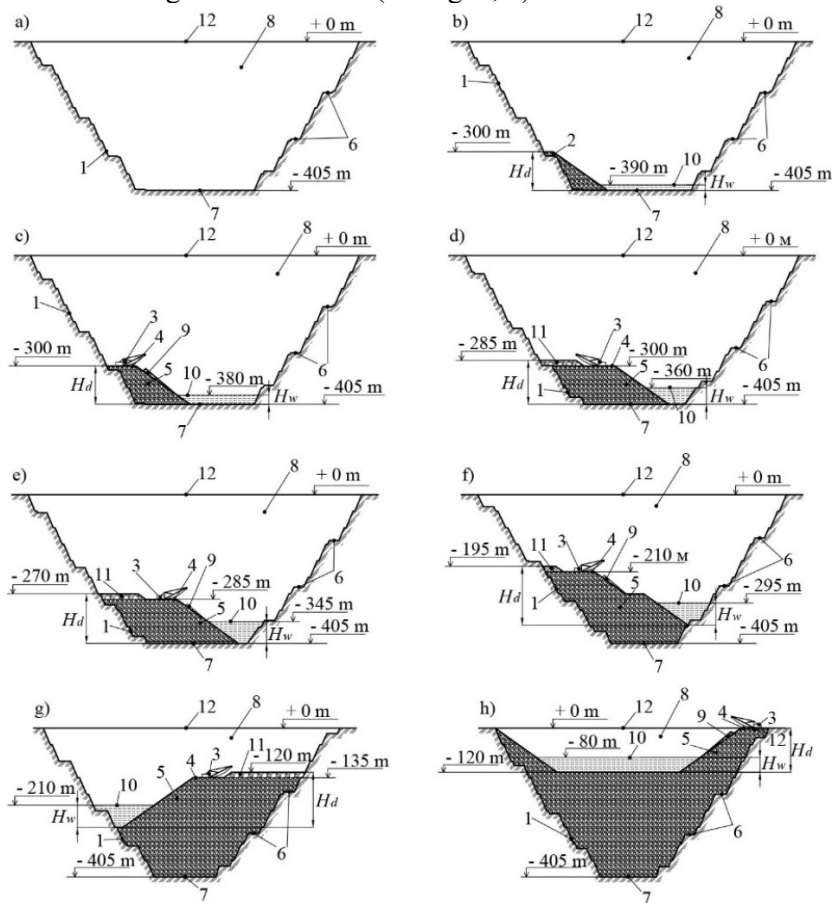


**Fig. 5.** Deep open-cast mine reclamation scheme: 1 - side of the quarry; 2 - pioneer dump; 3 - dragline excavator; 4 - prism of possible landslide; 5 - dump tier; 6 - transport berms; 7 - the bottom of the pit; 8 - developed intra-quarry; 9 - fallow back; 10 - height mark of the water level in the intra-quarry space; 11 - the next tier; 12 - surface

The value of the width of the prism of possible displacement (a, m) must meet the condition

$$a < R - (s + z), \quad (1)$$

where  $R$  - the unloading radius of the excavator-dragline, m;  $s$  - width of the safety embankment, m;  $z$  - is the distance from the axis of movement of the dragline excavator to the safety embankment, m.

The formation of a single-tier dump in the mined-out open pit space flooded with water consists of the following processes: transportation of the overburden rocks by haul trucks to the unloading site, unloading of the overburden rocks in heaps, selection of oversized pieces of rock from heaps and moving them outside the unloading of overburden rocks with bulldozer, planning of the dumped heaps into the ditch by the bulldozer, formation of the ditch by the dragline excavator, dumping of the overburden rocks planned in the ditch into the mined-out open pit space by the dragline excavator, movement of the dragline excavator.

The ditch for unloading of the overburden rocks is formed by the dragline excavator outside the prism of possible landslide with the unloading of rocks into the internal open pit space. The ditch width ( $b$ , m) must provide at least one place for unloading of the haul truck and the possibility for its maneuvers when directing for unloading. The ditch should be formed along the boundary of the prism of a possible landslide, and a utility road with a width of at least 5 m, or a technological road for passing haul trucks should be provided from the opposite site of the prism.

Overburden rocks from are transported from the open pit to the site of unloading by haul trucks. The width of the unloading site must take into account the width of the roadway, the area for maneuvers and the length of the unloading points. Upon reaching the unloading site, the rock-loaded haul truck reduces the speed to 10 km/h and, provided there is a free unloading place, begins maneuvering shunting operations with a speed of not more than 5 km/h, so as to move reverse under unloading beyond the prism of a possible landslide perpendicular to the upper edge of the ditch at a distance of at least 5 m from it to the wheel of the haul truck.

To ensure this, it is necessary to provide a safety embankment along the upper edge of the ditch having a height of at least a half of the diameter of the haul truck wheel. If there are no free places for unloading, the haul truck enters the unloading site in such a way as not to block the exit from the site to empty haul trucks. Subsequent haul trucks are outside the unloading site at a distance of 5 m from each

other. The distance between the haul trucks under loading must be at least 5 m.

Oversized pieces of the overburden rocks should not fall into the ditch, so they are selected by bulldozer and transported to the curb outside the unloading section. Selection and transportation of oversized pieces of the overburden rocks is allowed only outside the prism of possible landslide along the safety embankment.

The overburden rocks unloaded in heaps by haul trucks are transported by bulldozer to a ditch formed by a dragline excavator. The movement of the bulldozer is perpendicular to the upper edge of the dump towards the ditch. When planning the rock unloading site, the allowable distance from the upper edge of the ditch to the edge of the chains should be not less than 2 m. The surface of the rock unloading site is planned to be bulldozed at an angle of at least  $3^\circ$  from the upper edge of the ditch perpendicular to it at a distance of 10 m.

The dragline excavator must be installed on a solid level surface. The overburden rock is reloaded by the dragline excavator from the formed ditch into the mined-out space of the open pit. It is forbidden to stay in its bucket area during the operation of the dragline excavator. It is forbidden to carry the bucket over the roadway. The safe distance between mining equipment and the slopes of benches should be at least 1 m. Rock is dumped until the filling of the slope with unloading radius of the dragline excavator at its installation level.

Then the dragline excavator moves along the boundary of the prism of possible landslide, the boom herewith is installed in the direction opposite to the excavator movement, and the operations are repeated until the whole front of the slope is filled. In the event there is a threat of rock mass slide, dumping works should be stopped immediately, and the mining equipment should be moved to a safe area. To do this, a free exit for mining equipment must be provided.

To ensure the safety of the internal dump-formation in the mined-out space of the open pit, the mining equipment must be outside the prism of possible landslide, so the axis of movement of the dragline excavator must be located at such a distance from the prism of possible landslide ( $z, m$ ) which will provide an opportunity of formation of a safety embankment and construction a ditch of sufficient width by the dragline excavator (fig. 6).



Taking into account the parameters of the dragline excavator and the width of the ditch for unloading haul trucks, the distance from the axis of movement of the excavator to the safety embankment should be calculated according to the following author's formula

$$z = R_b \times \left[ \sqrt{1 - \frac{\left( R_b + R \sqrt{1 - \left( \frac{b_b}{2R_b} \right)^2} \right)^2}{\sqrt{R^2 + R_b^2 + 2RR_b \sqrt{1 - \left( \frac{b_b}{2R_b} \right)^2}}}} \right] \times \left[ \sqrt{1 - \frac{b - s - 1}{\sqrt{R^2 + R_b^2 + 2RR_b \sqrt{1 - \left( \frac{b_b}{2R_b} \right)^2}}}} \right]^2 + 1, \text{ m},$$

$$+ \frac{(b - s - 1) \left( R_b + R \sqrt{1 - \left( \frac{b_b}{2R_b} \right)^2} \right)}{R^2 + R_b^2 + 2RR_b \sqrt{1 - \left( \frac{b_b}{2R_b} \right)^2}} \quad (2)$$

where  $R$  - the digging radius of the excavator, m;  $R_b$  - the radius of rotation of the tail part of the turntable platform, m;  $b$  - the width of the ditch for upper unloading haul trucks, m;  $b_b$  - width of the body of the dragline excavator, m;  $s$  - the width of the safety embankment, m.

The width of the prism of possible landslide depends on the height of the internal dump, the level of its flooding (see fig. 3, 4), the overburden rocks that make it up, in particular, their physical and mechanical properties such as the angle of internal friction, specific gravity and adhesion, and is controlled the total height of the internal dump.

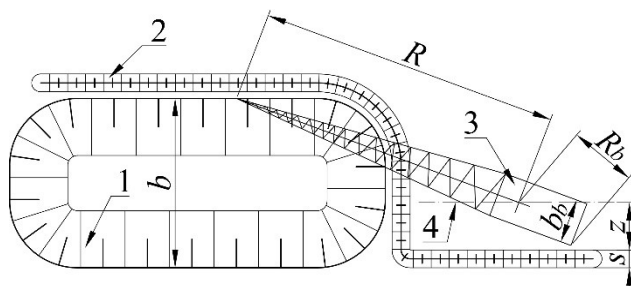


**Fig. 6.** Diagram for determining the distance from the safety embankment to the axis of movement of the excavator ( $z$ , m): 1 - the ditch for unloading haul trucks; 2 - safety embankment; 3 - dragline excavator; 4 - axis of movement of the dragline excavator.  $R$  - the digging radius of the excavator, m;  $R_b$  - the radius of rotation of the tail part of the turntable platform, m;  $b$  - the width of the ditch for upper unloading haul trucks, m;  $b_b$  - width of the body of the dragline excavator, m;  $z$  - the distance from the axis of movement of the excavator to the safety embankment, m;  $s$  - the width of the safety embankment, m

Next, the dump tier is formed by a dragline excavator by gradually increasing the height of the internal dump following the rise of the water level in the internal pit space in such a way that, based on the specified indicators, the height of the non-flooded part of the dump slope does not exceed approximately 70-110 m, according to studies [2], depending on the model of the dragline excavator and the physical and mechanical properties of the overburden rocks, and consists of the following technological operations.

First, a pioneer dump is formed on one of the sides of the mine to form a horizontal platform for setting up a dragline on it outside the prism of a possible shift with the possibility of dumping the tailing layer. The pioneer embankment is formed from overburden rocks, which are delivered to the quarry by dump trucks by transport berms and placed along them by bulldozers. The horizontal platform is separated from the prism of possible displacement by a safety embankment built outside of it. The difference between the marks of the formed site and the bottom should be equal to the height of the dump layer, at which it is possible to safely form it with the installation of a dragline outside the prism of possible displacement. The value of the width of which must meet the condition:

After the formation of the pioneer embankment, on the formed horizontal section on a firm, level base, the dragline excavator begins to form a pit for unloading dump trucks. The pit is formed outside the prism of a possible landslide with the unloading of rocks into the intra-quarry space. The rock is dumped until the dump pit is filled to the unloading radius of the dragline excavator at the level of its installation.

The width of the pit should provide at least one unloading place for the dump truck and the possibility for its maneuvers when feeding for unloading. The pit should be formed along the edge of the prism of possible displacement, and on the opposite side of it, along the pit, there should be an economic road. A safety embankment must be built between the utility road and the pit. It is forbidden to be in the area of action of its bucket during the operation of the dragline excavator.

After filling the backfill, it is necessary to move the excavator-dragline to a new position for further dumping of overburden rocks into the created space. The development of the front of dump works on one horizon of the installation of the dragline excavator is possible both parallel and fan depending on the height of the formed internal dump, the parameters of the spent pit and controlling the level of its flooding. It is prohibited to install a dragline excavator within the prism of possible displacement.

When the level of the specified mark of submergence is reached with a dragline excavator, the next tier is formed by adjusting the height of a single dump while maintaining the specified width of the prism of possible landslide in a continuous technological process.

When the front of the dump operations moves forward and with an increase in the level of submergence of the dump tier, the dragline excavator forms the next dump tier at the level of its installation on the opposite side of the slope of the first dump tier. For this, the excavator is installed outside the prism of possible displacement at a distance from the axis of movement of the dragline excavator to the safety embankment not less than

$$z = R_b + 1, \text{ m.} \quad (3)$$

Between the descent to the horizon of the installation of the dragline excavator and the next tier of the dump, space must be left for the passage of dump trucks. The height of the next layer is taken tak-

ing into account the maximum unloading height of the selected model of excavator-dragline 4, but in total with the unflooded part of the first dump layer no more than approximately 70-110 m. In addition, between the slope of the next dump layer and the safety embankment of the pit a utility road must be provided. The surface of the next tier is planned by a bulldozer with the formation of a horizontal platform for further work on it by a dragline excavator.

After reaching the difference between the water level marks in the intra-quarry space and the horizontal platform of the next dumping tier, approximately 70-110 m, and also provided that it is of sufficient size for the operation of the dragline excavator. The latter is moved to the horizontal platform of the next dump tier. At the same time, the space between the slope of the next dump layer and the slope is filled in the same way as when forming the pioneer embankment, ensuring the possibility of access for dump trucks to the new horizon of the installation of the dragline excavator.

After that, the two formed tiers are combined and form the next one. The operations are repeated in a continuous technological process until the difference in the marks of the day surface and the next dump layer approaches the value of the height of the stable dump, the formation of which is possible with the existing dragline excavator when it is installed outside the prism of possible displacement. After that, the increase in the height of the internal dump is stopped.

After filling the pit with rocks to a mark at which its difference with the surface mark approaches the value of the height of the stable dump, the excavator-dragline is installed on the surface and a pit is formed along the perimeter of the upper edge of the slope of the side of the pit with unloading into the produced intra-pit space. At the same time, all transport berms 8 in the intra-pit space are eliminated.

During this period of dump formation, it is possible to achieve the maximum productivity of stockpiling of overburden rocks, since the operation of the dragline excavator is not limited by the parameters of the backfilled pit, and the distance of transportation of overburden rocks to the pit is minimal. In addition, at this stage, it is possible to use railway transport, which can deliver overburden from distant quarries.

The formation of the internal dump in the intra-quarry space is carried out until it is filled with overburden rocks and water to the level of the day surface.

The use of the described method of reclamation of deep quarries allows:

- To place overburden rock with a depth of more than 200-300 m in the developed space with the maximum possible completeness of filling its volume;
- To achieve optimal parameters of internal dump formation from the point of view of the safety of the dragline excavator, its productivity, the distance of transportation of overburden rocks and the completeness of their filling of the spent pit;
- To apply the force of the weight of water in the intra-quarry space to the slope of the dump layer to increase its stability, instead of spending on its drainage;
- To restore lands disturbed by mining operations for agricultural or forestry purposes;
- To create a pond, the water from which can be used as technical water for various industries;
- To prevent the violation of external dumps by the area of land, the size of which is calculated according to the formula

$$S_d = \frac{100V_K}{0,6...0,7H_v} = \frac{100 \cdot 110}{0,6...0,7 \cdot 100} = 157...183 \text{ ha}, \quad (4)$$

where  $V_K$  - the volume of produced intra-pit space filled with overburden rocks, million  $m^3$ ;  $H_v$  - the height of the outer dump, m.

- To obtain the overall economic effect due to the preservation of land from disturbance, which is calculated according to the formula:

$$E = 0,0005 \left( \frac{V_K}{Q} + 1 \right) S_d c = \quad (5)$$

$$= 0,0005 \left( \frac{110}{10} + 1 \right) \cdot (157...183) \cdot (50...80) = 47,1...87,8 \text{ mln UAH},$$

where  $Q$  is the annual productivity from the storage of overburden rocks in the internal dump, million  $m^3$ /year;  $c$  – annual payments for land disturbance, thousand UAH/ha·year.

When completing the reserves of the deposit with the markings of the working zone significantly above the bottom of the pit, reduce the

distance of overburden rock transportation when forming an internal dump on the deep horizons of the pit according to the proposed method.

### **Conclusions**

1. The study of the obtained functions to the extremum revealed that the least stable position for the dumped overburden rock massif is achieved when the slope of the dumped rocks tier is flooded by 0,19 of its height.

2. It is established that when the slope of the dumped overburden rock mass is flooded with water, the physical and mechanical properties of the tier base change, and the stability of the slope begins to decrease, and the width of the prism of a possible landslide increases.

After reaching the critical point of flooding the slope with water, there is an increase in stability and a decrease in the width of the prism of a possible landslide due to the increased influence of the retaining forces of the water weight in the internal open pit space.

The slope acquires the greatest stability when it is maximally flooded by water.

3. The description of schemes of formation of a single-tier dump is given, their basic parameters are outlined and the author's formula of calculation of the distance from an axis of a dragline excavator movement to the border of a safety embankment taking into account dimensions of a dragline and the required width of a ditch for unloading haul trucks is offered.

Depending on the model of the excavator for a ditch with the width of 35-40 m, this distance is equal to 9.0-14.5 m.

4. The limits of efficiency of use of the dragline excavator for a certain height of a single-tier dump are substantiated.

Regarding the height of formation of a single-tier dump the dragline excavator can be effective, enough effective, not enough effective and ineffective.

5. By comparing the obtained dependences of the width of the prism of possible landslide on the height of the dumped overburden rock mass slope and the level of their flooding with the limits of efficiency of the dragline excavator use for a certain height of a single-tier dump, it was found that dragline excavators EK 6.5-45, EK 14-50 and EK 10-50 are effective for a tier height of 100 m regardless of the level of flooding, which is confirmed by the practice of dumping

in the mined-out space of the Open Pit No 1 of the “ArcelorMittal Kryvyi Rih”.

For the formation of a dump tier with a height of 150 m, the effective use of excavators EK 11-70 and EK 20/90 is possible when the slope is flooded with water by at least 70 m and 50 m, respectively.

6. For slopes of single-tier dumps of the overburden rocks higher than 150-200 m the dragline excavators EK 6.5-45, EK 14-50 and EK 10-50 are effective when the thickness of non-flooded part of a slope is 70-75 m, the dragline excavator EK 11-70 - 90-95 m, the dragline excavator EK 20/90 - 100-110 m.

7. The recommended height of the tier of the overburden rocks when forming it with a dragline excavator is not more than 100-150 m, which can be increased only in case of flooding the slope with water.

### *References*

1. **Adamchuk, A., & Shustov, O.** (2023). Control of dump stability lading rock on its edge. *Inżynieria Mineralna*, 1(1), 91–96. <https://doi.org/10.29227/IM-2023-01-11>

2. **Babets, Y. K., Adamchuk, A. A., Shustov, O. O., Anisimov, O. O., & Dmytruk, O. O.** (2020). Determining conditions of using draglines in single-tier internal dump formation. *Naukovyi Visnyk Natsionalnoho Hirnychoho Universytetu*, 6, 5–14. <https://doi.org/10.33271/nvngu/2020-6/005>

3. **Pavlychenko, A., Adamchuk, A., Shustov, O., & Anisimov, O.** (2020). Justification of dump parameters in conditions of high water saturation of soils. *Technology Audit and Production Reserves*, 6(3(56)), 22–26. <https://doi.org/10.15587/2706-5448.2020.218139>

4. **Dryzhenko, A. Yu., Adamchuk, A. A., Kozenko, H. V., & Nikiforova, N. A.** (2018). Sposib pidhotovky do rekultyvatsii vidroblenoho ta zatoplenoho vodoiu zalizorudnoho kar'ieru (Patent No. 117710).

5. **Dryzhenko, A.Yu., Adamchuk, A.A., Tamuia, S.A., & Telnov, V.H.** (2018). Research of inside dump parameters in worked-out area of deep opencast mines. *Collection of Research Papers of the National Mining University*, 53, 56–65.

6. **Dryzhenko, A., Shustov, O., & Adamchuk, A.** (2016). Prospects for future mining of steep iron-ore deposits in the context of Kryvbas. *Metallurgical and Mining Industry*, 10, 46–52. [http://nbuv.gov.ua/UJRN/metmi\\_2016\\_10\\_9](http://nbuv.gov.ua/UJRN/metmi_2016_10_9)

7. **Moldabayev, S., Sdvyzhkova, O., Babets, D., Kovrov, O., & Adil, T.** (2021). Numerical simulation of the open pit stability based on probabilistic approach. *Naukovyi Visnyk Natsionalnoho Hirnychoho Universytetu*, 6, 29–34. <https://doi.org/10.33271/nvngu/2021-6/029>

8. **Kovrov, O., Babiy, K., Rakishev, B., & Kuttybayev, A.** (2016). Influence of watering filled-up rock massif on geomechanical stability of the cyclic and pro-

gressive technology line. *Mining of Mineral Deposits*, 10(2), 55–63. <https://doi.org/10.15407/mining10.02.055>

9. **Kovrov, O., Kolesnyk, V., & Buchavyi, Y.** (2020). Development of the landslide risk classification for natural and man-made slopes based on soil watering and deformation extent. *Mining of Mineral Deposits*, 14(4), 105–112. <https://doi.org/10.33271/mining14.04.105>

10. **Babets, Y., Anisimov, O., Shustov, O., Komirna, V., & Melnikova, I.** (2021). Determination of economically viable option of liquidation the consequences of external dump deformation. *E3S Web of Conferences*, 280, 08014. <https://doi.org/10.1051/e3sconf/202128008014>

11. **Pysmennyi, S., Chukharev, S., Kyelgyenbai, K., Mutambo, V., & Matsui, A.** (2022). Iron ore underground mining under the internal overburden dump at the PJSC “Northern GZK.” IOP Conference Series: Earth and Environmental Science, 1049(1), 012008. <https://doi.org/10.1088/1755-1315/1049/1/012008>

12. **Pysmennyi, S., Fedko, M., Shvahaer, N., & Chukharev, S.** (2020). Mining of rich iron ore deposits of complex structure under the conditions of rock pressure development. *E3S Web of Conferences*, 201, 01022. <https://doi.org/10.1051/e3sconf/202020101022>

13. **Dryzhenko, A., Moldabayev, S., Shustov, A., Adamchuk, A., & Sarybayev, N.** (2017). Open pit mining technology of steeply dipping mineral occurrences by steeply inclined sublayers. *International Multidisciplinary Scientific GeoConference: SGEM: Surveying Geology & Mining Ecology Management*, 17(1.3), 599–605. <https://doi.org/10.5593/sgem2017/13/S03.076>

14. **Moldabayev, S. K., Sultanbekova, Z. Z., Adamchuk, A. A., Sarybaev, N. O., & Nurmanova, A. N.** (2022). Technology of an open pit refinement under limit stability of sides. *Naukovyi Visnyk Natsionalnoho Hirnychoho Universytetu*, 6, 5–10. <https://doi.org/10.33271/nvngu/2022-6/005>

15. **Moldabayev, S., Sultanbekova, Z., Adamchuk, A., & Sarybayev, N.** (2019). Method of optimizing cyclic and continuous technology complexes location during finalization of mining deep ore open pit mines. *International Multidisciplinary Scientific GeoConference Surveying Geology and Mining Ecology Management, SGEM*, 19(1.3), 407–414. <https://doi.org/10.5593/sgem2019/1.3/S03.052>

16. **Sdvyzhkova, O., Moldabayev, S., Bascetin, A., Babets, D., Kuldeyev, E., Sultanbekova, Z., Amankulov, M., & Issakov, B.** (2022). Probabilistic assessment of slope stability at ore mining with steep layers in deep open pits. *Mining of Mineral Deposits*, 16(4), 11–18. <https://doi.org/10.33271/mining16.04.011>

17. **Moldabayev, S., Rysbaiuly, B., Sultanbekova, Z., & Sarybayev, N.** (2019). Methodological approach to creation of the 3D model of an oval-shaped open pit mine. *E3S Web of Conferences*, 123, 01049. <https://doi.org/10.1051/e3sconf/201912301049>

18. **Moldabayev, S.K., Adamchuk, A.A., Toktarov, A.A., Aben, Y., & Shustov, O.O.** (2020). Approximation of the technology of efficient application of excavator-automobile complexes in the deep open mines. *Naukovyi Visnyk Natsionalnoho Hirnychoho Universytetu*, 4, 30–38. <https://doi.org/10.33271/nvngu/2020-4/030>

19. **Gorova, A., Pavlychenko, A., Kulyna, S., & Shkremetko, O.** (2012). Ecological problems of post-industrial mining areas. *Geomechanical Processes During*



Underground Mining - Proceedings of the School of Underground Mining, 35–40. <https://doi.org/10.1201/b13157-7>

20. **Gorova, A., Pavlychenko, A., & Borysovs'ka, O.** (2013). The study of ecological state of waste disposal areas of energy and mining companies. Annual Scientific-Technical Colletion - Mining of Mineral Deposits 2013, 169–171.

21. **Kovalenko, A., & Pavlychenko, A.** (2013). Analysis of ecology-social consequences of mining waste dumping. Mining of Mineral Deposits, 7(4), 405–408. <https://doi.org/10.15407/mining07.04.405>

22. **Hapich, H., Andrieiev, V., Kovalenko, V., Hrytsan, Y., & Pavlychenko, A.** (2022). Study of fragmentation impact of small riverbeds by artificial waters on the quality of water resources. Naukovyi Visnyk Natsionalnoho Hirnychoho Universytetu, 3, 185–189. <https://doi.org/10.33271/nvngu/2022-3/185>

23. **Lozhnikov, O., Sobko, B., & Pavlychenko, A.** (2023). Technological Solutions for Increasing the Efficiency of Beneficiation Processes at the Mining of Titanium-Zirconium Deposits. Inzhynieria Mineralna, 1(1). <https://doi.org/10.29227/IM-2023-01-07>

24. **Shustov, O. O., Pavlychenko, A. V., Bielov, O. P., Adamchuk, A. A., & Borysovska, O. O.** (2021). Calculation of the overburden ratio by the method of financial and mathematical averaged costs. Naukovyi Visnyk Natsionalnoho Hirnychoho Universytetu, 5, 30–36. <https://doi.org/10.33271/nvngu/2021-5/030>

25. **Pavlychenko, A., Kolosov, D., Adamchuk, A., Onyshchenko, S., & Dereviahina, N.** (2023). Regarding the issue of post-war development of mining regions and restoration of destroyed infrastructure facilities. In Key trends of integrated innovation-driven scientific and technological development of mining regions (pp. 612–644). UNIVERSITAS Publishing. <https://doi.org/doi.org/10.31713/m1226>

26. **Gorova, A., Pavlychenko, A., Borysovs'ka, O., & Krups'ka, L.** (2013). The development of methodology for assessment of environmental risk degree in mining regions. Annual Scientific-Technical Colletion – Mining of Mineral Deposits 2013, 207–209. <https://doi.org/10.1201/b16354-37>

27. **Dryzhenko, A. Yu.** (2014). Vidkryti hirnychi roboty: pidruchnyk. Natsionalnyi hirnychi universytet.

28. **Dryzhenko, A. Yu., Prosandiev, N. I., & Martynenko, V. P.** (n.d.). Sposib rekultyvatsii kar'ieru vnutrishnim vidvalnym ustupom, shcho vkluchaie yoho vidsypku (Patent No. 825771).

29. **Arsientiev, A. I., Bukin, I. Yu., & Myronenko, V. A.** (1982). Stiiikist bortiv i osushennia kar'ieriv. Nadra.

30. **Pavlychenko, A.V., Adamchuk, A.A., Anisimov, O.O., & Shustov, O.O.** (2022). Sposib rekultyvatsii hlybokykh karieriv (Patent No. 152133).

## **INCREASE OF FOREST PLANTATIONS PRODUCTIVITY IN PLACES OF ILLEGAL AMBER MINING OF WESTERN POLISSIA**



**Ihor FIZYK**

Associate Professor of the Department of ecology, environmental protection and forest technology, National University of Water and Environmental Engineering (NUWEE), Ukraine



**Vitalii ZAIETS**

Associate Professor of the Department of Mineral Deposits and Mining Engineering, National University of Water and Environmental Engineering (NUWEE), Ukraine



**Oleksandr VASYLCHUK**

Associate Professor of the Department of Mineral Deposits and Mining Engineering, National University of Water and Environmental Engineering (NUWEE), Ukraine



**Myroslava KUCHERUK**

Senior Lecturer of the Department of Mineral Deposits and Mining Engineering, National University of Water and Environmental Engineering (NUWEE), Ukraine

### **Summary**

The article reveals the problem of illegal amber mining in Ukraine, its negative impact on natural resources and increasing the productivity of forest plantations in both communal and state-owned forests. The main reasons for this phenomenon are considered: relative ease of access to amber deposits, their remoteness from populated areas, and the difficult accessibility of territories due to wetlands and dense afforestation.

The article notes the important role of forests, especially in the Polissia region, in ecosystems and emphasizes their ecological importance. It is noted that forests perform a variety of functions, such as sanitary and hygienic, water protection, rec-

reational, sanative, educational and aesthetic. The importance of forest areas for the preservation of rare species listed in the Red Book of Ukraine is noted.

The main focus is on the economic and environmental consequences of illegal amber mining. A large number of persons engaged in unauthorized mining is indicated, which leads to serious economic losses for the state and society. Emphasis is also placed on the need for reclamation of disturbed areas as a way to restore natural biotopes and improve the ecological situation.

The article calls for effective measures from the state and the public to solve the problem of illegal amber mining, in particular through the implementation of reclamation projects and increased control over the use of natural resources.

## **Introduction**

As known, amber is mined in Ukraine on lands occupied by forests, swamps, wetlands, as well as on lands of various agricultural purposes, such as hayfields, meadows, pastures, and arable land. Unauthorized extraction of amber will lead to partial or complete destruction of these natural objects and their environmental protection functions.

The vast majority of the forests of Ukrainian Polissia consist of conifers (scots pine), hardwoods, and soft-leaved trees (oak, birch, alder, aspen, ash, spruce, and linden). As a result of the photosynthesis process, 1 ha of mature forest releases oxygen and absorbs up to 8 kg of carbon dioxide (CO<sub>2</sub>) per hour. One hectare of forest can emit up to five kilograms of phytoncides and filter up to 70 tons of dust during the year [1-3].

According to their ecological significance, forests, as well as territories covered with tree and shrub vegetation, perform sanitary and hygienic, water protection, recreational, health, educational, aesthetic and other functions. A significant number of rare species listed in the Red Book of Ukraine grow in forest areas

### **The main reasons for illegal amber mining**

As of today, there are up to 300,000 citizens in Ukraine who engage in unauthorized extraction and/or sale of amber. The illegal activity of such "diggers" causes serious economic losses to the state and society, is accompanied by a worsening of the social climate, leads to the degradation of large areas of forest land, and the deterioration of the ecological situation. Since disturbed biotopes cannot be restored to their original state naturally, without human intervention, they require reclamation.

The main reasons for unauthorized extraction, processing and sale of amber in the conditions of Ukraine include the following:

- amber deposits are located relatively close to the surface and water bodies and at a considerable distance from populated areas;
- the territories are difficult to access due to characteristic wetlands and dense afforestation;
- insufficient effectiveness of legislative acts and their compliance during regulation of activities;
- high level of unemployment;
- low level of environmental awareness of the local population;
- recognition of amber as precious stones.

The state, in the form of central and local authorities, both legislative and executive, is forced to make efforts to solve the mentioned problem, but no noticeable progress has been achieved so far.

One of the areas of intervention in the situation by state bodies and the public is the practical implementation of the rehabilitation of disturbed areas. To this end, the Cabinet of Ministers adopted Resolution No. 1063 of the Cabinet of Ministers dated November 30, 2016, which approved the "Procedure for the implementation of the pilot project of reclamation of forestry lands disturbed by illegal amber mining." According to this resolution, the order of the State Forestry Agency of Ukraine No. 138 dated 21.04.2017 established the "List of forestry lands, within which there are parts disturbed due to illegal amber mining and in need of reclamation", which included 2,046 disturbed plots with a total area of 30,037.6 hectares.

### **Negative environmental consequences of illegal amber mining**

It is quite obvious that widespread methods of illegal amber mining, such as mining, underground water leaching, and water erosion in pits, have a significant negative impact on the ecological state of the development areas.

Illegal mining is uncontrolled, and this applies to both raw materials and the consequences of mining, which include the disturbance of natural areas. All parts of nature are closely related to each other as a complex system. Thus, the disturbance of the geological environment necessarily affects the neighboring environments [4-6].

"Artisan" extraction of amber from the subsoil of Polissia is carried out, as a rule, by individuals or organized groups of persons, in the absence of documents necessary for the development of deposits

or deposits of this type of minerals in accordance with current legislation. Thus, there are two main methods of amber extraction: mining and underground hydraulic leaching, which depend on geological conditions. The use of a particular approach is determined by a set of factors listed below:

- depth of amber deposits;
- the depth of groundwater and the presence of aquifers;
- the suitability of amber-containing deposits for erosion;
- amber content in amber-bearing deposits.

As a rule, amber deposits with a shallow (up to 5 m on average) occurrence in the aeration zone are mined by pits, among which there are the least floaters, as well as rich placers in water-resistant clay deposits that are not subject to hydroerosion. Deposits that lie deeper, among the permeable sediments covered by floaters, are developed by the method of underground hydraulic erosion.

Mining of amber by dredging makes, on average, about 55% of all Oligocene amber-bearing layers covered by small-scale industries. This method consists in the penetration from the day surface of vertical mine workings of various cross-sections and configurations among Quaternary and Oligocene deposits, aimed at the opening in the subsoil (partially or at full capacity) of amber-bearing horizons and at the same time mechanical extraction of lump amber from the emissions of the mining mass. The vast majority of pits are dug by hand with bayonet and scoop shovels using other tools similar in simplicity. That is why this method is a pioneer in artisanal amber mining in Ukrainian Polissia.

When using the mining method to extract amber, the grass and shrub layer of the forest is completely destroyed, and the root system of the trees is significantly damaged, and sometimes the trees are cut down and uprooted. Due to lack of soil and due to damage, the root system is not able to hold the trunk in a vertical position and the trees bend or even fall under their own weight. At the same time, neighboring plants can be damaged, the undergrowth dies. Over time, most trees die. In such areas, the main soil cover is almost completely absent. Instead, a large number of pits significantly reduces the area for the development of seeds and, therefore, young forest. Thus, the modern forest is being destroyed, and there are no conditions for its restoration.

In recent years, miners have begun to use preliminary exploration of the subsoil with the help of auger drilling wells to increase the efficiency of mining. If amber or organic-enriched siltstones and black clays are discovered during drilling, four more wells are drilled at a distance of 0.5-5.0 m around the prospecting well in order to establish the direction of the "vein" (that's what miners call productive lenses enriched in organic matter rocks with rich amber placers). In this way, the amber plume is contoured and miners can lay pits without going beyond the amber placer.

Digging of pits in the conditions of Polissia by diggers is carried out without prior storage of sod-podzolic soils of the vegetation layer. Sometimes technical means, such as small excavators or bulldozers, are involved in the digging of pits, which remove overburden, which are unproductive Quaternary deposits.

Usually, amber-bearing sandy deposits of the Oligocene contain water-pressure floats, which significantly complicate, and sometimes make it completely impossible, the passage of shafts. In connection with the floaters, the development of the productive horizon is limited to flooding, as there is a risk of the walls collapsing. As a result, miners develop mainly the upper part of the amber deposit layer, and the main volume of the productive horizon is not involved at all during the destruction of the pit.

A similar, but at the same time, different picture is observed in hydropump extraction of amber. At the same time, two types of negative consequences can be considered. The first is the creation of funnel-shaped cavities in the soil, covering it with washed material; the second - violation of the hydrogeological regime of this territory due to the influx of large volumes of water. Mechanical impact causes the soil to settle and lie under a layer of sandy-clay material. Additional moistening with technological waters increases the level of groundwater over a long period of time [7-9].

Thus, the root system of trees cannot maintain equilibrium in thin sandy soil due to the effects of these factors. In addition, the raised level of groundwater prevents the penetration of oxygen to the roots, and they die from waterlogging. When the number of dead roots reaches a critical limit, the plant dies completely. The difference of the hydropump method is only that the soil and rock are not moved

into dumps, but spread evenly over the territory by water flows, creating conditions for further self-renewal of the forest.

Underground hydraulic erosion is a set of measures aimed at extracting amber from the subsoil. This is achieved by disintegrating and destroying the productive amber layer with a pressure jet of water, after which pieces of amber are carried to the surface. This method came to Ukraine in the early 90s of the last century from neighboring Poland. Its essence consists in the vertical erosion of sandy-clay rocks by pressure water and the raising of amber together with the upward flows of the pulp.

Hydraulic pump units are used for hydraulic washing. These units consist of intake, supply and discharge parts. The source of water collection is a fire hose with a large diameter (140 mm), which is lowered into the water body. A powerful hydraulic pump based on BMW, Audi, Mercedes and Volkswagen engines and a fire hose with a diameter of 100 mm and a length of 20-300 m (from 500 to 800 m) with a reducer at the end. A rubber hose of small diameter (80 mm) with a cylindrical steel tip - fire nozzle, which has strong sharp-angled teeth at the end. This design allows you to create a water pressure with a flow rate of 800–1800 l/min at the outlet of the tip and wash away dense silty and clay rocks.

When conducting artisanal amber mining, the "test exploration" of a promising area is most often carried out not with an auger drill, but with a hydraulic pump unit itself, laying test wells along the profile or at random. The use of such a search method is popularly called "beating traffic jams". In this way, miners will immediately learn about the prospects of this or that deposit and the economic feasibility of its development based on the visually estimated output of amber.

The method of underground hydraulic erosion of amber has a number of advantages and disadvantages compared to mining. The advantages are its high productivity and efficiency in application, i.e., in the same time, you can cover an area ten times larger with hydraulic washing and, accordingly, extract more amber than with

pits. With this method, exploration and extraction of amber are combined, which saves material resources and efforts of miners.

The disadvantages of the hydro method are that it directly depends on the sources of water supply. This condition of application also determines the seasonality of hydropump extraction of amber, when there is no water in the amber-bearing areas in reservoirs, or it is scarce, in low-water periods of the year. This drawback is partially eliminated by the creation of artificial dams by diggers on watercourses, which retain and accumulate the necessary supply of water. Among the disadvantages of amber mining by the underground hydraulic erosion method, the low percentage of amber yield in relation to its natural concentration can also be attributed.

The combined mining of amber is used by diggers in the case of its extraction from the productive horizon by the method of underground hydraulic erosion at the site of previous pits dug up. Such mining takes place in those areas where the hydrogeological conditions did not allow to sufficiently develop a productive horizon by dredging, or where the area with a large amber content is poorly or incompletely excavated. In the first case, amber is extracted from the lower undisturbed part of the amber-bearing layer and the inter-pit space. In the second, mainly the inter-pit target is eroded, as well as the bottom of the pit to the bottom of the amber-bearing rocks.

Based on the analysis of the state of disturbed areas, it was established that the species similarity of the floristic composition of most forest communities after amber mining in the investigated areas is very low.

It should be noted that for the extraction of amber with pumps, deep channels were dug that drain forests on large areas, which leads to a change in the hydrological regime of the territory and a weakening of the ecological stability of forest ecosystems [10-12].

It was also found that, in most cases, the number of plant species in the disturbed areas was smaller compared to the original phytocenoses. This indicates the general destruction of phytodiversity as a result of illegal amber mining.



## Conclusions

Considerable reserves of amber are concentrated in the territory of Ukrainian Polissia. Almost 6% of the world's reserves of this mineral are concentrated in the Rivne region alone. Illegal mining of amber started due to a number of factors, the main of which were: recognition of amber as a precious stone, high level of unemployment of the local population, ineffectiveness of legislative acts regarding the regulation of this type of activity.

Illegal extraction of amber by diggers has a significant negative impact on the environment: soil degradation, destruction of forest lands, waterlogging, disturbance of the terrain. Due to the scale and nature of such impacts, even after the cessation of illegal activities, nature cannot restore itself (return to its original state) without human intervention.

That is why there is an urgent need for further reclamation of such disturbed lands by increasing forest plantations, both in communal and state-owned forests.

## References

1. **Malanchuk Ye. Z., Korniienko V.Ia., Volk P. P., Vasylchuk O. Yu., Semeniuk V. V.** Rekultyvatsiia porushenykh zemel vnaslidok nezakonnoho vydobutku burshtynu. Aktualnye nauchnye yssledovanyia v sovremennom myre // Zhurnal - Pereiaslav-Khmelnyskyi, 2018. Выр. 5(37), ch. 1 – 170 С., s.87-90.
2. **Korniienko V.Ia.** Suchasni tekhnolohii vydobutku burshtynu z rodovyshch. Visnyk NUVHP. Tekhnichni nauky: zb. nauk. prats. Vyp. 1 (65), Rivne, 2014, s. 449-457.
3. Promyslovi tekhnolohii vydobutku burshtynu. Monohrafiia. **Bulat A.F., Nadyuty V.P., Malanchuk Ye.Z. Malanchuk Z.R. Korniienko V.Ia.** Monohrafiia: – Dnipro - Rivne: IHTM-NUVHP, 2017, S. 237.
4. **Melnychuk V.H.** Burshtyn Polissia. Dovidnyk / **V.H. Melnychuk, M.V. Krynytsk4. a** – Rivne : NUVHP, 2018. – 236 s.
5. Modern geotechnical methods of management of the process of amber extraction. **Malanchuk E.Z., Malanchuk Z.R., Korniyenko V.Ya.** Monograph: "Innovative development of resource-saving technologies of mining of miner-

als" "St. Ivan Rilsky »Mining and Mining University of Geology (Sofia, Bulgaria), 2018, - 439p, 80-103 pp.

6. Physical-mechanical and technological features of amber extraction in the Rivne-Volyn region of Ukraine. **Malanchuk Z.R., Soroka V.S., Lahodniuk O.A., Marchuk M.M.** Topical scientific researches into resource-saving technologies of mineral mining and processing. Multi-authored monograph. – Sofia: Publishing House “St.Ivan Rilski”, 2020. - 6-24 pp., 446 p.

7. **Malanchuk, Z., Korniienko, V., Malanchuk, Y., Moshynskiy, V.** Analyzing vibration effect on amber buoying up velocity. E3S Web of Conferences 123, 01018 (2019). Ukrainian School of Mining Engineering - 2019. DOI: 10.1051/e3sconf/201912301018

8. **Malanchuk, Y., Korniienko, V., Moshynskiy, V., Soroka V., Khrystiuk, A., Malanchuk, Z.** Regularities of hydromechanical amber extraction from sandy deposits. Mining of mineral deposits. - 2019. DOI: 10.33271/mining13.01.049

9. **Z. Malanchuk, V. Moshynskiy, Y. Malanchuk, V. Korniienko.** Physico-Mechanical and Chemical Characteristics of Amber. Non-Traditional Technologies in the Mining Industry. Trans Tech Publications Inc. Solid State Phenomena (Volume 277), 2018, pp. 80-89 doi: <https://doi.org/10.4028/www.scientific.net/SSP.277>

10. **Malanchuk Z., Malanchuk Y., Khrystiuk A.** Mathematical Modeling Of Hydraulic Mining From Placer Deposits Of Minerals. Mining Of Mineral Deposits. Том: 10. Випуск: 2. 2016. С.: 18-24. DOI: 10.15407/mining10.02.013

11. **Malanchuk Z., Korniienko V., Malanchuk E., Khrystiuk A.** Results of experimental studies of amber extraction by hydromechanical method in Ukraine. Eastern – European Journal of Enterprise Technologies / PC «Technology Center», Kharkiv, Ukraine, Volume 3/10(81),– 2016, pp. 24-28.(SCOPUS) ISSN 1729-3774, UDC 622.232.5:622.2 DOI: 10.15587/1729-4061.2016.72404

12. **Nadutyi, V., Korniyenko, V., Malanchuk, Z., Cholyskhina, O.** Analytical presentation of the separation of dense suspensions for the extraction of amber. E3S Web of Conferences 109, 00059 (2019). Essays of Mining Science and Practice. DOI: 10.1051/e3sconf/20191090005

## **IMPACT ASSESSMENT OF THE JEBEL ALI POWER AND DESALINATION PLANT ON THE ENVIRONMENT**



**Jerom DANKERS**

BSc., Innovation Sciences at the University of Technology in Eindhoven, Netherlands; AGH University of Science & Technology in Krakow, Poland



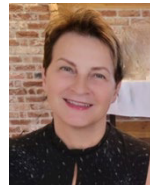
**Jiaqi LU**

BSc., China University of Mining and Technology; AGH University of Science & Technology in Krakow, Poland



**Sebastian ROTHER**

BSc. Graduate Student in mechanical engineering at the Ruhr-University-Bochum, currently on an exchange to the Faculty of Energy and Fuels of the AGH University of Science & Technology, Poland



**Wiktoria SOBCZYK**

Professor, DSc, PhD, Eng, Faculty of Energy and Fuels, AGH University of Science & Technology, Poland

### **Abstract**

The research aim of the article is to assess the impact of a large industrial facility on the environment: Jebel Ali Power Plant and Desalination Plant located in the United Arab Emirates.

We use AHP and Leopold Matrix principles and techniques to assess the impact of power plants on the environment. The combination of the two methods AHP and Leopold's Matrix ensures that decision-makers make informed choices towards sustainable solutions.

The analysis shows that the Jebel Ali power plant and desalination plant have little negative impact on the environment. Nevertheless, noticeable impacts on the hydrosphere and atmosphere were observed. The burning of fossil fuels has a direct impact on the atmosphere by emitting harmful substances. Desalination of salt water and returning by-products to the sea also has a direct negative impact on the hydro-

sphere. The combination of both factors also affects the biosphere. The power plant is of great importance in solving the problem of water shortages in the region. The problem is solved by combining power generation and water desalination.

**Keywords:** risk assessment, AHP Method, Leopold Matrix, Energetics

### Introduction

The Jebel Ali Power and Desalination Plant (Fig. 1, 2) has an installed capacity of 8.6 gigawatts. In 2021, the Complex was confirmed by Guinness World Records as the Largest Single-site Natural Gas Power Generation Facility in the World. The Complex has a power generation capacity of 9,547MW. And it can desalinate 2.228 million m<sup>3</sup> of seawater per day which corresponds to 490 million imperial gallons [1].

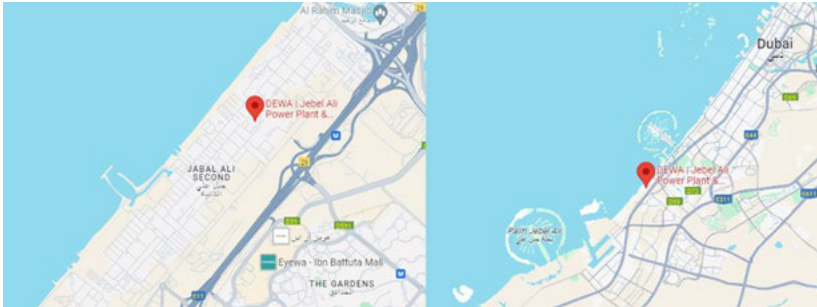


**Fig. 1.** Location Jebel Ali Power and Desalination Plant (zoomed-in, and out) [2, 3]



**Fig. 2.** Jebel Ali Power and Desalination Plant [3]

Desalination is becoming increasingly necessary due to drinking water scarcity, but the practice requires electricity, created by power plants that need large amounts of water. There is a mutual benefit for both in combining these two processes together. It's the ideal fit.

The power and desalination plant is located about 40 km southwest of Dubai in the United Arab Emirates. It is right next to the sea, and has direct access to the sea water. Which is necessary for their processes.

### **The power production process**

The primary fuel being used to power the plant is natural gas. In case of shortage of natural gas, the plant can also run on diesel. Electricity is generated through a gas turbine and a steam turbine. First, air is compressed by multi-stage blades, and the compressed air is mixed with natural gas fuel, which is then ignited to produce high temperature and high-pressure gas. The gas pushes the impeller to rotate, and the rotating shaft of the gas turbine is connected to a generator, which outputs power directly from the rotating shaft to the generator to produce electricity.

When the flue gases leave the gas turbine, there is still residual heat that can be utilised. In a heat recovery steam generator, high temperature flue gases heat water in a heat exchanger into water vapour, and the steam flows through a steam turbine. The steam turbine is also connected to a generator, which produces more electricity. The steam turbine is powered entirely by the high temperature flue gas from the tail end of the gas turbine.

### **The desalination processes**

Hot steam can be used to desalinate seawater, in addition to being used to generate further electricity. The main principle of distillation is the removal of salt from water by boiling it.

All distillation apparatus contain hot pipes into which hot steam is fed. Unheated seawater is then sprayed onto the surface of the hot pipes from the top and the seawater cools the hot steam. The hot steam condenses into fresh water inside the pipes and exits at the bottom of the pipes, while the steam from the heated seawater is transferred to the pipes in the next distillation section. The desalinated water is collected from the hot pipes within the distillation section, while the concentrated brine, exits through the bottom of the

still (Fig. 3). The vapour from the last section is reintroduced to the first distillation unit through a hot compressor [4].

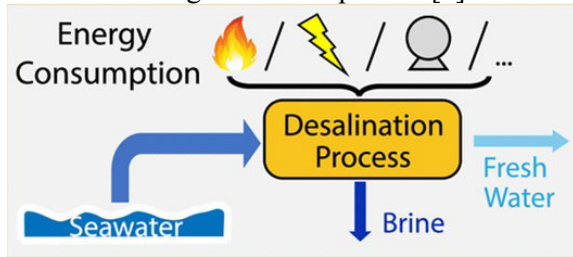


Fig. 3. Desalination process [1]

### The research methods

To evaluate and analyse the environmental impact of the subject power station we apply the AHP and Leopold Matrix principles and techniques. The AHP acronym stands for Analytic Hierarchy Process and is a multi-criteria decision making method. It translates the value of the impacts into measurable numeric relations. The main characteristic of the method is the use of pairwise comparisons; in our case we compare the impact on different elements of the environment one by one, pair by pair, in order to create a hierarchy showing the importance of the impact on different elements (biosphere, atmosphere, lithosphere...), giving a reasonable explanation to every comparison [5, 6, 7]. The valuations obtained were presented in the form of local weights (importance). The weight with a value close to zero means a small amount of impact. The weight close to 1 indicates a strong impact of the project on a given item. The sum of weights at each level is 1 (100%).

Each number represents a vector corresponding to the priority percentage of every element in the overall scheme: the higher the value of the vector the more important the item is [5].

The Leopold matrix is a framework method that enables us to do the environmental risk assessment of a project, on the basis of criteria related to significance, probability, and duration of the impact. Similarly to the AHP, it belongs to the multi-criteria decision making methodology. It consists of a two-dimensional matrix where individual actions are assessed in relation to the actual environmental features and conditions that could be affected by the project's operations. In this method we use the weights obtained in the AHP as a

reference in order to assess the actions that accompany the power station activities and affect each element, so that we are able to create a specific hierarchy of elements affected and specify actions taking place within the scope of the the subject power station of the study [5, 6].

**The course of the research**

To assess the environmental impact of the Jebel Ali Power and Desalination Plant in the UAE, we use AHP to prioritize factors like air and water quality, land impact, and ecosystem health. Then, the Leopold Matrix can be applied to evaluate the impact of each option on these factors. Combining these methods provides a straightforward and structured approach to understand and compare the environmental consequences of different alternatives for the Jebel Ali project.

In the case of the Jebel Ali Power and Desalination Plant, this method was also used to determine which attributes (lithosphere, hydrosphere, atmosphere, anthroposphere, biosphere and landscape aesthetics) are impacted the most by this power plant. The scores were given based upon the findings and information retrieved from the aerial images of the plant.

The consistency index (C.I.) of the assessment was 0.09, and therefore the results are sufficient and reliable. Filling in the AHP matrix resulted in weight scores for each element. In Table 1 the calculated weight score can be seen. The hydrosphere and atmosphere have the highest weight factor, whereas the lithosphere has the lowest weight factor. The results are as follows: lithosphere 0.03; hydrosphere 0.33; atmosphere 0.33; anthroposphere 0.07; biosphere 0.10; landscape aesthetics 0,15.

Table 1

Weight factors resulting from the AHP analysis	
Element	Weight
lithosphere	0,03
hydrosphere	0,33
atmosphere	0,33
anthroposphere	0,07
biosphere	0,10
landscape aesthetics	0,15

For each environmental element a score for each potential output factor of the plant is given. Ranging from 0 (no impact) to 5 (very strong impact). The given score is then multiplied by the corresponding importance factor, and results in a score.

The sum of these scores is then calculated per output factor, but also per environmental element.

In Table 2 importance per environmental element, ordered from highest to low-est sum the Leopold matrix can be seen.

Table 2

Importance per environmental element, ordered from highest to lowest sum

Rank	Environmental Elements	Importance	Sum
1	Hydrosphere	0.33	2.95
2	Atmosphere	0.33	1.97
3	Biosphere	0.10	1.43
4	Landscape aesthetics	0.15	1.04
5	Anthroposphere	0.07	0.87
6	Lithosphere	0.03	0.29
	<i>Sum</i>	<i>1.00</i>	<i>8.56</i>

## Results and Discussion

If we examine the results, we can look at two different things. Firstly, all the contributing factors from the plant (including water in the manufacturing process, infrastructure of the Power Plant, occupation of surface, unpleasant odors, vibration, and noise). We determined that the water in the manufacturing process impacts all the environmental elements the most (score of 3.27), whilst the infrastructure of the Power Plant also has a noticeable impact on the environmental elements (score of 2.95). This makes sense because the plant produces a lot of fresh water whilst using sea water. This has an impact on the sea water because some of the by-products of the process are being released back into the sea. The occupation of surface (score of 1.3) is significant due to it being large and close to a big city, and therefore also has impact. The impact of odors (score of 0.49), vibration (score of 0.32) and noise (score of 0.32) were deemed to be insignificant and were therefore given a lower score.

The impact score per factor from the plant can be seen in Fig. 4 (ordered by value from high to low).



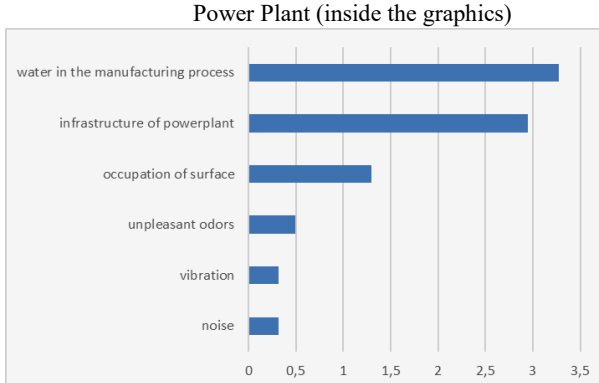


**Fig. 4.** Impact score per factor as derived from the Leopold matrix

The second thing we can examine is the sum of all impacting factors on the environmental elements. This was done by using the data from Table 2. In this table, we can see that the hydro- and atmosphere are impacted the most by the plant. In Fig. 5 an overview is provided. Due to the processes of the plant, it makes sense that the hydro-(score of 2.95) and atmosphere (score of 1.97) are impacted. The burning of fossil fuels has a direct impact on the atmosphere, and the desalination of salt water, whilst returning the by-product back to the sea also has an immediate impact on the hydrosphere. The combination of these both also has an impact on the biosphere (score of 1.43), and this impact is thereby also noticeable in the figure. The lithosphere (score of 0.29), anthroposphere (score of 0.87) and landscape aesthetics (1.04) are seemingly less impacted by the plant.

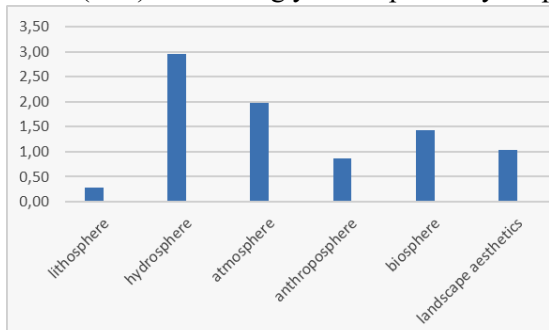


**Fig. 5.** Sum of impact per and on environmental element, derived from the Leopold matrix

And lastly a wind-rose can be used to visualize the differences in the average given score (ranging between 0, and 5) for each of the factors, as an impact on each of the environmental elements. This wind-rose can be seen in Fig. 6. On average, the biggest impact was on the biosphere (2.5 out of 5). The score of the impact on the anthroposphere was on average (2.17). The average score of the impact on the landscape aesthetics (1.17), lithosphere (1.5), hydrosphere (1.5), and atmosphere (1) are significantly lower than the average score of the impact on the bio- and anthroposphere.

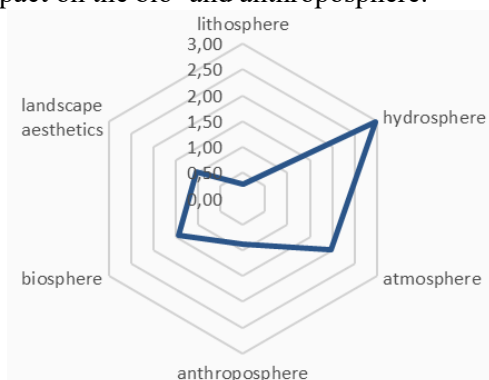


**Fig. 6.** Average given score (between 0, and 5) per factor, of the impact of the Power Plant on each environmental element

## Conclusions

In evaluating the environmental impact of the Jebel Ali Power and Desalination Plant using the AHP and the Leopold Matrix, several key insights came to light. The plant, recognized by Guinness World Records for its scale, plays a vital role in addressing water scarcity through the symbiotic coupling of power generation and desalination [8].

The AHP method facilitated a comprehensive assessment of environmental factors, assigning weights to elements such as lithosphere, hydrosphere, atmosphere, anthroposphere, biosphere, and landscape aesthetics. This structured analysis provided a nuanced understand-

ing of the relative importance of each element, with hydrosphere and atmosphere standing out as the most critical factors.

The Leopold Matrix, employing weights derived from AHP, delved into the plant's impact on specific environmental elements. The results underscored the significant influence on hydrosphere and atmosphere, aligning with expectations given the plant's desalination and power generation processes. Notably, water in the manufacturing process emerged as a primary contributor to environmental impact, emphasizing the interconnectedness of desalination and power production.

Considering factors such as infrastructure, occupation of surface, odors, vibration, and noise, the study revealed that water in the manufacturing process and infrastructure had the most substantial impact, while other factors were deemed relatively insignificant.

In summary, the Jebel Ali Power and Desalination Plant, while essential for addressing water scarcity challenges, imposes notable environmental effects, particularly on the hydrosphere and atmosphere. The integration of AHP and the Leopold Matrix provides a comprehensive framework for decision-makers to weigh the trade-offs and make informed choices toward sustainable energy and water solutions in the UAE.

W Sobczyk <https://orcid.org/0000-0003-2082-9644>

#### **Author Contributions:**

J. Dankers, J. Lu, S. Rother and W. Sobczyk authored the project and designed the study; J. Dankers, J. Lu, S. Rother contributed to the study design and discussed the data; J. Dankers, J. Lu, S. Rother and W. Sobczyk revised the data; J. Dankers, J. Lu, S. Rother and W. Sobczyk wrote the original draft of the paper; all authors contributed to the manuscript final form and approved the version to be submitted.

#### **Conflict of interest statement**

The authors declare no conflict of interest.

## References

1 **Wang L, Violet C, DuChanois RM and Elimelech M** 2020 Derivation of the Theoretical Minimum Energy of Separation of Desalination Processes. *J. of Chem. Education*, 4361-4369. <https://doi.org/10.1021/acs.jchemed.0c01194> (accessed on 6 Dec. 2023)

2 **Jebel Ali Power and Desalination Complex enhances generation efficiency and meets energy and water demand in Dubai.** Dubai Electricity & Water Authority. Dewa 2021, July 05. <https://www.dewa.gov.ae/en/about-us/media-publications/latest-news/2021/07/jebel-ali-power-and-desalination-complex> (accessed on 6 Dec. 2023)

3 **Google Maps.** <https://www.google.com/maps/place/DEWA+%7C+Jebel+Ali+Power+Plant+%26+Desalina-tion+Complex/@25.1549994,55.1735049,10.3z/data=!4m6!3m5!1s0x3e5f136a49da4399:0x964a121590d2d97!8m2!3d25.0591371!4d55.1182718!16s%2Fg%2F1210rxqm?hl=nl&entry=ttu> (accessed on 6 Dec. 2023)

4 **Jebel Ali Power Plant and Desalination Plant.** [https://en.wikipedia.org/wiki/List\\_of\\_largest\\_power\\_stations](https://en.wikipedia.org/wiki/List_of_largest_power_stations) (accessed on 6 Dec. 2023)

5 **Saaty TL** 2001 *The Analytic Network Process, Fundamentals of Decision Making and Priority Theory*, second ed. RWS Publications, Pittsburgh

6 **Saaty TL** 2004 *Decision making the analytic hierarchy and network processes (AHP/ANP)* *J. Syst. Sci. Syst. Eng.* 13 1

7 **Sobczyk W, Sobczyk EJ and Kowalska A** 2014 The use of AHP multi-criteria method and Leopold matrix to assess the impact of gravel and sand pits on the environment of the Jasiolka Valley. *Mineral Res. Manag.* 30 (2), 157-172

8 **Wang Q and Zhan I** 2019 *Science of The Total Environment* 692 529-545.

## UTILIZATION OF OVERBURDEN QUATERNARY ROCKS TO CREATE SOIL CUSHIONS FOR STRUCTURES



**Yuriy VYNNYKOV**

DSc, Professor, Head of the Department of Drilling and Geology, National University “Yuri Kondratyuk Poltava Polytechnic”, Ukraine



**Maksym KHARCHENKO**

PhD, Associated professor, Associate Professor of the Department of Drilling and Geology, National University “Yuri Kondratyuk Poltava Polytechnic”, Ukraine



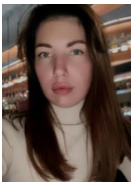
**Oleksandr MATYASH**

PhD, Associated professor, Associate Professor of the Department of Drilling and Geology, National University “Yuri Kondratyuk Poltava Polytechnic” Ukraine,



**Maryna VOVK**

Senior Lecturer of the Department of Drilling and Geology, National University «Yuri Kondratyuk Poltava Polytechnic», Ukraine



**Marina RYBALKO**

PhD, Assistant of the Department of Drilling and Geology, National University “Yuri Kondratyuk Poltava Polytechnic”, Ukraine

### **Abstract**

The article presents data on scientific and technical support of the construction of an embankment with an area of 1.9 million m<sup>2</sup> and a thickness of 4-6 m for the facilities of an electrometallurgical plant in the city of Horishni Plavni, Poltava region of Ukraine. The paper presents the results of comprehensive laboratory and

field studies of physical and mechanical parameters of compacted overburden of low-cohesion rocks, mainly sands, and their mixtures, and determines the influence of technological factors on the variation of these values. These rocks were formed as a result of the construction of quarries at the Yeristovo and Lavrykivka iron quartzite deposits. Practical possibilities of utilization of overburdened Quaternary low-cohesive rocks and their mixtures as a material for soil cushions of structures have been proved. Optimal methods of compaction of low-cohesive rocks using the vibration mode of rollers have been developed. The influence of technological parameters of compaction on the scatter of random variables of physical and mechanical characteristics of the soil cushion material was also determined. A certain inconsistency of the normative approach to quality control of compaction of overburden of low-cohesive rocks (standard laboratory test of Proctor) during the construction of pillows by modern mechanisms was established. The correct laws of distribution for random values of physical and mechanical properties of compacted low-cohesion overburden of quarries as a material of artificial foundations of structures have been substantiated by the tested methods of mathematical statistics.

**Keywords:** iron quartzite deposit, quarry, overburdened Quaternary low-cohesion rock, compaction, soil cushion, dispersion analysis.

## **Introduction**

Geotechnical engineers are forced to use flooded areas and sites composed of weak soils for modern facilities for various purposes [1]. Under these difficult conditions, artificial massifs with better geotechnical properties are a reliable and economical solution [2-4]. These design and technological solutions are enshrined in building codes [5].

In particular, the world geotechnical practice has already accumulated a very significant positive experience in the construction of geomasses by compacting soils and their mixtures. For example: artificial islands on the shelf territories, including international airports (Kansai, Chubu, Makao airports, Palm Island, World, Perl-Qatar, etc.) [6-8]; dams (Orovill, Serr-Ponson, etc. ) and dams [9]; port hydraulic structures; embankments of transport facilities [10, 11]; soil (sand) pillows, in particular for oil storage facilities [12, 13], and other critical structures [14, 15]; embankments for planning large areas [16-18], etc.

On the other hand, there is an urgent environmental and economic problem of utilization of mining and processing industry waste, including overburden generated by quarrying [18-20].

That's, it makes sense to assess the possibility of using overburden and their mixtures as geomass materials to reduce the cost of soil cushions.

### **1. Purpose and objectives of the study**

The aim of the work is to prove the practical possibility of utilizing overburdened Quaternary low-cohesion rocks and their mixtures as a material for ground cushions of structures. For this purpose, in particular, the following tasks were set:

- to substantiate the optimal method of compaction of overburden of low-cohesive rocks and their mixtures using the vibratory mode of rollers. To evaluate the influence of technological parameters of compaction on the spread of random variables of physical and mechanical characteristics of these rocks;

- to conduct comprehensive laboratory and field studies of the physical and mechanical properties of compacted overburden of low-cohesion rocks and experimentally obtain statistical data on the spread of these characteristics;

- to verify the compliance of the regulatory approach to quality control of overburden compaction of low-cohesion rocks during the construction of pillows with modern mechanisms. To study the influence of technological parameters on soil characteristics.

### **2. Methods of research of overburden compaction**

The experiment was conducted at a site for an electrometallurgical plant near the town of Horishni Plavni in Poltava Region. Alluvial sandy loam, loam, and sand lie on its surface, and the thickness of weak soils in some places reaches 2.5 meters. The area is flooded.

Therefore, the project for the preparation of the 1.9 million m<sup>2</sup> area included the removal of the soil and vegetation layer and the construction of a 4-5 m thick sand cushion by layer-by-layer compaction with self-propelled vibratory cam rollers or smooth and trailed pneumatic rollers. To strengthen the foundation for the embankment, the waterlogged and flooded massif was cut through with drainage trenches with a cross section of 1×1.5 m with a step of 3 m, which were filled with granite rubble.

The material for the artificial massif was Quaternary sands, which are overburden from the Yeristovo and Lavrykovo iron quartzite quarries. The rocks were delivered to the site by dump

trucks, leveled by bulldozers or graders, brought to optimum moisture content, and rolled.

The area for the embankment was divided into 58 borrow pits with an area of 16,000-20,000 m<sup>2</sup>. Due to the weak subsoil, the first layer of the cushion was compacted with pneumatic rollers. Its thickness ranged from 0.4 to 0.8 meters. Subsequent layers with a thickness of 0.3-0.6 m were compacted mainly with self-propelled rollers in a vibratory mode of operation, but in some grips - in a static mode.

Five grippers were made of a mixture of low-cohesion overburden and plastic sandy loam. The mixing of different types of rocks was performed as follows. Overburden (70-85% of the total mass) was delivered to the site. Next, sandy loam was added from the dumps formed during the drainage trenches. This mixture was then evenly leveled and mixed over the area of the bulldozer or grader.

The overburden compaction technology was tested in the field. It was found that low-cohesive overburden, when compacted in the vibration mode, reaches the design density of the soil skeleton faster if the work is performed in the following sequence. After the material of each layer was delivered and leveled, the first two passes with a roller were performed in a vibratory mode with oscillations of low frequency and amplitude. As a result, the rock particles take on a more compact position, and the massif becomes more homogeneous in density.

Compaction should be performed at the lowest possible speed of the roller (2-3 km/h). The next 2-3 passes in one trace were performed in a vibrating mode with a higher frequency and amplitude. At this stage, the soil is already dense enough for the equipment to move on it. Then, the rock was allowed to cool to the optimum moisture content and a technological break was scheduled for 2-3 hours so that the moisture was evenly distributed throughout the entire layer. After that, compaction was performed in both vibration and static mode.

To assess the physical and mechanical characteristics of the rocks and the optimal conditions for their compaction, comprehensive laboratory and field studies were carried out. Thus, the first stage included: sampling in quarries; determination in the laboratory of the



optimal parameters of their compaction according to the standard Proctor test in a stationary dynamic compaction device (optimal moisture content at different shock impulses, maximum density of the rock skeleton and values of mechanical characteristics when its design degree of compaction is reached).

The second stage included: controlling the type of rock delivered to the site; fixing the type of roller; the roller's operating mode; the number of passes in one trace; and measuring the thickness of the layers on the grippers before and after compaction. In accordance with the optimal parameters obtained, the material was compacted at the test sites.

After that, the geotechnical quality control of compaction was carried out, followed by standard laboratory determination of physical and mechanical parameters of rocks. In particular, during the quality control of the embankment compaction, rock samples were taken in rings with a cross-sectional area of 40 cm<sup>2</sup> and a volume of 140 cm<sup>3</sup> from the surface or pits. The number of samples depended on the compaction area and amounted to 12-30 for each layer of the gripper.

As a result, sufficient samples of random variables (RV) of rock characteristics and technological parameters were obtained. Their size was for: moisture content  $w$  and rock skeleton density  $\rho_d$ –3000; internal friction angle  $\varphi$  and specific cohesion  $c$ –50; strain modulus  $E$ –1500; number of measurements of passes along one roller track – 20, number of measurements of layer thickness  $h$ –50, etc.

After screening out the so-called "outliers", the statistical series was analyzed, the correct law of distribution of random variables was selected, and its parameters were determined. The coefficient of their variation was taken as the criterion for the variability of geotechnical properties of bedrock.

### **3. Results of overburden compaction studies**

From the analysis of the results of field and laboratory studies with a sample size of up to 3000 random variables, the following statistical data were obtained: variability of the values of the characteristics of compacted overburden and their mixtures from the variability of technological parameters of cushioning. This allowed us to make certain generalizations.

It makes sense to use waste generated as a result of open-pit mining in the mining and processing industry, in particular, overburden of low-cohesion rocks (sands and sandy loams), as a material for geotechnical massifs.

Field and laboratory studies have shown that in most cases, the actual value of the rock compaction coefficient  $k_s > 1$ . That is, the "standard" laboratory Proctor test does not provide a value for the maximum rock skeletal density and optimal moisture content. More accurate data was obtained using a modified Proctor test. The optimal compaction parameters for specific rocks (mixtures) and mechanisms should be determined by shock pulses that are close to the technical parameters of the seals.

Rock compaction performance significantly depends on the proximity of its moisture content to its optimum value, the thickness of the filled layer, the number of roller passes and its mode, which should be determined for each type of seal by full-scale experimental compaction. When arranging the leveling layer of cushions, it is not advisable to use the vibration mode at high groundwater levels.

The vibration mode allows to compact low-cohesive rocks in layers of 40-60 cm thick to the standard values: the first two passes should be performed with a low frequency and amplitude of oscillations at the lowest possible speed, and for subsequent passes, the frequency and amplitude should be increased.

With a decrease in the coefficients of variation of the thickness of the cushion layer and the moisture content of the rock in it, the variability of its skeletal density decreases. The most significant influence on this indicator is the type of rock and the content of impurities in it.

Therefore, statistical samples should be formed taking into account both the parameters of the mechanisms and the particle size distribution of the rock and the content of impurities in it.

The construction properties of the compacted soil mixture are not worse than those of homogeneous compacted rocks. There was an increase in the scatter of their values, and random values of the rock skeleton density of a poorly mixed mixture are characterized by the bimodality of the experimental graph of their distribution.

The technological mixing of different types of rocks and the vibration mode significantly affect the specific cohesion of compacted rocks and slightly affect their angle of internal friction; the value of

the deformation modulus of the compacted material depends on the density of the rock skeleton and the pressure interval in compression tests.

For the analytical description of the experimental distribution of random values of the physical characteristics of compacted overburden, it is advisable to use the normal distribution law. For the density of the soil skeleton of compacted mixtures, it is a polynomial exponential law. At the same time, the coefficient of variation of the soil skeleton density ranged from 2-4.4%, its moisture content from 23-36%, and the specific gravity of the rock from 4-4.6%.

The modulus of deformation of compacted rocks and their mixtures is best described by a logarithmic normal distribution law. The coefficient of variation of the deformation modulus is 33-57%.

The angle of internal friction  $\varphi$  and the specific cohesion  $c$  of compacted rocks and their mixtures are random vectors and are best described by a normal and logarithmically normal distribution law, respectively. The coefficient of variation of the internal friction angle was 11%, and the specific adhesion was 25%.

The distribution of random values of the specific resistance to penetration of compacted soil is best approximated by an exponential distribution law. The coefficient of variation of the values of the specific penetration resistance was 57%.

The horizontal strength of compacted overburden within the pillow is greater than the vertical strength. Thus, artificial geomasses are characterized by the above anisotropy of their mechanical characteristics.

#### **4. Recommendations for the design of overburden pillows**

By modeling the stress-strain state (SSS) of the cushions by the finite element method (FEM) using an elastic-plastic soil model with the involvement of Monte Carlo simulation, taking into account the experimentally established laws of distribution of RV physical and mechanical parameters of the overburden of the cushion, the statistical characteristics and laws of distribution of RV settlements  $S$  of the foundations were determined.

Based on the statistical analysis of the distribution of settlements of these foundation bases and their relative unevenness, the probability of their failure was obtained. In particular, it was found that the distributions of RV of the calculated and ultimate resistances

of compacted rocks are correctly approximated by Gauss's normal law.

The coefficient of variation  $RV$  of the calculated resistance of compacted soil ranges from 21.8-36.3%, and the  $RV$  of the ultimate resistance - from 34.4-37.5%.

The probabilistic approach to the calculation of foundation settlements on a cushion has established the following. There is a probability of linear and nonlinear stages of deformation of the foundation when the pressure under the foundation sole does not exceed the calculated resistance of the compacted soil in the deterministic approach.

This effect is due to the heterogeneity of physical and mechanical parameters of compacted rocks and the random nature of loads and impacts on foundations.

For a multilayer cushion, the value of the coefficient of variation of settlement is less than for a single-layer cushion. The mathematical expectation of settlement is 2.4 times higher.

The decrease in the coefficient of variation of settlement for the multilayer artificial massif can be explained by the fact that this value is the result of adding up a large number of random variations in settlement in individual layers that overlap.

The coefficient of variation of settlement also increases with increasing heterogeneity of the layers. The values of this coefficient depend on both the thickness of the individual layers and the ratios of the strain moduli in them.

This coefficient increases with increasing heterogeneity of the layers. In particular, with greater compressibility of the upper layers than the underlying layers and an increase in the ratio of their strain moduli.

The method of constructing a cushion with different degrees of compaction of its layers reduces the variability of foundation settlement on it.

It is established that the probability of failure of foundations on a cushion according to the first limit state is acceptable, since the safety characteristic  $\beta > 3-4$ , and according to the criterion of relative unevenness of their settlements on a single-layer cushion, it reaches 10% at the limit value  $(\Delta S/L)_u=0.002$  and 3% at  $(\Delta S/L)_u=0.004$ , but

for a multilayer cushion, these values are only 0.02% and 0.0006%, respectively.

Evaluation of FEM, SSS of artificial foundations using the Ansys 11.0 software package and its subsystem Probabilistic Design with the use of the Monte Carlo method at the number of iterations of  $10^4$  in the probabilistic formulation shows that the analytically determined probability of the existence of linear and nonlinear stages of soil deformation correctly describes the real processes occurring in overburden cushions when they are loaded.

### **Conclusions**

Thus, as a result of comprehensive laboratory and field studies, the possibilities of utilizing overburdened quaternary low-cohesion rocks formed as a result of quarrying iron quartzite deposits as a material for soil cushions for structures have been proved. The influence of technological factors on the scatter of random variables of physical and mechanical parameters of these compacted rocks and their mixtures is determined. It is statistically substantiated for the physical properties of the pillow rocks. The correctness of applying the normal law of distribution of mixtures - polynomial-exponential, for the deformation modulus of compacted rocks and mixtures – logarithmically normal, for the angle of internal friction – normal, for the specific adhesion - logarithmically normal, and for the specific resistance to penetration - exponential law of distribution.

Comparison of the coefficients of variation of physical and mechanical properties of compacted and natural rocks proves that when using overburden of low-cohesion rocks, waste from the mining and processing industry, they are more homogeneous in the pillow than in the natural state. Among the technological factors, the type of rock and the content of impurities in it have the greatest impact on the variability of the material properties of the new massif. The number of passes in one track and the vibration or static mode of operation of the mechanism have a smaller impact. And the smallest is the thickness of the layer before compaction.

It is proved that the optimal rock compaction parameters should be determined by pulses close to the technical characteristics of the mechanisms or natural seals. Since the standard laboratory Proctor test does not reach the maximum rock skeleton density that corresponds to the capabilities of modern seals, for example, in the vibration mode.

### *References*

1. **Briaud J.-L.** (2013). *Geotechnical Engineering: Unsaturated and Saturated Soils*. Hoboken: John Wiley & Sons.  
<https://doi.org/10.1002/9781118686195>
2. **Xing Y., Kulatilake P. & Sandbak L.** (2019). *Rock Mass Stability around Underground Excavations in a Mine*. London: CRC Press.  
<https://doi.org/10.1201/9780429343230>
3. **Das B.M.** (2019). *Advanced Soil Mechanics*. London: CRC Press.  
<https://doi.org/10.1201/9781351215183>
4. **Cheng Y.M., Law C.W. & Liu L.** (2021). *Analysis, Design and Construction of Foundations*. London: CRC Press.  
<https://doi.org/10.1201/9780429293450>
5. EN 1997-1<sup>^</sup>2003 (E); CEN/TC250. (2003). *Eurocode 7 Geotechnical design. Part 1: General rules. Final draft*.
6. **Chu J., Bo M.W. & Arulrajah A.** (2009). Soil Improvement works for an Offshore Land Reclamation. Proc. of the Institution of Civil Engineers, *Geotechnical Engineering*, №162(1), 21–32.
7. **Chu J., Varaksin S., Klotz U. & Mengé P.** (2009). *Construction Processes*. Proc. of the 17th Intern. Conf. on Soil Mechanics and Geotechnical Engineering. Amsterdam, Berlin, Tokyo, Washington: JOS Press, 3006–3135.
8. **Furudoi T.** (2005). Second phase construction project of Kansai International Airport. Large-scale reclamation works on soft deposits. Proc. 16<sup>th</sup> Intern. Conf. on Soil Mechanics and Geotechnical Engineering. Osaka, 329–332.
9. **Brito A. & Caldeira L.** (2008). Compaction control of soil-rock mixture at Odelouca Dam. Proc. of the 19<sup>th</sup> European Young Geotechnical Engineers' Conf. Hungary, 79–88.
10. **O'Brien A.S.** (2007). Rehabilitation of urban railway embankments: research, analysis and stabilization. Proc. of the 14<sup>th</sup> European Conf. on Soil Mechanics and Geotechnical Engineering. *Geotechnical Engineering in Urban Environments*. Madrid, 125–147.
11. **Vaniček I. & Vaniček M.** (2006). Embankment of transport infrastructure and waste or recycled materials. *Active Geotechnical Design in Infrastructure Development*: proc. of the XIII<sup>th</sup> Danube-European Conf. on Geotechnical Engineering. Ljubljana, Vol. 1, 905–911.
12. **Leira Velasco J.A. & Kropnick M.A.L.** (2007). Soil improvement under two LNG tanks at the port of Barcelona. Proc. of the 14<sup>th</sup> European Conf. on Soil

Mechanics and Geotechnical Engineering. Geotechnical Engineering in Urban Environments. Madrid, 1355–1360.

**13. Ong K., Yee K. & Wong L.T.** (2006). Dynamic compaction and dynamic replacement for large oil tank. Proc. of 16<sup>th</sup> Southeast Asian Geotechnical Conf. Kuala Lumpur, 591–595.

**14. Kryvosheiev P., Farenjuk G., Tytarenko V., Boyko I., Kornienko M., Zotsenko M., Vynnykov Yu., Siedin V., Shokarev V. & Krysan V.** (2017). Innovative projects in difficult soil conditions using artificial foundation and base, arranged without soil excavation. Proc. of 19<sup>th</sup> Intern. Conf. on Soil Mechanics and Geotechnical Engineering, Seoul. ICE Publishing, Seoul, 3007–3010.

<https://doi.org/10.1680/geot.1997.47.3.693>.

**15. Onyshchenko V., Vynnykov Y., Shchurov I. & Kharchenko M.** (2023). Case Study: Sites for the Drilling and Repair of Oil and Gas Wells. Lecture Notes in Civil Engineering, 299, 367–389.

<https://link.springer.com/book/10.1007/978-3-031-17385-1>

**16. Vynnykov Y., Kharchenko M., Dmytrenko V. & Manhura A.** (2020). Probabilistic calculation in terms of deformations of the formations consisting of compacted overburden of quarternary rocks. Mining of Mineral Deposits, 14(4), 122–129.

<https://doi.org/10.33271/mining14.04.122>.

**17. Forsman J., Napari M., Piispanen P., Lindroos N., Dettenborn T. & Suominen M.** (2017). Utilization of mass stabilized dredged mud and clay as fill and embankment construction material, case City of Helsinki. Proc. of 19<sup>th</sup> Intern. Conf. on Soil Mechanics and Geotechnical Engineering, Seoul. ICE Publishing, Seoul, 2977–2980.

**18. Vynnykov Yu.L., Kharchenko M.O., Lopan R.M. & Manzhaliy S.M.** (2017). Geotechnical properties of foundations for mining complex: Monograph. Poltava: PolNTU named after Yuri Kondratyuk. [in Ukrainian].

**19. Look B. & Lacey D.** (2013). Characteristics Values in Rock Socket Design. Proc. of 18<sup>th</sup> Intern. Conf. on soil Mechanics and Geotechnical Engineering, Paris, 2795 – 2798.

**20. Cherniaiev O., Pavlychenko A., Romanenko O. & Vovk Y.** (2021). Substantiation of resource-saving technology when mining the deposits for the production of crushed-stone products. Mining of Mineral Deposits, 15(4), 99–107.

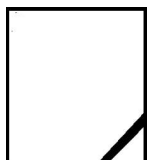
<https://doi.org/10.33271/mining15.04.099>

**THEORY AND PRACTICE OF UNDERGROUND  
LEACHING OF MINERAL RESOURCES**



**Nariman ZHALGASULY**

Head of the Department "Ecology and Safety of Mining" Institute of Mining. Kunaev, Ph.D., prof., academician of the International Academy "Ecology", (Almaty, Kazakhstan),



**Viktor YAZIKOV**

Doctor of Technical Sciences, Professor, First Vice President of Kazatomprom, Republic of Kazakhstan



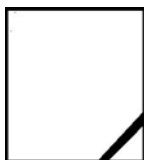
**Tulegen MUKHANOV**

First Deputy Executive director, Academician of the International Academy of information. Member of the National Scientific Council (Almaty, Kazakhstan)



**Uays BEKTIBAYEV**

Head of laboratory "Physical and chemical methods of processing of mineral raw materials", Institute of Mining after Kunaeva, Senior Researcher, (Almaty, Kazakhstan)



**Vladimir ZABAZNOV**

Candidate of Technical Sciences



### **Annotation**

The paper describes the vast experience of in-situ leaching in Kazakhstan, accumulated during 30 years of its application and improvement for mining, mainly uranium.

About half of the world's reliably explored uranium reserves are concentrated in the subsoil of Kazakhstan. A unique feature of the country's uranium reserves is that 75% of them are concentrated in deposits associated with regional zones of formation oxidation. This type of deposits is not widespread in the world. In Kazakhstan, these deposits are concentrated mainly in the Shu-Sarysu, Syrdarya and Ili uranium-ore provinces.

A number of deposits are currently being developed by the Stepny, Central and №6 ore departments of NAC Kazatomprom CJSC. Extraction is carried out by a relatively cheap and environmentally preferable method of in-situ leaching through a system of wells drilled from the surface underground borehole leaching (UBL).

For these purposes, a comprehensive research method is used, including: analysis and synthesis of practical and theoretical data in the field of uranium mining by underground leaching and the environmental problems arising in this case, mathematical modeling method, analytical calculations, analytical calculations, laboratory work and in-depth field experiments in production conditions, generalisation and transfer of the obtained scientific and practical data to design organisations and industrial enterprises dealing with uranium mining by in-situ leaching. The material from long-term observations of the process of aquifer self-regeneration is compelling and illustrative in the Irkol field of Syrdarya province in Kazakhstan.

The purpose of the work is to establish the patterns of natural demineralization of residual solutions of underground sulfuric acid leaching of uranium. For this purpose, at all operating UL enterprises, installations were designed and built to extract associated useful components from productive solutions.

In conclusion, it can be noted that the development and improvement, based on many theoretical and applied studies, of the method of borehole in-situ leaching of metals described in this work is the fruit of the creative efforts of a large number of specialists in various fields of knowledge both in the republic and abroad.

### **Introduction**

Underground leaching of metals is a method of development of ore deposits by selective conversion of useful component into liquid phase directly in the subsurface with subsequent processing of metal-containing (productive solutions). In this method the progressive technique of transferring one of the main hydrometallurgical processes - percolation - to the place of occurrence of ore material is successfully realised.

The scientific novelty is the establishment of theoretical and experimental substantiation of the regularities of the process of natural demineralization of residual solutions of underground leaching of

uranium and other components, the parameters of the formation and behavior over time of their halo under changing hydrodynamic conditions, as well as the scale of the demineralization zone.

Theoretical principles and methods for calculating the spreading parameters of technological solutions and their neutralization zones have been developed, and a general criterion for assessing the intensity of this process has been derived; a fundamentally new method has been created to intensify the process of natural demineralization of formation waters enriched with uranium leaching products, based on the displacement of the halo of residual solutions into rocks not affected by technogenesis.

The scientific significance of the work lies in the establishment by natural experiments of the basic laws of groundwater rehabilitation, the development of a theoretical method for predicting the spread of harmful new formations in waste horizons during uranium ISR.

The relevance of this study is that during underground borehole leaching (ISL) of uranium, the release of radioactivity into the atmosphere is significantly lower than with traditional mining methods of mining and processing uranium ore. Wells filled with liquid throughout the entire period of operation prevent the release of radon from the subsurface. During ISR, only about 20% of the main radioactive elements enter a mobile state in the subsurface and are brought to the surface, compared to 100% with traditional mining methods. There is also no need to build tailings dumps with a high level of radiation from the stored material. Solutions coming from leaching sites have a low level of radiation as a result of the poor solubility of radium and short-lived daughter products of the decay of U-238; only a very small part of Ra-226 and other radionuclides of the uranium-radium series is sorbed on the ion exchange resin simultaneously with uranium.

Moreover, it was in Kazakhstan that for the first time in the world the deepest deposits, with ore depths of more than 600 meters, were involved in mining using the UL method, and the profitability of their exploitation was proven primarily due to the production of richer productive solutions, the formation of which has a positive effect of natural autoclave - increased temperature and pressure in the area where the main leaching reactions occur.

It is difficult to overestimate the importance of the development and implementation of the UL method in Kazakhstan from an environmental and socio-economic point of view. Recently, one of the most pressing issues in mining production is its environmental assessment.

The idea of the work is to accelerate the process of natural demineralization and the depth of purification of residual uranium leaching solutions from harmful elements by forcibly shifting their halo from the zone of rocks disturbed by technogenesis to the zone with natural conditions.

The goal of the study is to mine uranium with the lowest content of radioactive substances. The fact is that during sulfuric acid leaching, as a result of the physicochemical interaction of the solvent with the host rocks and ores, in the process of multiple circulation of solutions between the above-ground and underground complexes, a complex anion-cation composition of technological solutions is formed, which far exceeds the maximum permissible concentrations for the waters used for drinking and household purposes. Significant amounts of sulfates, chlorides, bicarbonates, iron, aluminum, nitrates, radionuclides and other trace elements accumulate in EPS solutions. Contamination of groundwater with these solutions can occur in the event of their significant spreading beyond the boundaries of exhausted deposits or individual deposits along ore-bearing and adjacent aquifers. The ingress of hazardous listed and other components into drinking water can lead to serious environmental consequences.

### **1.1 Mineral resource base of uranium**

The material presented in this work allows us to get an idea of how large and diverse the uranium mineral resource base of Kazakhstan is. This is due to the peculiarities of the geotectonic position of the territory of the republic, the specifics of geological development, and the richness of geological and structural settings.

Industrial uranium deposits that make up the ore districts and provinces are found in deposits that are very different in age and structural and formational affiliation.

In the pre-Mesozoic formations of the Kazakh folded region and the spurs of the Tien Shan, the North Kazakhstan and Kendyktas-

Chu-Ili-Betpak-dala uranium provinces with a surprisingly diverse set of hydrothermal deposits are located, respectively.

Large soil-infiltration uranium-coal and bed-infiltration (sandstone) deposits of the Ili uranium province are localized in the coal-bearing terrigenous deposits of the Triassic-Jurassic depression structures.

The aquiferous sandy horizons of the Cretaceous-Paleogene host epigenetic reservoir-infiltration and uranium deposits of the regional zones of reservoir oxidation of the Chu-Sarysu and Syrdarya uranium-ore provinces, constituting one of the largest East Turanian megaprovinces in the world.

Finally, in the thickness of the Oligocene marine clays on the Mangystau Peninsula there is a uranium ore region of the same name with a unique phosphate-organogenic type of complex deposits associated with horizons of uranium-bearing fish and a variety of dinosaurs bone remains.

In addition to the noted uranium ore areas, a significant number of ore and uranium-bearing areas and individual objects (including other genetic types) that are currently in reserve have been identified, which in the future can be used to replenish the existing raw material base [1-2].

The evolution of the uranium raw material base in Kazakhstan is very indicative and interesting. From the 50s to the 70s, it was based on hydrothermal deposits localized in pre-Mesozoic formations, due to which its development and replenishment mainly took place.

Deposits of the organogenic-phosphate type on the Mangystau Peninsula also played a certain role. Other exogenous deposits (uranium-coal, reservoir-infiltration deposits in permeable aquifers of the Cretaceous and Paleogene) were not exploited due to the lack of acceptable technology.

Since the beginning of the 70s, with the introduction of a new progressive method of developing water-logged deposits - underground leaching, intensive searches, exploration and involvement in the exploitation of reservoir-infiltration deposits, large and unique in terms of the scale of distribution of raw materials, began.

It is difficult to overestimate the truly revolutionary role that the introduction of this method played in the creation of the mineral resource base of Kazakhstan.

In particular, the use of this method determined the amazing transformation of the unfavorable (for the mining method) features of epigenetic deposits, such as high water content and weak lithification of rocks and ores, into their main advantages, allowing the extraction of uranium and associated components without extracting the ore mass and host rocks at surface and thereby significantly reduce the negative impact on the natural environment. With the introduction of the UL method in the Mesozoic-Cenozoic depression structures of Kazakhstan, prospecting and evaluation work for uranium was again widely deployed, and the emphasis was placed on areas with already determined ore bearing Chu-Sarysu and Syrdarya uranium provinces.

As a result of the work carried out, the Chu-Sarysi depression by the end of the 70s took shape as the largest uranium ore province, representing a long-term mineral resource base for uranium mining using the underground leaching method. In this regard, it is advisable to note that the discovery of unique deposits of the Chu-Sarysu and Syrdarya ore provinces became possible only thanks to the development and prompt implementation into practice of the concept of regional ore-generating fronts of formation oxidation.

In particular, it was proven that the formation of epigenetic uranium deposits is associated not with individual Paleozoic uplifts, representing local areas of supply of oxygen-bearing uranium waters, as previously thought, but with the general development of the Tien Shan orogenic zone, which at the time of the latest tectonic activation caused the movement of formation waters immediately in all aquifers of the Cretaceous and Paleogene to the discharge centers. As already noted, in the initial period these deposits were explored for mining using the mining method (open pit or underground)

In terms of their industrial significance, they were considered monoelemental, where oxide uranium ores did not contain significant impurities of accompanying components. Accordingly, uranium was given the importance of the only metal capable of accumulating in industrial quantities at the boundaries of zones of formational limonitization.

The study of a number of elements localized together with uranium at the boundaries of the FOZ, in particular, selenium, molybdenum, and rhenium, was of a purely mineralogeochemical nature.

As a result of complex studies, the patterns of localization of uranium, selenium and molybdenum during the pinching out of the FOZ were outlined, and their place in epigenetic zoning was established.

However, when carrying out technical and economic calculations to determine the possibility of developing deposits and transferring them to industry for exploitation by mining, no practical interest arose in the accompanying elements, and these objects were still considered as monouranium, and not complex.

Again, the development by industry of the method of underground leaching at the location of ores through systems of geotechnological wells, made it possible to approach the problem of the possible use for the needs of the national economy of a number of useful components that are satellites of uranium in the exogenous epigenetic process from a fundamentally new position. It was shown for the first time that when implementing the IR method, when the working reagent (due to the specifics of the method) processes a larger volume of ore mass than necessary, the leaching processes should involve useful components contained not only in uranium ores, but also in the immediate vicinity of them in a single aquifer (rhenium, selenium, molybdenum, etc.).

Geological exploration work revealed, in addition to selenium, molybdenum, and rhenium, scandium, yttrium, lanthanides, and vanadium in the ores, and in the process of geotechnological research, the possibility of leaching the listed elements from ores of deposits of this type was in principle proven. By the beginning of the eighties, it became clear that the formation-infiltration deposits that were considered monouranium were polyelement deposits, and solving the problem of their detailed study, including complex geotechnological aspects, in preparation for industrial development in relation to the IW method is of great national economic importance.

Not only geological and operating organizations, but also industry and republican research institutes began to participate in the development of the problem

Thus, the structure of Kazakhstan's uranium raw material base began to steadily change in favor of deposits of this type, characterized by high competitiveness. By the beginning of the 90s, the basis of the uranium raw material base was formed by formation-infiltration deposits of regional 3POs. Hydrothermal deposits in pre-

Mesozoic formations are gradually being transferred to conservation for economic and especially environmental reasons. In addition, in recent years, the requirements for the profitability of deposits involved in development have sharply increased. In this regard, deposits of complex ores containing, in addition to uranium, other valuable associated components, began to attract maximum interest. The cost of uranium mined by the IR method in epigenetic reservoir-infiltration deposits is significantly lower than the cost of uranium mined by mining from most hydrothermal deposits.

The problem of negative technogenic impact on the environment as a result of the exploitation of deposits has now become of particular importance. In this regard, the UL method has a number of advantages over the mining method. Experts have clearly established that possible contamination of formation water during underground leaching can only occur as a result of a gross violation of the work technology. Existing methods of cleaning and reclamation of the natural environment, subject to compliance with all operating rules, ensure its environmental safety.

Currently, Kazakhstan has one of the world's largest uranium ore raw material bases, which not only makes it possible to fully meet domestic needs, even with maximum development programs for its own nuclear energy, but also makes the republic one of the largest potential suppliers of uranium to the world market.

In terms of total resources of natural uranium, the republic occupies one of the first places in the world, and in terms of resources and reliably explored reserves of uranium, suitable for mining uranium by underground leaching, it is a world leader. In the modern structure of Kazakhstan's uranium raw material base, the main place (about 73% in total resources and about 65% in reserves of categories B+C1+C2) belongs to deposits of reservoir oxidation zones, developed by the IW method. The explored reserves of soil-infiltration deposits account for 10%, of which 5.5% are complex molybdenum-uranium-coal deposits and 4.5% are deposits localized in sandy-clayey formations. About 3% are complex rare metal-uranium-phosphorus ores of organogenic-phosphate deposits of the Caspian region. The share of endogenous and polygenic deposits in pre-Mesozoic formations accounts for about 22%.

It should be emphasized that the decisive role in the creation of the uranium raw material base of the republic belongs to the Volkov-geologiya enterprise; at least 70% of the uranium resources suitable for mining using the UL method have been identified and prepared by its specialists.

Despite the fact that the stock of uranium deposits located in favorable conditions and especially easily discovered has significantly decreased, the prospects for replenishing and increasing the uranium mineral resource base in Kazakhstan are quite large. This applies both to epigenetic reservoir-infiltration deposits exploited by the IW method, and to deposits of other genetic types [3].

### **1.2 Copper mineral resource base**

The largest object of the cuprous sandstone formation in Kazakhstan is the Zhezkazgan copper deposit, which in this work will be considered as the most promising raw material base for underground leaching.

According to K.I. Satpayev, mineralization here is confined to the sand-shale strata of the Upper Carboniferous. The ore-bearing strata is exposed in the direction from south to north at a distance of 70 km.

The Upper Carboniferous sequence and the underlying Devonian Lower Carboniferous rocks are folded into a large synclinal fold, complicated by brachyanticlines broken by normal faults. The thickness of the Upper Carboniferous sandy-shale sequence is 900 m; it is subject to seven horizons with mineralization confined to the crest of the chest-type brachinticline.

Mineralization is concentrated in layers of gray sandstones with carbonate cement and is absent or poorly developed in layers of red sandstones and conglomerates with clayey-ferruginous cement. Ore bodies have the form of sheet-like deposits and flat lenses, their number is small. The largest deposits can be traced at a length of 1.5-2.0 km and a dip of 800 m, with a thickness of 1.5-4.0 m to 18 m. In addition to the deposits, there are separate mineralized zones “veins with breccia”, for example, the so-called Peter and Paul fault, traced along the strike for 500 m.

Composition of the ores: chalcopyrite, bornite, pyrite, fahlores, sphalerite, galena, calcite, quartz, barite, chalcocite, covellite, oxides and hydrous carbonates of copper. Ore minerals are scattered in the form of small impregnations in the cement of sandstones and in the



form of veinlets composed of rock crystal, calcite and large crystals of chalcopyrite, bornite, chalcocite, and galena. The ores contain up to several percent Cu (on average), and in places are enriched in Pb, Zn and Ag.

A characteristic feature of the Zhezkazgan deposit is the unevenness of mineralization and the qualitative heterogeneity of the chemical and mineralogical composition. Therefore, as a rule, areas with high copper content alternate with poor ones, and poor ones with substandard ores.

In the Zhezkazgan mines over the past 15 years, the average copper content in ore has decreased by almost 40%. In the total ore flow, the share of ore with low content (close to cut-off content) reaches 25-30%. It is known that during the enrichment of depleted ores, the removal of useful components into the tailings sharply increases.

One of the methods that allows the extraction of low-grade ores is their leaching in situ. Therefore, at present, numerous research and experimental work is being carried out on this problem [4-5]. The widespread introduction of heap leaching and especially underground leaching methods will make it possible to increase the raw material base of the Zhezkazgan deposit by more than double, as well as reduce the operational losses already committed by 5-6 times.



Table 1

List of countries by fuel uranium production according to data

№	A country	2015, tons	2016, tons	2017, tons	2018, tons	2019, tons	2020, tons	2021, tons	Share in the world, 2020, %
1	Kazakhstan	23607	24689	23321	21705	22808	19477	21819	45,1 %
2	Namibia	2993	3654	4224	5525	5476	5413	5753	11,9 %
3	Canada	13325	14039	13116	7001	6938	3885	4693	9,7
4	Australia	5654	6315	5882	6517	6613	6203	4192	8,7 %
5	Uzbekistan	2385	3325	3400	3450	3500	3500	3500	7,2 %
6	Russia	3055	3004	2917	2904	2911	2846	2635	5,5 %
7	Niger	4116	3479	3449	2911	2983	2991	2248	4,7 %
8	China	1616	1616	1692	1885	1885	1885	1885	3,9 %
9	India	385	385	421	423	308	400	615	1,3 %
10	Ukraine	1200	808	707	790	800	744	455	0,9 %
11	South Africa	393	490	308	346	346	250	385	0,7 %

12	Iran	38	0	40	71	71	71	75	0,2 %
13	Iran	45	45	45	45	45	45	45	< 0,1 %
14	Pakistan	40	44	0	0	0	15	29	< 0,1 %
15	Brazil	1256	1125	940	582	58	6	8	< 0,1 %
16	Czech	155	138	0	0	0	0	0	0 %
17	Romania	77	50	0	0	0	0	0	0 %
18	France	2	0	0	0	0	0	0	0 %
19	Germany	0	0	0	0	0	0	0	0 %
20	Malawi	0	0	0	0	0	0	0	0 %
	Total in the world, tons	<b>60304</b>	<b>63207</b>	<b>60514</b>	<b>54154</b>	<b>54742</b>	<b>47731</b>	<b>48332</b>	<b>100 %</b>
	Production U <sub>3</sub> O <sub>8</sub>	71113	74357	71361	63861	64554	56287	56995	
	% of global demand	98 %	96 %	93 %	80 %	81 %	74 %	77%	

Table 2  
The largest uranium deposits and their developers as of 2019

Field	A country	Company	Extraction method	Production (tons)	Share in the world
Cigar Lake	Canada	Cameco / Orano	underground	6924	13 %
Khusab	Namibia	Swakop Uranium	open	3400	6 %
Olympic Dam	 Australia	<a href="#">BHP Billiton</a>		3364	6 %
Muyunkum and Tortkuduk	Kazakhstan	Kazatomprom (49 %)/Orano (51 %)	in-situ leaching	3252	6 %
Inkai	Kazakhstan	Kazatomprom (60 %) / Cameco (40 %)	in-situ leaching	3209	6 %
Budenovskoe	Kazakhstan	Kazatomprom (51 %) / Uranium One (49 %)	in-situ leaching	2600	5 %
Rössing	Namibia	Rio Tinto	open	2076	4 %
Arlit	 Niger	<a href="#">Orano</a>	open	1912	4 %
Central Mynkuduk	Kazakhstan	Kazatomprom	in-situ leaching	1964	4 %
South Inkai	Kazakhstan	Kazatomprom / <a href="#">Uranium One</a>	in-situ leaching	1601	3 %

### 1.3 Basics of geotechnologies for underground leaching of useful components

The optimal way to exploit uranium deposits is in-situ leaching (IL) at the ore site through systems of technological wells constructed from the surface. The industry currently has two technologies for underground uranium leaching: sulfuric acid, widely used in Kazakhstan and the CIS countries and mainly suitable for ores with a low content of bound carbon dioxide, and bicarbonate (carbonate) with an oxidizer, widely used in the USA.

The fairly high efficiency of the underground leaching method has led to a reduction in industry requirements for the quality of uranium raw materials (for example, the minimum cut-off content of uranium in ores for the IW method is usually taken to be 0.01% and, apparently, can be reduced to 0.005%, while for mining method it is 0.03%). The use of underground leaching has made it possible to take a fundamentally new approach to the problem of extracting from the subsoil a number of important minerals, in particular, scandium, rhenium, yttrium, a number of lanthanides, molybdenum and others associated with the wedging out of formation oxidation zones in aquifers shared with uranium and contained in ores in lower concentrations than those established by industry requirements for the mining method of their extraction [6].

Analysis of the materials shows that the geological and hydrogeological conditions for the localization of multi-element mineralization in exogenous epigenetic deposits of Kazakhstan are favorable for the extraction of useful components by underground leaching, which is primarily due to:

- the very specificity of exogenous epigenetic ore formation, during which oxygen-containing waters, along the path of filtration, extract useful components from the host rocks of the productive horizon or areas of nutrition and, in a certain sequence, precipitate (concentrate) them under changing geochemical conditions on reduction or neutralization geochemical barriers in a form favorable for leaching with aqueous solutions of acids or alkali metal salts. Thus, in the natural conditions of Southern Kazakhstan, the first unique cycle of hydrometallurgical processing takes place, preparing elements for the subsequent cycle of underground leaching;

- compact arrangement of epigenetic concentrations of uranium and associated useful components in a single aquifer, which deter-

mines the possibility of developing them mainly through unified systems of technological wells:

- the confinement of ore concentrations to horizons of highly permeable gravel-sandy, highly watered rocks, not suitable for mining.

#### **1.4 Underground leaching of metals from ores of polyelement deposits**

The studies performed have shown that the process of underground leaching of useful components from ores of polyelement infiltration deposits is in many ways similar to exogenous epigenetic ore formation, differing from it in the reverse direction, the concentration of leaching reagents in solutions, the rate of chemical reactions, the content of useful components in solutions, and the time factor. This conclusion is of great importance for the development of underground leaching technology for the sequence (stages) of extracting useful components from the subsoil.

Underground leaching of useful components from ores of exogenous epigenetic deposits is considered as a reverse process of transferring metals into a mobile state as a result of their reactions with oxygen-containing solutions of reagents rich in sulfate sulfur or carbonate ion, which are fed into the formation through a system of injection technological wells with subsequent movement within the volume leaching and pumping of productive solutions from pumping (discharge) wells. Thus, the commonality of exogenous epigenetic ore formation and underground leaching of epigenetic concentrations of metals in hydrogenous deposits lies in the very nature of the processes under consideration, their physicochemical essence.

The movement of aqueous solutions in both cases is carried out in a filtration mode in rocks with natural permeability (filtration coefficient is usually more than 1 m/day) due to a pressure gradient: during the epigenetic process - from areas of formation piezomaximum to areas of groundwater discharge, during underground leaching - from areas injection wells to unloading areas. Hydraulic slopes and natural speeds of movement of formation waters are 2-3 orders of magnitude lower than those of UL solutions.

Both processes can be defined as heterogeneous chemical interactions, from a physicochemical point of view, accompanied by changes in the concentrations of reacting substances in the liquid and solid

phases during the filtration movement of the first within the leaching volume. Both processes obey the same laws of diffusion kinetics and physicochemical hydrodynamics.

It is obvious that technogenic UL solutions, differing from natural ones in a higher concentration of leaching reagents (primarily sulfate or carbonate components and oxidizing agents), are more chemically active. Concentrations of ore elements in UL solutions vary widely, being 2 - 4 orders of magnitude higher than in ore-forming formation waters. Thus, for uranium, molybdenum, vanadium and selenium, in the technogenic process they are 10<sup>-2</sup>-10<sup>-1</sup> g/l, and in the natural ore-forming process - from 10<sup>-6</sup> 10<sup>-3</sup> g/l; for rhenium and scandium - 10<sup>-4</sup>-10<sup>-3</sup> and 10<sup>-7</sup>-10<sup>-5</sup> g/l, respectively.

The forms of migration of useful components with the carbonate (bicarbonate) IW method, in process solutions are the same as in formation waters with a near-neutral and moderately alkaline environment: these are anions represented by dissociations of acids - molybdic acid  $\text{M004}$ , rhenium  $\text{Re04}$ , orthovanadium  $\text{H}_2\text{VO}_4$ , selenite  $\text{HSeO}_3$ , hydrogen selenide  $\text{HSe}$  or carbonate complexes - uranyl  $\text{UO}_2(\text{CO}_3)_2$ ,  $\text{UO}_2(\text{CO}_3)_3$  and scandium  $\text{Sc}(\text{CO}_3)_2$ .

Precipitation (concentration) of useful components from ore-forming aqueous solutions is carried out on the wedging out of zones of formation oxidation (on reduction or neutralization geochemical barriers) in a certain sequence: on a barrier of the first type - in accordance with the natural decrease in Eh of the environment from +200 to -200 mV:  $\text{Sc} > \text{V} > \text{U} > \text{Re} > \text{Mo}$ ; on a barrier of the second type - in accordance with a decrease in pH from 7.0-8.5 to 6.5 and a subsequent increase to ~7.5  $\text{V} > \text{Sc}$ , TR. Exogenous epigenetic concentrations refer to mineral forms that are quite easily soluble in aqueous solutions of acids or alkalis - these are finely dispersed oxides, hydroxides, disulfides, and native forms. The production of useful components from productive solutions is carried out on the surface as a result of various technological operations (sorption, precipitation, etc.).

The process of UL of useful components is opposite in its direction to the process of epigenetic ore deposition. Thus, with the carbonate leaching method, as the Eh of the medium increases, according to thermodynamic calculations and experiments, Mo should be extracted from the ores first, then Re, U, V, and finally, in the pres-

ence of a strong oxidizing agent, Se. With the sulfuric acid method, according to the same data, this sequence is generally preserved, but here it reflects not so much an increase in the Eh of the medium as a decrease in pH as the L:T indicator increases - Mo (pH<7), Re (pH<6.5), Sc (pH<5), U (pH<4), V (pH<3), Se (pH<6 in the presence of a strong oxidizing agent).

One of the features inherent in both the epigenetic process of ore formation and UL is the reprecipitation of useful components on mobile geochemical barriers along the path of filtration of ore-bearing solutions. For the conditions of natural ore formation, this effect is observed as long as there is a pressure gradient and the flow of oxygen uranium-bearing groundwater to geochemical barriers, and for the UL process - only during acidification of ore-bearing rocks or during the latent (hidden) period when preparing them for carbonate leaching. Responsible for the precipitation of useful components in natural conditions are mainly two types of geochemical barriers: for polyvalent elements - mainly reducing, for monovalent elements - neutralizing. Under technogenic conditions, two types of UL in the subsoil are also developed: with the acid method, the neutralization method predominates, and with the carbonate method, the reduction method predominates.

The intensity and duration of the processes of exogenous epigenetic ore formation and underground leaching are sharply different. If for the first it is millions and the first tens of millions of years, then for the second it is the first years. The relatively weak chemical activity and low degree of metal content of reservoir solutions when creating ore concentrations are compensated by the time factor - the duration of the ore formation process, and during operation (to achieve the design extraction of metals from the subsoil) its relatively short period is compensated by increased concentrations and chemical activity of working solutions, the creation of increased rates their movement within the mining volume and by other means.

Consequently, in the course of both natural ore-forming and technogenic processes of IR, one of the main cycles of hydrometallurgical processing is carried out directly in the subsoil, namely, the transfer of useful components into the liquid phase, and in the first, in addition, the concentration of elements in the solid phase at geochemical barriers in fairly easily soluble mineral form. The natural process

of exogenous epigenetic ore formation, as it were, prepares useful components for leaching and predetermines the possibility of using the IP method for the exploitation of multi-element deposits.

When developing geotechnological regimes of UL, the effect of precipitation of elements on the pinching out of formation oxidation zones in a certain paragenetic dependence is used. It is obvious that important for these regimes are the initial concentrations of the working reagent, the ratio of Liquid: Solid, the reagent capacity of the ore-hosting rocks and other factors that determine changes in the alkaline-acid index and the redox potential of the environment. It is recommended to extract useful components from polyelement ores in the reverse order of their deposition on geochemical barriers, according to the general scheme: Mo > Re > Sc, Y, TR, U > V > Se. Another important circumstance is the need to take into account the individual geochemical and mineralogical characteristics of useful components, which determines the choice of the environment and geotechnological conditions of the water supply, as well as environmental protection measures.

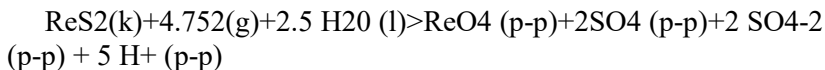
### **1.5 Thermodynamic prerequisites for the UL of useful components from ores**

The theoretical basis of the physicochemical conditions of the process of IR of useful components (molybdenum, rhenium, uranium, selenium, vanadium, scandium, yttrium, some lanthanides) is based on thermodynamic calculations of the fields of predominance of compounds in the liquid and solid phases, highlighting areas of favorable geotechnological conditions for their leaching

### **1.6 Polyvalent elements**

It is necessary to take into account that their ore epigenetic concentrations are associated with a reducing geochemical barrier in choosing geotechnological regimes for leaching useful components of this group (molybdenum, rhenium, uranium, parts of vanadium, selenium).

The assessment of geotechnological conditions for polyvalent elements is carried out in a sequence opposite to the order of their reductive precipitation, i.e., the sequence of their possible transition into the UL solution during oxidation. The interaction of leaching solutions with rhenium disulfide occurs according to the reaction equation:



Thermodynamically, this reaction, as in the leaching of molybdenum, does not depend on the alkalinity or acidity of the medium and for its implementation, in addition to the necessary kinetic factors, only the presence of oxygen or other oxidizing agents is required.

The most favorable geotechnological conditions for underground leaching of rhenium are mainly sulfuric acid and carbonate with an oxidizing agent, located in a vast field of perhenate ion  $\text{ReO}_4$ . Under these conditions, rhenium can be extracted from ores together with molybdenum and uranium.

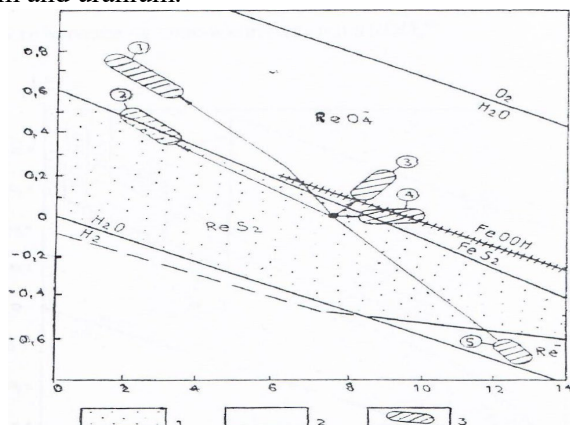


**Fig. 1.** Eh-pH diagram of the fields of dominance of the rhenium compound at = 25 °C and P = 1 bar. 1 - fields of liquid phases; 2 - fields of solid phases; 3 - geotechnological situation

The interaction of molybdenum leaching solutions occurs according to the reaction equations:



To implement these reactions, in addition to favorable kinetic factors, only the presence of an oxidizing agent is required. Favorable for underground leaching of molybdenum are mainly sulfuric acid and carbonate with an oxidizing geotechnological conditions, which



during the sulfuric acid method fall into the fields of liquid phases of hydromolybdate - ion  $\text{HMoO}_4^{2-}$  and molybdic acid  $\text{H}_4\text{MoO}_4$ , and for the carbonate method - into the field of molybdate - ion  $\text{MoO}_4^{2-}$ .

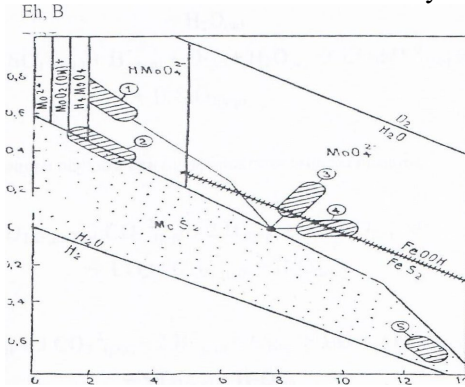
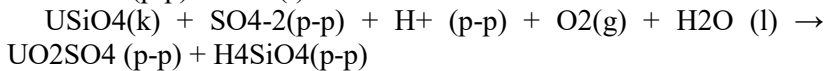
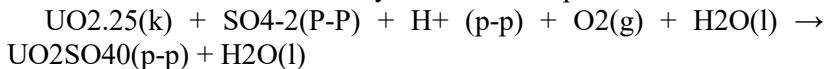


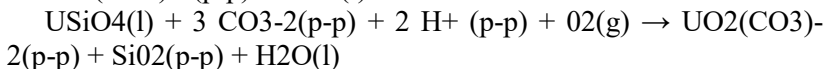
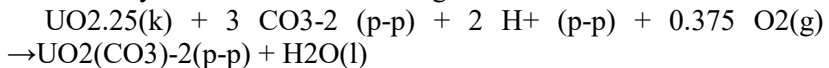
**Fig. 2.** Eh-pH - dominance field diagram molybdenum compounds at  $T = 25^\circ\text{C}$  and  $P = 1$  bar

Uranium is currently the main useful component in the deposits under consideration. The issues of geotechnology of underground leaching are the most developed for it. Depending on the mineral composition of the host rocks and the type of ore mineralization, acid (aqueous solutions of sulfuric acid) and carbonate, bicarbonate (aqueous solutions of sodium carbonate-bicarbonate, ammonium, etc.) methods are used for uranium leaching; Oxygen, hydrogen peroxide, and ferric iron are used as oxidizing agents.

The interaction of sulfuric acid working solutions with U (IV) oxides and silicates is described by the reaction equations:

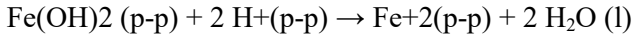
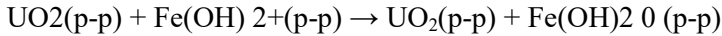
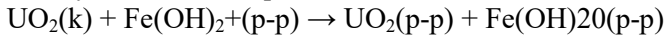


Similarly for bicarbonate leaching:



In an acidic environment, one of the oxidizing agents of U (IV) can be hydrolyzed forms of ferric iron:  $\text{Fe}(\text{OH})_2^+$ ,  $\text{Fe}(\text{OH})_3$

$\text{Fe}(\text{OH})_2^{2+}$  and, to a lesser extent,  $\text{Fe}^{3+}$  ions. The oxidation process of uranium oxides in an acidic environment is stepwise and is described by the reaction equations:



An additional oxidizing agent for uranium in a sulfuric acid environment is nitric acid, often supplied with sulfuric acid to passivate stainless steel materials and equipment.

Hexavalent uranium compounds are extracted from ores without an oxidizing agent in both acidic and carbonate environments.

In general, three geotechnological conditions are thermodynamically favorable for uranium leaching: sulfuric acid with an oxidizer and sulfuric acid without an oxidizer, located in the fields of uranyl sulfate complexes  $\text{UO}_2\text{SO}_4 - \text{UO}_2(\text{SO}_4)_2^{2-}$  and carbonate with an oxidizer - in the field of tricarbonatouranyl  $\text{UO}_2(\text{CO}_3)_3$ , the position of the latter above the hydrogoethite-pyrite equilibrium line determines the need to use an oxidizing agent. The release of uranium into solution when using sulfuric acid with an oxidizing agent is thermodynamically possible in the range  $\text{pH}=6.5-5.7$ , where it is in the form of dicarbonatouranyl, and then at a  $\text{pH}$  below 5.0; and without an oxidizing agent - at a  $\text{pH}$  below 4.5-4.0. With the carbonate IR method, uranium is released into solution at  $\text{pH} = 7.8-8.5$ . In a highly alkaline reducing environment, uranium leaching is impossible [7-9].

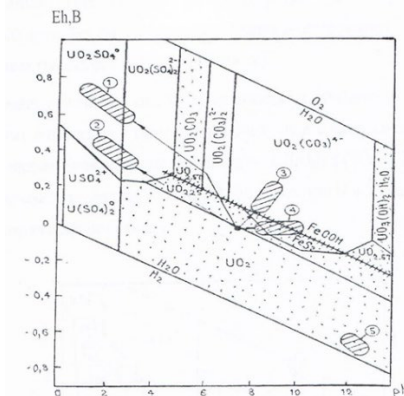
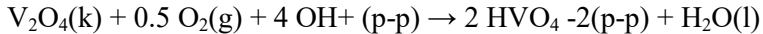
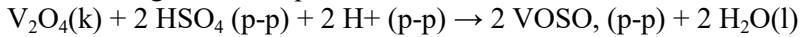


**Fig. 3.** Eh-pH - diagram of the fields of predominance of uranium compounds at  $T=25\text{ }^\circ\text{C}$  and  $P=1\text{ bar}$

Increasing the temperature of the uranium leaching process to 50°C does not change the position of the regions of solid and liquid phases observed at 25°C (Fig. No. 4), i.e., it has a positive effect only on the kinetics of the UL process. Favorable geotechnological conditions for uranium UL are the same for the entire temperature range from 25 to 50°C.

Leaching solutions react with vanadium compounds according to the following reaction equations:



Three geotechnological conditions are thermodynamically favorable for the leaching of vanadium: sulfuric acid with an oxidizing agent, sulfuric acid without an oxidizing agent, falling into the field of the monosulfate complex  $\text{VOSO}_4$ , and carbonate with an oxidizing agent - in the field of the dehydrogenate ion  $\text{H}_2\text{VO}_4^-$ . The through extraction of vanadium in sulfuric acid conditions at  $\text{pH} < 2$  is prevented by the  $\text{V}_2\text{O}_5$  field. In a carbonate environment without an oxidizer, leaching is unpromising due to the development of a field of solid phases  $\text{VO}_4$  and oxide  $\text{V}(\text{IV}+\text{V})$ .

The introduction of uranium into the calculation system leads to the disappearance of the field of soluble phases of vanadium in the alkaline region due to its displacement by the field of uranyl vanadates, for example, carnotite -  $\text{K}_2(\text{UO}_2)_2 \times (\text{VO}_4)_2 \times 3\text{H}_2\text{O}$ .

This limits the use of the UL method for the association of U and V, mainly by the sulfuric acid method.

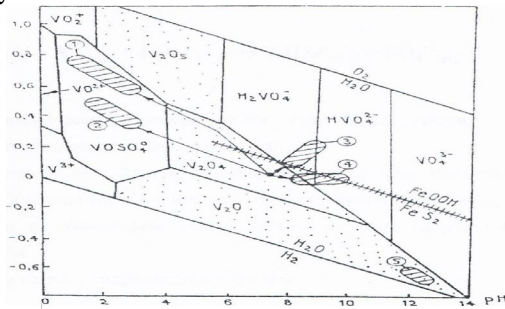
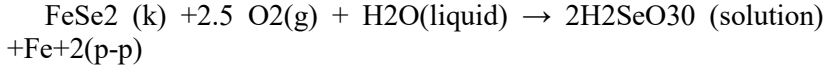
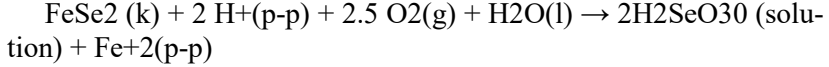
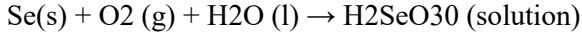


**Fig. 4.** Eh-pH - diagram of the fields of predominance of vanadium compounds at  $T = 22 \text{ }^\circ\text{C}$ ,  $P = 1 \text{ bar}$ .

The interaction of working solutions with mineral forms of selenium occurs according to the following reaction equation:

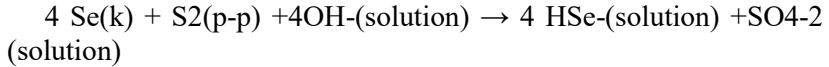
- during sulfuric acid leaching with an oxidizing agent;



- during carbonate leaching with an oxidizing agent;



- during sulfide leaching;



Three geotechnological conditions are thermodynamically favorable for selenium leaching:

-sulfuric acid with an oxidizing agent, falling into the field of undissociated selenous acid  $\text{H}_2\text{SeO}_3$  and partially hydroselenide - ion  $\text{HSeO}_3^-$ ;

-carbonate with an oxidizing agent, located in the fields of hydroselenide and selenide ion;

-sulfide - in the field of hydroselenide ion  $\text{HSe}^-$

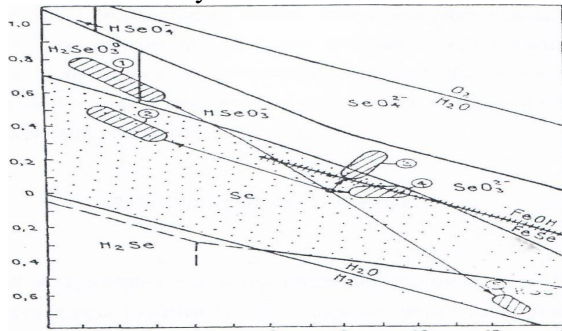
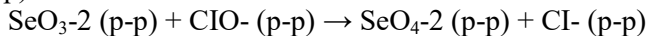
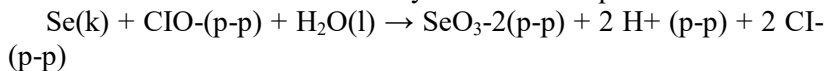


Fig. 5. Eh-pH - diagram of the fields of predominance of the selenium compound at T=25 degrees C and P=1bar.

Experiments have shown that oxidizing agents such as oxygen and hydrogen peroxide are not effective enough to completely convert selenium into the liquid phase from its elemental form. The pro-

cess proceeds more intensively when strong oxidizing agents are used, for example hypochloride, which is formed, in particular, in the presence of chlorine gas. The oxidation of selenium in an alkaline medium in this case is described by the reaction equations:



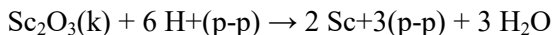
It can be seen that during the oxidation of selenium with hypochloride, both selenide and selenate-nones can be formed.

Sulfuric acid and carbonate environments without an oxidizing agent are unfavorable for the leaching of selenium. Leaching of selenium from ores of polyelement deposits using sulfuric acid and carbonate geotechnological conditions with a strong oxidizer can be carried out together with uranium, molybdenum, rhenium, vanadium, and in alkaline sulfide conditions - only with rhenium.

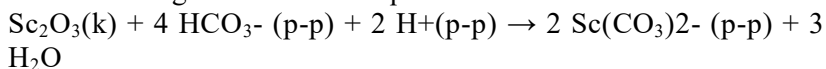
### 1.7 Monovalent elements

In choosing a geotechnology for leaching useful components of this group, it is necessary to take into account that their ore concentrations (scandium, yttrium, lanthanides, etc.) are associated primarily with the neutralization (alkaline) barrier. Consequently, the main role in extracting the elements under consideration from the subsoil should belong to the sulfuric acid UL method.

Thus, the solubility of scandium oxide increases sharply with a decrease in pH to less than 5.0-4.5, when the bicarbonate complex  $\text{Sc}(\text{CO}_3)_2$ , characteristic of near-neutral formation waters, and the monohydroxide ion  $\text{ScOH}^+$ , characteristic of weakly acidic environments, are replaced by the  $\text{Sc}^{3+}$  cation. According to thermodynamic calculations, the concentrations of this cation in equilibrium with crystalline  $\text{Sc}_2\text{O}_3$  are about 30 mg/l at pH=4, and more than 10 g/l at pH=3. The following reaction corresponds to the dissolution of the oxide:



In a near-neutral, weakly alkaline environment, the release of scandium into the process bicarbonate solution is fundamentally possible according to the reaction equation:



However, in this case, the maximum solubility of  $\text{Sc}_2\text{O}_3$  does not exceed -2.5 mg/l, and therefore the bicarbonate IR method for the

industrial extraction of scandium from multi-element formation-infiltration ores should be considered ineffective.

According to calculated data, the yield of scandium in both acidic and bicarbonate solutions will increase sharply if its mineral phase is represented by  $\text{Sc}(\text{OH})_3$  hydroxide, the solubility of which is 4 orders of magnitude higher than that of the anhydrous oxide. At the same time, if the metal in question enters the crystal lattice of apatite or other newly formed or syngenetic minerals, the efficiency of its extraction will sharply decrease [10].

Similarly, the sulfuric acid environment favors the effective leaching of yttrium and lanthanides from ores. All these rare earth metals, as mentioned above, form monosulfate complexes  $\text{MeSO}_4$ , the stability of which consistently increases with increasing acidity of the medium.

Thermodynamically, the most favorable for the UL of scandium, yttrium and lanthanides is the sulfuric acid geotechnological region. At the same time, according to the calculations performed, with an increase in the L:T ratio and a drop in the pH of the medium below 5.0-4.5, the first of the elements under consideration in significant concentrations can pass into solution cerium and ytterbium, then lanthanum, scandium and yttrium. At the same time, due to different levels of content of these metals and the initial solid phase - in ores and host rocks, they can change places, giving primacy to those elements that create the most significant epigenetic accumulations and, accordingly, are in easily soluble mineral forms and (or) have more high clarke.

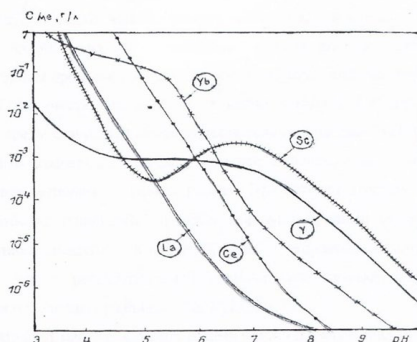
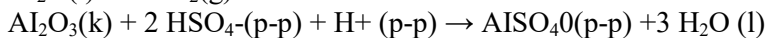
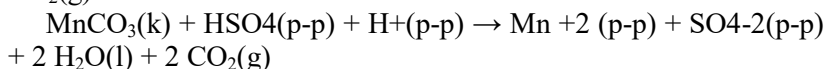
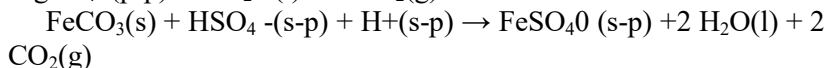
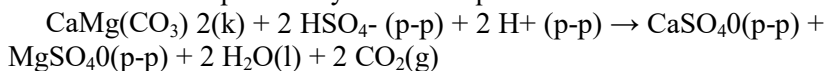


**Fig. 6.** Dependence on pH value of scandium concentrations and solutions (in the form of  $\text{Sc}_2\text{O}_3$ ,  $\text{Sc}(\text{OH})_3$  and  $\text{Sc}(\text{CO}_3)_2$ ); yttrium (in the form of  $\text{Y}_2\text{O}_3$ ); lanthanum (in the form of  $\text{La}_2\text{O}_3$  and  $\text{LaCO}_3$ ); cerium (in the form of  $\text{Ce}_2\text{O}_3$ ) and ytterbium (in the form of  $\text{Yb}_2\text{O}_3$ ) T-25 degrees C; P=1 bar

## 1.8 Possibilities for leaching of uranium associated components

In the process of underground leaching, working solutions react not only with ore concentrations of the elements discussed above, but also with a number of epigenetic and syngenetic accumulations, other metals, as well as with some rock-forming minerals. The largest amount of metals goes into solution with the acid UL method; the capabilities of the carbonate and sulfide methods in this regard are limited. A large group of elements is associated with the acidic migration environment, in addition to the Sc.Y described above. TR - aluminum, calcium, magnesium, manganese, nickel, cobalt, as well as iron, phosphorus, zinc, copper, partially lead, niobium, beryllium, cadmium, capable of participating in the formation-infiltration process during acidification of groundwater starting from pH = 7,0-6.5. If we take into account that under sulfuric acid AF conditions the scale of acidification of the environment becomes more significant (pH decrease to 1.0), then the above list should be supplemented with vanadium, indium, chromium, gallium, thorium, strontium, barium, radium. These metals in a strongly acidic environment with an excess of SO<sub>4</sub><sup>2-</sup> and HSO<sub>4</sub><sup>-</sup> ions form strong sulfate complexes, or are in the form of simple and hydroxide cations. Naturally, in the water-salt system under consideration, the concentrations of alkali metals - Na, K, Li, Rb, Cs - will also increase.

The concentrations of magnesium, calcium, iron, manganese, aluminum (in the form of MeSO<sub>4</sub>) in equilibrium with their mineral carbonate or oxide phases in sulfuric acid technological solutions become thermodynamically almost unlimited. Their transition into solution can be expressed by reaction equations:



The situation is similar with cobalt and nickel. According to thermodynamic calculations, in concentrations exceeding 1 mg/l, the following can pass into the sulfuric acid solution:

at pH<7.5 - zinc; at pH<6.4 - copper; at pH<4.8 - vanadium and niobium; at pH<4.4 indium,

at pH 2.9- gallium, at pH<6.8- cadmium; at pH<5.3\_ lead; at pH<4.5 - beryllium; at pH<3.3-chromium; at pH<2.0 – thorium.

Dependence of solubility on pH of the most stable mineral phases: chromium CrO<sub>3</sub> (eskolaite); indium In(OH)<sub>3</sub> (gilindite); cadmium CdSO<sub>4</sub>; zinc ZnSO<sub>4</sub> (morenosite); ZnCO<sub>3</sub> (smithsonite) and ZnO (zincite); T=25°C and P=1 bar, without taking into account the ionic strength of solutions (below the curves the limit of the predominance of the forms of occurrence of metals in solutions is shown).

It is clear that the intensity of the release of the listed metals into solution will be determined not only by the thermodynamic limits of solubility of their most stable mineral phases, but also by the contents of these metals in the host sand rocks, the presence of their easily leached epigenetic additive, the kinetics of the dissolution process of the initial mineral components, etc. .

According to calculations made on the basis of available thermodynamic constants, silver, tin, bismuth, antimony, tungsten, gold, platinum (the last two in the absence of organic acids), as well as the most important rock-forming component - silicic acid, practically do not react to a decrease in the pH of the environment. Elements that are relatively inert in the sulfuric acid treatment of formation-infiltration ores can also include germanium, zirconium, hafnium and, probably, tantalum, the solubility of their oxides increases at pH less than 1.0, i.e. in relatively concentrated acids.

In the case of the bicarbonate (carbonate) UB process, technological solutions can additionally extract from rocks those elements that (in addition to uranium and rare earths) form carbonate complexes: lead, copper, cadmium, beryllium, however, as calculations show, this enrichment will be negligible.

The introduction of an oxidizing agent into the working sulfuric acid or carbonate solution, which causes an increase in the Eh value of the aqueous medium, in all cases stimulates leaching from ores, in addition to Mo, Re, U, V, Se, tellurium, palladium, a complex of chalcophile elements that migrate well in oxygen conditions in favorable acidity ranges.



Thus, the main amount of metals is transferred into the liquid phase under sulfuric acid geotechnological conditions without an oxidizing agent.

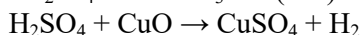
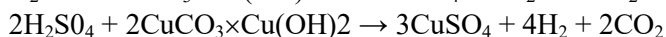
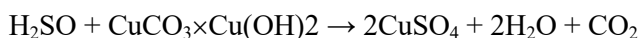
The use of a sulfuric acid environment with an oxidizer makes it possible to additionally extract tellurium, palladium, and a number of chalcophile elements from the subsurface. The carbonate geotechnological situation is generally unfavorable for the transfer of most metals into the liquid phase. The geotechnological conditions established during thermodynamic calculations that are favorable for each of the useful components are confirmed by the results of laboratory studies, field experiments at underground leaching sites and during the industrial exploitation of uranium deposits.

### **1.9 Obtaining copper-containing solutions from underground leaching**

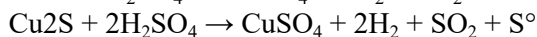
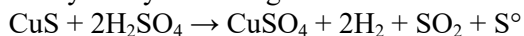
The conversion of natural insoluble copper compounds into a soluble (mobile) form occurs under the influence of chemical reagents.

These can be, first of all, acids - sulfuric, hydrochloric, nitric, alkaline reagents NaOH, Na<sub>2</sub>CO<sub>3</sub>, active gases, such as chlorine, chemical compounds of higher valence metals, such as ferric sulfate Fe<sub>2</sub>(SO<sub>4</sub>)<sub>3</sub>, chlorine iron FeCl<sub>3</sub>, copper chloride CuCl<sub>2</sub>, etc. Without going into the advantages and disadvantages of this or that solvent, we note that currently the ubiquitous solvent in geotechnological processes for copper minerals is sulfuric acid [11].

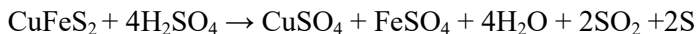
Not all copper minerals dissolve at the same rate. It has been established that copper oxides and carbonates dissolve at the highest speed, since the interaction of these compounds with sulfuric acid appears as a neutralization reaction that takes place with a large exothermic effect



The secondary copper sulfides covellite and chalcocite dissolve relatively easily according to the reactions:



Primary sulfides dissolve through complex multi-stage reactions:  
- chalcopyrite:



- bornite dissolves only in the presence of oxygen:



These equations characterize reactions from a qualitative point of view. For quantitative judgment, it is necessary to have data on the rate of dissolution of minerals, which are determined specifically for each mineral.

### **1.10 Socio-economic and environmental aspects of the UL method**

Over the past 30 years, in the mining of metals, the method of in-situ leaching (IF) has become widespread through a system of boreholes drilled from the surface or from underground mine workings.

The essence of underground leaching of minerals is the selective transfer of a useful component into the liquid phase by controlled movement of a solvent through the ore in its natural occurrence or through a pre-crushed ore mass, lifting a solution enriched with metal to the surface. And for this purpose, through wells drilled from the surface, a chemical reagent is supplied to the ore zone, capable of converting minerals of the mineral into a soluble form. The solution, having passed the path from the injection well to the pumping well, is lifted to the surface using technical means and then transported through pipelines to processing plants.

A necessary condition for using the UL method is the possibility of movement of the leaching reagent in the ore zone, i.e. ore-bearing rocks must have natural or artificially created permeability. Unlike the traditional scheme of ore mining and processing, the technological scheme of underground leaching from reservoir deposits, the productive horizon of which is flooded, does not require a complex set of structures for water supply and treatment of industrial wastewater, since the latter are absent in the process. From an environmental point of view, the UL method can be classified as a waste-free method of mining.

Water for preparing leaching solutions comes from the watered productive horizon through technological wells, and after extracting the metal from the productive solutions, they are further strengthened with a solvent reagent.

Injection of leaching solutions into the formation and lifting of productive solutions is carried out in a closed cycle, and the balance

of injected and pumped out solutions is maintained. Sometimes a slight imbalance in the operation of the system in the direction of increasing the pumped out solutions is planned in advance, which prevents the spreading of process solutions beyond the boundaries of the mining allotment contour.

In-situ leaching enterprises include two main complexes: a mining and processing plant.

A mining complex is a technology and technical means for extracting minerals from the subsoil in the form of solutions and delivering them to a processing plant. The mining complex consists of two parts: underground and surface.

The underground part includes technological wells and their equipment, with the help of which the opening of the productive horizon, preparation of the ore body for leaching, the leaching process itself and the rise of the productive solution are ensured (K.Ch. Kozhagulov et al., 2023)).

The equipment of the surface part of the mining complex includes technological pipelines for transporting leaching and productive solutions, reagents, air ducts, pumping stations for pumping solutions over long distances and settling tanks for cleaning solutions from mechanical suspensions.

### **1.11 Development system in aquiferous permeable rocks**

The method of underground leaching is most widely developed in the development of infiltration-type deposits with natural permeability of ores. The process is implemented through systems of technological wells constructed from the surface.

Wells are the main link in the technical equipment of underground leaching enterprises. The share of drilling costs in the cost of the final product is 15-30%, depending on the depth of the deposit.

With the help of wells, exploration is carried out and the reserves of the deposit are determined, the geometric shapes of ore bodies are specified, and ore deposits are opened and prepared for leaching.

In the technological process, a leaching solution is supplied into the formation through wells and productive metal-containing solutions are taken from the formation, the movement of technological solutions in the productive horizon and the completeness of mineral extraction are controlled. Various measures are also carried out through wells in order to protect the subsoil and the environment

from pollution. Deposit development by in-situ leaching, depending on its scale, requires the construction of several hundred to several thousand wells.

In recent years, the technical and economic indicators of well construction have improved significantly. Unified well designs using the same type of parts and assemblies have been developed. New pipe materials are being used that make it possible to equip wells up to 650 m deep and improve the quality of their operation (Zhalgasuly N. et al., 2023).

The following requirements are imposed on wells when extracting UL metal:

1. The location of wells and their operating mode must ensure maximum extraction of metal from ores with minimal unproductive losses of productive solutions and solvent.

2. Wells must be designed and operated with the highest possible productivity under the given natural conditions.

3. With the help of wells, a controlled process of movement of solutions in the subsurface must be ensured.

4. The service life of wells should not be less than the operating time of a cell (operational block or section).

5. When choosing the number of wells and determining their cost, it is necessary to proceed from the economic feasibility of mining using the UL method in order to obtain an acceptable cost of the metal deposit.

6. When constructing wells, the manufacturability of all operations performed must be ensured, using standard equipment and tools.

7. Wells should not be a source of environmental pollution.

All drilling wells used in opening and developing deposits using the UL method are, to one degree or another, involved in the technological process and are therefore called technological. Depending on their functional purpose, technological wells are divided into two groups: production and auxiliary.

Production wells are directly involved in the extraction of metal from the subsoil. Through them, solutions are transported and the hydrodynamic regime in the productive formation is regulated. Based on their purpose, production wells are divided into pumping and injection wells.

Pumping wells (sometimes called unloading wells) are designed to lift productive (metal-containing) solutions from the productive formation to the surface.

Injection wells are designed to supply leaching solutions (solvent) into the productive formation (ore deposit). The group of auxiliary wells does not directly participate in metal extraction. They play a large role in studying the deposit, preparing the formation for leaching, protecting and cleaning the subsoil from contamination, monitoring the water recovery process, etc.

Exploration wells are drilled for detailed exploration of a deposit or its individual deposits, clarifying mineral reserves, determining the shape of ore bodies in plan and section, and studying the properties of rocks along the IW process route.

Observation wells are intended for observation and control of the conditions for the formation of productive solutions within production blocks, the hydrodynamic state of the productive horizon, the spreading of technological solutions beyond the boundaries of production areas and their possible flow into higher or underlying horizons.

Monitoring wells are drilled in mined-out areas to monitor the completeness of extraction of useful components from the subsoil, as well as to solve other problems (studying changes in ore-bearing rocks, monitoring possible contamination of groundwater and the environment, etc.) .

Depending on their purpose, geotechnological wells have significant differences in design, drilling technology and technology, and equipment. They are also subject to various reliability and durability requirements.

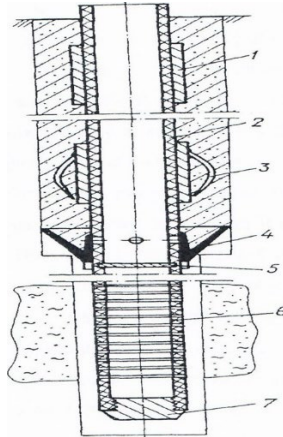


**Fig. 7.** Typical design of a technological well (column layout):

- 1 - weighting agent; 2 - production string; 3 - centralizer; 4 - disconnecting cuff;  
5 - cement diaphragm; 6 - filter; 7 - plug

The borehole system is the most effective, as it allows you to sharply reduce the number of capital construction projects and reduce capital costs compared to the conventional mining method.

A borehole leaching enterprise can be created in successive stages, using a modular principle, when each stage includes a full set of necessary structures for mining the corresponding areas, and an increase in productivity is ensured by the parallel operation of several module blocks; the cost of production of such an enterprise is practically constant and does not depend on productivity.

In general, the cost of production at borehole leaching enterprises turns out to be 2-6 times less than at mining enterprises.

It is important to emphasize the significant difference not only in the magnitude, but also in the cost structure of the cost of a leaching enterprise and a mining enterprise with a traditional mining method. If at enterprises with a mining method of extraction the share of operating costs in the cost of production is 65-70%, and the depreciation of capital investments is 30-35%, then at borehole leaching enterprises the share of operating costs in the cost of production is always much higher and reaches 77-90% with a decrease the share of depreciation capital investments up to 23-10%. Moreover, the

amount of capital investment in the latter case is 2-4 times lower than in enterprises with a mining method of extraction.

The structure of operating costs of borehole leaching enterprises is also unique and consists of the costs of drilling and equipping wells with surface pipelines (17-23%), costs of reagents (30-45%) and energy (8-15%).

Downhole in-situ leaching systems also make it possible to sharply reduce the requirements for the content of useful components in ores and effectively involve poor and poor ore deposits in the development.

The nature of labor in production processes under the UL method has also changed significantly. All work on the preparation of ore bodies, drilling and casing wells, constructing simple trestles and laying pipelines, can easily be fully mechanized. All metal mining processes - injection and pumping out of solutions, their transportation, sorption and desorption - are easily automated.

With a significant reduction in tension and labor intensity compared to mining methods, the UL method makes it possible to increase labor productivity for the final product by 2-4 times. At the same time, the old problem of bringing production personnel directly to the surface of the earth has been solved.

Underground leaching is the most environmentally friendly, virtually waste-free production, since its use eliminates:

- delivery of ore and rock mass to the surface, creation of dumps and tailings of hydrometallurgical plants;
- release of contaminated drainage groundwater to the surface and discharge it into surface watercourses,
- air pollution with dust and harmful gases.

Essentially, the entire technogenic impact of this method is limited to ore-bearing aquifers, where natural waters are replaced by working solutions during operation. Both are distinguished by increased concentrations of uranium and a number of satellite elements (radium, selenium, vanadium, etc.). Technogenic impact on the ore-bearing horizon therefore does not create additional environmental hazards, since in areas of infiltration deposits, groundwater and in natural conditions are initially contaminated with the same complex of elements in concentrations significantly exceeding the MPC,

which makes them unsuitable for use for domestic and drinking purposes.

Recently, the issue of environmentally safe underground disposal of liquid industrial waste has become a problem; with underground leaching, the disposal of residual solutions at such objects is carried out as if automatically, which over time, according to numerous experiments, are actively self-cleaning.

### **1.12 Rock-based mining systems**

Deposits confined to rocks, under certain conditions, are also suitable for mining by underground leaching. Moreover, unlike reservoir infiltration deposits, they require the creation of mine or combined (underground mine workings plus wells) systems for development.

For underground leaching with a combined system, the most suitable sites are those where it is technically difficult to extract ore, where there has been a collapse, and finally where the content of the useful component is quite low. All of these objects can be defined as lost ores.

Let's consider some objects suitable for underground leaching at the Zhezkazgan copper deposit. The field has ten flexural zones located almost parallel at a distance of 200-300 and up to 800-1200 from each other, which can be traced from north to south from 2 to 9.5 km. The vertical amplitude of the displacement is from 15 to 200 m. Copper reserves in flexure zones account for about 6% of the total reserves of the deposit.

The stability of ores and rocks of the flexural part of the deposit is reduced due to large tectonic disturbances, therefore, mining of flexures using a room-and-pillar system, which is widely used in the deposit, is impossible due to the danger of working in an open mining space.

At the Kresto-Zapad mine in 1963, 4 blocks were mined in a steeply dipping flexure deposit using a forced block caving system.

This system is characterized by significant ore losses and dilution, and therefore the introduction of this system at the Zhezkazganok deposit was limited to the development of pilot blocks.

At present, when the preparation of the raw material base for the Zhezkazgan deposit lags behind the needs of metallurgical enterpris-



es, there is a need to develop reserves in flexural zones, which are classified as temporary reserves.

Currently, when the preparation of the raw material base for the Zhezkazgan deposit lags behind the needs of metallurgical enterprises, there is a need to develop reserves in flexure zones, which are classified as temporary reserves.

Based on the results of enlarged laboratory studies, the ZhezkazganNIPItsvetmet Institute compiled a technical and working design for the development of a pilot section of the 3-bis flexural mine, the "Cresto-Zapad" zone.

The site of the Western Krestovskaya flexure is located between the shaft of mine 3-bis and the failure of blocks No. 2 and No. 4. The steeply falling part of the flexure in the field of the site has access to the surface. Intense fracturing is widespread near and inside the flexure zone; the ores are destroyed by natural cracks of three separate systems with edge sizes not exceeding 0.8 m. In the oxidized zone there are sliding and secant cracks running at right angles to the rock bedding.

Ore-bearing gray sandstones are developed throughout the entire area of the site and almost everywhere contain copper mineralization with a content of 0.2%.

There are two types of ores: oxidized (about 29%) and sulfide. The maximum oxidation depth reaches 40-65 m, the rocks are porous and the filtration coefficient varies over a fairly wide range. Near the daytime surface it is 3 m/day. at a depth of 80 m - 1.1 m/day and decreases to 0.1 m/day at a depth of 120 m.

When choosing in-situ leaching technology for the pilot site, two options were considered. The first option includes a combined system in which the ore of the oxidized zone, due to its intense fracturing, is leached without crushing, and the ore of the sulfide zone is crushed by drilling and blasting.

According to the method of breaking ores in the sulfide system of the zone in a combined zone, it can be associated with a system with staged breaking of ore in chambers. Its peculiarity is the creation of compensation spaces over the entire height of the floor, into which the ore mass is broken using deep wells in a compressed environment. The total height of the floor is equal to the height of the sulfide zone. The chamber is limited from above by the thickness of the oxi-

dized zone, and from the failure of previously mined blocks - by the whole between the blocks; an overcut pillar is left at the bottom of the chamber in order to preserve the chamber bed and drainage catching wells.

Separate saturation of the oxidized and sulfide zones with a leaching solution is provided. For the first, injection wells are drilled from the surface to a depth of H-45 m with a double-row arrangement at a distance of 20 m between their mouths, with a solution supplied to them under pressure of  $P=3$  atm. Due to pressure filtration of solutions through cracks, they saturate ore particles and enter into chemical reactions with ore minerals. The enriched solution, seeping through the thickness of the oxidized zone, flows into the ore stored in the chamber and, filtered, together with the solution supplied for leaching the crushed ore, exits through ore passes and ore outlets into the cross-cut. Some of the solution is drained through collection wells.

Along the groove, it moves into the settling tank of the pumping chamber and through the unloading well it is discharged to the surface into the main settling tank and then to the hydrometallurgical installation.

To irrigate the ores of the sulfide zone, wells are also drilled from the surface along a 5x5 m grid and go into the chamber. The solution supplied from the surface into cased wells through nozzles irrigates the crushed

Treatment work includes the preparation of compensation slots with the release of ore at the bottom of the crosscut 3-bis horizon 295 and the release of ore to the surface, breaking in a compressed environment of a volume of rock mass in the chamber and storing this volume for leaching.

The loosening coefficient of stored ore is Kr-1.2. The main amount of ore has a size of 200 mm. In order to preserve injection wells drilled from the surface, they are drilled after blasting in the chamber. To prevent unirrigated areas from remaining in the chamber, injection wells along the hanging side are located outside the contour of the flexure zone.

The advantages of the combined in-situ leaching system are as follows:

- a small volume of ore released to the surface when preparing chambers for leaching in the sulfide zone, amounting to 5% (with mining preparation and cutting operations) of the volume of ore in the chamber; efficiency of the process of leaching of crushed rock mass by infiltration flow.

However, the system has the following disadvantages: a significant amount of drilling work in preparing raw materials for leaching; the need to leave an inter-block and cross-cut pillar, which leads to the loss of a useful component in the subsoil, the need to supply a large amount of leaching solution for irrigation in order to cover the leached raw material in the chamber; significant costs for preliminary crushing of ore.

In order to reduce the cost of the system, a second option for underground leaching of naturally occurring ores has been developed.

Studies of the filtration properties of ore, carried out in laboratory conditions, for the first time using the method of electrohydrodynamic analogy, as well as the study of the mass transfer process in the "solid-liquid" system, where the solid denotes copper minerals, and the liquid. sulfuric acid solution showed that the experimental section of the flexure zone can be leached without preliminary crushing of the ores. To do this, the leaching solution under pressure is fed into injection wells to a depth of 100 m, where the filtration coefficient is 0.5 m/day and then until the crosscut, the solution will be filtered due to the pressure coming from the end of the wells.

During the leaching process, when the materials filling the cracks are largely destroyed as a result of chemical reactions, the filtration permeability of solutions along the cracks will increase.

The rate of filtration of sulfuric acid solutions through ore and ore materials - crack fillers is  $\sim 0.02$  m/day, with the solution diffusion rate for ore units being 0.016 m/day, solution concentration  $H_2SO_4 = 14$  g/l.

The advantages of this system are the following:

- a small number of workers - 25 people with a site productivity of 350 tons of cementation copper;
- there is no surface collapse;
- the minimum sufficient technical base for developing the site is: one drilling rig of the SBU-ZIF-300 m brand; polyethylene casing

pipes with a diameter of up to 100 mm; surface main pipeline (polyethylene);

- two chemical pumps (one of them is a backup);
- completeness of metal extraction;
- simplicity and convenience in organizing work; lack of mining preparation work during ore preparation.

The system has one serious drawback;

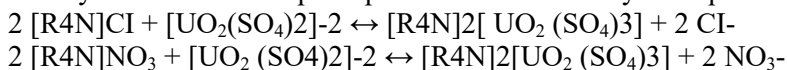
- Quite a long service life.

It will be possible to intensify and accelerate the leaching process by introducing ferric iron sulfate into the leaching solution.

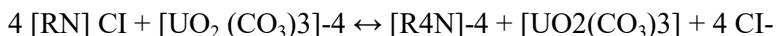
### **1.13 Technology for extracting uranium from UL solutions**

Currently, when processing sulfuric acid and bicarbonate (carbonate) UL solutions, preference is given to sorption methods.

In sulfuric acid solutions, uranium is in the form of uranyl-sulfate complexes, for example  $[\text{UO}_2(\text{SO}_4)_2]^{-2}$ , the pH of the medium is usually below 3. The sorption process is described by the equations:



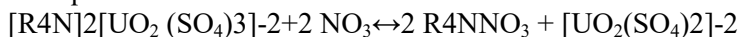
When using the carbonate UL method, the sorption process is reduced to the absorption of tricarbonatouranyl  $[\text{UO}_2(\text{CO}_3)_3]^{-4}$  by the resin



Depending on the salt composition of productive solutions, excess acidity or carbonate content, strongly basic anion exchangers are widely used. Competition for anionic forms of uranium during sorption consists of nitrate, fluoride, dihydrogen phosphate, sulfate and chloride ions. The depressant effect of a number of reagents is also used in the desorption of uranium from resin (in addition to sulfuric acid, nitric and hydrochloric, chloride and nitrate solutions, and in some cases some mixtures of them, are used).

When desorption of uranium by eluting, for example, uranyl sulfate ions absorbed during the processing of sulfuric acid solutions of PV, sulfuric acid eluents are effective. In this case, after desorption, the regenerated sorbent remains in the salt form used in the sorption processing of the solution. For desorption, 10-15% sulfuric acid solutions are used, the concentration of uranium in the commercial regenerate is 10-15 g/l. [14-15].

The best results are obtained by desorption of uranyl sulfate ions with nitrate solutions. The process of nitrate desorption is described by the equation:



After desorption, the treated ammonite must be converted into a working ionic form. Nitrate desorption is widely used at industrial water supply facilities of NAC Kazatomprom. The initial desorption solution usually consists of ammonium nitrate and nitric acid or melange.

Uranium is usually extracted from eluates using a precipitation method. This operation is determined by the type of solution used in the desorption step. Ammonia and alkaline precipitation are often used with finished products and in the form of polyuranates (diuranates).



The yellow cake is separated from the remaining solution by thickening and filtration. For transportation to further cleaning operations, the cake is dried or deoxidized in solutions (20-30 g/l) of sulfuric acid.

Thus, directly at the UL facilities, as a result of the redistribution of productive solutions, a significant concentration of uranium occurs in comparison with the initial one (10-500 mg/l); The finished products have a fairly high quality of uranium (30-40%).

#### **1.14 Methods for processing multicomponent productive solutions of UL**

The transfer of useful components into solution during underground leaching is carried out in the subsurface. Productive uranium solutions with a number of accompanying components (Re, Mo, V, S, Y, TR, etc.), depending on the recovery method, are pumped to the surface through a system of unloading (pumping) wells, settled and supplied to surface processing units to obtain marketable products (concentrates).

To process the combination of productive UL solutions, various methods are used - sorption, extraction, precipitation.

The main requirements for the implementation of individual technological schemes for the redistribution of productive solutions include: the most complete extraction of components converted into useful components; solution of technological schemes, the use of

methods and providing the minimum possible number of operations, reagents and modes for concentrating useful components to obtain enough (concentrates), as well as cost-effective, clean finished products, economically advantageous processing. The methods for extracting useful components existing in the Republic of Kazakhstan, near and far abroad countries are close to each other. Specific indicators and parameters of technological processes at different enterprises may vary due to the mineral and chemical composition of the ores, the IP method used and the conditions of the process, the set of useful components, etc.

Useful components from ores of polyelement deposits using sulfuric acid, productive solutions pumped to the surface may contain, in addition to uranium (10-500 mg/l), rhenium (0.1-0.3 mg/l), scandium (0.2-1.0 mg/l or more), yttrium (2-10 mg/l or more), lanthanides (fractions of milligrams and milligrams per liter), vanadium (up to 200 mg/l in the Zhutan type of ores), in a number of deposits molybdenum (3-10 mg/l). With a carbonate (bicarbonate) PV with an oxidizing agent, the amount of useful components in solutions is usually lower than with an acidic one: uranium - up to 200 mg/l, mainly 30-100 mg/t, rhenium 0.3-1.0 mg/l; yttrium, lanthanides and scandium are practically absent [12-13].

Productive sulfuric acid solutions have a total mineralization of 10-30 g/l, including concentrations (g/l): H<sub>2</sub>SO<sub>4</sub> - 8-22, free acid 1-5; Al - 0.2-1.5; Mn - 0.1-0.5; Fe - 0.7-2.0; Ca - 0.5-2.0; Mg - 0.2-1.0; H<sub>2</sub>SiO<sub>4</sub> - 0.1-0.3; Cl - 0.1-1.5; R - up to 1.0. Na, K, Rb, Cs, Be, Sr, Ba, B, Ti, Nb, Co, Cu, Zn, Cd, Hg, As, Pb, NOg, Ni, etc. are present in various concentrations. pH value of productive sulfuric acid solutions 1, 2-3.0. In productive bicarbonate solutions, the total mineralization is 3-7 g/l, rarely more, including concentrations (g/l): HCO<sub>3</sub> - 0.8-2.0; SO<sub>4</sub> - 2-1-3; NH<sub>4</sub> - 0.4-0.6; Na+K - 0.5-1.0; Cl - 0.8-1.2; Cu - 0.6-1; Mg-0.1-0.3. The concentrations of F, Pb, Cu, Zn, Cd, Ga, Ge, H<sub>4</sub> SiO<sub>4</sub> are low.

In accordance with the complex chemical composition of productive UL solutions and the low content of useful components in them, their processing and initial concentration are based on sorption methods for extracting elements with subsequent use for greater concentration and purification from impurities of extraction, precipitation, and in some cases, again sorption methods .

### 1.15 Sorption methods

Sorption methods for the extraction of uranium and associated components are based on the use of the ion exchange process on ion exchange resins. Ion exchangers are solid, practically insoluble in aqueous solutions of acids, alkalis, and organic media, artificial (or natural) materials that ensure the extraction of metals in cationic or anionic forms from solutions. Horse exchange consists of two stages: saturation and desorption. At the first stage, the productive solution comes into contact with the sorbent, and useful components are quite selectively absorbed by the ion exchanger. Upon reaching equilibrium capacity for one or more metals, the sorbent is transferred to the desorption stage; during the latter, it comes into contact with a chemical solution, which removes metals from the ion exchanger, after which it returns to the saturation stage. The concentrated productive solution is sent for further processing. The volume of solutions of useful components after desorption is significantly less than the volume of the initial ones received for sorption, which, in turn, allows for their further concentration to be effectively carried out.

The process of sorption exchange obeys the law of mass action. One of the main requirements is selectivity for extracted metals and maximum resin capacity with fairly good kinetic parameters of sorption and regeneration. The efficiency of the sorption stage is assessed by the sorption capacity of the resin, the degree of metal extraction from UL solutions, the number of sorption stages, the one-time loading of the ion exchanger, the duration of contact of the solution with the ion exchanger, and the desorption conditions. All these parameters are usually interconnected and reflect the basic physical and chemical laws of sorption, and also depend on the instrumental design of the process. In modern processes of sorption extraction of uranium, rhenium, molybdenum, gold, rare and trace elements from acidic and carbonate solutions and ore pulps, strongly basic styrene-based dinonites are most widely used; AM, AMP, vinylpyridine anion exchanger BP-1 Ap, as well as macroporous anion exchanger AMI-25, which have increased selectivity and distribution coefficient of uranium, especially in the region of low concentrations (1-50 mg/l). This ensures a decrease in the uranium content in sorption mother liquors (to less than 1 mg/l) and an increase of 1.5-2 times in

eluates, with a corresponding increase in the efficiency of concentration and purification of uranium-containing compounds.

Of particular interest for the extraction and concentration of scandium and rhenium from PB solutions are 8H cation exchangers, in particular phosphorus-containing SF-3, SF-4, SF-5, sulfopolystyrene KU-2, KU-2-N, KMDR, etc., ampholytes of the Afl type.

For the extraction of alkaline and alkaline earth elements, R3E and heavy metals, KMDF cation exchanger is intended, which is recommended for sorption of scandium and thorium from UL solutions. It has high chemical and osmotic stability and can be effectively used in processes involving alternating operations for treating the ion exchanger with solutions of acids and alkalis

Ampholytes with nitrogen-phosphorus-containing groups API-21 and API-22 are used for the sorption of uranium, scandium, rhenium, thorium from PV solutions, industrial waters and the capture of valuable components for the purification of natural components from industrial wastewater. In addition to being used for scandium sorption, ampholyte API-22 can be effectively used for the extraction of other metals. It has increased selectivity to vanadium, tungsten and platinum.

To extract uranium and rare metals (Re, Sc, Y) from productive UL solutions of complex salt composition, it is possible to use impregnated sorbents (C) created in recent years, the so-called productive solid extractants (TVEX).

Thus, a synthesis technology has now been developed, and the production of various sorbents - anion- and cation-exchange resins and ampholytes, solid extractants and various types of mitregnate resins for the sorption extraction of uranium, rare (Re, so, U). noble and most non-ferrous metals from solutions and remote control, including productive UL solutions. These sorbents have high exchange capacity, selectivity, mechanical and osmotic strength, chemical, thermal and radiation resistance, ensuring fairly effective extraction of useful components from solutions.

The sorbed metal from the ion exchanger is removed in the desorption stage; nitrate or chloride solutions, as well as acids (sulfuric, hydrochloric, nitric) are used for it. During desorption, the contents of useful components in the ion exchanger are gradually reduced to certain maximum permissible values, ensuring the production of



waste solutions containing valuable components. When filtrating eluting solutions through an ion exchanger layer, solutions with variable concentrations of metals are obtained, of which portions with the highest indicators are removed as a commercial fraction for further processing, and the remaining fractions with low concentrations of PC are used as recycled ones.

There are a number of methods for desorption of metals from ion exchangers: elution, displacement, conversion, extraction desorption. During elution, the metal is washed out from a saturated sorbent with a pure solvent (for example, uranyl sulfate complexes are eluted with 10–15% sulfuric acid solutions). As the eluent temperature increases, the amount of desorbed metal increases. Displacement occurs during desorption by a more sorbed ion or substance. The spent ion exchanger remains in the form of a desorbing ion and, therefore, requires special treatment to remove this tone from the ion exchanger in order to convert it into a working ionic form, which ensures the most effective extraction of the valuable component. For example, the displacement of uranyl sulfate complexes from anion exchangers by nitrates and chlorides is widely used. During conversion, a sorbed metal complex, for example, sulfate, in the ion exchanger phase is converted into a chloride or nitrate complex when the ion exchanger is treated with concentrated solutions of nitrates or chlorides. Extraction desorption is used to extract metal from anion exchangers, for which solutions of mineral acids with an extractant (tributyl phosphate, trialkylamine, etc.) are used.

Methods for extracting metal from commercial reclaims are different and depend on the composition of the desorbent used. For example, after nitrate desorption, fractional separation of metals from the solution is carried out by gradual neutralization with ammonia. If the metal is eluted with an acidic salt solution, then precipitation is performed by direct neutralization with ammonia. When used for desorption of alkali carbonate, acid additives are used to destroy it before uranium precipitation. The cake obtained after the remaining solution is thickened and settled is separated from the remaining solution by drying and filtering.

### **1.16 Extraction methods**

To process multicomponent productive solutions of PV, it is fundamentally possible to use extraction methods - the extraction of

metal compounds from aqueous solutions, where they are in the form of salts of inorganic acids into organic solutions that are immiscible with water. Compared to sorption technology, extraction has a number of advantages - simplicity of technology, high efficiency and selectivity. It allows you to selectively extract useful components with similar properties and effectively get rid of impurities.

In extraction processes, inert diluents of organic phases (kerosene, hexane, benzene, white spirit, etc.) are widely used. After this stage, the resulting extract (organic phase saturated with metal) is washed with water and subjected to stripping - extraction of the metal from the organic phase, followed by the return of the regenerated extractant to a new extraction cycle. Depending on the properties of the extractant and the stability of the resulting salt, ordinary water or water slightly acidified with nitric acid (hot), concentrated or diluted hydrochloric and fluoric acids, table salt, sodium and ammonium carbonate are used for re-extraction. Particularly pure final products are obtained when re-extraction is carried out in the solid-phase version.

Depending on the concentration of useful components and the required quality of the finished product, it is possible to combine sorption and extraction methods, as well as the use of several stages of sorption and extraction in the process of obtaining the finished product.

### **1.17 Precipitation methods**

Precipitation methods for processing productive solutions are usually implemented at the final stages of the technological process. The precipitation reagent must be cheap and available. Ammonia or alkaline precipitation methods are used to isolate components from purified acidic solutions, such as uranium. When a solution of  $\text{NH}_4\text{OH}$  or  $\text{NaOH}$  is added to a solution of uranyl salt, as the pH increases, hydroxouranyl complexes are formed with varying degrees of polymerization, which depends on the pH of the medium and uranium concentrations. When alkali or ammonia is added to a solution of uranyl sulfate, nitrate, or chloride, what usually precipitates is not uranyl hydroxide, but the corresponding salt of uranium acid (diuranate, more precisely polyuranate). This has certain advantages for further processing of the precipitate to obtain (by calcination) uranium oxide.

Uranium can be extracted from carbonate solutions by several precipitation methods, in particular: acid decomposition (acidification, precipitation of sodium diuranate with ammonia, calcination), decomposition of sodium uranyl carbonate salt with excess sodium hydroxide (the resulting precipitate of sodium diuranate is filtered off), etc.

### **1.18 Technology for extracting molybdenum from UL solutions**

Sorptive extraction of molybdenum from sulfuric acid media, including together with uranium, has been quite well studied and is successfully used in industrial practice.

It has been established that with a decrease in the concentration of sulfuric acid in the solution, the exchange capacity of anion exchangers for molybdenum increases, and the sorption front decreases.

According to the efficiency of ion exchange extraction of molybdenum from solutions

pH-1-2 (equilibrium concentration of molybdenum is about 0.1 g/l) known ion exchangers are arranged in a row:

BP-IAp		AM		
BP-Ip	>	MP	>	AFI-22
AM-p		BP-3Ap		
		AM-26		

Desorption of molybdenum can be effectively carried out with aqueous solutions of ammonia (30 g/l NH<sub>4</sub>OH), while the addition of NO<sub>3</sub> to eluents improves the process performance. Ammonia solutions containing ammonium sulfate can also be used for desorption of molybdenum. The finished product is obtained in the form of technical ammonium paramolybdate with a molybdenum content of more than 20%.

### **1.19 Technology for extracting rhenium from UL solutions**

Sorptive extraction of rhenium from UL solution is carried out using both ion-exchange resins and activated carbons. Sorption of perhenate ions is most effectively carried out by resins from solutions at pH=5-6. With an increase in the acidity of solutions to 5-15 g/l, their working capacity for rhenium decreases by 8-10 times, especially in the region of its low equilibrium concentrations. Sorbents based on the efficiency of rhenium extraction from solutions can be

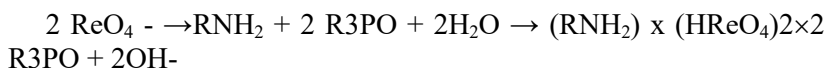
as follows: VP-1p>AM-3>AN-21>AM(AM-p)>activated carbons. One of the productive rhenium sorbents is the anion exchanger VTs-14KR, the elution of rhenium from which is carried out with ammonia.

With sufficiently high rates, rhenium can be extracted from acidic, alkaline and neutral solutions by extraction. The existence of rhenium in aqueous solutions only in the form of perrhenate ions determines the use of organic solvents for the extraction of anions (aliphatic, amines, quaternary ammonium bases and alkyl phosphates) for their extraction.

Rhenium is extracted from sulfuric acid solutions with aliphatic alcohols, ketones, amines, and TBP, depending on the ion concentration.

For the extraction of rhenium from carbonate media, a mixture of ANP -2 + FOR is widely used, and at pH = 11 - ANP -2 + TBP + FOR, which allows in one stage to double the extraction of rhenium in comparison with the mentioned double mixture of extractants, bringing it up to 92%.

In this case, rhenium extraction proceeds according to the equation:



Re-extraction of rhenium by approximately 90% can be accomplished in one stage with an ammonia solution. The finished rhenium product is ammonium perrhenate grade AR-O.

### **1.20 Technology for extracting vanadium from UL solutions**

The extraction of vanadium from solutions to obtain its technical compounds is carried out by sorption, extraction and precipitation methods, and the last two are usually used when processing solutions that are relatively rich (10-200 g/l) in vanadium. When processing its poor (less than 1 g/l) solutions, sorption technology is preferable.

When extracting vanadium with anion exchangers VG1-1p and VG-1 Ap from sulfuric acid

media with a pH of 1.6-1.8 (after preliminary sorption of uranium from them), the degree of vanadium extraction is -90%. Its desorption with sufficient completeness can be carried out with aqueous solutions of ammonia.

The elution of vanadium from the VP-1Ap anion exchanger is improved by adding mineral salts, in particular  $(\text{NH}_4)_2\text{SO}_4$ ,  $\text{NaCl}$ , to desorbing ammonia solutions.

$\text{VO}^{2+}$  ions, which are stable in aqueous solutions, are sorbed from sulfate and chloride solutions by cation exchangers, for example KU-2.

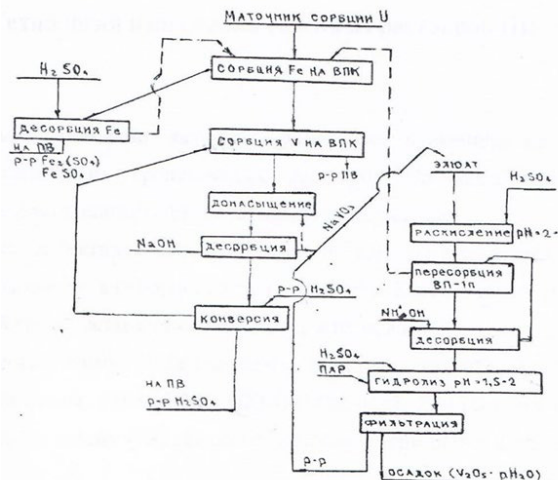


**Fig. 8.** Schematic diagram of the associated extraction of vanadium from underground uranium leaching solutions

Cation exchangers practically do not sorb vanadium either from dilute alkaline media or from solutions obtained by acidification to relatively high concentrations due to the presence of vanadium, respectively, in the form of negatively charged particles.

### 1.21 Technology for selenium extraction from UL solutions

The main methods are physical and chemical. For the extraction of selenium from productive UL solutions, chemical methods are currently the most acceptable and tested.

The sorption of selenium from carbonate solutions is most effective if it is in an oxidation state of 6. The capacity of VP-1A resin in a carbonate environment is about 88 mg/l, in a neutral environment - 130 mg/l.

Selenium is also quite efficiently extracted from sulfuric acid solutions into resins:  $\text{AN} > \text{AN-2F} > \text{EDE-10P} > \text{AV-17x8}$ . For all anion exchangers, sorption for selenium (IV) reaches a maximum at pH-

3, and for selenium (VI) decreases at pH = 1-3 and remains constant at pH more than 3. The capacity of anion exchangers is high (170-700 mg/l).

Ampholytes may be of practical interest for selenium sorption. This direction is fundamentally possible for the redistribution of selenium solutions (Zhalgasuly et al., 2018).

For the desorption of sorbed selenium, acids (hydrochloric and sulfuric), anion exchangers AM, AMP, VP-1Ap, EDE-10P etc. are used; Selenium is well desorbed by alkali solutions.

When obtaining high-purity selenium from hydrochloric acid solutions, it is possible to use cation exchanger KU-2, Dauex-50 and anion exchanger AI-1, AV-17×8, Dauex-2.

### **1.22 Technology for extracting scandium, yttrium, lanthanides from UL solutions**

Scandium and rare earth elements are extracted from leaching solutions of ore concentrates by a combination of sorption and extraction methods: the elements are concentrated on a strong acid sulfation exchanger KU-2, and then separated and purified by extraction of TBP from nitric acid eluates.

The extraction of scandium from very poor (up to 1 mg/d) sulfuric acid productive solutions of UL is most effectively carried out according to a combined scheme using sorption and extraction methods.

To extract scandium from poor UL solutions, it is effective to use anion exchangers such as AMP, VP-Ap and VP-3Ap. Experiments have shown that during the sorption of scandium from sulfuric acid solutions (pH - 1.6-2.2), its 75% recovery can be achieved when the anion exchanger is saturated with AMP to 0.3-0.4 kg/t, and with subsequent desorption of scandium Using nitric-sulfate solutions, obtain eluates containing up to 40 mg/l.

The principle scheme for extracting useful components from complex UL solutions involves first removing uranium (according to one of the known methods), then scandium, and then yttrium and lanthanides.

As experiments show, the sorption of scandium from sulfuric acid solutions of UL containing only 0.1 - 0.7 mg/l Sc should be carried out on apholytes of the API type (API-21 and API-22). At pH 1.2-2.5, the capacity of ampholyte API-22 for scandium reaches 0.2-0.5

kg/ton of sorbent. Carbonate ( $\text{Na}_2\text{CO}_3$ ) desorption of scandium and its subsequent resorption onto API-22 from deoxidized eluates makes it possible to concentrate up to 30-40 mg/l. which is sufficient for subsequent effective extraction and purification of scandium from impurities.

Primary scandium concentrate with a  $\text{Sc}_2\text{O}_3$  content of 1 to 5% can be obtained directly at IP facilities. Its further processing is recommended under stationary conditions at any of the processing plants in the industry, where, depending on the requirements for the finished product and using existing extraction, precipitation and sorption methods, scandium oxide corresponding to the SKO-3, OS-1, SKI-3 grades is obtained.

Available technical and economic studies allow a minimum on-board concentration of scandium in productive UL solutions at the level of 0.1 mg/l.

The concentrations of the sum of rare earth elements and yttrium in UL solutions are usually low and amount to 5-25 mg/l, less often - 55-60 mg/l.

For the sorption of rare earth elements from ISL solutions from the available set of sorbents, cation exchangers KU-2 are preferred; KU-2 x 8N; KU-23.

Desorption of lanthanides is carried out with a sulfate-nitric acid solution. The extraction cycle of solutions is carried out using synthetic fatty acids, dioctyl methylphosphonate in hydrocarbons and other extractants to concentrate the amount of P3E and remove impurities. Re-extraction is carried out with solutions of nitric acid, nitric acid, technical water. An ammonia solution is used to precipitate divalent metals from the strip extract.

The finished product is obtained in the form of a hydrate cake with a total lanthanide and yttrium content of about 20-28%. Subsequently, at one of the hydrometallurgical enterprises, the hydrate cake is dissolved in nitric acid, followed by complex extraction purification of rare-earth metal nitrates and the separation of individual lanthanides, and then the production of rare-earth metal concentrate of the cerium group, neodymium oxide (NOK-1), concentrate P3M of the yttrium group, neodymium oxide (ItO-Lum), samarium and europium concentrate, gadolinium and lutetium, samarium oxide (SMO-M), europium oxide (EvO-Zh). The most important indicator

of the profitability of hydrate cake production and especially its further processing is the concentration of the amount of P3E in UL solutions (usually not lower than 15-20 mg/l) and individual elements.

### **1.23 Technology for extracting copper from UL solutions**

Sorption technology for extracting copper from solutions is best carried out using an ion exchanger and extraordinary sorption-desorption equipment, developed and tested in industrial conditions by specialists of the Tselinny Mining and Chemical Combine at the KV and UL facilities. The results of desorption of various metals obtained on an SDK column are several times higher than their concentrations in commercial reclaims achieved on traditional desorption columns.

The main operations of the technological scheme for processing productive solutions of heap or underground leaching can be called the following.

Sorption of copper from productive solutions is carried out on ampholyte ANBK-35 in columns of the SVNK-2400 type and, partially, in SDK-1500 columns. The copper sorption capacity of the ion exchanger is 40-50 g/kg, the copper content in the sorption mother liquor is 35-45 mg/l. It is planned to saturate the sorbent with copper in one of the branches of the SDK-1500 column.

Desorption of the fully saturated ion exchanger is carried out with a sulfuric acid solution, which makes it possible to obtain a sulphate regenerate rich in copper, suitable for subsequent extraction of copper by electrolysis or cementation, or separation of copper sulfate.

The technological scheme for processing productive solutions does not have liquid and solid discharges. All solutions are in circulation and do not enter the environment. To ensure the cleanliness of the air basin, the scheme excludes airlift pumping of ion exchanger with sulfuric acid solutions.

### **1.24 Practical results**

The fundamental basis of the method of geotechnological extraction of metals in Kazakhstan was the sulfuric acid method of uranium extraction by borehole systems, developed and implemented in the late 70s and early 80s.

As already indicated, it is difficult to overestimate its revolutionary role both in the development and dramatic expansion of the republic's mineral resource base, and in the creation of a technologi-



cally new, science-based progressive direction in the development of scientific and technological progress.

The first, not entirely successful, experimental work on underground leaching of uranium was undertaken in 1973-1975. at small uranium deposits of the South Kazakhstan region of Kyzylkol and Chayan by the Leninabad Mining and Chemical Combine and the Krasnokholm expedition. The complex geological conditions of these deposits, the lack of necessary experience, the lack of specific equipment and materials in the mining industry of those years, etc. became the reason that the results of the experimental work were not very promising.

However, the undoubted attractiveness of the IP method and certain successes of these studies achieved in neighboring Uzbekistan served as the basis for the launch in 1977 of full-scale, methodically developed pilot work at two large deposits in Kazakhstan - Uvanas and Northern Karamurun.

The Uvanas deposit had ideal geological and technical features for the underground leaching method, and Northern Karamurun was then the deepest deposit in the world where uranium geotechnology was tested.

Upon completion of more than successful pilot tests, both of these deposits were involved in industrial development and a few years later, on their basis, the first large UL mines were built - Stepnoye in the Suzak region of the South Kazakhstan region and Mining Department No. 6 in the Kyzylorda region. These enterprises are successfully operating to this day.

During these same years, the Volkov expedition, together with the Kyrgyz Mining Combine, successfully carried out a full-scale experiment on underground leaching of uranium in the Eastern section of the Mynkuduk deposit, which is unique in terms of reserves, which since 1985 has become the second operational mine of the Steppe RU.

The large Kanzhugan deposit, discovered in the 70s by the Volkov expedition, became the raw material base for the organization of another mining operation in the UL - Central.

Thus, by the mid-80s in Kazakhstan, as part of a fairly powerful, previously created uranium mining sub-industry, a fundamentally new industrial type of enterprises was formed that successfully ex-

tracted uranium using the underground leaching method. Until the beginning of the 90s, production volumes at these mines were constantly increasing and already accounted for about 50% of the total uranium production in the republic.

The introduction of a new progressive method of uranium mining and the creation of a large and long-term raw material base for it constantly reduced the competitiveness of both other types of uranium deposits and existing mining operations, which were significantly inferior in profitability to underground leaching. With the fall in uranium prices around the world in recent years, the profitability of developing a number of deposits using the traditional mining method has sharply decreased, and as the economy of Kazakhstan transitioned to market relations, most of the mines and mines here were mothballed.

To date, almost all of the uranium produced in the republic is mined by underground leaching. Since the organization of the first, quite modest in terms of production volumes, pilot tests of this method, to this day Kazakhstan is one of the leaders in uranium mining.

In this regard, it is very indicative to compare the role of underground uranium leaching in the overall production of uranium in the republic and in the world as a whole. As can be seen from Fig. No. 2, its share in the world does not exceed 15% of total production and does not yet have a noticeable tendency to increase. This situation is, first of all, evidence of the uniqueness of the republic's mineral resource base, where, as stated earlier, about 10% of all available uranium reserves are suitable for mining using this method, as well as a fairly developed production infrastructure that carries out the IR process.

In some years, Kazakhstan ranked first in the world in terms of uranium mining volumes using the UL method and retains its leadership to this day; moreover, NAC Kazatomprom's immediate plans provide for a sharp increase in production volumes based on the modernization of existing and the creation of new in-situ leaching facilities.

Over the past two decades of intensive development of the uranium irradiation method, mining and geological exploration organizations of the republic have accumulated enormous practical and theoretical experience in this area.

In addition to improving the geotechnological uranium theme, already at the first stages of operational and experimental work it was established that in productive solutions, together with uranium, industrially significant concentrations form some valuable rare elements: rhenium, scandium, vanadium, lanthanides, selenium, yttrium, etc., which caused In life, a whole area of research is the selection of geotechnological techniques and methods that provide the possibility of the most comprehensive extraction, the development and implementation of methods for obtaining commercial concentrates of associated components for uranium processing plants, and much more related to this problem.

All this, naturally, could only be carried out on the basis of a thorough study of the complex geochemical transformations occurring both at the stage of complex uranium ore formation, and directly during the process of active leaching itself. The basic testing grounds for these studies were numerous experiments carried out in dozens of deposits at the stage of geological exploration, as well as during the exploitation of such elements as rhenium scandium, vanadium and rare earth metals that had already been produced on an industrial scale.

For this purpose, at all operating UL enterprises, installations were designed and built to extract associated useful components from productive solutions. In some fields in the south of Kazakhstan, extraction was organized by borehole leaching, for example, of lanthanides and vanadium, where uranium was already regarded as an associated component. For the first time in world UL practice, pilot industrial production of selenium, etc., was carried out at the Northern Karamurun deposit.

At each stage of the enterprise's scientific and technical activities, the latest achievements of world and domestic science and technology were used when choosing directions and methods of work. This became possible thanks to the high qualifications and professionalism of the majority of specialists, many of whom defended dissertations on this topic, made dozens of inventions, received patents, and wrote numerous scientific publications.

The authors of this work were direct participants in this long process, holding various positions at the level of chief specialists in scientific institutions since the early 70s.

The destruction of the entire economic system and the severance of scientific and practical ties, with the collapse of the Soviet Union, sharply reduced interest and demand for many rare useful components, and the general global drop in prices for non-ferrous metals in recent years has made their extraction, even incidentally the main production of uranium, unprofitable. Recently, however, there has been a tendency for world prices to increase for such metals as rhenium and vanadium, therefore NAC Kazatomprom does not include in its plans for the coming years, given favorable market conditions, the continuation of their associated production.

Significant volumes of solutions productive in uranium and other components at operating UL enterprises, despite their relatively low concentrations, make it possible to extract hundreds of tons of uranium, hundreds of kilograms of rhenium and scandium, the first tens of tons of yttrium and lanthanides, tens and hundreds of tons of vanadium per year from each developed multi-element deposit. The profit from extracting from the subsoil the entire possible complex of useful components at just one UL enterprise can amount to millions of dollars.

The use of the leaching process as one of the most currently developed geotechnological methods for mining minerals can significantly improve the technical and economic performance of existing mining enterprises.

The relevance of underground leaching, for example, of Zhezkazgan ores using various technological schemes described in this work, is confirmed by a number of patents issued recently in Kazakhstan.

Thus, in one of the latest technical solutions, based on an optimal combination of means, methods and processes that ensure resource-saving use of mineral raw materials, a new technology for selective mining and processing of ore mass using traditional and geotechnological methods has been developed in relation to the conditions of the Zhezkazgan deposit.

The essence of the developed technology is to separate the broken ore in the working face into two ore flows:

One with a low metal content (0.4-0.6%) and the other with a higher one. In this case, sorted higher-grade ore is transported to the surface for subsequent beneficiation, and ore with a low metal con-

tent is subjected to leaching in underground conditions, followed by processing of the solutions using hydrometallurgical methods.

The authors' calculations show that processing ore with low copper content that has already been crushed and left in the mine workings by leaching will increase the total profit of LPA "Kazakhmys" by no less than 3-5%.

### **Conclusion**

The development and improvement, based on many theoretical and applied studies, of the method of borehole underground leaching and metals described in this work is the result of the creative efforts of a large number of specialists in various fields of knowledge both in the republic and abroad.

Over the past two decades, specialists from the mining institutes named after D.A. Kunaev, NAC Kazatomprom of Kazakhstan, geological prospectors, operators, representatives of fundamental and applied science have made perhaps the most significant contribution to the development of this progressive direction of scientific and technical improvement.

The result of this was a radical restructuring of the uranium mining industry of the republic and Kazakhstan becoming a world leader in the use of geotechnological methods of mining in mining. Over the years, no other country in the world has produced as much uranium and its accompanying useful components using the UL method as Kazakhstan.

In recent, difficult times for all metallurgists in the world, when prices for almost all non-ferrous and rare metals have fallen and there is a widespread decline in mining production, the basis for maintaining and even increasing the volume of production of uranium, copper and rare metals for the republic will be the widely introduced highly profitable geotechnological method of IR.

In 1998, NAC Kazatomprom, together with the Academy of Sciences of the Republic of Kazakhstan and other scientific and production organizations, developed the "State Program for the Develop-

ment of Nuclear Energy and Industry of the Republic of Kazakhstan until 2030,” which received approval from the Government.

The basis for the development of the uranium industry, laid down in the program, is the systematic expansion of natural uranium production, using underground leaching methods, which will allow the country in a few years to take one of the first places in the world in the production of uranium compounds.

The widespread introduction of borehole underground leaching methods in general at the Zhezkazgan ore field will significantly improve the main technical and economic indicators of this important industrial facility for the republic.

All this, along with the purely scientific value of the research presented in the work, will help accelerate the economic and social development of Kazakhstan in accordance with the strategy of the 2030 Program.

The article was prepared within the framework of grant funding for scientific and (or) scientific and technical projects "Technology for obtaining an adaptogen drug based on humates from coal and extracts of wild plants to create a sustainable vegetation cover on man-made objects 2022-2024 y. (AP14871298)

### *References*

1. **Zabaznov V.L., Yazikov V.G.** (1998) Opyt reabilitatsii rudovmeshchayushchikh vo-ponosnykh gorizontov posle podzemnogo vyshchelachivaniya urana gidrogeokhi-kucheskimi metodami. Kazakhstanskii kruglyi stol po chistomu proizvodstvu. Almaty, 29.11 - 2.12 1999, 8 s.
2. **Yazikov V.G.** Geologo-promyshlennyye tipy mestorozhdenii urana Respubliki Kazakhstan i perspektivy vkhozheniya v mirovoi uranovyi rynek. Tomsk, 1995.- 82 S.
3. **Zabaznov V.L., Yazikov V.G.** (2000). Experience of restoration of Bearing aquifers In-Leach (ISL) Uranium Mining by hydrogeochemical methods. International Symposium on the Production and Environmental // Viena. Austria 2-6 October 2000 (Book Extended Synopses) – JAEM-SM-P. 169-170.
4. **Zhalgasuly N., Ismailova A.A., Bektybaev U.A.**(2023). Intensifikatsiya protsessa kuchnogo vyshchelachivaniya mednykh rud Zhezkazganskogo mestorozhdeniya//Mezhdunardonaya nauchno-prakticheskaya konferentsiya «Innovatsii v gornodobyvayushchei promyshlennosti»,posv.pamyati akademika Inzhenernoi

akademii Kyrgyzskoi Respubliki, d.t.n., professora Mambetova Sh.A.- Bishkek, 2023.-S.138-144

5. **Metaksa A.S., Izbai A.I., Bektibaev U.A., Metaksa G.P., Ismailova A.A.** (2023) Obosnovanie novykh tekhnologicheskikh priemov dobychi rud vyshchelachivaniem // 16 Mezhdunarodnaya nauchnaya shkola molodykh uchenykh i spetsialistov. «problemy osvoeniya nedr v xxi veke glazami molodykh»- Moskva, 2023.-S.376-378

6. **N. Zhalgasuly, A.A. Asanov, S.V. Efremova, U.A. Bektibaev, A.A. Ismailova** (2023). The significance of modern brown coal processing technologies for the development of agricultural production and public heat power. Известия НАН РК. Геология и технические науки, ISSN 2224-5278, Volume 6 (462).-2023, Pp. 89-100.

7. **K.Ch. Kozhagulov, N. Zhalgasuly, U.A. Bektibaev, A.A. Ismailova.** (2023). Zavisimost' izvlecheniya metalla ot kharaktera drobleniya// Sovremennye problemy geomekhaniki. Nauchno-tekhnicheskii zhurnal № 52(2),2023.-S.55-70

8. **K.Ch. Kozhagulov, N. Zhalgasuly, U.A. Bektibaev.** (2023). Pererabotka khvostov obogashcheniya Zhezdinskoi obogatitel'noi fabriki vyshchelachivaniem//Sovremennye problemy geomekhaniki. Nauchno-tekhnicheskii zhurnal № 52(2),2023.-S.3-20

9. **K.Ch. Kozhagulov, N. Zhalgasuly, U.A. Bektibaev.**(2023).Pererabotka svintsya i tsinka iz otval'nykh rud Karagailinskogo mestorozhdeniya// Sovremennye problemy geomekhaniki. Nauchno-tekhnicheskii zhurnal № 52(2),2023.-S.20-34.

10. **Zhalgasuly N., A.A. Ismailova, G.K. Kazbekova.** Podzemnoe vyshchelachivanie medi s napravlyennym gidrodinamicheskim potokom rastvoritelei (2020).// Institut geomekhaniki i osvoeniya nedr NAN Kyrgyzskoi Respubliki. Nauchno-tekhnicheskii zhurnal №41(3).- Bishkek-2020.-S.65-79

11. **Bektibaev U.A.** Metody podgotovki rudy k vyshchelachivaniyu (2023). Mezhdunarodnoi nauchno-prakticheskoi konferentsii «Innovatsii i kompleksnaya pererabotka mineral'nogo syr'ya –aktual'nye sostavlyayushchie diversifikatsii ekonomiki», posvyashchennoi 30-letiyu Natsional'nogo tsentra po kompleksnoi pererabotke mineral'nogo syr'ya Respubliki Kazakhstan.-Almaty, 2023.-S. 113-115.

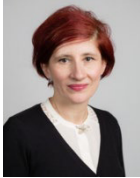
12. **Zhalgasuly N., Skripchenko L N.** i dr. Ratsional'noe ispol'zovanie mineral'nykh resursov Zhezkazganskoj oblasti (1995) // V sbornike «Nauchno-prakticheskaya konferentsiya posvyashchennaya 25-letiyu ZhNIPItsvetmeta " chast' Zhezkazgan, 1995.

13. **Zhalgasuly, N., Kogut, A.V., Ismailova, A.A.** (2018) Study of leachability of zhezkazgan deposit copper ores Mining Science and Technology (Russian Federation), 2018, (2), страницы 14–20.

14. **Zabaznov V. L., Dzhakishev M.E., Yazikov V.G.** Uranovaya promyshlennost' Kazakhstana: v XXI vk -navstrechu miru, svobodnomu ot yadernogo oruzhiya. Tezisy mezhdunarodnoi konferentsii, Almaty, 29.07.-10.08.2001.-S. 74-75.

15. **Zabaznov V. L., Yazikov V.G.** Opyt reabilitatsii rudovmeshayushchikh vodonosnykh gorizontov posle podzemnogo skvazhinnoho vyshchelachivaniya urana gidrokhimicheskimi metodami. Tezisy dokladov mezhdunarodnogo simpoziuma po geologii urana. Uran na rubezhe vekov: prirodnye resursy, proizvodstvo, potreblenie. -M.-2000.-S. 178-180.

## REVIEW OF ENERGY INVESTMENTS FOR STRENGTHENING RESILIENCE IN ENERGY SYSTEM



**Maria Daniela STOCHITOIU**  
Associate Professor,  
University of Petrosani, Romania



**Ilie UTU**  
Associate Professor,  
University of Petrosani, Romania

**Abstract.** The provoked shock in the energy system came into a moment in which climate impact is more and more visible and took several types. The rise of prices has determined economic incentives for increasing the offer and for choosing the alternative or more efficient ways to satisfy the demands. The shocks due to energetic security have created strong incentives for politic decisional factors for reducing the dependences and vulnerabilities, but in the same time for a lot of developing countries, the financial resources are depleted. The last years were a period of extreme perturbation for energy sector.

### 1. Introduction

EU governments and decisional factors are still discussed how best to contain the dramatic impact of high energy prices on households, industry and the whole economy, when winter has come [1],[2]. In the same time the European Commission has indicated its intention to formulate proposals for longer-term adjustments to Europe's current electricity market design, the importance of distinguishing between short-term crisis management and long-term market reform initiatives.

It has to take into account the capital flows in energy sector and the way in which investors can evaluate the risks and the opportunities in all supplying domains with combustible and electrical energy, critic minerals, efficiency, research and also finance in energy domain.

The characteristics of climate crisis solutions are:



- the current policies which consolidate incentives for green energy costs;
- the energy security perspectives;
- general pressure above costs and inflation;
- the major increase of incomes to traditional suppliers due to high prices of fuels;
- growing expectations that the investments will be aligned to climate crisis solutions.

The recovery due to Covid-19 pandemic and the answer to global energy crisis have given a significant boost for investments in clean energy. As well, it is essential to distinguish between pure market project elements and complementary mechanisms aiming to address remaining market failures [2],[3].

The future investments have to shape a European electricity market that is resilient to shocks and supports the accelerated implementation of renewables over the next three decades.

## **2. Review of energy investments**

The annual investments in clean energy have risen faster than investments in fossil fuel between 2021 and estimated for 2023 (24% for green energy and 15% for fossil fuel). This analyse emphasises the way in which the intense volatility period on fossil fuel market has accelerated the impulse behind technological investments in clean energy caused by the Russian invasion in Ukraine. Wartime interventions should be proportionate, short-term and reversible, while sensible long-term reform proposals that support the energy transition may not help with the current crisis.

It is estimated that were invested about 2800 billion of dollars in energy in 2023. More than, about 1700 billion of dollars were invested in clean energy, included the renewable resources, nuclear, energy storage systems, the combustible with low emissions, increasing efficiency and final energy using from renewable sources and electrification. Only 1000 billion of dollars were allocated for fossil fuel and electrical energy supply (15% for hard coal and lignite and 85% for petroleum and gas). For every dollar spent of fossil fuel about 1,7 dollars are spent for green energy. Five years ago, the percentage was 1:1. During the global energy crisis, the investments in renewable energy, grids and energy storage systems have been accelerated

but the capital costs for energy generated from fossil fuel were increased (fig. 1).

The investments in energy sector have increased with 12% in 2022, and for the first time overtook about 1000 billion of dollars and increasing was about 1200 billion of dollars in 2023.

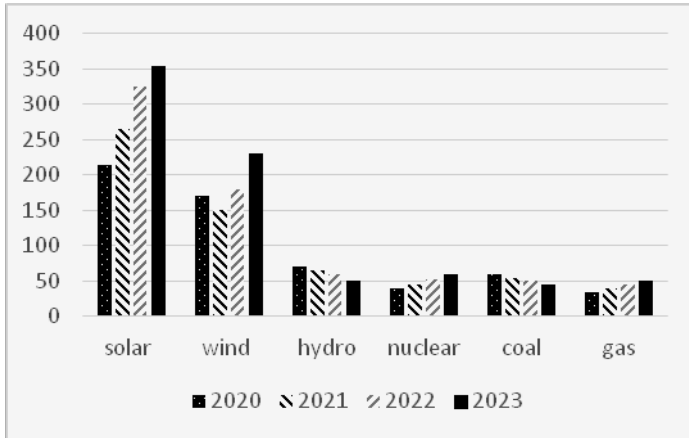


**Fig. 1.** Electric energy global annual investment (billions of dollars) for different technologies

The abundant incomes and also the increased prices have determined the growing investments in fossil combustibles but of course, the costs are limited by the concerning of costs and demands on long terms. 2022 was an extraordinary year for carburant suppliers and dealers. The Russian invasion in Ukraine has determined growth of gas prices over the record levels all around the world, but the petroleum prices have returned of 2010 level. The net incomes have increased from fossil fuel sales, as the world petroleum and gas industry gained about 4000 billion of dollars.

The increased prices have stimulated a growth of investments in fossil combustible. Taking into account some ratings, the investments in new supply sources based on fossil combustible grow up with 6% till 950 billion of dollars [4],[5].

The world energy crisis has stimulated the costs for efficiency, electrification and final energy from renewable sources with 16% in 2022. Emerging market economies recorded a growth of investments

about 19%, China being the only one which recorded a decreasing of investments in energy efficiency due to continuous jam of Covid-19 and real estate crisis. Also, the growth of investments was made for heat pump installations. The investments in electrification of transport systems were about 60% in 2020 and the electric vehicles sales reached record levels more than ten million of units.

The costs of energy research and developing grow with 10% in 2022 reaching about 44 billion of dollars and 80% of them for green energy domain. It is a trend which push the innovation in spite of macroeconomic doubts (as Net Zero industry Act and Industrial Plan Green Deal). Also, in European Union, Innovation Fund has given a direct financing of 1,8 billion euros for seventeen projects for batteries, Hydrogen, solar energy and wind energy. As a response of actual energy crisis, next budget was doubled at 3 billion of euros.

The financial community has an important role in massive growth of outgoings for clean energy, necessary for fulfilling the climate objectives and for relocation of capital budget without of fossil fuel.

The promotion of sustainable financing is a strong key due to the high number of financial institutes which align the financing to net zero scenarios. The global value of the fund's assets decreased in 2022 but the sustainable funds proved more resistance and recovered at the beginning of 2023 despite of some exits from huge funds ESG (Environmental, Social and Governance).

### **3. Strengthening resilience in energy system**

The extreme climate phenomena are increasing as frequency as the extend challenging damages physical assets to gas transport infrastructure or electric energy infrastructure. The extreme weather conditions affect the renewable discontinuous disponible as wind or solar energy as the energy demand volatility.

The European electrical energy and gases systems also became interdependence due to reaching the net zero objectives for achieving a just transition and a carbon-neutral economy by 2050 requires unprecedented joint efforts, which determines efficiencies in the same time with vulnerabilities resulting from introduced distributed systems.

A reliable and resilience has appeared as a new paradigm applying across many energies sector and infrastructures. Resilience can be defined as the ability of infrastructures to overcome ex-

treme events with minimum disruptions, including duration of the restoration phase system.

Resilience is the essence for European energy transition, which has to resist, to adapt and to fast return when is affected by the climate hazards. So, it is essential to search an answer for how can the European Union settlements and legislations to support and to create incentives for a resistant infrastructure [4].

The Report “Strengthening resilience in European energy system” emphasizes the consequences of hazards due to climate changes and how the extreme climatic events can increase both in terms of frequency and scale, causing serious damage to physical assets such as gas and electricity transport infrastructure. Different ways of bringing the required investments, costs will, however, almost certainly increase the quality and reliability of energy supply Europe accustomed to is to be maintained [3,4,5].

The divergent approaches of national regulatory show there is not a clarity on methodologies regulators use to monitor operators’ resilience assessment and investments, and also in terms of guidance as to the prioritisation of investments to consolidate the resilience.

It has to promote a more comprehensive and more integrated understanding. The European energy regulatory approaches in specific way some resilience features as: energy grid planning; operational system manage; technical performance. This is a good start, but resilience has to be more integrated and defined as an evaluation and mandatory demand, determining strong incentives for investments for limiting the over costs in case of major breakdown. So, it is necessary a larger evaluation domain (as flexibility) and a long-term perspective.

An essential role for network operators remains to identify and evaluate the risks which are the base of investment decisions and plans.

Moreover planning, preparation for urgent situations, restauration and technical performance, the resilience building must be better integrated through cooperation markets level, plus a strong interaction between grid operators and other operators (flexibility suppliers, auxiliar and equilibrium services) which contribute to resilience.

The projects of Intergovernmental Panel on Climate Change should show an extra growth of frequency of hazard while Europe made faces with higher incidence of climate hazard in the last decades (fig. 2).

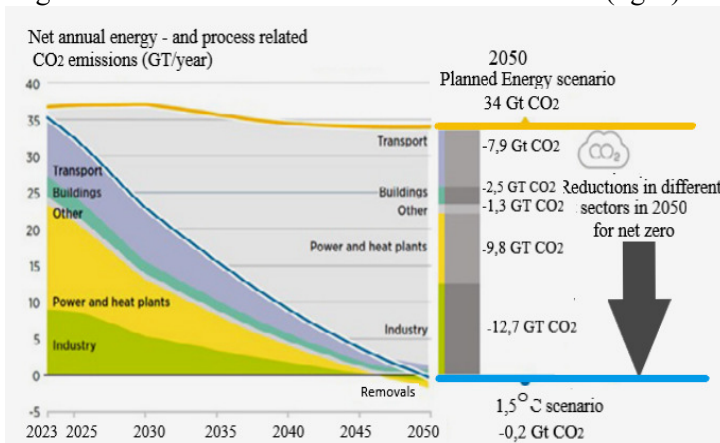


Fig. 2. Estimated trends for CO<sub>2</sub> Emissions for

### 1,5°C Scenario 2023-2050, Source: [www.irena.org](http://www.irena.org)

The impact will be in dependence with the success of climate reduction significant efforts for the global warming to be limited at 1,5°C. The higher levels of warming would have a stronger impact. So, the extreme temperatures phenomena frequency, which can determine a huge risk of forest fire and can affect the underground electrical lines, will increase probably with 50% in comparison with the actual level and more than fourth times without warming; the abundance of rains on shores will increase with 15% and could be probable with 50% more than present warming level of 1°C.

Europe has established the ambitious goal to become neutral from climate point of view till 2050. An intermediary goal is to reduce with 55% the emissions till 2030 in comparison with 1990. European Commission has proposed that the energy percentage of renewable resources to be double into decade from 20% to 40% in 2030 as a component of this goal.

The resilience strengthens and ensuring have necessary of structural steps. The investments are urgent and vital for realise the energy sector resilience as well as functional methods adaptation to “new normality” of extreme events. This reality is relevant in

the climate changes as well as the wartime, energy crisis and the growth of bound of gas and electricity sectors. Due to the increased nature of bounding between the gas and electricity sectors, new gas and electricity resilience metrics may be needed that reflect increasing inter-dependence and feedback between the two sectors and how one sector can support resilience of the other sector.

The resilience of gas systems and electrical systems can be affected by a several factors in the climate changes context.[4] The natural gases system resilience is in dependence with:

- vulnerability to extreme weather events (as suddenly drop air temperature resulting the increase in demand for space heating, hurricane disrupting offshore gas production facilities, etc.) that can increase demand and disrupt supply and delivery infrastructure system;
- the dependence on a limited number of suppliers, transportation routes and storage facilities should increase the risk of supply disruptions due to war and geopolitical situations;
- leakage of methane during production and transportation, which can negatively impact the environment (for example explosion of the Nord Stream offshore gas pipeline).

The electricity system resilience is in dependence with [5],[6]:

- vulnerability to extreme weather events (as hurricanes, heat waves) that can impact power generation, transmission and distribution networks;
- dependence on centralised generation and transmission infrastructure, which can be vulnerable to cascade failure and cause widespread interruptions;
- increasing integration of renewable energy sources, such as wind and solar, which can be distributed and weather-dependent so require additional investments in grid infrastructure and storage solutions to increase resilience.

It is considered that in 2050 Romania will allocate around 10TWh with purpose of suppling the electrolysis for the production of hydrogen; the construction of electrolysis about 1500MW will be required as a production of about 0,2Mt H<sub>2</sub>/year. Making a comparison between emissions the hydrogen produced by electrolysis of water causes the lowest emissions as: solar 1,0kg CO<sub>2</sub> equivalent/kg H<sub>2</sub>; wind 0,5kg CO<sub>2</sub>equivalent/kg H<sub>2</sub>; nuclear 0,6 CO<sub>2</sub>equivalent/kg H<sub>2</sub> and 0,115g nuclear waste; hydro 0,3 CO<sub>2</sub> equivalent/kg H<sub>2</sub>.

The energy efficiency has to preserve the same level of operating, safety and performances for energetical system and some possible measurements could be applied to diminish the energy crisis in Romania [6,7,8]:

- the resources allocation by the central and local authorities for professionalisation and increase of the skills of the workers in the energy field and for combating climate change in the context where investments in these sectors are significant;

- updating by training institutions, including those of higher education, of curricula for energy and environment with an emphasis on cooperation and interdisciplinarity;

- significantly more consistent funding for fundamental and applied scientific research for energy efficiency technologies, renewable sources and low emission mobility;

- partnerships between professional associations with tradition and professional associations with an energy profile for information sessions in the field of energy transition towards decarbonize [9], [10].

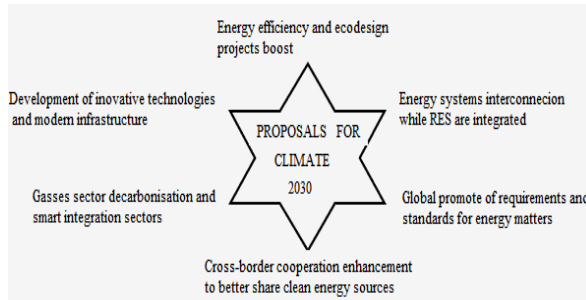


**Fig. 3.** The Romania climate objectives

In the last years, almost of 3000MW were put out of operating another 1475MW till 2025 and 2300 MW will put out of operating till 2030 in Romania.

It has to take account the bound between geography and existed resources of every state or region isolated. Poland and Germany have coal, Denmark, Finland and Romania have access and gas resources off-shore, states from the Carpathian and the Alps have hydroelectric potential as well as the states from North Sea have wind potential or the states from south of Europe have solar potential, so, not all states could have the same energetical mix.

Romania is ready to meet tight deadlines for European funding, increasing energy independence from Russia, decrease the effects of the European energy crisis and decarbonize its economy. In Arad in Romania's west, will be installed the largest photovoltaic plant in Europe as it joined a 1.04 GW project developed by Monsson [6,9,10].

### Conclusions

The existing structure of the European market has produced an integrated, or "coupled," European market where production and distribution are handled by a range of different companies competing for customers. The energy system has to responsibly rethink for assuring the energy independence. The renewable sources alone will not be able to ensure a constant and sufficient level of electricity supply and a flexible balance with classical sources will be ensured, avoiding their elimination before securing a replacement.

In the context of the drastic reduction of oil and natural gas reserved, with consequences on the prices of petroleum production and delays in finding solutions for storage electricity, obtained from renewable sources or the emergence of geopolitical events with major economic implications for national without immediate solutions to equilibrate the balance, coal remains a bridge in the medium term, during which adopting the problems of adapting the new types of resources must be gradually resolved.

While some of the reform proposals for the power market make sense, these won't address the scope of the energy crisis in a timely manner. But speeding up some of them would advance their advantages. Such adjustments must be considered in the medium term in light of the 2030 and 2050 climate goals.

### References

1. [www.energynomics.ro](http://www.energynomics.ro)
2. [www.irena.org](http://www.irena.org)
3. **E. Cazacu**, s.a. (2020) Elemente de calitate și eficiența a energiei în instalațiile electrice modern Editura Matrixrom, București,
  1. [www.energy.ec.europa.eu](http://www.energy.ec.europa.eu)
  2. [www.eurelectric.org](http://www.eurelectric.org)
  3. [www.balkangreenenergynews.com](http://www.balkangreenenergynews.com)
4. **Utu I., Stochitoiu M.D.** (2023), Aspects concerning the energy crisis in Romania, vol. XXV, Annals of the University of Petrosani, Universitas Publishing House
5. **V. Vaida**, (2015) Politici, strategii, dezvoltare, Editura. Agir, București
6. **N. Golovanov**, s.a. (2017) Eficiența energetică. Mediul. Economia modernă, Editura Agir, București
7. **Stochitoiu M.D, Utu I**, (2022) Challenges of the European energy transition, vol XXIV, Annals of the University of Petrosani, Universitas Publishing House



**MANAGING THE LOCALIZATION PROCESS  
POLLUTION WITHIN THE INFLUENCE OF LANDFILLS  
MINING PRODUCTION LOCALIZATION OF POLLUTION  
WITHIN THE LIMITS OF INFLUENCE OF MINING DUMPS**



**Ruslan ZHOMYRUK**

Candidate of Technical Sciences, Associate Professor, Associate Professor of the Department of Automation, Electrical and Computer Integrated Technologies, National University of Water and Environmental Engineering, Ukraine

**Abstract**

As a result of the intensive development of science and technology, a large number of various industries, which use the most modern technologies, have emerged. The complexity of technological processes increases the risk of situations that can cause irreparable damage to the environment. Therefore, the primary task of modern times has become the prevention of environmental problems and the reduction of the consequences to which their appearance may lead, or has already led. In particular, one of the important issues that need to be solved as soon as possible is the protection of underground sources from pollution that gets there as a result of active industrial activity of mankind, which significantly affects people's health.

Thus, managing the process of localization of soil and groundwater contamination is an important and urgent task. Its solution will increase the reliability of engineering systems for the environmentally safe operation of waste storage facilities, which will significantly reduce the morbidity of people within the limits of their influence.

**Introduction**

Ensuring the ecologically safe existence of all natural objects is one of the main problems of modern times. No one doubts this provision, especially since an adequate solution to this issue and its subsequent implementation will ensure not only comfortable living conditions for people and optimal sanitary and hygienic conditions for their production activities, but also the very possibility of the existence of the biosphere. That is why environmental safety is currently considered an integral element of national security, which is very relevant for almost all countries of the world. Various aspects of the problem of environmental safety are the object of attention of many researchers.

Unfortunately, anthropogenic changes have so far affected almost the entire ecosystem of the planet. Trying to actively adapt the environment to their needs, a person with his activity initiates a huge number of not only primary, but also secondary, as well as combined effects, many of which become dangerous for the normal functioning of various components of nature and society. The very emergence and active development of such situations is caused, first of all, by the rapidly growing pace of scientific and technical progress without sufficient consideration of the objective laws of development and renewal of natural resource complexes, which brings increasing pollution of the environment and destruction of natural landscapes. In many areas of the world, the threshold of invariance of natural objects has already been crossed, as a result of which the dynamic balance of the environment has been disturbed, as human activity has come into conflict with nature itself.

### **1. Ecological condition of soils and groundwater in the areas where man-made dumps are located**

The problem of coordination of relations between production, on the one hand, and nature, on the other, becomes central to ensuring the environmentally safe existence of all its components. At the same time, it should be noted that compliance with these provisions is useful not only for the biosphere: the use of the principles of sustainable development of the environment in the formation of the strategy of any enterprise helps to achieve an optimal combination of economic and non-economic goals, which is a necessary condition for its long-term and successful functioning.

Ukraine, unfortunately, is not an exception in this regard, and the problems of environmental security affecting all its regions are no less, and sometimes more acute, than in other countries of the world, since the current state of the environment in our country is beginning to acquire negative properties, becoming a direct source of threat to the biosphere itself, as well as to the health and even life of its citizens. The main reason for this situation is still the same: excessive man-made load on natural objects without the appropriate level of environmental responsibility of those who manage the development of production - both agricultural and industrial to the same extent, which is increased by the current economic state of the state. Due to

this, the rate of environmental degradation, and not only in the radius of direct influence of specific enterprises, begins to exceed (and in some areas has already exceeded) the adaptive capabilities of its components.

Pollution of surface and ground water can most often be observed within highly developed regions of both agriculture and industrial complexes. Very often, the presence of harmful substances in groundwater becomes known only after a long time since they entered the soil. One of the reasons why this happens is the slow rate of groundwater movement through aquifers. In soil flows, substances do not mix and spread as quickly as in surface flows. Therefore, pollution can remain for a long time in the form of concentrated localized spots that persist for many years. There are known cases when harmful substances that got under the surface of the soil more than 10 years ago became known only very recently. That is, today's practice can have a significant impact on water quality in the distant future.

In relation to groundwater, until recently, the prevailing opinion among researchers was that the soil creates a protective filter or barrier that does not allow pollution to penetrate deep into the earth's surface and thus protects underground sources from their negative effects. However, when pesticides and other chemical substances were found in groundwater, it became clear that natural filters do not provide reliable protection of underground sources from pollution that enters there as a result of active industrial activity of mankind.

During the development of mineral deposits, their extraction and processing, highly toxic waste is formed, which pollutes the environment, soils and groundwater.

These problems became especially acute during the implementation of the Program for the closure of unpromising coal mines and cuttings. In fact, immediately there were problems related to the flooding and waterlogging of the territories, the expansion of the leakage zones of highly mineralized mine waters, and the deterioration of the properties of rocks and soils.

Due to the fact that mine waters are highly mineralized (average mineralization is  $2.0-4.0 \text{ g/dm}^3$ ) and contain a significant amount of toxic substances, there is a real threat of contamination of aquifers and the fertile soil layer.

The greatest threat to the quality of groundwater is represented by

those organic compounds that are relatively soluble, do not evaporate and do not decompose chemically or biologically. In water, organic substances are eliminated under the action of bacteria. Their decomposition leads to a decrease in the concentration of dissolved oxygen in the water, thereby exposing the ecological balance of the water body to danger.

During the construction of large industrial enterprises, especially chemical ones, there is a need for safe and economical disposal of harmful industrial effluents, often of very high toxicity. This is a very serious problem that must be solved when designing an enterprise.

During the operation of the enterprise, damage to protective hydrotechnical structures may occur, which include: leaching of the cement curtain, formation of karsts at the base of the dam due to chemical suffusion, etc.

As a result of such damage and violations of environmental legislation, soil and groundwater may be contaminated with untreated water, which will inevitably lead to the deterioration of the ecological state of the environment.

Regarding the Rivne region, according to the materials of the geological exploration expedition, there are almost 1,200 stationary sources of potential groundwater pollution in the region. Of the entire mass of particularly dangerous waste generated, only about 2% is reused or disposed of. The lack of centralized points of storage, disposal, disposal and burial of hazardous waste contributes to their accumulation on the territory of industrial enterprises [ 1 ].

Almost 512,000 tons of toxic waste alone was generated in the region, of which 25 tons belong to the first class of danger, 4.29 thousand tons to the second class, which primarily included waste containing formaldehyde, petroleum compounds, polymer resins, etc. . Up to 70% of first-class waste was transferred to other enterprises for further use, and the rest was sent to organized storage facilities. Waste of the second class is less alarming, since most of it is neutralized, and the rest is sent to other enterprises for further use [2] .

The lion's share of toxic waste is made up of substances of the third (0.19 thousand tons ) and fourth (507.0 thousand tons) hazard classes. The third class mainly includes "OPAK" oil from the production of adipic acid, to a lesser extent - sediments after dewatering

sewage sludge, various solvents and dyes. The bulk of waste of this class (98%) is neutralized, the rest is transferred to other enterprises for further use or stored. Waste of the fourth class of danger is represented mainly by phosphorus oxides, which accumulate in phosphogypsum dumps located near the production site of OJSC "Rivneazot" [3].

16.8 million tons are stored in the warehouses of the organized storage of enterprises of the region. toxic waste.

A special threat to the residents of Rivne and surrounding villages, as well as the basin of the Horyn River, is posed by phosphogypsum dumps located on the territory of Rivneazot OJSC, which is 20 km west of Rivne. 98.97% of all waste in the Rivne region is accumulated here. Therefore, solving the problem of industrial waste disposal in the region largely depends on how successfully this problem will be solved at this enterprise [4].

A comprehensive assessment of the state of the soil systems in the areas where waste is located at enterprises and a forecast of the effects of technogenic factors initiated by these objects on them were carried out at this object.

This choice is justified by the fact that the object is the most problematic from the point of view of the ecological situation - the largest repository of solid toxic waste in the Rivne region. This waste of the fourth class of danger is mainly represented by phosphorus oxides. Dumps of phosphogypsum are typical for other objects that pose a threat to soil and groundwater pollution and are suitable for field studies and solving scientific problems related to the prevention of soil and groundwater pollution. The results obtained during the research can be extrapolated to other objects that pose a threat to the environment.

## **2. Review of the methods of forecasting the migration of pollutants in the area of man-made dumps**

According to the studies carried out in the works of such researchers as P. Ya. Polubarina-Kochyna and R. Collins, it is almost impossible to determine the distribution of velocities in the pore space, especially for heterogeneous media. When solving practical problems, it is enough to know only the flow rates, velocities and pressures of the liquid within small volumes, which at the same time are much larger than the pore sizes. For this, you can use the contin-

uous filtration flow model, in which it is assumed that the liquid moves, filling the entire space: both pores and soil particles. Thus, the real liquid flow is replaced by its fictitious filtration flow, which completely fills the entire volume. The flow line of the filtration flow is a line whose tangent at each point coincides with the direction of the filtration velocity.

The basic law of filtration relates the fluid movement speed to the pressure difference  $H$  in the filtration flow. In the differential form, the law has the form

$$V = -K \text{grad} H. \quad (1)$$

The filtering coefficient  $K$  is determined by the formula

$$K = \frac{k\gamma}{\mu} = \frac{kg}{\nu}, \quad (2)$$

where  $\mu$  and  $\nu$  are dynamic and kinematic viscosity;  $\rho$  - liquid density;  $k$  - medium permeability.

If compressibility is neglected, the equation of the filtration flow will be written down

$$\frac{\partial}{\partial x} \left( K \frac{\partial H}{\partial x} \right) + \frac{\partial}{\partial y} \left( K \frac{\partial H}{\partial y} \right) + \frac{\partial}{\partial z} \left( K \frac{\partial H}{\partial z} \right) = 0. \quad (3)$$

Polubarynoy-Kochynoy P.Ya. [7] considered in detail the nonlinear condition on the free surface. The author considered the filtration of a liquid with a free surface above an impermeable water barrier. The equation for the upper free  $z=f(x,y)$  which has a slight slope is written in the form

$$\frac{\partial}{\partial x} \left( Kh \frac{\partial H}{\partial x} \right) + \frac{\partial}{\partial y} \left( Kh \frac{\partial H}{\partial y} \right) + \frac{\partial}{\partial z} \left( Kh \frac{\partial H}{\partial z} \right) + \varepsilon = n \frac{\partial h}{\partial t}. \quad (4)$$

For horizontal waterproofing  $h = H$ , then when  $K = \text{const}$ :

$$K \left( \frac{\partial^2 h^2}{\partial x^2} + \frac{\partial^2 h^2}{\partial y^2} \right) + 2\varepsilon = 2n \frac{\partial h}{\partial t}. \quad (5)$$

Analytical solution of the nonlinear equations (4) and (5) is faced with difficulties of a mathematical nature, although a number of exact solutions have been obtained for a number of one-dimensional problems Berentblatgom G.I. [8]. There are ways to linearize equation (5), for example V.I. Aravin, S.N. Numerov. [9] convert it to an equation of the heat conduction type.

Equation (4) is written for the case of an absolutely impermeable water stop. A "relative water resistance " occurs quite often , due to which a weak movement of liquid through cracks and pores is possible. Flow intensity  $\varepsilon_d$  through the lower boundary (sole of the aquifer) is due to the difference in pressure in the upper and lower - aquifers  $\varepsilon_d = K_0(H-H_1)/t_0$  (Fig. 1). Here  $H_1$  is the pressure in the lower layer,  $K_0$  is the filtration coefficient of the water resistance ,  $t_0$  is its thickness (power).

Taking into account the overflow, equation (4) will be written as follows

$$\frac{\partial}{\partial x} \left( Kh \frac{\partial H}{\partial x} \right) + \frac{\partial}{\partial y} \left( Kh \frac{\partial H}{\partial y} \right) + \frac{\partial}{\partial z} \left( Kh \frac{\partial H}{\partial z} \right) + \varepsilon - \frac{K_0}{m_0} (H - H_1) = n \frac{\partial h}{\partial t}.$$

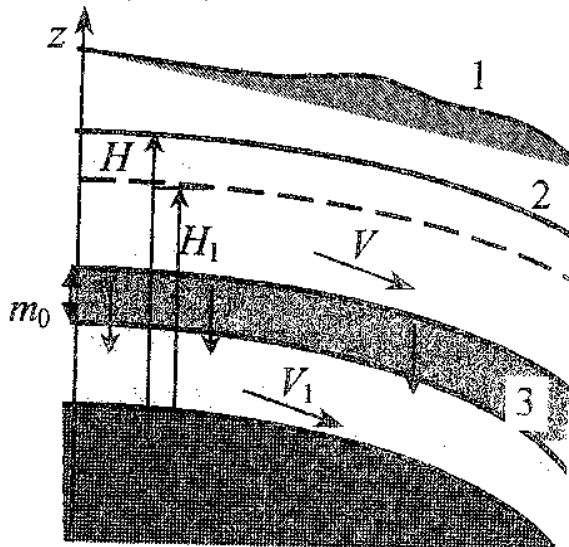


Fig. 1. Scheme of flow through a poorly permeable layer:  
1 - ground surface; 2 - free surface; 3 - poorly permeable layer

Mass transfer in the filtration flow is a set of processes of mechanical transfer of dissolved or emulsified substances, their physical and chemical transformations, and mass exchange with the porous medium. The main factors of mass transfer are: 1) mechanical (forced) convection, 2) hydrodynamic dispersion (convective diffusion), 3) sorption and mass transfer, 4) physical and chemical transformations (decay, formation of new substances) [8].

Under the influence of forced convection, there is a mechanical movement of particles of matter in the form of solutions or colloids along the flow lines of the filtration flow. The speed of movement - of the substance front in the absence of mass exchange with the porous medium is determined by the filtration speed along the flow line  $V(\xi)$  and the active porosity  $n_a$ :  $d(\xi)/dt=V(\xi)$  here  $\xi$  is - a curvilinear coordinate measured along the flow line. A particle of matter will move along the streamline during the time interval  $[t_1, t_2]$  by the distance  $\xi_2 - \xi_1$ , which is determined from the equation [8]

$$t_2 - t_1 = \int_{\xi_1}^{\xi_2} \frac{d\xi}{V^*(\xi)}, V^*(\xi) = \frac{V(\xi)}{n_a}.$$

The heterogeneity of the porous medium leads to the fact that forced convection is accompanied by the formation of a transition zone between the areas of the flow with maximum and minimum concentrations. The intensity of the formation of the transition zone is quantitatively characterized by the coefficient of hydrodynamic dispersion, which is a tensor of the second rank. In a homogeneous porous medium, the longitudinal (along the flow direction) and transverse (perpendicular to the flow) dispersion coefficients  $D_L$  and  $D_T$  are distinguished,  $m^2/\text{day}$ . It was experimentally established [9] that

$$D_L = D_0 + \delta_L |v|, \quad D_T = D_0 + \delta_T |v|, \quad (6)$$

where  $\delta_L$  and  $\delta_T$  are parameters of longitudinal and transverse dispersion,  $m$ ;  $D_0 \sim$  coefficient of molecular diffusion. Longitudinal dispersion, as a rule, is an order of magnitude greater than transverse. Since it is practically impossible to theoretically determine the value of the dispersion parameters, the results of experimental measurements  $D_L$  and  $D_T$  are used when solving practical problems.

Sorption (desorption) is a process of binding (release) of a substance on the surface of a porous medium. Sorption processes are caused by surface phenomena at the boundary of the "liquid-solid" separation. According to the Nernst model (diffusion boundary layer) [10], a thin ( $\mu\text{m}$  particles), practically immobile layer of liquid is formed on the surface of the sorbent grains, where particles of matter from the liquid medium are attracted and retained due to the difference in electric charge.

exchange capacity  $N_0$ ,  $\text{mg-equiv-g}^{-1}$ , which is defined as the



mass of dissolved substance that can be bound (absorbed) by a sorbent weighing 1g. Due to the tortuosity of the pore channels, the presence of dead-end chambers at not the entire capacity is actually used in the exchange. When the particle size of the porous medium decreases, the parameter  $N_0$  increases, reaching several tens of mg-eq /100 g of dry mass of the sorbent in clayey rocks [10].

The parameter of sorption kinetics is the mass transfer rate  $\gamma$ , day<sup>-1</sup>, which is inversely proportional to the duration of the time interval during which equilibrium is established between the solution and the sorbent. During ion exchange, physical adsorption, equilibrium is reached within several hours, during sorption with the formation of chemical bonds - several days [10]. Therefore, mass transfer lasting - months and years is usually described using equilibrium sorption isotherms of the form  $N=f(\varphi)$ , where  $N$  is the concentration of the substance in the sorbent,  $\varphi$  is in the solution. At low concentrations, a fair linear dependence was obtained by A. B. Sytnikov [11].

Non-equilibrium mass transfer, which is described by differential equations of the form  $dN/dt = f(\varphi, N)$ , is generally nonlinear. At low concentrations, Henry's linear isotherm of the form  $dN/dt = \gamma(K_d \varphi - N)$  can be used. When  $\varphi > N/K_d$  ( $dN/dt > 0$ ) sorption occurs, when  $\varphi < N/K_d$  ( $dN/dt < 0$ ) - desorption. Irreversible sorption with strong fixation of a substance by a sorbent can be described by the equation of the form  $dN/dt = a\varphi$ , dissolution and crystallization - by the equation  $dN/dt = \gamma(\varphi_{max} - \varphi)N\beta$  where  $\varphi_{max}$  is the maximum - possible solubility of substances,  $a$ ,  $\beta$ ,  $\gamma$  are empirical parameters of these processes.

The sought-after functions when solving problems of mass transfer in filtration flows are the concentration of the substance in the pore solution  $\varphi$  and in the solid phase  $N$ . When studying the mass transfer of soluble substances in groundwater, along with the equations of filtration, the equations of transport and diffusion, as well as the mass balance of the substance in the elementary volumes of the porous medium.

For a filtration flow, the horizontal dimensions of which are one or two orders of magnitude larger than its vertical dimensions, which is the most common, Rudakov D.V. [10] averaged the concentration of the substance over the thickness of the aquifer and obtained a two-dimensional equation

$$\frac{\partial}{\partial x} \left( D_x \frac{\partial \bar{\phi}}{\partial x} - u \bar{\phi} \right) + \frac{\partial}{\partial y} \left( D_y \frac{\partial \bar{\phi}}{\partial y} - v \bar{\phi} \right) + \frac{q}{m} - q_M - q_d = (1 - n_1) \frac{\partial N}{\partial t} + n \frac{\partial \bar{\phi}}{\partial t}. \quad (7)$$

where  $t$  is the flow depth (thickness of the aquifer);  $q_u$ ,  $q_d$  - mass flows through its upper and lower boundaries;  $u$ ,  $v$ , - filtration speed components;  $D_x$ ,  $D_y$  - dispersion (diffusion) components;  $\bar{\phi}(x, y, t) = \frac{1}{m} \int_{m_0}^m \varphi(x, y, z, t) dz$  - vertically averaged concentration.

Among the problems of underground water dynamics, calculations of drains that intercept filtering (including polluted) groundwater flows have gained great practical importance.

Under the conditions of a steady two-dimensional flow of groundwater for a single well with a constant flow (flow rate)  $Q$ , located in a homogeneous layer of average thickness  $t$  and with a filtration coefficient  $K$  at a point with coordinates  $(x_0, y_0)$ , the distribution of groundwater decline  $H$  is described by equation

$$Km \left( \frac{\partial^2 h}{\partial x^2} + \frac{\partial^2 h}{\partial y^2} \right) = Q \delta(x - x_0, y - y_0), \quad (8)$$

where  $h = H_0 - H_3$ ;  $H_0$  - the level of groundwater formed without the influence of the well;  $H_3$  - their reduced level.

The solution to equation (8), first obtained by Forchheimer for the semi-bounded region  $x > 0$ , on the border of which  $x = 0$  a constant level ( $h = 0$ ) is maintained, has the form

$$h(x, y) = \frac{Q}{2\pi Km} \ln \frac{\rho}{r}, \quad (9)$$

$$r = \sqrt{(x - x_0)^2 + (y - y_0)^2}, \quad \rho = \sqrt{(x + x_0)^2 + (y + y_0)^2}$$

For a group of  $n$  arbitrarily located wells, the distribution of reduction in a semi-confined layer ( $x > 0$ ) is calculated by summing up the reductions from individual wells according to the formula

$$h(x, y) = \frac{1}{2\pi Km} \sum_{i=1}^n Q \ln \frac{\rho_i}{r_i}, \quad (10)$$

Unsteady filtration in the case of a single well is described by the equation

$$Km \left( \frac{\partial^2 h}{\partial x^2} + \frac{\partial^2 h}{\partial y^2} \right) - Q \delta(x - x_0, y - y_0) = \sum \frac{\partial h}{\partial t}, \quad (11)$$

where  $\Sigma = \beta \cdot m$  is the elastic capacity of the pressure layer. It is defined as the ratio of the change in water volume in the aquifer per unit area to the corresponding change in head. The solution of equation (11), first obtained by Theis for an unbounded layer, has the form

$$h(x, y) = -\frac{Q}{2\pi Km} Ei\left(-\frac{r^2}{4at}\right),$$

$$r^2 = (x - x_0)^2 + (y - y_0)^2 \quad (12)$$

where  $a = Kt/\lambda$  - coefficient of piezoconductivity of the layer,  $Ei(\xi)$  - integral exponential function. For a semi-bounded region

$$h(x, y) = -\frac{Q}{2\pi Km} \left\{ Ei\left(-\frac{r_1^2}{4at}\right) - Ei\left(-\frac{r_2^2}{4at}\right) \right\},$$

$$r_{1,2}^2 = (x \pm x_0)^2 + (y - y_0)^2$$

The reduction calculation for a group of wells is performed similarly to formula (10).

In practice, both vertical and horizontal drainage systems are used. Depending on the dimensions of the solved problem, the drain is schematically shown as a point or linear drain [7]. Calculation formulas for linear flow are derived by integrating the corresponding solution for point flow along the drainage contour. For a horizontal drain, the contour of which is given by the equations  $y=f(x)$  or  $x=f(y)$ , it is written

$$h(x, y, t) = \int_{x_1}^{x_2} Q_1(\xi) h(x - \xi, y - f(\xi), t) d\xi = \int_{y_1}^{y_2} Q_1(\eta) h(x - g(\eta), y - \eta, t) d\eta \quad (13)$$

where  $h(x, y, t)$  is the solution of the problem with respect to the decrease caused by the influence of a point flow of unit intensity;  $(x_1, y_1)$ ,  $(x_2, y_2)$  - endpoints of the contour;  $Q_1$  - the specific flow rate of the drain, which can vary along it. Calculations of drainage under various conditions were considered in detail in many works, including V.I. Aravin, S.M. Numerov [9], F.M. Bochever, N.N. Lapshin, A.Ya. Oradovskaya [8], V. S. Usenko [12].

Formula (13) for linear drains is also used to predict flooding, which in urban conditions is often caused by leaks from water and heat supply systems. Then  $Q_l$  means the intensity of leaks, and the

equations  $y=f(x)$  and  $x=f(y)$  describe the position of the section of the water supply line where leaks occur.

When choosing a model for forecasting the spread of pollutants in groundwater flows, the following assumptions can be used. At low concentrations of pollutants, their transfer does not have a significant impact on the dynamics of the filtration flow, so the filtration problem can be considered independently of the migration problem. If the filtration flow is constant, then the migration problem can be solved separately on the basis of a predefined field of filtration velocities. For long-term migration predictions, sorption kinetics can be neglected, and at low concentrations, a linear sorption isotherm can be used to describe mass transfer with a porous medium. Depending on the volume of leaks of solutions containing pollutants, the sources of pollution in groundwater can be schematized as hydrodynamically active and passive. The most complete representation of the spread of pollution in groundwater is given by the field of filtration current velocities, on the basis of which the problem of mass transfer is solved

Preliminary estimates of the zone of groundwater contamination can be made using the "piston model" [9], in which the influence of diffusion is neglected. For a plane-parallel flow between intersections 1 and 2 (Fig. 2) with an average depth  $t$ , the horizontal components of the filtration rate are equal to

$$u = -K \frac{(H_2 - H_1)}{l} - \frac{Q_n}{mn} = const, \quad v = 0.$$

where  $Q_n$  is the filtration flow rate per unit of its width. If pollution begins to flow through section 1 after the moment  $t=0$ , then the length of the zone of pollution at the moment  $t_1$  is  $x_1 = Q_n t / (n_e m)$ , and the time for the pollution front to reach point  $x_\phi$  is equal to  $t_\phi = (n_e m n x_\phi) / Q_n$ . Here the speed of migration  $u_m = u / n_e$ . The concentration at point  $x$  is equal to

$$\varphi(x, t) = \varphi_0 (1 - \theta(t - t_\phi)),$$

$$\theta(\xi) = \begin{cases} 0, & t < 0, \\ 1, & t > 0. \end{cases}$$

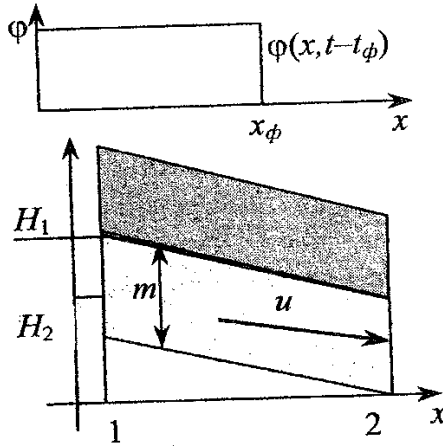


Fig. 2. Scheme of piston displacement in undisturbed unidirectional flow

The migration forecast based on the diffusion model takes into account the erosion of the contamination front. Most of the analytical solutions were obtained for simplified schemes of plane-parallel and radial flows.

A fairly common case is migration in a semi-infinite region, at the entrance boundary of which  $x=0$ , the concentration  $\phi_0$  is set. The process of solute transport is described by a one-dimensional equation

$$D \frac{\partial^2 \phi}{\partial x^2} - u \frac{\partial \phi}{\partial x} = n_e \frac{\partial \phi}{\partial t}. \quad (13)$$

The solution of equation (14) was first obtained by Samuelson [8] and has the form

$$\phi(x, y) = 0.5\phi_0 \left\{ \operatorname{erfc}(\xi - \eta) + e^{4\xi\eta} \operatorname{erfc}(\xi + \eta) \right\}, \quad (14)$$

$$\eta = \frac{u\sqrt{t}}{2\sqrt{Dn_e}}, \quad \xi = \frac{x}{2\sqrt{Dt/n_e}}$$

Numerical analysis [6] shows that when  $D/(ux) < 0.005$  the second term with an error of 4% can be rejected. The coordinate of a point with a concentration of  $0.5\phi_0$  moves with a constant speed  $u/n_e$  which corresponds to the scheme of piston displacement. When the pollution front moves, three zones are formed: 1) a zone of high concentrations close to  $\phi_0$ ; 2) the mixing zone, where the concentration

changes from 0 to  $\varphi_0$ ;

3) uncontaminated zone, where  $\varphi=0$ . The width of the mixing zone  $L$  between the points with a concentration of  $0.99\varphi_0$  and  $0.01\varphi_0$ , which is  $6.6 \sqrt{Dt/n_e}$ , increases over time.

To describe non-stationary mass transfer in two and three-dimensional plane -parallel flows in the presence of continuously operating plane sources of inflow of pollutants, the formulas obtained by F.M. Bochever [8] are used

$$\varphi(x, y, t) = \frac{1}{mn_e} \int_0^t q(t(1-\theta))\varphi_x(x, t\theta)\varphi_y(y, t\theta)d\theta, \quad (15)$$

$$\varphi(x, y, z, t) = \frac{1}{n_e} \int_0^t q(t(1-\theta))\varphi_x(x, t\theta)\varphi_y(y, t\theta)\varphi_z(z, t\theta)d\theta,$$

where  $\varphi_x, \varphi_y, \varphi_z$  - solutions of one-dimensional problems of mass transfer along the  $O_x, O_y, O_z$  axes after "instant" contamination of a local area.

For an unlimited aquifer in terms of  $\varphi_x$  an expression can be used

$$\varphi(x, t) = 0,5 \left\{ erf \left( \frac{x-x_1-u^*t}{2\sqrt{D_x^*t}} \right) - erf \left( \frac{x-x_2-u^*t}{2\sqrt{D_x^*t}} \right) \right\}. \quad (16)$$

For  $\varphi_y$ , you can take the given formula by replacing the corresponding notations. In fig.3 shows an example of the distribution zone of the substance in groundwater, calculated according to the two-dimensional model.

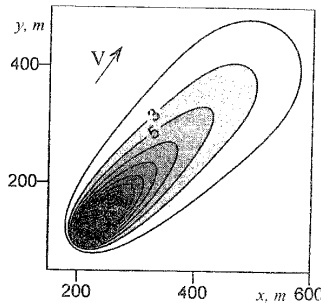


**Fig. 3.** Concentration distribution  $\varphi$  obtained according to the two-dimensional model for a certain moment in time

So, there is a well-developed mathematical apparatus for describ-

ing the migration of pollutants in the filtration streams of groundwater, but their use in each case requires adaptation of the approach to the boundary conditions and physico-chemical features of the object being studied.

### **3. Overview of technical pollution prevention systems in the conditions under study**

Water filtration through the body of protective structures is always undesirable. With significant sizes, or when highly mineralized water is filtered, it can pose a serious threat to both the environment and the hydrotechnical structure itself.

A large number of hydrotechnical structures, which are intended for the protection of soils and groundwater, are built from permeable materials that are separated by structural or technological seams, or are placed on a filtering basis, so their integral structural part is anti-filtration devices, the role of which is to prevent penetration of water into the body of the structure or foundation, or to reduce filtration losses to acceptable safe limits.

Today, anti-filtration devices of various designs are used in production - screens, sumps, sheet pile walls, diaphragms, cores, linings, etc., and are made of various materials - clay, bitumen, wood, metals, reinforced concrete, rubber, etc. .

All traditional materials used for anti-filtration devices have one or another disadvantages. Constructions with their use are either time-consuming, complex and expensive, or limited by a narrow range of structures, conditions of their work and construction.

Polymer films as a material for anti-filtration devices of hydro-technical structures have a number of advantages: practical impermeability of the material itself and high resistance of polyethylene and polynyl chloride films to the aggressive effects of common chemical reagents, high deformability of films, low material consumption and high manufacturability. The advantages of polymer films include the fact that the formation of waterproof elements in them depends little on local construction conditions.

At the same time, polymer anti-filtration devices have a number of disadvantages and features. This is primarily a tendency to aging, which proceeds at a sharply different speed depending on the conditions in which they are found, weak aggression towards other materials, a significant change in properties when the temperature changes, etc.

Film anti-filtration devices must be reliable in operation during the entire service life of the structure. Reliability of operation is determined primarily by the properties of the polymer film element. These properties should be such as to distinguish the types of influences (mechanical stress, water influence, temperature fluctuations, etc.), possible both during operational and construction periods, that would not cause changes in the material or its damage, unacceptable from the point of view of reliability anti-filtration device.

In buildings, for example, in which there should be no place for water loss (storage of aggressive liquids, etc. ), in film anti-filtration elements, not only punctures, cuts, but also changes that would lead to a violation of the integrity of the films and, hence, loss water-proofing in a period shorter than the service life of the structure.

In fig. 4. the scheme of protection of phosphogypsum dumps with a polyethylene diaphragm is shown.

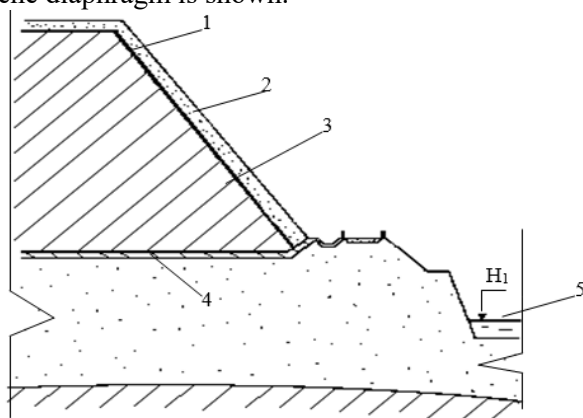


**Fig. 4.** Scheme of a protective structure with a polyethylene diaphragm:

1 - polyethylene diaphragm; 2 - loading layer of large stone; 3 - dumps of phosphogypsum; 4 - concrete curtain; 5 - fishing channel

In the absence of mechanical damage to the film due to its low porosity, the movement of water through the film is possible only in the form of diffusion of water molecules and substances soluble in it. Diffusion losses of water, however, are quite insignificant, but in some cases they have to be taken into account (for example, when



designing storage facilities for highly toxic substances).

Since protective screens during operation can lose their protective functions due to soil deformation, erosion, suffusion, the main attention in the work is devoted to substantiating the parameters of drainage structures that will intercept the soil flow of highly mineralized water coming from the object of study.

In fig. 5 shows the scheme of interception of the soil flow from the massif of phosphogypsum dumps by one drainage line.

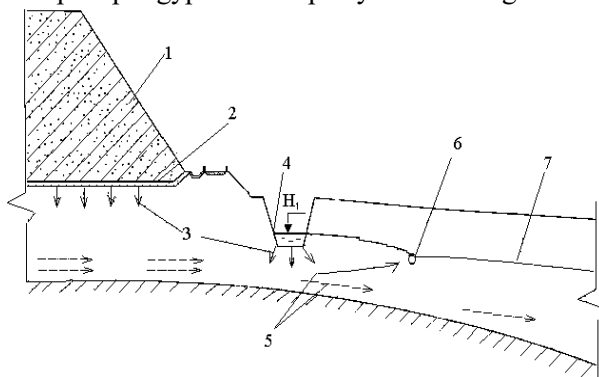


**Fig. 5.** Scheme of the arrangement of the drainage line for intercepting the soil flow from the massif of phosphogypsum dumps: 1 – phosphogypsum dumps; 2 – concrete curtain; 3 – migration flow; 4 – fishing channel; 5 – the direction of the filtration current; 6 - drain; 7 – the level of groundwater after installing drainage

It is possible to arrange *the nth* number of drains [1] (Fig. 6).

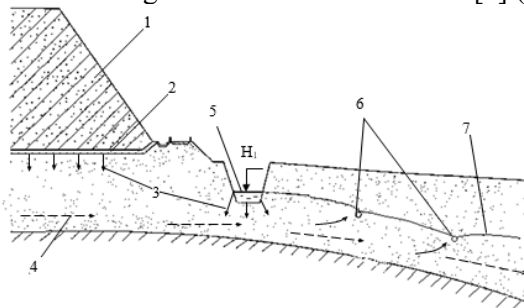


**Fig. 6.** Scheme of arrangement of the *nth* number of drains to intercept the soil flow from the massif of phosphogypsum dumps: 1 – phosphogypsum dumps; 2 – concrete curtain; 3 – migration flow; 4 – the direction of the filtration current; 5 – fishing channel; 6 - drain; 7 – groundwater level after drainage installation

In the practice of hydrotechnical construction, with the artificial

interception of contaminated groundwater in order to prevent soil pollution, it is possible to apply a scheme for arranging a group of wells, the mutual location of which may be different.

The scheme of groundwater interception by a series of wells is presented in Fig. 7. In this case, the wells can be located in several rows after washing the contaminated object. The number of wells and their placement is optimized by appropriate hydrotechnical and migration calculations.

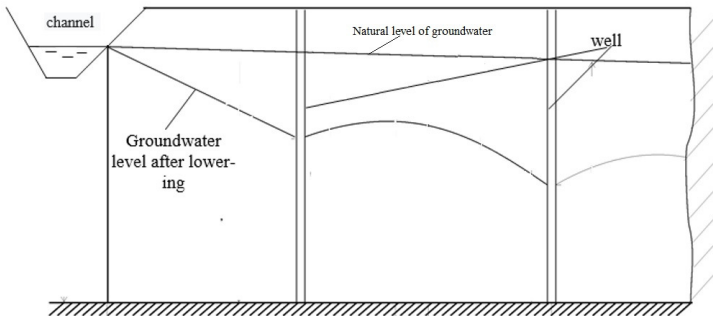


**Fig. 7.** Scheme of interception of the soil flow of contaminated water from the object of pollution by a series of wells

For more effective interception of groundwater, the horizontal drainage can be reinforced with vertical wells that will discharge into the drains (Fig. 8).

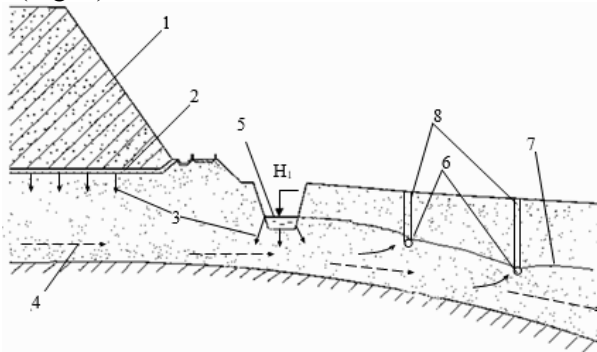


**Fig. 8.** Scheme of interception of polluted water by drainage reinforced with vertical wells: 1 – phosphogypsum dumps; 2 – concrete curtain; 3 – migration flow; 4 – the direction of the filtration current; 5 – fishing channel; 6 – drain; 7 – ground water level after installing drainage; 8 – well

Strengthening of drainage with vertical wells is recommended in the case when the soil mass from which the polluted water is drained is represented by soils with a low filtration coefficient.

One of the options for cleaning the water that is wedged out of the waste layer can be: cleaning the drains in 2-step biological ponds with natural aeration and aquatic vegetation; - interception of heavy metals from filtrates with the help of a natural sorbent in a geochemical screen (loam of a defined chemical and mineralogical composition, laid at the base of the catch channel); combination of the proposed combination of two cleaning methods - biogeochemical and geochemical.

The biochemical method involves the use of aquatic vegetation grown in ponds, at the base of which screens of rocks are placed. Based on the results of a comparative analysis of the accumulation of heavy metals in the system "aquatic deposits - aquatic vegetation", it was established that reed is a better natural sorbent than sedge and cattail for the following metal content: chromium >copper>nickel >cadmium>cobalt>manganese. The best sorbent that accumulates metals among studied aquatic plants is watercress. The accumulation coefficients, calculated as the ratio of the metal content in watercress to the metal content in water, range from 16,000 to 24,000 for manganese, and from 4,000 to 8,000 for iron. Since the main pollutant components for this object are iron, manganese, and chromium, then the combination of reed and duckweed allows to reduce pollution by the listed metals.

The main burden of reducing the content of pollutant components in the waters of the fishing channel is borne by the geochemical screen. Geochemical screens are used in the form of soil dams that enclose ponds. An anti-filtration tray is installed along the bottom and slopes of the dams. A geochemical screen made of natural sorption material is placed in the biopond of the second stage of purification. The filtrate, having passed through a layer of sorption material, enters the drainage layer and enters the biopond of the third stage through pipes, where it is further purified, after which the excess of purified filtrate is discharged into the drainage channel.

The scheme of the preliminary assessment of the validity of the geochemical screen is based on the determination of the value of the limit sorption capacity in relation to the pollutant components toxic

for the given source for the specified type of rocks.

To reduce pollution of the fertile soil layer, you can use a layer of loess loam with a thickness of 0.5 m in combination with layers of chernozem of different thicknesses (30, 50, 70 cm). The conducted studies made it possible to conclude that the use of a shielding layer of loess loam reduces the entry of lead and zinc into the black soil by 2 times, copper, cobalt and cadmium - by 1.6 times. The concentration of iron, manganese and chromium in the soil in the contact zone with the loess rock does not change. A decrease in the number of mobile forms of metal entering the soil layer from the rock leads to a decrease in the content of metals in agricultural products.

In the reclamation of territories, carbonate loams are widely used both independently and together with sand as ameliorants. Carbonate ameliorant improves the chemical composition of rocks, increases the supply of fine soil, increases moisture capacity, porosity, water permeability.

Methodological approaches and criteria for evaluating geoecological indicators of safety and minimization of water and soil contamination by heavy metals in the territory of phosphogypsum dumps include:

- creation of geochemical screens;
- engineering and technical measures - installation of drainage structures to intercept polluted water coming from phosphogypsum dumps, installation of film screens;
- the use of perennial grasses (alfalfa and safflower) as test crops and buffer crops on reclamation sites;
- creation of a methodology for determining the parameters of absorption of heavy metals by soils and rocks and its implementation in the practice of predicting groundwater pollution;
- of highly mineralized waters discussed above are designed to intercept the flow of clean water. And we are dealing with a liquid that has a concentration different from the concentration of groundwater.

The schemes do not take into account diffusive transport, as well as sorption and desorption of the soils of the massif on which the studies are conducted.

#### **4. Justification of the technological parameters of interception and removal of polluted waters**

highly mineralized water from the territory of phosphogypsum dumps of JSC " Rivneazot " is filtered in the experimental area , which leads to soil, groundwater and Horyn River water pollution.

According to experimental research data, the source of pollution is not only the phosphogypsum dumps of JSC " Rivneazot ", but also the surrounding area. As a result of the spread of phosphogypsum by wind erosion and groundwater, the content of soil contamination in a radius of 1 km around the dumps exceeded the maximum permissible standards. The content of nitrates in the soil exceeds the maximum allowable concentration of MPC (45 mg/dm<sup>3</sup>) and ranges from 30 to 90 mg/dm<sup>3</sup>. The content of manganese in groundwater within the study area in all samples exceeds the MPC (0.1 mg/dm<sup>3</sup>). An area with a manganese content in groundwater of 50-300 mg/dm<sup>3</sup> has been allocated directly on the territory of the solid household waste site. The content of iron in groundwater directly within the waste site is within 2000-1000 mg/kg (MPC-0.3 mg/dm<sup>3</sup>). The content of lead, zinc, copper, cadmium, nickel, cobalt, and nitrites in groundwater everywhere exceeds the MPC. The results of chemical analysis of water samples taken from the site show that the water has a mineralization of 8.3 mg/dm<sup>3</sup>. The content of total chromium exceeds the MPC (1.0 mg/dm<sup>3</sup>) and is 3.0-6.0 mg/dm<sup>3</sup>.

To prevent the spread of pollution, we have developed and proposed an engineering network for the interception of highly mineralized waters from the territory of phosphogypsum dumps (Fig. 9). According to this scheme, it is proposed to arrange a network of drainage around the dumps, which will intercept and divert contaminated groundwater to the treatment facilities of OJSC " Rivneazot", located 5 km from the territory of the research object. Catch channels (3) are designed around the perimeter of the object to intercept the polluted water coming from the territory of the phosphogypsum dumps, which accumulates in the dumps due to atmospheric precipitation in the form of rain and snow. From the catch channels, the highly mineralized solution is fed by the pumping station (5) into the pond, which is located on top of the dumps (V=406,000 m<sup>3</sup>). The installation of a settling tank on top of the dumps is due to the prevention of the highly mineralized solution from entering the soil and the further spread of groundwater pollution in the Horyn River.

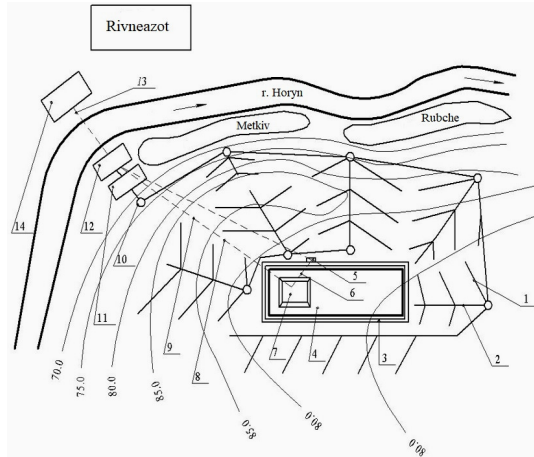


**Fig. 9.** Engineering network of pollution prevention within the influence of phosphogypsum dumps: 1 - drains; 2 - collective collector; 3 - fishing channels; 4 - dumps of phosphogypsum; 5 - pumping station; 6, 13 - pressure pipeline; 7 - storage pool; 8, 9 - gravity pipeline; 10 - drainage well; 11 - collection pool; 12 - pumping station; 14 - treatment facilities

To evaluate the parameters of drainage systems for the localization of migratory currents, theoretical developments [2] were used to determine the one-way inflow to the drain by the point flow method and calculated dependencies to determine the parameters of the closed drainage. A sufficiently generalized version of the hydrodynamic scheme reflects the most common situation with layers differing in permeability and partial pressure (fig. 10), which, however, is easily simplified to a single-pressure scheme.

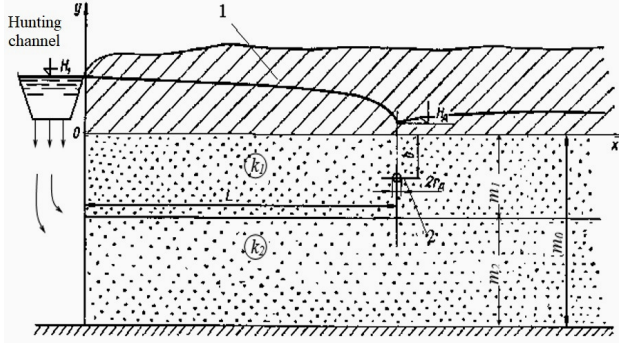


**Fig. 10.** Calculation scheme of one-way inflow to the drain:  
1 - depression curve; 2 - drain

The solution of the problem for the flow located at a point with coordinates  $(L, -b)$  and having a flow rate  $q$  is expressed by the equation

$$\begin{aligned}
 H(x, y) = & \frac{q}{4\pi k_1} \left\{ \ln[(x-L)^2 + (y+b)^2] + \ln[(x-L)^2 + (y-b)^2] \right\} + \\
 & + \frac{q}{4\pi k_1} \sum_{n=1}^{\infty} c'_n \left\{ \ln[(x-L)^2 + (y+2nm_0-b)^2] + \ln[(x-L)^2 + (y+2nm_0+b)^2] \right\} + \\
 & + \ln[(x-L)^2 + (y-2nm_0+b)^2] + \ln[(x-L)^2 + (y-2nm_0-b)^2] \left\} + C_1
 \end{aligned} \quad (17)$$

The solution of the problem for a fictitious source located at the point  $(-L, -b)$  and which has a flow  $-q$ , will be as follows

$$\begin{aligned}
 H(x, y) = & -\frac{q}{4\pi k_1} \left\{ \ln[(x+L)^2 + (y+b)^2] + \ln[(x+L)^2 + (y-b)^2] \right\} - \\
 & - \frac{q}{4\pi k_1} \sum_{n=1}^{\infty} c'_n \left\{ \ln[(x+L)^2 + (y+2nm_0-b)^2] + \ln[(x+L)^2 + (y+2nm_0+b)^2] \right\} + \\
 & + \ln[(x+L)^2 + (y-2nm_0+b)^2] + \ln[(x+L)^2 + (y-2nm_0-b)^2] \left\} + C
 \end{aligned} \quad (18)$$

Summing expressions (17) and (18), we find the level function for an arbitrary coordinate

$$\begin{aligned}
 H(x, y) = & \frac{q}{4\pi k_1} \left\{ \ln \frac{[(x-L)^2 + (y+b)^2][(x-L)^2 + (y-b)^2]}{[(x+L)^2 + (y+b)^2][(x+L)^2 + (y-b)^2]} \right\} + \\
 & \sum_{n=1}^{\infty} c'_n \ln \frac{[(x-L)^2 + (y+2nm_0-b)^2][(x-L)^2 + (y+2nm_0+b)^2]}{[(x+L)^2 + (y+2nm_0-b)^2][(x+L)^2 + (y+2nm_0+b)^2]} \times
 \end{aligned}$$

$$\times \left\{ \frac{\left[ (x-L)^2 + (y-2nm_0+b)^2 \right] \left[ (x-L)^2 + (y-2nm_0-b)^2 \right]}{\left[ (x+L)^2 + (y-2nm_0+b)^2 \right] \left[ (x+L)^2 + (y-2nm_0-b)^2 \right]} \right\} + C \quad (19)$$

In order to satisfy the condition  $H=H_1$  at  $x=0$ , the constant value  $C$  must be taken equal to  $H_1$ . The pressure  $H_d$  on the contour of the tubular drain with a radius  $r_D$  we determine from expression (19), substituting  $x=L-r_D$  and  $y=-b$  into it

$$H_d = \frac{q}{4\pi k_1} \left\{ \ln \frac{r_d^2 (r_d^2 + 4b^2)}{(2L - r_d)^2 [(2L - r_d) + 4b^2]} + \right. \\ \left. + \sum_{n=1}^{\infty} c'_n \ln \frac{[r_d^2 + 4(nm_0 - b)^2] (r_d^2 + 4n^2 m_0^2)^2}{[(2L - r_d)^2 + 4(nm_0 + b)^2] [(2L - r_d)^2 + 4n^2 m_0^2]} \right\} \times \\ \times \frac{[r_d^2 + 4(nm_0 + b)^2]}{[(2L - r_d)^2 + 4(nm_0 + b)^2]} \left. \right\} + H_1. \quad (20)$$

From formula (20), taking into account that  $r_d < m_1$  and  $r_d < L$ , we obtain for the consumption  $q=q_d$  per unit length of the drain

$$q_d = 4\pi k_1 (H_1 - H_d) \left\{ \ln \frac{16L^2 (L^2 + b^2)}{r_d^2 (r_d^2 + 4b^2)} + \right. \\ \left. + \sum_{n=1}^{\infty} c'_n \left[ \ln \left( 1 + \frac{L^2}{(nm_0 - b)^2} \right) + 2 \ln \left( 1 + \frac{L^2}{n^2 m_0^2} \right) + \ln \left( 1 + \frac{L^2}{(nm_0 + b)^2} \right) \right] \right\}^{-1}. \quad (21)$$

When  $k_2=0$  and  $k_1=k_2$  from the obtained formulas, the known dependences for head and linear flow in the case of a homogeneous pressure reservoir with capacities  $m_1$  and  $m$

$$q_d = \frac{k_1 (H_1 - H_d)}{\frac{L}{m_1} + \frac{1}{2\pi} \ln \frac{m_1}{2\pi r_d \sin \frac{\pi(2b + r_d)}{2m_1}}}, \quad (22)$$

When  $k_2=0$

$$q_d = \frac{k_1 (H_1 - H_d)}{\frac{L}{m_1} + \frac{1}{\pi} \ln \frac{m_1}{\pi r_d}}. \quad (23)$$

Consider the scheme of inflow to the  $n$ th number of drains (Fig. 11).



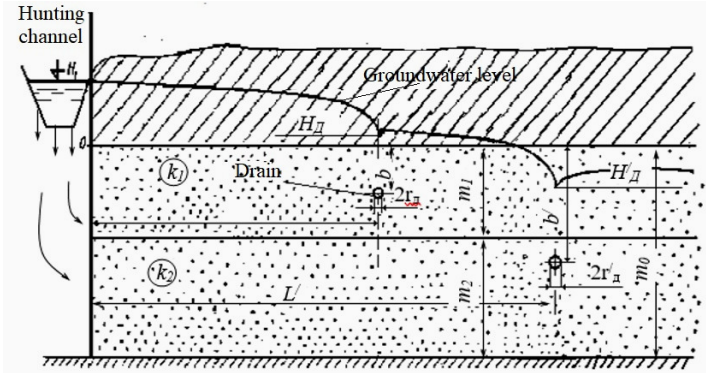


**Fig. 11.** Calculation scheme for interception of soil flow by the drain system

To solve problems of this type for the second drain, let's assume that the Y axis passes through the center of the first drain. Then it can be written when  $k_1=k_2$

$$q'_д = 4\pi k_1 (H_д - H'_д) \left( \frac{4\pi(L' - L)}{m_0} + \ln \frac{m_0}{2\pi r'_д} - 2 \ln \sin \pi B - 2 \ln \frac{\sin \pi B}{4} \right)^{-1}; \quad (24)$$

$$B = \frac{2b' + r'_д}{2m_0}$$

where  $q'_д$  is the flow intensity of the second drain,  $m^3/s$ ;  $H'_д$  - pressure over the second drain, m;  $r'_д$  - radius of the cross-section of the second drain, m;  $L'$  - distance from the second drain to the power source, m;  $b'$  - the depth of the second drain, m.

For complete interception of the soil flow, it is necessary that the condition  $H'_д=0$  be fulfilled, that is, the pressure above the drain should be equal to zero.

$$H'_д = H_д - \frac{4\pi k_1 \left( \frac{4\pi(L' - L)}{m_0} + 2 \ln \frac{m_0}{4\pi r'_д} - 2 \ln \sin \pi B - 2 \ln \frac{\sin \pi B}{4} \right)^{-1}}{q'_д} = 0; \quad (25)$$

For the  $n$ th drains dependence (25) can be rewritten

$$H_{\Delta}^n = H_{\Delta}^{n-1} - \frac{4\pi k_1 \left( \frac{4\pi(L^n - L^{n-1})}{m_0} + 2 \ln \frac{m_0}{4\pi r_{\Delta}^n} - 2 \ln \sin \pi B - 2 \ln \frac{\sin \pi B}{4} \right)^{-1}}{q'_{\Delta}} = 0; \quad (26)$$

performing the necessary mathematical operations in equation (26) we obtain

$$H'_{\Delta} = H_{\Delta} - \frac{4\pi k_1 \left( \frac{4\pi(L' - L)}{m_0} + 2 \ln \frac{m_0}{4\pi r'_{\Delta}} - 4 \ln 2 \right)^{-1}}{q'_{\Delta}} = 0; \quad (27)$$

$$H'_{\Delta} = H_{\Delta} - \frac{4\pi k_1 \left( \frac{4\pi(L' - L)}{m_0} + 2 \ln \frac{m_0}{16\pi r'_{\Delta}} \right)^{-1}}{q'_{\Delta}} = 0; \quad (28)$$

$$H_{\Delta}^n = H_{\Delta}^{n-1} - \frac{4\pi k_1 \left( \frac{4\pi(L^n - L^{n-1})}{m_0} + 2 \ln \frac{m_0}{16\pi r_{\Delta}^n} \right)^{-1}}{q^n_{\Delta}} = 0; \quad (29)$$

where  $q^n_{\Delta}$  is the flow intensity of the  $n$  drain,  $\text{m}^3/\text{s}$ ;  $H_{\Delta}^n$  - pressure over the  $n$  drain,  $\text{m}$ ;  $r_{\Delta}^n$  - radius of the cross section of the  $n$  drain,  $\text{m}$ ;  $L^n$  - distance from the  $n$  drain to the power source,  $\text{m}$ ;  $b^n$  - the depth of the  $n$  drain,  $\text{m}$ .

To intercept highly mineralized water coming from phosphogypsum dumps, we will calculate the installation of a drainage line along the contour of the object under consideration. The drainage is arranged at a distance of 20 m from the fishing channel, the depth of which is 0.5 m. The calculation scheme is presented in fig. 12. For complete interception of contaminated water, the drain will be arranged on the sole of the waterproof layer at a depth of 5 m from the ground surface. The difference in pressure between the mark of laying the drain and the mark of the water level in the catch channel is 2 m. To prevent soil and groundwater contamination, the pressure above the drain  $H_{\Delta}$  should be equal to 0.

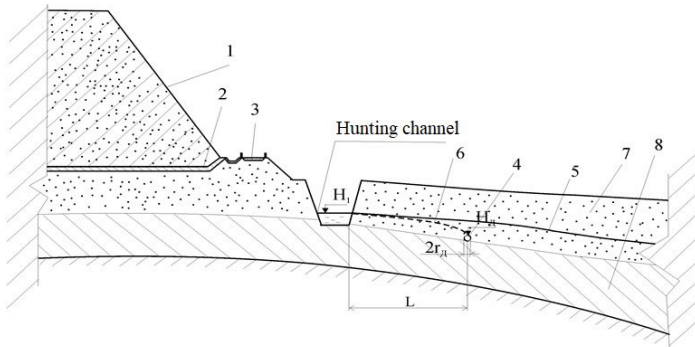


**Fig. 12.** Scheme for calculating the installation of a drainage line for intercepting soil flow from an array of phosphogypsum dumps: 1 – phosphogypsum dumps; 2 – concrete curtain; 3 – road; 4 – drain; 5 – natural level of groundwater; 6 – ground water level after installing drainage; 7 – sand; 8 – loam

In order to intercept the drainage water as much as possible, the radius of the drainage should be such that it can pass the drainage flow. To calculate the required radius of the drainage line, we will use dependence (23). After transformations, we get

$$r_D = \frac{m_1}{\left( \frac{\pi \kappa_1 (H_1 - H_D)}{q_D} - \frac{\pi L}{m_1} \right) \pi e} \quad (30)$$

Fig. 13, 14 show the results of calculations for possible ranges of parameters in the form  $r_D = f(\kappa_1; L; m)$ .

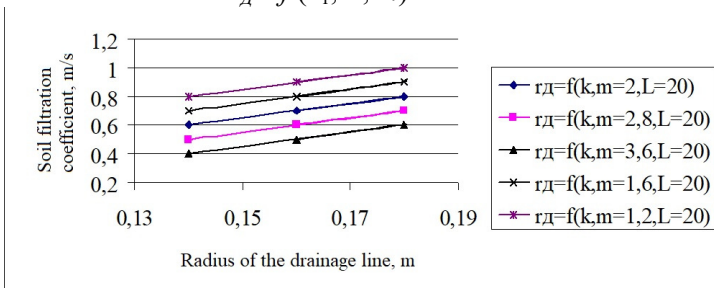


**Fig. 13** Dependence of the drainage radius of the line on the filtration coefficient at different values of the capacity of the aquifer

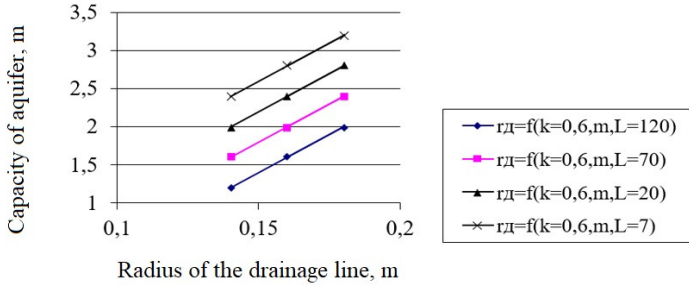


**Fig. 14.** Dependence of the radius of the drainage on the capacity of the aquifer at different values of the distance of laying the drainage from the catch channel

For more effective interception of groundwater, the horizontal drainage can be reinforced with vertical wells that will discharge into the drains (Fig. 15).

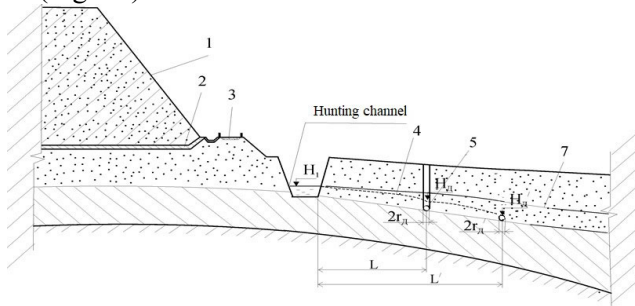


**Fig. 15.** Scheme of interception of polluted water by drainage reinforced with vertical wells: 1 – phosphogypsum dumps; 2 – concrete curtain; 3 – road; 4 – ground water level after installing drainage; 5 – drain; 6 – well; 7 – natural level of groundwater

To determine the diameter of the well, it is advisable to use the theoretical developments of M.M. Veregin on the lowering of groundwater.

In the case of one well, the pressure (water depth)  $h$  at any point of the soil flow is expressed by the following equation

$$h^2 = H_e^2 - \frac{q}{\pi k} \left[ \ln \frac{\rho_k}{r_k} + 0,5 \zeta \left( \frac{l}{m}, \frac{m}{r_k} \right) \right]. \quad (31)$$

where  $k$  is the filtering coefficient.

Here we note only that at  $l=m$  (perfect well), and also at  $m/r_k \leq l$  value  $\sigma=0$ .

Therefore, for the case when the well reaches a water-impermeable layer, dependence (31) can be rewritten

$$h^2 = H_e^2 - \frac{q}{\pi k} \left( \ln \frac{\rho_k}{r_k} \right). \quad (32)$$

The values  $\rho_k$  and  $r_k$  are expressed in the following way

$$r_k = \sqrt{(x - b - \rho)^2 + (y - \rho \sin \alpha)^2}, \quad (33)$$

$$\rho_k = \sqrt{(x + b + \rho)^2 + (y - \rho \sin \alpha)^2}. \quad (34)$$

$\rho_k$  and  $r_k$  - bipolar coordinates of any point, correspondingly equal to its distance to the center of an arbitrary well and to its mirror image relative to the water cut;  $q$  - flow rate of the well.

The value of  $H_e$  is equal to the depth of water at any point in natural conditions (before the start of the wells).  $H_e = 1$  m - above the drainage line.

With the action of all  $n$  wells based on the principle of addition of currents, the pressure  $h$  at the same point will be expressed as follows

$$h^2 = H_e^2 - \frac{q}{\pi k} \left( \sum_{k=0}^{k=n-1} \ln \frac{\rho_k}{r_k} \right), \quad (35)$$

To determine the radius of the well, which is necessary for complete interception of the soil flow of contaminated water, we will use the dependence

$$H^2 - h^2 = \frac{Q}{\pi r} \ln \left( \frac{2l}{r_0} \right) \quad (36)$$

Taking  $h=0$ , we get  $r_0=0.1$  m.

$$\ln r_0 = \ln(2l) - \frac{H^2 \cdot \pi r}{q}.$$

In fig. 16 gives the results of calculations for a possible range of parameters  $r_D = f(L; l; r_0)$ .

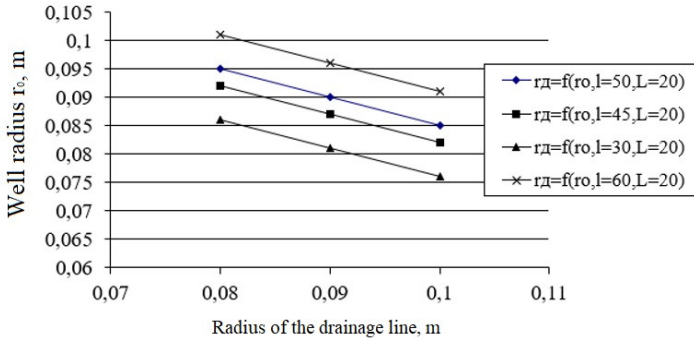


**Fig. 16.** Dependence of the drainage radius on the radius of the well at different values of the distance between the wells  $l$

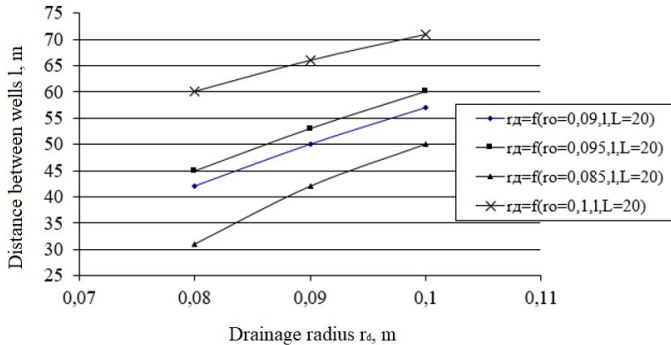


**Fig. 17.** Dependence of the drainage radius on the distance between the wells at different values of the well radius

Strengthening of drainage with vertical wells is recommended in the case when the soil massif from which the polluted water is drained is represented by soils with a low filtration coefficient.

### 5. Justification of optimal parameters of volumetric drainage filters for interception of polluted waters

When choosing the optimal parameters (thickness and density) of drainage filters, it is necessary to solve the technical and economic optimization problem. On the one hand, increasing the thickness of the filter makes it possible to increase the distance between the drains due to the reduction of filtration resistance, that is, to reduce construction costs per unit area. On the other hand, material costs for filter production are increasing. In addition, reducing the density of the filter allows you to reduce material consumption and increase the

distance between the drains. But, with a certain load on the filter, it begins to deform, which reduces the intensity of drying. Therefore, among many values of different thickness, density, diameter of drains, type of filtration scheme, it is necessary to choose the most optimal option both from the point of view of economy and from the point of view of ensuring the required drainage effect.

Reducing the density of the filter allows you to reduce the consumption of material and increase the distance between the drains, but due to the load on the filter, it begins to deform. Therefore, among the many values of different filter thickness, density and diameter of drains, it is necessary to choose the option with the lowest costs for the construction of the drain, taking into account the cost of the filter material.

According to the methodology developed by L.F. Kozhushko [13], the criterion of optimality is the minimum capital investment in the construction of drainage with volumetric filters, with the mandatory provision of the calculated module of drainage flow

$$K=ZD+ZF=>min, \quad (37)$$

where  $ZD$  - drainage construction costs without taking into account the cost of the filter, hryvnias/ha;  $ZF$  - filter manufacturing costs and material cost, hryvnias/ha

$$ZD=K_{ZD} \cdot L_0, \quad (38)$$

$$ZF=K_{ZF} \cdot P_0, \quad (39)$$

where  $K_{ZD}$  is the cost of construction of 1 m of drainage without a filter, determined by calculation, UAH/ha;  $K_{ZF}$  - the cost of the volumetric filter, taking into account the cost of the material and the costs of manufacturing the filter, hryvnias/ha;  $L_0$  - length of drains per unit area, m/ha;  $P_0$  - filter material consumption per unit area, kg/ha.

$$L_0 = \frac{10000}{E}, \quad (40)$$

$$P_0 = \pi(t(D+t))\rho \cdot L_0, \quad (41)$$

where  $E$  is the distance between drains, m;  $t$  - filter thickness, m;  $D$  - diameter of drains, m;  $\rho$  - filter density, kg/m<sup>3</sup>.

The calculation is performed taking into account soil and hydrogeological conditions in the following sequence:

1. Given the known diameters of the drain and the type of filter

material, we set different values of the initial thickness of the filter:  $t_1, t_2, \dots, t_n$  and the initial density:  $\rho_1, \rho_2, \dots, \rho_n$ ;

2. For each of the values of  $t_{and}$  and  $\rho_i$ , determine the load of the backfill of the drainage trench per 1 p.m of the drain

$$P_i = \frac{2jHb}{\pi(D + 2t_i)}, \quad (42)$$

where  $j$  is the volumetric mass of the backfill soil,  $\text{kg/m}^3$ ;  $H$  - trench depth, m;  $b$  - trench width, m.

3. Depending on the type of filtration material, its filtration coefficient is determined at  $\rho = \rho_\phi$ ;

$$k_\phi = a \cdot \rho^b, \quad (43)$$

where  $a, c$  are empirical coefficients depending on the type of material,  $\text{kg/m}^3$ ;

4. Determine the actual thickness of the filter, taking into account the deformation  $t_\phi$ , and the actual density  $\rho_\phi$

$$t_\phi = t_0 \left( 1 - a \frac{P^m}{P_0^n} \right), \quad (44)$$

$$\rho_\phi = \rho_0 \frac{2t_0(D + t_0)}{t_0(D + 2t_\phi) + Dt_\phi}, \quad (45)$$

where  $D$  is the pipe diameter, m;  $P$  - load,  $\text{kg/cm}^2$ ;  $m, n$  - empirical coefficients depend on the type of material.

5. At  $t = t_\phi$  and  $\rho = \rho_\phi$  we calculate the filtration resistance according to the nature of the opening of the aquifer  $\Phi_i$ ;

$$\Phi_i = 2\Pi \cdot K_{cp}^n \cdot \rho_\phi^k (a_0 + a_1 t_\phi + a_2 t_\phi^2 + a_3 t_\phi^3) - \ln 4H_o / D. \quad (46)$$

6. Taking into account the filtration scheme, we determine the general filtration resistances according to the degree and nature of the opening of the aquifer [13].

7. Determine the distance between the drains using the formulas:

$a$  - when the water resistance is relatively shallow

$$B = 4 \left( \sqrt{L_{no}^2 + \frac{H_p T}{2q}} - L_{no} \right) \quad (47)$$

the waterproofing is deep

$$B = \frac{2\pi K_{cp} H_p}{q(\ln(2E / \pi D) + \Phi_i)} \quad (48)$$



where  $K_{sp}$  - soil filtration coefficient, m/day;  $H_p$  - calculated pressure above the drain, m;  $q$  - inflow of water to the drain, m/day;  $L_{no}$  - total filtration resistance according to the degree and nature of formation opening ( $\Phi_0 + \Phi_\phi$ ).

8. According to formula (40), the length of drains per 1 ha is determined and according to (45) at  $t=t_\phi$ ,  $\rho=\rho_\phi$  calculate  $\rho_0$ ;

9. With the known values of  $ZD$  and  $ZF$ , we determine the value of the optimization criterion  $K$  by formulas (38) and (39);

10. According to the minimum value of the criterion, we determine the optimal initial parameters  $t$  and  $\rho_i$ , and the distance between the drains that corresponds to them.

According to this method, the optimal parameters of volumetric drainage filters are given (Tab. 1).

Table 1  
Optimal parameters of volumetric drainage filters

Parameters	Filtering materials			
	straw	flax - kostrytsia	a mixture of fire- wood and sawdust	a mixture of straw and artificial fibers
Filter density, g/ cm <sup>3</sup>	0.16-0.20	0.18-0.22	0.18-0.22	0.18-0.22
Filter thickness, mm	10-12	10-12	10-12	10-12

The use of volumetric filters made of organic materials allows to reduce the cost of drainage construction by 1.3-1.4 times compared to the option of a filter made of non-woven fabric [13].

### **5. Recommendations for environmentally safe operation and disposal of phosphogypsum dumps of JSC "Rivneazot"**

After the analysis of the research object, which included topographic surveying, determination of the chemical and mechanical composition of the soil and groundwater, water-physical properties of the soil of the adjacent territory, three stages are proposed that will ensure the environmentally safe functioning of the phosphogypsum dumps of JSC "Rivneazot"[14].

At the first stage, in order to prevent the spread of pollution, a scheme for intercepting polluted waters from the territory of phosphogypsum dumps is proposed. In the territory around the dumps, it is necessary to install a collector and drainage network that will in-

tercept and divert contaminated groundwater to the treatment facilities of OJSC "Rivneazot", located 5 km from the territory of the research object.

Remedial measures will intercept soil and surface flows of polluted water, which in turn will prevent their entry into the soil, groundwater, and in the Horyn River, drinking water wells in the village of Metkiv et al. Rubche.

At the second stage, it is recommended to cover the phosphogypsum dumps with a protective film followed by sprinkling with a fertile layer of soil with planting of vegetation, which will prevent wind erosion and contamination of the adjacent territories. Vegetation that is recommended for planting in a one-meter layer of soil - small bushes with herbs.

The third stage is designed for a longer perspective - it is the processing of phosphogypsum into building materials (wall blocks, floor panels, binder with strength greater than concrete grade 500) with simultaneous disinfection of phosphogypsum from harmful elements and extraction of rare earth metals that are part of phosphogypsum - up to 1%.

### **Conclusion**

In the work, an actual scientific and practical task is solved, which consists in establishing the regularities of the distribution of pollution in the soil massif during the filtration of groundwater from the source of pollution, based on which methods of assessment and analysis of the impact of man-made objects on the environment and calculation of rational parameters of pollution localization have been created within the influence of phosphogypsum dumps, developed technological solutions for the localization of such pollution.

The implementation of these solutions will increase the level of environmental safety through the use of more reliable engineering systems for environmentally safe storage of phosphogypsum dumps and reduce the morbidity of the population living within the limits of the dumps.

### *References*

1. Moshynskiy V., Malanchuk Z., Tsybaliuk V., Malanchuk L., Zhomyruk R., & Vasylchuk O. (2020). Research into the process of storage and recycling technogenic phosphogypsum placers. *Mining of Mineral Deposits*, 14(2), 95-102. <https://doi.org/10.33271/mining14.02.095>

2. **Moshynskiy V., Zhomyruk R., Vasylychuk O., Semeniuk V., Okseniuk R.** Investigation of technogenic deposits of phosphogypsum dumps. E3S Web of Conferences; Les Ulis , R ifi 280, (2020). DOI:10.1051/e3sconf/202128008008
3. **Yevhenii Malanchuk , Sergiy Stets, Ruslan Zhomyruk , Andriy Stets.** Modeling of the process of mining of zeolite-smectite tuffs by hydro-well method / Topical scientific researches into resource-saving technologies of mineral mining and processing. Multi-authored monograph - Sofia: Publishing House " St. Ivan Rilski ", 2020. - 446 i. ISBN 978-954-353-408-1. UDq 622.002. (P.244-260)
4. **Zhomyruk RV, Malanchuk EZ, Stets SE, Khrystiuk A.J.** Localization of pollution of soils and groundwater within the influence of the technogenic switches / Resource-saving technologies of raw-material base development in mineral mining and processing. Multi-authored monograph. Roland MORARU - Petroşani , Romania: UNIVERSITAS Publishing, 2020. - 514 i. ISBN 978-973-741-694-0. (p. 224-238)
5. **E. Malanchuk , R. Zhomyruk , R. Okseniuk** Alternative solutions for disposal of technogenic phosphogypsum dumps // Proceedings of the 3 nd International Scientific and Technical Internet Conference ""Innovative development of resource-saving technologies and sustainable use of natural resources". Book of Abstracts. - Petroşani , Romania: UNIVERSITAS Publishing, 2020. - p.153-155
6. **Malanchuk , Z., Moshynskiy , V., Malanchuk , Y., Korniienko , V, Koziar , M.** (2020). Results of Research into the Content of Rare Earth Materials in ManMade Phosphogypsum Deposits. Key Engineering Materials, (844), 77-87. <https://doi.org/10.4028/www.scientist.net/KEM.844.77> .
7. **Polubarina-Kochina P.Ya.** \_ Theory of groundwater movement. - M.: Energoizdat , 1975. - 561 p.
8. **Bochever FM, Lapshin NN, Oradovskaya A. Ya .** Protection of groundwater from pollution. - M.: Nedra, 1979. - 224 p.
9. **Aravin VI, Numerov SN** The theory of the movement of liquids and gases in a non-deformable porous medium. - M.: GITTL, 1953. - 616 pp.
10. **Rudakov DV** Mathematical models in environmental protection. - Dnipropetrovsk: National State University, 2004. - 160 p.
11. **Sitnikov AB** Dynamics of moisture and salts in soils of the aeration zone. - K.: Naukova Dumka, 1986. - 152 p..
12. **Usenko VS** Questions of the theory of filtration calculations of drainage and water wells. - M.: Kolos , 1968. - 301 p.
13. **Kozhushko LF** Improvement of drainage systems. - Rivne: RDTU Publishing House, 2001. - 279 p. 7
14. **Malanchuk, Z., Korniyenko, V., Malanchuk, Y., & Khrystyuk, A.** (2016). Results of experimental studies of amber extraction by hydromechanical method in Ukraine. Eastern-European Journal of Enterprise Technologies, 3(10(81)), 24-28. <https://doi.org/10.15587/1729-4061.2016.72404>

## **THE INFLUENCE OF BIOGAS CONTENT ON THE EMISSION OF HARMFUL IMPURITIES AND THE INTRODUCTION OF GREENHOUSE GAS EMISSION METHODOLOGY IN UKRAINE**



**Yury KURIS**

PhD (Engineering), Professor, Lecturer,  
Zaporizhzhia National University, Ukraine



**Yana VIDLOHA**

master, student, Zaporizhzhia National University,  
Ukraine.

### **Abstract**

One of the main goals of biogas energy use, as mentioned above, is to reduce greenhouse gas emissions when replacing fossil fuels. This implies determination of emissions before and after biogas use. The calculation of emissions is based on a systematic approach, when the calculation is made taking into account emissions from fuel extraction, its transportation, fuel consumption for equipment manufacturing, etc. At the same time, the life cycle of equipment and capital facilities is considered.

In this regard, the development of performance indicators for the ecological use of biofuels becomes relevant from this point of view. The above-mentioned developments are computer programmes with relevant databases. One of the peculiarities of using these programmes, in our opinion, is that, on the one hand, they allow for a specific calculation with maximum detail and assessment of the "integral" result. At the same time, the analysis of the interaction of various factors remains hidden, which can often lead to erroneous conclusions. This is especially true for generalised (strategic) analysis. Therefore, computational studies should be supplemented by analytical studies that allow identifying the main relationships between parameters.

**The scientific novelty** is as follows:

A methodology has been developed that allows analysing the environmental efficiency of energy use of biogas produced from anaer-

obic digestion of biomass based on the indicator of specific greenhouse gas emission reduction. This indicator allows an objective comparison of existing and proposed technologies and equipment for the use of bioenergy fuels, while fully taking into account the complex effect of the type and quality of the substitute fuel on the emissions and efficiency of thermal units.

Combustion kinetics calculations were carried out with the output of intermediate concentrations up to the time  $\tau=0.5$  s, when the burning process of the slowest components formed after the decomposition of hydrocarbon components is almost complete, and the CO<sub>2</sub> content in the combustion products is levelled and reaches a maximum. Thus, the processes occurring directly in the combustion zone are considered.

Based on the results of the computer calculations, we have constructed graphs (Fi. 1-3) that clearly illustrate the process of decomposition of the input and formation of new components. To avoid cluttering the figures, only the main reaction products (CO<sub>2</sub>, H<sub>2</sub>O, CO), as well as NO, NO<sub>2</sub> and components that affect their formation are shown in the graphs: NH, HCN, NSO, O, NO<sub>2</sub>, CN.

Let's compare the results obtained for natural gas NG (see Fig. 2) and biogas without nitrogen-containing impurities, which corresponds to the composition of municipal wastewater digester gas BG (see Fig. 3). As can be seen from the graphs, 0.5 seconds before the end of the calculation, the carbon dioxide content reached 10.42% for GHG and 15.53% for BG, with CO<sub>2</sub> concentrations continuously increasing to 10.3% (GHG,  $\tau=0.05$  s) and 16.52% (BG,  $\tau=0.1$  s), respectively, and then levelling off. A similar pattern is observed in the formation of H<sub>2</sub>O: a continuous increase to 18.24% (PG,  $\tau=10-3$ s) and 17.24% (BG,  $\tau=10-3$ s), followed by slow dissociation to 18.04% (PG,  $\tau=0.3$ s) and 17.16% (BG,  $\tau=0.5$ s).

The intensive formation of CO in NG begins at time  $\tau=0.5-10^{-6}$ s and reaches a maximum of 7.27% at  $\tau=0.5-10^{-5}$ s, followed by a rapid burnout to 0.13% at  $\tau=0.05$  s and then gradually decreases to  $3.7-10^{-2}$  at  $\tau=0.3$  s. The process of CO formation in the BG is somewhat slower: a maximum of 4.41% is reached at  $\tau=10^{-4}$ s, and by the time  $\tau=0.3$ s, the CO content becomes  $1.28-10^{-3}$ . The absolute content of CO during the combustion of BG, as we can see, is less than during the combustion of GHG until the time close to the end of the com-

bustion process by about an order of magnitude, which can be explained by the longer duration of the biogas combustion process.

Let's trace the formation of nitrogen oxides. The nature of the increase in nitrogen dioxide concentrations is the same for GHG and BG: at first, there is a slow increase to  $3.05 \cdot 10^{-6} \%$  at  $\tau=10^{-3}$  s for GHG and  $3.86 \cdot 10^{-7} \%$  at  $\tau=10^{-2}$  s for BG, and then there is a sharp increase by the time  $\tau=0.3$  s to  $2.69 \cdot 10^{-5} \%$  for GHG and  $1.81 \cdot 10^{-5} \%$  for BG.

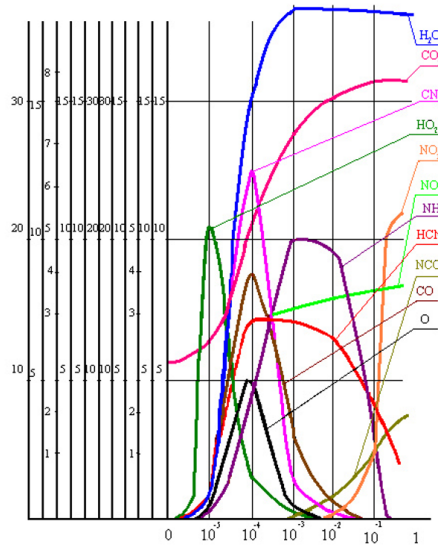


**Fig. 1.** Results of computer calculation of the kinetics of biogas combustion without nitrogen additives

This change in nitrogen oxide concentrations is explained by the "behavior" of  $\text{NO}_2$  and  $\text{O}$  by the time nitrogen dioxide formation begins, the concentrations of peroxide reach a maximum of  $3.66 \cdot 10^{-4} \%$  at  $\tau=10^{-6}$  in PG and  $1.04 \cdot 10^{-4} \%$  at  $\tau=10^{-5}$  s in BG, then decrease by about an order of magnitude to  $3.5 \cdot 10^{-5} \%$  at  $\tau = 0.5 \cdot 10^{-5}$  s in PG and  $6.40 \cdot 10^{-6} \%$  at  $\tau=10^{-3}$  in BG, and then by the time  $\tau=0.3$  the concentration decreases by another order of magnitude: to  $6.2 \cdot 10^{-7} \%$  for GHG and  $1.05 \cdot 10^{-7}$  for BG. The maximum  $\text{O}$  concentration is observed a little later:  $1.28 \%$  at  $\tau=0.5 \cdot 10^{-5}$  s in PG and  $0.25 \%$  at  $\tau=10^{-4}$  s in BG, then the concentration decreases to  $0.37 \%$  at  $\tau=0.3$  s in PG

and 1.2·10<sup>-5</sup> % in BG. Thus, the time of nitrogen dioxide formation in BG is shorter than in PG, since this formation starts later, therefore, a smaller amount of nitrogen dioxide is obtained at the end of combustion.

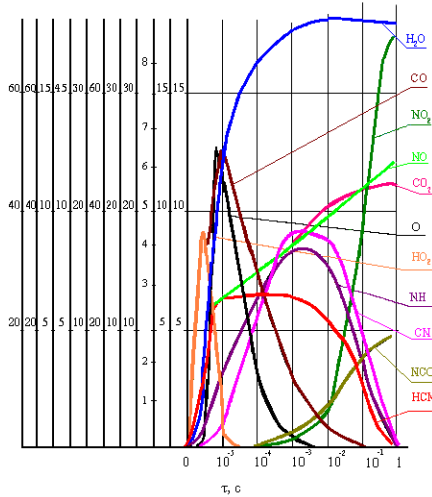


**Fig. 2.** Results of a computer calculation of the kinetics of natural gas combustion

In contrast to nitrogen dioxide, the nature of nitrogen oxide formation is different for NG and BG. The similarity of the curves is maintained at the beginning of combustion, when "fast" nitrogen oxide is formed. This occurs for GHG at  $\tau=0.5 \cdot 10^{-5}$  s (increase to  $1.25 \cdot 10^{-2}\%$ ) and for BG at  $\tau=10^{-4}$  s (increase to  $7.21 \cdot 10^{-3}\%$ ). At subsequent time points, the nitrogen oxide content for BG slightly increases and by  $\tau=0.5$  s is  $8.40 \cdot 10^{-3}\%$ . During the combustion of NG, a rather intense increase in the nitrogen oxide content continues, which by  $\tau=0.3$  s is  $2.4 \cdot 10^{-2}\%$ . At the same time, there are differences for GHG and BG in the curves of HCN, NH, CN concentrations, which are more striking for GHG.

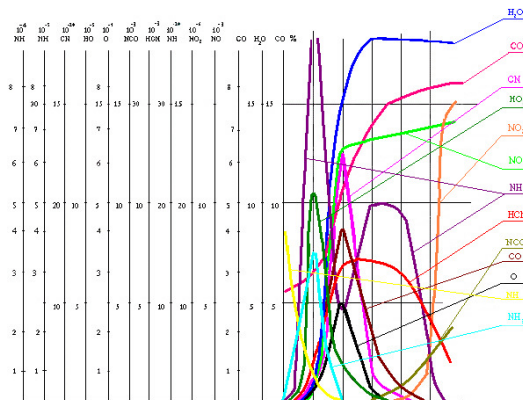


**Fig. 3.** Results of computer calculation of the kinetics of biogas combustion with an admixture of 0.004%  $\text{NH}_3$

The formation of HCN and the increase in its concentration practically "repeats" the formation of nitrogen oxide by the "fast" mechanism. The maximum value of  $1.27 \cdot 10^{-20}\%$  for GHG is achieved at  $\tau = 10^{-5}$  s, for BG -  $7.2 \cdot 10^{-3}\%$  at  $\tau = 10^{-4}$  s, which coincides with the completion of the formation of "fast" nitric oxide. At the same time, a peak of CN was observed -  $4.49 \cdot 10^{-6}\%$  in PG and  $2.49 \cdot 10^{-7}\%$  in BG. Subsequently, the decrease in HCN and CN content for BG is more gradual than for GHG. For some time, the concentration of HCN almost does not change: at  $\tau = 10^{-3}$  s, the content of CN is  $1.25 \cdot 10^{-2}\%$  for PG and  $7.16 \cdot 10^{-3}\%$  for BG. By  $\tau = 0.3$  s, the HCN content for BG changes slightly to  $3.66 \cdot 10^{-3}\%$ , while for NG it decreases by an order of magnitude to  $3.11 \cdot 10^{-3}\%$ . The maximum value of NH is reached at  $\tau = 10^{-3}$  s and amounts to  $3.75 \cdot 10^{-9}\%$  in PG and  $2.0 \cdot 10^{-9}\%$  in BG, up to  $\tau = 10^{-2}$  s this value almost does not change, then it decreases by  $\tau = 0.3$  s to  $1.18 \cdot 10^{-9}\%$  in PG and  $5.57 \cdot 10^{-10}\%$  in BG. In the final stage, the concentration of NCO increases to  $7.88 \cdot 10^{-3}\%$  for PG and  $3.22 \cdot 10^{-3}\%$  for BG by the time  $\tau = 0.3$  s.

Thus, it can be concluded that a shift in the time of nitrogen oxide turnover in BG without nitrogen-containing impurities leads to a twofold reduction in "fast" nitrogen oxides, while the total amount of NO is also reduced by almost half.



Now let's consider the combustion of biogas with nitrogen-containing impurities, the presence of which is typical for biogas from agricultural biogas plants.

The results of calculating the kinetics of the biogas combustion process with an impurity of 0.004%  $\text{NH}_3$  are shown in Fig. 3, and with an impurity of 0.0008%  $\text{NO}$  - in Fig. 4.

Comparison of the graphs for biogas without impurities and biogas with impurities shows that the pattern of changes in the concentrations of all components is preserved, but the amount of nitrogen oxides increases with the addition of  $\text{NH}_3$  and  $\text{NO}$  to the gas. The increase in nitrogen oxide concentration occurs in the area of "fast" nitrogen oxide formation up to  $\tau=10^{-4}$ s. For biogas with an admixture of ammonia only at  $\tau=10^{-4}$ s, the nitrogen oxide content reaches  $1.28 \cdot 10^{-2}\%$  and weakly increases to  $1.40 \cdot 10^{-2}\%$  at  $\tau=0.05$ s, after which it does not change. Simultaneous admixture of  $\text{NH}_3$  and  $\text{NO}$  leads to an increase in the nitric oxide content by an amount equal to the initial content, while maintaining the character of the curves.

The decomposition of  $\text{NH}_3$  occurs in both cases in the same way. The lifetime of  $\text{NH}_3$  is only  $10^{-4}$ s. By this point, all ammonia is converted to the rapidly decaying radicals  $\text{NH}_2$  and  $\text{NH}$ , whose maximums are observed at  $\tau=10^{-5}$  s and are  $3.6 \cdot 10^{-4}\%$  for  $\text{NH}_2$  and  $1.77 \cdot 10^{-5}\%$  for  $\text{NH}$ . At  $\tau=10^{-4}$  s,  $\text{NH}_2$  decomposes completely, and the  $\text{NH}$  content decreases to  $9.16 \cdot 10^{-10}\%$ ; then the  $\text{NH}$  change curve is identical to the corresponding curve for biogas without impurities. The decay time of ammonia and amine radicals is equal to the period of formation of "fast" nitric oxide, which confirms their participation in the increase of "fast" nitric oxide content. Thus, the introduction of ammonia directly into the combustion zone does not have a predominant effect on nitric oxide, but rather causes a slight increase in concentrations. Probably, the addition of  $\text{NH}_3$  as a method of nitrogen oxide suppression is effective only in the flame zone.

The pattern of change in the nitrogen dioxide curves is maintained with a slight increase in concentrations to a level that does not exceed the values for natural gas.

It should be noted that the total amount of nitrogen oxides at the outlet of the combustion zone during biogas combustion is lower than for natural gas. A comparative picture of nitrogen oxides formation for natural gas, biogas and their mixture is shown in Fig. 5.

At the time point  $\tau=0.3$  s, the content of nitrogen oxide for unadulterated biogas is 65% lower and nitrogen dioxide 50% lower than for natural gas. Biogas admixture to natural gas in the proportion of NG: NG=1:1 results in a 45% reduction in nitrogen oxide and 22% reduction in nitrogen dioxide. Even for biogas containing  $\text{NH}_3$  admixtures, the yield of nitrogen oxides is lower than that of natural gas, by 41% NO and 15%  $\text{NO}_2$ . Accordingly, for biogas with  $\text{NH}_3$  and NO impurities, this reduction is 36% of nitrogen oxide and 17.5% of nitrogen dioxide.

All the results above were obtained in the calculations of combustion of stoichiometric gas-air mixtures of gas and air, with an excess air coefficient  $\alpha=1.0$ . To verify the reliability of the chosen model, similar calculations were additionally carried out for biogas containing  $\text{NH}_3$  and NO impurities at values of the excess air ratio from 1.0 to 1.4. Based on the results of the calculations, graphs of the dependence of the nitrogen oxides content at the outlet of the combustion zone at  $\tau=0.5$  s were constructed (Fig. 5). The maximum value of NO content equal to  $1.53 \cdot 10^{-2}$  % was obtained at  $\alpha=1.0$  and then decreases to  $8.31 \cdot 10^{-3}$  % with an increase in  $\alpha$  to 1.4. The highest amount of  $\text{NO}_2$  ( $9.62 \cdot 10^{-5}$  %) occurs at  $\alpha=1.1$ , and then decreases and becomes equal to  $2.61 \cdot 10^{-5}$  % at  $\alpha=1.4$ .

The type of graphs coincides with the data of other researchers [1-5], which confirms the reliability of the calculation results.

Thus, the addition of biogas to natural gas can be recommended as one of the ways to reduce the yield of nitrogen oxides during combustion.

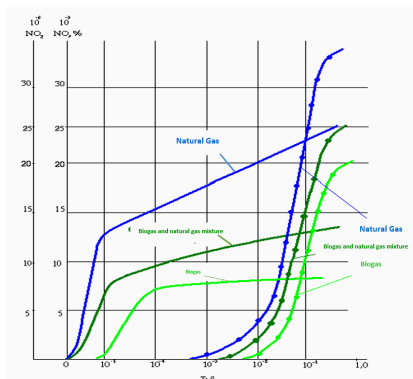


**Fig. 4.** Content of nitrogen oxides in the combustion products of natural gas, biogas and their mixture of NO and  $\text{NO}_2$

Unfortunately, insufficient information on the kinetics of carcinogenic compounds (surfactants, N-nitrosamines) formation does not allow us to trace the nature of changes in the concentration of these components in the flame using the presented mathematical model. To determine their amount in the combustion products, field studies in thermal installations are required.

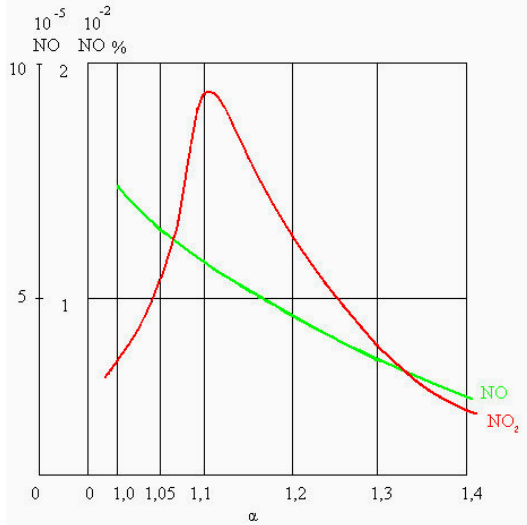


**Fig. 5.** Dependence of the nitrogen oxides content at the outlet of the combustion zone on the excess air ratio during the combustion of biogas containing  $\text{NH}_3$  and NO impurities

### Conclusions

The environmental characteristics of biogas, natural gas and their mixtures can be determined on the basis of the results of mathematical modelling of the dynamics of decomposition and formation of various components that affect the appearance of harmful substances.

The formation of harmful impurities in the combustion products of biogas, natural gas and their mixtures was studied using a mathematical model. According to computer calculations, it was found that the amount of carbon monoxide in biogas combustion is an order of magnitude less than in natural gas combustion products and amounts to  $1,28 \cdot 10^{-2}\%$ .

The main harmful components in the combustion products of gaseous fuels are nitrogen oxides. Calculations have shown that the con-

tent of nitrogen oxides in biogas combustion products is 1.5-2 times lower than in natural gas combustion products due to the lower combustion temperature, the presence of CO<sub>2</sub> and H<sub>2</sub>O in biogas. Adding biogas to natural gas in the proportion of BG: NG=1:1 results in a 45% reduction of NO and 22% reduction of NO<sub>2</sub>. Even for biogas containing NH<sub>3</sub> and NO impurities, which is typical for biogas from agricultural BGUs, the yield of nitrogen oxides is lower than that of natural gas, by 36% NO and 17.5% NO<sub>2</sub>.

Thus, the addition of biogas to natural gas can be recommended as one of the ways to reduce the yield of nitrogen oxides during the combustion of gaseous fuels is nitrogen oxide.

## **2. Determination of greenhouse gas emissions from the use of biomass.**

The greenhouse gas emission rate for the energy use of biomass is determined by the emissions from fossil fuel combustion during the collection, processing and transportation of biomass. Given that biomass suitable for energy use in Ukraine refers to waste production, GHG emissions associated with harvesting and collection of biomass were not considered, as energy costs were fully attributed to the production of main products. In this case, the emission figure for biomass  $e_{CO_2}^{BM}$  is composed of two components

$$e_{CO_2}^{BM} = e_{Transp}^{BM} + e_{proc}^{BM}, \quad (2.1)$$

where  $e_{Transp}^{BM}$  - the greenhouse gas emission rate associated with biomass transport, gCO<sub>2</sub>-eq/(kg tce of biomass);

$e_{proc}^{BM}$  - the greenhouse gas emission rate associated with biomass processing and preparation, gCO<sub>2</sub> - eq/(kg tce of biomass).

Due to low bulk density of biomass of 100-150 kg/m<sup>3</sup>, its transportation over long distances is not very efficient, therefore in calculations maximum transportation distance is assumed to be 100 km, and vehicles are used for transportation. Fuel costs for transportation of biomass  $Q_{VTr}^{BM}$  and greenhouse gas emission rate  $e_{CO_2}^{NP}$  according to [8]

$$e_{Transp}^{BM} = e_{CO_2}^{VTr-BM} = Q_{VTr}^{BM} \cdot e_{CO_2}^{NP}, \quad (2.2)$$

and

$$Q_{VTr}^{BM} = 0,1S_{Vtr}^{BM} [H_z + H_W \cdot G_{BM}] = (1 + \sum i), \quad (2.3)$$

Table 2.1

Specific energy consumption for biomass shredding [5]					
Particle size, mm	>25	>15	>10	>5	>3
Specific energy consumption, $b_{ee}^{sherd \cdot BM}$ , kWh/t	10-25	20-35	25-45	40-80	60-130

where  $Q_{VTr}^{BM}$  - fuel consumption for biomass transportation, l;

$H_z$  - basic linear fuel consumption rate [138], l/100 km;

$H_W$  - norm of fuel consumption for transport work, for petrol vehicle equals 2.0 l/t km, for diesel vehicle - 1.3 l/t km;

$G_{BM}$  - mass of biomass transported by vehicle, t;

$S_{Vtr}^{BM}$  - distance travelled, km;

$K_i$  - coefficients taking into account additional fuel costs when transporting cargo within the city limits equal to 0.1-0.05;

$$e_{CO_2}^{pp} = e_{CO_2}^{VTr \cdot pp} + e_{CO_2}^{rTr \cdot pp} + e_{prod}^{pp} + e_{transp}^{pp} + e_{comb}^{pp} + e_{CO_2}^{combpp}, \quad (2.4)$$

where  $e_{CO_2}^{pp}$  - emission factor for petroleum products (petrol, diesel fuel, fuel oil), gCO<sub>2</sub>-eq/kg tce of petroleum product;

$e_{CO_2}^{VTr \cdot pp}$  - emission factor for transportation of oil products (gasoline, diesel fuel, fuel oil) in tank trucks, gCO<sub>2</sub>-eq/kg t of oil product;

$e_{CO_2}^{rTr \cdot pp}$  - emission rate during transportation of petroleum products by rail, gCO<sub>2</sub>-eq/kg tce of petroleum product;

$e_{prod}^{pp} + e_{transp}^{pp} + e_{comb}^{pp}$  - emission factor for refining, transportation and extraction of oil, respectively, gCO<sub>2</sub>-eq/kg tce of oil product;

$+ e_{CO_2}^{combpp}$  - emission factor during petroleum product combustion, gCO<sub>2</sub>-eq/kg tce of petroleum product.

In the calculations, the volume of the truck body was varied from 8 m<sup>3</sup> (MAZ-53) to 52 m<sup>3</sup> (KAMAZ-54 specialized truck for grain transportation) [3, 4].

Processes for the preparation of biomass, as an energy fuel, include two alternative processes: shredding and pressing (briquetting).

Consequently, the total greenhouse gas emissions for biomass preparation and processing are as follows

$$e_{prod}^{BM} = e_{CO_2}^{prezBM} + e_{CO_2}^{shred \cdot BM} . \quad (2.5)$$

The energy consumption for shredding depends on the final biomass particle size (Table 2.1 [145]) and the type of biomass. The maximum energy input refers to the shredding of woody biomass, the minimum to straw.

Accordingly, the greenhouse gas emissions associated with biomass  $e_{CO_2}^{shred \cdot BM}$  shredding were determined using the relationship

$$e_{CO_2}^{shrd \cdot BM} = b_{ee}^{shrd \cdot BM} \cdot E_{ee} . \quad (2.6)$$

Biomass baling and pelletising can be carried out using several well-known processes, the names of which determine the type of equipment used (Figure 2.2 [6]). Electricity consumption directly for biomass pressing is 20-70 kWh/t (Table 2.2 [6, 7]).

Table 2.2

Energy consumption for briquetting and pelletizing of biomass

Type of equipment used	Rolling press	Screw press
Electricity costs, $b_{ee}^{press \cdot BM}$ , kWh/t	20-60	50- 0

In addition to energy costs, biomass baling technology involves drying the biomass to a predetermined moisture content. In this case,

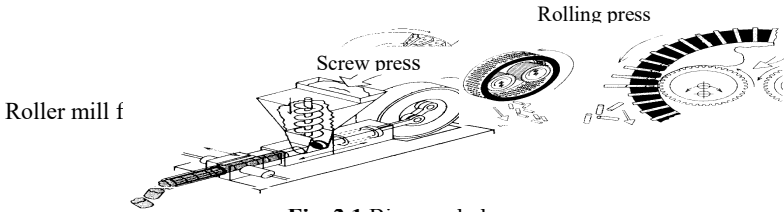


Fig. 2.1 Biomass bal

the thermal energy consumption is  $b_{Tem}^{hress \cdot BM} = 0,02 - 0,08$  Gcal/(t biomass) [7].

Accordingly, the greenhouse gas emissions from biomass  $e_{CO_2}^{press \cdot BM}$  baling include emissions associated with both heat and electricity use

$$e_{CO_2}^{press-BM} = EMBEDE_{Equation.3} \Theta E_{66} + b_{Tem}^{press-BM} E_{Tem}. \quad (2.7)$$

The above methodology made it possible to estimate greenhouse gas emission values for various fossil fuels and biomass, on the basis of which various options of technologies and equipment for biomass energy use were compared.

## 2.1 Study of greenhouse gas emissions in energy production in Ukraine

### 2.1.1 Study of greenhouse gas emissions during the use of fossil fuels.

The methodology described above and the calculation of greenhouse gas emission rates were not meant to make an inventory of greenhouse gas emissions in the Ukraine, but to obtain quantitative data enabling evaluation of the efficiency of fossil fuels replacement with biomass. In this regard, the range of variation of emission indicators was calculated, both for main fossil fuels and biomass waste. Attention was also paid to studying the structure of the components of greenhouse gas emission indicators.

The values of greenhouse gas emission indicators for the main types of fossil fuels in European countries, California and Ukraine are shown in figure 2.5 and table 2.5.

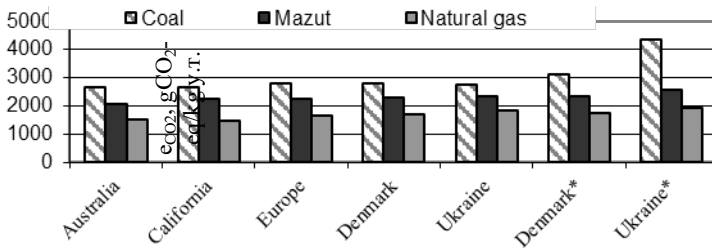


Fig. 2.2. Fossil fuel greenhouse gas emission rates

The emission values in Fig. 2.5 for Australia (148), California (149), Europe (150), Denmark (151) and Ukraine are given for the combustion stage only. Values for Denmark\* (152) and Ukraine\* include energy inputs for the whole fuel production cycle. Thus, we can say that emissions related to fossil fuel combustion for different countries are almost the same. The marginal deviation of emission figures does not exceed 5%. The main difference in fossil fuel emis-

sions is due to the indirect greenhouse gas emission component in the upstream and downstream stages. Comparison of this component for Ukraine and Denmark shows that indirect greenhouse gas emissions at coal use in Ukraine are 2-5 times higher.

Analysis of the structure of the indirect component of greenhouse gas emissions for coal (table 2.3 and fig. 2.3) shows, that the share of coal mine methane emission constitutes from 47% to 96% of the total emissions. At the same time the emission value associated with heat and electric energy consumption during coal extraction may vary by tens of times. The main share of emissions is attributable to carbon dioxide CO<sub>2</sub> (Fig. 2.4).

Table 2.3  
Greenhouse gas emission values for the main fossil fuels in Ukraine

Type fuel	Coal		Petrol		Mazut		Diesel fuel		Natural gas		
	gC O <sub>2</sub> / kg y.T.	%	gCO <sub>2</sub> /kg y.T.	%	gCO <sub>2</sub> /kg y.T.		gCO <sub>2</sub> /k g y.T.	%	gCO <sub>2</sub> /k g y.T.	%	
max	$e_{CO_2}^{prod}$	1531	35,2	1,9	0,1	1,9	0,1	1,9	0,1	-	-
	$e_{CO_2}^{transp}$	34	0,8	2,0	0,1	2,1	0,1	2,0	0,1	95,7	5,0
	$e_{CO_2}^{proc}$	-	-	150,5	6,5	143,4	5,6	152	6,2	-	-
	$e_{CO_2}^{tr}$	-	-	63,0	2,7	19,0	0,7	64,1	2,5	-	-
	$e_{CO_2}^{comb}$	2785	65,0	2117	90,6	2375	93,2	2225	91,0	1812	95,0
	$e_{CO_2}$	<b>4350</b>	<b>100</b>	<b>2334</b>	<b>100</b>	<b>2555</b>	<b>100</b>	<b>2446</b>	<b>100</b>	<b>1908</b>	<b>100</b>
min	$e_{CO_2}^{prod}$	763	22,7	1,4	0,1	1,4	0,1	1,4	0,1	-	-
	$e_{CO_2}^{transp}$	-	-	0,1	0,0	0,1	0,0	0,1	0,0	73,1	4,3
	$e_{CO_2}^{proc}$	-	-	77,6	3,5	75,8	3,1	78,8	3,4	-	-
	$e_{CO_2}^{tr}$	-	-	1,0	0,0	-	-	1,0	0,0	-	-
	$e_{CO_2}^{comb}$	2601	77,3	2117	96,4	2330	96,7	2225	96,5	1641	95,7
	$e_{CO_2}$	<b>3364</b>	<b>100</b>	<b>2197</b>	<b>100</b>	<b>2501</b>	<b>100</b>	<b>2685</b>	<b>100</b>	<b>1714</b>	<b>00</b>

It is 81% for coal, 99% for fuel oil and 96% for natural gas, respectively. At the same time, the total N<sub>2</sub>O component does not exceed 4 percent for all fossil fuels, and the methane share for fuel oil and natural gas does not exceed 0.5 percent. Hence, the lack of relia-



ble data on N<sub>2</sub>O and CH<sub>4</sub> emissions cannot lead to significant inaccuracies in the emission factor calculations for fossil fuels.

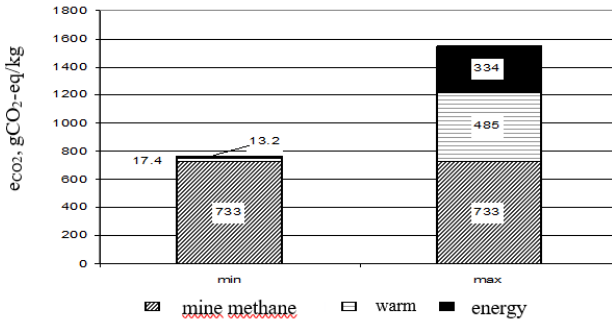


**Fig. 2.3.** Structure of the indirect component of greenhouse gas emissions

A similar conclusion can be drawn for emissions caused by the consumption of fuel during transport. This is primarily true for coal and fuel oil transport (Fig. 2.3).

### 2.1.2 Research into greenhouse gas emission while using biomass

The greenhouse gas emission indicator for biomass is associated with the technology of its preparation for combustion. The main preparation stages are: transportation, shredding, briquetting (pelletizing) or various combinations of these stages. The calculations were applied to waste biomass with bulk density 100-150 kg/m<sup>3</sup>, which includes sunflower husk, rice and buckwheat husk, and sawdust. Thus, the maximum value of the indicator of greenhouse gas emission in consideration of transportation, shredding and the following granulation is 125.2 gCO<sub>2</sub>-eq/kg t, and the minimum value, supposing just the transportation on 10 km by the specialized transport, is 0.8 gCO<sub>2</sub>-eq/kg t. The part of carbon dioxide in the total emission is from 95% to 98%.

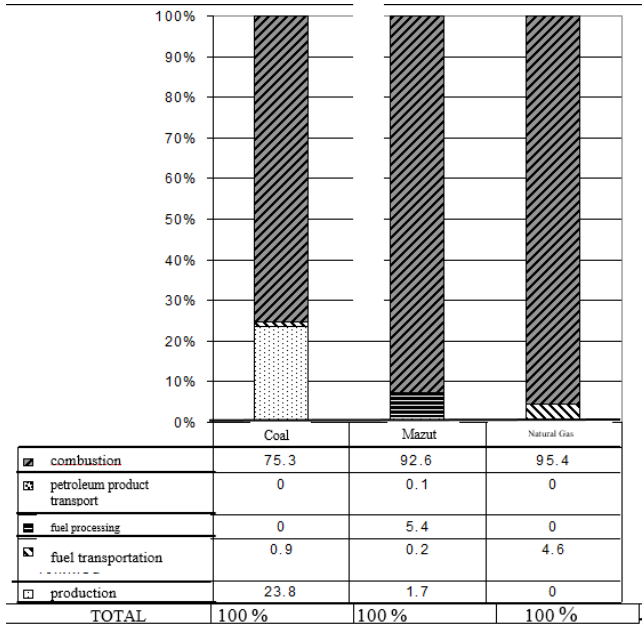


Fig. 2.4. Ratio of greenhouse gas emission components for different fossil fuels

## 2.2 Investigation of the environmental efficiency of various technologies and equipment for biomass energy use

Analysis of dependence of specific GHG emission reduction value (2.1) shows that it is determined by three values: ratio of emission indicators and efficiency of energy units, as well as absolute value of fossil fuel emission indicator.

Based on data (Tables 2.3 and 2.4) on emission figures, the ratio  $e_{CO_2}^{BM}/e_{CO_2}^{ff}$  varies between 0.00018 and 0.073. For each fossil fuel, the value of the ratio is given in Table 2.4.

Given that the ratio of efficiencies in dependency (2.4) is not significantly different from unity, it can be argued that the biomass GHG emission value can change the final result by 3-8%.

Table 2.4

Value ratios of biomass emission rates and fossil fuels,  $e_{CO_2}^{BM}/e_{CO_2}^{ff}$

Type of fuel to be replaced	coal	Mazut	Natural gas
Maximum value	0,037	0,050	0,073
Minimum value	0,00018	0,00031	0,00042

Based on the efficiency values of hot water boilers burning fossil fuels and biomass (Table 1.1, Chapter 1), it follows that the ratio  $\eta_{\Sigma BM}/\eta_{\Sigma ff}$  can vary from 1.34 to 0.753 (Table 2.5). In other words, the efficiency of energy units significantly affects the result of replacing fossil fuels with biomass.

The range of possible changes in specific GHG emission reduction in case fossil fuels are replaced by biomass using direct combustion technology for thermal energy generation is shown in Fig. 2.5.

Table 2.5

Efficiency ratios for hot-water boilers fired by biomass and fossil fuels on biomass and fossil fuels  $\eta_{\Sigma BM}/\eta_{\Sigma ff}$

Boiler heat output	Value	Replaceable fuel		
		Coal	Mazut	Natural gas
Up to 100 kW	max	1,169	–	1,071
	min	0,833	–	0,76
From 100 kW to 10 MW	max	1.34	1,084	1,059
	min	0,854	0,753	0,735

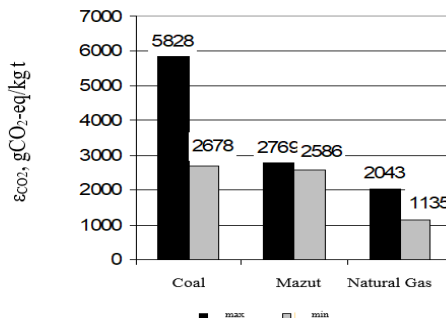


**Fig 2.5.** Specific reduction of greenhouse gas emissions  $\epsilon CO_2$  when replacing fossil fuels with biomass in heat production

An analysis of co-combustion of fossil fuels and biomass is of interest. When fossil fuels are partially replaced by biomass, the emission rate for the mixture of fuels decreases proportionally to the share of biomass (Fig. 2.6). With direct combustion of biomass, the substitution with coal is most likely and most efficient. In this case, the efficiency of the boiler and the whole plant changes as well. This is connected, first of all, with the change of heat losses with flue gases ( $q_2$ ) and bottom ash ( $q_6$ ).

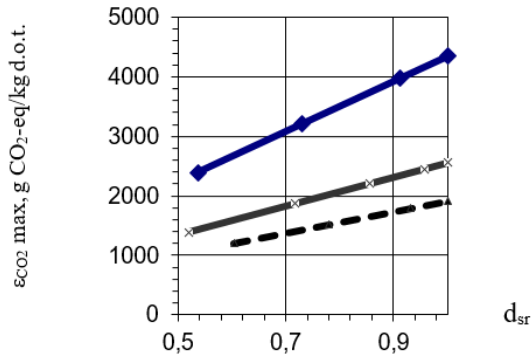


**Fig. 2.6.** Emission value  $\epsilon_{CO_2}$  as a function of energy fraction  $d$  of fossil fuel co-combustion with biomass: 1 - coal + biomass; 2 - fuel oil + biomass; 3 - natural gas + biomass

In modelling the boiler operation with partial replacement of coal by biomass, exactly these factors were taken into account. The calculation results showed that the change in boiler efficiency does not exceed 1% (tab. 2.6). Real experience of combined combustion of coal and biomass confirms the obtained results of insignificant change of boiler efficiency [6-8].

Table 2.6

Boiler operation indicators at partial substitution of coal for biomass

Boiler heat output	Value	Replaceable fuel		
		Coal		
Up to 100 kW	max	1,169	–	1,071
	min	0,833	–	0,76
From 100 kW to 10 MW	max	1.34	1,084	1,059
	min	0,854	0,753	0,735
Mass fraction of coal in the fuel mix-	0,7	0,8	0,9	1

ture				
Boiler efficiency,%	88,9	89,2	89,4	89,6
$\eta_{\Sigma}^{CM} / \eta_{\Sigma}^{HCK}$	0,992	0,995	0,998	1
$\epsilon_{CO_2}$ max g CO <sub>2</sub> -eq/kg o.t	3208,6	3594,7	3980,1	–

Gasification and pyrolysis are additional thermal processing steps and therefore reduce the overall efficiency of the biomass energy use process.

When using both chemical and physical energy from the generator gas, e.g. by burning it in boilers, gasification efficiencies range from 60% to 90%. The maximum values apply to medium power plants and the minimum values to low power plants. At use of generator gas in engines and turbines additional losses are connected with necessity of cooling of generator gas for the purpose of its cleaning [7].

Thus, at production of thermal energy the efficiency of boiler units, using direct combustion of biomass, is higher, on average, by 5-10 %, than at use of gasification. This is clearly seen in the presented data in table 2.7.

Table 2.7  
Overall efficiency of district heating system in the gasifier+boiler scheme, %

Gasification efficiency, %	Boiler efficiency 85%	Boiler efficiency 90%	Boiler efficiency 95%
70	59,5	63,0	66,5
80	68,0	72,0	76,0
90	76,5	81,0	85,5

A similar reduction in overall efficiency applies to pyrolysis processes. For example, the efficiency of liquid fuel production by fast pyrolysis using the RTPtm process is, according to real data, 85%. Naturally, this reduces the overall efficiency of energy production by 12-14%.

The analysis of the proposed pyrolysis technology in the hot air flow showed that the process efficiency is determined by the loss of physical heat of hot coke residue removed from the system. As the

pyrolysis gas is used in hot state without cooling. Taking into account that residue mass is 30-40% of the original fuel, and its heat capacity is 1,01 kJ/(kg-K) , portion of losses from heat of biomass combustion is 8-10 % at residue discharge temperature 500-700 °C. Therefore, the pyrolysis efficiency would be 90-92 %.

Taking into account the obtained efficiencies of biomass gasification and pyrolysis energy production processes, the limit values of specific greenhouse gas emission reduction indicator  $\epsilon_{CO_2}$  , presented in fig. 2.7, are determined.

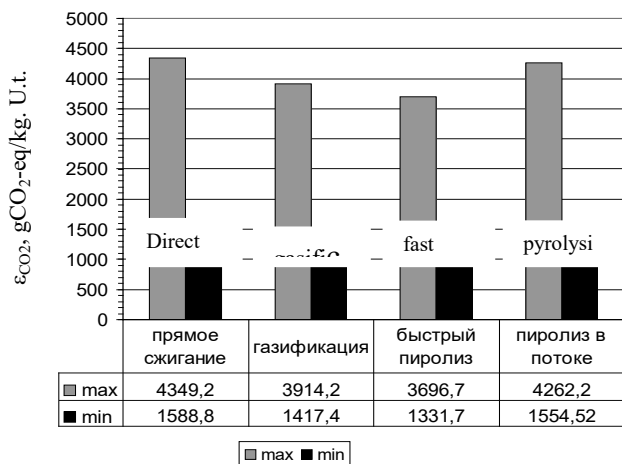


Fig. 2.7. Values of specific greenhouse gas emission reductions  $\epsilon_{CO_2}$

It follows that the most efficient technologies for the energy use of biomass are direct combustion technologies. Pyrolysis technology in a hot air stream is close to them and is competitive in terms of environmental efficiency. All of the above shows the relevance of the development of pyrolysis technology and further research in this field.

### General conclusions

1. A methodology has been developed that allows analysing the environmental efficiency of energy use of biogas obtained from anaerobic digestion of biomass based on the indicator of specific greenhouse gas emission reduction. This indicator allows for an ob-

jective comparison of existing and proposed technologies and equipment for the use of bioenergy fuels, while fully taking into account the complex effect of the type and quality of the substitute fuel on the emissions and efficiency of thermal units.

2. Using the developed methodology, quantitative data on the change in greenhouse gas emissions  $kCO_2$  for the conditions of Ukraine were determined, which were: for petrol -  $2188 \div 2329$   $gCO_2$ -eq/kg d.o.w., fuel oil -  $2414 \div 2552$   $gCO_2$ -eq/kg d.o.w, natural gas -  $1712 \div 1910$   $gCO_2$ -eq/kg d.o.w. and combustion of biogas produced by anaerobic digestion of biomass -  $1037 \div 1253$   $gCO_2$ -eq/kg d.o.w. Based on the studies performed, the ranges of possible specific reduction of greenhouse gas emissions when replacing natural gas with bioenergy fuel produced by anaerobic digestion of biomass were determined.

### *References*

1. **Edited by Prof. Malyarenko V.A** (2002) Power plants and environment. Study guide. - Kharkiv: Kharkiv State University of Geology and Geophysics. 398 p.
2. **Sigal I.Y.** (1988) Protection of the **air basin during fuel combustion - L.: Nedra. -312 p.**
3. **Margaret K. Mann, Pamela L. Spath** (August 29-September 2 1999) The net  $CO_2$  emissions and energy balances of biomass and coal-fired power systems/ Proceedings of the Fourth Biomass Conference of Americas, - Oakland, California, - Elsevier Science, - pp.379-385.
4. **Karnatsevich L.V., Khazhmuradov M.A., (2000) Grigorova T.K.** et al. Anaerobic processing of organic biogas production and utilisation: Informational and bibliographic reference. Kharkiv: NSCPHTI. - 155 p.
5. **Dubrovsky V.S., Viestur U.E.** (1998) Methane digestion of agricultural waste. - Riga: Zinatne, 204 p.
6. **Geletukha G.G., Zhel'zna T.A., Tishaev S.V., Kobzar S.G., Kop'yekin K.O.** (2001) Concept of Bioenergetics Development in Ukraine. Ukraine, 14 p.
7. **Geletukha G.G., Zheleznaya T.A., Martsenyuk Z.A.** (1999) Concept of bioenergy development in Ukraine / Industrial Heat Engineering, vol.6, T.21 <sup>1</sup> pp. 94-102.
8. **Geletukha G.G., Zheleznaya T.A., Borisov I.I., Khalatov A.A.** (1997) Prospects of using in Ukraine the modern technologies of thermochemical gasification and pyrolysis of biomass // Industrial Heat Engineering. -. - T. 19, (Vols 4-5). p. 115-120.

**INTERACTION OF CONICAL MONOLITHIC THIN-WALLED REINFORCED CONCRETE SHELLS WITH THE SOIL OF THE FOUNDATION AND THEIR STRESS STATE UNDER THE ACTION OF STATIC LOADING**



**Volodymyr PANTELEIENKO**

PhD (Engineering), Associate Professor State Higher Educational Institution "Prydniprovsk State Academy of Civil Engineering and Architecture", Ukraine



**Serhii KARPUSHYN**

PhD (Engineering), Associate Professor Central Ukrainian National Technical University, Ukraine



**Andrii CHERVONOSHTAN**

Graduate student of the Department of Construction and Road Machinery, State Higher Educational Institution "Prydniprovsk State Academy of Civil Engineering and Architecture", Ukraine

**Abstract**

The use of monolithic thin-walled spatial reinforced concrete shells as foundations for low-rise technological or residential facilities is economically feasible, in terms of reducing the volume of earthworks. Compared to classical types of foundations, it provides a significant reduction of costs of concrete, reinforcement, and labor costs. However, the issues of interaction of monolithic thin-walled spatial reinforced concrete shells with the base soil remain insufficiently researched.

The work substantiates the dynamic model of the "hammer-head-shell-soil" system when interacting with the base soil. It demonstrates that it is reasonable to use the elastic-viscous-plastic model taking into account the attached soil mass.

Based on that, the calculation scheme of this system was developed, considering the main connections between the colliding bodies and the interaction with the soil.

Taking into account the above, the mathematical model "hammer-head-shell-soil" is developed and demonstrated, which is a system of nonlinear differential equations of second order.



The solution of the system of equations gives the displacement and speed of all bodies, as well as the value of the forces acting on the contacts of colliding bodies at any moment of the time.

The presence of an oscillating process in the "hammer-head-shell-soil" system was experimentally established. The headrest oscillations are unstable.

They occur only in the event of impact and are extinguished as the load decreases. The analysis of the obtained dependencies when solving the mathematical model showed that the impact force is mainly determined by the height of the impact part and the stiffness of the elastic gasket. The ratio of the masses of the hammer and the shell has a smaller influence on the immersion process. The influence of the physical and mechanical properties of the soil base is insignificant.

Despite the periodic nature of the force impact, the shell sinks into the soil base quite smoothly.

This is explained by the significant mass of the shell, as well as the inertial stabilization properties of the soil base.

To find out the qualitative regularities and the physical essence of the process of immersion of conical blocks in natural conditions, a specially designed stand was used, which made it possible to determine the shape and dimensions of the compacted zone in different soils.

Concrete block designs of various types were developed and presented. A static load study using the "SolidWorks" program showed that concrete blocks can withstand tests for fatigue failure, for loss of stability, and have a safety margin for deformations that occur during loading. For the manufacture of concrete blocks, as the research on the material showed, it is advisable to use M300 concrete.

## **Introduction**

Monolithic and prefabricated reinforced concrete foundations traditionally used at the moment, along with the known advantages, have great complexity of erection on the construction site, high material consumption and, accordingly, cost. The use of monolithic thin-walled spatial reinforced concrete shells (MTWCS) as foundations for low-rise technological or residential objects is economically feasible in terms of: reducing the volume of earthworks by up to 90%, saving on formwork, idle time for the concrete to gain strength. In addition, the use of MTWCS in comparison with classical types and methods of arranging foundations allows you to significantly reduce the costs of concrete, reinforcement, and labour costs, which ultimately leads to a decrease in the estimated cost of zero-cycle works by up to 40% [1, 6-8].

## **Statement of the problem and formation of tasks.**

The issues of interaction processes of MTWCS with the foundation soil during dynamic or static immersion, as well as during build-

ing operation, remain insufficiently researched and highlighted in the scientific literature.

Immersion of MTWCS is possible by impact and static loading in the form of discrete or continuous gradual loading. Immersion by impact is a complex energy process, during which the potential energy of the hammer is transformed into the kinetic energy of the impact, which leads to the overcoming of the resistance forces of the soil base to the residual and elastic movements under the surface of the MTWCS [9, 10].

This study provides an analytical review of the methods, machines and their working bodies existing in construction practice for local form-forming compaction to intensify the process of constructing zero-cycle buildings and structures.

#### **Justification of the type of hammer-shell interaction model.**

At the same time, the impact energy developed by the falling load (hammer) is partially lost during the co-impact through the damper between the hammer and the shell, shaking the surrounding soil of the foundation, and only a part of it determines the residual movements of the MTWCS.

During the impact of the shock load, the elastic deformation of the head  $C_1$ , then the shell  $C_2$  itself, and the soil of the base  $C_3$  occurs, and only after that does the final vertical movement (immersion) of shell  $e$  occur. After the shock pulse is exhausted, the elastic deformations are restored. Thus, the total elastic deformation is equal to

$$C = C_1 + C_2 + C_3 \quad (1)$$

The values of  $C_1$  and  $C_2$  are usually small and can be neglected in many cases, i.e. take  $C=C_3$ . In the idealized schemes of changes in  $C$  and  $e$  as the impact energy of the hammer  $N$  increases, the elastic part of failure  $C$  increases at  $e=0$ , until it reaches the limit value  $C$  (Fig. 1). With a further increase in  $N$ , the value of  $C$  remains constant and the final failure  $e$  begins to increase. Thus, the ultimate elastic deformation of the soil  $C$  does not depend on the immersion parameters  $Q$  and  $H$  and is a characteristic of the soil.

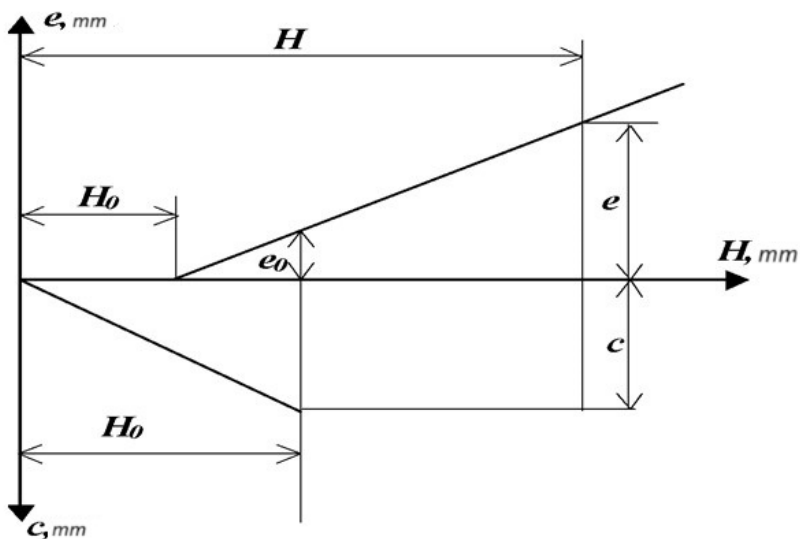
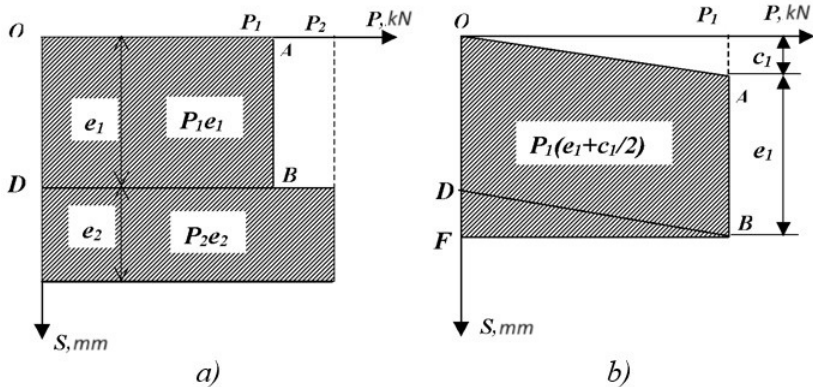


Fig. 1. Scheme of the dependence of  $C$  and  $e$  failures on the height of the fall of the hammer  $H$

The dynamic nature of the load application, which qualitatively changes depending on the ratio of the three phases of the soil base, has a significant influence on the deformation and resistance of the soil to the immersion of the shells. In connection with the impossibility of taking into account all the features of the upper layers of the soil base of the building site and obtaining accurate analytical expressions of dynamic resistance, it seems appropriate to use modeling methods for this purpose. At the same time, it is proposed to apply simple models that could reflect only the main properties of the system, and a large number of temporary features would be taken into account in a generalized way or through the values of calculated indicators.

To simplify this model, the initial state of the soil and the features of its changes during deformation may not be taken into account, but only the final influence of the features of this soil on the development of resistance forces may be reflected. The simplest soil models for the analysis of the "hammer-head-shell-soil" system are plastic and elastically plastic (Fig. 2).



**Fig. 2.** Dependence between the frontal resistance to movement of the shell  $P$  and its settlement  $S$  with different models of interaction: *a* - plastic model; *b* - elastic-plastic model

The plastic model is built taking into account the following assumptions (see Fig. 2*a*). It is an absolutely solid body, and the soil surrounding it is motionless. The resistance along the side and the top is  $P_b$ , i.e. friction between the side surfaces of the shell and the ground, reduced to the equivalent Coulomb dry friction of all types (it is assumed that  $P_b$  does not depend on the speed of the shell movement). As the tests showed, bringing the dynamic side friction to the equivalent dry friction makes it possible to obtain fairly stable soil resistance values.

The frontal resistance  $P_l$  is imagined as a pinched weightless bottom. Overcoming the friction that develops on the side surface, the shell affects the bottom, which sinks if the force applied to it exceeds  $P_l$ .

The relationship between the frontal resistance to the movement of the shell and its subsidence is given in a simplified form - in the form of a broken line OAB, and it is assumed that the force  $P_l$  does not depend on the speed of the shell movement. The area of the OABD diagram represents the work for one cycle of  $Pe$  (see Fig. 2, *a*). Despite its simplicity, this scheme can be quite useful, as it does not require the establishment of many uncertain parameters of elasticity and viscosity.

The elastic-plastic model is distinguished by the presence of elasticities that simulate the elasticity of the soil and intermediate ele-

ments (see Fig. 2*b*). At this stage of research, it is assumed that the elasticity of the soil is manifested mainly at the point of contact of the end of the shell with the soil. Therefore, the assumption that the lateral resistance to immersion is characterized by dry friction remains valid for the scheme.

The mechanical model of frontal resistance is simplified in the form of a bottom with a linear spring. When the casing is struck, the elastic deformation of the soil OA (compression of the spring) first occurs, and after the force in it reaches the value of the frontal resistance  $P_b$ , irreversible compression of the bottom AB begins (see Fig. 2*b*). After the load is finished, the BD is restored. This graph generally shows well the interaction of the shell with the soil.

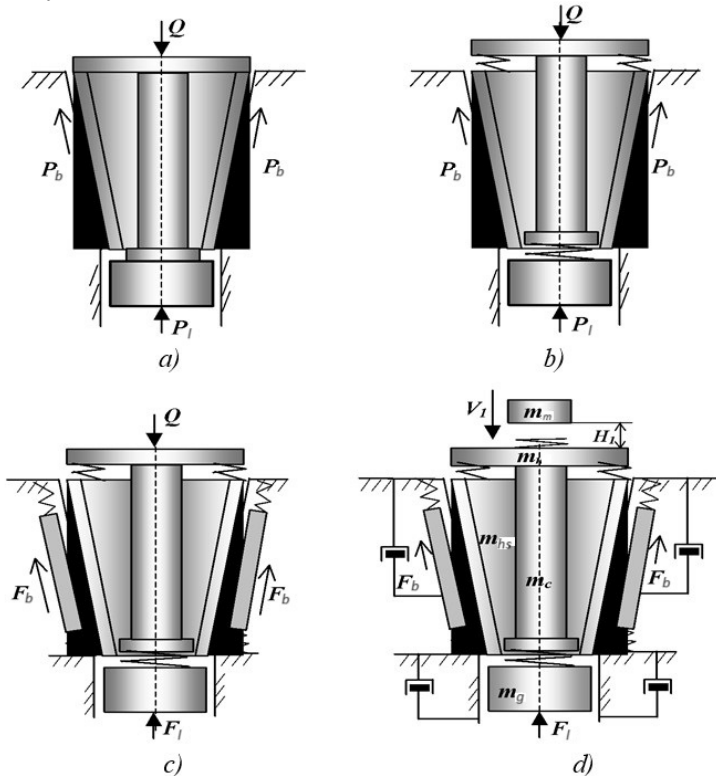


**Fig. 3.** Dynamic models of the "hammer-head-shell-soil" system: *a* - plastic model; *b* - elastic-plastic model; *c* - elastic-plastic model with attached soil mass; *d* - elastic-viscous-plastic model with attached soil mass

The positive properties of this model are also that when using the energy approach to determine energy costs, i.e. the area of the force-displacement diagram, the contours of this diagram, as well as the condition that  $C=0$  do not affect the accuracy of the results.

The considered model does not take into account the influence of soil inertia, which is quite significant.

Therefore, for further clarification, an elastic-plastic model with an attached soil mass is adopted (Fig. 3c). In this model, the surrounding attached soil mass is represented by an equivalent elastic body resting on elastic supports. In this case, the weight of the body is equal to the weight of the attached soil.

When the shell moves after the impact, the attached mass moves together with the shell until the elastic forces of the springs reach the resistance values on the side surface  $P_b$ . After that, the shell begins to slip relative to these elements. Further interaction is similar to the interaction of the previous model.

The elastic-viscous-plastic model (Fig. 3d) allows you to additionally take into account the viscous resistance of the soil. Further, it is possible to clarify the nature of the change in the frontal resistance of the soil depending on the settlement during loading and unloading, i.e. apply instead of a simple Prandtl elastic-plastic model, an elastic-plastic model with compaction, etc. Thus, the number of possible variants of dynamic models can be quite large. These models will more and more fully reflect the influence of the main factors and their role in the immersion process.

In all models analyzed above, the shell is considered a completely rigid body. However, upon impact, the shell has an elastic deformation. In addition, the usual impact on the shell is performed through the elastic headband.

Therefore, the elasticity of the shell and the headrest can be represented by a spring.

Evaluating the possibility of using complex models for practical calculations, it should be pointed out that currently there is not a sufficient amount of experimental data for a reasonable assignment of the numerical values of many indicators characterizing these models. In addition, the resulting mathematical expressions of the interaction of the "hammer-shell-soil" system will become more and more com-

plex with the complexity of the models, and this will not always contribute to increasing accuracy, i.e. practical purposes.

Considering the above, for further research it is most appropriate to use the elastic-visco-plastic model, taking into account the attached mass of the soil, the elasticity of the shell and the head (see Fig. 3*d*).

This scheme allows you to take into account the change in the value of the attached mass of the soil and the change in the interaction in connection with this.

### **Theoretical features of the interaction between the hammer and the shell.**

Thus, the dynamic model of the "hammer-head-shell-soil" system with elastic-viscous-plastic resistance of the soil is presented as follows. The elastic shell, which is in the soil, is struck with a hard undeformed hammer through the elastic head.

Under the influence of the impact, the shell acquires a reserve of kinetic energy, which is spent on overcoming soil resistance: with each impact, the shell sinks, initially elastically deforming the soil by the amount  $C$ , and then the plate moves in the soil by the amount of final failure  $e$ .

Elastic deformations after are restored with each hit. Each blow is considered as a single one, isolated from others, i.e. before each subsequent impact, the shell, hammer and soil are at rest.

The shock is absorbed by the reduced mass of the shell, taking into account part of the mass of the soil attached to it, and the subsequent movement is carried out only by the shell.

The hammer impact effect is represented as the transfer of some part of the kinetic energy of the impact  $N$ , which goes directly to the immersion of the shell [2-4].

For the development of a mathematical model of the process of immersion in the ground base of conical-reinforced concrete shells, a calculation scheme is proposed (Fig. 4).

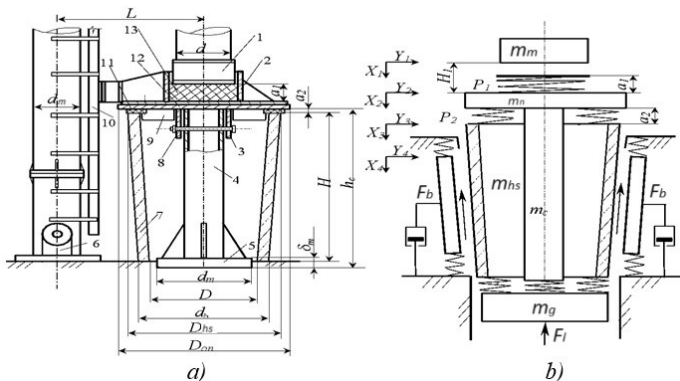


**Fig. 4.** System "hammer-head-shell-soil": *a)* - real system; *b)* - calculation scheme: 1 - hammer; 2 - headrest; 3 - conductor; 4 - core; 5 - tamping plate; 6 - mast; 7 - shell; 8 - finger; 9 - stops; 10 - guides; 11 - gasket; 12 - transmission plate; 13 - shock absorber

The mathematical model of this process is a system of nonlinear differential equations, which consist of the equations of the "hammer-head" and "shell-soil" subsystems, which must be solved jointly.

The mathematical model "hammer-head-shell-soil" is a system of nonlinear differential equations of the second order

$$\left\{ \begin{array}{l} m_2 d^2 X_2 / dt^2 = Q_2 + P_{12} - P_{23}, \\ (m_3 + m_4) d^2 X_3 / dt^2 = Q_3 + Q_4 + P_{23} - F_1 - F_b, \quad \text{при } F_b \leq R_b \\ X_3 = X_4, \\ m_1 d^2 X_1 / dt^2 = Q_1 - P_{12}, \\ m_3 d^2 X_3 / dt^2 = Q_3 + Q_4 + P_{23} - F_1 - F_b, \\ m_4 d^2 X_4 / dt^2 = Q_4 + F_b - K_b X_4, \end{array} \right. \quad \text{при } F_b < R_b \quad (2)$$

where  $m_1, m_2, m_3, m_4$  are the masses of the hammer, the head, the shell with the core, and the soil, respectively;

$Q_1, Q_2, Q_3, Q_4$  - respectively, the weight of the hammer, the head, the shell with the core and the soil;

$P_{12}, P_{23}$  - respectively, the forces acting on the contacts of the bodies, which collide;

$X_1, X_2, X_3, X_4$  are, respectively, the coordinates of the hammer, the head, the shell and the soil;



$F_f, F_b$  – frontal and lateral soil resistance, respectively;

$R_b$  is the ultimate resistance of the soil on the side surface.

The solution of this system of equations gives the displacement and speed of all bodies, as well as the value of the forces acting on the contacts of colliding bodies at any moment in time.

Mathematical model (2) belongs to the class of simulation models, as it simulates in detail the process of submersion of shells by impact load. This nature of the model allows you to use it to study the process of computer immersion. In addition, the implementation of full-scale experiments on the immersion of shells is a rather expensive method that requires a lot of machine time [5, 6].

Experience shows that the most interesting for practice is the study of the influence of the following factors on the immersion process:

- 1 - the ultimate resistance of the shell on the soil;
- 2 - the ratio of the mass of the striking part to the mass of the submerged shell;
- 3 - the thickness of the elastic gasket in the headrest;
- 4 - lifting height of the impact part.

Wood or conveyor rubber can be used as cushioning material in the headrest. The stiffness of the soil depends on the value of the lateral resistance so that the elastic failure does not exceed 1 cm. This value of elastic failure is most often encountered in practice.

Calculations on a computer were carried out for a hammer with a striking part weighing 500 kg.

Mathematical planning of the experiment was used to organize calculations on a computer. The Hartley-Cohn four-factor plan [3] was adopted. In order to obtain analytical dependencies between the parameters of the studied system, a correlation analysis of the obtained data was carried out. For the analysis, regression equations of the type are applied

$$y = A + \sum_{i=1}^n B_i X_i; \quad (3)$$

$$y = A + \sum_{i=1}^n (B_i X_i + C_i X_i^2); \quad (4)$$

$$y = A \prod_{i=1}^n X_i^B \quad (5)$$

Co-impacts in the "hammer-head-shell-soil" system are characterized by forces arising at the contacts of the elements that are in direct contact during the impact. In Fig. 5.a,b,c, the graphs of the change in time of these forces, calculated with the same initial data for a time interval equal to 0,03 s after the first contact of the hammer with the head, are given. The impulse of impact forces is characterized by several peaks and has a complex damping character. The contact of the shock part with the head is irregular. Thus, for a period of 0,06 s, 11 collisions occurred at the "hammer-headpiece" contact, and 10 at the "headpiece-shell" contact.

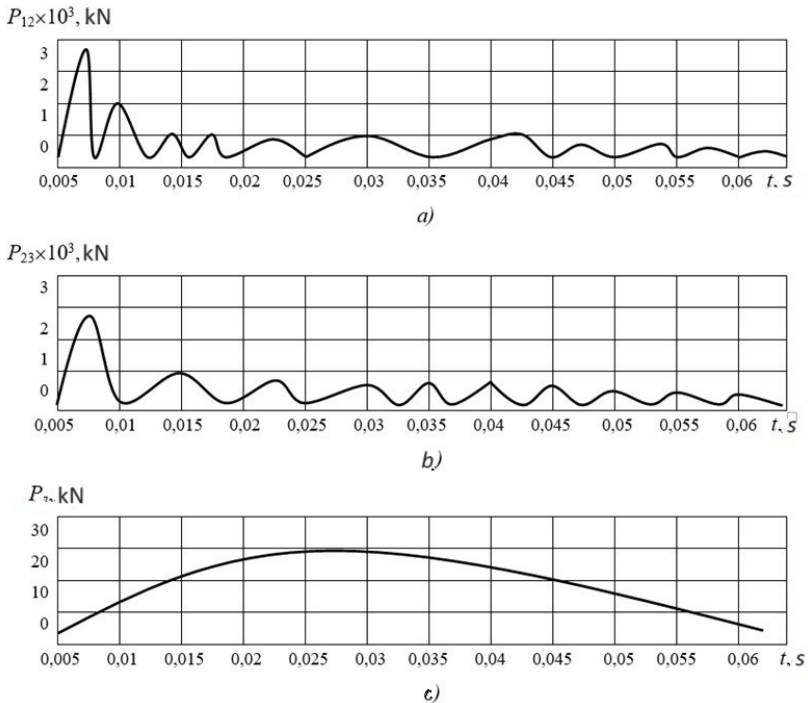


**Fig. 5.** Forces acting on the contacts of colliding bodies: *a* – hammer-head; *b* – a head-shell; *c* - is the frontal resistance of the soil

In this way, we can talk about the existence of an oscillatory process in the "hammer-head-shell-shell-soil" system. Oscillations of the headrest are unstable. This follows from the fact that during slow,

quasi-static immersion, oscillations do not occur, they occur only during impact and die out as the load decreases.

In real conditions, due to the inevitable eccentricities of load application, the headrest carries out not only forward movement along the vertical axis but also angular oscillations. In the mathematical model, following the accepted assumptions, all movements occur only along the vertical axis, so the graph of the impact force on the shell is divided into several separate co-impacts.

The observed multiple collisions of the headpiece with the shell are due to a significantly shorter period of the headpiece's own oscillations compared to the duration of the force impact. Therefore, the headpiece can be represented as a mechanical oscillator, brought out of equilibrium by mechanical collision with the striking part, and then oscillating between two massive bodies: the striking part and the shell.

The regularities noted above were reflected in the correlation dependences for the impact force. The impact force on the "hammer-headset" and "headset-shell" contacts can be determined by the following dependencies

$$P_1 = 314m_M H_1 + 0,7R + 212 \frac{m_M}{m_H} + 6131 \frac{a_1}{S_1} + 950, \quad (6)$$

$$P_2 = 245m_M H_1 + 0,97R + 522 \frac{m_M}{m_c + m_{hs}} + 9231 \frac{a_2}{S_2} + 637, \quad (7)$$

where  $m_M$ ,  $m_H$ ,  $m_{hs}$ ,  $m_c$  - respectively, the mass of the hammer, head, shell, and core;

$a_1$ ,  $S_1$ , and  $a_2$ ,  $S_2$  - respectively, the thickness and area of the cushioning pads at the "hammer-headrest" and "headrest-shell" contacts;

$H_1$  - hammer lift height;

$R$  - soil resistance.

The correlation ratio of these formulas is at least 0,95. This testifies to the correct selection of varied parameters.

The analysis of the given dependencies shows that the force of the impact is mainly determined by the height of the impact part and the stiffness of the elastic gasket. The ratio of the masses of the hammer and the shell has a smaller influence on the immersion process. The

influence of the physical and mechanical properties of the soil base is insignificant.

Despite the periodic nature of the force impact, the shell sinks into the soil base quite smoothly. This is explained by the significant mass of the shell, as well as the inertial stabilization properties of the soil base. The shell receives a positive acceleration under the influence of the first co-impact, then the shell acceleration changes its sign, i.e. the shell's movement slows down.

For the value of the final failure, the best result is given by the dependence of the form:

$$e = 1,2 \frac{m_M H_1 \left( \frac{m_M}{m_h + m_c + m_{hs}} \right)^{0,2}}{R^{1,3} (10a_1)^{0,64}} . \quad (8)$$

Analysis of the influence of various factors on the size of the failure shows that the impact of the stiffness of the shock absorber can be neglected, since the reduction in failure when the thickness of the lining increases from 0,05m to 0,25m does not exceed 10%. Therefore, for practical purposes, dependence (8) can be simplified

$$e = ,2 \frac{m_M H_1 \left( \frac{m_h}{m_h + m_c + m_{hs}} \right)^{0,2}}{R^{1,3}} . \quad (9)$$

### **Experimental part and modeling in Solid Works.**

The study of the process of immersing conical blocks in the soil Fig. 6, was carried out in the immediate vicinity of erected houses and structures on construction sites in places that are characteristic from the point of view of the geological structure and the main characteristics of the soil, located within the boundaries of the construction site. A specially developed stand [3, 5] was used to clarify the qualitative regularities and physical essence of the process of submersion of conical blocks in natural conditions.

The research stand (Fig. 7) consists of: anchor piles 1, reinforced concrete blocks 2, transverse beams 3, fittings 4 and clamps 7 connecting anchor piles with transverse beams. Clamps 5, which hold the transverse beam 8 with mounting brackets 6 in a fixed position, the tested block 9 with a supporting bridge 10, a support plate 11, a hydraulic jack 12 with a load capacity of up to 500 t with a rod 13,

concrete slabs 14 for transferring the load to the transverse thrust beam 8, pumping unit 15, shock absorber 16 and wells 17, which provide the possibility of soaking the soil to a depth of 5 m and a metal insert 18 for distributing the load over the volume of the shell.

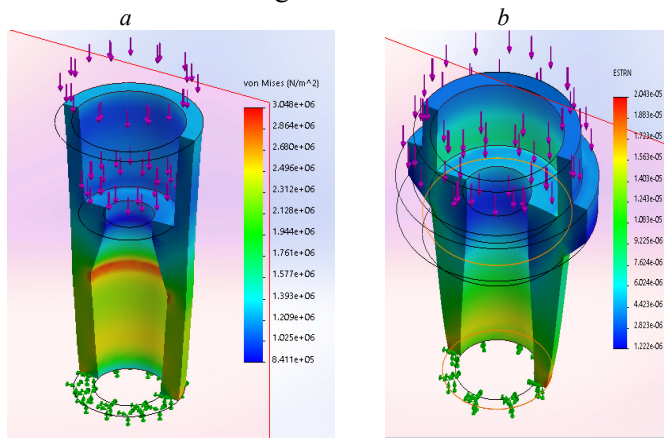


**Fig. 6.** Conical concrete blocks of various types for erecting foundations for buildings: *a* - conical block for columns of frame buildings; *b* - conical block with an extended upper part

During experiments in type II soils, soil soaking was carried out. For this, boreholes with a diameter of 200 mm and a depth that is 2 times greater than the height of the stamp were drilled around the block in a radius of 2 m with a step of 2 m. The sequence of the experiment includes the following:

1. The main physical and mechanical properties of the soil are determined with the help of the Lytvynov field laboratory (PLL-9).
2. The soil is soaked using pre-drilled wells to a depth that is 2 times greater than the height of the stamp.
3. A submersible stamp is installed on the design mark, on the upper section of which a transfer plate with a hydraulic jack is mounted.
4. The jack is turned on, the force of which is transmitted through the rod and the support beam to the upper section of the block, through the base plate and through the metal insert on the bridge, which allows unloading the upper part of the block, as a result, the stamp sinks into the soil by the stroke of the rod equal to 200 mm.

5. The hydraulic jack rod returns to its original position. A concrete slab with a thickness equal to the working stroke of the hydraulic jack rod of 200 mm is placed under the base plate, then the working fluid is fed into the piston cavity and the next stage of immersion takes place.

6. Immersion is carried out to a depth at which the deformation of the soil stabilizes in the longitudinal and vertical directions, while a compacted zone with areas of different densities and shapes is formed.

7. After sinking to the design mark with the help of a crane, the block is pulled out of the soil and the dimensions and physical and mechanical properties of the compacted zone are determined in the pit.

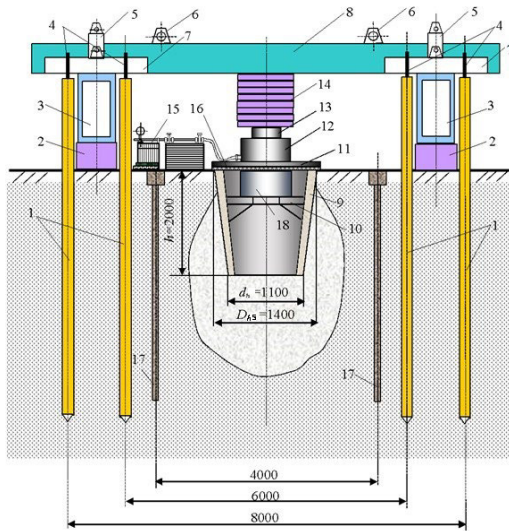


Fig. 7. Structural diagram of the stand for studying the immersion process

The resistance of the soil during the immersion of concrete blocks is determined by the degree of its compaction, the dimensions of the compacted zone, the strength and deformation characteristics of the soil.

As a result of the experiments carried out in the conditions of various construction sites, the study of the density of forest-like and clayey soils, it was established that with an area of the lower base

equal to  $0,2-0,3 \text{ m}^2$  (Fig. 8), the compacted zone extends to the clay –  $0,8 \text{ m}$  from the lower section of the block.

In terms of its shape, the compacted zone in various soils approaches an ellipsoid of rotation (Fig. 8), the major axis of which coincides with the vertical axis of the block. At the same time, a significant part of the compacted zone is formed under the base of the block. This is one of the differences in the formation of a compacted zone in comparison with piles, which have a much smaller area of the lower base. When submerging blocks whose area is close to  $0,2-0,3 \text{ m}^2$  (Fig. 8, *a, b*), the compacted zone is characterized by the presence of four areas with different densities: the area with the highest density in the form of an elongated ellipsoid of rotation in the horizontal plane with a density of about  $2 \text{ g/cm}^3$  (cork). Below the cork is an area with a density of  $1,9 \text{ g/cm}^3$  (core), it is located directly under the base of the element that is immersed, and is close in shape to a sphere, the diameter of which is approximately equal to:  $d_j = 1,1d_b$ , where  $d_b$  is the diameter the basics of the block. A compacted core with a density equal to  $1,9 \text{ g/cm}^3$  for loams and sandy loams is adjacent to a region with a lower density, approximately  $1,8 \text{ g/cm}^3$ . Next, the area with a density of about  $1,7 \text{ g/cm}^3$ , while the density of the soil of natural composition can be equal to  $1,6-1,5 \text{ g/cm}^3$ .

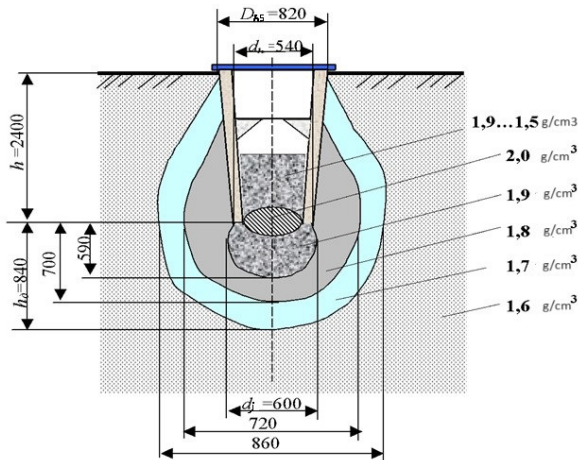


**Fig. 8.** The formation of a compacted zone during the immersion of conical concrete blocks with a base area of  $0,2-0,3 \text{ m}^2$  in forest-like and clayey soils

Immersion of concrete blocks can be carried out both by shock and static load. At this stage, preference is given to machines that perform immersion by the compression method. At the same time, the force developed by this machine is in the range of 100...120 t and more.

The graphs of the stress state of various concrete blocks under the action of static load are presented below. The plots were built using the SolidWorks computer program [14-17]. The initial data, in this case, were the following parameters: geometric dimensions of the block, wall thickness, material (concrete M300) and static load of 60 tons.

It should be noted that the study of the stress state was carried out at the moment of the greatest soil resistance on the side and front surfaces of the block. This condition can be observed when the block is completely immersed in the soil base. At this moment, the stress in the material reaches its maximum value.

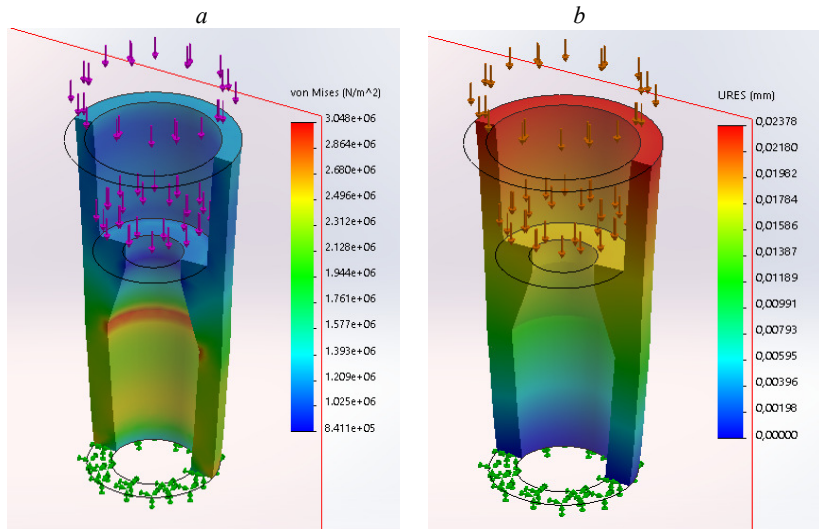


**Fig. 9.** Plots of stresses *a* - and displacement *b* - of a conical block under the columns of frame buildings.

The stress diagram (Fig. 9a) allows you to plot the resulting stress in different places of the structure under static and dynamic loads



according to the Mises criterion. It can be seen from the plot that the greatest stress according to this criterion occurs in the middle part of the conical block at the end of the internal structural element. Closer to the upper section of the shell, the stress decreases, towards the lower supported ring it will also be smaller.

In fig. (Fig. 9b) shows the diagram of movements, which characterizes the stability of the block under loads, provides the possibility of obtaining the results of the movement and researching the structure for loss of stability. It can be seen from the displacement graph that the most significant displacements during loading will occur in the upper and middle parts of the block.

A concrete block (Fig. 10) with an expanded upper part has a higher bearing capacity. In addition to the formation of a compacted zone under its base and support on the side surface, it rests on the soil with its upper, wider part, which increases its bearing capacity by approximately 10-15%.

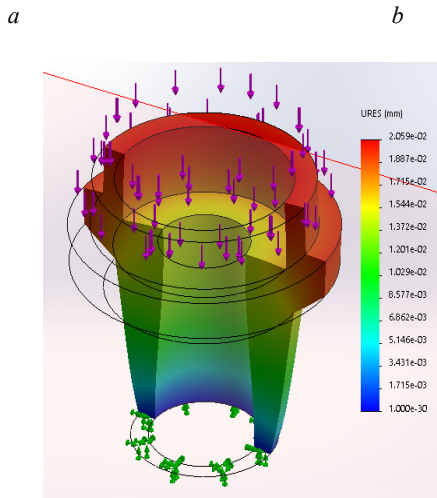


**Fig. 10.** Plots of stresses *a* - and displacement *b* - of a conical block with an extended upper part under the columns of frame buildings

It can be seen from the stress plot (Fig. 10a) that the greatest stress will be at the base of the conical shell. Closer to the upper section of the shell, the stress decreases [11-13].

In fig. (Fig. 10b) shows the diagram of movements, which characterizes the stability of the shell under loads, and provides the possibility of obtaining the results of the movement and researching the structure for loss of stability. It can be seen from the displacement graph that the most significant displacements under loads will occur in the upper part of the conical block. In the lower part, they will be minimal.

### **Conclusions**

1. The proposed dynamic model and calculation scheme of the "hammer-head-shell-soil" system with elastic-viscous-plastic resistance with attached soil mass.

2. The mathematical model of the researched process is formed, which is a system of nonlinear differential equations, which consists of the equations of the "hammer-head" and "shell-soil" subsystems, which must be solved jointly.

3. Determined dependences for the impact force on the "hammer-headrest" and "headrest-shell" contacts.

4. To clarify the qualitative regularities and the physical essence of the process of immersion of conical blocks in natural conditions, a specially designed stand is proposed and research methods are presented.

5. As a result of the experiments carried out in the conditions of various construction sites in forest-like and clayey soils, the dimensions, shape and density of the soil core formed under the base of the shells were determined.

6. The study of the stress state of concrete blocks of various types using the SolidWorks program showed that their construction withstands tests for fatigue failure, loss of stability, margin of strength, and deformations that occur under load.

### *References*

1. Machines and equipment for the arrangement of recess for foundations of

quickly installed technological mining facilities without digging: Monograph /V.I. **Panteleienko, S.O. Karpushyn** – Petrosani, Romania: UNIVERSITAS Publishing, 2022. – 63 p.

2. **Panteleyenکو V.I., Karpushyn S.O., Chervonoshtan A.L., Ihnatov A.B.** Do-slidzhennya napruzhenoho stanu metalevykh shtampiv pid fundamenti dlya budi-vel' riznogo pryznachennya / Naukovyy visnyk budivnytstva. Naukovotekhnichnyy zhurnal Kharkivs'koho natsional'noho universytetu budivnytstva ta arkhitektury KHNUBA. Kharkiv 2020, t.101 №3, S 99-107.

[doi.org/10.29295/2311-7257-2018-101-3-99-107](https://doi.org/10.29295/2311-7257-2018-101-3-99-107)..

3. **Panteleienکو V.I., Karpushyn S.O.** Doslidzhennya procesu zanurennya tonkostinny'x fundamentiv-obolonok pry' zvedenni nul'ovogo cy'klu budivel' i sporud.// Naukovi zapy'sky' KNTU Vy'pusk 10, Naukovi zapy'sky': zb. nauk. pr. - Kirovograd: KNTU, 2010. - Vy'p. 10, ch. 3. - S. 228-225. URL: <http://dspace.kntu.kr.ua/jspui/handle/123456789/5654>

4. **Khmara L.A., Shypilov O.S., Musiyko V.D., Kuz'minets' M.P., Panteleyenکو V.I., Karpushyn S.O.** Dorozhni mashyny. Mashyny dlya budivnytstva, remontu ta utrymannya avtomobil'nykh dorih. Navch. Posibnyk. Chast. II. Kyiv-Dnipropetrovs'k: NTU, 2013. 400s.: tabl., skhemy, rys..

5. **Panteleienکو V.I., Karpushyn S.O.** Spetsializirovannoye oborudovaniye dlya pogruzheniya svay i fundamentov-obolochek. / Materialy Mizhnarodnoyi naukovopraktychnoyi konferentsiyi, prysvyachenoyi 40-richchyu kafedry budivel'nykh, dorozhnikh mashyn i budivnytstva. «Problemy rozvytku dorozhn'o-transportnoho i budivel'noho kompleksiv» 03-05 zhovtnya 2013r. – Kirovohrad, PP Eksklyuzyv-System, 2013. S.337-340.

6. Patent na korynsnu model' 148700 Ukrayina, MPK (2006) E02D 7/00 Prystriy dlya zanurennya obolonok. **Panteleyenکو V.I., Chervonoshtan A.L., Karpushyn S.O., Pushenko V.A.**; zayavnyk i vlasnyk patentu DVNZ PDABtaA; zayavleno 15.03.2021; opublikovano 08.09.2021, byuleten' №36.

7. Mashyny dlia pohruzheniya svai, fundamentov-obolochek y ustroystva uhlubleniy bez vyemky hrunta: Monohrafiya / L.A.Khmara, V.Y. Panteleenکو, M.H.Malich – Pavlohrad, TOV «IMA-pres». 2017 – 205s.

8. **Khmara L.A., Panteleienکو V.I., Kulik I.A.** Opredeleniye parametrov mashin dlya pogruzheniya svay i fundamentov-obolochek. Dnepropetrovsk: OOO «ENEM», 2005. 144s.: tabl., skhemi, ris.

9. **V.I. Panteleienکو, S.O. Karpushyn** Energy-effective method of installation of foundations under objects of mine surfaces. UDC 622:658.589 (063) 2 nd International Scientific and Technical Internet Conference “Innovative Development of

Resource-Saving Technologies of Mineral Mining and Processing”. Book of Abstracts. - Petrosani, Romania: UNIVERSITAS Publishing, 2019. - 220 p. ISBN 978-973-741-656-8 (Print) ISBN 978-973-741-663-9 (Online) S.104-107. URL: <http://surl.li/bbfuw>.

10. Patent na korysnu model' 147297 Ukrayina, MPK (2006) E05D 13/00 Stend dlya doslidzhennya yakisnykh zakonmirmnostey protsesu zanurennya modeley obolonok v hrunt. Panteleyenکو V.I., Chervonoshtan A.L., Ihnatov A.B.; zayavnyk i vlasnyk patentu DVNZ PDABtaA; zayavleno 06.11.2020; opublikovano 28.04.2021, byuleten' №17.

11. Patent na korysnu model' 147293 Ukrayina, MPK (2021.01) E05D 13/00 Stend dlya doslidzhennya protsesu zanurennya obolonok v hrunt v naturnykh umovakh. **Panteleyenکو V.I., Karpushyn S.O., Chervonoshtan A.L., Danylenko I.O.**; zayavnyk i vlasnyk patentu DVNZ PDABtaA; zayavleno 06.11.2020; opublikovano 28.04.2021, byuleten' №17.

12. **V.I. Panteleienکو, A.L. Chervonoshtan M.S. Khomchyk** Doslidzhennia napruzhenoho stanu konichnykh betonnykh blokiv ta osoblyvosti formuvannia ushchilnenoi zony pry yikh zanurenni u hrunt. Naukovyi visnyk budivnytstva. – Kharkiv, 2020. S. 36-41.

13. V.I. Panteleienکو, S.O. Karpushyn., A.L. Chervonoshtan, A.B. Ihnatov Doslidzhennia napruzhenoho stanu metalevykh shtampiv pid fundamenti dlia budivel riznoho pryznachennia. Naukovyi visnyk budivnytstva. – Kharkiv, 2020. S. 99-107.

14. Patent na korysnu model' 148692 Ukrayina, MPK (2021.01) G01M 7/08. E02D 17/00 Stend dlya doslidzhennya protsesu vytrambovuvannya zahlyblen' u hrunti. **Panteleyenکو V.I., Karpushyn S.O., Chervonoshtan A.L., Matsevych I.M., Abyel'tsev YE.D.**; zayavnyk i vlasnyk patentu DVNZ PDABtaA – № a 2008 08807; zayavleno 18.01.2021; opublikovano 08.09.2021, byuleten' № 36.

15. **Aliamovskyi A.A.**, COSMOSWorks. Osnovy rozrakhunku konstruktsii na tryvkist v seredovyshchi SolidWorks, DMK Pres, 2010, 784 c.

16. Trokhmirne modeliuвання u prohrami SolidWORK. Metodychni vkazivky ta instruktsiia do vykonannia indyvidualnykh kontrolnykh robot. // **Shpak Ya.V., Lanets O.S., Hurskyi V.M.** – Lviv: Rukopys, 2011. – 30 s.

17. **Polishchuk I.N.** SOLID WORK 2001 v oryhinali. S.- P., 2003.

18. **Prokhorenکو V.P.** SolidWorks. Praktychne kerivnytstvo. – M.: OOO «Binom-Pres», 2004 r. – 448 s.

**MODELS AND METHODS OF OPERATIONAL  
MANAGEMENT IN MINING PRODUCTION**



**Oleksandr Krukovskiy**

Corresponding Member of NAS of Ukraine, Doctor of Technical Sciences (D. Sc), Deputy Director of the institute, M.S. Polyakov Institute of Geotechnical Mechanics under the National Academy of Sciences of Ukraine, Dnipro, Ukraine



**Andrii Khorolskiy**

Candidate of Technical Science, Head of the Department of Field Development Problems, Branch for Physics of Mining Processes of the M.S. Poliakov Institute of Geotechnical Mechanics the National Academy of Sciences of Ukraine, Dnipro, Ukraine



**Oleksandra Ashcheulova**

Candidate of Economic Science, Associate Professor, Dnipro University of Technology, Dnipro, Ukraine



**Volodymyr Medianyk**

Candidate of Technical Science, Dnipro University of Technology, Associate Professor of the Mining Engineering and Education Department, Dnipro, Ukraine



**Oleksandr Mamaikin**

Candidate of Technical Science, Dnipro University of Technology, Associate Professor of the Mining Engineering and Education Department, Dnipro, Ukraine

## **Abstract**

The goal of the work is to develop and verify a new methodological approach for the comprehensive assessment of the technological potential of coal mining enterprises.

To address this task, a comprehensive approach has been applied, based on the implementation of the neoclassical production function in the form of the Solow model to analyze the state of the coal mining industry. It also involves evaluating the economic reliability coefficient to develop recommendations for improving techno-economic indicators.

The efficiency of enterprise functioning can be assessed by the ratio of input (capital) to output (production level) flows of resources, with a significant role played by the innovative component. Analyzing the relationships between resource flows allows selecting optimal production development scenarios and forming principles for designing production at a certain stage of development.

For the first time in the paper, a model for evaluating parameters of mining production is proposed, demonstrating the relationship between production functions and resources. Using the developed model, it is possible to track the efficiency of the use of production resources over time, determine production volumes, calculate the main parameters of coal mines' functioning, and investigate the resources contributing to increased productivity.

Regularities in the formation of the efficiency level of coal mining enterprises are established for the first time, and approaches to production design considering the area of rational exploitation are developed.

Methods of combined management of processes of simple and extended reproduction of technological schemes of mines are proposed by regulating the resource potential of mines. The procedure of gradient reduction of the limit on technological resources and adjusting the functional value to approach results in mine operation to a possible breakeven threshold is a widely recognized form of sensitivity analysis of modeling results. The comprehensive assessment of the technological scheme of the mine in four directions significantly increases the objectivity level of the final result compared to evaluating it with only one indicator.

## **Introduction**

The features of the management system of coal mining enterprises at the present stage are closely tied to the change in their strategic orientations. The primary economic goal of enterprises in market conditions is to enhance production efficiency through various influencing factors, including the formation of internal economic reserves. The potential utilization of these reserves enables the implementation of a policy to abandon budgetary support for loss-making coal mining enterprises. In this context, the ability to extract a certain volume of coal and increase reserves without significant reliance on state budget funds, achieving breakeven, ensuring a certain level of

profitability, reducing subsidy levels, and creating conditions for investment attractiveness becomes particularly crucial.

Hence, there is a need to develop new methodological approaches to stabilize the situation. To achieve this, it is necessary to:

- analyze innovative prospects for underground deposit exploitation and identify key factors shaping the overall production level, as well as possible ways to enhance efficiency;

- identify the main factors for replenishing internal reserves of coal enterprises;

- propose methodological approaches for evaluating the level of coal mining enterprises.

The aforementioned work is dedicated to addressing these tasks.

The key to improving the efficiency of coal mining enterprises lies in creating conditions that allow for the operational management of production activities. This requires the development of tools and approaches.

### **Existing Approaches to Mining Production Management**

Before delving into the main material, it is necessary to analyze existing approaches to design. This will allow for a concise overview of a multitude of approaches. But before doing so, let's characterize the models that can describe production processes. Management and design processes in mining production can be divided into 6 types of models: optimization, informational, deterministic, probabilistic, static, and dynamic.

Optimization models encompass the description of the functioning conditions of the object in the form of equations and inequalities that represent constraints of the task and reflect the balance of resources (material, labor, financial, etc.). The distinctive feature of optimization models is that there is a set of feasible solutions (sometimes an infinite majority), among which the optimal solution needs to be identified.

Informational models contain the necessary output information for decision-making. With these models, it is possible to establish a regression relationship between the influencing and outcome features. In these types of models, the functioning of the object is described by equations that establish a quantitative connection between the input and output parameter systems.

Deterministic models presuppose a cause-and-effect relationship in the model, which is interrelated and can be expressed analytically. In other words, randomness is considered insignificant in deterministic models.

Probabilistic models take into account the influence of random factors on economic and organizational phenomena and processes. Models of reliability theory, mass servicing, forecasting of mining equipment indicators, quarry transport, etc., fall under probabilistic models.

Static models are applied when the parameters of a specific system, within a defined time interval describing the operation and conditions of the object, practically do not change.

In cases where system parameters undergo significant changes over time, dynamic models are applied.

It is worth noting that mathematical programming methods differ only in the requirements for constraints. If the constraints of the objective function are linear, linear programming methods are applied. If the constraints or the objective function are specified by nonlinear constraints, nonlinear programming is employed. If there is a requirement for the components of the solution vector  $X$  to be integers, then integer programming is used. If randomness is considered, stochastic programming is applied. To account for time, dynamic programming is utilized.

After this, we can proceed to the analysis of tasks, which have been classified based on different types.

There are several classifications that can be conditionally divided into:

1. Classification based on the application of economic-mathematical methods. This involves a subdivision into models such as probabilistic, stochastic, deterministic, static, dynamic, etc.

2. Classification based on the type of obtained solution: informational and optimization models.

3. Classification based on the forecasting duration (short-term, long-term) and the method of obtaining the solution (using software, simulation modeling).

Let's delve into each classification separately and analyze the main works in each category.



The classification based on economic-mathematical methods [1] is grounded on the tools (mathematical) employed for model construction. The following methods are known: mathematical programming, which is divided into linear [2], quadratic [3], integer [4], stochastic [5], dynamic [6], and geometric [7]; inventory management [8], game theory [9], network models [10], correlation models [11], queuing theory [12], reliability theory [13], forecasting [14], and simulation modeling [15]. When applying linear, quadratic, and integer programming, optimization, deterministic, and static models can be implemented. For stochastic programming: optimization, probabilistic, and static models. For dynamic programming: optimization, deterministic, probabilistic, and dynamic models. For geometric programming: optimization, deterministic, static, and dynamic models. Inventory management implements optimization, deterministic, probabilistic, static, and dynamic models. Game theory realizes optimization, deterministic, probabilistic, static, and dynamic models. For network models as an economic-mathematical method, optimization, informational, deterministic, probabilistic, and static models are possible. Correlation methods, like queuing theory, implement informational, probabilistic, and static models. Reliability theory, forecasting, and simulation modeling realize informational, probabilistic, static, and dynamic models.

One drawback of this classification is the division of methods based on the type of objective function and decision-making tool, without describing the application area or "rationality of the approach." Additionally, it does not consider the interconnection of production processes.

Examining works [1-15] and methods, it becomes apparent that these can be applied to short-term planning. However, decision-making processes are influenced not only by economic, technological, and social factors but also by qualitative ones. If, for instance, the specific cost or transportation costs [16] are taken as the objective function, the decision will be optimal in terms of the defined parameter. Still, there is a high probability that it will not correspond to the "quality" characteristic - a set of features that characterize the object.

Therefore, a classification of methods based on the type of obtained solution [17] was considered. According to this classification,

methods are divided into optimization and informational. Optimization models answer the question of which solution is optimal from a quantitative point of view, while informational models address the qualitative aspect. Optimization methods include all the aforementioned mathematical programming methods [2-7], as well as game theory, network, and correlation models. Informational models are based on the Analytic Hierarchy Process (AHP) method [18] and its variations, such as PROMETHEE [19], ELECTRE [20], TODIM [21], VICOR [22], Fuzzy-AHP [23], Grey-AHP [24], fuzzy set methods [25]. These approaches prioritize and build hierarchies, resulting in a qualitative solution but heavily dependent on the level of expertise. However, situations may arise where it's impossible to construct a connectivity matrix [26]. To address the drawbacks of the first two groups of methods, another classification was considered [27], which is based on planning terms and tools. This classification divides methods into long-term and short-term planning, which are all based on the methods described earlier [2-15, 18-25]. It highlights a group of approaches based on simulation modeling [28] of production parameters. These parameters can consider qualitative or economic indicators, allowing for production activity planning. The difference lies in the simulation modeling method.

The last set of works [29–32] suggests trends in the creation of approaches to designing processes for the development of mineral deposits:

- the optimality criterion is "quality" but distinguished by various quantitative indicators;
- general tasks are divided into local ones; only after optimizing the tasks at the first stage do they move on to optimization at the second and beyond.

With this analysis, we can proceed directly to the development of the operational management model for mining production.

### **Development of Operational Management Model**

Innovative aspects of production can be described using the Solow model [33]. Concerning mining production, this model offers several advantages:

1. Firstly, it is based on the application of a single type of good Y, as in the conditions of Ukraine, mines are considered enterprises for

coal extraction, not components in the energy or metal production system.

2. Secondly, the model takes into account the relationship between capital, labor, and the level of workers' qualifications, thus aligning with fundamental technical and economic indicators that define enterprise efficiency.

3. Thirdly, the introduction of new innovations  $A$  is closely associated with the volume of labor resources  $L$ , a decisive factor in the production design process.

In its general form, the Solow model considers a neoclassical production function of the form

$$Y=f(K,L,A)$$

де  $K$  - the level of engaged capital;

$L$  - the volume of labor resources;

$A$  - the efficiency of one worker, depending on the level of qualification and knowledge.

In this context, the variable  $A$  reflects technological progress and innovations in production, correlating with the volume of labor resources. Considering constant returns from investments, the production function can be expressed in per capita variables, reflecting efficiency per unit of labor

$$\frac{Y}{LA} = f\left(\frac{K}{KA}\right) \Rightarrow y = f(k)$$

where  $y$  - productivity,  $k$  - denotes capital investment with constant efficiency.

The provided model demonstrates the change in the marginal product, i.e., the additional output of production from the application of an additional unit of resources. In other words, the proposed function illustrates the efficiency of implementing innovations.

To enhance production efficiency, it is necessary to balance the flows of input and output resources depending on the production scenario. Let's consider each scenario separately:

"Scenario  $I$ " involves transitioning from a crisis to stability and describes the current state of the coal industry in Ukraine, where the pace of mechanization is low, yet it surpasses the rate of workforce reduction in enterprises. In terms of the Solow model, this can be formulated as follows: there is a scarcity of capital, while labor re-

sources are abundant. This situation only exacerbates the state of affairs. For coal mines, the situation is further complicated by the fact that the production cycle is subordinated to a sectional labor organization system. Therefore, reducing the group of workers involved in coal mining or preparatory blasting will lead not to savings but to the uncontrolled collapse of the entire production cycle. To stabilize the situation, it is necessary to implement mechanization, giving preference to domestic analogs. Thus, any innovations aimed at improving the technological process will contribute to the restoration of enterprise potential, leading to a transition from a crisis state to a stable one (Scenario II).

- "Scenario II" describes a stable production level where the pace of capital depreciation hinders process efficiency. To improve techno-economic indicators, it is necessary to either introduce radically new technologies, achieve a breakthrough, or significantly increase labor productivity. In this case, the implementation of mechanization without justifying a rational area of operation and optimizing operational parameters will not improve the situation. This scenario corresponds to the attempt to technically re-equip coal mines in Ukraine from 2005 to 2009 when the lack of approaches to selecting equipment based on operating conditions prevented an increase in the daily coal production rate.

- "Scenario III" involves a transition from stability to crisis, describing a production level where innovations do not contribute to improving production efficiency. Accumulation of substantial funds in enterprises hinders productivity enhancement. This situation may arise in Ukraine when the indicators of average daily output in ore processing increase to 3200 tons/day (as of 2012, it was 847 tons/day, currently lower), and there is a need for foreign counterparts of equipment if they fail to ensure productivity exceeding 8000 tons/day [34]. The transition from stability to crisis will occur in such a scenario. Therefore, for the mining-geological conditions of the Donbas region, innovations will either involve the implementation of new technologies significantly boosting productivity or further optimization of the technological process [35, 36].

To maintain stability, continuous operational management of production should be carried out, aiming to minimize risks and losses. To achieve this, it is necessary to identify the key factors in forming

and reproducing internal reserves. We have proposed a methodology for assessing the utilization of internal technological resources in mines, considering the main factors of the production function. Additionally, results regarding the model verification for the Luhansk region are presented [37].

### Methodology for assessing the utilization of internal technological resources

The methodology for assessing the utilization of internal technological resources in mines is designed to identify production resources that are not being utilized (reserved). The establishment of such a regulating mechanism will allow for a comparison of mine capabilities based on key parameters (advancement of workings, concentration level of mining operations, labor productivity of the extraction worker). The results of the calculation are presented in Table 1.

Table 1

Calculation of economic reliability parameters  
for the Dovzhansko-Rovenetska group of mines

Mines	Reliability Components			Economic Reliability
	Technological	Economic	Geological	
"Komsomolska"	0,4	0,13	0,68	0,72
"Partyzanska"	0,9	1,16	0,49	1,55
No. 81 "Kyivska"	0,7	0,86	0,59	1,20
Named after Frunze	0,5	0,49	0,61	0,83
Named after Cosmonauts	0,7	0,76	0,52	1,07
1-2 "Rovenkivska"	0,3	0,41	0,58	0,71
Named after Dzerzhinsky	0,9	0,86	0,46	1,20
"Centrosoyuz"	0,9	1,0	0,46	1,36
"Luhanska"	0,5	0,41	0,2	0,40

Table 2 presents the overall scheme for constructing a direct and dual economic-mathematical model. The goal of this model is to minimize production costs and determine the efficiency of using each technological resource.

In Table 2,  $U_i$  represents the objectively determined assessment of a specific technological resource;  $C_i$  is the cost of 1 ton of finished coal production;  $V$ ,  $K$ , and  $P$  are the respective parameters for ad-

vancing the mining faces, the level of concentration of mining works, and the labor productivity of a worker in coal extraction per 1 ton.

The calculation is performed as follows:

1. Enter the initial data into Microsoft Excel.
2. Define the objective function with the aim of minimizing extraction costs.
3. Introduce and set constraints on the enterprise's resources.
4. Calculate the optimal level of extraction.

Table 2

Modeling Initial Data

Direct problem						
№	Resource Name	Costs per 1 ton				Resource constraints
		1	2	...	$n$	
1	Advancement of longwalls, m/month	$v_{11}$	$v_{12}$	...	$v_{1n}$	$V$
2	Concentration level of the processing line per 1 km of supported output, m	$k_{21}$	$k_{22}$	...	$k_{2n}$	$K$
3	Labor productivity, t/month	$p_{31}$	$p_{32}$	...	$p_{3n}$	$P$
4	Coal cost, UAH	$C_1$	$C_2$	...	$C_n$	$min$

Dual Problem			
Resource Names			Resource constraints
Advancement of longwalls, m/month	Concentration level of the processing line per 1 km of supported output, m	Labor productivity, t/month	
$v_{11}$	$k_{21}$	$p_{31}$	$C_1$
$v_{12}$	$k_{22}$	$p_{32}$	$C_2$
...	...	...	
$v_{1n}$	$k_{2n}$	$p_{3n}$	$C_n$
$U_1$	$U_2$	$U_3$	$max$

5

Having the results of solving the direct and dual problem, it is possible to assess the efficiency of the mine's operation (Table 3).

A comprehensive evaluation across the four specified directions allows minimizing the objective function based on only one indicator, even if it is relatively synthetic, such as the cost of coal extraction. Additionally, an assessment based on technical characteristics,

including the production capacity of the enterprise and remaining geological reserves, is deemed insufficient [38, 39].

We found it practical and convenient for practical use to compose three components of the quantitative assessment of the mine's technological scheme ( $V$ ,  $K$ , and  $P$ ) and adjust their sum with the parameter  $E$  - the probability of the enterprise's evolutionary development. In other words, the structure of the mine's technological scheme passport can be represented as  $M_i=(V_i+K_i+P_i)E_i$ .

The results of the calculations are presented in Table 3.

Table 3

Level of "objective-oriented" assessments of resource utilization degree				
Mine	Concentration of work, 1/1000 t	Advancement of longwalls, m/1000 t	Labor productivity, t/1000 t	Objective- oriented assessment
«Shakhtarska Hlyboka»	12,1	2,00	1,10	0,91
«Progress»	14,0	1,32	0,90	1,95
«Zorya»	14,3	1,30	0,65	0,95
«Komsomolska»	9,4	1,33	0,08	3,80
«Partyzanska»	9,8	1,90	0,04	0,82
No. 81 "Ky- ivska"	6,3	1,30	0,70	1,73
Named after Frunze	10,7	1,15	0,43	5,28
Named after Cosmonauts	11,2	1,33	0,74	1,56
1-2 "Roven- kivska"	7,3	1,66	0,10	0,74
Named after Dzerzhinsky	8,8	1,69	0,16	0,80
"Centrosoyuz"	8,90	1,32	0,69	1,85
"Luhanska"	9,2	2,00	0,08	0,70

Table 4 presents the characteristics of the technological scheme passport for 12 anthracite mines.

Thus, by collectively using these indicators, it is possible to quantitatively assess the capabilities of providing the specified production volumes with this technological scheme. Additionally, the level (passport) of the technological scheme allows assessing the investment level needed to support each ton of installed capacity.

Table 4

Potential of technological schemes for the group of anthracite mines

Mine	Components of the technological passport potential				Level of the technological scheme passport
	Probability		Reliability		
	Evolutionary	Innovative	Economic	Resource	
«Shakhtarska Hlyboka»	0,68	2,53	0,91	1,34	3,25
«Progress»	0,78	2,53	1,95	1,33	4,53
«Zorya»	0,35	1,95	0,95	0,72	1,27
«Komsomolska»	0,80	3,65	3,80	0,72	6,54
«Partyzanska»	0,25	2,34	0,82	1,55	1,18
No. 81 "Kyivska"	0,81	3,37	1,73	1,20	5,10
Named after Frunze	0,87	3,70	5,28	0,83	8,53
Named after Cosmonauts	0,82	2,90	1,56	1,07	4,53
1-2 "Rovenkivska"	0,28	1,76	0,74	0,71	0,90
Named after Dzerzhinsky	0,61	1,73	0,80	1,20	2,27
"Centrosoyuz"	0,69	4,26	1,85	1,36	5,15
"Luhanska"	0,03	1,43	0,70	0,40	0,08

The interest is sparked by the extreme values of the technological scheme's quality and its passport components. In the real conditions of the coal industry in Ukraine, for mines of the first type, the economic reliability parameter can reach a level of 2.0 [35]. The level of the innovative component reaches a value of 6.0, while the resource utilization level is 3.0. Considering that the probability of evolutionary development cannot exceed 1.0, the highest level of the technological scheme for Ukrainian mines can be calculated as  $(2+6+3)*1.0=12$ .

While this example is not conclusive evidence, it provides a basis to assert that in actual conditions, the maximum level of the privatization passport should not exceed 10-12 points. The closer this indicator is to 10, the more attractive the mine is for privatization and



corporate development of reserves, requiring fewer expenses for each ton of capacity increment.

The essence of the technological passport lies in its ability to offer a comprehensive evaluation of the mine based on its technical level and the manifestation of topological features, including solutions for diversification of mining production, such as the processing of mining waste and beneficiation plants. Thus, the obtained tool is versatile and applicable in the conditions of mines operated by PJSC «DTEK Pavlogradvuhillia».

### **Conclusions**

This work has introduced a novel approach to assess the innovative prospects of exploiting coal deposits. A comprehensive methodology was applied, relying on the incorporation of neoclassical production functions in the form of the Solow model for analyzing the state of the coal mining industry. Additionally, economic reliability was considered to develop recommendations for enhancing techno-economic indicators. It was established that the efficiency of enterprise functioning can be evaluated by the ratio of input (capital) to output (production level) resources, with a significant emphasis on the innovative component. Analyzing the relationships between these resource flows enables the selection of optimal development scenarios and the formulation of principles for designing production at various stages of development.

For the analysis of sustainable development prospects of the technological scheme of a mine, simulation modeling was employed to assess the dynamics of changes in the volume of reserves prepared for extraction. This approach practically aligns the simulation model with optimal programming models, making it versatile for analyzing the rules of mine object actions and their structures.

The comprehensive assessment of the state of the mine's technological scheme along four directions significantly increases the objectivity of the final results compared to using only one indicator, even if that indicator is relatively synthetic, such as the cost of coal production. Therefore, based on the obtained results, it can be argued that the maximum level of the privatization passport for the technological scheme, in real conditions, does not exceed 10-12 points. The closer this indicator is to 10, the more attractive the enterprise is for privatization and corporate development, with lower costs for each ton of capacity increment.

### *References*

1. **Amosha, O. I., Salli, V. I., Tryfonova, O. V., & Symonenko, O. I. (2007).** Kil'kisini parametry investytsiynoyi pryvabyvosti vuhil'nykh shakht. Dnipropetrovs'k: NHU. 110 p. (in Ukrainian)

2. **Huang, S., Li, G., Ben-Awuah, E., Afum, B. O., & Hu, N. (2020).** A robust mixed integer linear programming framework for underground cut-and-fill mining production scheduling. *International Journal of Mining, Reclamation and Environment*, 34(6), 397-414. <https://doi.org/10.1080/17480930.2019.1576576>

3. **Khodayari, F., & Pourrahimian, Y. (2016, October).** Quadratic programming application in block-cave mining. In 1st International Conference on underground Mining, Santiago, Chile (pp. 427-438).

4. **Topal, J. L. E. (2011).** Strategies to assist in obtaining an optimal solution for an underground mine planning problem using Mixed Integer Programming. *International Journal of Mining and Mineral Engineering*, 3(2), 152-172. <https://doi.org/10.1504/IJMME.2011.042429>

5. **MacNeil, J. A., & Dimitrakopoulos, R. G. (2017).** A stochastic optimization formulation for the transition from open pit to underground mining. *Optimization and Engineering*, 18, 793-813. <https://doi.org/10.1007/s11081-017-9361-6>

6. **Khorolskyi, A., Hrinov, V., & Kaliushenko, O. (2019).** Network models for searching for optimal economic and environmental strategies for field development. *Procedia Environmental Science, Engineering and Management*, 6(3), 463-471.

7. **Balezentis, T., Streimikiene, D., & Siksnylyte-Butkiene, I. (2021).** Energy storage selection for sustainable energy development: The multi-criteria utility analysis based on the ideal solutions and integer geometric programming for coordination degree. *Environmental Impact Assessment Review*, 91, 106675. <https://doi.org/10.1016/j.eiar.2021.106675>

8. **Hill, A., Brickey, A. J., Cipriano, I., Goycoolea, M., & Newman, A. (2022).** Optimization Strategies for Resource-Constrained Project Scheduling Problems in Underground Mining. *INFORMS Journal on Computing*, 34(6), 3042-3058. <https://doi.org/10.1287/ijoc.2022.1222>

9. **Özyurt, M. C., & Karadogan, A. (2020).** A new model based on artificial neural networks and game theory for the selection of underground mining method. *Journal of Mining Science*, 56, 66-78. <https://doi.org/10.1134/S1062739120016491>

10. **Khorolskyi, A., Hrinov, V., Mamaikin, O., & Fomychova, L. (2020).** Research into optimization model for balancing the technological flows at mining enterprises. In *E3S Web of Conferences (Vol. 201, p. 01030)*. EDP Sciences. <https://doi.org/10.1051/e3sconf/202020101030>

11. **Petlovanyi, M., Sai, K., Malashkevych, D., Popovych, V., & Khorolskyi, A. (2023, April).** Influence of waste rock dump placement on the geomechanical state of underground mine workings. In *IOP Conference Series: Earth and Environmental Science (Vol. 1156, No. 1, p. 012007)*. IOP Publishing. DOI 10.1088/1755-1315/1156/1/012007

12. **Kwinta, A., & Gradka, R. (2020).** Analysis of the damage influence range generated by underground mining. *International Journal of Rock Mechanics and Mining Sciences*, 128, 104263. <https://doi.org/10.1016/j.ijrmms.2020.104263>

13. **Vayenas, N., & Peng, S. (2014).** Reliability analysis of underground mining equipment using genetic algorithms: A case study of two mine hoists. *Journal of Quality in maintenance Engineering*, 20(1), 32-50. <https://doi.org/10.1108/JQME-02-2013-0006>

14. **Zarebska, K., Baran, P., Cygankiewicz, J., & Dudzińska, A.** (2012). Prognosticating fire hazards in goafs in Polish collieries. *AGH Drilling, Oil, Gas*, 29(4).
15. **Yueze, L., Akhtar, S., Sasmito, A. P., & Kurnia, J. C.** (2017). Prediction of air flow, methane, and coal dust dispersion in a room and pillar mining face. *International Journal of Mining Science and Technology*, 27(4), 657-662. <https://doi.org/10.1016/j.ijmst.2017.05.019>
16. **Bazaluk, O., Ashcheulova, O., Mamaikin, O., Khorolskiy, A., Lozynski, V., & Saik, P.** (2022). Innovative activities in the sphere of mining process management. *Frontiers in Environmental Science*, 304. <https://doi.org/10.3389/fenvs.2022.878977>
17. **Hrinov, V., & Khorolskiy, A.** (2018). Improving the process of coal extraction based on the parameter optimization of mining equipment. In *E3S Web of Conferences* (Vol. 60, p. 00017). EDP Sciences. <https://doi.org/10.1051/e3sconf/20186000017>
18. **Saaty, T. L., Vargas, L. G., Saaty, T. L., & Vargas, L. G.** (2013). The analytic network process (pp. 1-40). Springer US.
19. **Balusa, B. C., & Singam, J.** (2018). Underground mining method selection using WPM and PROMETHEE. *Journal of the Institution of Engineers (India): Series D*, 99, 165-171. <https://doi.org/10.1007/s40033-017-0137-0>
20. **Balusa, B. C., & Gorai, A. K.** (2019). A comparative study of various multi-criteria decision-making models in underground mining method selection. *Journal of The Institution of Engineers (India): Series D*, 100, 105-121. <https://doi.org/10.1007/s40033-018-0169-0>
21. **Liang, W., Zhao, G., Wu, H., & Chen, Y.** (2019). Assessing the risk degree of goafs by employing hybrid TODIM method under uncertainty. *Bulletin of Engineering Geology and the Environment*, 78, 3767-3782. <https://doi.org/10.1007/s10064-018-1340-4>
22. **Pak, M. C., Han, U. C., & Kim, D. I.** (2022). Suitable Mining Method Selection using HFGDM-TOPSIS Method: a Case Study of an Apatite Mine. *Journal of Mining and Environment*, 13(2), 357-374. <https://doi.org/10.22044/jme.2022.11713.2163>
23. **Alavi, I., & Alinejad-Rokny, H.** (2011). Comparison of Fuzzy AHP and Fuzzy TOPSIS methods for plant species selection (case study: reclamation plan of sungun Copper Mine; Iran). *Australian journal of basic and applied sciences*, 5(12), 1104-1113.
24. **Sahoo, S., Dhar, A., Kar, A., & Ram, P.** (2017). Grey analytic hierarchy process applied to effectiveness evaluation for groundwater potential zone delineation. *Geocarto International*, 32(11), 1188-1205. <https://doi.org/10.1080/10106049.2016.1195888>
25. **Yang, W., Xia, X., Pan, B., Gu, C., & Yue, J.** (2016). The fuzzy comprehensive evaluation of water and sand inrush risk during underground mining. *Journal of Intelligent & Fuzzy Systems*, 30(4), 2289-2295. DOI: 10.3233/IFS-151998
26. **Pérez, J., Jimeno, J. L., & Mokotoff, E.** (2006). Another potential shortcoming of AHP. *Top*, 14, 99-111. <https://doi.org/10.1007/BF02579004>
27. **Paravarzar, S., Pourrahimian, Y., Askari-Nasab, H., & Emery, X.** (2021). Short-term underground mine planning: a review. *International Journal of Mining and Mineral Engineering*, 12(1), 1-33. <https://doi.org/10.1504/IJMME.2021.114902>

28. **Reinhart, R., Dang, T., Hand, E., Papachristos, C., & Alexis, K.** (2020, May). Learning-based path planning for autonomous exploration of subterranean environments. In 2020 IEEE International Conference on Robotics and Automation (ICRA) (pp. 1215-1221). IEEE. <https://doi.org/10.1109/ICRA40945.2020.9196662>
29. **Li, S., Huang, Q., Hu, B., Pan, J., Chen, J., Yang, J., ... & Yu, H.** (2023). Mining method optimization of difficult-to-mine complicated orebody using Pythagorean fuzzy sets and TOPSIS method. *Sustainability*, 15(4), 3692. <https://doi.org/10.3390/su15043692>
30. **Erdogan, G., & Yavuz, M.** (2017, December). Application of Three Existing Stope Boundary Optimisation Methods in an Operating Underground Mine. In IOP Conference Series: Earth and Environmental Science (Vol. 95, No. 4, p. 042077). IOP Publishing. DOI 10.1088/1755-1315/95/4/042077
31. **Brazil, M., & Grossman, P.** (2008, September). Access layout optimization for underground mines. In Australian Mining Technology Conference, Queensland, 119-128.
32. **Emdini Gliwan, S., & Crowe, K.** (2022). A Network Flow Model for Operational Planning in an Underground Gold Mine. *Mining*, 2(4), 712-724. <https://doi.org/10.3390/mining2040039>
33. **Durlauf, S. N., Kourtellos, A., & Minkin, A.** (2001). The local Solow growth model. *European Economic Review*, 45(4-6), 928-940.
34. **Khorolskyi, A., Mamaikin, O., Fomychova, L., Pochevov, V., & Lapko, V.** (2022). Developing and implementation a new model optimizing the parameters of coal mines under diversification. *ARP Journal of Engineering and Applied Sciences*, 17(16), 1544-1553.
35. **Khorolskyi, A., Mamaikin, O., Medianyuk, V., Lapko, V., & Sushkova, V.** (2021). Development and implementation of technical and economic model of the potential of operation schedules of coal mines. *ARP Journal of Engineering and Applied Sciences*, 16(18), 1890-1899.
36. **Fomychov, V., Fomychova, L., Khorolskyi, A., Mamaikin, O., & Pochevov, V.** (2020). Determining optimal border parameters to design a reused mine working. *ARP Journal of Engineering and Applied Sciences*, 15(24), 3039-3049.
37. **Khorolskyi, A., Hrinov, V., Mamaikin, O., & Demchenko, Y.** (2019). Models and methods to make decisions while mining production scheduling. *Mining of Mineral Deposits*, 13 (4), 53-62.
38. **Moldabayev, S., Sultanbekova, Z., Adamchuk, A., & Sarybayev, N.** (2019). Method of optimizing cyclic and continuous technology complexes location during finalization of mining deep ore open pit mines. *International Multidisciplinary Scientific GeoConference Surveying Geology and Mining Ecology Management, SGEM*, 19(1.3), 407-414. <https://doi.org/10.5593/sgem2019/1.3/S03.052>
39. **Babets, Ye. K., Adamchuk, A. A., Shustov, O. O., Anisimov, O. O., & Dmytruk, O. O.** (2020). Determining conditions of using draglines in single-tier internal dump formation. *Naukovyi Visnyk Natsionalnoho Hirnychoho Universytetu*, 6, 5-14. <https://doi.org/10.33271/nvngu/2020-6/005>

**THE SCOOP FEEDER AS A MEANS OF RESOURCE  
SAVING IN BALL MILL GRINDING OF FEED ORE WITH  
CLASSIFIER SANDS**



**Vasyi KONDRATETS**

Doctor of Technical Sciences, Professor, Professor of the Department of Automation of Production Processes, Central Ukrainian National Technical University, Ukraine



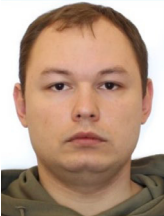
**Anatolii MATSUI**

Doctor of Technical Sciences, Professor, Associate Professor of the Department of Automation of Production Processes, Central Ukrainian National Technical University, Ukraine



**Oleksandr SERBUL**

Ph.D, Associate Professor, Associate Professor of the Department of Automation of Production Processes, Central Ukrainian National Technical University, Ukraine



**Oles IZOVITA**

Postgraduate Student of the Department of Automation of Production Processes, Central Ukrainian National Technical University, Ukraine



**Volodymyr YARMOLENKO**

Postgraduate Student of the Department of Automation of Production Processes, Central Ukrainian National Technical University, Ukraine

**Abstract.** The subject of the research is a new approach of resource-saving adaptive distributed control of ore grinding with sands of mechanical single-spiral classifier in ball mills on the basis of taking into account the role of scoop feeder, influence on material flows, estimation of technological parameters with increased accuracy and new mathematical models of water dosing in the technological process and algorithm of estimation of solid concentration in the pulp of technological unit. Within the framework of the adopted research methodology a number of methods of different accessory groups have been applied. Comparison method – when studying the statics of the scoop feeder and its operation with one and two gripping bodies. Method of analysis – at increase of resource saving in the process of grinding of raw materials, means and approaches of stabilisation of pulp liquefaction in ball mills, prediction of errors of solid/liquid ratio, inclusion of the initial section of the mill in active work. Method of mathematical modelling – in the development of a mathematical model for finding the mass flow rate of solid in the sand flow, finding the water flow rate into the ball mill at various technological points. Method of the theory of algorithmic estimation – in the development of an approach for identification of the solid/liquid ratio in the ball mill. Method of error theory – in measuring pulp volumetric flow rate. Flowmeter theory methods – in measuring the volumetric flow rate of water and slurry. Methods of the theory of scanning devices – at creation of volumetric flow meter of pulp in open flow. The aim of the publication is to investigate the scoop feeder as a means of resource saving in a ball mill when grinding ore with classifier sands based on the application of new models of the technological process, a new algorithm for assessing the concentration of solid in the pulp, control of the oscillation of material flows and models of water flow rate stabilisation. The purpose of the research has been achieved. The obtained results are a theoretical basis for the creation of a system of adaptive separate resource-saving control of ore grinding with classifier sands in the first stages of ore preparation.

## **1. Introduction**

Ukraine is among the top ten countries producing ferrous metallurgy products. The products of domestic metallurgical and mining and processing plants account for the overwhelming share of export revenues. At the same time, the industry's products are characterised by high production costs, compared to those of foreign partners, and are of somewhat lower quality and significantly higher specific costs of electrical energy and materials. Therefore, there is an urgent need to solve the problem of overcoming the insufficient level of competitiveness of these types of domestic products in the world market. Since now the share of magnetite concentrates in iron ore raw materials is more than half, providing a lower cost of metal compared to smelting it from rich ores, and rich ores at this stage also need beneficiation, the relevant technological processes need to be transformed in the direction of improving their economic performance.

## **2. Actuality of the paper**

Depending on the quality of the initial ore and the final product size, power consumption for grinding accounts for 55-70% of the total expenditure of this type of energy at the concentrator. The determining technological parameter is pulp liquefaction in ball mills, because only at a certain value of this parameter optimal conditions for the operation of balls and material movement along the mill drum are created. The pulp liquefaction in a ball mill depends on the type of ore and its size. As it is known, the necessary optimal pulp liquefaction in ball mills can be achieved and maintained only automatically. However, no effective systems of automatic control of this process have been created so far, and the capabilities of the scoop feeder as a controlled object have not been utilised, despite the considerable amount of research carried out in this direction. Successful solution of the automation issue would open prospects for realisation of a number of potential opportunities - increase in productivity of ball mills, significant reduction of power, ball and lining consumption, improvement of quality of the finished product, reduction of iron losses. This is especially important in the first stages of grinding, where the expenditure of energy and materials in the form of balls and linings is the most significant.

### **3. Unresolved parts of a common problem**

Among the unresolved parts of the problem we can single out the processes of control of technological redesigns of ball grinding of iron ore at ore dressing plants in closed cycles, including ball mill, mechanical single-spiral classifier and scoop feeder, as well as a set of automated systems for energy-efficient control of ore grinding-classification as part of the automated control system of the technological process of the first stage of ore preparation on the basis of the developed methodology. The role of the scoop feeder in resource saving in ore preparation processes is not disclosed.

### **4. Aim of the research**

The aim of the publication is to study the scoop feeder as a means of resource saving in a ball mill during grinding of initial ore with sands of mechanical single-spiral classifier on the basis of application of new models of technological process, a new algorithm for estimation of solid concentration in the pulp of technological unit, control of material flow oscillation and models of water flow rate stabilisation.

In order to achieve the above objective, the following main tasks need to be accomplished:

- consider the ball mill as the main unit for resource saving;
- characterise the scoop feeder as an important means of resource saving;
- review the status of slurry rarefaction stabilisation in ball mills operating in closed cycles with a mechanical single-spiral classifier;
- reveal a distinctive transition in stabilising pulp liquefaction in ball mills;
- outline the essence of an algorithmic method for estimating the solid/liquid ratio for the communications of a ball mill operating in a closed cycle with a mechanical single-spiral classifier;
- investigate the features of implementation of the proposed algorithm for identification of pulp liquefaction in a ball mill operating in a closed cycle with a mechanical single-spiral classifier;
- simulate the conditions of resource saving at grinding of initial ore with sands of mechanical single-spiral classifier.

## **5. Method**

### **5.1 The ball mill is the main unit for resource saving**

Grinding of raw materials at iron ore dressing plants in the first stages is mainly carried out according to the technological scheme, where the ball mill operates in a closed cycle with a mechanical single-spiral classifier. For such technological cycles in [1] the necessary stabilisation at appropriate levels of ball mill loading with ore and pulp density in it is proved. The importance of stabilisation of pulp liquefaction stabilisation in ball mills is also pointed out in [2, 3] and others. That is, only at a certain ore load of the ball mill and specifically necessary liquefaction of the pulp in the drum there will be resource-saving grinding of raw materials. However, these are only the initial conditions for effective grinding. At the entrance of the ball mill at the same time receives dry initial crushed ore, water and sands of mechanical single-spiral classifier, fed by scoop feeder. Although the ball mill is an efficient agitator, the material is not averaged in the initial section of the drum. Such material cannot be effectively pulverised. That is, it must be averaged (mixed) to a uniformly coarse solid state, which will occupy a certain length of the drum - at least one third of it.



With average material, three cases can arise. If there is a lot of solid material, the impact of the balls will not effectively break the raw material – this is overloading the mill and inefficient use of the energy used to lift the balls and the balls themselves, which wear out but do not break the ore well enough. If there is little material, it is underloading the mill with raw material. The ball energy is not fully utilised for breaking, little raw material is broken, and the residual energy is consumed for breaking the grinding body itself and the lining. Consequently, resource saving will only occur at a certain volume of material in the ball working areas and this must be maintained. The material, normally averaged and normally loaded, moves along the drum and is gradually pulverised. At the output, the coarseness must correspond to the set value. Both the required travelling speeds and the coarseness of the solids in the mill discharge can only be achieved at a certain concentration of solids in the pulp, appropriate to the process. This is also stated by the authors of [4].

At the initial section of the drum, irrespective of the optimality of the mill loading with ore, due to the nonconcentration of large pieces of solid, classifier sands and water, zones are created where large pieces are over-concentrated and where their arrangement is almost opposite. This character of the arrangement of the feed ore in the mixture practically excludes the creation of zones with nominal concentration of coarse solids. This corresponds to inefficient ball operating conditions. It is therefore important to effectively mix the material almost from the point of loading.

Material flows - feed ore, water, classifier sands – are characterised by a certain instability, which can excite oscillations of the liquid mixture in the mill drum. This also worsens the conditions for grinding large particles of solid. Fluctuations of the liquid mixture in the drum are determined by the frequency and amplitude at the inlet. With the help of special programmes, computer modelling has established the areas of variation of oscillatory parameters of ore streams and water at the inlet of the technological unit, when the ratio of the mass value of the parameter to the mass of the liquid product in the drum does not exceed 3,0% [5]. It is known that at such deviations, the technological unit does not leave the nominal operating mode. The boundaries of the obtained areas of variation of oscillatory parameters at the input of the technological unit allow us to set limits in

the implementation of automatic control of ore grinding. From the considered it can be seen that resource saving in the ball mill is determined by the state of the material in the drum and oscillatory input flows of the initial ore, water and sands of the mechanical single-spiral classifier. The analysis established that it is possible to increase resource saving during grinding of raw materials in a ball mill only through the influence on the input material flows. Studies have shown that the flows of feed ore and water into the drum do not change the technological mode of operation of the ball mill so much that the oscillatory parameters go beyond the established areas. The influence of other factors on the resource efficiency of the mill during the grinding of feed ore should be checked.

### **5.2 Scoop feeder - a means of resource saving**

The scoop feeder is an integral component of the ball mill in this ore grinding cycle. It, in turn, is an integral part of the drum feeder that feeds ore, water and balls into the process unit. The scoop feeder is a spiral-shaped gripping organ, endowed with a round hole in the side wall for reloading the captured at the bottom mark liquid sands of the classifier into the ball mill drum [6]. It includes two spiral-shaped sidewalls, parallel spaced at a certain distance and rigidly fixed on the side of the spiral part by a metal profile bottom, and a flange in the vicinity of the outlet round hole for bolting to the drum trunnion of the technological unit. The scoop feeder has a rectangular cross-section between the sidewalls, which width should be greater than the diameter of the largest ball and sufficient to move the sands at their highest productivity. The body of the feeder's gripping body is cast from alloyed cast iron or made of sheet steel. The inner surface of the gripper is lined with steel plates. A replaceable visor made of manganese steel or alloyed cast iron is installed on the end of the gripping body to protect it from wear. Scoop feeders are made with one, two or three gripping bodies. The scoop feeder rotates together with the mill drum.

Schematic representation of scoop feeder in the technological scheme is shown in Fig. 1.

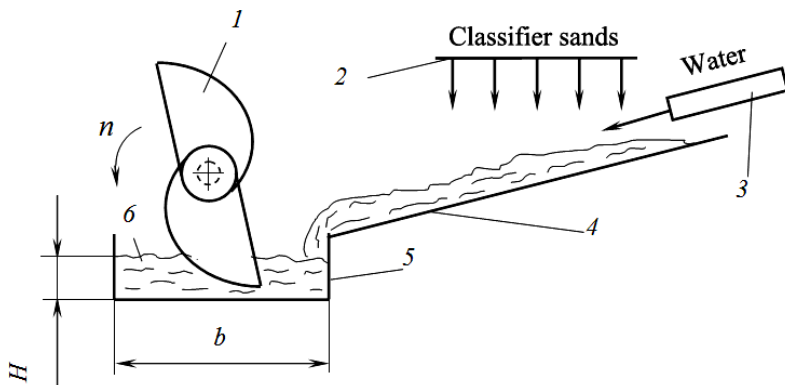


**Fig. 1.** Schematic representation of the scoop feeder in the process flow diagram: 1 – scoop feeder; 2 – threshold of mechanical single-spiral classifier; 3 – water supply pipeline to the classifier sand chute; 4 – classifier sand chute; 5 – scoop feeder receiving device; 6 – pulp

The scoop feeder 1 rotates together with the mill drum, making  $n$  revolutions per minute. The sands of the mechanical single-spiral classifier are discharged through the sand sill 2 into the sand chute 4, where at its beginning water is supplied through pipe 3 to ensure their movement and create a pulp. The pulp 6 contains the hard sands, the water which is discharged from the classifier with them, and the added water from pipe 3. It is accumulated in the receiving device 5, which has a length  $b$ . At any volumetric capacity in the receiving device 5, certain values of the pulp level  $H$  are set. That is, in the steady-state mode of operation, the volume of pulp coming from the classifier per unit of time will correspond to the quantity removed from the receiving device 5. Therefore, the scoop feeder is a kind of transfer link between the mechanical single-spiral classifier and the ball mill.

Scientists have paid little attention to the study of spiral feeders. Therefore, it is necessary to investigate the nature of sand feeding of mechanical single-spiral classifier into the ball mill. We will carry out researches according to the considered approach with attraction of the received diagrams of non-exit of the technological unit from 3% zone of deviations of pulsations of liquid material in the drum. The research was carried out on the real test data of the technological scheme in the conditions of one of the ore dressing plants. Let's take the smallest 163,2 t/h and the largest 329,0 t/h values of circulating

load, fixed in experiments [7]. It is established that it is inadmissible to feed the sand stream directly from the classifier into the ball mill, due to large oscillations of the material in the drum of the technological unit. When using a scoop feeder with one gripping element, ore and water pulsations do not leave the zone of 3,0% deviations. The use of a scoop feeder with two gripping elements significantly improves the indicators. So, in terms of pulsations, all material flows into the ball mill meet the process requirements, as the scoop feeder significantly improves the sand flow by converting it.

### **5.3 Status of stabilisation of pulp liquefaction in the mill**

As it has been shown, resource-saving ball milling of initial ore will be carried out if the oscillation of material flows does not exceed the established limits and qualitative averaging of solids by size. However, a necessary condition is still the maintenance of a specific value of solid particle concentration for a certain technological ore type, i.e., in general, at the beginning of the process it is necessary to stabilise the solid/liquid ratio at a given level. The solid/liquid ratio can be set as the ratio of the total flow rate of ore and sands from the classifier (circulating load) to the water flow rate to the ball mill. Water flow rate is measured by a number of known types of flow meters, and the mass flow rate of ore into the ball mill is estimated by conveyor scales with a stated relative error of  $\pm 1,0\%$ , which, as it was found in practice is not quite confirmed. Improvements to the conveyor scales outlined in the works [8-10], which guarantee the measurement of ore flow rate into the ball mill with an error somewhat less than 1,0%. Circulating load measurement is more problematic. The development of these techniques has received considerable attention. The most weighty of them are published in the works [11-16]. Devices and methods of estimation of this technological parameter realise various approaches, but it was not possible to achieve the necessary accuracy.

When measuring the circulating load, the accuracy was mainly influenced by the flow dynamics. The static sand conditions are maintained in the classifier spirals, where the sands do not pulsate, but only gradually move towards the sand threshold. Therefore, attention was drawn to this feature of sand condition and subsequently started to carry out research in this part of the process flow diagram. Ways to evaluate the performance of spiral classifier on sands were pro-

posed [17-19]. Since these methods had disadvantages, such studies were subsequently continued. Improved methods for determining the performance of spiral classifier on sands were proposed [20-22], but the disadvantages of previous approaches could not be completely eliminated and these technical solutions, containing elements of assumptions, also gave an error, which does not quite meet the requirements of the technological process. This forced researchers to develop solid/liquid stabilisation systems.

A group of researchers (V.I. Dmitriev and others) proposed three systems of automatic control of the solid/liquid ratio in closed cycles of initial ore grinding [23-25]. These systems are very different from each other, so let us consider them separately.

Among the disadvantages of the system of automatic control of the ratio of liquid and solid phase flow rates in the mill feed with setting the necessary averaging time intervals and data delay [23] are the following. Firstly, significant errors are allowed when determining the solid and liquid flow rates. The system contains a large number of computational blocks – converters, adders, comparison blocks, which also introduce error. Secondly, measuring pulp density at the mill drain is currently not technically feasible. In addition, there is a significant delay in signal acquisition. Thirdly, the determination of the solid/liquid ratio from the measured value of the pulp density and other parameters also introduces additional error. Fourthly, the scheme proposes to use an experimental delay time which cannot be set accurately – different situations will have different delay intervals, so it is not practically possible to apply this approach of stabilising the solid/liquid ratio under these conditions.

The system of automatic regulation of the ratio of solid and liquid phase flow rates in the mill feed with preliminary determination of the optimum value of pulp density [24] also has certain drawbacks. In particular, the solid flow rate is determined with a large error, since the flow rate of sands cannot be accurately measured. Also, the system involves the use of many elements that introduce additional errors - these are adders, moisture content determination unit, ratio determination unit.

Finally, let us consider a system of automatic control of the ratio of the flow rate of inlet streams into the mill with determination of the total mass flow rate of solid phase and water [25]. It is character-

ised by shortcomings of technical nature. This concerns the impossibility of measuring the mass flow rate of pulp in open streams at high values of densities due to the lack of such means. Existing devices for mass flow rate determination are not suitable for such measurements [26]. Also, there are no means of measuring sand density today. The system is overloaded with a large number of parameter determination blocks, which introduces a significant additional error.

Therefore, several approaches to create automatic systems for stabilising the solid/liquid ratio for closed cycles of ball milling of initial ore with classifier sands have been proposed; however, as the analysis has shown, none of them can be implemented for various reasons. Therefore, the search for approaches to overcome this technical contradiction should be continued.

#### 5.4 Excellent approach in stabilising pulp liquefaction

Let's consider the device for automatic control of loading and stabilisation of pulp liquefaction in the mill in accordance with the copyright certificate [27] №388790 (USSR) and Fig. 2. The sands of the classifier by spiral 11 are discharged into the sand chute 1, where water is fed through pipeline 2, creating a pulp. The pulp, moving in the sand chute 1 falls into the accumulating tank 10 and further - into the pulp outlet 9, and then - into the receiving device 8 of the scoop feeder. The volumetric flow meter 7 measures the pulp flow rate  $Q_{vn}$  in the sand chute 1, and the flow meter 6 measures the water flow rate  $Q_{B1}$  into the sand chute. Their signals are fed to the input of the computing device 6, which determines the ore flow rate  $Q_{qp}$  according to the equation

$$Q_{qp} = \frac{\delta_T}{1 + k_p \frac{\delta_T}{\delta_B}} (Q_{vn} - Q_{B1}) = A(Q_{vn} - Q_{B1}), \quad (1)$$

where  $\delta_T$ ,  $\delta_B$  - ore and water densities, respectively;  $k_p$  - moisture content of classifier sands;  $A$  - constant for a certain technological ore type.

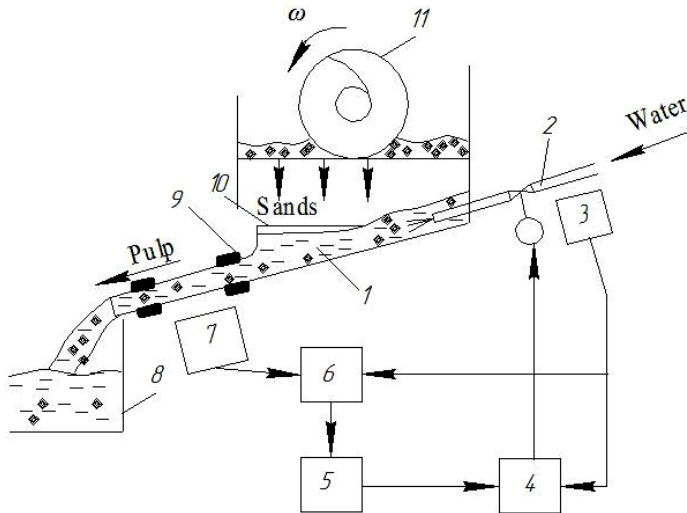


**Fig.2.** Device for automatic control of loading and stabilisation of pulp liquefaction in the mill: 1 - classifier sand chute; 2 - pipeline; 3 - water flow meter; 4 - ore and water feed ratio regulator; 5 - device showing the amount of material loaded into the mill; 6 - computing device; 7 - pulp volume flow meter; 8 - scoop feeder receiving device; 9 - pulp outlet; 10 - accumulating tank; 11 - classifier spiral

The signal formed at the output of the computing device 6 is measured by the device 8, which shows the value of the mass flow rate of ore  $Q_{qp}$  into the mill. This signal and the flow meter signal are fed to the input of the ratio regulator 4, which by adjusting the water flow rate  $Q_{Bl}$  maintains constant pulp liquefaction in the mill.

The accuracy of the control is determined by the accuracy of the slurry and water flow meters. If the pulp outlet is well filled with liquid, it is possible to measure the volume flow rate of the pulp with sufficient accuracy. The water flow rate can be measured with standard devices. The wiring diagram of the device is simple and practically accommodates standard devices that provide the required accuracy in industrial applications.

The distinctive feature of this approach is that instead of a mass flow meter, a device that measures the pulp volume flow rate in the classifier sand chute is used. The slurry flowmeter with an accumulating tank has proven to be a good solution, but requires complex measures to protect it from scrap and other foreign objects. In addition, it is characterised by significant metal consumption, complexity

of installation. Subsequently, a solution was found to estimate the volume flow rate of pulp in the sand chute by scanning its surface [28]. It is shown that it is expedient to scan open surfaces of streams by devices realising the method of measuring surface coordinates by rays of constant length, which change their position in space. Their length should be several times greater than the maximum flow height. The control of the flow height should be carried out at four points along its width - at a distance of 0,1 and 0,4 from the edges. This provides the highest accuracy of cross-sectional area measurement. However, the check showed that the relative error of pulp volume flow measurement can be within 3-5%, which requires further search.

### 5.5 Algorithmic method for pulp liquefaction identification

Adaptive methods based on the invariance principle are used to improve the measurement accuracy of individual parameters. Recently, the algorithmic method of increasing the measurement accuracy has been developed, which is also based on the invariant principle, where the measured value is determined in the computing device in accordance with the developed algorithm. When creating automatic control systems, the expediency of incomplete satisfaction of invariance conditions has long been recognised. This allows to apply the algorithmic method of increasing the accuracy of parameter determination directly in the identification process, if the problem can be reduced to an algorithm of the necessary type. It is proved that the algorithmic method can, under certain conditions, provide the necessary accuracy of estimation of the technological parameter when measuring one of the values with a significant error.

For the communications of a ball mill operating in closed loop with a mechanical single-spiral classifier, the following algorithm has been formulated

$$K_{T/P} = \frac{A \cdot (Q_n - Q_{B1}) + Q_p}{\delta_B Q_B + \delta_B Q_{B1} + K_n [A \cdot (Q_n - Q_{B1})]}, \quad (2)$$

where

$$A = \frac{\delta_T}{\left(1 + K_n \frac{\delta_T}{\delta_B}\right)} = \frac{\delta_T \delta_B}{\delta_B + K_n \delta_T}, \quad (3)$$



$K_n$  – relative moisture content in classifier sands;  $Q_n$  – volume flow rate of pulp in the classifier sand chute;  $Q_{BI}$  – volume flow rate of water into the sand chute;  $Q_B$  – volume flow rate of water into the ball mill;  $Q_P$  – mass flow rate of ore into the ball mill.

Algorithm (2) shows that its expression includes the parameter  $Q_n$  – volume flow rate of pulp in the sand chute of the classifier, which is estimated with a significant error. There is also a mechanism to compensate for the error in determining this parameter, since  $Q_n$  is included in both the numerator and denominator of the expression. To identify the solid/liquid  $K_{TP}$  ratio, it is necessary to have information on the pulp volume flow rates  $Q_n$  in the classifier sand chute, ore mass flow rate to the ball mill, water flow rate  $Q_B$  to the ball mill, water flow rate  $Q_{BI}$  to the sand chute, moisture content of the classifier sands  $K_n$  and ore density  $\delta_T$ . The final identification result will be affected by the errors in the determination of each of these parameters.

Let us consider the influence of parameter determination errors in algorithm (2) on the accuracy of predicting the solid/liquid  $K_{TP}$  ratio. Let us introduce the concept of the base value  $K_{(TP)B}$ , which is determined at parameter values without error. In this case, it is equal to  $K_{(TP)B}=4,3$ . If any of the six parameters ( $\delta_T$ ,  $K_n$ ,  $Q_{BI}$ ,  $Q_n$ ,  $Q_P$ ,  $Q_B$ ) does not correspond to the base value, the solid/liquid ratio according to algorithm (2) will be predicted with error. At computer modelling of the given process dependences of a relative error of prediction of a ratio solid/liquid on algorithm (2) from a relative error of definition of one of parameters for the case when the last corresponds to base value (fig.3) are received. The dependences of Fig. 3 show that algorithm (2) has the property of error compensation for all six parameters, but the degree of compensation for each of them is different. The greatest influence on the  $K_{TP}$  prediction error is the accuracy of measurement of water flow rate into the mill, the least - the ore density. At a certain direction of measurement error deviation, three parameters in the result of  $K_{TP}$  prediction contribute negative error, and three - positive error. All these factors in pairs contribute almost the same influence on  $K_{TP}$  with opposite signs.

It is also evident from the graphs in Fig. 3 that all parameters introduce a certain error when predicting the solid/liquid ratio in the mill. Without taking special measures, the resulting error in predict-

ing the solid/liquid ratio in the mill can be quite high. Therefore, it is necessary to make a more detailed analysis of the influence of parameter measurement errors on the result of the  $K_{TP}$  identification.

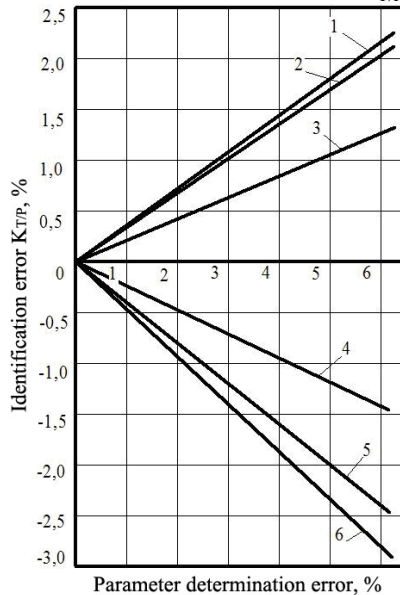


**Fig.3.** Dependence of the relative error of predicting the solid/liquid ratio in the mill on the error of determining one of the parameters:

1 -  $Q_P$ ; 2 -  $Q_n$ ; 3 -  $\delta_T$ ; 4 -  $Q_{B1}$ ; 5 -  $K_n$ ; 6 -  $Q_B$

### 5.6 Features of the implementation of the proposed algorithm

It is clear that at each moment of time the error of measurement or deviation of this or that technological parameter from the prescribed value can take the sign "plus" or "minus". This will be a random process. Since the sign of the parameter determination error affects the resulting solid/liquid ratio error differently,  $\delta_{K_{TP}}$  will also be a random process. However, it is possible to set limits to the variation of the relative solid/liquid ratio error in this process. The limiting value of the resulting error of the solid/liquid ratio will be at the unlikely situation - when all errors of measurement of technological parameters take the same sign. The second unlikely situation corresponds to another limiting condition. It will take place when the measurement errors take different signs and the most unfavourable combination of them.

If all process parameters are measured with the same errors, which have the same sign, then even with a relative error of 5%, the relative error in determining the solid/liquid ratio does not exceed 1,1%. This would be the lower limit of the parameter identification error. This error can be practically halved if in the technological process the moisture content of the classifier sands, ore density and water flow rate into the sand chute are unchanged and precisely set.

If all technological parameters are measured with the same errors, and their signs take the most unfavourable combination, the resulting error of identification of the solid/liquid ratio increases significantly. When measuring technological parameters, for example, with the same error of 5%, the resulting error of identification of solid/liquid ratio will be more than 10%. It can be significantly reduced provided that the values of classifier sands moisture content, ore density and water flow rate into the classifier sand chute are constant and highly accurate. This will be the upper (theoretical) limit of the prediction error of the solid/liquid ratio in the ball mill, as it cannot really exist even in unlikely situations due to the much higher accuracy of most existing measuring instruments.

The actual prediction error of the  $K_{T/P}$  parameter will be somewhere between certain limits, since the real situation of measuring process parameters is unlikely to approach the limiting conditions. Such actual error should satisfy the requirements of the technological process.

Thus, it follows from the analysis that when implementing algorithm (2), it is desirable to ensure that the moisture content of the classifier sands, ore density and water flow rate into the classifier sand chute remain constant. At present, it has been concluded that it is expedient to process separate technological ore types in separate technological complexes [29]. Under these conditions, the ore density will be unchanged, and the moisture content of the classifier sands will also be constant [30]. In process schemes where the ball mill operates in a closed cycle with a mechanical single-spiral classifier, it is possible to maintain the conditions of supplying a constant water flow rate into the sand chute [31]. The authors of this publication have developed approaches and a means of stabilising the water flow rate into the sand chute of the classifier, which ensures a dosing error of less than 1% [32-34]. Therefore, it is necessary to ensure a suffi-

ciently high accuracy of measuring the mass flow rate of ore in the mill, water into the mill with a relatively inaccurate flow meter of pulp volume flow rate in the sand chute of the classifier. The best results of predicting the solid/liquid  $K_{T/P}$  ratio by the algorithm (2) can be obtained on the basis of optimisation of the choice of measuring instruments by their permissible error. Table 1 shows the absolute errors of identification of the solid/liquid ratio in the mill at the accepted values of parameters in dependence (2), arising under the influence of water flow measurement with a certain relative error. It follows from the data of Table 1 that the absolute error of  $K_{T/P}$  prediction increases with increasing relative error of ore flow measurement. The best results will be at the lowest measurement error. In the process of optimisation it was established that the ore flow meter, water flow meters to the mill and sand chute should have a measurement error of  $\pm 1\%$ , and the pulp flow meter –  $\pm(3...5)\%$  with the error of the ore density and moisture content in the classifier sands  $\pm 1\%$  [35]. With such means, the solid/liquid ratio identification errors are 0,951% for a pulp flow meter error of  $\pm 3\%$  and – 1,626% for a pulp flow meter error of  $\pm 5\%$ . It is possible to provide the mill water flow rate with standard instruments and the ore flow rate with advanced conveyor scales [8-10].

Table 1

Absolute errors in predicting the solid/liquid ratio in the mill when varying parameters are measured with different uncertainties

Variable parameter	Relative errors of measurement of varying parameters, %				
	1	2	3	4	5
Ore flow to the mill	<b>0,01580</b>	0,03159	0,04730	0,06321	0,07912
Water flow to the mill	<b>-0,02069</b>	-0,04110	-0,06106	-0,08084	-0,10105
Pulp flow rate in the sand chute	0,01520	0,03038	<b>0,04515</b>	0,06020	0,07482

### 5.7 Conditions for resource saving during ore grinding

To obtain the above results of solid/liquid ratio prediction according to algorithm (2) is possible, moreover, if all process parameters are measured at the same process point, i.e. when the process is not affected by different lags. Delays can be influenced in the ore feed, water to the mill, pulp and water to the sand chute of the classifier. If

the classifier sand chute is fed with a constant water flow rate, there is no lag in this channel. If the pulp volume flow rate is measured at the end of the sand chute, this information regarding the material flow entering the ball mill will be lagged by the lag time in the scoop feeder, which is constant and is determined by its design and operating characteristics. That is, the scoop feeder in the technological communications of the ball mill is a key element, as it guarantees the conditions of equalisation of the lag in all channels of the material flow into the ball mill. To exclude the influence of lag on the result of  $K_{TP}$  prediction by algorithm (2) it is necessary to equate the lag time in the ore and water supply lines to the mill with the value of the parameter in the scoop feeder. This can easily be done by installing conveyor scales at a certain point or by selecting the belt speed and choosing the length and slope of the chute feeding water to the mill.

Therefore, the prerequisites for ensuring the necessary concentration of solid in the ball mill slurry have been considered, but to achieve resource saving in the ball mill when grinding the initial ore with sands of a single-spiral classifier, it is still necessary to ensure the inclusion of the initial section of the mill drum in active operation. The analysis has shown that this can be realised only by influencing the ore and sand flows into the mill [36]. That is, as the analysis has shown, the total water flow rate into the ball mill, determining the given solid/liquid ratio, should be divided into three unequal streams, the first of which is fed directly to the ore directed to the technological unit, automatically changing the amount of liquid according to the solid surface flow rate in the ore stream, multiplied by the thickness of the water film held by molecular adhesion forces, with the determination of the regulated value according to the dependency

$$Q_{PB} = \frac{6\alpha_P}{L_\delta^2 \delta_T^2} \cdot \frac{P_L^2 \cdot v \cdot \Delta n}{S_{pm}}, \quad (4)$$

second - according to the flow rate of added water at the inlet of the scoop feeder receiving device, which is possible due to its unchanged lag time, with its calculation according to the equation

$$Q_{BD} = \frac{Q_n - Q_{B1}}{\left( \frac{\delta_B}{\delta_T} + K_n \right)} \cdot \left( \frac{1}{K_{(T/P)G}} - K_n \right) - Q_{B1} \quad (5)$$

third - in accordance with the condition  $Q_{DBM} = Q_{BM} - Q_{PB} - Q_{BD}$  where  $\alpha_p$  is a constant characterising the ore loosening during destruction;  $L_\delta$  is the base distance on conveyor scales;  $P_L$  is the ore mass measured by conveyor scales at the base distance  $L_\delta$ ;  $v$  is the conveyor line speed;  $S_{pn}$  is the cross-sectional area of the ore stream;  $K_n$  is a constant characterising the moisture content in the classifier sands;  $K_{(T/P)G}$  is the limiting value of the solid/liquid ratio in the pulp of the scoop feeder receiving device;  $\Delta n$  is the thickness of water film held on the surface of ore pieces by molecular adhesion forces;  $Q_n$  is the volume flow rate of pulp in the classifier sand chute;  $Q_{B1}$  is the volume flow rate of water supplied to the sand chute;  $Q_{PB}$  is the volume flow rate of water proportional to the surface of ore pieces;  $Q_{BD}$  is the volume flow rate of water added to the mill;  $Q_{BM}$  is the total volume flow rate of water to the mill.

These effects of water on the material flows in the ball mill prepare them for rapid penetration into each other and active mixing from the very beginning of the drum through its rotation, the movement of the balls and the entire material along the inclined surface. In this section, the active grinding of solids in a resource-efficient manner begins immediately.

## 6. Conclusions

The conducted research allows us to draw the following conclusions:

1. It is established that resource-saving grinding of raw materials will occur only at a certain ore loading of the ball mill and specifically necessary liquefaction of pulp in the drum. Despite the fact that the ball mill is an efficient agitator, the material is not averaged in the initial section up to 1/3 of the drum length and is therefore poorly pulverised. Resource saving will only be achieved with a certain volume of material in the ball areas and this volume must be maintained. Both the required travelling speed and the required solid size in the mill discharge can only be achieved with a certain concentration of solids in the pulp, which is appropriate for the process. Fluc-

tuations of the liquid mixture in the drum are determined by the frequency and amplitude at the inlet. They must be such that the process unit does not leave the nominal operating mode. Resource conservation in a ball mill is determined by the state of the material in the drum and the oscillating inlet streams. Flows of initial ore and water into the drum do not appreciably change the technological mode of the ball mill. To increase the resource saving during the grinding of raw materials in the ball mill is possible only through the influence on the input material flows.

2. A scoop feeder is a spiral shaped gripper for transferring the classifier liquid sands captured at the bottom mark into the ball mill drum. Scoop feeders are used with one, two or three gripping bodies. The scoop feeder rotates together with the mill drum. In steady state operation, the volume of pulp coming from the classifier per unit time will correspond to the quantity removed from the intake. So far, scientists have paid little study to scoop feeders. It has been established that directly from the classifier the sand flow into the ball mill is inadmissible due to large oscillations of the material in the drum. When using a scoop feeder with one gripper, the ore and water pulsations do not exceed the 3% deviation zone. The performance is significantly improved by a scoop feeder with two grippers. Consequently, since the scoop feeder significantly improves the sand flow by converting it, all material flows to the ball mill meet the process requirements in terms of pulsations.

3. Several approaches for creating automated systems for stabilising the solid/liquid ratio for closed cycles of ball milling of initial ore with classifier sands have been proposed, but, as the analysis has shown, none of them can be implemented for various reasons. Therefore, the search for approaches to overcome the technical contradiction should be continued.

4. A mathematical model of a device for stabilising pulp liquefaction in a ball mill is proposed, the distinguishing feature of which is the use of a volumetric pulp flow meter in a sand chute instead of a mass flow meter. A solution for estimating the volumetric flow rate of pulp in the sand chute of a classifier by scanning the flow surface is found. The relative error of pulp volume flow rate measurement is within 3...5%, which requires further search.

5. A solid/liquid ratio prediction algorithm is proposed for the communications of a ball mill operating in a closed loop with a mechanical single-spiral classifier, which includes the densities of water and ore, the relative moisture content of the classifier sands, the volume flow rate of pulp in the classifier sand chute, the volume flow rate of water into the ball mill and sand chute, and the mass flow rate of ore into the ball mill.

It is shown that this algorithm has the property of error compensation for all parameters, but the degree of compensation for each parameter is different. Therefore, without special measures, the resulting error in predicting the solid/liquid ratio in the mill can be quite high.

6. It is established that the limiting errors of estimating the solid/liquid ratio when measuring all parameters in the algorithm with an error of  $\pm 5\%$  will be within 1,1%-10%.

If in the technological process the moisture content of the classifier sands, ore density and water flow rate into the sand chute will be unchanged and accurate, then the specified errors are halved, which is easily possible to realise, since the moisture content of the sands is unchanged and ore density is unchanged when processing one technological different types of ore, and the developed water flow meter into the sand chute provides a small error, which is less than 1%.

Therefore, it is necessary to ensure a sufficiently high accuracy of measurement of the mass flow rate of ore into the mill, water into the mill with a relatively inaccurate flow meter of pulp volume flow rate in the sand chute of the classifier. In the process of optimisation it was established that the ore flowmeter, water flowmeter into the mill and sand chute should have a measurement error of  $\pm 1\%$ , and the pulp flowmeter –  $\pm(3-5\%)$  with the error of the ore density and moisture content in the sands of the classifier  $\pm 1\%$ . With these means, the solid/liquid ratio identification error is 0,951% with the slurry flowmeter error of  $\pm 3\%$  and - 1,626% with the slurry flowmeter error of  $\pm 5\%$ .



7. It is possible to obtain high accuracy of solid/liquid ratio estimation only under conditions of equal or no lag in all material flows. Using the invariability of the lag in the scoop feeder and the non-variability of the water supply conditions (stabilisation) in the classifier sand chute, this problem can be solved by selecting the mode of ore flow measurement by conveyor scales and water supply to the ball mill.

8. To include the initial section of the ball mill in active grinding with resource saving, three mathematical models of water flow rate into the ball mill have been developed - to the feed ore, into the scoop feeder receiving device and directly into the ball mill.

9. All this provides resource-saving grinding of ore with sands of mechanical single-spiral classifier with saving of consumption of electric energy, balls and lining and increase of productivity of ball mill and reduction of losses of useful component.

The direction of further research is the development of a system of adaptive distributed resource-saving control of grinding of initial ore with sands of mechanical single-spiral classifier in the first stages of ore preparation.

### *References*

1. **Bogdanov, O.S., Revniltsev, V.I.** (1983). Reference book on ore dressing. Special and auxiliary processes, enrichment tests, control and automation. Moscow: Nedra.
2. **Bonch-Bruevich, A.M., Bykov, V.L., Chinaev P.I.** (1967). Non-contact elements of self-tuning systems. Moscow: Mashinostroenie.
3. **Malyarov, P.V.** (2004). Fundamentals of intensification of ore preparation processes. Rostov-on-Don: Rostizdat.
4. **Ivanov, A.B., Kuvaev, V.N., Kuvaev, Ya.G.** (2010). Perspective directions of automation of processes of crushing and grinding of ore. Moscow: Publishing House "Ore and Metals".
5. **Kondratets, V.O., Serbul, O.M.** (2006). Computer-integrated system of automatic control of ore/water ratio in ball mills with circulating load. Kryvyi Rih: KTU.

6. **Sokur, M.I.** et al. (2017). Preparation of minerals for enrichment. Kremenchuk: Shcherbatykh O.V.

7. **Matsui, A.M., Kondratets, V.O.** (2017). Modelling of the weighted average particle size of solids in the ball mill load with ore and sands of the classifier. Kamianske: DGTU.

8. **Kondratets, V.O., Serbul, O.M.** (2014). Conveyor scales. Patent of Ukraine №93639.

9. **Kondratets, V.O., Matsui, A.M.** (2017). Conveyor scales. Patent of Ukraine №113083.

10. **Matsui, A.M., Kondratets, V.O.** (2017). Conveyor scales for bulk material with variable characteristics. Patent of Ukraine №118205.

11. **Mariuta, A.N., Obletsov, E.I., Eleseev, A.K.** (1968). Device for measurement of circulation load in a closed grinding cycle. Copyright certificate №229346.

12. **Gulenko, T.I., Kondratets, V.A.** (1969). Method of continuous measurement of circulating load. Copyright certificate №329905.

13. **Arkhangelskaya, I.N., Vaisberg, V.M., Brevde, G.M.** (1983). Method of determination of circulating load in a closed grinding cycle. Copyright certificate №1011263.

14. **Arkhangelskaya, I.N., Vaisberg, V.M., Brevde, G.M.** (1983). Method of determination of circulating load in a closed grinding cycle. Copyright certificate №1036373.

15. **Bessonnikova, I.V., Weisberg, V.M., Kornienko, Y.P.** (1979). Method for determining the circulating load. Copyright certificate №694214.

16. **Degtyarev, F.N.** et al. (1977). A device for measuring circulating load. Copyright certificate №570398.

17. **Dmitriev, V.I.** (1986). Method of determination of productivity of spiral classifier on sands. Copyright certificate №1269838.

18. **Morozov, E.F.** (1989). Method for determining the productivity of a spiral classifier for sands. Copyright certificate №1530258.

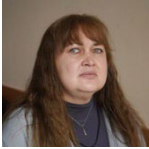
19. **Dmitriev, V.I.** (1991). Method of operative determination of productivity of spiral classifier on sands. Copyright certificate №1659102.

20. **Kondratets, V.O., Matsui, A.M.** (2016). Method for determining the performance of a spiral classifier for sands. Patent of Ukraine №107479.

21. **Kondratets, V.O., Matsui, A.M.** (2017). Method for determining the performance of a spiral classifier for sands. Patent of Ukraine №114305.

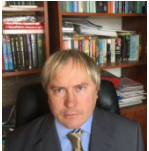
22. **Kondratets, V.O., Matsui, A.M.** (2017). A method for determining the performance of a spiral classifier for sands during the operational operation of the spiral working elements. Patent of Ukraine №121446.
23. **Savilov, A.P.** et al. (1989). Method of automatic control of the ratio of liquid and solid phase flow rates in the mill feed. Copyright certificate №1526829.
24. **Dmitriev, V.I., Savilov, A.P., Saganenko, A.A.** (1987). System of automatic regulation of the ratio of solid and liquid phase flow rates in the mill feed. Copyright certificate No. 1326335.
25. **Dmitriev, V.I., Saganenko, A.A., Savilov, A.P.** (1988). Method of automatic regulation of the ratio of flow rates of inlet streams into the mill. Copyright certificate №1416179.
26. **Ilyinsky, V.M.** (1973). Measurements of mass flow rates. Moscow: Energia.
27. **Degtyarev, F.N.** et al. (1973). Device for automatic control of loading and stabilisation of pulp liquefaction in a mill. Copyright certificate №388790.
28. **Kondratets, V.O.** (2013). Theoretical study of scanning the surface of open material flows by beams of constant length. Kryvyi Rih: KNU.
29. **Matsui, A.M., Kondratets, V.O.** (2017). Modelling of approaches to grinding ore varieties of a particular deposit in closed-cycle ball mills. Kamianske: DDTU.
30. **Kondratets, V.A.** (2014). Study of moisture content of sands of double-spiral mechanical classifiers in industrial conditions. Kriviy Rig: KNU.
31. **Kondratets, V.O., Serbul, O.M.** (2013). Theoretical study of the liquefaction of sands of a single-spiral classifier by a source with a constant water consumption. Kirovograd: KNTU.
32. **Kondratets, V.O., Serbul, O.M.** (2003). Theoretical study of the hydraulic fluid flow transducer as a regulated object of the flow stabilisation system. Kirovograd: KDTU.
33. **Kondratets, V.O., Serbul, O.M.** (2003). Theoretical studies of the statics of invariant SAR of the liquid level in a hydraulic transducer. Kirovograd: KDTU.
34. **Kondratets, V.O., Serbul, O.M.** (2003). Device for automatic stabilisation of liquid flow rates. Patent of Ukraine №74393.
35. **Kondratets, V.O., Serbul, O.M.** (2009). Device for automatic stabilisation of pulp dilution in circulating load mills. Patent of Ukraine №40465.
36. **Kondratets, V.O.** (2014). Method of automatic stabilisation of pulp liquefaction in circulating load mills. Patent of Ukraine №90851.

**DEVELOPMENT OF A MODEL OF FAILURE  
RELATIONSHIPS FOR COMPLEX TECHNICAL FACILITY  
FOR RESOURCE-SAVING TECHNOLOGIES FOR MINING  
AND PROCESSING OF MINERALS**



**Oksana BANZAK**

Doctor of technical sciences, professor, professor of department Electronics, transport technologies and logistics, State university of intellectual technologies and communications, Odessa, Ukraine



**Hehhadii BANZAK**

Candidate of technical sciences, assistant professor, assistant professor of department Metrology, quality and standardization, State university of intellectual technologies and communications, Odessa, Ukraine



**Oleg LESHCHENKO**

Candidate of technical sciences, assistant professor, head of department Electronics, transport technologies and logistics, State university of intellectual technologies and communications, Odessa, Ukraine



**Oleg GRABOVSKY**

Candidate of technical sciences, assistant professor, dean of faculty Electronics, automation and metrology, State university of intellectual technologies and communications, Odessa, Ukraine



**Antonina GABER**

Candidate of technical sciences, assistant professor, head of department Metrology, quality and standardization, State university of intellectual technologies and communications, Odessa, Ukraine

### Annotation

Complex technical objects in modern society are extremely important. Such objects belong to the class of recoverable objects of long-term multiple use. They tend to be expensive and require significant maintenance costs. To ensure the required level of reliability during their operation, maintenance is usually carried out, the essence of which is the timely preventive replacement of elements that are in a pre-failure state, which is very important for military equipment.

The problem is that when developing such objects of military equipment, all issues related to maintainability and maintenance should be addressed already at the early stages of designing an object. If you do not provide in advance the necessary hardware and software for the built-in monitoring of the technical condition (TC) of the object, do not develop and “embed” the maintenance technology into the object, then it will not be possible to realize in the future a possible gain in the reliability of the object due to the maintenance. Since all these issues must be resolved at the stage of creating an object (when the object does not yet exist), mathematical models of the maintenance process are needed, with the help of which it would be possible to calculate the possible gain in the level of reliability the object due to maintenance, to estimate the cost costs required for this. In this paper, we develop a methodology for optimizing the parameters of the strategy for regulated maintenance of military equipment.

**Keywords:** maintenance, object of military equipment, regulated maintenance of military equipment, costs for the cost military equipment

### Model of failure-free operation of a non-recoverable object.

The model being developed is intended to obtain probability functions of failure-free operation  $P(t)$  (or time-to-failure  $F(t)=1-P(t)$  distribution functions) for the object as a whole and all its structural elements based on the available information on the failure-free performance of component elements. The functions  $P(t)$  and  $F(t)$  indicators of the reliability of non-recoverable objects, therefore we will call the model the model of failure-free operation (MF) of a non-recoverable object.

The structural structure of a complex technical object is almost always hierarchical. Elements belonging to different design levels can be called, for example, units (cabinets), devices (blocks), nodes (boards), etc. In this case, an object can consist of units, units - of devices, devices - of nodes, etc.

Let us denote  $E_{ijk}^u$   $k$ -th element of  $u$ -th structural level, which is part of  $j$ -th element of  $(u-1)$  level. The index  $ij-k$  in this case indicates a chain of numbers elements of higher levels (including this one) in the sequence of their occurrence in elements of previous

(higher) levels. Numbering of levels starts from the top, starting from the object level ( $u=0$ ). The numbering of  $u$ -th level elements included in ( $u-1$ )-th level element is independent within this element. Thus, the number of numbers in the lower index is always equal to the value of the upper index  $u$ -the number of design level.

The object as a whole is treated as a level zero element  $E^0$ . It is always unique and is not included in any other elements. In figure 1 shows a fragment of the hierarchical structural structure of the object.

Each structural element of some  $u$ -th level  $E_{ijk}^u$  can include structural elements of next ( $u+1$ )-th level  $E_{ijkl}^{u+1}$ . In fig. 1, elements of the lower level are indicated by circles, all other elements are indicated by rectangles.

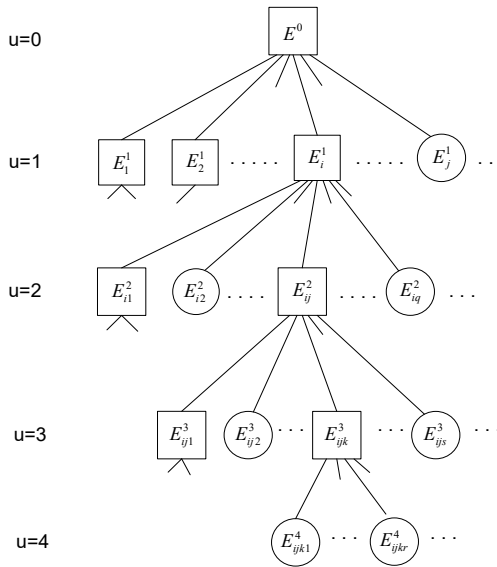


**Fig. 1.** Fragment of the hierarchical structural structure of the object

We will use the term structural element in the case when it is necessary to pay attention to the place occupied in the structural structure of an object. Structural elements of the lower level, following the terminology adopted in [1], we will agree to call zero-rank prod-

ucts (ZRP). An ZRP can be either a very complex device or consist of a single simplest element (for example, a resistor, microcircuit, transformer, bearing, etc.). ZRP is an inseparable element and is always considered as one whole.

We will formally represent the constructive structure of an object as a hierarchical list structure. Each structural element  $E_{ij\dots r}^u$  is treated as a list

$$E_{ij\dots r}^u = \{E_{ij\dots r0}^{u+1}, E_{ij\dots r1}^{u+1}, \dots, E_{ij\dots rs}^{u+1}, \dots\}; s = \overline{0, |E_{ij\dots r}^u|}; u = \overline{0, U}, \quad (1)$$

where  $E_{ij\dots rs}^{u+1}$  - is  $(u+1)$ -level element included in the element  $E_{ij\dots r}^u$ ;  $U$  - maximum level (nesting) of structural elements for a given RET object.

The object as a whole is represented by a list of 1-st level elements

$$E^0 = \{E_0^1, E_1^1, \dots, E_i^1, \dots\}; i = \overline{0, |E^0|}. \quad (2)$$

ZRP elements are represented as empty lists.

The set of all nested lists of the form (1) represents a mathematical model of the constructive structure of an object.

The reliability structure of an object can be an arbitrary series-parallel structure. This means that each structural element  $E_{ij\dots k}^u$  can be either an ZRP-element, or represent a series connection of its constituent elements, or be a redundant group of elements - a group of elements connected in parallel in the sense of reliability. Elements of a reserved group can only be elements of the same type. Reservations in groups can be loaded (permanent) or unloaded (replacement).

If an element  $E_{ij\dots k}^u$  consists of series-connected elements of  $(u+1)$  level, then the probability of failure-free operation of this element is defined as the product

$$P(t / E_{ij\dots k}^u) = \prod_{\forall E_{ij\dots kr}^{u+1} \in E_{ij\dots k}^u} P(t / E_{ij\dots kr}^{u+1}), \quad (3)$$

where  $r$  - is the number of  $(u+1)$ -level element  $E_{ij\dots kr}^{u+1}$  included in  $u$ -th level element  $E_{ij\dots k}^u$ ;

$P(t / E_{ij...kr}^{u+1})$  - probability of failure-free operation elements  $E_{ij...kr}^{u+1}$ .

If an element  $E_{ij...k}^u$  is a redundant group consisting of  $n$  identical elements  $E_{ij...k0}^{u+1}$  connected in parallel, then in the case of a constant reserve the probability of failure-free operation for it is equal to [2]

$$P(t / E_{ij...k}^u) = 1 - [1 - P(t / E_{ij...k0}^{u+1})]^n. \quad (4)$$

The model does not take into account the possibility of multiple failures, since within the framework of the tasks for which this model is developed, the probability of multiple failures can be neglected.

From what has been considered, it is clear that the initial information for the model should be the probability functions of failure-free operation of ZRP  $P(t/e)$  ( $e_m$  - designation of an arbitrary ZRP). For all structural elements of higher levels, including the object as a whole, functions  $P(t / E_{ij...r}^u)$  must be calculated.

In practice, functions  $P(t/e_m)$  are rarely known exactly. At best, the first two moments are known and there are certain assumptions about the class of distribution laws to which the function  $P(t/e_m)$  may belong. As a rule, only the estimate of the first moment (the mathematical expectation of time to failure) is known. In the worst case, neither the distribution function nor its moments are known. Therefore, in practice, one has to make an assumption about the form of the distribution law, taking into account the type of a given element and the available information about the physical laws of failure for elements of this type. The average time to failure of elements must be estimated based on information about analogue-elements.

The model being developed is intended to solve problems of assessing the reliability of aging objects, so we need to use the laws of time-to-failure distribution that take into account degradation processes in materials of different types of elements. Failures generated by various degradation processes are usually called gradual [5, 6]. It has now become generally accepted that gradual failures occur due to the fact that the value of some defining parameter reaches the maximum permissible value. Failure models based on the concept of a defining parameter are usually called probabilistic-physical (*WF*-models) [6,8].

The most universal model of gradual failures is the diffusion



nonmonotonic distribution (*DN*-distribution) [6].

For *DN*-distribution, the probability density has the following form

$$f(t) = f(t; \mu, \nu) = \frac{\sqrt{\mu}}{\nu\sqrt{2\pi t}} \exp\left(-\frac{(t-\mu)^2}{2\nu^2\mu t}\right), \quad (5)$$

where  $\mu$  - is the scale parameter (mean time to failure);

$\nu$ - coefficient of variation.

The density function (5) corresponds to the integral function of *DN*-distribution

$$\begin{aligned} F(t) = DN(t; \mu, \nu) &= \Phi\left(\frac{t-\mu}{\nu\sqrt{\mu t}}\right) + \exp\left(\frac{2}{\nu^2}\right)\Phi\left(-\frac{t+\mu}{\nu\sqrt{\mu t}}\right) = \\ &= \Phi\left(\frac{at-1}{\nu\sqrt{at}}\right) + \exp\left(\frac{2}{\nu^2}\right)\Phi\left(-\frac{at+1}{\nu\sqrt{at}}\right) \end{aligned} \quad (6)$$

where  $\Phi(z) = \frac{1}{\sqrt{2\pi}} \int_{-\infty}^z \exp\left(-\frac{x^2}{2}\right) dx$  - is the normalized normal distribution;

$a$  - average rate of the degradation process (average rate of change of the defining parameter), equal  $t a=1/\mu$ .

*DN*-distribution has one important property, which is that the coefficient of variation of the distribution of time to failure coincides with the coefficient of variation of the distribution of the random variable of the determining parameter. This property, combined with the fact that the mean time to failure is equal to the reciprocal of the mean degradation rate of the governing parameter, opens up great opportunities for the use of *DN*-distribution in maintenance modeling problems.

The universality of *DN*-distribution lies in the fact that its coefficient of variation (shape parameter) practically coincides with the shape parameters of *DN*-distribution and is approximately equal to the inverse value of the shape parameter of Weibull distribution and alpha distribution [6]. This makes it possible to use *DN*-distribution as a model of failures of elements of various types that have different physical mechanisms of degradation processes. To ensure the adequacy of the failure model, it is enough to correctly set the value of the coefficient of variation. Recommendations for choosing the coef-

efficient of variation are given in [8]. In table 1 shows some data taken from [8] on the characteristic values of the coefficient of variation.

Table 1

Generalized estimates of the coefficients variation various physical processes

Type of degradation process	Coefficient of variations destruction process	Name of elements undergoing destruction
Fatigue (high-cycle)	0,40–1,00	Housing parts, rolling bearings, shafts, axles, springs, connecting rods, bolts, etc.
Wear (mechanical-chemical)	0,20–0,50	Sliding bearings, shafts, axles, guides, bushings, etc.
Aging	0,40–1,00	Elements and parts made of metals, polymers, rubber products, seals, semiconductors, etc.
Electrical (electrolysis, charge migration, electrodiffusion)	0,70–1,50	Semiconductor devices, integrated circuits, capacitors and other electronic products.

The choice of a numerical value of the coefficient of variation from the specified range in each specific case can be carried out taking into account the following general considerations: the greater the average ratio of load to endurance limit (strength), the lower the coefficient of variation, and vice versa, that is, the lower the loading coefficient, the higher coefficient of variation.

Taking into account everything considered as a failure model for all structural elements and the object as a whole, we choose  $WF$ -model of  $DN$ - distribution. The initial information for MB in this case is the set of pairs of parameters  $\langle \mu_i, \nu_i \rangle$  of all elements-ZRP. Based on this information, the corresponding parameters for all other structural elements of higher levels must be calculated.

In [8] it is proved that if a system consists of elements whose failures are subject to  $DN$ -distribution, then the failures of the system are also subject to the  $DN$  distribution. The parameters of  $DN$ -distribution of system time to failure (scale parameter  $\mu$  and shape parameter  $\nu$ ), depending on the method of reliable connection of elements in the system, are calculated using the following formulas.

Calculation formulas for determining the scale  $\mu$  parameter and shape parameter for structural elements of higher levels (not ZRP):

Series connection of different types of elements

$$\mu = 1 / \sqrt{\sum_{i=1}^N \frac{n_i}{\mu_i^2}} ; \quad (7)$$

$$\nu = \sqrt{\sum_{i=1}^N \frac{n_i \nu_i^2}{\mu_i^2}} / \sqrt{\sum_{i=1}^N \frac{n_i}{\mu_i^2}} , \quad (8)$$

where  $n_i$  - is the number of elements  $i$ -th type;

$\mu_i$  - scale parameter  $DN$ -distribution of time to failure of elements  $i$ -th type (average time to failure of elements  $i$ -th type);

$\nu_i$  - parameter of form  $DN$ -distribution of time to failure elements  $i$ -th type (variation coefficient);

$N$  - is the number of element types in system.

Series connection of identical elements

$$\mu = \mu_0 / \sqrt{n} ; \quad (9)$$

$$\nu = \nu_0 , \quad (10)$$

where  $\mu_0$  - is the scale parameter of  $DN$ -distribution of elements included in the system (average time to failure of one element);

$n$  - is the number of identical elements in the system.

Loaded (permanent) reservation

$$\mu = \mu_0 \sqrt{n} ; \quad (11)$$

$$\nu = \nu_0 / \sqrt{n} . \quad (12)$$

Unloaded (replacement) reservation

$$\mu = \mu_0 n ; \quad (13)$$

$$\nu = \nu_0 / \sqrt{n} . \quad (14)$$

The formal descriptions of the structural and reliability structures of an object introduced above, the expression for probability of failure of an object (or element)  $F(t)$  (6) and the calculation expressions (7)-(14) together represent a mathematical model of the failure-free operation of a non-repairable object.

The prototype of the considered MB can be considered the model described in [6]. The main difference between MB and the

prototype is use of the important property of  $DN$ -distribution to preserve the type of distribution when transforming the reliability structure of structural elements (when moving from a sequential structure to a parallel one, and vice versa).

Model of failure-free operation of a restored object.

In previous section, MB was developed for the case when an object is considered unrecoverable. In the developed model

*a* - hierarchical structural structure of the object is represented;

*b* - reliability structure is determined by specifying the redundant group attribute for each structural element;

*c* - automatic (software) calculation of the parameters  $DN$ -distribution of time to failure is carried out for each elements of object.

Thus, MB contains all the necessary information for modeling failures of any of the structural elements of the object.

However, this is not enough for IMS, in which maintenance processes must be modeled. For IMS, it is necessary to indicate specific elements whose failures and recovery should be modeled.

Let us introduce the concept of a set recoverable elements  $E_g$  as follows. The set  $E_g$  must include structural elements that will be replaced in case of failure of the object. The set  $E_g$  includes the most repairable elements, that is, elements whose replacement time is minimal, these are the so-called standard replacement elements (SRE). The set  $E_g$  must satisfy the requirements of completeness and non-redundancy.

The completeness requirement is that the set must include all elements whose failures can lead to the failure of the object. Formally, the requirement of completeness is ensured by the following condition: there should not be a single path between the root of the tree (object) and the hanging node (INR element) that does not contain an element belonging to set  $E_g$  (such an element must be unique).

The nonredundancy requirement is that set  $E_g$  must not contain more than one element that belongs to the path between the root of tree and any hanging node.

With this definition of set  $E_g$  and with the previously accepted assumption about the sequential reliable connection of structural elements, the probability of failure-free operation of the object is equal to

$$P(t) = \prod_{i \in E_n} [1 - F_i(t)], \quad (15)$$

where  $F_i(t)$ - is the probability of failure  $i$ -th element from set  $.E_\theta$

The probability  $P(t)$  does not depend on the choice of set  $.E_\theta$

In the same way, value of  $E_\theta$  average time to failure does not depend on

$$T_{cp} = \int_0^{\infty} P(t) dt. \quad (16)$$

If an object is considered as recoverable, then the failure flow parameter  $\omega(t)$  and average time between failures should be used as indicators of failure  $T_0$  [7].

When connecting elements in series, the failure flow parameter is defined as the sum

$$\omega(t) = \sum_{i \in E_n} \omega_i(t), \quad (17)$$

where  $\omega_i(t)$  - is failure flow parameter of  $i$ -th element from the set  $E_\theta$ .

The failure flow parameter of  $i$ -th element  $\omega_i(t)$  is found as a solution to the integral equation of the following form [7]:

$$\omega_i(t) = f_i(t) + \int_0^t f_i(t-x) \omega_i(x) dx. \quad (18)$$

where  $f_i(t)$  - is the probability density of failure of  $i$ -th element ( $i \in E_\theta$ ).

The failure flow parameter always has a steady-state value

$$\omega^\infty = \lim_{t \rightarrow \infty} \omega(t).$$

In this case, the average time between failures of the object is equal to  $T_0 = 1 / \omega^\infty$ .

For real technical objects, within the operating period of interest to the user  $T_0$ , the steady-state value of the failure flow parameter may not occur. In this case, the average time to failure of an object is determined by the formula:

$$T_0 = T_0(T_3) = 1 / \left( \frac{1}{T_3} \int_0^{T_3} \omega(t) dt \right). \quad (19)$$

The value  $T_0$  (in contrast to  $T_{cp}$ ) significantly depends on the choice of set  $E_g$ . The higher the average level of elements included in  $E_g$ , greater the value. This is easily explained, since when larger structural elements are replaced, a larger number of serviceable elements are simultaneously updated. Consequently, the higher the structural level of the restored elements (lower the level number  $u$ ), the greater proportion of elements that are updated after ongoing repairs, which leads to an increase in the indicator  $T_0$ .

### **Model database.**

For software implementation of MB and ensuring its application for real technical objects, a database (DB) is required in which information about the object (composition, structural and reliability structure, failure-free performance indicators of ZRP, etc.) could be stored. As is known, information in the database is presented in the form of tables [4]. The following tables were created in the developed database for MB:

- tbEu tables - contain information about the structural elements of an object at level  $u$ . The number of tables tbEu is equal to the maximum number of levels of structural elements that can be represented in database: tbE1 - for 1-st level elements included in object, tbKE2 - 2-nd level elements included in 1-st level elements, etc.d. One table entry contains information about one  $u$ -level structural element.

- tables tbKEu - contain information about elements that are ZRP and related to the design level  $u$  : tbKE1 - ZRP included directly in the object; tbKE2 - ZRP included directly in the structural elements of the 1st level; tbKE3 - ZRP included directly in the structural elements of the 2nd level, etc. One record contains information about one element -  $u$ -level ZRP. The number of tbKEu  $u$  tables is equal to the number of tbKEu tables plus one;

- table tbTipKE – contains information about the types of component elements - ZRP and their reliability indicators (information is taken from reference books and product passports);

- tbGTipKE – contains information about groups of ZRP types. Type groups were introduced for convenience of working with the database;

- tbSprav – table containing a list of reference books from which information about the reliability indicators of ZRP was taken.

In table 2-6 shows the structure of these tables. Only information that is directly used by MB is indicated.

Table 2

Structure of tbEu tables (parameters of structural elements)

Field name	Data type	Key attribute	Field purpose
i1	INTEGER	*	Structural element code
I2	INTEGER		Code of the "higher" level structural element that includes this element
NAME	VARCHAR		Element name
PZ	CHAR(1)		Restoration attribute (0 – attribute is not defined; 1 – element is restored (replaced) in case of failures; 2 – element is replaced and serviced during maintenance)
TG	CHAR(1)		Type of connection in the group (0 – separate element; 1 – serial connection; 2 – loaded reserve; 3 – unloaded reserve)
N	INTEGER		Number of elements in the group.
....	....		.....

Table 3

Structure of tbKEu tables (parameters of elements - ZRP)

Field name	Data type	Key attribute	Field purpose
Kod	INTEGER	*	Element code – ZRP
I2	INTEGER		Code of the "senior" level structural element that includes this element
NAME	VARCHAR		Item name
KOD GTIP	INTEGER		ZRP type group code
KOD TIP	INTEGER		ZRP type code
N	INTEGER		The purpose of the fields is the same as tblEu table fields of the same name
PZ	CHAR(1)		
TG	CHAR(1)		
....	....		

Table 4

Structure of tbGTipKE table (ZRP type groups)

Field name	Data type	Key attribute	Field purpose
Kod GTipKE	INTEGER	*	ZRP type group code
name	VARCHAR		Name of the group ZRP types

Table 5

Structure of tbTipKE table (ZRP reliability indicators)

Field name	Data type	Key attribute	Field purpose
Kod_TipKE	INTEGER	*	ZRP type code
Kod_GTipKE	INTEGER		ZRP type group code
name	VARCHAR		Element type name
Mu	FLOAT		Average time to failure, h
Nu	FLOAT		The coefficient of variation
z	INTEGER		Distribution law code
Kod_Sprav	INTEGER		Directory code - source of information

Table 6

Structure of tbSprav table (list of reference books)

Field name	Data type	Key attribute	Field purpose
Kod_Sprav	INTEGER	*	Directory code
name	VARCHAR		Name

Relationships of “master-slave” type have been created between the database tables (they are also called “one-to-many” relationships). In fig. 2. shows a diagram of connections “master-slave” type between the tables tbEu and tbKEu.

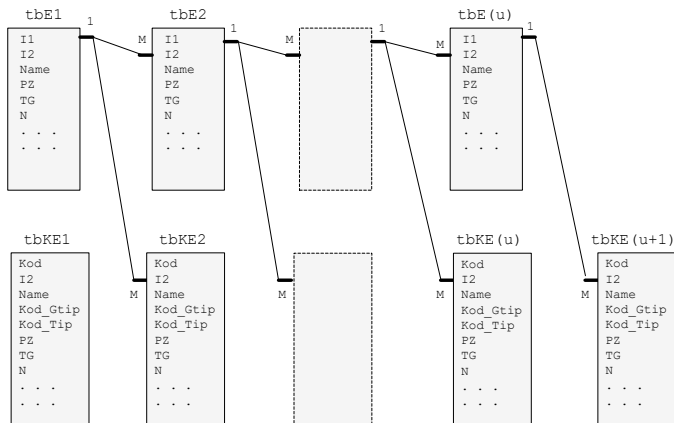


Fig. 2. Master-slave relationships between tables tbEu and tbKEu



A 1:M relationship means that one record in the main table corresponds to 0 or more records in the slave table. For example, tables tbE2 and tbKE2 are subordinate to table tbE1. The link key in subtables tbEu and tbKEu is the key field I2.

Relationships between tables are created to ensure data integrity as well as ease of data management. The linked records in table tbE2 contain data about the 2nd level structural elements that are part of the 1st level structural element, the data for which is contained in the linked record in table tbE1. In the same way, the related records of table tbKE2 contain data on ZRP, which are elements of 2-nd level and are parts same structural element of 1-st level.

Thanks to the presence of relationships in subordinate tables, it is easy to find only those records that are related to the current, currently selected record in the main table.

Connections were also created between the tables tbGTipKE and tbTipKE and between tbSprav and tbTipKE (fig. 3).

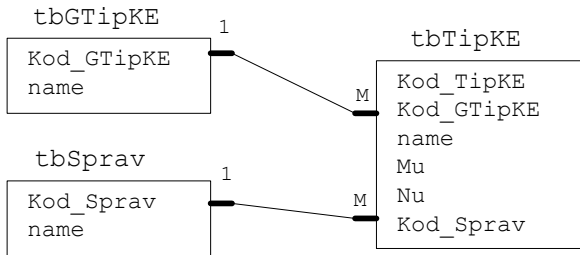


**Fig. 3.** Diagram of relationships between tables tbGTipKE, tbSprav and tbTipKE

One record in tbGTipKE table (one group of types) can correspond to 0 or more records in tbGTipKE table (0 or more ZRP types). In the same way, one record in tbKEu table (one directory) can correspond to 0 or more records in the tbTipKE table (data of the same ZRP type is always taken from one directory).

There are also M:1 type connections between tbKEu tables and tbTipKE table (not shown in the figures). The communication keys here are Kod\_Tip and Kod\_TipKE fields. Using this connection, each ZRP presented in tbKEu table is associated with a single entry in tbTipKE table, containing information about the reliability parameters of an element of this type.

Thus, the constructive structure of an object in the database is represented by placing data on elements of various levels in various tables and creating appropriate connections between the tables. Information about the reliability structure of structural elements is presented using the TG field (group type), which is available in tbEu and tbKEu tables.

A brief description of MB database, as well as information on possible ways to improve it, is given [5].

Reliability model user interface.

The MB is implemented in such a way that when the software is launched, all data structures used in the model are immediately (automatically) created in the PC OS and become available to other models. At the same time, indicators of the reliability of the object and all its elements are immediately formed.

In the "Database" mode, it is possible to create a database and correct previously entered information. The PC screen view in this mode is shown in fig. 5.

The left side of the screen displays the object's structural structure tree. In this tree, you can collapse or expand the internal structure of any of the elements. When you select (by clicking) any of the elements in this tree, the tables located on the right display information about elements that make up selected element. The top table displays data about the constituent structural elements that make up the selected element. The lower table displays data on ZRP that is directly included in the selected element. You can edit the data in these tables.

At the bottom left (under the tree) a panel with data is displayed:

- average time to failure of the selected element ( $h$ );
- cost of element (c.u);
- number of structural elements included in the selected element;
- total number of ZRP -elements in the selected element.

At the bottom of the screen (under the tables) a histogram of the density  $DN$ -distribution of the selected element is displayed.

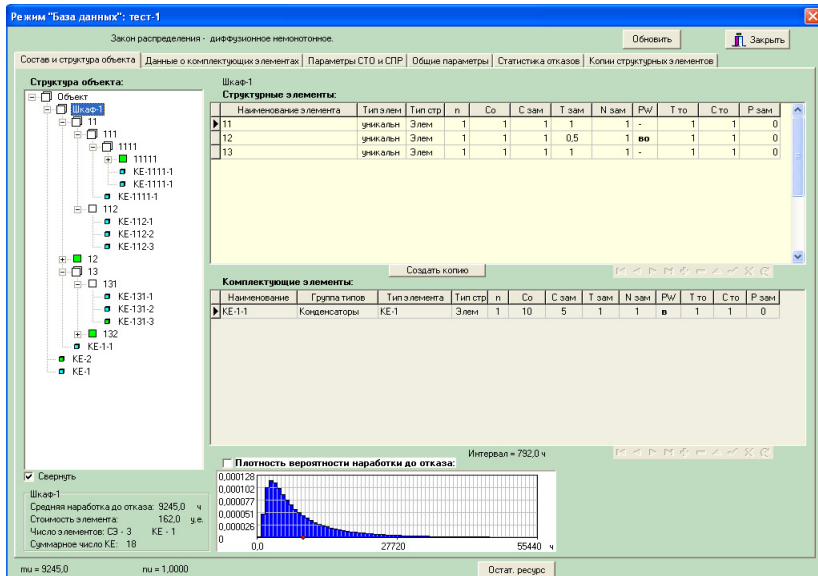
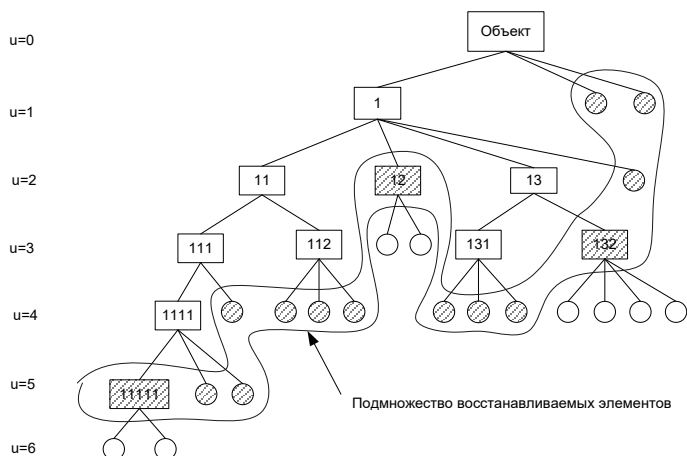


Fig. 4. PC screen view in "Database" mode

### Examples of using the model for test objects.

To verify and study the developed models and methods, test objects with different structures and reliability were used. The characteristics of test objects are selected in such a way as to cover all typical cases of possible real objects encountered in practice. Using test objects, the following sections demonstrate the application features of the developed models and their capabilities. This section provides the main characteristics of the test objects, as well as the simulation results obtained for them using MB software.

The Test-1 object is an example of the simplest object that has a consistent reliability structure and a design structure with 6 nesting levels (fig. 5). It consists of 20 elements- ZRP, which are part of other structural elements of higher levels. ZRP elements are indicated by circles. All ZRP have the same reliability characteristics:  $T_{cp}=20,000$  h;  $\nu=1$ . Elements included in the set  $E_g$  are marked with shading.



**Fig. 5.** Constructive structure of the Test-1 object

Object Test-2 is an example of a low-reliability object that uses redundancy to improve reliability. The structural structure of the object is shown in fig. 5. The three least reliable elements have reserve: 11 ( $n=3$ ), 12 ( $n=3$ ) and 131 ( $n=2$ ). All other elements represent a sequence (in terms of reliability) of all the elements included in them. The total number of ZRP is 900. Elements included in the set of restored elements  $E_{\theta}$  are also marked with shading.

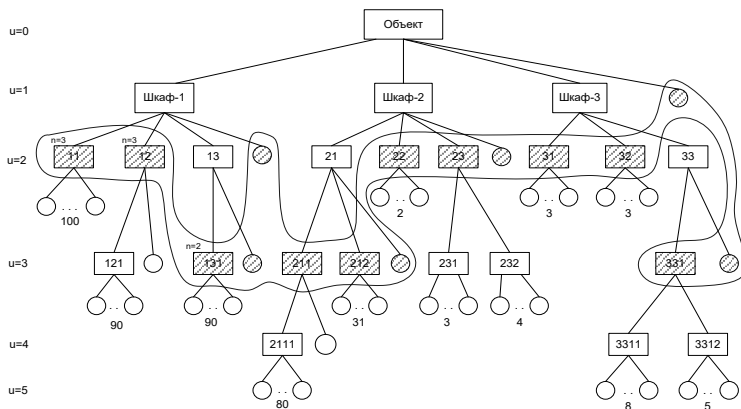


**Fig. 6.** Constructive structure of the Test-2 object

Objects Test-3 and Test-4 are examples of objects that have a single-level structural structure (fig. 7). The number of all elements is 50. The elements of objects differ significantly in their level of reliability. Object Test-3 is an example of an object with a high level of reliability, object Test-4 is an example of an object with low reliability. Since the structural structure is single-level, all elements are ZRP, and all of them are restored.

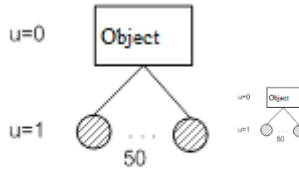


Fig. 7. Constructive structure of objects Test-3 and Test-4

For each of test objects, a separate database was created, into which the necessary information about object was entered. For all ZRP, the coefficient of variation is set to the same, equal to 1.

In table 7 presents the main characteristics of the test Characteristics of test objects

Object	Number of INR	Number of re-stored elements	Average time to failure, h	Variation coefficient
Test-1	20	15	4472,1	1,0
Test-2	900	16	745,8	0,726
Test-3	50	50	29930,7	1,0
Test-4	50	50	1783,2	1,0

The values of reliability indicators given in the table (mean time to failure and coefficient of variation) are generated automatically when DB program is launched and are displayed on PC screen (fig. 4). For Test-2 object, the resulting coefficient of variation is not equal to 1 due to the presence of reserved groups elements in the object.

The most important characteristic of an object that affects the operational reliability and cost of object is the distribution of object's failure-free performance indicators among its elements. In fig. 8

shows histograms of the distribution of the average time to failure of elements test objects. The grouping intervals are shown horizontally, and the number of elements in the intervals are shown vertically.

The histograms shown in the figures were generated using model software in “Database” mode.

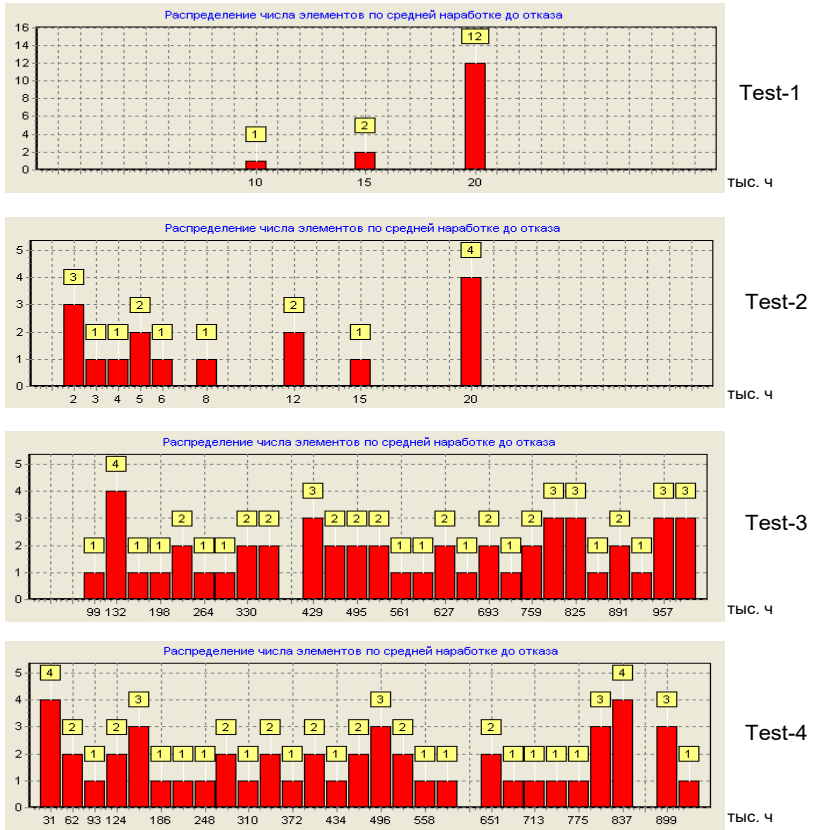


**Fig. 8.** Histograms of distribution of average time to failure of restored elements of test objects

## Conclusions

1. The reliability model (RM) allows you to obtain estimates of the reliability indicators (RI) of individual structural elements and the object as a whole based on information about RI of elements of

the lower structural level. The RM represents the hierarchical structural structure of the object. Structural elements of some  $u$ -th structural level are a sequential (in the sense of reliability) connection of its constituent elements of  $(u+1)$ -th level. Individual structural elements can be a redundant group (parallel connection) of similar elements. Thus, with the help of RM, the representation of a hierarchical structural structure is combined with an arbitrary serial-parallel reliability structure of an object, which is an acceptable representation for most technical objects encountered in practice.

2. The *DN*-distribution is used as a failure model for all elements and the object as a whole. The *DN*-distribution is considered an adequate gradual failure model for both electronic products and various mechanical components and elements. An important advantage of *DN*-distribution is that its appearance is preserved during transformations of the reliability structure of the system. It is this feature of *DN*-distribution that made it possible to apply it to a system with a hierarchical structure.

3. The software implementation of the MB was developed in Delphi programming system. The hierarchical constructive structure of an object is represented programmatically using list data structures (TList are used). The elements of the lists are objects (instances of Delphi classes) representing individual structural elements of a technical object. Such objects encapsulate all the necessary data related to individual structural elements, including the parameters of *DN*-distributions of mean time to failure.

Information about the composition, structure and reliability indicators of the object elements is stored in the model database, built using tables in the InterBase DBMS format.

## *References*

1. Optimization of parameters maintenance process of an electronic equipment facility / **O.V. Banzak, H.V. Banzak, O.I. , Leshchenko, N.A. Khlevny** \ The 4th International scientific and practical conference “Innovative development of science, technology and education” (January 18-20, 2024) Perfect Publishing, Vancouver, Canada. 2024.

2. Forecasting to reliability complex object radio-electronic technology and optimization parameter their technical usage with use the simulation statistical models: [monography] in English / **Sergey Lenkov, Konstantin Borjak, Gennady Banzak, Vadim Braun, ets.; under edition S.V. Lenkov.** – Odessa: Publishing house “VMV”, 2014. – 252 p.

**DEVELOPMENT OF METHODS FOR FORECASTING  
THE DURATION OF RECOVERY GROUNDWATER LEVEL**



**Elvira FILATIEVA**  
PhD, Independed researcher, Ukraine



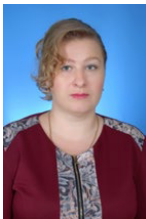
**Oleksandr OLEINICHENKO**  
Senior Lecturer, Volodymyr Dahl East Ukrainian  
National University, Ukraine



**Mikhail FILATIEV**  
Dr. engineering sciences, Independed researcher,  
Ukraine



**Inna MAKSYUK**  
PhD, Independed researcher, Ukraine



**Olga FURSOVA**  
Assistant, Independed researcher, Ukraine



## **Abstract**

The change in the natural balance of surface, ground and underground waters is one of the urgent environmental problems of coal-mining regions, which is associated with negative phenomena and processes that accompany the exploitation and liquidation of mines. Management of groundwater inflows at various stages of the post-exploitation existence of mines that are being liquidated is difficult due to the lack of study of water migration in the disturbed massif. The purpose of the work is to develop methods of forecasting the time of restoration of the natural surface of depressed groundwater wells in the regions of mine closure. The hydrofiltration scheme of coal mine flooding was considered, and its connection with the shift of artificial rocks and the earth's surface during cleaning operations was carried out. A hydrogeological forecast of the ecological consequences of the exploitation and closure of coal mines has been made. Based on the monitoring of the water surface level in the vertical shafts of mines that are being liquidated, methods have been developed for determining the duration of restoration of the natural level of groundwater for a separate mine and the region as a whole.

## **Introduction**

For more than two hundred years, over 21 billion tons (up to 12 km<sup>3</sup>) of rocks, including about 15 billion tons (10 km<sup>3</sup>) of coal, have been extracted from the depths of Donbas by coal mines. As a result of such activity, deformations occurred with a violation of the geomechanical balance and integrity of 600 km<sup>3</sup> of the rock massif in the zones affected by mining operations, and on 50% of the area, the subsidence of the day surface amounted to an average of 1.5÷2.0 m, with a simultaneous increase in the permeability of the rocks and an increase in the interaction of surface and groundwater [1]. During the historical development of Donbas, approximately 970 mines were built, of which about two hundred are currently in operation at a maximum depth of 1,450 m [2]. The critical acceleration of the closure and liquidation of coal mining enterprises, starting from the 1990s, mainly by the method of wet conservation (self-rehabilitation flooding), led to imperfect accounting of object-territorial and regional changes in environmental parameters of natural-technogenic geosystems "mining area - geological environment". As a result of these circumstances, a large complex of irreversible and dangerous changes in the ecological state of the subsoil was accumulated.

The most dynamic changes in the geological environment of Donbas are associated with significant inflows of underground water into mining operations. Their total volume at the maximum development of mining operations was 25.0 m<sup>3</sup>/s (1990). Of these,

12.0 m<sup>3</sup>/s were natural resources, which indicates active drainage of surface water sources and hydraulic interconnection of mines [2].

The intensification of man-made environmental changes in Donbass was influenced by the mining of 129 rivers and creeks, 26 reservoirs (683 cases), as well as continuous subsidence of the earth's surface on an area of up to 8,000 km<sup>2</sup>.

A significant complication for the mine closure process is the presence of about 250 previously flooded and semi-flooded mines that are hydraulically connected to the working ones. According to the available estimate, the total volume of mining products of these mines exceeds 2.3 km<sup>3</sup> and contains up to 1.6 km<sup>3</sup> of water, which can significantly accelerate the regional intensification of the flooding of the territories of cities and towns, the migration of pollutants into surface and underground water intakes and the river network, as well as increase the danger of emergency water breakthroughs into working mines.

The total water inflow to the mine consists of: inflow of underground water (aquifers drained by mining operations); mine waters coming from flooded workings and neighboring mines; water supplied to the mine for laying, irrigation, drilling wells and for other purposes; surface water and precipitation. The mode of water entering the workings depends on a set of interacting natural (climatic, geomorphological, hydrogeological) and technological (shape and size of mining workings, depth and intensity of deposit development, development systems) factors [3].

The zone of water cracks is a disturbed massif of rocks, through the cracks of which underground and surface waters enter the mine workings. There are zones of natural water supply cracks associated with large tectonic disturbances and karst phenomena, and artificial ones - with the displacement of mining rocks over the produced space and the deformation of rocks, as a result of which cracks are formed, which cause the connection of aquifers and surface waters with the produced space .

In the Donetsk pool, on an area of up to 15,000 km<sup>2</sup>, as the depth of mining operations increased (up to 900÷1300 m) and the ground-water level decreased under the influence of mine drainage, the regional imbalance in the "mineral skeleton of rocks - underground water" system grew. The consequence of the new hydrogeological

conditions was the development of the local-regional depressed surface of groundwater. The deepening of the zones of active water exchange from 150÷250 to 450÷550 m with the corresponding increase in the infiltration of atmospheric precipitation and the inflow of man-made surface waters from rivers, reservoirs, ponds and other water bodies into aquifers led to a change in the natural balance. As a result of the mine water exchange, the leveling of hydrochemical conditions due to the mixing of surface and underground waters and the increase in their mineralization due to the leaching of salts from rocks and pore solutions was noted. As a result of long-term drainage in the area of mining operations in the zone of pressure-free filtration (cracked soil horizon), a regional pit of depression with a depth of 40÷50 m was formed. Within the mine fields, the depth of local lower pits of depression of groundwater levels in the coal complex reaches the depth of coal working layers, that is, 800-1000 m. The volume of drained rocks is 150-200 km<sup>3</sup> [1]. Large radii of influence of depressed surfaces indicate a high level of depletion of water resources in the area of activity of mining enterprises and water intake structures [4]. In Donbas, a quasi-equilibrium system "mine water - mineral skeleton" was formed for some time in the upper zone of the geological environment. This led to a change in the natural configuration and direction of underground water flows, man-made increase in the activity of interconnection with surface waters, and a change in the structure of the sources of the formation of their resources [1].

A change in hydrogeological conditions causes the following negative changes in the geological environment and ecosystem: depletion of underground water reserves; separation of gravity water from water-resistant rocks; drainage of wells, watercourses and reservoirs; violation of the water-salt regime of the rocks of the aeration zone; deterioration of the quality of underground and surface waters.

Negative phenomena and processes accompanying the liquidation of mines and cuttings belong to one of the urgent environmental problems of the coal-mining regions. They have a multi-vector nature and are in one way or another related to the restoration of natural levels of groundwater drained during the period of exploitation. The main ones include flooding and waterlogging of the earth's surface, changes in the chemical composition of underground and surface waters, activation of the shift of the earth's surface above

workings, deterioration of the physical and mechanical properties of mining rocks, as well as the extrusion of mine gases [5].

Human intervention with the use of powerful machinery for the extraction of minerals, their transportation and processing has changed not only the landscape, but also the massif of rocks [6].

The flooding of mines in Donbas from 1996 to 2014 led to the flooding of 20 to 40% of the areas adjacent to them. Management of groundwater inflows at various stages of the post-exploitation existence of mines that are being liquidated is difficult due to the lack of study of water migration in the disturbed massif [7]. The issues related to the restoration of the surface of underground water depressions in the regions of mine closures during the restoration of the natural level of underground water, which were drained during the period of exploitation, remain practically unexplored. This situation is caused by the fact that during the period of operation of individual sites and mines in general, the possible level of underground water was not determined purposefully. At the stage of closing and liquidation of coal mines, the study of this issue is relevant, since the reliability of the hydrogeological forecast and the development of measures to mitigate environmental consequences depend on the degree of its study.

To achieve the goal, the basic hydrogeofiltration scheme of coal mine flooding was previously considered and a scheme of a possible circular cycle of surface, soil and underground water circulation under the influence of treatment works was developed.

### **Principle hydrogeofiltration scheme of coal mine flooding**

According to the environmental condition, all mining regions of Ukraine can be divided into three groups: 1 - partial, 2 - significant, 3 - critical deterioration of the environment [2].

Mining regions with a partially deteriorated state of ecological parameters of the environment include those where ecological threats to the population and the environment occur mainly in limited areas and are of a short-term nature. These are the majority of construction materials extraction areas, some chemical raw materials (due to the small depths and areas of mining operations), lignite, as well as the majority of oil and gas extraction areas.

Mining regions and areas with a significantly deteriorated state of the environment are territories where the deterioration of the eco-parameters

of the natural environment has a steady development and in some areas or objects exceeds the standards for its components (geological environment, soils, surface and underground waters, air, biodiversity) within the influence zones of individual mining enterprises and their complexes. This group may include areas of extraction of manganese ores, uranium, mercury, and partially iron ores.

Mining regions with a critical state of the environment are the oldest and spatially developed complexes of a predominantly underground method of deposit development, where environmental problems have been accumulating for decades due to the use of imperfect mining technologies with irreversible violations of the environmentally safe state of the subsoil over large areas (thousand km<sup>2</sup>) and depths (up to 1.5 km) with the simultaneous accumulation on the earth's surface of areas of its subsidence and large volumes of solid and liquid waste. In these conditions, any further development of mining operations or their termination due to the closure of mining enterprises with subsequent uncontrolled flooding can be the impetus for emergency situations and environmental disasters of various levels, in particular transboundary ones. Such areas in Ukraine include the Donetsk, partially Lviv-Volyn coal and Kryvorizka iron ore basins.

The main factors that determine the ecological state of the mining regions of Ukraine are [2]:

1 - violation of the geomechanical and hydrogeofiltration equilibrium of the rock massifs due to mining operations with the extraction of large volumes of mineral raw materials and groundwater, the formation of water-permeable zones of man-made fracturing;

2 - accumulation of waste from mining and processing complexes;

3 - violation of the hydrogeological regime of the territory.

All other factors (development of dangerous geological processes, pollution of the surface atmosphere, soil, underground and surface water, reduction of biodiversity, etc.) are mostly derived from these three [2].

The most critical state of the environment has developed in Donbas as a result of the accelerated decommissioning of mines and

the influence of factors of the armed conflict (disruption of energy supply, reduction of environmental monitoring points, etc.).

The most indicative of the complexity and complexity of the factors of the transition to the post-mining state is the mining region of Donbass (Donetsk coal basin) together with the Western Donetsk coal district, which covers an area of up to 15,000 km<sup>2</sup> within three regions - Luhansk, Donetsk, Dnipropetrovsk and forms one from the largest technological and geological systems. At present, the "Principle hydrogeofiltration scheme for the flooding of a Donbas coal mine" has been developed [2]. This scheme (Fig. 1) shows that the violation of the equilibrium geomechanical state of the subsoil, the level and hydrogeochemical regime of underground waters and the deformation of the earth's surface are the main factors in the development of potential ecological and technogenic threats of post-mining under the scheme of self-rehabilitation flooding (wet conservation).

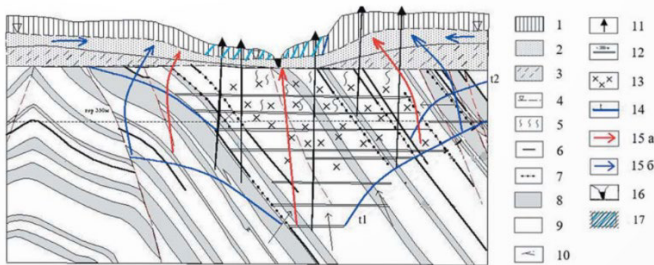


**Fig. 1.** Basic hydrogeofiltration scheme of coal mine flooding in Donbas [2]:

1 - zone of downward unsaturated filtration (aeration zone); 2 - zone of distribution of groundwater; 3 - poorly permeable rocks of the bottom of the soil aquifer; 4 - the level of the soil aquifer; 5 - zone of development of regional water-permeable fracturing in the covering part of coal-bearing rocks (area of lateral filtration); 6 - coal seams; 7 - worked coal seams; 8 - sandstones; 9 - siltstones; 10 - tectonic disturbances; 11 - surface mine structures; 12 - underground mine workings; 13 - zones of man-made fracturing; 14 - underground water level of deep horizons during mine flooding for different periods of time (*t*); 15a - directions of mineralized groundwater movement; 15b - directions of underground water movement during mine flooding (radial and lateral streams); 16 - river bed (regional groundwater drain); 17 - areas of flooding and active surface subsidence

The schematic diagram of the movement of surface, soil and underground water (Fig. 1) made it possible to develop on its basis the movement of water flows that occur directly under the influence

of treatment works during coal mining and after its termination. This allows us to move from a qualitative assessment of the water exchange processes taking place to the quantitative parameters of the shift of artificial rocks and the conditions for the formation of mold on the earth's surface.

### **Groundwater level change during treatment works and after their completion and flooding of mining works**

Over half a century, a significant amount of experimental material has been accumulated on the shear parameters of rocks forged by treatment works and the conditions for the formation of shear molds on the Earth's surface [8-17]. These and some other information were summarized, which made it possible to propose, for various mining technical and mining-geological conditions, empirical dependences for determining the parameters of the displacement processes of artificial rocks and the earth's surface for engineering calculations [18]. In particular, it is possible to determine the dimensions of the workings  $LH$  at which the shift of the earth's surface begins and its maximum subsidence occurs  $\eta_m$ . In addition, for various mining and geological conditions, the angles of total displacements  $\psi$  and limit angles  $\delta$  are known. Knowing these parameters allows one to determine [18] the dimensions of the zone of forged rocks with a break in their continuity (I) and the zone of parallel subsidence of rock layers (II) with the possible formation of horizontal delamination cracks along the layering (Fig. 2).

The following circumstances were taken into account during the development of the principle scheme for changes in the level of groundwater during clean-up operations and after the flooding of mine workings:

- the water pumped out of the mine workings during mine operation contains almost 50% of surface water [2]. The main amount of surface and ground water enters the mine workings from the zones of influence of the mine workings and to a large extent under the influence of cleaning works;
- volumes of drained rocks under the influence of cleaning works are several times larger than the sizes of the zones that fall into the zone of their possible landslide. Taking into account the usually insignificant size of coal seams between the boundaries of mine

fields (20÷100 m), it can be argued that when mines are flooded in one region, in almost all cases, a hydraulic connection will be observed between mining workings and drained rocks in the zones of influence of cleaning workings individual mines of the region;

- the depressed surface of groundwater (the free surface of pressure-free or piezometric surface of groundwater) decreases at the point of its exit to the surface of the earth or water pumping. For drainage and water intake wells, the radius of influence of the depressed surface is usually hundreds of meters, and for mines and quarries - several kilometers (sometimes several tens of km). Large radii of influence of the depressed surface indicate a high level of depletion of water resources in the area of activity of mining enterprises [4].

Based on the above circumstances, for a separate mine during its operation, the lower part of the depressed surface of groundwater (8) will be at the level of the sump of the shaft or the water surface in the mine reservoir (Fig. 2).

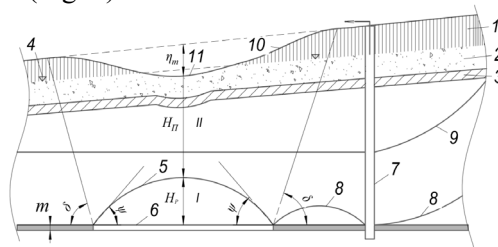


**Fig. 2.** Schematic diagram of changes in the level of underground water during the cleaning works and after their completion and flooding of the works: 1 - zone of downward unsaturated filtration (aeration zone); 2 - zone of distribution of groundwater; 3 - poorly permeable rocks of the bottom of the soil aquifer; 4 - the level of the soil aquifer; 5 - boundary of the zone of forged rocks with a break in their integrity; 6 - layer being developed; 7 - a vertical trunk through which water is pumped during mine operation; 8 - the level (piezometric surface) of underground water during the period of operation of the mine; 9 - groundwater level (piezometric surface) in different periods of flooding ( $t$ ); 10 - displacement trough on the earth's surface; 11 - areas of flooding of the displacement trough in the zone of maximum ( ) displacement of the earth's surface;  $m$  - capacity of the developed layer; - angles of complete shifts of forged rocks;  $\delta$  - limit angles; I - zone of rocks with a break in their integrity; II - a zone of parallel subsidence of rock layers with possible stratification

When water pumping is stopped (flooding of the mine), the level of water in the shaft will rise when it comes from the zones of



directly forged rocks, as well as from zones that were not subject to displacement during cleaning operations, but were previously drained. The current level of water in the shaft characterizes the degree of flooding of fake rocks by the liquidated mine. It determines the position of the lower part of the depressed surface (9), which in configuration is close to the horizontal surface. During the period of incomplete flooding of the mine, the water levels in different parts of the mine field may differ slightly from each other due to the different composition of the coal seam.

The final flooding of the mine must be considered taking into account the position of the depressed surface in the neighboring mine fields. Depending on the ratio of the position of the depressed surfaces in the forged rocks of the neighboring mines and the degree of their flooding, the possibility of flooding the earth's surface of some part of the mine (11) will depend to a large extent.

Monitoring the position of the water surface in the shafts of mines that are being closed, taking into account the peculiarities of the formation of the depressed surface of groundwater in the region as a whole and the maximum subsidence of the earth's surface, allows to make a geological forecast of the environmental consequences of the operation and closure of coal mines.

### **Methods of determining the period of restoration of natural water levels**

The methodology for a separate mine was developed based on the results of monitoring the water surface level in the shafts of the May Day group of coal mines of the Luhansk region as of November 1, 2017.

According to data [19], it is known that shaft No. 1 of the "Pervomaiska" mine was flooded to the mark -156 m. The sump of this shaft is located at the mark -602 m. The shaft was flooded at 446 meters (602-156). The flooding period from September 2015 to November 1, 2017 was 769 days. The average rate of water level rise in the trunk was 0.58 m/day (446:769). In this period, the water inflow occurred only from the zones of influence of the Pervomaiska mine's cleaning workings. This was caused by the lack of hydraulic connection with other mines during this period. If we conditionally assume that the hydraulic connection with the workings of other mines will continue to be absent, then the rate of raising the level in

the shaft will decrease proportionally as the area - the depressed surface - increases. The area of the depressed surface before the outfall was stopped was equal to the area of the treatment works on the lower horizon (-602 m). The area of drained rocks near the earth's surface is approximately 3-4 times greater than the area of the treatment works (Fig. 2). Therefore, the area of the depressed surface will also be 3-4 times greater than the area of the cleaning products. With a constant influx of underground water entering the mine from various sources and an increasing depression surface, the rate of rise of the water level in the shaft will decrease. Such a decrease in speed is inversely proportional to the areas of depressed surfaces at the beginning of flooding and after the complete end of this process. In this case, the rate of water level rise depends on the ratio of the areas of depressed surfaces

$$\frac{S_1}{S_2} = \frac{V_1}{V_2}, \quad (1)$$

where  $S_1$  is the area of treatment works on the lower horizon;  
 $S_2$  - the area of the depressed surface at the time of complete flooding of the mine;

$V_1, V_2$  are the rates of water level rise in the trunk, respectively, for areas  $S_1$  and  $S_2$ .

It follows from equation (1) that

$$V_2 = \frac{S_1 \times V_1}{S_2}. \quad (2)$$

If we take the final depressed surface ( $S_2$ ) by analogy with its shape around the water pumping points close to the circle, then its area will be equal to

$$S_2 = \frac{\pi R_2^2}{4}, \quad (3)$$

$$S_1 = \frac{\pi R_1^2}{4}. \quad (4)$$

With the approximate ratio  $R_2 \approx 4R_1$ , equation (2) can be reduced to the form

$$V_2 = \frac{V_1}{16}. \quad (5)$$

In this case, before the restoration of the natural groundwater level, the average rate of water rise in the trunk was according to equation (5)  $V_2 = V_1/16 = 0.58/16 = 0.036$  m(day)

With this average speed, the water level in the shaft should rise in the absence of hydraulic communication with other mines. According to the absolute marks (-156 and 162 m), the length of the flooded part of the trunk after November 1, 2017, is 318 m. The duration of flooding of this part ( $t_2$ ) at the average rate of rise of the water level in the trunk  $((0.200 + 0.036)/2 = 0.118$  m/day) will be  $t_2 = 318/0.118 = 2695$  days or 7.4 years. The total duration of flooding up to the -156 m mark,  $t_0 = 7.4 + 2.1 = 9.5$  years.

Such a technique is valid only under the condition of complete absence of hydraulic connection with productions of other mines, which does not correspond to reality.

A completely different technique is needed to predict the duration of recovery of the natural water level after the exploitation and flooding of a group of mines in a region that are hydraulically interconnected. Let's consider this technique using the example of the initial position of the depression surface for the primordial group of mines as of November 1, 2017.

The location of the depressed surface in the region of the closing mines and its maintenance at this level is ensured by pumping water through shaft № 3 of the "Zolote" mine. The total depth of this shaft according to the markings (-707.9 and +157.1) is 865 m. If you stop pumping water through shaft № 3, then the inflow of water in it to the level of -156.0 m will occur faster compared to the inflow into the shaft № 1 of the "Pervomaiska" mine. This will be caused by an additional water inflow of 1060 m<sup>3</sup>/h. from the side of already flooded mines [19]. Based on the ratio of the total inflow to shaft № 3 (1,500 m<sup>3</sup>/h) and from previously flooded mines (1,060 m<sup>3</sup>/h), the average speed of its flooding will exceed the increase in the water level in shaft № 1 of the Pervomaiska mine. In quantitative terms, the average speed of flooding of trunk № 3 to the -156 m mark will be

$$V_1 = 0,58 \times \frac{1500}{1060} = 0,82 \text{ m/day}$$

The depth of the flooded part of shaft № 3 to the -156 m mark is:

$$H_1 = 707.9 - 156.0 = 551.9 \text{ m.}$$

Time of flooding of this part of the trunk:

$$t_1 = 551.9 / 0.82 = 673 \text{ days or 1.8 years.}$$

The depth of the unflooded part of the trunk № 3:

$$H_2 = 865.0 - 551.9 = 313.1 \text{ m.}$$

If we take the shape of depression surfaces at the time of restoration of the underground water level for the "Zolote" mine and the entire region as close to circles, then the ratio of their radii, based on Fig. 3, is approximately 1:6.9 (Fig. 3).

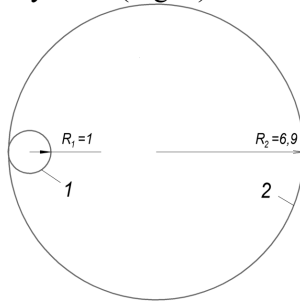


**Fig. 3.** The ratio between the areas and radii of depression surfaces at the time of the end of mine flooding: 1, 2 - circles of depressed surfaces, respectively, for the "Zolote" mine and the entire region;  $R_1$ ,  $R_2$  are the radii of depression surfaces, respectively, for the "Zolote" mine and the entire region

If  $R_1=1$  is accepted, then  $R_2=6.9$  and  $S_1 \cdot V_1 = S_2 \cdot V_2$ , and  $V_2 = V_1 / 6.9^2 = 0.82 / 47.61 = 0.017 \text{ m}(\text{day})$

The  $V_2$  flooding rate remains approximately constant for all mines in the region, as  $S_2$  varies little. The time for flooding the remaining part (313.1 m) of trunk № 3 will be

$$t_2 = 313.1 / 0.017 = 18418 \text{ days or 50.5 years.}$$

The total duration of restoration of the natural level of underground water in the region after the cessation of water pumping through shaft № 3 of the "Zolote" mine will be

$$t_0 = t_1 + t_2 = 1.8 + 50.5 = 52.3 \text{ years.}$$

Thus, the forecast for the restoration period of the natural water level in the regions of Donbas is long-term, as it can last more than fifty years.

The lack of smoothness of curved depression surfaces for the mines of the Central District of Donbass is associated with mining-geological conditions (steeply falling layers) and low permeability of rocks in the direction perpendicular to their layering. This circumstance causes an increase in the duration of the leveling of the curve of the depression surface, and therefore will lead to an even longer period of restoration of the natural level of underground water in case of complete flooding of the mines of this region. The duration of the process for mines working steeply dipping layers can significantly exceed the period of restoration of the natural water level for mines with gently lying layers.

It should be noted the possible catastrophic environmental consequences in the event of stopping the pumping of groundwater through the shafts of the "Yuny Komunar" coal mine and the 2-bis mine from cinnabar extraction. In this case, the threat of duration of negative environmental consequences will increase for several tens of years.

### **Conclusions**

On the basis of the conducted research, the peculiarities of the duration of recovery of the groundwater level during the flooding of coal mines in the regions of Donbas have been determined. They are as follows:

1. The duration of restoration of the underground water level during the flooding of a separate mine, which is not hydraulically connected with other enterprises, is about 10 years.

2. Taking into account the insignificant coal targets of coal between the boundaries of mine fields, practically all mines of each region of Donbas are hydraulically interconnected due to the saturation of drained rocks.

3. The duration of the natural recovery of the underground water level in the regions of the closure of mines in the case of gently lying layers is not less than fifty years. This period is significantly increased for the region of mines that developed steeply falling layers, and is caused by the hydrogeological features of the restoration of the depressed surface of groundwater to the natural level.

### *References*

1. Slyadnev V.A., Yakovlev E.A., Yurkova N.A. Mine waters as a factor of technogenic risk of changes in the state of the geological environment. Coal of Ukraine. 2007. № 3. P. 43-46.

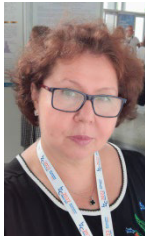
2. **Rudko G.I., Yakovlev E.O.** Post-mining of mining regions of Ukraine as a new direction of ecologically safe use of mineral resources. *Mineral resources of Ukraine*. 2020. № 3. P. 37-44.
3. Mining encyclopedia. Volume 1. Aa - Lava - Geosystem. Moscow: Publishing House "Soviet Encyclopedia". 1984. 560 p.
4. Mining encyclopedia. Volume 2. Geosphere-Kenai. Moscow: Publishing House "Soviet Encyclopedia". 1986. 575p.
5. **Zaboryn M.S., Bohun L.D., Voevoda B.I.** Geodynamics and its influence on restoration of hydrogeological conditions within closed mines. *Coal of Ukraine*. 2007. № 2. P. 31-33.
6. **Gontarevsky V.P., Kuleshov V.M., Kush O.A., Maltsev B.K.** Some aspects of the ecological and hydraulic situation in the mine closure areas. *Coal of Ukraine*. 2003. No. 12. P. 24-27.
7. **Fomin V.O.** Forecasting changes in the inflow of groundwater into a liquidated mine. *Coal of Ukraine*. 2015. № 5. P. 20-24.
8. Rock movement during underground mining of coal and shale deposits / **A.G. Akimov** et al. Moscow: Nedra, 1970. 224 p.
9. **Iofis M. A., Shmelyov A. I.** Engineering geomechanics at underground developments. Moscow: Nedra, 1985. 248 p.
10. **Borzykh A.F., Horovoy E.P.** The influence of the width of the developed space on the activation of the movement of the coal-bearing massif. *Coal of Ukraine*. 1999. № 9. P. 26-30.
11. **V. G. Larchenko**, Stages of deformation and displacement zones of modified rock thickness. *Herald of MANEB*. 2001. № 1 (37). P. 127–130.
12. **Larchenko V. G.** Influence of underground mining of coal seams on the state of the earth's surface. *Herald of MANEB*. 1998. № 4 (12). P. 39–41.
13. **Kulibaba, S.B., Rozhko, M.D., and Khokhlov, B.V.** The nature of the development of the process of movement of the earth's surface in time over a moving cleaning wall. *Scientific works of the UkrNDMI of the National Academy of Sciences of Ukraine*. 2010. № 7. P. 40–54.
14. **Havrylenko Y.N.** Prediction of displacement of the Earth's surface in time. *Coal of Ukraine*. 2011. № 6. P. 45-49.
15. **Nazarenko V.A., Yoshchenko N.V.** Patterns of development of the maximum subsidence and surface slopes in the mulde. Dnipropetrovsk: NSU. 2011. 91 p.
16. **Averin G.A., Kiryazev N.N., Dotsenko O.G.** The influence of stratification on the subsidence of the earth's surface. *Coal of Ukraine*. 2010. № 10. P. 34-35.
17. **Babenko E. V.** Setting up a model for modeling seismic events of man-made nature. *Problems of mountain pressure, DonNTU*. 2009. №17. P. 67–93.
18. **Dubovik A. I., Filatiev M. V., Filatyeva E. N.** Engineering geomechanics when mining coal seams. Lysychansk: DonHTU, 2017. 250 p.
19. **Shcherbak V.V., Arsenyuk S.Yu.** Analysis of threats and environmental risks arising from damage to mining enterprises in the zone of local military conflict in the East of Ukraine. *Collection of scientific papers of the Donbas State Technical University*. 2018. Issue 1 (47). P. 40-46.

## **STORAGES OF INDUSTRIAL WASTE ARE DANGER AND SECONDARY RAW MATERIALS SOURCES: PATHWAYS TO USE IN THE CIRCULAR ECONOMY**



**Viktoriya MOKHONKO**

candidate of geological sciences, associate professor,  
Volodymyr Dahl East Ukrainian National University,  
Ukraine



**Olena KORCHUGANOVA**

candidate of technical sciences, associate professor,  
Volodymyr Dahl East Ukrainian National University,  
Ukraine

### **Abstract**

The work highlights the dangers caused by industrial waste that is stored for a long time in repositories. The largest waste storage site of the chemical industry in the Luhansk region is described in detail.

More than 100 types of waste are stored at the landfill. PJSC “Severodonetsky Azot” is considered the owner of the landfill, but nearby are the waste storage facilities of other largest enterprises of the region: “Rubizhansky Krasytel”, Scientific and Industrial Association “Zarya”, Lysychansk Plant of Rubber and Technical Products, and Scientific and Industrial Association “Skloplastik”.

The impact of landfill waste on the environment is determined not only by the duration of waste storage and the technical imperfection of the repository but also by the geological structure of the location region. The most dangerous impact of storage is on the state of water bodies in the region and on underground sources of drinking water supply. This fact is evidenced by long-term observations of water quality in water supply sources given in the work.

Ways of processing certain types of waste contained in the landfill are proposed. The general characteristics of solid industrial waste processing methods are given, a description of the possible utilization of certain types of industrial waste into marketable products is given.

### **Introduction**

The war in Ukraine has been going on for a long time, but it will end and the occupied territories will have to be restored. Resource-intensive and energy-intensive industries play a key role in the for-

mation of Ukraine's GDP, so the priorities of state policy on the path to sustainable development should be the optimization of the use of natural resources and minimization of the negative impact on the environment by transitioning to a green economy model.

The National Waste Management Strategy in Ukraine until 2030 refers to the waste problem as a large-scale problem caused by the dominance of multi-waste technologies in the national economy, as well as the lack of effective waste management. In particular, among the main trends associated with ineffective waste management in Ukraine are the following:

1 - significant amounts of waste generation and accumulation in both the industrial and household sectors;

2 - focus on landfill disposal of waste;

3- placement of waste in landfills and/or natural landfills, most of which do not meet the requirements of environmental safety.

The territory of the Luhansk region has been characterized by a tense ecological situation for quite some time. The situation is exacerbated, first of all, by the difficult socio-political situation, namely, the conduct of the antiterrorist operation in the territory of the Luhansk region, and then the war.

In 2017, the OSCE issued a technical report on the impact of military operations on the surrounding natural environment in the East of Ukraine. Among the most dangerous factors that worsen the ecological condition of the territories under the influence of military actions were the following:

- intentional or unintentional damage to production facilities;

- flooding of Donbas mines;

- disruption of industrial enterprises;

- violation of regular activities of water supply enterprises;

- fires in natural and agricultural landscapes;

- damage to nature conservation areas.

Since 2022, the influence of these factors has increased significantly, the ecological situation is becoming worse. To a large extent, the deterioration of the ecological situation is associated with another dangerous factor, namely, it's the accumulation of a significant amount of industrial waste in storage facilities of various types, which leads to a sharp deterioration in the quality of drinking groundwater, increased pollution processes in the areas where stor-



age facilities are located, as well as to a reduction in the resource of the geological space in terms of long-term unsuitability of disturbed lands for most types of economic use.

Potentially dangerous facilities include industrial waste storage located in Luhansk and Donetsk regions. According to the UN report, the amount of accumulated industrial waste in Ukraine is one of the largest in the world. According to the results of the OSCE Report on the state of storage facilities in Donbas, there are 200 storage facilities containing 939 million tons of industrial waste in the territory of Donetsk and Luhansk regions alone.

Repositories of industrial waste are territorially close to industrially developed and mining regions, with a high level of technogenic influence on the geological environment. A classic example of such a region is the so-called Lysychansk-Rubizhne-Severodonetsk triangle. The fact that the district has been in the area of active hostilities since February 24, 2022, and is now in the occupied territory, only complicates the environmental situation.

Fig. 1 shows the layout of industry enterprises.

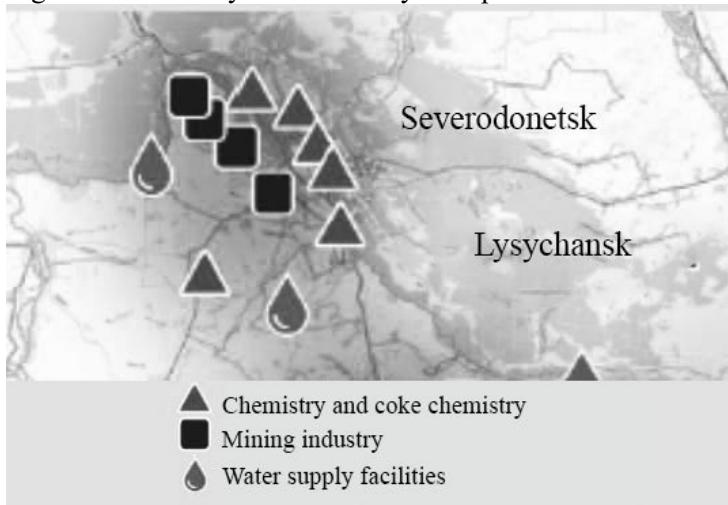


**Fig. 1.** Scheme of location of industry enterprises in the region



Fig. 2. Map of the location of waste storage facilities in Donbas

### **The largest storage of chemical industry waste in the Luhansk region: Description**

Near the village of Vovchoyarivka (formerly Fugarivka) of the Popasnya district, at a distance of 0.43 km from it, on the site of the former Loskutivka sand pit, one of the largest landfills for industrial waste is located, owned by PJSC “Severodonetsk Azot”. The landfill occupies an area of 6.52 hectares and was put into operation in 1969. Next to the landfill site, other industrial enterprises of the region, for example, LLC “NVP Zarya” and LLC “NVO “Skloplastik” etc., placed their waste. It also stores the waste of already defunct enterprises namely, they are LLC “Rubizhanskyi Krasitel”, Lysychansk production of rubber products, etc. Water intake facilities are located 1 km from the landfill. It’s water supply was carried out from the Berestova River through special catchments (water intake facilities), in the southern direction from the landfill.



**Fig. 3.** The industrial site of the landfill

Designation of storage units of the enterprises: 1 -PJSC "Severodonetsk Azot", 2 - Lysychansk production of rubber products, 3 and 4 - LLC "Rubizhansky Krasitel", 5 - NPO "Zorya", 6 - NPO "Severodonetsk Skloplastik"

Information on the accumulators of three enterprises located within the boundaries of the landfill - PJSC "Severodonetsk Azot", LLC "Rubizhansky Krasitel" and LLC "NVO Zorya" according to the data of the Register of waste disposal sites of the Luhansk region is provided in table 1. (*Register of waste generation, treatment and disposal facilities of Luhansk region (as amended in 2017)*, 2017).

The total amount of waste accumulated from the activities of these enterprises is 375,268,749 tons.

The list of waste to be disposed of at the landfill includes 139 items of industrial waste, most of which belong to the hazardous type, including spent catalysts for the production of ammonia, nitric and acetic acid, spent ionic resins, activated carbon, carbon black from the production of acetylene, sludges of various industries, that formed in the process of dissolution and filtration, waste insulating materials (asbestos, rubber), thermal insulation waste.

Table 1

The main characteristics of storage units located within the landfill (*Zvit pro vikonannya robot po ob'ektu: «Provedennya robot z monitoringu pidzemnih vod na teritoriyi oblasti., 2019*)

№	The Characteristic	Storage of “Severodonetsk Azot”	Storage of “Rubizhansky Krasitel”	Storage of “NPO Zorya”
1	Year of commissioning	1968 <sup>45</sup>	1969	1982 reconstruction in 1998
2	The actual period of operation as of 2020	52 years	51 years	38 years
3	Estimated useful life (as of 2020)	21 years	10 years	15 years
4	The area of the object according to the passport	6.52 hectares (project area is 11.5 hectares)	10,8103 hectares	10,3674 hectares
5	Volume of removed waste as of 2020	161 050,638 t (146409,671 m <sup>3</sup> )	143 486,82 t (119 572,35 m <sup>3</sup> )	70 731,291 t
6	Volume of removed waste for the previous year 2019	0	0	1 387,560 t
7	Project volume of waste removal	228 800 t (208 000 m <sup>3</sup> )	- 325 300 m <sup>3</sup>	- 160 000 m <sup>3</sup>
8	Part of storage volume filling (as of 2020)	70%	37%	47 %
9	The waste, that stored	192 appellations I-IV classes of danger*	149 appellations I-IV classes of danger*	33 appellations I-IV classes of danger*
10	Aggregate state of waste	solide	solid, sludge/ spread like	solid, sludge/ spread like
11	Gas evaporation	absent	Aniline nitroproducts phenol	nitrogen oxides, sulfuric anhydride, sulfuric acid

\* According to the Procedure for the Classification of Harmful Substances established in GOST 12.1.007-76.

According to Art. 7 of the recently adopted Law of Ukraine "On Waste Management" (*Law of Ukraine, 2023*) waste is divided into two classes: 1) hazardous waste; 2) harmless waste.

The term "hazardous waste" is defined by Art. 1 of the Law: hazardous waste - waste that has one or more properties that make it dangerous, specified in the List of properties that make waste dangerous (explosiveness, oxidizing capacity, flammability, irritation, selective toxicity for certain target organs, acute toxicity) (*Law of Ukraine, 2023*).

It should be noted that the Procedure for the classification of harmful substances was established in GOST 12.1.007-76, the validity of which was terminated in Ukraine on 01.01.2019. According to this Procedure, according to the degree of impact on the human body, harmful substances were divided into four classes of danger: 1st - substances extremely dangerous; 2nd – highly dangerous substances; 3rd – moderately dangerous substances;

4th - low-hazard substances, the Standard applied to harmful substances contained in raw materials, products, semi-products and production waste, and established general safety requirements for their production, use and storage. According to GOST 12.1.007-76, waste of the first class of danger was considered the most harmful and was characterized by the maximum degree of environmental pollution. However, no regulatory document has been developed to replace this Standard. Therefore, this standard can continue to be used as an instruction, if it is not intended to make reference to it in the relevant field of activity (according to the Explanation of the Ministry of Economic Development and Trade of Ukraine on the application of standards).

**Geological conditions of storage location.** According to the geomorphological zoning, the waste storage of the "Severodonetsk Azot" is confined to the northern slope of the Main Waterparting of Donetsk Ridge.

The Donetsk Ridge is a geomorphological region bounded in the north by the Prydonetska terrace plain (the border runs along the right high bank of the Siversky Dinets), in the south by the Azov Upland. It has a complex and quite diverse relief, which is characterized by the presence of a dense river network. Watershed spaces are narrow, and elongated in the meridional direction. The depth of the ero-

sion cutting here is 100 m. The density of the beam network is 0.5-1.0 kilometers per square kilometer.

The relief of the Donetsk highlands is determined by the peculiarities of the geological history of its development, geological structure, and recent tectonic movements, which played a major role in the formation of the relief. The processes of weathering, denudation, and accumulation in the later geological period gave the relief of the highlands its modern features.

The Donetsk Upland is characterized by a close connection of the relief with the geological structure. Cleavage on significant areas of the day surface of intensely dislocated deposits of the Lower and Middle Carboniferous, represented by alternating rocks (limestones, sandstones), caused the development of a peculiar Donetsk type of relief, the so-called maned. (*Zvit pro vikonannya robit po ob'ektu: «Provedennya robit z monitoringu pidzemnih vod na teritoriyi oblasti.*, 2019).

From a geostructural point of view, the territory of the landfill site belongs to the northern zone of fine folds of the Donetsk folded structure, which has a complex multiphase structure because the deforming forces here were 1.6 times greater than those of the entire Donetsk region.

A characteristic feature of the zone is the unidirectional extension of the folds and the significant development of regional thrusts that have a general extension with folded structures. The main ones are Severodonetsk, Maryinsky, Almazny, Illichivsky. Stratigraphic amplitudes of oversteps decrease with depth.

The rocks that make up the site of the landfill form a brachianticline uplift cut in the northeast direction by the Maryinsky thrust. In the upper part of the elevation, deposits of the Horlivsky Carboniferous measures ( $C_2^7$ ) are exposed, which is represented by intercalation of limestones, siltstones, and argillites, with interlayers of sandstones and coal. On the southern and eastern slopes of the brachyantocline, there are significant outcrops on the  $M_5$  limestone surface. In the quarry, where it was developed, there is a drive of JSC "Krasitel", the active filling of the first map which began in 1975-1976.

Deposits of the Horlivsky set have dip angles varying from 25-30° to 75° or more in some areas.

Rocks of the Horlivska set are overlapped by deposited of the Carboniferous Isayevska set ( $C_3^1$ ), which are preserved only at the base of the brachianticline and can be traced on the left bank of the Berestova river, west of the village of Fugarivka. This is a stratum of mudstones and siltstones with thin layers of sandstones and limestones ( $I_1-I_5$ ).

To the north of the Maryiv thrust, coal deposits are overlain by rocks of Mesozoic and Cenozoic age, which fill the core of the synclinal fold.

Near the northeastern outskirts of the village of Vovchoyarivka, on the right bank of the Berestova River, in the upper part of the geological section, there are deposits of the Santonian stage of the Upper Cretaceous  $K_{2S}$ , represented by micaceous marls and white chalk-like marls. The thickness of the Santonian layer is about 80 m. In the eastern direction, they overlap with Paleogene deposits. These are hard clays with layers of marl. Quaternary deposits are found in the form of scree and deluvium on the slopes. Modern diluvial deposits with a thickness of 2-3 m are close to the foot of the gentle slopes of the beams and are represented by loess-like loams with lenses of rubble of native rocks.

To the north of the training ground is the Maryinsky thrust. The thrust amplitude is almost 1200 m, the dip is southwest at an angle of  $38-50^\circ$ . It should be noted that the entire described dome structure is torn by numerous resets and thrusts in both sublatitudinal and submeridional directions.

The hydrogeological conditions of the landfill site are characterized by the presence in the upper cracked zone of the carbon weathering crust of the aquifer complex with a thickness of 15 to 20 m (Fig. 4). The average thickness of the aquifer is 17 m. The active porosity of water-bearing rocks is 0.03-0.031. Pressurized and non-pressurized water. Flow rates of wells are from 1 to 20 l/s, springs - 0.3-0.5 l/s. Groundwater is fed by precipitation. Drainage of the aquifer is carried out in streams and rivers, as well as in mining operations. Their mineralization ranges from 0.3 to 3.6 g/dm<sup>3</sup>. The class of water in natural conditions relates mainly to calcium bicarbonate. The level and hydrochemical regime of the aquifer complex is sub-

ject to seasonal changes. The amplitude of level fluctuations reaches 5-6 m.

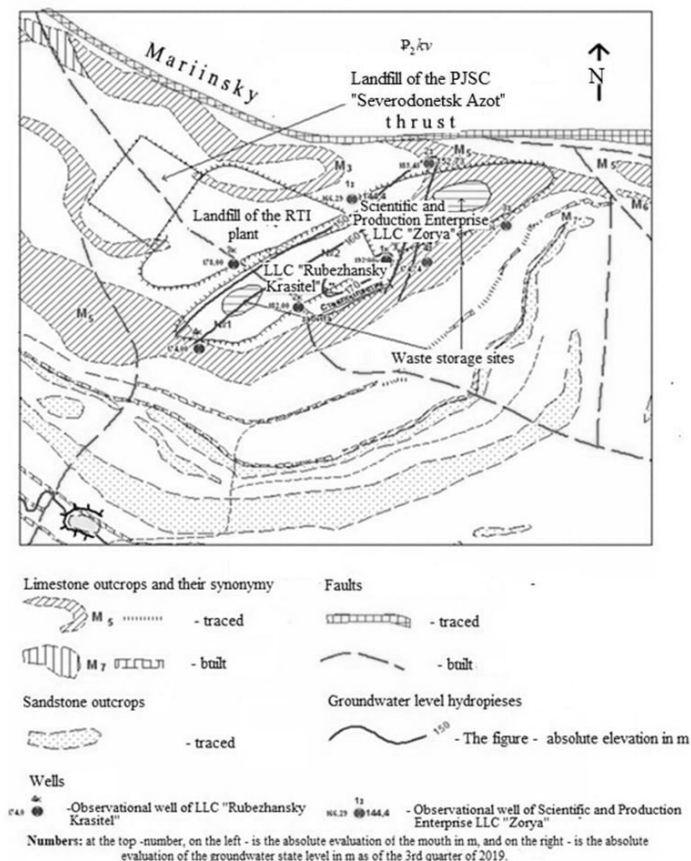


**Fig. 4.** Schematic hydrogeological map of the industrial landfill area in the village of Fugarivka

Groundwater of the aquifer complex belongs to the category of unprotected, that is, vulnerable to pollution.

In the area of the industrial waste landfill of PJSC "Severodonetsk Azot" at a distance of 0.44 km from the landfill, the Berestova River flows, which is a tributary of the White River and flows into Sivversky Donets together with it. It originates from sources that have an outlet to the south of the landfill and flows throughout the contami-



nation zone (*Zvit pro vikonannya robot po ob'ektu: «Provedennya robot z monitoringu pidzemnih vod na teritoriyi oblasti.»*, 2019).

**Impact of storage on the environment.** Among the environmental hazard factors associated with the features of the geological environment of the landfill site, it is possible to note its location in the zone of major tectonic disturbances, the development of dangerous geological processes as a result, as well as the presence of conditionally unprotected underground aquifers.

It should be noted that water supply to the population and enterprises of the Luhansk region is carried out mainly from underground sources. Currently, only 20-25% of the total amount of groundwater extracted for the economic and drinking needs of the region meets the standard requirements (*Sanitarni pravyla i normy*, 2010). There is a shortage of potable water in the region, which leads to the need to use substandard groundwater, especially in the north of the region.

The quality of groundwater in the territory of Luhansk region is very different due to many objective reasons (formation conditions, operation of large water intakes, man-made loading, influence of pollution sources, etc.). The main reserves of underground water used for drinking water supply are confined to the Upper Cretaceous deposits and are located on the left bank of the Siversky Donets River. Groundwater on the right bank of the river, in the territory controlled by Ukraine, is rarely used for centralized drinking water supply due to substandard quality and low productivity of aquifers. The best quality in this territory is noted for underground water confined to the carbon weathering crust zone and distributed on the northern and southern wings of the Main Syncline of Donbass. They are used as a source of local water supply. It is in the area where they lie that an industrial waste landfill is located.

Long-term operation (38-52 years) led to the loss of waterproofing properties of landfill structures, and, as a result, the ingress of harmful substances into unprotected aquifers and contamination of local water supply sources - wells in the village. Vovchovarivka, which drains underground waters of beam alluvium and carbon weathering zones.

The presence of polluting components in the well water, which made it unsuitable for domestic and drinking water supply, is a consequence of the cumulative effect of the waste storage facilities of

chemical enterprises located within the boundaries of the landfill upstream of the groundwater.

Deterioration of the composition of the water in the wells of the Vovchoyarivka village was observed starting in 1974, when the water in the wells acquired an unpleasant smell and taste. Testing carried out in 1975 showed an increased content of ammonium in the amount of  $115 \text{ mg/dm}^3$ . In a well located on the eastern outskirts of the village, the content of ammonium nitrogen reached  $334.4 \text{ mg/dm}^3$ .

Until 2013, the state of pollution at the landfill was controlled by local networks of wells drilled by each enterprise in the areas affected by storage facilities. There is a network of 12 wells in the area of the Nitrogen reservoir, one of which is located along the contour of the reservoir, the other on the right-bank slope of the valley of the Berestova River, on which the village of Vovchoyarivka is located.

According to the data of departmental regime observations, the formation of the dynamic circlets of multicomponent chemical pollution of all natural environments around waste storage facilities was monitored. An important indicator of the anthropogenic impact of reservoirs on the environment is the characteristic scale of landscape-hydrodynamic and landscape-hydrochemical redistribution of pollutants between different components of the natural environment.

The results of regular observations conducted by PJSC "Azot" indicated that practically the entire coal aquifer complex, as well as the Quaternary alluvial aquifer, became contaminated in the area of influence of the Nitrogen accumulator. Groundwater was characterized by a high dry residue, which exceeded the norm by more than 9 times. The main part of mineralization consisted of sulfates (Table 2). Ammonium content above the MPC was observed in individual wells and exceeded the MPC value by almost 40 times (well 3A). As of the IV quarter. In 2013, the area of ammonium pollution was  $0.1 \text{ km}^2$ , total salt pollution was  $0.65 \text{ km}^2$ . The concentration of nitrates and nitrites during the entire observation period had a periodic character. An increase in their concentration in groundwater was observed in the period from the II quarter to the III quarter (this trend was maintained for almost all types of pollution). The area of this contamination was stable, had local distribution and amounted to  $0.02 \text{ km}^2$ . Of the microelements, lithium was constantly present in

groundwater in all monitoring wells in concentrations above the MPC, and nickel was observed in individual wells. The area of groundwater with a lithium content above the MPC was 0.5 km<sup>2</sup>, nickel - 0.03 km<sup>2</sup>.

There have been changes in the chemical composition of underground waters of the coal aquifer complex. It became more banded:

- mainly sodium chloride-sulfate magnesium and hydrogen carbonate-chloride-sulfate magnesium-sodium under the storage;
- around the storage – calcium-magnesium-sodium bicarbonate-chloride-sulfate and sodium-magnesium bicarbonate-sulfate-chloride.

The ionic chemical composition of water remained stable throughout the year.

According to the regime observations, it was established that the water quality in the Berestova River in terms of sanitary and chemical indicators also did not meet the regulatory requirements (Document 4630-88 "Sanitary rules for the protection of surface waters from pollution") in terms of sulfate content, dry residue all year round and in some months - by the content of chlorides, ammonium nitrogen, MPC (Table 2) (*Informacia o sostoyanii kachestva podzemnyih vod na promplotshadke PJSC «Severodonetsk Azot» i poligona TPO (c. Fugarovka) za IV kv. 2013, 2013*).

Table 2

Summary data of chemical analyzes of underground and surface waters in the area of the landfill site for 2013

Place of sampling (indicator)	Unit	Normative value, not more	Average value
Полігон ТПВ (грунтова вода)			
Hydrogen index	pH	not standardized	7,48
Odor at 20°C	ball	not standardized	2
Odor at 60°C	ball	not standardized	2
Color	grad.	not standardized	13,4
Transparency	cm	not standardized	29,5
Ammonia nitrogen	mg/dm <sup>3</sup>	not standardized	24,0
Nitrates	mg/dm <sup>3</sup>	not standardized	6,4
Chlorides	mg/dm <sup>3</sup>	not standardized	497
Sulphates	mg/dm <sup>3</sup>	not standardized	889
Hardness	mg-equiv/dm <sup>3</sup>	not standardized	18,2
Dry residue	mg/dm <sup>3</sup>	not standardized	2839
ChAO	mg O <sub>2</sub> /dm <sup>3</sup>	not standardized	21,0

BAO <sub>5</sub>	mg O <sub>2</sub> /dm <sup>3</sup>	not standardized	<3
Berestova River			
Hydrogen index	pH	6,5 – 8,5	7,85
Odor at 20°C	ball	not standardized	0
Odor at 60°C	ball	not standardized	0
Color	grad.	not standardized	18,4
Transparency	cm	not standardized	24,8
Ammonia nitrogen	mg/dm <sup>3</sup>	0,39	0,22
Nitrates	mg/dm <sup>3</sup>	45	5,5
Chlorides	mg/dm <sup>3</sup>	300	229,2
Sulphates	mg/dm <sup>3</sup>	100	733
Hardness	mg-equiv/dm <sup>3</sup>	not standardized	15,1
Dry residue	mg/dm <sup>3</sup>	1000	1648
ChAO	mg O <sub>2</sub> /dm <sup>3</sup>	15	15,5
BAO <sub>5</sub>	mg O <sub>2</sub> /dm <sup>3</sup>	3,0	2,2

Therefore, in the area of Vovchoyarivka village, the water in the Berestova River is not subject to any type of water use. The use of water from wells is also prohibited.

Since the beginning of the armed conflict, regular routine monitoring of monitoring wells of the departmental network of PJSC "Severodonetsk Azot" has not been carried out, which is unacceptable from the point of view of the threat posed by the storage to drinking aquifers, there is no information about the hydrochemical situation in the area of the storage.

In 2017, "East of DRGP", according to the project "Maintenance of DEC, state accounting of the use of groundwater, monitoring of resources and reserves of groundwater in the territory of Luhansk region", one-time works were carried out to survey the state of groundwater in the area of the solid industrial waste landfill of PJSC Severodonetsk association "Azot". Water samples were taken and examined from 4 wells of the departmental monitoring network: Nos. 2A, 3A, 5A, 12A, located downstream of the groundwater flow from the industrial waste landfill in the direction of the Berestova River.

The highest water mineralization and total hardness were noted in well No. 3A, the highest indicators of ammonium, nitrates, and phenol content were in well № 5A. These wells are located right next to the storage contour. In the other two wells, located downstream of the groundwater flow, the indicators of groundwater pollution are

lower, but high enough to pose a threat to local water consumers – residents of the Vovchoyarivka village.

In the area of the solid industrial waste storage facility of "NVP "Zorya" LLC, regular monitoring (quarterly) has been carried out by "Luhansk Geococenter" LLC for many years. Surveys were carried out on 2 observation wells No. 1z, 2z of the departmental regime network located around the storage.

As of the III quarter. In 2019 (according to the data of "Luhansk Geococenter" LLC), the underground water level of the coal aquifer was at a depth of 21.89-30.72 m at absolute elevations +144.4 to +152.73 m, which is 0.25-0.57 m higher compared to the same period of 2018.

According to the chemical composition, the groundwater had a dry residue of 1180-1960 mg/dm<sup>3</sup>, total hardness - 6.4-11.2 mmol/dm<sup>3</sup>, chloride concentration - 232.2-500 mg/dm<sup>3</sup>, sulfate concentration - 345-395.5 mg /dm<sup>3</sup>, ammonium concentration - 0.8 - 1.50 mg/dm<sup>3</sup>, nitrate - 11.2-46.5 mg/dm<sup>3</sup>, iron concentration - 2.0-2.9 mg/dm<sup>3</sup>. Phenols, amino nitro products are not found.

According to the chemical composition, underground waters belong to the class of sulfate-hydrocarbonate-chloride calcium-sodium and chloride-sulfate-hydrocarbonate calcium.

The highest water mineralization, total hardness, concentration of chlorides, ammonium nitrates, and iron are noted in well No. 1z, located near the western corner of the storage contour, downstream of the groundwater flow, the highest rate of sulfates is in well No. 2z.

Compared to 2018 in III quarter In 2019, there was an increase in the indicators of dry residue (2420 mg/dm<sup>3</sup> in well No. 1z), sulfates (425.3-486 mg/dm<sup>3</sup> in wells Nos. 1z, 2z), chlorides (758.3 mg/dm<sup>3</sup> in well No. 1z), and iron (5.3 mg/dm<sup>3</sup> well No. 2z). The fairly high content of ammonium (0.8-1.50 mg/dm<sup>3</sup>), iron (2.0-2.9 mg/dm<sup>3</sup>), which is direct evidence of the impact of the storage on underground water, attracts attention. A comparison of the given indicators with the normative values of DSanPiN 2.2.4-171-10 (*Sanitarni pravyla i normy*, 2010) showed an excess of such indicators as dry residue (1.3 MPC), total hardness (1.1 MPC), chlorides (1.4 MPC) and iron (2.9 MPC).

Areas of groundwater contamination by various components in the zone of influence of the industrial waste storage facility of LLC

"NVP "Zorya" were not counted (*Zvit pro vikonannya robot po ob'ektu: «Provedennya robot z monitoringu pidzemnih vod na teritoriyi oblasti.*, 2019).

According to the interviews, in 2014-2015, there were active military actions in the area of the training ground, the territories adjacent to the facility were mined, but there is no information about damage to the training ground structures as a result of projectiles.

In 2019, under the project of the OSCE Project Coordinator in Ukraine "Strengthening the Capacity for monitoring and Management of water resources in the East of Ukraine", a study of the current state of tailings storage facilities in the Donbas was conducted regarding their possible emergency impact on water bodies, the task of which was to investigate the current state of storage tanks of industrial waste, determine hazard factors and identify existing threats to the environment in probable emergency scenarios.

A comprehensive study of the storage facilities, which included a review of the natural conditions of the territory and the specifics of the location of the storage facilities of enterprises, determination of the volume and toxicity of waste, study of the current state of the facilities and analysis of the available monitoring results, made it possible to outline the following types of landfill hazards:

- fire - the presence of gaseous, liquid, and solid substances, materials or mixtures capable of sustaining combustion;
- chemical - the presence of toxic, harmful, highly effective poisonous substances, poisonous chemicals, chemical means of plant protection and mineral fertilizers;
- ecological - the possibility of an adverse effect on the environment of man-made and natural factors, as a result of which the adaptation of living systems to the usual conditions of existence is disturbed (I Nikolayeva et al., 2021).

Internal factors of ecological danger included:

- probable unsatisfactory state of structures (instability of dams, loss of waterproofing properties), associated with a long period of operation of storage tanks (38-52 years);
- the presence of hazardous substances in the composition of waste: metals, non-metals and their compounds, salts of perchloric acid and nitrous acid, organic solvents, ethers, etc.;
- gas evaporation: aniline, nitro products, phenol, nitrogen oxides,

sulfuric anhydride, sulfuric acid;

- a significant total amount of accumulated waste.

The cited results of monitoring observations and complex studies indicate that even in the absence of direct discharge of pollutants directly from the reservoirs, the anthropogenic load from their long-term operation led to a change in the state of underground and surface waters. In addition, the location of industrial waste storages of various chemical enterprises on the same site of the landfill can lead to an increase in their influence and the successive occurrence of accidents at these facilities. The location of the pumping station of the Western Filtering Station next to the landfill in the event of an accident at the landfill can lead to disruption of the water supply to the region.

Therefore, in the near future, it is necessary to develop and implement appropriate technical and management measures that will lead to the minimization of the ecological threat of the industrial waste landfill to the environment. One of these measures is the search for ways of further handling of accumulated waste: reuse and/or neutralization of waste.

**Main directions of waste processing.** The directions of waste processing are determined by the demand for waste components and the possibility of obtaining products of commercial quality from them. In the case of chemical processing, a number of typical technological operations are used: dissolution, sedimentation, and filtration, which allow to separation of waste components from each other for further processing.

Approximately from the end of the 60s to the beginning of the 70s, in connection with the aggravation of the energy and raw material problems of developed foreign countries, there has been an acceleration of growth in the use of production and consumption waste. And this becomes an important task for the development of their economy. The process of growth in the volume of waste processing was determined by a number of factors: firstly, the negative impact of accumulated waste on the ecological situation in certain regions and in the world as a whole; secondly, the increase in economic interest in the processing of secondary raw materials, which is mainly due to the depletion of mineral deposits and the increase in the price of natural raw materials; thirdly, by political factors related to the

desire of states to increase independence from the import of natural raw materials.

A significant obstacle in the way of waste disposal was the slow improvement of the technique and technology of their processing. The traditional problem of waste processing is wasteability. Waste usually differs from primary raw materials in terms of chemical composition and contains other types and amounts of impurities. Therefore, in order to obtain the same products, a change in technology and a complex approach are needed - the use of not only the most valuable component, but also all the others with the aim of their as complete utilization as possible.

The most common types of hazardous waste of the 1st class of danger are:

- lead batteries are damaged or worn out;
- fluorescent lamps and waste containing mercury.

Disposal of these products, which have lost their consumer value, has long been successfully carried out in many countries of the world.

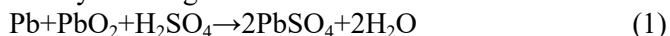
Lead is an important metal for the industrial development of the automotive industry, for storage and backup power in the field of alternative energy. The processing of lead in the developed countries of the world significantly exceeds its extraction from the sources of primary raw materials. Spent lead-acid batteries are intensively processed, their component part in recycled materials is about 85%.

The first acid batteries were proposed in 1860 by G. Plante. Until now, they are widely used due to the simplicity and stability of work. Their body was originally made of ebonite, now it is made of acid-resistant plastics. The electrolyte is an aqueous solution of sulfuric acid (density 1.28-1.30 g / cm<sup>3</sup> or 37.5 - 39 wt. %). The cathode is made of ribbed lead plates, and the anode is made of lead grids, the cells of which are filled with PbO<sub>2</sub> paste.

Spent lead paste consists of lead sulfate (~60 wt.%), as well as lead dioxide (~28 wt.%), lead oxide (~9 wt.%) and a small amount of metallic lead (~3 wt.%).

The operation of a lead-acid battery is described by the following total chemical reactions:

In case of battery discharge





In the case of charging the battery, the course of the reverse reaction is carried out.

The utilization of lead batteries is as follows:

- First, the electrolyte is drained, which is an aggressive acid solution.
- The plastic case is cut or crushed to remove the metal parts.
- Plastic is separated from metal on a special device.
- Smelting takes place for the production of secondary raw materials.

Traditional disposal of pastes can be carried out in two (Zhang et al., 2016) ways:

1 - Direct smelting, in which the lead paste was directly processed in a melting furnace at a temperature above 1000 °C to decompose and melt the lead compounds with or without desulfurization in the furnace.

2 - Desulfurization at lower temperatures followed by melting. The spent paste is treated with a desulfurizing agent such as  $\text{Na}_2\text{CO}_3$  or  $\text{NaOH}$  in aqueous solutions close to ambient temperatures. A common feature is the use of aqueous solutions of  $\text{NaOH}$  or  $\text{Na}_2\text{CO}_3$  to fix S as soluble  $\text{Na}_2\text{SO}_4$ , which can be crystallized as a commercial by-product. Insoluble  $\text{PbCO}_3$  or  $\text{Pb}(\text{OH})_2$  is collected in the form of sludge and sent to the smelter.

It is now practiced to harvest and recycle fluorescent lamps on an industrial scale for mercury separation and safe disposal (Dhawan & Tanvar, 2022). However, processing phosphor powder rich in rare earth compounds is still developing. A luminophore consisting of several rare earth minerals (Y, Eu, Ce, Tb, La) can be considered as a potential secondary raw material. The latest scientific publications indicate that research tends towards combined pyrohydrometallurgical processes as the most effective.

The phosphors in fluorescent lamps are a source of critical rare earth elements such as Y, Eu, Tb, and Ce, and almost 79% and 63% of the global consumption of Y and Eu are from phosphors, so their recycling is crucial for resource conservation (Hua et al., 2019).

The phosphor used for luminescence is up to 2 wt.% of the lighting fixture and contains 9 to 26% REE, which is significantly higher than in REE ore deposits. Currently, recycling rates in some major

lamp producing countries are 4%, Canada 7%, Japan 9%, USA 20% and South Korea 28%.

A typical technological scheme of crushing and separation of used FD components on an industrial scale is presented in fig. 5.

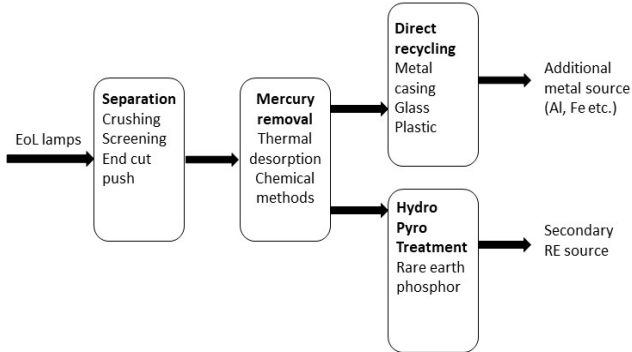


**Fig. 5** Typical technological scheme of recycling fluorescent lamps

There are two widely used FL recycling processes:

1) Method of end pushing. With this method, the end caps made of aluminum in the FL are removed or cut off, and phosphor waste on the inner walls of the glass is pushed out using a scraper, high-pressure air, or water. Metallic mercury and phosphor are captured and mercury vapor is captured by activated carbon filters. Metal caps and glass are crushed to extract metals and make glass products or new lamps. The luminophore collected by this method does not contain impurities. The disadvantage of this process is the use of manual operations and considerable processing time. On an industrial scale, the process has reached a productivity of 300 million lamps per year. Several companies have commercialized this method, namely Mercury Recovery Technology Company in Holland, WEREC, OSRAM, BISON and OSRAM (owned by Siemens).

2) Another method was implemented by companies in Germany, Switzerland, and Finland. This method involves wet crushing, in which the tubes are crushed in ethanol or 30% aqueous acetone to capture mercury vapor and prevent environmental contamination. However, many small glass particles contaminate the phosphor. Therefore, the extracted phosphor requires additional resources to remove these impurities. Around the world, companies like Eco Re-

cycling Ltd. in India, Fluorescent Lamp Recyclers Technologies Inc. in Canada, AERC Recycling Solutions, Veola Environmental Services in the US, and Lampcare in the UK have developed special crushing equipment to avoid mercury leakage (*Eco Recycling Limited Lamp Recycling*, n.d.).

One of the most important properties of waste, which determines possible successful processing, is not only the presence of valuable components in the waste but also a stable chemical composition. These requirements are met by spent catalysts, which make up a fairly large part of the waste of chemical industry enterprises. The landfill contains not only catalysts used at PJSC "Severodonetsk Azot" but also catalysts and metal-containing waste from other enterprises in the region are stored there. Spent catalysts have lost their active properties due to the processes carried out in the technological equipment. The loss of catalytic activity is a consequence of the action of temperature, pressure, and the action of so-called catalytic poisons – compounds that form a surface layer of inactive substances with the catalyst components. Examples of such poisons can be residual sulfur contained in natural gas, which enters for conversion in the production of ammonia. Also, the most common cause of the loss of catalytic activity is the formation of a carbon layer on the surface of the catalysts, which is formed from the components of the reaction mixture.

Spent catalysts are classified as a waste of hazard classes 1-3, depending on their chemical composition.

The waste contains vanadium, copper, nickel, cobalt, molybdenum, and platinum group metals.

The amount of generated waste catalysts depends on their service life and the size of the equipment. Usually, the service life (Scott, 2018) of catalysts ranges from several months to several years. The volume of the spent catalyst depends on the production capacity, type, and operating conditions of the catalyst. But for more than 50 years of operation of the industrial waste landfill, their number is already quite large. The estimated amount of waste is indicated in the regional reports of the Department of Ecology and Natural Resources and the registers created by this organization (*Register of waste generation, treatment and disposal facilities of Luhansk region (as amended in 2017)*, 2017).

Unfortunately, the open information is quite concise and does not contain all the necessary data to decide on the choice of disposal method. However, some information on the chemical composition of the waste can be obtained from the registers using the names of the processes and the catalysts used to carry out these processes.

Thus, by the information from the above-mentioned register, information on spent catalysts stored at the sites of individual enterprises was determined: Thus, spent catalysts of the hydrogenation process of natural gas in the production of ammonia are stored at the landfill, mostly aluminum-cobalt-molybdenum containing the components CoO - 2-6%, MoO<sub>3</sub> 10-16%. More precisely, unfortunately, it is impossible to find out the chemical composition, because the manufacturers of catalysts for the entire period of existence of the waste storage landfill are unknown. Vanadium-containing catalysts at sites owned by LLC "Zorya" and PJSC "Severodonetsk Azot" differ in chemical composition and content of active components. At the first enterprise, the catalysts were used for contact oxidation of sulfur (IV) oxide and contained 7-10% V<sub>2</sub>O<sub>5</sub>, at another enterprise they were used for cleaning exhaust gases from nitrogen oxides and contained 12-15% V<sub>2</sub>O<sub>5</sub>.

Silver catalysts contain 7-20% silver, depending on the process in which they were used at Zorya LLC.

Many researchers have been engaged in the processing of catalysts to extract the most expensive and valuable components, proposing mainly the hydrometallurgical method (Sittig, 1980) as a series of sequential leaching and precipitation operations, as well as the possible use of ion exchange processes and electrochemical purification.

Table 3

Components of some spent catalysts			
Spent catalyst	Source	Active Componentets	Клас небезпеки
Spent silver catalyst	Government Plant "Zorya"	Ag	4
Catalyst of sulfuric acid production AVC-10 IC-1-6	LLC "Zorya"	V2O5	4

Catalysts of manufactures of ammonia, nitric acid, acetic acid, methanol RKS-2-7H, RKS-2P, NCM-1, NCM-1C, NCM-C, GO-70, CNM-Y, RKN-3, GPC-4III, IT-305 etc.	PJSC “Severodonetsk Azot”	Co, Mo, Ni, Cu, Zn, Cr, C, Al, V	1, 2, 3, 4
---	------------------------------	--	------------

One of the limitations of the use of waste is related to the possibility of obtaining products of commercial quality from it. Thus, the processing of spent catalysts into fresh ones does not always give a positive result due to the difficulty of extracting some impurities that reduce the catalytic activity of such materials.

Obtaining nano-sized materials can help in solving such a problem. Particle size affects three main groups of properties of any material. Firstly, on structural characteristics (lattice symmetry and cell parameters), secondly, on electronic properties of oxides. Structural and electronic properties determine the third group of properties: physical and chemical.

The spent catalyst disposal scheme can be seen on the example of spent alumina-nickel catalyst (Korchuganova et al., 2020) (Fig. 6).

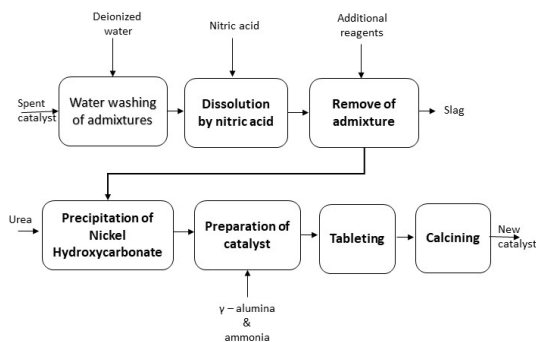


**Fig. 6.** Scheme of disposal of spent aluminum-nickel catalyst

Each stage of the production process generates a certain type of waste. Each waste product requires a specific management solution.

Processing of industrial waste is carried out using various technologies, the main of which are (Arockiam JeyaSundar et al., 2020): physico-chemical, thermal, and biotechnologies.

Physico-chemical technologies are not universal but can lead to the best result for the use of waste as secondary raw materials. By physicochemical methods, some types of industrial waste are processed into fertilizers, building materials, ceramics, etc.

Thermal technologies are used to dispose of many types of solid, soluble, liquid, and gaseous waste. The method consists in heat treatment of waste with a high-temperature coolant, which uses combustion products, a plasma stream, molten metal or oxide, and microwave heating of waste. Products of thermal decomposition undergo oxidation and other chemical interactions with the formation of non-toxic products.

Biotechnologies used in the processing of metal-containing waste and low-grade ores, such as chalcopyrite, are among the most promising waste disposal and processing technologies (Dong et al., 2020). Recently, a direction in non-ferrous metallurgy - biohydrometallurgy has been developing quite actively.

Reducing the amount of waste, we generate is a priority today. This means changing our consumption patterns, for example by choosing products that use recycled material ("Waste at Every Stage," 2002). It also means recycling – sorting, collecting, processing, and reusing materials that would otherwise be treated as waste.

Recently, various countries have been using waste as materials for artificial geochemical barriers (Perel'man, 1986):

- mining complex waste (overburden, beneficiation tailings) containing chemically active minerals;
- mixtures of chemically active or differently modified minerals;
- products and wastes of deep chemical and metallurgical processing of ores and concentrates.

There are different ways of applying geochemical barriers:

- arrangement of anti-filtration screens;
- filtration of solutions through a barrier with deposition of pollutants;

-adding a barrier substance to the solution (in natural reservoirs, tailings ponds, settling tanks, etc.).

Among the areas of use of artificial geochemical barriers, in addition to the purification of natural and wastewater from heavy metals, radioactive elements, and petroleum products, the following can be distinguished:

- extraction of valuable components from natural and man-made raw materials by physical and chemical methods;
- waterproofing of tailings and sludge storage facilities, accumulators, sedimentation tanks, etc.;
- oil consolidation in construction.

Of the natural minerals, carbonates have found the most widespread use for geochemical barriers. Examples of successful use of calcite, dolomite, and magnesite are considered in several studies (Bennett et al., 2000).

In addition to natural carbonates, there is a fairly large amount of waste containing them. An example of such waste can be the liming sludge of natural water treatment and wastewater treatment plants. Lime sludges usually contain more than 70% calcium carbonate. Quite acceptable methods are the use of sediments in the natural environment to be applied to the soil to reduce acidity (Cheng et al., 2014), or in the man-made environment to improve wastewater treatment (Hua et al., 2019). In (Hua et al., 2019), a water treatment method of reusing the upper clarified part of lime sludge to simultaneously remove COD, nitrogen, and phosphorus was investigated. The upper clarified part of the lime sludge is alkaline wastewater containing a high concentration of calcium ions, alkalinity, biodegradable chemicals, and ammonium nitrogen. Using the method in denitrification processes allows you to fully compensate for alkalinity for nitrification, as well as save the costs of phosphorous precipitators, external carbon, and alkalinity. Therefore, this method is technically and economically effective.

It is also shown that water purification can be effectively carried out with the help of carbonate-containing tripels. Carbonate cherts with a 20-30% calcite content are highly effective sorbents of heavy and non-ferrous metal ions, radionuclides Sr, and Cs (Yurmazova et al., 2016).

Various layered hydrosilicates have also found widespread use as

geochemical barrier materials.

Different types of barriers with anti-filtration and anti-migration properties are used to prevent the spread of toxic elements in natural waters and to protect the environment in areas where ground waste storage facilities are located.

The authors substantiated the following priority directions for the use of waterproofing compositions based on nepheline:

- construction, repair and operation of wells in the oil and gas industry;
- solidification of liquid waste, including those containing various toxic and radioactive substances;
- creation of anti-filtration curtains in loose and cracked rocks in quarries, dams, dams, in the roof of various gas, oil, and waste storage facilities;
- isolation of sand-gravel foundations and rock fissures from the surface for waste storage, creation of artificial reservoirs; - neutralization and dehydration of acidic effluents of chemical enterprises.

In addition to the use of chemically active rocks and minerals, it is possible to use their artificial mixtures. Thus, in the work (Chanturiya et al., 2011) a mixture of serpentine and carbonates is proposed.

Amorphous silica can also be considered as a large-tonnage by-product of the acid processing of many ores and concentrates. The use of active silica as a barrier ensures the formation of a precipitate of mainly non-ferrous hydrosilicates, for example, nickel and cobalt. Carbonate in the barrier plays the role of an environment regulator, neutralizing the sulfuric acid formed during the synthesis of hydrosilicates and ensuring a stable alkaline reaction of the solutions. This barrier is also effective in natural and wastewater treatment technologies (Labus et al., 2020).

One of the most popular areas of research is the use of waste as raw materials for building materials, such as bricks and cement.

Brick is a widely used building and construction material all over the world. It is common knowledge that the production of bricks is extremely energy-intensive and emits a significant amount of greenhouse gases. Production of 1 kg of product requires about 1.5 kWh of energy and results in emissions of about 1 kg of CO<sub>2</sub> into the atmosphere. At the same time, in many areas of the world there is already a



shortage of natural raw materials for the production of bricks (Chen et al., 2011).

Cement production accounts for about 7% of all CO<sub>2</sub> emissions (Gjorv & Sakai, 1999). Thus, the production of concrete bricks also consumes a lot of energy and emits a significant amount of CO<sub>2</sub>.

For environmental protection and sustainable development, many researchers have studied the possibility of using waste for brick production (Chou et al., 2001).

A wide range of wastes were studied, including fly ash, mine tailings, slag, construction and processing industry waste, wood sawdust, cotton waste, limestone powder, paper residues, waste oil sludge, kraft pulp residues, cigarette residues, tea waste, rice husk ash, rubber crumb and dust for cement kilns.

There are several groups of methods for producing bricks from waste:

- high-temperature (firing, etc.);
- cementation (using binding materials);
- geopolymerization.

High-temperature methods involve the use of waste to replace part or all of the clay (primary raw material) and then bricks are made in the traditional way. Thus, the use of iron ore tailings (Chen et al., 2011) and ash with clay for the manufacture of bricks has been tested. Lingling et al. (Lingling et al., 2005) investigated the production of fired bricks using fly ash to replace most of the clay. Fired bricks with a high ash content are characterized by high compressive strength, low water absorption, no cracking and high frost resistance.

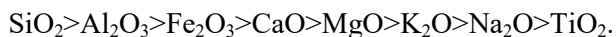
In addition to bricks, there are developments in the production of other building materials. Thus, the authors of the work (Sahu et al., 2017) developed a technology for manufacturing paving tiles from a mixture of ash and lime sludge. The optimal composition of the mixture of ash and sludge was determined. The composite turned out to be strong, without leaching of heavy metals and suitable for designing flexible pavements. A mixture of ash and water treatment sludge is also used to make bricks. The organic component is first burned from the sludge, and then mixed with ash and further processed (Minh Trang et al., 2021).

A large number of works (Lin & Lin, 2005; Pavlík et al., 2016) are devoted to the possibility of using sludge in cement production. The

authors of the work (Pavlík et al., 2016) suggest replacing part of the cement with calcined sediment, unfortunately, the results of these studies revealed that the technological properties of the waste are not good enough. The publication (Lin & Lin, 2005) gives the results of experiments on the production of eco-cements using waste, including water treatment. The waste was pre-calcined to burn out the organic component. According to the results of the research, the best quality was cement made with the addition of limestone.

Alkaline activation of aluminosilicates is a technology often called geopolymerization. It was first developed in the 1970s by Joseph Davidowitz. It involves a chemical reaction between oxides of aluminosilicates and solutions of alkaline silicates under conditions of high alkalinity. This gives amorphous or semi-crystalline polymer structures of Si-O-Al bonds. Geopolymers demonstrate good physical, chemical, and mechanical properties: among them low density, micro- and nanoporosity, low shrinkage, high mechanical strength, good thermal resistance, durability, surface hardness, and fire, and chemical resistance. Given these desirable properties, they are considered potential alternative materials for industrial applications such as construction, transportation, aerospace, mining, and metallurgical engineering (Barbosa & MacKenzie, 2003; Swanepoel & Strydom, 2002). Alkaline activation of aluminosilicate material can be described as the reaction of a liquid with a high alkaline concentration and a solid with a high proportion of reactive silicate and aluminate. Ash geopolymers harden quickly at room temperature, they are characterized by high strength. Large-scale application of such geopolymers is much more difficult, but high-performance geopolymer concretes are beginning to be commercialized (Van Deventer et al., 2012).

Coal ash, which is produced after burning coal, is a very powerful industrial and energy solid waste (Blissett & Rowson, 2012). Ash is a mixture of combustion products of inorganic and organic components of coal. It usually contains the following oxides in decreasing order of their content in the ash



Ashes of different origins are quite different from each other in terms of the content of the listed oxides. Depending on its chemical and mineralogical composition, several main directions of its use are

proposed. One of the most common is the use for cement production. There is also a direction of use called geotechnical. It covers its use as an asphalt filler, creating a road surface base, filling structures, changing soil properties (González et al., 2009). Ash is used as a soil stabilizer because of its properties. It was found that the addition of ash to soils, as a rule, reduces the tendency to absorb water into the soil. High water absorption of soils can lead to cracking of pavements, basements, driveways, pipelines and foundations. As a result of adding ash to the soil, through the pozzolanic reaction, the soil becomes more granular and contains less water (Zha et al., 2008).

The method of "disposing of waste using other waste" seems very promising. An example of such a method is coal ash.

Thanks to its chemical and mineralogical composition, ash can perform the role of a sorbent. In the paper (Panday et al., 1985), its adsorption properties in gaseous and aqueous media were studied. The use of ash mixtures with different chemical compositions for the removal of various metal wastes was recently evaluated: Cu (Alinor, 2007), Pb (Cho et al., 2005), Zn (Itskos et al., 2010), Mn, Cd, Cr, and Ni (Mohan & Gandhimathi, 2009). A recent review of the use of low-cost adsorbents for the removal of heavy metals from industrial wastewater concluded that fly ash has great potential for wastewater treatment; this potential is limited by the variability of ash chemistry and the large volumes that may be required for its effectiveness (Ahmaruzzaman, 2011).

Aksu and Yener (1999) investigated the potential for using fly ash instead of activated carbon for phenol adsorption. They reported the adsorption capacity compared to the properties of activated carbon. Flue gas desulfurization sorbents were obtained by mixing  $\text{Ca}(\text{OH})_2$  with ash (Lee et al., 2021). The results show that the desulfurization properties of the sorbents increase with the ash/ $\text{Ca}(\text{OH})_2$  ratio. This field of application promises to be a promising direction, since the process of gas formation will lie in close proximity to the generation of ash.

Considering the chemical and mineralogical composition of zeolites, there are many attempts to produce zeolites from them (Querol et al., 2002).

The next method of using waste is to extract the most valuable components from it. Ash contains 30-35% silica, 5-15% aluminum,

some titanium and other elements.

Several methods of extracting aluminum from ash have been proposed. Direct leaching with sulfuric acid of low concentration and at ambient temperatures (Matjie et al., 2005). A more effective option, according to which preliminary treatment is carried out: ash is granulated with fine coal and lime, then aluminum is leached with sulfuric acid.

Shabtai and Mukmenev (Shabtai & Mukmenev, 1996) described a new process for extracting titanium and aluminum. The authors used concentrated sulfuric acid for extraction. Extraction of titanium was carried out simultaneously with the process of biomagnetic adsorption. *Rhodococcus* bacteria were cultured and added to a suspension containing magnetic particles, resulting in the adsorption of the bacteria on the magnetic particles. As titanium falls out of solution, it is adsorbed together with magnetite on the bacteria.

Another example of the implementation of this direction is the recycling of coagulants from the sludge of water treatment plants, which are a necessary component of water treatment and wastewater treatment processes. Recycling is usually performed by acid leaching of iron or aluminum compounds and subsequent separation of the mixed solution. In the work (Petruzzelli, 2000) it is proposed to carry out separation with the help of ion-exchange resins, in this way the solutions are purified to a conditioned state. The authors of the paper (Jangkorn et al., 2011) tried to reduce the use of fresh coagulants by adding sludge to the coagulation process.

For the comprehensive utilization of ash, it is proposed to produce several products from it (Little et al., 2008): concrete, fertilizers, mesoporous silicate material/zeolite. The authors show how by placing an ash processing plant in the center of an industrial ecosystem, waste generation is limited. Sodium hydroxide, anode process waste, and limestone are used as additional raw materials.

### **Conclusions**

Therefore, waste processing can solve not only the problems of raw material sustainability but also reduce anthropogenic impact on the natural environment, and improve the condition of water bodies and the quality of drinking water.

Of course, not all waste is acceptable in terms of recyclability, it depends on several reasons and characteristics of the waste.

Yes, spent catalysts are convenient for processing, their advantages for recycling are stability of composition, limited number of components, ease of storage, and transportation. However, the stability of the composition is also a characteristic feature of some other wastes, including sludges from water treatment and wastewater treatment from metal impurities. An approximate list of components of spent catalysts is presented in the table

Accumulation of industrial waste from various chemical enterprises in one area of the landfill can lead to successive accidents at these facilities and provoke an increase in their impact, causing the so-called "domino" effect.

As a result of hostilities, it is quite likely that industrial enterprises will be disrupted and emergencies will arise. With the beginning of hostilities, the observation posts for water and air quality stopped working.

### *References*

1. **Ahmaruzzaman, M.** (2011). Industrial wastes as low-cost potential adsorbents for the treatment of wastewater laden with heavy metals. *Advances in Colloid and Interface Science*, 166(1–2), 36–59. <https://doi.org/10.1016/j.cis.2011.04.005>
2. **Alinnor, I. J.** (2007). Adsorption of heavy metal ions from aqueous solution by fly ash. *Fuel*, 86(5–6), 853–857. <https://doi.org/10.1016/j.fuel.2006.08.019>
3. **Arockiam JeyaSundar, P. G. S., Ali, A., Guo, D., & Zhang, Z.** (2020). Waste treatment approaches for environmental sustainability. In *Microorganisms for Sustainable Environment and Health* (pp. 119–135). Elsevier. <https://doi.org/10.1016/B978-0-12-819001-2.00006-1>
4. **Barbosa, V. F. F., & MacKenzie, K. J. D.** (2003). Thermal behaviour of inorganic geopolymers and composites derived from sodium polysialate. *Materials Research Bulletin*, 38(2), 319–331. [https://doi.org/10.1016/S0025-5408\(02\)01022-X](https://doi.org/10.1016/S0025-5408(02)01022-X)
5. **Bennett, P. J., Longstaffe, F. J., & Rowe, R. K.** (2000). The stability of dolomite in landfill leachate-collection systems. *Canadian Geotechnical Journal*, 37(2), 371–378. <https://doi.org/10.1139/t99-110>
6. **Blissett, R. S., & Rowson, N. A.** (2012). A review of the multi-component utilisation of coal fly ash. *Fuel*, 97, 1–23. <https://doi.org/10.1016/j.fuel.2012.03.024>
7. **Chanturiya, V., Masloboev, V., Makarov, D., Mazukhina, S., Nesterov, D., & Men'shikov, Y.** (2011). Artificial geochemical barriers for additional recovery of non-ferrous metals and reduction of ecological hazard from the mining industry waste. *Journal of Environmental Science and Health, Part A*, 46(13), 1579–1587. <https://doi.org/10.1080/10934529.2011.609435>
8. **Chen, Y., Zhang, Y., Chen, T., Zhao, Y., & Bao, S.** (2011). Preparation of eco-friendly construction bricks from hematite tailings. *Construction and Building Materials*, 25(4), 2107–2111. <https://doi.org/10.1016/j.conbuildmat.2010.11.025>

9. **Cheng, W., Roessler, J., Blaisi, N. I., & Townsend, T. G.** (2014). Effect of water treatment additives on lime softening residual trace chemical composition – Implications for disposal and reuse. *Journal of Environmental Management*, 145, 240–248. <https://doi.org/10.1016/j.jenvman.2014.07.004>
10. **Cho, H., Oh, D., & Kim, K.** (2005). A study on removal characteristics of heavy metals from aqueous solution by fly ash. *Journal of Hazardous Materials*, 127(1–3), 187–195. <https://doi.org/10.1016/j.jhazmat.2005.07.019>
11. **Chou, M.-In. M., Patel, V., Laird, C. J., & Ho, K. K.** (2001). Chemical and Engineering Properties of Fired Bricks Containing 50 Weight Percent of Class F Fly Ash. *Energy Sources*, 23(7), 665–673. <https://doi.org/10.1080/00908310152004764>
12. **Dhawan, N., & Tanvar, H.** (2022). A critical review of end-of-life fluorescent lamps recycling for recovery of rare earth values. *Sustainable Materials and Technologies*, 32, e00401. <https://doi.org/10.1016/j.susmat.2022.e00401>
13. **Dong, B., Jia, Y., Tan, Q., Sun, H., & Ruan, R.** (2020). Contributions of Microbial “Contact Leaching” to Pyrite Oxidation under Different Controlled Redox Potentials. *Minerals*, 10(10), 856. <https://doi.org/10.3390/min10100856>
14. **Eco Recycling Limited Lamp Recycling.** (n.d.). *ECORECO*. <https://ecoreco.com/services-lamp-recycling.aspx>
15. **Gjorv, O. E., & Sakai, K.** (Eds.). (1999). *Concrete Technology for a Sustainable Development in the 21st Century* (0 ed.). CRC Press. <https://doi.org/10.1201/9781482272215>
16. **González, A., Navia, R., & Moreno, N.** (2009). Fly ashes from coal and petroleum coke combustion: Current and innovative potential applications. *Waste Management & Research: The Journal for a Sustainable Circular Economy*, 27(10), 976–987. <https://doi.org/10.1177/0734242X09103190>
17. **Hua, Z., Geng, A., Tang, Z., Zhao, Z., Liu, H., Yao, Y., & Yang, Y.** (2019). Decomposition behavior and reaction mechanism of Ce0.67Tb0.33MgAl11O19 during Na2CO3 assisted roasting: Toward efficient recycling of Ce and Tb from waste phosphor. *Journal of Environmental Management*, 249, 109383. <https://doi.org/10.1016/j.jenvman.2019.109383>
18. **I Nikolayeva, H Lenko, D Averyn, & O Lobodzinsky.** (2021). Review of the Current State of Tailing Storage Facilities in Donetsk and Luhansk Oblasts. Summary (p. 51). Organization for Security and Co-operation in Europe. <https://www.osce.org/files/f/documents/9/9/486259.pdf>
19. **Informacia o sostoyanii kachestva podzemnyih vod na promplotshadke PJSC «Severodonetsk Azot» i poligona TPO (c. Fugarovka) za IV kv. 2013.** (2013). OOO “Vostokgeologia.”
20. **Itskos, G., Koukouzias, N., Vasilatos, C., Megremi, I., & Moutsatsou, A.** (2010). Comparative uptake study of toxic elements from aqueous media by the different particle-size-fractions of fly ash. *Journal of Hazardous Materials*, 183(1–3), 787–792. <https://doi.org/10.1016/j.jhazmat.2010.07.095>
21. **Jangkorn, S., Kuhakaew, S., Theantanoo, S., Klinla-or, H., & Sriwiri-yarat, T.** (2011). Evaluation of reusing alum sludge for the coagulation of industrial wastewater containing mixed anionic surfactants. *Journal of Environmental Sciences*, 23(4), 587–594. [https://doi.org/10.1016/S1001-0742\(10\)60451-2](https://doi.org/10.1016/S1001-0742(10)60451-2)

22. **Korchuganova, O., Tantsiura, E., Ozheredova, M., & Afonina, I.** (2020). The Non-Sodium Nickel Hydroxycarbonate for Nanosized Catalysts. *Chemistry & Chemical Technology*, 14(1), 7–13. <https://doi.org/10.23939/chcht14.01.007>
23. **Labus, K., Cicha-Szot, R., & Falkowicz, S.** (2020). Injected silicate horizontal barriers for protection of shallow groundwater—Technological and geochemical issues. *Applied Geochemistry*, 116, 104577. <https://doi.org/10.1016/j.apgeochem.2020.104577>
24. **Lee, X. J., Ong, H. C., Gao, W., Ok, Y. S., Chen, W.-H., Goh, B. H. H., & Chong, C. T.** (2021). Solid biofuel production from spent coffee ground wastes: Process optimisation, characterisation and kinetic studies. *Fuel*, 292, 120309. <https://doi.org/10.1016/j.fuel.2021.120309>
25. **Lin, K.-L., & Lin, C.-Y.** (2005). Hydration characteristics of waste sludge ash utilized as raw cement material. *Cement and Concrete Research*, 35(10), 1999–2007. <https://doi.org/10.1016/j.cemconres.2005.06.008>
26. **Lingling, X., Wei, G., Tao, W., & Nanru, Y.** (2005). Study on fired bricks with replacing clay by fly ash in high volume ratio. *Construction and Building Materials*, 19(3), 243–247. <https://doi.org/10.1016/j.conbuildmat.2004.05.017>
27. **Little, M. R., Adell, V., Boccaccini, A. R., & Cheeseman, C. R.** (2008). Production of novel ceramic materials from coal fly ash and metal finishing wastes. *Resources, Conservation and Recycling*, 52(11), 1329–1335. <https://doi.org/10.1016/j.resconrec.2008.07.017>
28. **Matjie, R. H., Bunt, J. R., & Van Heerden, J. H. P.** (2005). Extraction of alumina from coal fly ash generated from a selected low rank bituminous South African coal. *Minerals Engineering*, 18(3), 299–310. <https://doi.org/10.1016/j.mineng.2004.06.013>
29. **Minh Trang, N. T., Dao Ho, N. A., & Babel, S.** (2021). Reuse of waste sludge from water treatment plants and fly ash for manufacturing of adobe bricks. *Chemosphere*, 284, 131367. <https://doi.org/10.1016/j.chemosphere.2021.131367>
30. **Mohan, S., & Gandhimathi, R.** (2009). Removal of heavy metal ions from municipal solid waste leachate using coal fly ash as an adsorbent. *Journal of Hazardous Materials*, 169(1–3), 351–359. <https://doi.org/10.1016/j.jhazmat.2009.03.104>
- On Waste Management. (2023). <https://zakon.rada.gov.ua/laws/show/2320-20#top>
31. **Panday, K. K., Prasad, G., & Singh, V. N.** (1985). Copper(II) removal from aqueous solutions by fly ash. *Water Research*, 19(7), 869–873. [https://doi.org/10.1016/0043-1354\(85\)90145-9](https://doi.org/10.1016/0043-1354(85)90145-9)
32. **Pavlik, Z., Fořt, J., Záleská, M., Pavlíková, M., Trník, A., Medved, I., Keppert, M., Koutsoukos, P. G., & Černý, R.** (2016). Energy-efficient thermal treatment of sewage sludge for its application in blended cements. *Journal of Cleaner Production*, 112, 409–419. <https://doi.org/10.1016/j.jclepro.2015.09.072>
33. **Perel'man, A. I.** (1986). Geochemical barriers: Theory and practical applications. *Applied Geochemistry*, 1(6), 669–680. [https://doi.org/10.1016/0883-2927\(86\)90088-0](https://doi.org/10.1016/0883-2927(86)90088-0)

34. **Petruzzelli, D.** (2000). Coagulants removal and recovery from water clarifier sludge. *Water Research*, 34(7), 2177–2182. [https://doi.org/10.1016/S0043-1354\(99\)00357-7](https://doi.org/10.1016/S0043-1354(99)00357-7)
35. **Querol, X., Moreno, N., Umaña, J. C., Alastuey, A., Hernández, E., López-Soler, A., & Plana, F.** (2002). Synthesis of zeolites from coal fly ash: An overview. *International Journal of Coal Geology*, 50(1–4), 413–423. [https://doi.org/10.1016/S0166-5162\(02\)00124-6](https://doi.org/10.1016/S0166-5162(02)00124-6)
36. Register of waste generation, treatment and disposal facilities of Luhansk region (as amended in 2017). (2017). Luhansk War Civil Administration. [ecolugansk.gov.ua/2013-12-12-00-50-06-3/2013-12-12-00-50-06/povodzhennya-z-vidkhodami](http://ecolugansk.gov.ua/2013-12-12-00-50-06-3/2013-12-12-00-50-06/povodzhennya-z-vidkhodami)
37. **Sahu, V., Srivastava, A., Misra, A. K., & Sharma, A. K.** (2017). Stabilization of fly ash and lime sludge composites: Assessment of its performance as base course material. *Archives of Civil and Mechanical Engineering*, 17(3), 475–485. <https://doi.org/10.1016/j.acme.2016.12.010>
38. **Scott, S. L.** (Ed.). (2018). A Matter of Life(time) and Death. *ACS Catalysis*, 8(9), 8597–8599. <https://doi.org/10.1021/acscatal.8b03199>
39. **Shabtai, Y., & Mukmenev, I.** (1996). A combined chemical-biotechnological treatment of coal fly ash (CFA). *Journal of Biotechnology*, 51(3), 209–217. [https://doi.org/10.1016/S0168-1656\(96\)01598-2](https://doi.org/10.1016/S0168-1656(96)01598-2)
40. **Sittig, M.** (1980). Metal and inorganic waste reclaiming encyclopedia. Noyes Data Corp.
41. **Swanepoel, J. C., & Strydom, C. A.** (2002). Utilisation of fly ash in a geopolymeric material. *Applied Geochemistry*, 17(8), 1143–1148. [https://doi.org/10.1016/S0883-2927\(02\)00005-7](https://doi.org/10.1016/S0883-2927(02)00005-7)
42. **Van Deventer, J. S. J., Provis, J. L., & Duxson, P.** (2012). Technical and commercial progress in the adoption of geopolymer cement. *Minerals Engineering*, 29, 89–104. <https://doi.org/10.1016/j.mineng.2011.09.009>
43. Voda pytna, hihiiienichni vymohy do yakosti vody tsentralizovanoho hospodarsko-pytnoho vodopostachannia. (2010). K.: Vyd-vo standartiv.
44. Waste at every stage. (2002). Vital Waste Graphics. <http://www.grid.unep.ch/waste/index.html>
45. **Yurmazova, T., Shakhova, N., & Tuan, H. T.** (2016). Adsorption of inorganic ions from aqueous solutions using mineral sorbent—Tripoli. *MATEC Web of Conferences*, 85, 01017. <https://doi.org/10.1051/mateconf/20168501017>
46. **Zha, F., Liu, S., Du, Y., & Cui, K.** (2008). Behavior of expansive soils stabilized with fly ash. *Natural Hazards*, 47(3), 509–523. <https://doi.org/10.1007/s11069-008-9236-4>
47. **Zhang, W., Yang, J., Wu, X., Hu, Y., Yu, W., Wang, J., Dong, J., Li, M., Liang, S., Hu, J., & Kumar, R. V.** (2016). A critical review on secondary lead recycling technology and its prospect. *Renewable and Sustainable Energy Reviews*, 61, 108–122. <https://doi.org/10.1016/j.rser.2016.03.046>
48. Zvit pro vikonannya robot po ob'ektu: «Provedennya robot z monitoringu pidzemnih vod na teritoriyi oblasti. (p. 265). (2019). ShId DRGP.



## **JUSTIFICATION OF THE CHOICE OF PNEUMATIC STRUCTURES FOR THE FORMATION OF GROUND STORAGE FACILITIES FOR THE GAS HYDRATES STORAGE**



**Larysa PEDCHENKO**

PhD, Associate Professor of the Department of Oil and Gas Engineering and Technologies, National University «Yuri Kondratuk Poltava Polytechnic», Ukraine



**Mykhailo PEDCHENKO**

PhD, Associate Professor of the Department of Oil and Gas Engineering and Technologies, National University «Yuri Kondratuk Poltava Polytechnic», Ukraine



**Nazar PEDCHENKO**

PhD, Senior lecturer of the Department of Oil and Gas Engineering and Technologies, National University «Yuri Kondratuk Poltava Polytechnic», Ukraine

### **Abstract**

Natural gas can exist not only in gaseous, but also in liquefied and solid aggregate states. Natural gas in a solid state - gas hydrates of natural gas. It is in the solid state - in the form of gas hydrates - that natural gas can be stored in improved casing gas-resistant structures. In order to improve the pneumatic structures and the method of operation of these structures, the features of such storage are substantiated. The design and operation technology of the ground storage facility for the accumulation and storage of natural gas as part of the gas hydrate includes the main and some auxiliary elements. Compulsory components of a pneumatic structure include a fence, pumping equipment and a foundation. However, the main element of the ground pneumatic structure is a frameless gas-resistant shelter in the form of at least two dome-shaped gas-tight soft shells on a thermally insulated base. A necessary condition for the storage of gas hydrates of natural gas is the creation of thermobaric conditions higher than the dissociation parameters of gas hydrates of this composition. For increase the thermal resistance of the pneumatic coating, it is

suggested to fill the space between the shells with a porous substance with low thermal conductivity. Liquid compression foam is offered as a thermal insulation material. The use of liquid foams will increase the thermal resistance of soft shells and reduce the heat exchange between gas hydrates and the air outside. The use of these hydrate storages will significantly increase the efficiency and competitiveness of natural gas storage technology in the form of gas hydrates.

## **I. Introduction**

As is known, at relatively low temperatures and a certain pressure, water molecules form a three-dimensional structure that can be occupied by gas molecules (for example, methane, ethane, carbon dioxide, etc.) [1]. This type of compounds are known as clathrates or inclusion compounds [2]. Today, a number of technologies are known in which gas hydrates are an intermediate or target product. These are the so-called gas hydrate technologies (transportation and storage of natural gas in gas hydrate form [1], gas hydrate fractionation, concentration using gas hydrates of any aqueous solutions [3, 4], etc.).

At the same time, the natural gas storage in gas hydrate form in many cases becomes a real alternative to traditional technologies.

Storage of gas hydrate requires maintenance of appropriate thermobaric conditions. However, gas hydrate can exist in a metastable state for some time as a result of the self-preservation effect or due to preservation by a ice layer of [4-6].

In addition, a compulsory condition for the reliable gas hydrate storage is the organization its high-quality thermal insulation and sealing. Such conditions should be ensured in specialized hydrate shelters. There are a number of projects, for example described in patent №US5964093, which involve the use of surface or partially buried capital structures built from traditional building materials.

However, warehouses made of traditional metal or reinforced concrete structures cannot provide effective sealing and thermal insulation. In fact, these structures can only perform the role of a skeleton for attaching insulating and sealing elements.

## **2. Theoretical substantiation**

Taking into account the results of research on the development of parameters proposed in the work on the production of gas-hydrate blocks, the level of development of construction technologies and problems related to the provision of natural gas to consumers, an

analysis of the structures of potential storage facilities for the accumulation and long-term storage of blocks until the moment of consumption of dissociated gas was performed.

Light membrane structures best meet the specified storage parameters, among which pneumatic structures should be chosen (Fig. 1).

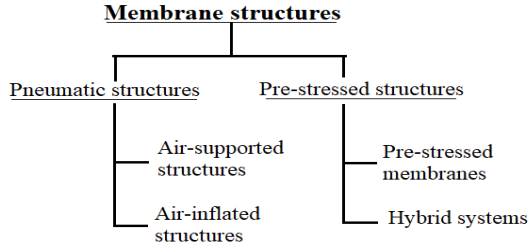


**Fig. 1.** Classification of membrane structures

A pneumatic structure is defined as a structure in which pressure drops of gas or air control and ensure shape stability [7]. Pneumatic structures are one of the most effective known structural forms. Constructions that use pressure as a stabilizing medium have been used for a long time, but they began to be used in the construction industry relatively recently [8].

Pneumatic structures are divided into two main types: air-controlled structures and air-stabilized structures. Among them, the construction with air stabilization is the most relevant for architectural applications [9].

Air-supported structures consist of only one membrane, which is supported by a small internal pressure difference. Thus, the internal air volume of the structure is under a pressure higher than atmospheric.

Air structures in which the enclosing membrane is supported by a small air pressure drop, such as stadium roofs, inflated storages. Pressure is created inside the entire structure. A low pressure is required to maintain a membrane-type structure; however, air leakage is very common because it is not possible to maintain a sealed structure. Therefore, membrane-type structures must have a constant supply of air to replenish the escaping air.

Air-inflated structures are supported by pressurized air contained

inside the inflated element of the building. The internal air volume of the building remains under atmospheric pressure.

Inflated structural elements are under high pressure and are used as structural elements in spatial construction. In this type of construction, high air pressure is maintained only inside the inflated members, which are the main load-bearing components of the structure. This system is more airtight than the membrane type, as it can be closed after inflation. The beam-type design is also more economical, as there is no need for constant air replenishment and less material is required.

The shape and stability of the air-stabilized structure is controlled by pressure differences across the membrane. In this type of pneumatic structures, there are several structures related to the number of membranes, types and magnitude of the pressure drop [8]. Therefore, in air-stabilized structures there are single-wall air structures and air-inflated structures (single wall air-supported structures and air-inflated structures) (Fig. 2).

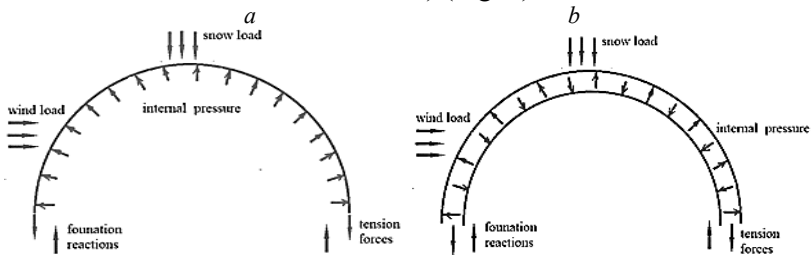


Fig. 2. Types of pneumatic structures: a - air support; b - air - inflated

Pneumatic designs are based on the theory of soap bubbles. A new roof construction technique, called pneumatic structures, is able to take a heavy load and withstand the effects of high-speed wind due to the pressure that holds the air inside the structure.

Forms created with soap bubbles are "ideal" pneumatic molds in which the membrane stresses are the same at every point on the surface. Such forms have the largest volumes and the smallest possible surface areas.

Obligatory components of pneumatic construction are enclosure, pumping equipment and foundation. Depending on the functional purpose, pneumatic structures also have other structural elements:

inlets, anchoring devices, power belts, fan and climate systems, reinforcing ropes, diaphragms, etc. [10]. Pumping equipment for an air-inflatable structure can be fans, blowers or compressors. First of all, pressure is created in the inner volume of the shell with the help of pumping equipment. This equipment is also used to maintain a stable pressure in the event of an air leak.

Structures are fixed to the ground with heavy anchors or attached to the foundation. Material weight and wind loads are used to determine the most suitable fastening system. For a small independent structure, ballast, concrete blocks or bricks can be placed around the perimeter of the sealing skirt to stabilize the structure. A larger and wider pneumatic structure requires reinforcing cables or nets to secure and stabilize it.

The main element of gas-resistant structures is a soft shell. There are many types of membranes used as roofs in pneumatic structures, including fabrics, hyperelastic materials (like rubber), composites, and more. The classification of membranes and tissues is shown in Fig. 3 [10].

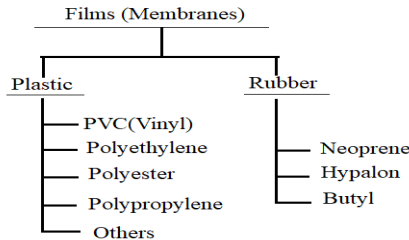


**Fig.3.** The classification of membranes and fabrics

It consists of the shell itself with a support contour and a number of technological components (fittings, non-return and ventilation valves, flanges, nodes for fastening power elements and equipment, etc.) [11]. However, the thermal performance of gas-resistant shells is low. Thin shells are not able to provide a sufficient level of thermal resistance. Therefore, to improve their thermal performance, it is advisable to cover these buildings with a two- and three-layer coating.

In addition, the amount of excess, relative to the environment, pressure in pneumatic two- and three-layer structures can be gradually changed from layer to layer, distributing the estimated total

excess pressure between the inflatable layers. This allows you to increase the load-bearing capacity and stability of the structure without increasing the strength of the structural material, while simultaneously maintaining increased tightness. At the same time, the inner shell is supported by the pressure difference between the room and the intershell space.

Modern technologies make it possible to obtain multi-layered and combined materials based on polymer films and synthetic high-strength fabrics. The main scheme of their design consists of three layers: a gas-tight film, a reinforcing base and a heat-welding layer. The two-layer gas-tight film is two orders of magnitude better than the performance of vulcanized rubbers. This is achieved by metallizing one or both sides of the film by vacuum spraying. However, the disadvantage of film materials is insufficient strength. Therefore, they are reinforced with fabrics [12].

In [13], it was indicated that the total coefficient of thermal conductivity of their two-layer shelters was  $2.8-3.4 \text{ W}/(\text{m}^2\cdot\text{K})$ , and when using internal reflective cladding it could be reduced to  $1.7 \text{ W}/(\text{m}^2\cdot\text{K})$ . Similar results can be obtained when using a suspension of a light shell, which forms a closed (isolated) air layer. Since the second dome is not structural, very light materials can be used for it. Even better insulating properties are achieved when an additional substrate (film) with a mirror coating is placed under the shell, for effective reflection of thermal radiation.

Thanks to the air layer, the overall coefficient of thermal conductivity decreases and thus heat loss decreases.

Single-layer or double-layer membranes can be made of industrial fabrics such as fiberglass or polyester, which provides great stability. The shell shape is a very important aspect in pneumatic designs. If the pressure on the pneumatic structure is uneven, the membrane creates wrinkles and stress points, which will lead to its destruction. However, the membrane (covering) of structures with such fabrics is quite unreasonably expensive.

Therefore, the most widely used material for air-resistant structures is a fabric made of nylon or polyester fibers covered with plasticized polyvinyl chloride (PVC) or chlorosulfonated polyethylene (hypalon) [13, 14]. The service life when using ordinary materials is usually 7-10 years. However, with high-quality

operation, pneumatic structures have been in continuous operation for more than 15 years, at the same time withstanding stormy winds without damage [13]. Fluorine-containing polymers are successfully used to create more durable materials.

Based on the features of gas storage in gas-hydrate form, it is suggested to use a two-layer coating with a barrier layer of non-flammable gas or gas mixture for gas-resistant hydrate storages. Also, in order to limit the supply of energy from the soil to the storage, it is necessary to provide thermal insulation of its base.

In addition, information on the composition of the non-flammable gas mixture injected between the layers of the coating, divided into separate isolated sectors, is proposed to be used to control their integrity. The nature of the change in the composition of the gas will indicate a violation of the tightness of the outer or inner shell, respectively.

In gas-resistant structures, which are proposed to be used as hydrate storage, it is necessary to maintain a temperature regime that allows the gas hydrate to be in a stable state at a pressure close to atmospheric. It is proposed to ensure the necessary temperature regime of the storage for the cold and warm periods of the year due to the accumulated cold in the gas-hydrate blocks and the additional cooling system.

Effective thermal insulation can be provided by a relatively thin layer of porous material (foam, mineral wool, etc.), and high-quality sealing by a polymer film [10, 12, 13].

Based on this, it is proposed to use gas-resistant pneumatic structures as hydrate storages [10, 14]. At the same time, modern coatings allow maintaining their operational characteristics for a long time (up to 15-20 years) [10]. In addition, they can be easily dismantled, transported and quickly assembled, that is, they can be considered as mobile technological objects.

These buildings are structures supported by a gas cushion. However, the pressure in them is higher than atmospheric only to ensure the force for the formation of a dome-shaped form and to compensate for the mass of the shell itself (in the range of pressure – 0.01-1.0 MPa) [9].

However, the thermal resistance of such structures is insignificant [15]. Therefore, they need their conditioning (cooling). Taking into

account the costs of cold production, it is impractical to operate such buildings without the organization of additional thermal insulation.

A variant of increasing the thermal resistance of these structures is the use of two- and three-layer coatings. However, the thermal resistance of the barrier gas layer increases noticeably only up to its thickness of 0.3 m [16, 17]. For example, the coefficient of thermal conductivity of the two-layer shelters considered in [18] was 2.8-3.4 W/(m<sup>2</sup>·K). Therefore, regardless of the external temperature, a significant heat flow will enter the storage even through a double-layer coating.

Taking into account the results of research on the development of the parameters of the gas hydrate blocks proposed in the work, the level of development of construction technologies, and problems related to the provision of natural gas to consumers, it is proposed to accumulate and store it for a long time until the moment of consumption in ground hydrate storage facilities in the form of gas-resistant structures covered with soft shell. These structures are closed structures that "lie" on an air (gas) cushion, the pressure in which is excessive, but exceeds the atmospheric pressure only to overcome the effort of forming (bending) and compensating the shell's own weight. They are operational in the region of the so-called Laplacian overpressure (0.01-1.0 MPa), which belongs to the low level [14]. The use of this type of surface hydrate storage can significantly smooth out the seasonal unevenness in gas production and in some cases be a serious alternative to underground gas storage.

### **2.1. Improvement of the storage thermal insulation system**

It is known that the thermal insulation properties of materials are determined by their porosity. The pores are filled with gas of low thermal conductivity. As thermal insulation, among others, materials are used, which are polymers, foamed before the start of hardening. Hardening, in this case, is required for the production of heat-insulating panels of a certain shape and size for the convenience of their use and transportation.

However, the phase state of material bubbles does not affect its thermal insulation properties. Therefore, the use of solid porous thermal insulation materials is due to the convenience of their use. In the case of gas-resistant shell structures, the use of solid heat-



insulating materials will be unacceptable, as this will significantly complicate the construction and duration of the shelter installation.

Therefore, it is proposed to use liquid polymer foams as a material for thermal insulation of gas-resistant shell structures - storage of gas hydrates. At the same time, in the case of using a transparent shell-shelter, the foam will allow part of the scattered sunlight into the storage. This will make it possible to regulate the supply of energy to the storage to some extent.

Foams are coarsely dispersed highly concentrated systems in which the dispersed phase is gas bubbles, and the dispersion medium is liquid in the form of thin films. The concentration of gas bubbles should be more than 74% (by volume). Foams are thermodynamically unstable systems.

In foams, gas bubbles are pressed against each other by a thin layer of dispersion medium - foam films. The system is in stable equilibrium when contact is made between three bubbles. Liquid films between these bubbles form a Plateau triangle, and the contact points of the films and their thickening are Plateau-Gibbs channels (Fig. 4).



**Fig.4.** Cross-section of the Plateau channel: 1 – liquid films; 2 – Plateau-Gibbs channel

The main characteristics of foams are: multiplicity, dispersibility, stability over time. The ratio of the volume of the formed foam to the volume of the dispersion medium characterizes the multiplicity of the foam. The multiplicity of the foam increases with the increase in the size of the gas bubbles (cells) and the thinning of their walls.

The dispersion of the foam is estimated by the size (radii) of the bubbles. Usually, real foam is polydisperse and gas bubbles in it are of different sizes. Polydispersity of foams affects its stability over time [19].

The stability (stability) of the foam is its ability to maintain the total volume, dispersion and prevent the outflow of liquid (syneresis). The stability of the foam increases as the cell size decreases and the thickness and strength of the polymer film that

forms the cell increases.

Foam stability is divided into two types:

- kinetic (sedimentation) stability – the ability of the system to keep the distribution of particles of the dispersed phase unchanged over time in the volume of the entire dispersed system, the ability of the system to resist the force of gravity;

- aggregative stability - the ability to keep the size of particles of the dispersed phase unchanged (maintain dispersity).

Violation of the sedimentation resistance of the foam is caused by the action of gravity and capillary suction forces. There is a process of spontaneous swelling of the liquid in the foam film, its thinning and rupture. The movement of fluid against gravity is explained by capillary effects due to the fluid pressure gradient in the Plateau channels.

Aggregative stability of the foam is formed by the mono- or polydispersity of gas bubbles and occurs under the influence of gas diffusion. The smaller the gas bubble, the greater the pressure in it. Over time, there is a process of gas diffusion from small bubbles to large ones, while the small bubbles decrease in size and the large ones increase in size. This leads to a change in the stability of the foam, the foam "ages" and breaks down. The destruction of the foam structure (change in its dispersed composition) occurs as a result of the diffusion transfer of gas between the foam bubbles and the destruction of the bubble films, which leads to their fusion (coalescence). A higher degree of polydispersity causes a significant manifestation of gas diffusion, although this process is quite slow.

Foams are typical lyophobic systems. Thermodynamically, they are not stable due to the diffusional transfer of gas and the swelling of the dispersion medium under the influence of gravity, which lead to a change in the structure and gradual destruction of the foam.

It is known that the size of the foam bubbles and their homogeneity [20] depend on the type and concentration of the foaming agent, the presence of a stabilizing substance, the ratio of the consumption of the aqueous solution of the foaming agent and air, and the methods of their formation. One of the most promising in terms of aggregate resistance is compressed air foam - a homogeneous, fine-structured foam of low multiplicity, obtained by mixing a foaming agent, water and compressed air or nitrogen. The

stability of the compression foam increases when the diameter of the bubble decreases [21].

The main components of foaming agents are surfactants (surfactants). Colloidal surfactants or high molecular structures (HMS) are usually used as a foaming agent. Usually, middle members of homologous series are used as foaming agents, and anionic surfactants are better than cationic and nonionic surfactants. Polyelectrolytes, such as proteins, are the best foaming agents among high molecular structures (HMS).

An important role is played by the concentration of the foaming agent. For foaming agents - colloidal surfactants, the maximum foaming capacity is reached in a certain interval of concentrations, and with its further growth, it remains constant or even decreases. In the case of HMS, the foaming ability increases with increasing concentration.

A change in the properties of the foam is possible when stabilizers are added to surfactant solutions. Their action is based on increasing the viscosity of solutions and slowing down the flow of liquid due to this, i.e., a structural-mechanical factor is added to the action of the kinetic stability factor characteristic of foaming agents - surfactants. For example, substances that increase the viscosity of the foaming solution itself (thickeners) can be used as such stabilizers for surfactants or HMS for thermal insulation of gas-resistant shell structures. They are added in large concentrations. These are glycerin, ethylene glycol, methyl cellulose. Cellulose derivatives already in the amount of 1-2% increase the viscosity of the solution and the stability of the foam tenfold, which leads to a strong slowdown in the process of dehydration of films. Colloidal stabilizers are more effective than thickeners. These include: gelatin, glue, starch, agar-agar. These substances, taken in the amount of 0.2-0.3% of the mass of surfactant, increase the viscosity of the liquid in the films by more than 100 times, and the stability of the foam increases by 2-8 times.

In addition, substances that polymerize in the volume of the foam can be used. Polymerization significantly increases the strength of films, but their transition to a solid state is possible. These are the most effective stabilizers. These can be polymer compositions - synthetic resins, for example, urea or latex.

Stabilizers can be substances that participate in the construction

of adsorption layers at the boundary of the "liquid-gas" separation. The main representatives are fatty alcohols, mainly tetradecyl alcohol. The introduction of only 0.05% alcohol into solutions of foaming agents greatly reduces the surface tension, which leads to an increase in the stability of foams

Mineralized (three-phase) foams can also be used [20, 21]. They are obtained when finely ground solids are added to the foam to increase its strength - talc, asbestos, quartz, carbon black, which, when evenly distributed on the surface of the bubbles, strengthen the films and extend the life of the foam. The strengthening of the foam occurs due to the adhesion of solid mineral particles to the foam bubbles, due to the interaction between the surface of the solid particle and the polar groups of the surfactant. Fine powders give strong foam films. The stabilization mechanism of three-phase foams (gas-liquid-solid particles) is primarily explained by the narrowing of the Plateau channels. As a result of decreasing the diameter of the channel, the rate of outflow of the solution decreases and corks made of grains that did not stick to the bubbles additionally clog these channels.

Taking into account the above, for the thermal insulation of gas-resistant shell structures, surfactants or HMS can be used together with any of the named stabilizers or three-phase foams.

The schematic diagram of such a storage-shelter, supplemented by a complex of appropriate equipment for the implementation of the technological process of gas hydrate storage and regasification, is presented in Fig. 5.

Its main elements are shelter, base and auxiliary equipment. The shelter of the hydrate storage-shelter consists of a liquid foam layer between several impermeable to gas and water canvases 2 and 4 with a sun-reflective layer on top. The shelter is fixed by a net made of ropes 5. The storage-shelter is equipped with the following systems: foam generation and selection of products its destruction; storage conditioning (cooling and heating); gas and water selection. The foam generation system involves supplying the produced foam to the upper part of the space between the inner and outer shells. At the same time, a system for selecting of foam destruction products is placed between the shells at the base level.

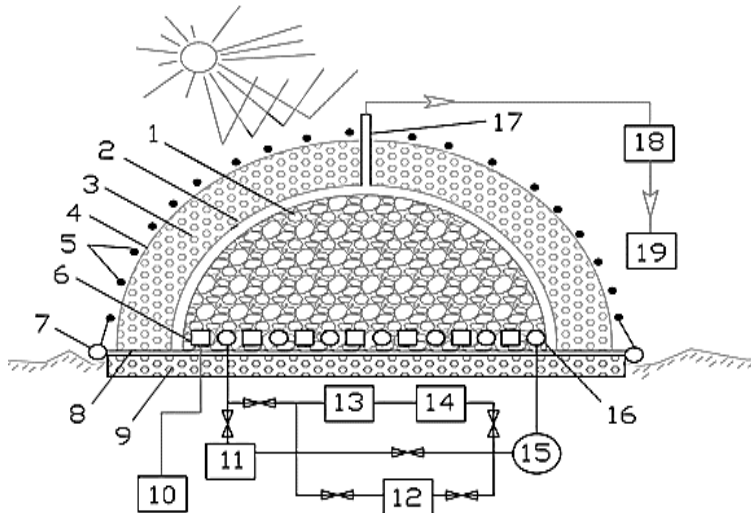


**Fig 5.** Schematic diagram of hydrate storage-shelter at the gas hydrate storage stage: 1 – gas hydrate; 2 – the lower fabric for the shelter; 3 – a liquid foam layer; 4 – the upper fabric for the shelter; 5 – a system of external reinforcement of the shelter in the form of a net made of ropes; 6 – perforated pipes of the gas and water extraction system from under the gas hydrate stack; 7 – a hermetic connection system of the cover sheets and the base; 8 – base covering made of material impermeable to gas and water; 9 – heat-insulating coating of the base; 10 – water collection tank; 11 – system of heating the coolant based on the solar collector; 12 – coolant heating block; 13 – unit of the refrigerating unit; 14 – air cooling system; 15 – circulation pump; 16 – heat exchanger pipe system; 17 – gas selection system; 18 – gas compression unit; 19 – gas consumer [9]

For the maximum energy efficiency of the technology, the level of gas hydrate cooling in the production process is determined, taking into account the duration and parameters of transportation and storage.

The flow of thermal energy from the ground through the base of the storage at its average value of  $17 \text{ W/m}^2$  [22] will be 0.03 MW. Thermal insulation of the base will allow to reduce it to 9 kW. After the preparation of the site, the base of the storage-shelter is arranged by sequentially laying a layer of thermal insulation 9 (Fig. 5), a coating of water- and gas-tight material 8, a heat exchanger in the form of a system of pipes 16, a system of gutters and perforated pipes 6 for the removal of gas and water.

For reliable sealing of the hydrate storage-shelter, system 7 seals the connection between the shelter sheets and the base. The isolated space formed is connected to the compressor 18 by the gas discharge line 17. The temperature regime of the hydrate storage is ensured by the accumulated cold in the gas hydrate and the additional air conditioning system. Hydrate dissociation is proposed to be carried out directly in the storage at the expense of solar energy. The temperature of the gas hydrate (cooling during storage and heating in the process of gas extraction) is maintained by pumping the cooled or heated coolant through the heat exchanger 16 at the base of the hydrate storage-shelter.

The coolant is cooled by a refrigerating unit 13 or an air cooling system 14. Cooling or heating of the coolant is carried out in the solar collector 11, heater 12, refrigerating unit 13, air cooling system 14. Gas selection is carried out as a result of controlled dissociation of gas hydrate when pumping the coolant through the heat exchanger 16. Water is discharged from the storage-shelter to the tank 10 by the collector 6. (In addition, it is possible to organize the inflow of solar energy through the transparent areas of the shelter).

Gas through the selection line 17 enters the compression unit 18. Then it is consumed by the gas distribution network. The pressure in the line is limited by the mechanical strength of the shelter and lies within 0.2-0.4 MPa. The mobility of the storage-shelter will allow them to be placed directly near the objects of consumption. This will allow the gas during pressure dissociation to be sent to the gas distribution network without additional compression.

### 3. Calculation of storage-shelter operational parameters

The thermal resistance of the coating, which characterizes the heat-shielding characteristics of the gas-resistant storage-shelter, is determined by the formula

$$R_{stor} = \frac{1}{\alpha_1} + \frac{2\delta_{shel}}{\lambda_{shel}} + R_{barr} + \frac{1}{\alpha_2}, \quad (1)$$

where  $R_{stor}$  - reduced thermal resistance of the storage-shelter shell,  $m^2 \cdot K/W$ ;  $\alpha_1$  i  $\alpha_2$  - coefficients of heat transfer of external and internal air, respectively  $W/m^2 \cdot K$ ;  $\delta_{shel}$  - thickness of the gas-tight shell fabric, m;  $R_{barr}$  - thermal resistance of the barrier layer,  $m^2 \cdot K/W$ ;  $\lambda_{shel}$  - coefficient of thermal conductivity of the shell fabric,  $W/m \cdot K$ .

The average temperature for the forest-steppe zone of Ukraine for January is 265 K, July - 293 K [14, 15]. The thermal resistance of the storage-shelter cover ( $R_{stor}$ ) in summer will be  $0.27 \text{ m}^2 \cdot \text{K}/\text{W}$ , in winter -  $0.35 \text{ m}^2 \cdot \text{K}/\text{W}$ . Then, during the winter period, energy will flow into the storage-shelter

$$q_W = \frac{1}{R_{stor}} (t_{out} - t_{in\ stor}) \left( \frac{W}{m^2} \right) \quad (2)$$

where  $t_{out}$  i  $t_{in\ stor}$  - air temperature, respectively, outside and in the storage-shelter, K.

$$q_W = \frac{1}{0,35} (265 - 248) = 48,6 \text{ (W / m}^2\text{)}.$$

The heat flow in the hydrate storage in the summer ( $q_s$ ) will be [16]

$$q_s = q_{av.d} + k \cdot A_d = 1 / R_{stor.s}(((t_s + p_{rad} \cdot I_{rad} / \alpha_{surf}) - t_{in\ stor}) + k \cdot (0.5 \cdot A \cdot K_m + p_{rad} (I_m - I_{rad}) / \alpha_{surf})), \quad (3)$$

$$q_s = 105.0 \text{ (W/m}^2\text{)},$$

where  $A_d$  - daily fluctuation of heat energy flow,  $\text{W/m}^2$ ;  $q_{av.d}$  - average daily heat energy input to the storage,  $\text{W/m}^2$ ;  $k$  - daily coefficient of change of heat flow  $A_d$ ;  $t_s$ ,  $t_{in\ stor}$  - the temperature of the outside air in July and inside the storage, respectively, K;  $p_{rad}$  - coefficient of absorption of heat of solar radiation by the external surface of the storage;  $I_{rad}$  - average daily amount of solar radiation reaching the storage surface in the warmest month,  $\text{MJ/m}^2$ ;  $\alpha_{surf}$  - coefficient of heat absorption of the external surface of the storage for the warm period of the year;  $K_m$  - the maximum amplitude of daily air temperature fluctuations in the warmest month of the year,  $^\circ\text{K}$ ;  $I_m$ ,  $I_{av.d}$  - maximum and average daily value of the amount of solar radiation, respectively,  $\text{MJ/m}^2$ .

The results of calculations of thermodynamic parameters for gas hydrate storage in a storage-shelter with a two-layer coating and an air barrier layer are given in table. 1.

Table 1

Gas hydrate storage parameters in a double-layered storage with an air barrier layer

Thermodynamic parameters	Calculations for the average monthly temperature	
	winter	summer
Thermal resistance of the storage-shelter shell, $R_{stor}$ , $m^2 \cdot K/W$	0.35	0.27
Heat flow to gas hydrate without thermal insulation layer, $q$ , $W/m^2$	48.6	105.0

Taking into account the thermal resistance, the thermal inertia of the two-layer cover of the hydrate reservoir will be [11]

$$D_{ther.in} - 0.27 \cdot R_{stor} \sqrt{\lambda \rho c} \quad (4)$$

where  $D_{ther.in}$  - thermal inertia;  $R_{stor}$  - thermal resistance,  $m^2 \cdot K/W$ .

$$D_{ther.in} - 0.27 \cdot 0.27 \div \sqrt{0.0244 \cdot 1.29 \div 717} = 0.4 D_{ther.in} < 1.5$$

Therefore, such a coating is inertialess. Let's consider the option of reducing the heat flow through a two-layer coating when filling the space between them with stable foam (foam density  $4.0 \text{ kg/m}^3$ , layer thickness ( $\delta_{coat1}$ ) - 1.5 m, coefficient of thermal conductivity ( $\lambda_{coat1}$ ) -  $0.041 \text{ W/(m}\cdot\text{K)}$ ) using an example storage with a capacity of 3,000 tons of gas hydrate (5.4 million cubic meters of natural gas).

The coefficient of thermal conductivity  $\lambda_{coat1}$  of a two-layer reinforced coating with a thickness of 2 mm is  $0.16 \text{ W/m}\cdot\text{K}$  [17]. Then its thermal resistance  $R_{coat1}$  will be at the level of  $0.0125 \text{ m}^2 \cdot \text{K/W}$ . The thermal balance of the storage-shelter is described by the equation

$$Q_1 + Q_2 - Q_3 - Q_{add} = 0, \quad (5)$$

where  $Q_1$  - heat flow into the storage through the shell, J;  $Q_2$  - heat flow from the base of the storage, J;  $Q_3$  - cold accumulated by gas hydrate, J,  $Q_{add}$  - additional heat removal (cooling), J.

The reduced thermal resistance of the coating is determined by the formula

$$R_{stor\ coat} = \frac{1}{\alpha_{out}} + \frac{2\delta_{coat1}}{\lambda_{coat1}} + \frac{\delta_{coat2}}{\lambda_{coat2}},$$

where  $R_{stor.coat}$  - reduced thermal resistance of the storage-shelter coating,  $m^2 \cdot K/W$ ;  $\alpha_{out}$  - coefficient of heat transfer of outside air,



Bt/(m<sup>2</sup>·K);  $\delta_{coat1}$  - coating layer thickness, m;  $\lambda_{coat1}$ - thermal conductivity coefficient coating, W/m·K;  $\delta_{coat2}$  - thickness of the foam layer, m;  $\lambda_{coat2}$  - coefficient of thermal conductivity of the foam layer, W/m·K.

Therefore, the reduced thermal resistance of the storage-shelter cover ( $R_{stor.coat1}$  and  $R_{stor.coat2}$ ) for winter and summer will be 37.78 and 37.62 m<sup>2</sup>·K/W, respectively. Then, in winter, the heat flow into the storage from the outside will be

$$q_{w1} = \frac{1}{R_{stor.coat1}} (t_{out} - t_{in.stor}) (W/m^2) \quad (7)$$

where  $t_{out}$  and  $t_{in.stor}$  - air temperature, respectively, outside and in the storage, K.

$$q_{w1} = \frac{1}{37,78} (265 - 248) = 0,45 (W/m^2)$$

The total heat flow into the storage-shelter through the coating  $Q_{w1}$  in the winter period will be 1.76 kW.

The heat flow to the storage in the summer ( $q_{s1}$ ) was determined by the formula

$$q_{s1} = 1/R_{stor.coat2}(((t_{out} + p_{rad} \cdot I_{rad} / \alpha_{surf}) - t_{in.stor}) + k(0.5 \cdot A \cdot K_m + p_{rad}(I_m - I_{rad}) / \alpha_{surf})), \quad (8)$$

$$q_{s1} = 1.33 \text{ W/m}^2.$$

The total heat flow into the storage through the coating ( $Q_{s1}$ ) in the summer period will be 5.23 kW.

The heat flow that enters the gas hydrate from the base ( $Q_2$ ), with its average annual value for mid-latitudes of 0.17 W/m<sup>2</sup> [15], will be 0.3 kW. Its insulation will reduce heat input to 0.25 kW.

In the table 2 shows a comparison of the calculated parameters of gas hydrate storage in ground-based gas-resistant storages in variants of the air layer between shells and foam.

Therefore, the required capacity of the additional cooling system of the storage-shelter for storage of gas hydrate without its dissociation (at a temperature of 258 K) is 0.9 kW in the winter period, and 4.44 kW in the summer period.

Table 2

Comparison of gas hydrate storage parameters in ground gas-resistant storage-shelters depending on the level of thermal insulation

Thermodynamic parameters	Calculations for the average monthly temperature <sup>en</sup>	
	winter	winter
Thermal resistances, $R_{stor.coat}$ , $m^2 \cdot K/W$ :		
- air between the fabrics of the shell	0.27	0.35
- a layer of foam between the fabrics of the shell	37.78	37.62
Heat flow to storage-shelter, $q$ , $W/m^2$ :		
- air between the fabrics of the shell	48.6	105.0
- a layer of foam between the fabrics of the shell	0.45	1.33
Heat flow to storage-shelter, $Q_t$ , kW:		
- air between the fabrics of the shell	189	408.0
- a layer of foam between the fabrics of the shell	1.76	5.23
Energy costs for cooling, $Q_3$ , kW:		
- air between the fabrics of the shell	190.2	409.2
- a layer of foam between the fabrics of the shell	2.1	5.5

#### 4. Modeling of heat exchange processes

Let's set the temperature on the surface of the gas hydrate as a result of the arrival of heat flow, as a process of heat transfer through a multilayer coating. On one side of the coating is the external environment with a temperature of  $T_p$ , and on the other – cooled to a temperature of  $T_g$ . gas hydrate (Fig. 6).

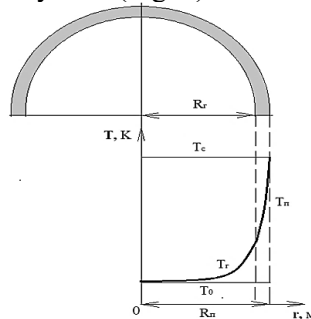


Fig. 6. Scheme of the gas hydrate heating process in the storage-shelter

Formulation of the problem. Let's assume: the initial temperature of the gas hydrate ( $T_0$ ) is 248 K; the gas hydrate stack has the shape

of a hemisphere with a base radius ( $R_g$ ) of 23.5 m; the surface of the gas hydrate is covered with a 1.5 m layer of foam ( $R_s - R_g = 1.5$  m); the initial temperature of the foam is 248 K; there is thermal contact between the foam and the hydrate; the temperature of the outer surface of the storage-shelter ( $T_{out}$ ) is constant and is 293 and 265 K for summer and winter, respectively.

It is necessary to find the temperature distribution over time and establish the moment when the temperature of the surface of the gas hydrate reaches 258 K (equilibrium temperature).

This process is described by a system of differential equations.

The change in gas hydrate temperature is described by the equation

$$\frac{\partial [rT_g(r, \tau)]}{\partial \tau} = a_g \frac{\partial^2 [r, T_g(r, \tau)]}{\partial r^2} (\tau > 0, 0 < r < R_g); \quad (9)$$

Temperature change in the foam layer as a result of heat exchange with the gas hydrate and the external environment

$$\frac{\partial [rT_g(r, \tau)]}{\partial \tau} = a_g \frac{\partial^2 [r, T_g(r, \tau)]}{\partial r^2} (\tau > 0, R_g < r < R_s); \quad (10)$$

$$\frac{\partial [rT_{\downarrow}(r, \tau)]}{\partial t} + \alpha(T_{out} - T(R, \tau)) = 0 \quad T_{out} - T(R, \tau) = 0; \quad (11)$$

Initial conditions of the process

$$T_g(r, 0) = T_o; \quad T_s(r, 0) = T_o; \quad (12)$$

Boundary conditions of the process

$$T_g(R_g, \tau) = T_s(R_g, \tau); \quad \lambda_g \frac{\partial T_g(R_g, \tau)}{\partial \tau} = \lambda \frac{\partial T_s(R_g, \tau)}{\partial \tau}$$

$$T_s(R_s, \tau) = T_{out}; \quad T_s(R_s, \tau) = T_{out}; \quad T_g(0, \tau) \neq \infty \quad (13)$$

where  $r$  - variable (current) value of the radius of the storage base, m;  $R_g$  - radius of the base of the storage-shelter located under the gas hydrate embankment, m;  $R_s$  - the radius of the base of the storage-shelter, which is located under the gas hydrate mound and the foam layer, m;  $T_o$  - storage temperature of gas hydrate, initial temperature of gas hydrate and foam layer, ( $T_o = 248$ ), K;  $T_{out}$  ambient temperature (293 K in summer, 255 K in winter);  $T_g$  variable over time (current) gas hydrate temperature, K;  $T_s$  - variable over time (current) temperature of the foam layer, K;  $\tau$  - the time of the heating (cooling)

process of gas hydrate and foam;  $\lambda_g$  - coefficient of thermal conductivity of gas hydrate, W/(m K);  $\lambda_s$  - coefficient of thermal conductivity of foam, W/(m K);  $a_g$  - coefficient of thermal conductivity of gas hydrate,  $m^2/s$ ;  $\alpha$  - heat transfer coefficient, W/( $m^2$  K);  $a_s$  - coefficient of gas hydrate thermal conductivity,  $m^2/s$ .

In order to evaluate the thermal insulation characteristics of the foam and the dynamics of the temperature change of the gas hydrate in the gas-resistant storage-shelter, its computer simulation was carried out (Fig. 7-10). The above storage calculation parameters were taken as the starting point.

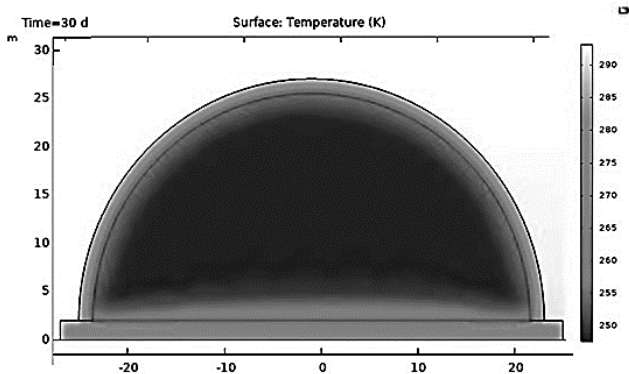


**Fig. 7.** Simulation of heat exchange in summer (external temperature 293 K) of gas-resistant hydrate storage-shelter thermally insulated with liquid foam without additional cooling after 30 days of storage

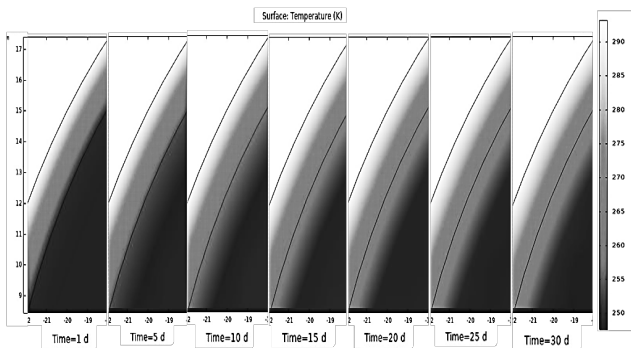


**Fig. 8.** Dynamics of changes in the temperature of the gas hydrate surface and the foam layer in the hydrate storage-shelter in the summer ( $T= 293$  K) without additional cooling

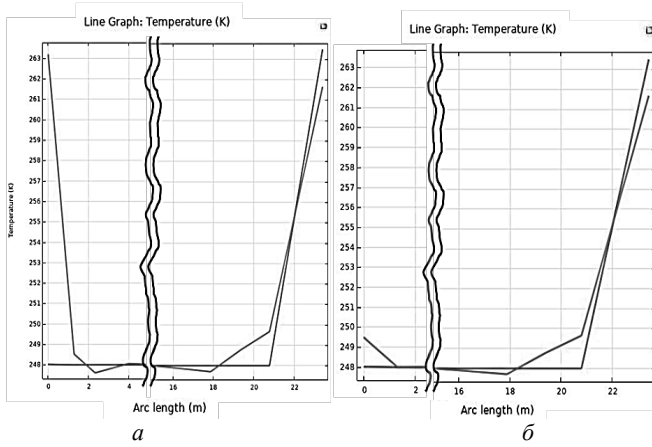


**Fig. 9.** Dynamics of changes in the temperature of the gas hydrate (with an initial temperature of 248 K) from the surface to the center of the sole of the stack in the summer period of storage ( $T = 293$  K) without additional cooling, provided that it is thermally insulated with a layer of foam 1.5 m thick: a) at the end of the first days of storage; b) at the end of the thirtieth day of storage

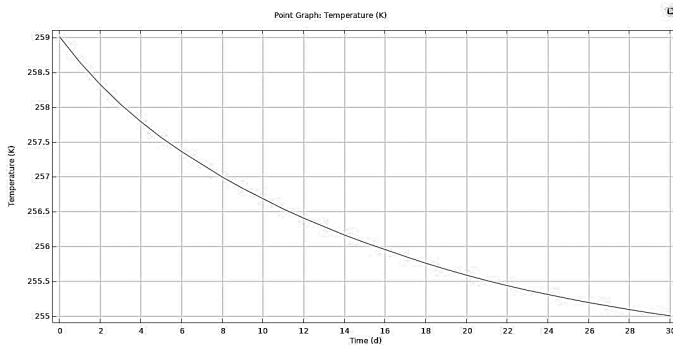


**Fig. 10.** Dynamics of changes in the temperature of the gas hydrate surface (with an initial temperature of 248 K) during thirty days in the summer storage period ( $T = 293$  K) without additional cooling, provided that it is thermally insulated with a layer of foam 1.5 m thick

Therefore, with an initial temperature of gas hydrates of 248 K, its additional cooling when stored in a storage-shelter facility insulated with foam, even in the summer months, will be necessary after 30 days of storage (to maintain the temperature of the gas hydrate at a level not higher than 258 K).

In winter, at an average air temperature of 265 K, storage of gas hydrate is possible without additional cooling.

At the same time, under the condition of gradual selection of gas, which will be released from the surface of the gas hydrate layer, the storage-shelter can be operated without cooling during the entire storage cycle.

### Conclusions

Thus, gas storage in gas hydrate form is proposed to be implemented in improved shell gas-bearing structures.

This improvement consists in the use of liquid stable foams as a thermal insulation material.

The main design elements of this storage-shelter facility are a frameless gas-resistant shelter in the form of at least two dome-shaped gas-tight soft shells on a thermally insulated base, the space between which is filled with liquid foam.

The use of these hydrate storages will significantly increase the efficiency and competitiveness of natural gas storage technology in the form of gas hydrates.

### References

1. **Sloan, E. D.** (2003) Fundamental Principles and Applications of Natural Gas Hydrates. *Nature*, 426 (6964), 353-363. Retrieved from <https://www.nature.com/articles/nature02135>
2. **Carroll, J.J.**, (2002). *Natural Gas Hydrate: A Guide for Engineers*. Gulf Professional Publishing, Elsevier.
3. **Sloan, E. D., Jr., Koh, C., Sum A. K.** (2009) Natural Gas Hydrates in Flow Assurance. Colorado School of Mines, Summer workshop. June 10-12, 2009. Colorado. Retrieved from [http://hydrates.mines.edu/CHR/Workshop\\_files/Natural%20Gas%20Hydrates%20Workshop%202009.pdf](http://hydrates.mines.edu/CHR/Workshop_files/Natural%20Gas%20Hydrates%20Workshop%202009.pdf)
4. **Gudmundsson, J.-S., Parlaktuna, M., Khokhar, A.A.** (1994). Storage of Natural Gas as Frozen Hydrate. *SPE Production & Facilities*, 9(1), 69-73. <https://doi.org/10.2118/24924-pa>
5. **Gudmundsson, J.S., Parlaktuna, M.** (1991) Gas-in-ice: Concept evaluation. Technical report, Department of Petroleum Engineering and Applied Geophysics, Norwegian University of Science and Technology. Trondheim.
6. **Takeya, S., Ebinuma, T., Uchida T. et al.** (2002) Self-preservation effect and dissociation rates of CH<sub>4</sub> hydrate. *J. Crystal Growth*, V. 237 – 239, 379 -382.
7. **Riches, C.G., Gosling, P.D.**, (1998d). *Pneumatic Structures: A Review of Concepts, Applications and Analytical Methods*, 1998 Symposium of the Interna-

tional Association for Shell and Spatial Structures (IASS), v.2, Sydney, Australia, 5-8 October, 883-894.

8. **Herzog, T.** (1976), *Pneumatic Structures – a handbook for the architect and engineer* / Oxford University Press, New York

9. **Kawabata, M. and Ishii, K.** (1994), *Study on Structural Characteristics of Air-Inflated Beam Structures/ Proc of IASSASCE Int Symp on Spatial, Lattice and Tension Struct*, Atlanta, pp. 742-751

10. **Rehan Jamil, M. Atif Shehzad, Nasir Mehmood, Muhammad Atif Shehzad** (2005) *Study and adaptability of pneumatic structures*. Military College of Engineering, Risalpur National University of Sciences and Technology, Rawalpindi Pakistan, April 2005, 171.

11. **Raisinghani, M. and Tanwani, N.** (1986), *Pneumatic Structures-A Study/ J of Inst of Engineers (India), Part AR, Vol. 67, pp. 1-7*

12. **Subramanian, N.** (2019) *Building materials. Nesting and Sustainability*. Oxford university press, 386.

[13] **Pashchenko, T.M., Svitla, Z.I.** (2005) *Budivelne materialoznavstvo. K.*, 330p.

[14] *Pneumatic Structures: A Handbook of Inflatable Architecture* / Thomas Herzog, Gernot Minke, H. Eggers // Oxford University Press, 1986, 192 p.

[15] **Zhvan V. D.** *Zvedennia i montazh budivel i sporud: navch. posibnyk* / V. D. Zhvan, M. D. Pomazan, O. V. Zhvan; Khark. nats. akad. misk. hosp.-va. – Kh.: KhNAMH, 2011. – 395p.

[16] **Fedorov, A.B., Tiutiunnykov, A.Y.** (2004). *Терпозашчутные характеристики оhrzhdaiushchykh konstruksyi karkasno-tentovykh y naduvnykh sooruzheniy. Myr stroytelstva y nedvyzhymosti*, 4, 30–31p.

[17] **Ponomarchuk, I.A., Voloshyn, O.B.** (2004). *Ventyliatsiia ta kondytsiuvannia povitria. Vinnytsia: VNTU*, 121 p.

[18] *Budivelna klimatolohiia. Zakhyst vid nebezpechnykh heolohichnykh protsesiv, shkidlyvykh ekspluatatsiinykh vplyviv, vid pozhezhi. Natsionalnyi standart Ukrainy. DSTU – NBV.1.1-27:2010. Kyiv, Minrehionbud Ukrainy, 2011, 123 p.*

[19] **Ehorov Y. A.** *Yssledovanyia v oblasti razrabotky tekhnolohyy prouyzvodstva pennykh aэrozolei. – Kharkov, 1977.*

[20] **Shakhov, S. M., Kodryk, A. I., Nikulin, O. F., Titenko, O. M., Vinogradov, S. A., & Stylyk I. G.** (2019). *Визначення залежності характеристик компресійної піни. Науковий вісник НЛТУ України, 29(5), 103-106.*

<https://doi.org/10.15421/40290520>

[21] **Nikulin, O. F., Kodrik, A. I., Titenko, O. M., & Prisyazhnyuk, V. V.** (2018). *Rozroblennya eksperimentalnogo laboratornogo zrazka sistemi pinnogo pozhezhogasynnya, scho spozhivae stisnene povitrya. Naukoviy visnik: Tsvilniy zahist ta pozhezhna bezpeka*, 2(6), 4–9.

[22] *DBN V.2.6-31:2006 iz zm. №1 vid 1.07.2013r. Teplova izoliatsiia budivel./ Minbud Ukrainy.- K.: DP „Ukrarkhbudinformat”, 2006.- 70 p.*

**PROCESSING OF WASTE SHEET GLASS INTO  
SECONDARY RAW MATERIALS**



**Olena FEDOSKINA**

Candidate of Technical Sciences (Ph.D), Associate Professor in the Engineering and Generative Design Department, Dnipro University of Technology, Ukraine



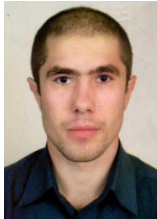
**Olena SVIETKINA**

Professor, Doctor of Technical Sciences (D.Sc.), Department of Chemistry, Dnipro University of Technology, Ukraine



**Kirill ZIBOROV**

Candidate of Technical Sciences (Ph.D), Associate Professor in the Engineering and Generative Design Department, Dnipro University of Technology, Ukraine



**Mikola YERISOV**

Assistant Lecturer of the Department of Automobiles and Automobile Economy, Dnipro University of Technology, Ukraine



**Valeriy FEDOSKIN**

Candidate of Technical Sciences (Ph.D), Associate Professor in the of the Department of Automobiles and Automobile Economy, Dnipro University of Technology, Ukraine



## **Abstract**

Hundreds of thousands of tons of flat glass waste are generated around the world every year. A huge amount of broken glass resulted from military operations. Recycling construction waste into secondary raw materials is an urgent task, the solution of which will save vast areas of land and natural resources. The purpose of the work is to determine the effectiveness of an innovative technological process for processing construction waste sheet glass into secondary raw materials using small-sized vibration equipment. The research was carried out according to the developed technological scheme, including a vibratory jaw crusher with an inclined crushing chamber, a vibratory dryer, a vibratory screen, and a vibratory mixer. The design features of the laboratory equipment make it possible to install a technological line for processing waste sheet glass at the zero level of the installation site, excluding the use of multi-level metal structures. Taking into account the degree of contamination of flat glass waste and the requirements of production technologies, a limit grain size is established, dividing the crushed product into two classes by size. When processing waste glass according to the developed technological scheme, it is possible to obtain clean glass with a sharp or rounded edge. Laboratory testing of an innovative technological scheme for obtaining secondary raw materials from sheet glass waste using small-sized vibration equipment showed the feasibility and effectiveness of the dry method of processing the source material.

## **Introduction**

Sheet glass is a widely used material based on natural resources, mainly quartz sand, soda ash and limestone. Glass is a durable, inert and brittle material [1, 2], which can be recycled and reused countless times without loss of quality or purity. Currently, the global flat glass market volume is 11.2 billion square meters. According to the forecast of the international analytical company Freedonia, consumption of flat glass will increase by 4.9% annually, reaching 14.3 billion square meters in 2027. An increase in glass production also predetermines an increase in waste, the annual generation of which amounts to hundreds of thousands of tons, but only a small part of it becomes secondary raw materials [3]. Glass waste is a serious environmental problem worldwide [4, 5, 6]. They occupy vast areas of the earth's surface suitable for agricultural and industrial production, and pollute the air, water and soil. Almost without decomposing and retaining sharp chips, cullet is dangerous for animals and people.

Recycling this waste and reusing glass can conserve vast areas of land and natural resources, minimize landfill space and save significant amounts of energy. Producing 1 ton of glass from sand, soda and other materials requires 3 times more energy than using recycled glass. One ton of cullet saves 1.5 tons of mineral glass raw materials,

incl. 100-130 kg of soda ash, 40-50 kg of sodium sulfate and 300-350 kg of quartz sand. [7, 8]. In addition, it helps reduce greenhouse gas emissions.

The sources of glass waste are the production process of products at glass factories, municipal solid waste, trimmings during sheet cutting and installation work, modernization, repair and demolition of buildings. A huge amount of glass waste was generated as a result of hostilities. According to calculations of the Kyiv School of Economics, as of the end of 2022, there were more than 150 thousand damaged or destroyed residential buildings in Ukraine [9], and this is hundreds of thousands of tons of glass waste, which it is advisable to process at the site of their generation into secondary raw materials and use them during construction new buildings.

In order to effectively use recycled glass raw materials, a large amount of research is being carried out and the search for new areas of its application is being carried out. One of the most widely used materials in the world is concrete and its constituent cement. Today, annual global cement production has exceeded 3 billion tons and continues to increase [10].

The cement industry is one of the largest industrial sources of greenhouse gas emissions. It has been estimated that each ton of clinker produces one ton of CO<sub>2</sub> [11, 12].

Waste glass and natural sand have approximately the same physical properties, which served as the basis for a possible partial replacement of sand in the production of concrete. Despite the fact that the percentage of glass introduced into the concrete mixture is insignificant, hundreds of thousands of tons of recycled glass raw materials will be used in the overall production of concrete.

Currently, a large amount of research is being carried out on the use of glass waste as aggregate in concrete [13]. One of the research objectives is aimed at determining the rational percentage of glass waste that is acceptable for use as a filler without any impact on the properties of the resulting concrete. In [14], partial replacement of sand with 10%, 15% and 20% was considered. The results confirmed 80% pozzolanic strength activity of the waste glass after 28 days. The flexural strength and compressive strength of the samples containing 20% glass waste were 10.99% and 4.23% higher, respectively, than the control sample after 28 days [15]. Tests using mortar

showed that finely ground glass helped reduce expansion by 66% compared to the control mixture. The size of glass waste aggregate particles has a significant impact on the quality of concrete.

Studies were carried out for a wide range of crushed glass grains 0.15-4.75 mm [16, 17], and in [18] it was shown that it is safe to use glass waste with a particle size of 36-50 mm as filler. One of the main uses of glass waste is adding it to the batch of glass melting furnaces. However, in this case, the cullet introduced into the charge must be sorted from foreign impurities, washed, dried and sorted by color in order to match its chemical composition to the composition of the glass being produced. The penetration rate and homogeneity of the glass mass when using glass chips is higher compared to uncrushed glass.

Currently, glass waste is used for the production of fiberglass, foam glass, glass-ceramics and glass-ceramic tiles, characterized by durability, frost and weather resistance, construction and facing bricks, they are used for road construction, as fillers for plastics, rubber, paints and other materials. Currently existing glass processing technologies do not have any noticeable differences; obsolete equipment is used in the form of jaw, rotary, and roller crushers with a low degree of crushing and a multi-stage technological process.

At the same time, in the technological process chain, the crushing and grinding operation is the most expensive due to the consumption of a significant amount of electricity, the high cost of repairs, and the replacement of rapidly wearing crushing elements.

This necessitates the creation of highly efficient small-sized installations that provide a complete technological process for processing minerals, including the preparation of source material, crushing and grinding operations and the separation of a commercial product and indicates the relevance and need for analytical, experimental, design developments aimed at increasing the efficiency of obtaining fine-grained and powder materials directly from glass waste.

**Goal of the work.** To determine the effectiveness of an innovative technological process for processing construction waste sheet glass into secondary raw materials using small-sized vibration equipment.

**Method and materials.** The studies were carried out on laboratory samples of the developed innovative equipment according to the technological diagram presented below (Fig. 1).

Glass sorting is the most labor-intensive process; it is done manually and can be performed directly on the site of a destroyed building or at a construction waste site.

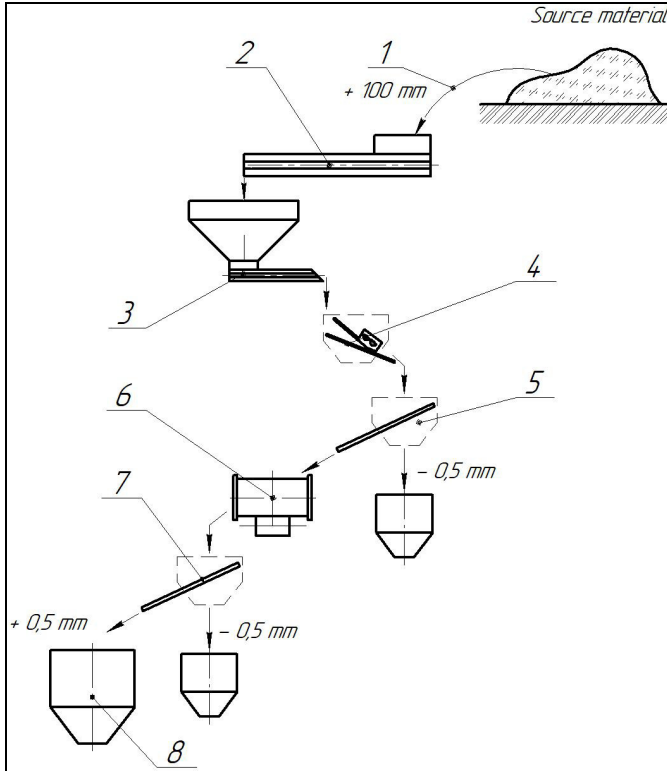


**Fig. 1.** Circuit diagram of the equipment line for the production of commercial glass chips: 1 - sorting, 2 - vibrating dryer, 3 - feeder, 4 - vibrating crusher, 5 - under-size product hopper, 6 - mixer, 7 - vibrating screen, 8 - secondary raw material hopper

Depending on the degree of destruction of the building [19, 20, 21], the complexity of sorting construction waste is estimated. The least time-consuming and most productive sorting of waste is in buildings of the first category, with up to 40% destroyed (Fig. 2a). In

the presence of a mobile mobile crushing plant, in most cases, it is possible to dispense with the storage of glass by loading the waste directly into the crusher. Serious difficulties arise during the disassembly of those that have the third category of destroyed (Fig. 2*b*). At the same time, a complete sampling of glass waste is not always possible, a site is required for storage and drying of waste before loading it into the crusher.

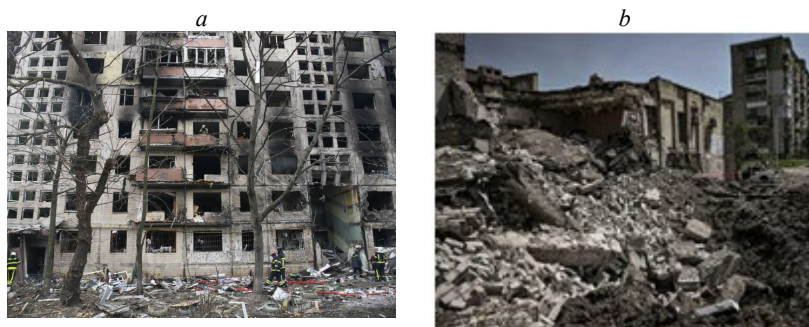


**Fig. 2.** Destroyed buildings: *a* - minor damage to the enclosing structures; *b* - load-bearing objects that are not suitable for use as intended

Drying can be carried out naturally with the placement of waste under a canopy or with the use of a drying unit. In this study, a laboratory vibro-drying installation of conductive action was considered. The dryer (Fig. 3) contains a vibrating conveyor 1, fixed with the possibility of relative rotation on a heat-insulating frame 2, which rests on supporting elastic elements 3 and is driven into oscillating motion by a vibration exciter 4 of directional action. Shades are installed under the flat working surface 5, which provide heating of the work surface and drying of the material. In fig. 3 the upper cover of the vibrating conveyor, which forms the drying chamber, is conditionally not shown.

If the initial humidity of the glass waste is high, the flat working surface 5 of the vibrating conveyor can be replaced with a perforated one and a convective drying method can be installed. A special feature of the vibration drying unit is the end location of the loading and unloading window, which eliminates the need to install vertical bins and large metal structures.

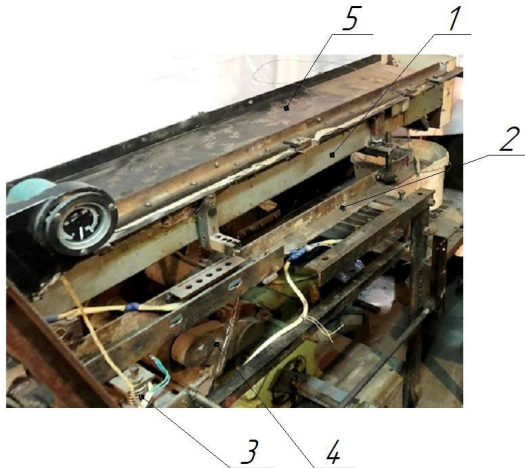


**Fig. 3.** Vibration drying unit: 1 - vibration conveyor, 2 - thermal insulating frame, 3 - elastic elements, 4 - self-balanced vibration exciter, 5 - working surface

Crushing was carried out on a laboratory sample of a vibrating jaw crusher with an inclined chamber [22]. This type of crusher has a pronounced impact nature of the application of load to the crushed material, and has the advantages of jaw and rotary crushers. Having a large set of adjustable parameters, the process of material destruction is effectively controlled.

In general, the design diagram of the vibratory crusher represents an oscillatory system in which vibrations with a frequency of 16-32 Hz are transmitted to the jaws. The crusher (Fig. 4) includes a passive (lower) crushing jaw 1, mounted on elastic elements 5 and simultaneously serving as a housing.

The active jaw 3 is installed in the racks of the passive jaw by means of the suspension axis 2, relative to which it can perform rotational oscillations. The vibrations of the jaws are generated by a two-shaft inertial vibration exciter 4. The destruction of the material occurs in the crushing chamber formed by the working surfaces of the passive 1 and active 3 jaws. The design feature of the crusher allows loading of the source material and unloading of the crushed product in a horizontal plane, which is especially important when processing sheet material.

*a*

*b*

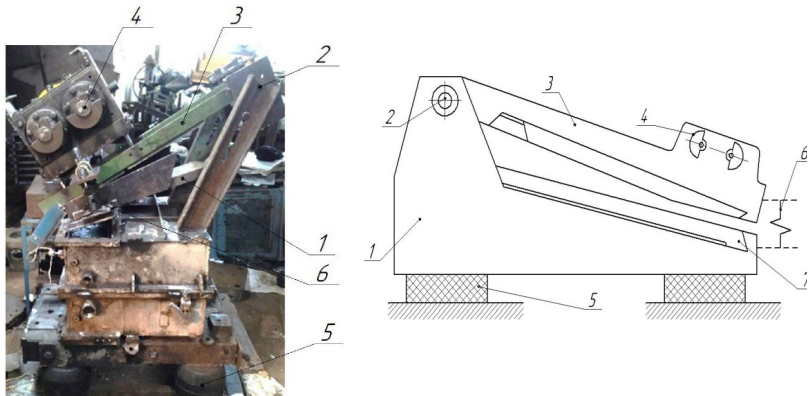


**Fig. 4.** Vibrating jaw crusher with an inclined chamber: *a* – general view of the crusher, *b* – structural diagram: 1 - passive jaw; 2 - suspension axis; 3 - active jaw; 4 - vibration exciter; 5 - elastic elements; 6 - elastic element; 7 - lining

#### Technical characteristics of the crusher

Dimensions of the receiving window, mm	130×100
Height of unloading slot, mm	0-50
Crushing chamber length, mm	500
Angle of inclination of the lower jaw, Rad	0-0.9
Jaw vibration frequency, Hz	0-25
Dimensions, mm	
length	1000
width	600
height	1200

The technical characteristics of the crusher, as the main unit of the technological chain, are the basis for determining the parameters of related equipment. Separation of crushed material was carried out on a screen with end docking windows.

The source material was sorted from a construction waste dump and is 4 mm thick sheet glass. Taking into account the width of the crushing chamber of a laboratory sample of a vibrating jaw crusher, following the destruction of glass on a impactor, pieces (Fig. 5) with a particle size of 100-130 mm were selected



**Fig. 5.** Primary state of glass waste

The broken glass has a sharp chip, the flat surface is covered with mud and paint in places, the edges contain putty residues. In the process of crushing the material, the vibration frequency of the cheeks was 16.7 Hz, the width of the unloading gap in a stationary position was taken to be 0 mm and 10 mm. Such limiting values of the slot width are taken from the condition of assessing the influence of one of the crusher control parameters on the particle size distribution of the crushed product.

A qualitative picture of the surface of crushed glass (Fig. 6*a,b*) shows different densities of grains, depending on the width of the unloading slot. On the surface there are dark grains of the broken mud component of the original material.

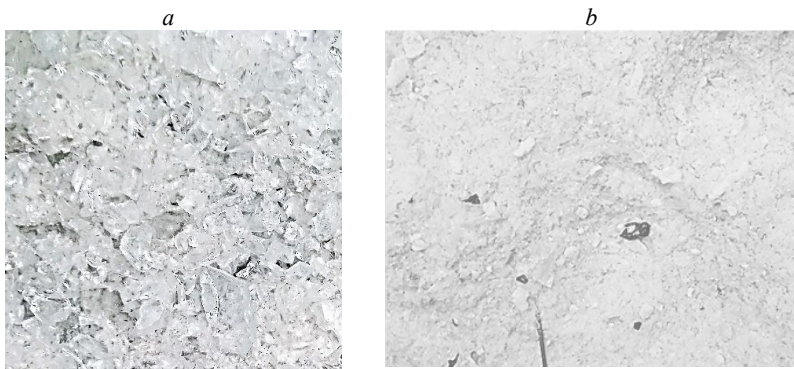


**Fig. 6.** Crushed waste sheet glass at the discharge slot: *a* – 10 mm; *b* – 0 mm



Some manufacturing processes do not allow sharp chipping of glass chips. In this regard, a vibrating mixer was introduced into the technological chain under study. The qualitative picture (Fig. 6*a,b*) of the results obtained shows a high degree of roundness (Fig. 6*b*) and the feasibility of using a vibrating mixer to change the surface shape of crushed glass

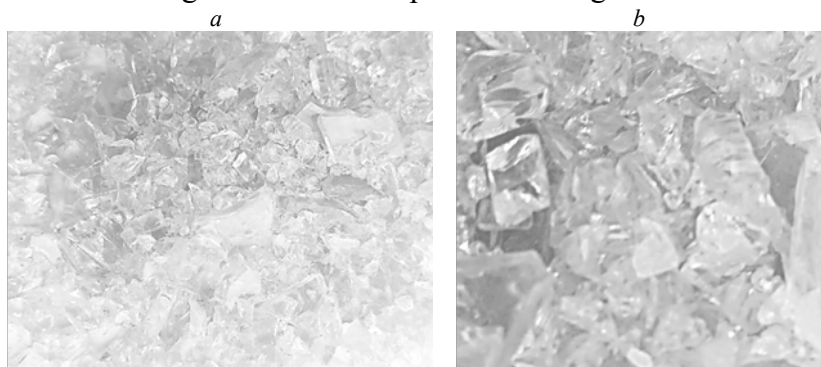


**Fig. 7.** Shape of the end surface of the glass: *a* – sharp chip; *b* – rounded chip

The crushed material on a vibrating screen was separated into a size of 0.56 mm, corresponding to one of the standard size classes of graded sand.

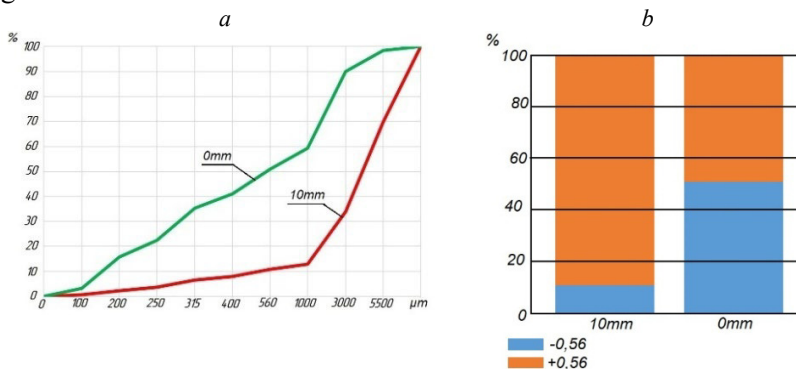


**Fig. 8.** Characteristics of crushed glass size: *a* – graphical dependence; *b* – diagram

As can be seen from the graphical dependence (Fig. 8a), the width of the unloading slot significantly affects the granulometric composition of the crushed material, which shows the possibility of changing the content of the required size class in the finished product. If we take the size of the finished secondary raw material +0.56 mm (based on production or other requirements), its percentage content differs by 5 times.

### **Conclusions**

1. Laboratory testing of an innovative technological scheme for obtaining secondary raw materials from sheet glass waste using small-sized vibration equipment showed the feasibility and effectiveness of the dry method of processing the source material.

2. The limiting grain size dividing the crushed product into two classes by size is taken into account the degree of contamination of flat glass waste and the requirements of production technologies.

3. The design features of the tested laboratory equipment make it possible to install a technological line for processing waste sheet glass at zero level of the installation site, excluding the use of multi-level metal structures.

4. The technological capabilities of the tested laboratory equipment make it possible to obtain clean glass with a sharp or rounded edge.

### *References*

1. **Shelby, J.E.** (2020). Introduction to glass science and technology. Cambridge: Royal society of chemistry.

2. **Musgraves J. D., Hu J. & Calvez L.** (Eds.). (2019). Springer handbook of glass. Cham : Springer.

3. **Meyer, C.** (2001). Recycled glass - from waste material to valuable resource. Int.Symposium on Recycling and Reuse of Glass Cullet , University of Dundee, Scotland.

4. **Du, H. & Tan, K.H.** (2013). Use of waste glass as sand in mortar: Part II – Alkali–silica reaction and mitigation methods. Cement and Concrete Composites, 35,118–126, <http://dx.doi.org/10.1016/j.cemconcomp.2012.08.029>.

5. **Tamanna, N., Sutan, N.M., Lee, D. T. C. & Yakub, I.** (2013). Utilization of waste glass in concrete. 6th International Engineering Conference, Energy and Environment (ENCON), Kuching, Sarawak, Malaysia [http://dx.doi.org/10.3850/978-981-07-6059-5\\_090](http://dx.doi.org/10.3850/978-981-07-6059-5_090)
6. **Kvasha, T., Paladchenko, O. & Molchanova, I.** (2020). Perspektivni svitovi naukovi ta tekhnolohichni napriamy doslidzhen u sferi «Vidkholdy»: monohrafiia. [Promising global scientific and technological directions of research in the field of "Waste": monograph]. <http://doi.org/10.35668/978-966-479-113-4>. (in Ukr.).
7. **Hogland, W.** (2002). Remediation of an old landfill site. *ESPR-Environmental Science*, 9, 49–54.
8. **Mutafela, R.N., Mantero, J., Jani, Y., Rimon, T., Holm, E. & Hogland, W.** (2020). Radiometrical and physico-chemical characterisation of contaminated glass waste from a glass dump in Sweden. *Chemosphere*, 241, 124964. <https://doi.org/10.1016/j.chemosphere.2019.124964>.
9. **Nastych, I.** (2023). Budivselne smittia: vyrishennia problemy zalezhyt vid politychnoi voli ta hotovnosti vprovadzhuvaty reform. [Construction waste: solving the problem depends on political will and willingness to implement reforms]. [https://propertytimes.com.ua/spetsproekti/budivselne\\_smittya\\_vyrishennya\\_problemi\\_zalezhit\\_vid\\_politychnoyi\\_voli\\_ta\\_gotovnosti\\_vprovadzhuvaty\\_reformi](https://propertytimes.com.ua/spetsproekti/budivselne_smittya_vyrishennya_problemi_zalezhit_vid_politychnoyi_voli_ta_gotovnosti_vprovadzhuvaty_reformi). (in Ukr.).
10. **Schneider, M., Romer, M., Tschudin, M. & Bolio, H.** (2011). Sustainable cement production—present and future. *Cement and Concrete Research*, 41, 642–650. <http://dx.doi.org/10.1016/j.cemconres.2011.03.019>.
11. **Ali, M.B., Saidur, R. & Hossain, M.S.** (2011). A review on emission analysis in cement industries. *Renewable and Sustainable Energy Reviews*, 15, 2252–2256. <http://dx.doi.org/10.1016/j.rser.2011.02.014>.
12. **Rehan, R. & Nehdi, M.** (2005). Carbon dioxide emissions and climate change: policy implications for the cement industry. *Environmental Science & policy*, 8, 105–114. <http://dx.doi.org/10.1016/j.envsci.2004.12.006>
13. **Jani, Y. & Hogland, W.** (2014). Waste glass in the production of cement and concrete – A review. *Journal of Environmental Chemical Engineering*, 2, 1767–1775. doi:10.1016/j.jece.2014.03.016
14. **Ismail, Z.Z. & Al-Hashmi, E. A.** (2009). Recycling of waste glass as a partial replacement for fine aggregate in concrete. *Wastemanagement*, Vol.29, 2, 655–659.
15. **Ucol-Ganiron Jr, T.** (2012). Recycled window glass for non-load bearing walls. *International Journal of Innovation, Management and Technology*, Vol.3, 6, 725–730. doi: 10.7763/IJIMT.2012.V3.327.
16. **Takata, R., Sato, S., Nonaka, T., Ogata, H., & Hattori, K.** (2004, August). Investigation on alkali–silicic acid reaction utilizing waste glass in concrete and

suppression effect by naturalzeolite. In 29th Conference on our world in concrete and structures . Vol. 25, 26.

17. **Idir, R., Cyr, M. & Tagnit-Hamou, A.** (2010). Use of fine glass as ASR inhibitor in glass aggregate mortars. *Construction and Building Materials*, Vol. 24, 7, 1309-1312. <https://doi.org/10.1016/j.conbuildmat.2009.12.030>.

18. **Corinaldesi, V., Gnappi, G., Moriconi, G. & Montenero, A.** (2005). Re-use of ground waste glass as aggregate for mortars. *Waste Management*, Vol. 25, 2, 197–201. <https://doi.org/10.1016/j.wasman.2004.12.009>.

19. **Beliukina, N.** (2023). Praktychni rekomendatsii za rezultatamy realizatsii proiektu «Stvorennia interaktyvnoi onlain-platfomy dlia kartohrafuvannia zbytkiv, poviazanykh iz viinoiu, iz klasyfikatsiieiu zruinovanykh ob'ektiv za typom i stupenem poshkodzhennia u 20 pilotnykh hromadakh iz vykorystanniam heoinformatsiinykh system». [Practical recommendations based on the results of the implementation of the project “Creation of an interactive online platform for mapping conflicts associated with the war, from the classification of constructed objects by type and stage by harm in 20 urban communities from the use of geographic information systems.”]. [https://www.undp.org/sites/g/files/zskgke326/files/2023-10/practical\\_recommendations\\_on\\_determining\\_the\\_destruction\\_of\\_buildings.pdf](https://www.undp.org/sites/g/files/zskgke326/files/2023-10/practical_recommendations_on_determining_the_destruction_of_buildings.pdf). (in Ukr.).

20. Cabinet of ministers of Ukraine (2022, June 24). Postanova №726 Pro realizatsiiu eksperymentalnoho proektu shchodo monitorynhu zavdanykh poshkodzhen ta ruinuvan za rehionamy Ukrainy vnaslidok zbroinoi ahresii Rosiiskoi Federatsii na osnovi heoinformatsiinoi systemy. [Resolution No. 726 On the implementation of an experimental project on monitoring the damage and destruction caused by the regions of Ukraine as a result of the armed aggression of the Russian Federation on the basis of the geoinformation system]. <https://zakon.rada.gov.ua/laws/show/726-2022-%D0%BF#Text>. (in Ukr.).

21. Ministry of development of communities and territories of Ukraine (2022, April 24). Nakaz № 65 Metodyka obstezhennia budivel ta sporud, poshkodzhenykh vnaslidok nadzvychainykh sytuatsii, boiovykh dii ta terorystychnykh aktiv. [Decree No. 65 Methodology for the inspection of buildings and structures damaged as a result of emergency situations, hostilities and acts of terrorism.]. <https://advokat-bti.com.ua/ua/obstezhennya-budivel-i-sporud-shho-zaznaly-poshkodzhen-i-rujnuvan-vnaslidok-zbrojnoyi-agresiyi-rosijskoyi-federatsiyi/> (in Ukr.).

22. **Fedoskina, O.V., Franchuk, V.P., Fedoskin, V.O. & Haddad J.S.** (2022). Improving the efficiency of the impact crusher with inclined working chamber. *Geo-Technical Mechanics*, 161, 66-74.

**CONSTRUCTION AND DESIGN OF BUILDINGS AND STRUCTURES UNDER MARTIAL LAW. NEW CHALLENGES AND WAYS TO ADDRESS THEM**



**Oleksandr SHASHENKO**

Doctor of Technical Sciences, Professor of the Department of Building, Geotechnics and Geomechanics of Dnipro University of Technology, Ukraine



**Volodymyr SHAPOVAL**

Doctor of Technical Sciences, Professor of the Department of Building, Geotechnics and Geomechanics of Dnipro University of Technology, Ukraine



**Oleksandr SKOBENKO**

Candidate of Technical Sciences, Associate Professor of the Department of Building, Geotechnics and Geomechanics, Dean of the Faculty of Architecture, Building and Land Management of Dnipro University of Technology, Ukraine



**Bohdan MORKLIANYK**

Doctor of Technical Sciences, Professor of the Department of Strength of Materials and Structural Mechanics Lviv Polytechnic National University, Ukraine



**Sofiia BARSUKOVA**

PhD student of the Department of Building, Geotechnics and Geomechanics of Dnipro University of Technology, Ukraine

**Abstract**

This paper is a result of the detailed analysis, carried out by a group of scientists at Dnipro University of Technology, of the circumstances and situation in the field

of construction, operation, and design of residential, communal, and industrial infrastructure facilities, which emerged after the full-scale invasion of Russia into Ukraine.

It formulates the new requirements that we devised for the construction of new, and reconstruction of existing buildings and structures, as well as for design and construction documentation.

The material presented in the current paper can be conditionally divided into 5 parts:

1. Legal and organizational foundations of the civil protection system.
2. Patterns of damage to civilian population in the course of military operations of various types and under various conditions.
3. Tendencies and patterns of destruction and damage to buildings and structures of various purposes and with various structural features during modern hostilities.
4. Modern principles, methods, and structures designed to protect civilian population in different countries.
5. Conclusions and recommendations regarding the calculation and design of cities, towns, buildings, and structures under conditions of the danger of conducting military operations.

## **Introduction**

First, we shall consider the legal provisions based on which protection of the population (including civilians) of Ukraine should be carried out [1].

According to the Code of Civil Protection of Ukraine [2], every citizen of Ukraine has the right to protect his/her life and health from the consequences of accidents, disasters, fires, natural disasters, as well as for guarantees of ensuring the implementation of this right, including by sheltering in protective structures.

To ensure this right, Ukraine currently employs a Unified State System of Civil Protection, which has a rather complex and extensive organizational structure (Fig. 1). One of the important links in ensuring the safety of civilian population is the presence of protective structures. In the case of emergencies (technical, military, etc.), these structures provide civil protection of the population. It should also be noted that protective facilities are included in the civil defense system of Ukraine, as well as in the engineering service and the storage and shelter service.

In order to understand the need for certain properties that protective structures and shelters must possess under modern conditions, let us consider the data given in [3]. The authors analyzed the nature and type of population damage depending on the location

in relation to the front of hostilities (see also [4, 5, 6, 7, 8]). At the same time, the time range from World War I to the present time is considered (Table 1, Figs. 2 and 3).

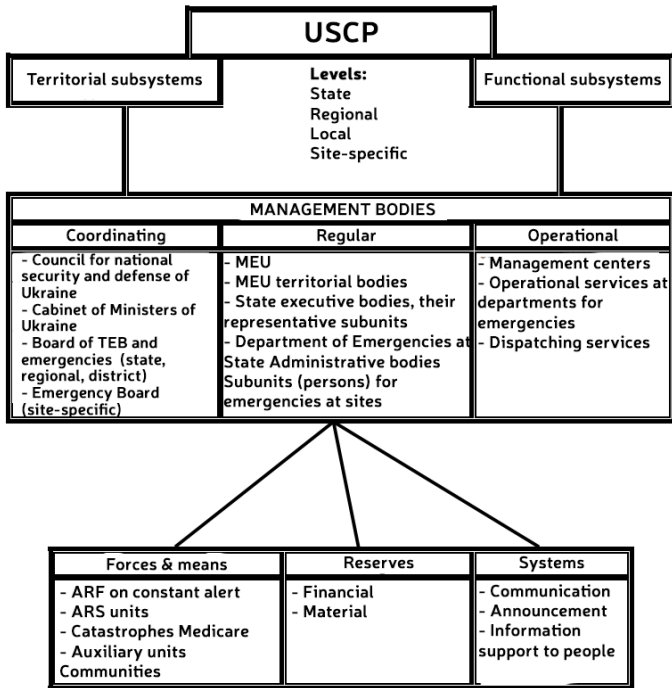


**Fig. 1.** Structure of the Unified State System of Civil Protection

Table 1

The percentage of injuries to the personnel of the armed forces and civilian population in the course of various conflicts

Damage type	The percentage of injuries to the personnel of the armed forces and civilian population during various conflicts									
	I		II		III		IV		V	
	Fatalities, %	Injured, %	Fatalities, %	Injured, %	Fatalities, %	Injured, %	Fatalities, %	Injured, %	Fatalities, %	Injured, %
1	35	42	50	32	49	40	67	34	-	-
2	65	58	12	46	41	43,2	18	51	-	-
3	-	-	38	22	10	16,8	15	16	5	5
4	-	-	-	-	-	-	-	-	-	95

Notes. The following designations are used in the table:1. In the first column of this table: 1 - bullet injuries; 2 - shrapnel damage; 3 - mine-explosive injuries; 4 - damage by powerful explosive devices with a large radius of action. I - losses during World War II (1941-1945); II - losses of the USSR during the Afghan war (1979-1989); III - losses of the Russian Federation during the first Chechen war (1994-1996); IV - losses of the Russian Federation during the second Chechen war (1999-2001); V - victims among civilians in Ukraine from February 24 to October 2, 2022 (according to the UN Human Rights Monitoring Mission in Ukraine).

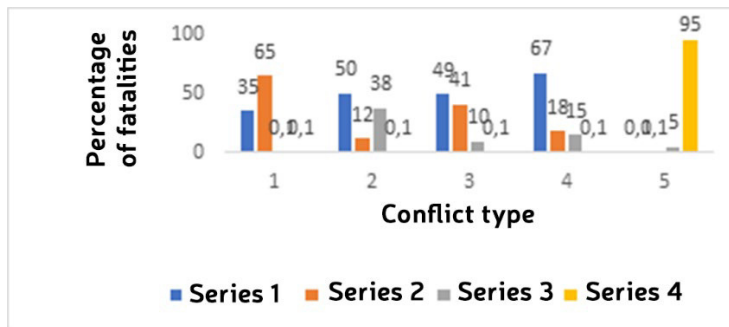


Fig. 2. The percentage of fatalities during military operations

Notes. In Fig. 1, the following notations are used: series; 1 - bullet injuries; series; 2 - the same, shrapnel; series 3 - the same, mines - explosive; 4 - damage by powerful explosive devices with a large radius of action. The following designations are used along the abscissa axis: 1 - losses during World War II (1941-1945); 2 - losses of the USSR during the Afghan war (1979-1989); 2 - losses of the Russian Federation during the first Chechen war (1994-1996); 4 - losses of the Russian Federation during the second Chechen war (1999-2001); 5 - victims among civilians in Ukraine from February 24 to October 2, 2022 (according to the UN Human Rights Monitoring Mission in Ukraine).



Analysis of the data given in Table 1 and Fig. 2 and 3 allowed us to conclude that there is a clear trend of increasing injuries to population by shrapnel (a consequence of artillery and mortar attacks), as well as injuries by powerful explosive devices with a large radius of action.

This trend holds both for fatalities (Fig. 2) and for injuries to people (Fig. 3).

It was concluded that modern protective structures should protect the population from shrapnel injuries, as well as from explosions of great force.

At the same time, it is understandable that protection against potential threats from nuclear, chemical, and bacteriological weapons should be provided for.

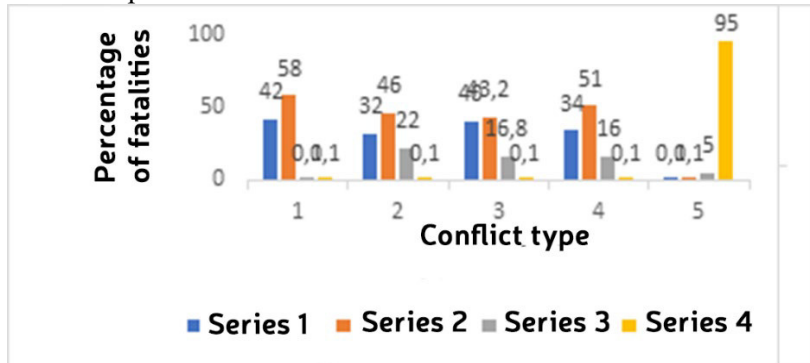


**Fig. 3.** Percentage of injuries during military operations. Notes: Series 1, 2, 3, and 4; numbers 1, 2, 3, 4, 5 along the abscissa axis refer to explanations in Fig. 2

Next, we shall consider modern trends in the destruction of buildings and structures of various purposes in the course of military operations, as well as damage to their various parts and structures on the example of such cities as Kyiv, Kharkiv, Odesa, Mariupol, Chernihiv, and Irpin [5, 6, 7, 8, 9, 10].

In this case, the destruction and damage to buildings and structures in such cities as Kharkiv and Mariupol are the most characteristic.

This data is valuable from the point of view that the shelling and bombardment of these places was carried out using aviation, field and long-range artillery, rocket launchers and mortars.

In addition, during the street fighting in Mariupol, small arms were used very intensively.

The structure of damage and destruction of buildings and structures in the city of Kharkiv is shown in Fig. 4. Analysis of the presented data allowed us to conclude that windows are most often destroyed in the shelling zone. Next (in descending order) are roofs, walls, and porches.

Next, we shall analyze the regularities of the destruction in the city of Mariupol. According to the UN, up to 90 % of residential buildings and up to 60 % of private houses in the city were damaged or destroyed as a result of the fighting.

In addition, a clear tendency was revealed to launch rocket and artillery strikes on critical infrastructure objects, as well as on high-rise and other residential buildings, grocery stores, and objects of other civil infrastructure, in particular, a drama theater, maternity hospitals, etc.

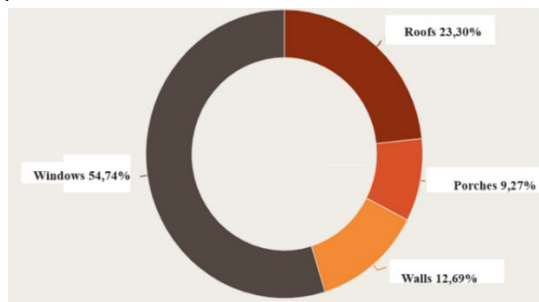


**Fig. 4.** Distribution of damage to various elements of buildings and structures in the city of Kharkiv as a result of military actions

At the same time, there were issues of damage to the population by fragments of explosive devices, fragments of glass and building structures.

Such damage took place both in the open space (on the streets and squares of the city) and inside the premises.

In addition, a huge problem was the need to liberate the civilian population hiding in the underground parts of buildings and structures, from under the debris of buildings and facilities destroyed during shelling (that is, rubble).

It also turned out to be a big surprise that a large part of the civilian population refused to move to premises safer than their apartments (i.e., bomb shelters, underground parking lots, subway stations, and other protective structures) after the announcement of the air raid alert. At the same time, the motivation behind this behavior turned out to be the following:

1. Health status of the elderly.
2. Long distance from the place of residence to protective structures.
3. The danger of being hit by fragments of explosive devices, buildings, structures, and other objects on the way from the place of residence to the protective structure.
4. The impossibility of evacuating people from under the rubble above protective structures located under residential buildings.
5. Insufficient thickness of ceilings above bomb shelters located in the basements of residential buildings and structures.



**Fig. 5.** Nature of damage and scheme of destruction of a panel building in the town of Borodyanka



**Fig. 6.** Nature of damage and scheme of destruction of a panel building in the city of Mariupol

In general, it was concluded that when designing structures for the protection of civilian population, it is necessary to ensure their protection from bullets, debris, and high-power explosions, and to ensure the possibility of evacuation from under the debris of structures of buildings and facilities destroyed during hostilities.

Next, we shall analyze the nature of damage to buildings and facilities with different structural implementation of load-bearing structures made of different materials [10].

The buildings were divided into the following groups:

- panel houses in the cities of Borodyanka and Mariupol with carrying or transverse load-bearing walls and floors made of precast reinforced concrete;

- brick buildings in the cities of Chasiv Yar, Kharkiv, and Chernihiv with carrying or transverse load-bearing walls and floors made of precast reinforced concrete;

- buildings in the cities of Kyiv and Odesa made of monolithic reinforced concrete with a spatial frame and a rigid reinforced concrete core (the functions of the core are performed by an elevator shaft).

Fig. 5 and 6 show photographs and diagrams of damage to panel buildings in Borodyanka (Fig. 5) and Mariupol (Fig. 6). These houses are built from reinforced concrete wall panels on which reinforced concrete floor slabs rest.

The destruction of these buildings includes the following common features:

- windows, doors, and partitions destroyed by the blast wave;
- traces of fires;
- avalanche-like destruction of load-bearing structures.

The essence of an avalanche-like destruction is that due to the action of weight from the structures of the destroyed upper floors, the load on the lower floor of the building increases. This leads to its destruction, due to which the load on the lower floor of the building increases. This process continues until the porch or house is completely destroyed. The procedures (more precisely, express methods) for determining the additional pressure on the inter-floor ceiling from the destroyed structures located above the floors and the method for determining the thickness of the ceiling above bomb shelters are given, respectively, in works [11] and [12].

In general, it was concluded that the main problems of panel buildings in the case of their damage by explosive devices are the destruction of windows, doors, partitions, fire, and avalanche-like destruction of supporting structures.

Fig. 7, 8, and 9 show photographs and diagrams of damage to brick buildings in the town of Chasiv-Yar (Fig. 7), in the city of Kharkiv (Fig. 8), and in the city of Chernihiv (Fig. 9). These houses have brick walls supported by reinforced concrete floor slabs.

On July 10, 2022, a brick dormitory building was destroyed in the town of Chasiv Yar in Donetsk region as a result of rocket fire. 4 rockets hit the house. 48 people died from the raids.

The photograph and the diagram in Fig. 7 demonstrate that the reinforced concrete inter-floor ceilings rest on brick load-bearing longitudinal walls. In this case, as a result of the destruction of the front wall of the building, the supports under the floor slabs were destroyed, as a result of which the building collapsed.

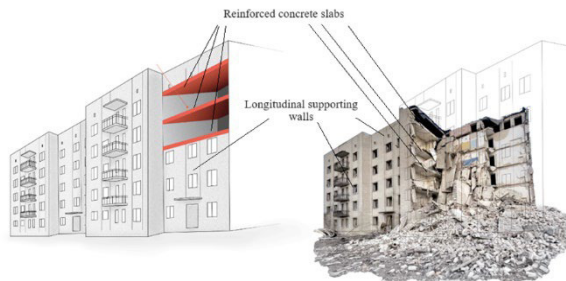


**Fig. 7.** Nature of damage and scheme of destruction of a brick building in the town of Chasiv-Yar

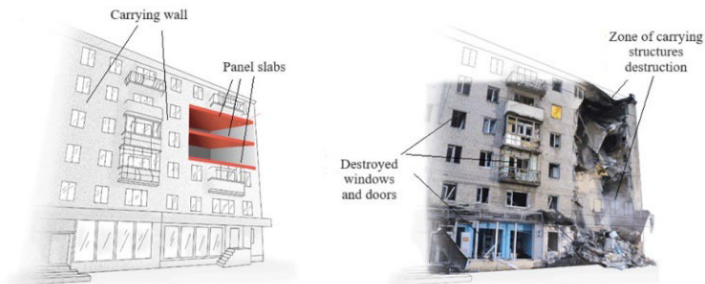


**Fig. 8.** Nature of damage and scheme of destruction of a brick building in the city of Kharkiv

In the city of Kharkiv, as a result of rocket fire on July 11, 2022, a brick building built in the 1960s in the historical center of Kharkiv was destroyed, and there were no casualties.

The photograph and the diagram in Fig. 8 demonstrate that the reinforced concrete inter-floor ceilings rest on brick load-bearing longitudinal walls.

In this case, as a result of the destruction of the front wall of the building, the supports under the floor slabs were destroyed, as a result of which the building collapsed. Thus, the nature and causes of the destruction in this case are completely identical to those discussed earlier (that is, the building in Chasiv Yar).

The "Ukraine" hotel building destroyed on the night of March 12, 2022, in Chernihiv is of interest in the sense that it was probably destroyed with the use of an Iskander missile (Fig. 9).

Also, in this case, there are the following differences from the cases considered above:

- reinforced concrete floor slabs are made of narrow slabs of the beam type;
- the walls of the building are much thicker than in the two considered cases.

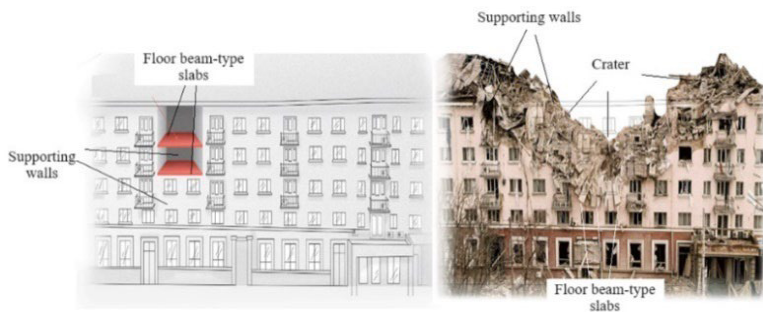


**Fig. 9.** Nature of damage and the scheme of destruction of the brick building of the "Ukraine" hotel in the city of Chernihiv



**Fig. 10.** Nature of damage and the scheme of destruction of the brick building of the "Ukraine" hotel in the city of Chernihiv

In this case, the destruction repeats the contour of the crater, as if the explosive device fell to the ground. One can see that, in this case, the rather strong and thick walls on the lower floors stayed put while the floor slabs were completely destroyed.

In general, it was concluded that the main problems of brick buildings in the case of their damage by explosive devices are the destruction of windows, doors, partitions, fire, avalanche-like destruction of load-bearing structures, and the destruction of slab supports and beams of floor coverings.

Next, we shall consider the characteristic damage to buildings that had been built according to the frame scheme.

The damage to the building in Irpin near Kyiv in the residential complex "Irpinski Lypky" (Fig. 10) is interesting from the point of view that this building was mostly damaged by fire, and not by explosions. In this case, there was damage to concrete (deterioration of properties, cracking, peeling, etc.), exposure and deterioration of the properties of reinforcement.



**Fig. 11.** Nature of damage to a multi-story building with a reinforced concrete frame

Such consequences of the fire are due to the fact that because of shelling it could not be extinguished within the standard time (1–2 hours). If the building had been equipped with an automatic fire extinguishing system, severe damage and destruction of its supporting structures would not have occurred.

In conclusion, we shall consider the structures of buildings, which are very promising from the point of view of living under wartime conditions.

These are buildings made of reinforced concrete, on a slab or pile foundation, with a monolithic frame and a monolithic stiffness core, the functions of which are performed by the elevator shaft and capital walls around the stairs.

First, let us consider a building located in the city of Kyiv near Zhuliany airport (Fig. 11), which was hit by a Russian missile on February 26 at the level of 17–20 floors. 2 people died, and 4 were injured. Fig. 11 shows that the damage to the building is local and there are no avalanche-like destructions of the floors above and below the place where the rocket hit.

Exactly the same picture was observed after a missile launched from a Tu-95 aircraft hit a high-rise building in Odesa on April 23 (Fig. 12). The rocket hit between the fourth and fifth floors, 8 people died, 18 were injured.



For comparison, the same figure (i.e., Fig. 12) shows the consequences of a rocket hitting a panel house in the city of Dnipro (it happened on January 14, 2023, at the level of the third floor), as a result of which 46 people died (11 of them were not identified and 11 were missing), and 80 people were injured [13].



**Fig. 12.** Nature of damage to multi-story buildings: panel (left image) and reinforced concrete frame (right image)

Fig.12 demonstrates the difference in the destruction of panel and frame buildings under approximately the same conditions of their damage.

In addition to the fact that the destruction of a panel building is much greater than that of a frame house, about seven times as many people died and went missing inside it, and four times as many people were injured. This clearly shows the significant advantages of buildings made of monolithic concrete and spatial frames over panel ones.

Also, the images shown in Figs. 5-12 testify to the following:

1. The most vulnerable are the buildings, the above-ground part of which is built from factory-ready reinforced concrete slabs, and the least vulnerable are the buildings with a monolithic spatial frame and a rigid core.

2. In all considered cases, the damage to the underground part of the buildings was minimal.

Considering the second conclusion, the data reported in [14] regarding the relationship between the excess pressure at the front of the air blast wave and the pressure in the soil layer caused by the explosion are of interest (Fig. 13).

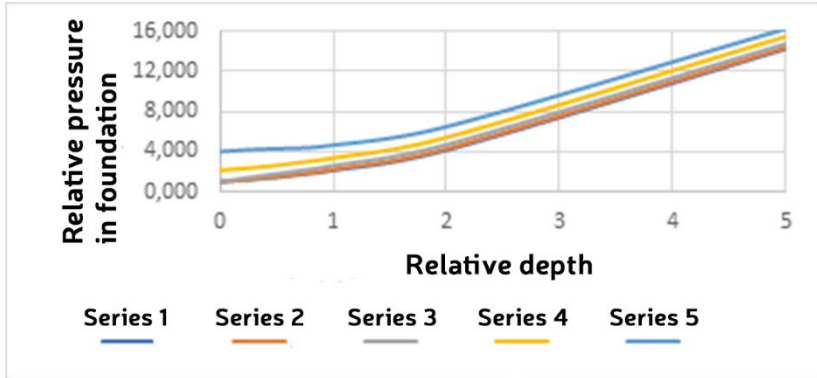


**Fig. 13.** Relative pressure  $p_0$  at relative depth  $z_0$  and relative distance from the explosion site  $r_0$ . Notes: the following designations are used: series 1 -  $r_0=0$ ; series 2 -  $r_0=0,5$ ; series 3 -  $r_0=1$ ; series 4 -  $r_0=1,5$ ; series 5 -  $r_0=1,5$

2. The relative parameters (that is, pressure, depth, and distance from the site of explosion on the surface of the base) should be determined according to formulas (1).

The solution was derived in a cylindrical coordinate system for dimensionless pressure, depth, and distance from the explosion site. In this case, the following relationship holds between the relative, actual coordinates, and the energy of the explosion

$$r_0 = \frac{r}{\sqrt[3]{\lambda \cdot Q}}; \quad z_0 = \frac{z}{\sqrt[3]{\lambda \cdot Q}}; \quad (1)$$

$$\bar{P}(r_0, z_0) = \frac{P(1,0)}{P(r_0, z_0)}.$$

The following designations are used in the formula:  $r$  and  $z$ , accordingly, are the actual horizontal distance from the center of the explosion and the depth at which the actual pressure in the soil base is determined;  $P(r_0, z_0)=1$  if the explosion occurred in the air and  $\lambda=2$  if the explosion occurred on the surface of the earth;  $Q$  - explosion energy in calories.

Analysis of data shown in Fig. 13 allowed us to conclude that the location of civil structures below the soil surface makes it possible to significantly (many times) reduce the destructive energy of blast waves. This conclusion is not new. It is confirmed by the entire

previous practice of building fortification facilities and civil defense structures [15, 16].



**Fig. 14.** The world's largest Doomsday community has built an entire city with 575 underground bunkers. The photograph on the left is the general view of the town from the side of the soil surface, and on the right – the interior



**Fig. 15.** Individual bomb shelter [18]

Fig. 14, 15, and 16 show options for underground structures for the protection of civilian population, built in different countries and under different conditions.

In particular, Fig. 14 displays a photograph of an underground city with 575 bunkers with arched supporting structures [17]. A characteristic feature of the town is the increased comfort of residential premises. Also worthy of attention are the latest Ukrainian advancements of factory-ready individual shelters (Fig. 15), which perform the same functions as the bunkers of the "Doomsday" community [18]. These structures have an advantage in speed and manufacturability of construction (a minimum of operations under

field conditions). In this case, in our opinion, the issues of thermal insulation, corrosion, location in depth, and protection against direct impact on these buildings need further clarification [12, 14].



**Fig. 16.** Example of the conversion of industrial facilities into structures for the protection of civilian population. Cozy apartments in an abandoned mine [19]

It is also of interest to convert abandoned civil and military facilities into structures for the protection of civilian population (Fig. 16).

In this case, the following goals were achieved:

- disposal of an abandoned building (thus saving funds for its destruction);
- reduction of costs for maintenance of abandoned structures in proper condition;
- construction of new comfortable housing;
- construction of new civil defense facilities.

Here, a clear trend of combining different functions in structures intended for the protection of civilian population is observed [20-32]. This is due to the high cost of construction and operation of purely civil protection facilities. In this case, the provision of several functions to protective structures makes it possible to significantly reduce the costs of their operation and pay off the costs of their construction. Successful examples of such dual use of civil defense facilities are subways, underground parking lots, shopping centers, technical and storage facilities, etc.

Thus, the data presented in this part of the paper allow us to formulate the following conclusions:

1. The structures intended for the protection of civilian population should be located below the level of soil surface (that is, underground).

2. The combination of various functions in structures intended for the protection of civilian population makes it possible to significantly reduce the costs of their operation and pay off the costs of their construction.

In some cases, the construction of underground civil defense structures is either impossible or impractical. This is due to the following reasons:

1. High level of underground water (in this case, there are problems of their constant pumping or complete sealing of the structure of the building, mold, flood safety in case of damage to the enclosing structures of the storage, etc.).

2. A long distance or a dangerous path from the structure of civil protection to the place of people residence.

3. Impossibility or reluctance of people to leave homes during an air raid period.

Considering the issues discussed, the experience of using the so-called mamad and mamak in Israel deserves attention [33, 34, 35]. The difference in these definitions is that mamad (abbreviation of merhav mugan dirati - "protected space of the apartment") is a fortified room in a private apartment, while mamak is a fortified room in public facilities. The difference between mamaks and our bomb shelters in the traditional sense is that mamaks are placed on each floor.

According to the requirements given in [35], mamads should have the following minimum properties:

- the area of mamad must be at least 9 square m;
- ceiling height – 2.5 m;
- the walls of mamad should be reinforced concrete, 25-30 cm thick or more;
- mamad must have metal hermetic doors that can withstand the blast wave;
- mamad must be equipped with filters to protect against attacks using chemical, biological, and nuclear weapons (in the latter case, radioactive dust is meant).

Of interest is the experience accumulated at Dnipro University of Technology in the course of master's theses in redesigning residential buildings into houses with mamads, Fig. 17.

In this case, the following goals are achieved by adding mamad (or mamak) to the existing building:

1. In this way, the safety of the people living in the house increases.

2. The living space increases and, thus, its value increases.

In our opinion, it is expedient to add monolithic concrete mamads to all existing panel and brick buildings.

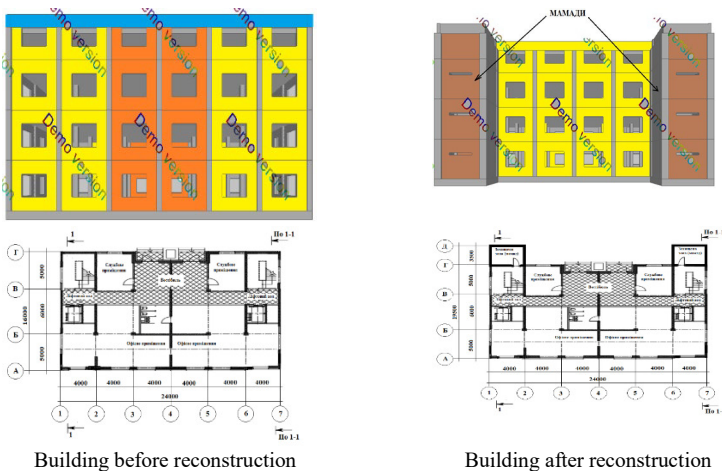


**Fig. 17.** Schematic of mamad attachment to the existing building

## Conclusions

1. According to the Code of Civil Protection of Ukraine, every citizen of Ukraine has the right to protect his/her life and health from the consequences of accidents, disasters, fires, natural disasters, and for guarantees to ensure the implementation of this right, including by sheltering in protective structures. To ensure this right, the Unified State System of Civil Protection currently operates in Ukraine.

2. One of the important links in ensuring the security of civilian population is the presence of protective structures that are included in the civil defense system of Ukraine, as well as in the engineering service and the storage and shelter service.

3. There is a clear trend of growth (compared to previous conflicts) of injuries to people by shrapnel (this is a consequence of artillery and mortar attacks), as well as injuries by powerful explosive devices with a large radius of action and high explosive energy. Injuries to the population by fragments of explosive devices, fragments of glass and building structures took place both in the open space (on the streets and squares of the city) and inside the premises.

In this case, the largest number of fatal injuries to civilian population occurs in the places of its greatest concentration (the most characteristic example is the bombing of the Mariupol Drama Theater [9]).

4. A huge problem is the need to liberate civilian population hiding in the underground parts of buildings and structures, from under the debris of buildings and structures destroyed during shelling (that is, rubble).

5. There is also the issue of the refusal of a large part of civilian population to move to premises that are safer than their apartments (that is, to bomb shelters, underground parking lots, subway stations, and other protective structures) after the announcement of an air raid alert. In this case, according to the population survey, the motivation behind such unusual behavior turned out to be the following factors:

5.1. Health condition of the elderly.

5.2. A long distance from the place of residence to protective structures.

5.3. The danger of being hit by fragments of explosive devices, buildings, structures, and other objects on the way from the place of residence to the protective structure.

5.4. The impossibility of evacuating people from under the rubble above protective structures located under residential buildings.

5.5. Insufficient thickness of ceilings above bomb shelters located in the basements of residential buildings and structures (this reduces the protective properties of bomb shelters).

6. In the zone of shelling, windows are most often destroyed. Next (in descending order) are roofs, walls, and porches. Also, in places of explosions of concentrated charges of high power, entire entrances and buildings are destroyed. In this case, the underground part of buildings and structures is the most protected from damage.

7. Under wartime conditions, the most dangerous are panel buildings, and the most promising from the point of view of safety are buildings built from monolithic reinforced concrete and having the following design features:

- slab or pile foundation;
- reinforced concrete spatial frame;
- reinforced concrete core of rigidity.

Brick buildings and buildings with other structural schemes occupy an intermediate position between panel and frame buildings from the point of view of safety.

8. More modern buildings give more chances of salvation for more people. However, they do not guarantee complete security. This should be kept in mind when choosing a shelter during an air raid and a possible missile attack.

9. An important factor in improving the quality of protection of civilian population, civil defense facilities, and the national economy (in particular, trade, critical infrastructure, and industry) is their location below the soil surface level (that is, underground).

10. There is a positive world experience of using ordinary buildings and facilities of high-security zones, the so-called mamad and mamak.

This method of protecting civilian population under the conditions of hostilities has an advantage over the ones discussed above in the close proximity of the underground water to the soil surface and the short flight time of the means of destruction to the object in which civilian population is located.

The disadvantage of such structures is the possibility of defeat by concentrated explosive devices of high power.

11. There is also the problem of using modern construction standards in the design, construction, and reconstruction of buildings and facilities, taking into account the situation that arose as a result of the armed attack of the Russian Federation on Ukraine. The essence of this problem is the fact that the state building regulations currently in force on the territory of Ukraine (i.e., SBR) do not include strict requirements for the construction and operation of structures intended for the protection of people during military operations.



Also, the issue of dual use of civil protection facilities, for example, additionally as production, trade, warehouse, technical, and other premises, has not been worked out in SBR.

The following recommendations and suggestions follow from the above conclusions:

1. To justify the legal basis of actions during the design, construction, reconstruction, and operation of structures, the data given in points 1 and 2 of the conclusions should be used.

2. The planning of settlements must meet the following requirements:

- maximum separation of residential and industrial facilities in the plan (this could reduce the destructive effect of high-power explosions with a high concentration of explosives);

- the height of residential buildings, in the basements of which shelters intended for the protection of civilian population are located, and the distances between them should allow trouble-free placement of ways for emergency exits from shelters in accordance with SBR requirements;

- transport highways should have above-ground (bridges) and underground (tunnels) sections, which, in the case of danger after detonation, should act as obstacles for enemy equipment;

- the height of buildings and structures should be limited to 4-5 above-ground floors (this is the experience of Israel), while the number of underground floors can be as large as desired;

- new small architectural forms should be introduced into design practice - structures designed to protect civilian population in places of their concentration (public transport stops, platforms in front of shopping facilities, etc.).

3. Premises for the protection of civilian population, shopping centers, objects of critical infrastructure, especially important productions, and other facilities important for the national economy of Ukraine should be placed below the level of soil surface. This will provide them with additional (compared to their above-ground placement) protection.

4. New buildings and structures must be made mainly of monolithic reinforced concrete and have the following structure:

- slab or pile foundation;
- reinforced concrete spatial frame;

- reinforced concrete core of rigidity;
- underground parking and (or) premises for the protection of civilian population with a monolithic reinforced concrete floor above them with a thickness of at least 1000 mm.

In this case, the following should be placed inside the monolithic reinforced concrete core:

- elevator shaft;
- explosion-proof staircases connecting adjacent floors;
- comfortable rooms with reinforced walls and ceilings, designed to protect people from the effects of blast waves, debris, chemical weapons, fires, etc. (analogous of Israeli mamad and mamak).

5. During the construction, design of new, and reconstruction of old structures, the following basic rules should be observed:

5.1. Each of the residential buildings must have a civil defense facility (i.e., shelter).

5.1.1. This structure, if possible, must be underground. It should create comfortable conditions for the long-term living of people.

5.1.2. Each of the civil protection facilities must have several emergency exits. The outer ends of these exits must be located in such a way and at such a distance that guarantees the impossibility of their being filled with debris from nearby destroyed buildings and structures.

5.1.3. The monolithic reinforced concrete floor over shelters for the protection of civilian population must withstand the additional load from the weight of the destroyed floors and the action of the explosion of the estimated charge. Its structural thickness should be at least 1000 mm.

5.2. A very promising direction is the arrangement of protected premises on each floor in buildings and structures. This practice has become widespread in Israel. There, such premises are called mamad and mamak [33, 34].

5.3. Windows should be made either completely protected from the blast wave, or from such materials that cause minimal damage when destroyed (film, tempered glass, etc.).

5.4. Roofs of buildings should be made in a reinforced version, or in such a way that they can be quickly restored with minimal costs (a combined version is also promising).

5.5. The walls of buildings should also be made in a reinforced version, such that they can withstand the pressure of the blast wave and damage from the fragments of the blast wave.

5.6. Entrances and exits from destroyed buildings and structures (in particular, entrances) are also a weak point of pre-war buildings. In our opinion, the solution to this problem is the presence of one or more emergency exits, as well as inter-floor stairs protected from fragments of explosive devices and bullets.

6. The protective properties of existing buildings and structures should be increased using the following methods:

6.1. By means of reconstruction of already existing basements (increasing the comfort of staying in them, arranging additional emergency exits, strengthening the floors above the basement, etc.).

6.2. By adding to existing buildings and structures premises with reinforced structures that withstand the impact of shock waves, fragments of explosive devices and fragments of buildings and structures, fires, chemical attacks, etc. (there is a positive experience of using such structures in Israel, where they are called mamad or mamak).

6.3. By expanding underground communications in such a way that it was possible to use them to leave basements and shelters under rubble. This allows one to achieve the following goals:

- to increase the safety of people in densely built-up areas;
- to improve the operating conditions of tunnels in which communications are laid.

7. When designing and reconstructing buildings and structures, it is imperative to combine several functions with structures intended to protect the civilian population. In this case, there is a significant improvement in payback and a reduction in the cost of operating such facilities. Successful examples of such a combination are the use of subway stations and underground passages, which house commercial enterprises that are operated as:

- transport arteries;
- trade enterprises;
- structures intended for the protection of civilian population.

8. It is necessary to adapt the state building regulations (SBR) currently in force on the territory of Ukraine to modern conditions.

This is achieved by adding relevant sections or amendments to the currently valid documents.

Examples:

- SBR B.1.2-2:2006 "Loads and impacts" should be supplemented with a section that allows one to calculate the load from the explosive shock wave, from the weight of structures destroyed by the explosion, etc.;

- SBR B.2.2-9:2018 "Buildings and structures" should be supplemented with sections "underground and above-ground facilities intended for the protection of civilian population", "design of additional emergency exits", etc.

## *References*

1. **O. Shashenko, V. Shapoval, O. Skobenko & V. Konoval.** (2023). The 2th International scientific and practical conference "Modern education using the latest technologies". Zakhysni sporudy-skladova systemy tsyvilnoho zakhystu naselennia (pp. 498-502). Lisbon: International Science Group.

2. Kodeks tsyvilnoho zakhystu Ukrainy. Retrieved from <https://www.uzhnu.edu.ua/en/infocentre/get/732>

3. **V. Shapoval, O. Skobenko, S. Hapieiev & O. Khalymendyk.** (2023). Proceedings of the V International Scientific and Practical Conference "Formation of perceptions of the structure of scientific methodology". Zakonomirnosti travmuvaniia naselennia ta ruinuvania budivelnykh ob'iektiv v riznykh umovakh vedennia voiennykh dii (pp. 51-55). Vienna: InterSci.

4. Battle suit. Wound statistics, bullets and splinters. Retrieved from <https://topwar.ru/166022-boevoj-skafandr-statistika-ranenij-puli-i-oskolki.html>

5. Novyny upravlinnia verkhovnoho komisara z prav liudyny. Ukraina: onovleni dani shchodo kilkosti zhertv sered myrnykh zhyteliv na 3 zhovtnia 2022 r. Retrieved from <https://www.ohchr.org/ru/news/2022/10/ukraine-civiliancasualty-update-3-october-2022>

6. Ruinuvannia Kharkova. Infografika. Retrieved from <https://www.sq.com.ua/rus/novosti/26.10.2022/razruseniya-xarkova-infografika>

7. Boi za Mariupol. Retrieved from [https://ru.wikipedia.org/wiki/%D0%91%D0%BE%D0%B8\\_%D0%B7%D0%B0\\_%D0%9C%D0%B0%D1%80%D0%B8%D1%83%D0%BF%D0%BE%D0%BB%D1%8C\\_\(2022\)](https://ru.wikipedia.org/wiki/%D0%91%D0%BE%D0%B8_%D0%B7%D0%B0_%D0%9C%D0%B0%D1%80%D0%B8%D1%83%D0%BF%D0%BE%D0%BB%D1%8C_(2022))

8. Verkhovnyi komisar nadala Radi z prav liudyny onovlenu informatsiiu pro sytuatsiiu v Mariupoli, Ukraina. Upravlinnia Verkhovnoho komisara OON z prav liudyny (16 chervnia 2022 roku). Retrieved from <https://www.ohchr.org/ru/statements/2022/06/high-commissioner-updates-humanrights-council-mariupol-ukrain>

9. Aviaudar po Mariupolskomu teatru. Retrieved from [https://uk.wikipedia.org/wiki/%D0%90%D0%B2%D1%96%D0%B0%D1%83%D0%B4%D0%B0%D1%80\\_%D0%BF%D0%BE\\_%D0%9C%D0%B0%D1%80%D1%96%D1%83%D0%BF%D0%BE%D0%BB%D1%8C%D1%81%D1%8C%D0%BA%D0%BE%D0%BC%D1%83\\_%D1%82%D0%B5%D0%B0%D1%82%D1%80%D1%83](https://uk.wikipedia.org/wiki/%D0%90%D0%B2%D1%96%D0%B0%D1%83%D0%B4%D0%B0%D1%80_%D0%BF%D0%BE_%D0%9C%D0%B0%D1%80%D1%96%D1%83%D0%BF%D0%BE%D0%BB%D1%8C%D1%81%D1%8C%D0%BA%D0%BE%D0%BC%D1%83_%D1%82%D0%B5%D0%B0%D1%82%D1%80%D1%83)

10. Yak rosiiski udary ruiniuiut bahatopoverkhivky. Visim prykladiv z komentariamy inzhenera-konstruktora. Retrieved from <https://texty.org.ua/projects/107604/yak-ros-udary-ruiniuiut-budynky/>

11. **O. Shashenko, V. Shapoval, O. Skobenko & V. Konoval.** (2023). Proceedings of the III International Scientific and Practical Conference Theoretical and practical aspects of science. Ekspres-metod vyznachennia normatyvnoho navantazhennia na zalizobetonne perekryttia nad bomboskhovyshchem vid ulamkiv zruinovanykh budynkiv (pp. 116-120). Prague, Czech Republic.

12. **O. Shashenko, V. Shapoval, O. Skobenko & V. Konoval.** (2023). Proceedings of the II International Scientific and Practical Conference "General regularities and models of science development". Ekspres-metod vyznachennia normatyvnoi tovshchyny zalizobetonnoho perekryttia nad bomboskhovyshchem (pp. 135-140). Zagreb: Inter.Sci.

13. U Dnipri vzhe 46 zahybylykh vid udaru rakety po zhytlovomu budynku. Retrieved from <https://interfax.com.ua/news/general/885623.html>

14. **O. Shashenko, V. Shapoval, O. Skobenko, Ye. Sherstiuk & V. Kulivar.** (2023). The 5th International scientific and practical conference "Prospects of modern science and education". Zakonomirnosti rozpovsiudzhennia tysku vid povitrianoi vybukhovoi khvyli v hruntovii osnovi (pp. 643-647). Stockholm: International Science Group.

15. Inzhenerno-tekhnicni zakhody tsyvilnoho zakhystu (DSK). (2019). DBN V.1.2-4:2019 from 26<sup>th</sup> March 2019.

16. Fortyfikatsiia Retrieved from <https://uk.wikipedia.org/wiki/%D0%A4%D0%BE%D1%80%D1%82%D0%B8%D1%84%D1%96%D0%BA%D0%B0%D1%86%D1%96%D1%8F>

17. Naibilshe u sviti spivtovarystvo «Sudnoho dnia» zbuduvaly mini misto z 575 pidzemnymy bunkeramy. Retrieved from <https://building-tech.org/%D0%A1%D0%BE%D0%BE%D0%B1%D1%89%D0%B5%D1%81%D1%82%D0%B2%D0%BE/krupneyshee-v-myre-soobshchestvo-%C2%ABSudnogo-dnya%C2%BB-postroyly-myny-gorod-s-575-podzemnyy-bunkeramy>

18. U Kharkovi zapustyly proekt budivnytstva avtonomnykh pidzemnykh bomboskhovyshch «Skhov» Retrieved from <https://building-tech.org/%D0%A1%D0%BE%D0%BE%D0%B1%D1%89%D0%B5%D1%81%D1%82%D0%B2%D0%BE/v-kharkove-zapustyly-proekt-po-stroytelstvu-avtonomnikh-podzemnikh-bomboubezhyshch-%C2%ABskhov%C2%BB>

19. Amerykanets Larri Kholll pobuduvav zatyshni kvartyry u zanedbanii raketni shakhti. Retrieved from <https://building-tech.org/%D0%90%D1%80%D1%85%D0%B8%D1%82%D0%B5%D0%BA%D1%82%D1%83%D1%80%D0%B0/amerykanets-larry-kholll-postroyl-uyutnie-kvartyri-v-zabroshennoy-raketnoy-shakhte->
20. Obiekty narodnoho hospodarstva u pidzemnykh hirnychykh vyrobkakh. SNiP 2.01.55-85 from 1<sup>st</sup> July 1986.
21. Teplofizychni rozrakhunky obektiv narodnoho hospodarstva, shcho rozmishchuiutsia u hirnychykh vyrobkakh. Posibnyk do SNyP 2.01.55-85.
22. **B. Morklianyk, V. Shapoval, A. Khalimendyk & V. Ivaskevych.** (2019). Zbirnyk naukovykh prats Natsionalnoho hirnychoho universytetu. Perspektyvy vykorystannia pidzemnykh sporud yak dzherela teplovoi enerhii (pp. 98-112). Dnipro: Dnipro University of Technology.
23. **I. Malkov, T. Titkova.** (2009). Ispolzovanie podzemnykh prostranstv v hradostroytelstve: ucheb.-metod. posobie. Homel: Beloruskiy hosudarstvenniy unyversitet transporta, 46.
24. **H. Holubiev.** (1979). Ispolzovanie podzemnogo prostranstva v zhiloy zastroyke. Moskva: Stroyizdat, 23.
25. **H. Holubiev.** (1979). Podzemnaya urbanystika: (hradostroytelnye osobennosti razvitiya ssstem podzemnykh sooruzheniy). Moskva: Stroyizdat, 231.
26. **A. Tetior, V. Lohinov.** (1990). Proektuvannia ta budivnytstvo pidzemnykh budivel ta sporud. Kyiv: Budivelnik, 168.
27. **D. Koniukhov.** (2004). Ispolzovanie podzemnogo mesta: ucheb.-metod. posobie. Moskva: Arkhitektura-S, 296.
28. **L. Makovskiy.** (1985). Horodskie podzemnye transportnye sooruzheniya: ucheb.-metod. posobie. Moskva: Stroyizdat, 439.
29. **Ye. Mykhailova.** (2007). Arkhitekturne osvoennia pidzemnogo prostoru mista. (pp. 40-41)
30. **P. Shvetsov, A. Zilberbord, M. Papernov.** (1992). Podzemnoe prostranstvo i ego osvoenie. Moskva: Nauka, 196.
31. Rekomendatsii po proektyrovaniyu kompleksov torgovo-bytovogo obsluzhivaniya pri podzemnykh peshekhodnykh zonakh. Moskva: Tsentralniy nauchno-issledovatel'skiy i proektniy instytut tipichnogo i eksperimentalnogo proektirovaniya shkol, doskolnykh uchrezhdeniy, srednykh i visshykh uchebnykh zavedeniy, 78.
32. Desing Considerations for Earth- Integrated Education Center in Israeli Desert // Tunnelling and Underground Space Technology. - 1987. - № 1. 28 Burnaby Gamatkhna // Architectura and Urbanism. - 1986. - № 4.
33. Munytsypalityet Yekhuda. Retrieved from <https://local.oryehuda.muni.il/ru/6/>
34. Izrail'ski ukryttia: shcho take mamady i mamaky ta vid choho vony zakhyshchali. Retrieved from [https://realestate.24tv.ua/shho-take-mamadi-mamaki-izrayili-vid-chogo-voni-zahishhayut\\_n2181368](https://realestate.24tv.ua/shho-take-mamadi-mamaki-izrayili-vid-chogo-voni-zahishhayut_n2181368)
35. Mamaky y mamady: ukryttia Izrailiu ta shcho planuietsia v Ukraini. Retrieved from <https://vikna.tv/dlia-tebe/bezpeka/mamaky-j-mamady-ukryttia-izrayilyu-ta-shho-planuyetsya-v-ukrayini/>

**STRESS STATE MODELLING FOR COMPOSITE  
TRACTIVE ELEMENT WITH BREAKAGES OF CABLE  
REINFORCEMENT AND CHANGE IN MECHANICAL  
PROPERTIES OF ELASTOMER SHELL**



**Ivan BELMAS**

Dr. Sc. (Tech.), Prof., Head of Department of Mechanical Engineering Technology, Dniprovsk State Technical University, Kamianske, Ukraine



**Dmytro KOLOSOV**

Dr. Sc. (Tech.), Prof., Head of Department of Mechanical and Biomedical Engineering, Dnipro University of Technology, Dnipro, Ukraine



**Serhii ONYSHCHENKO**

Cand. Sc. (Tech.), Associate Professor of Department of Mechanical and Biomedical Engineering, Dnipro University of Technology, Dnipro, Ukraine



**Olena BILOUS**

Cand. Sc. (Tech.), Associate Prof., Associate Prof. of Department of Industrial Engineering, Dniprovsk State Technical University, Kamianske, , Ukraine



**Hanna TANTSURA**

Cand. Sc. (Tech.), Associate Prof., Associate Prof. of Department of Industrial Engineering, Dniprovsk State Technical University, Kamianske, Ukraine

**Abstract.** The purpose of research is determination of a dependency of a stress state for composite elastomer-cable tractive element with a broken structure on a nonlinear dependency of shear modulus on deformations in the elastomeric shell. Research methodology is in analytical solution of a model of a composite tractive element with disturbed structure and a deformation-dependent shear modulus of an elastomeric shell. Results are in constructing an algorithm for determining a stress state of a composite tractive element with broken structure and a deformation-dependent shear modulus. Scientific novelty is in determining a character of dependency for a stress state of a composite tractive element on a nonlinear dependency of shear modulus on deformations. Practical application of research is in a possibility to determine the dependency of a stress state of a composite elastomer-cable tractive element on a nonlinear shear modulus allows considering the effect of this phenomenon on the tractive element strength and ensures an increase of its operational safety.

### **Introduction**

Continuous improvement of technical systems in the fields of mining technologies [1-9], transportation and hoisting [10-12], deep-sea mining [13, 14], and dynamics of technical systems [15-19] facilitate wider and more thorough development of analytical and computational simulation methods of processes and phenomena occurring within the systems. Currently, researchers in many countries are conducting complex scientific studies aimed at developing methods and means of modernizing lifting and transporting complexes with the aim of increasing operational efficiency and safety of mining transport equipment. Composite elastomer-cable tractive elements, in particular rubber-cable ropes (RCR), also known as steel cord belts, are widely used in hoisting and transporting machines [20-24]. At the same time, these tractive elements have significant lengths. Conveyor belts of a closed shape are created by connecting ends of belts. Cables at belt ends in such connections are not mechanically connected and interact through rubber layers. Damage accumulates in ropes during use. One type of damage is rupture of one of reinforcing elements (cables). Rupture of continuity of cables and presence of non-continuing cables, in accordance with the Saint-Venant's principle, are sources of disturbance of a stress-strain state in a rope (belt).

### **State of Question and Research Problem**

Rope strength in the cross-section of cable breakage is much lower [25-27], it is also lower in butt joints [28]. In paper [29], it is suggested to determine a stress-strain state of spatial structures reinforced with parallel elements by means of electrical modelling. A



method of determining characteristics of materials with a system of regularly arranged parallel reinforcing elements is suggested in the article [30]. The papers [31-40] are devoted to investigation of features of a rope (belt) stress state, considering its interaction with structural elements of a machine. Experience indicates that there is a nonlinear dependency of stresses in elastic materials on their deformations, and rubber is no exception to this. Rubber layers in rubber-cable ropes ensure the connection of cables, determine a mechanism of redistribution of forces between the cables, which affects the operational characteristics of the entire rope. In these papers, the issue of a nonlinear law of rubber deformation is not considered. At the same time, it constitutes an actual scientific and technical problem of considering the specified feature during the design and continuous control of the condition of hoisting and transporting machines with a rubber-cable tractive element. The solution allows considering the influence of deformation character in rubber on rope strength and provides a possibility of increasing operational safety of rubber-cable ropes (belts).

Generally, the dependency graph of stresses on deformations has a shape of a curved line. The main factor in the occurrence of shear stresses in rubber layers of a rope or belt is breakage of continuity of cables. Discontinuity of cables occurs in the event of cable breakage and in butt joints of rubber-cable ropes and belts. In butt-joint connections, no cables at both ends of the connected belts continue. A cable break or a cable end is a source of stress-strain state disturbance in a rope (belt). Well-known studies [26] indicate that deformations of rubber take place practically only in the layers adjacent to the broken cable. Deformation values are maximum in the cross-section of cable continuity breakage and decrease exponentially with increasing distance from the specified cross-section.

### **Consideration of Natural Changes in Mechanical Properties of Elastic Shell on Stress-Strain State of a Rope**

Loading forces on cables and their displacements without considering rubber aging, according to [26] are determined by dependencies

$$p_i = E F \sum_{m=1}^{M-1} \left( A_m e^{\beta_m x} - B_m e^{-\beta_m x} \right) \beta_m \cos(\mu_m (i - 0.5)) + P, \quad (1)$$

$$u_i = \sum_{m=1}^{M-1} \left( A_m e^{\beta_m x} + B_m e^{-\beta_m x} \right) \cos(\mu_m (i-0.5)) + \alpha + \frac{P x}{E F}, \quad (2)$$

where  $M$  is amount of cables in a rope,  $i$  is cable number ( $1 \leq i \leq M$ );  $A_m, B_m$  are integration constants;  $E, F$  are, respectively, reduced tensile modulus of elasticity and cross-sectional area of a cable in a rope (belt);  $x$  is coordinate axis directed along the rope,  $P$  is average load

on a cable in a rope;  $\beta_m = \sqrt{2 \frac{G b k_G}{(h-d) E F} [1 - \cos(\mu_m)]}$ ;  $\mu_m = \frac{\pi m}{M}$ ;

$h$  is distance between cables;  $b$  is rope thickness;  $d$  is cable diameter;  $G$  is shear modulus of elastic (rubber) layer connecting the cables,  $k_G$  is coefficient of shape influence of rubber located between cables on shear rigidity;  $\alpha$  is cable displacement as a rigid body.

Natural change in mechanical properties during aging process of an elastic shell is associated with a change in modulus of elasticity and shear modulus. According to (1) and (2), shear modulus affects a stress-strain state of a rope. Assume that a law of change of shear modulus of an elastic (rubber) layer is known. Its value is given by the following expression

$$G = G_0 f(t), \quad (3)$$

where  $G_0$  is shear modulus right after rope (belt) production ( $t=0$ ).

Formulate a physical model of rope deformation made of  $M$  cables of considerable length. Cable with number  $J$  has a continuity breakage. This breakage is located at an infinitely large distance from rope edges. Rope is loaded with a tensile force. Tensile force ensures an average loading on cables equal to one. Direct an  $x$ -axis along the rope. Place axis origin point at a cross-section of cable breakage. Consider a rope part for which ( $0 \leq x \leq \infty$ ).

From a condition of limited displacements of cables and limited loading forces on cables for an infinite growth of  $x$ -coordinate, assume that  $A_m=0$ . Consider rope displacement as a rigid body equal to zero. Then, expressions (1) and (2) obtain the following forms

$$p_i = -E F \sum_{m=1}^{M-1} B_m e^{-\beta_m^* x} \beta_m^* \cos(\mu_m (i-0.5)) + P, \quad (4)$$

$$u_i = \sum_{m=1}^{M-1} B_m e^{-\beta_m^* x} \cos(\mu_m (i-0.5)) + \frac{P x}{EF}, \quad (1 \leq i \leq M), \quad (5)$$

where  $\beta_m^* = \sqrt{\frac{2G_0 f(t) b k_G}{(h-d)EF} [1 - \cos(\mu_m)]}$ .

Displacements of all cables, except for the broken one, in the cross-section  $x=0$  are absent. Displacement of a broken cable is denoted as  $U_0$ . Displacements of cables in the cross-section  $x=0$  are defined as product of  $U_0$  and  $\delta$ -function on a limited axis length of discrete cable numbers. This makes it possible to determine the vector of unknown constants of integration from expression (5) through one unknown quantity

$$B_m = \frac{2}{M} U_0 \cos(\mu_m (J-0.5)). \quad (6)$$

The unknown  $U_0$  is determined from a condition that a loading force (4) of a broken cable is zero

$$U_0 = \frac{P M}{2 EF \sum_{m=1}^{M-1} \cos^2(\mu_m (J-0.5)) \beta_m^*}. \quad (7)$$

Expressions (4) - (7) make it possible to determine a stress-strain state of a rope of considerable length on a hoisting machine and a conveyor belt of considerable length in case of breakage of an arbitrary cable, considering the aging period of their elastic shell at the moment of cable breaking.

Known displacements of cables (5) allow determining relative shear of cables. Difference in shear of adjacent cables is accompanied by occurrence of tangent stresses in an elastic shell. The tangent stresses are at their maximum values in a plane of axes of rope cables. The distances between the nearest points on surfaces of adjacent cables are minimal in this plane. Tangents of shear angles are determined by the following expression

$$\tan(\gamma_j) = \frac{u_j - u_{j+1}}{h}, \quad (1 \leq j < M), \quad (8)$$

where  $j$  is layer number.

For a rope of RCR-3150 type consisting of five cables, determine a distribution of internal forces and tangents of shear angles for an elastic shell in a plane where centers of cross-sections in cables are located. Assume that as a result of natural changes in rubber properties, a shear modulus has doubled. Apply an external load so that the average load on cables is equal to one. The noted internal loading forces on cables in this case are equal to a coefficient of uneven loading on cables. Results for cases  $f(T)=2$  (curve 1) and  $f(0)=1$  (curve 2) are indicated in Fig. 1 and 2.

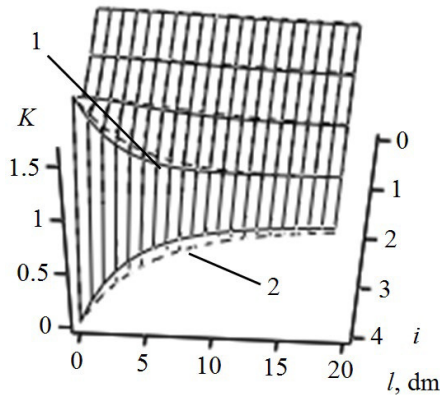


**Fig. 1.** Distribution of coefficients of uneven loading on cables with numbers  $i$  along rope length  $l$

According to graphs shown in the Figure 1, loads on cables caused by continuity breakage in of one of them lead to a local redistribution of forces practically only between two cables - the broken one and the one adjacent to it. Accordingly, in a case of breakage in a non-extreme cable, the forces practically change only in three cables - the broken one and two adjacent ones to it. The forces change significantly over a length of up to 2 m. The extreme values of internal loading forces on cables do not depend on change in shear modulus of rubber material over time.

Distribution of tangents of shear angles in rubber (Fig. 2) also indicates an insignificant effect on rubber shear angles between cables.

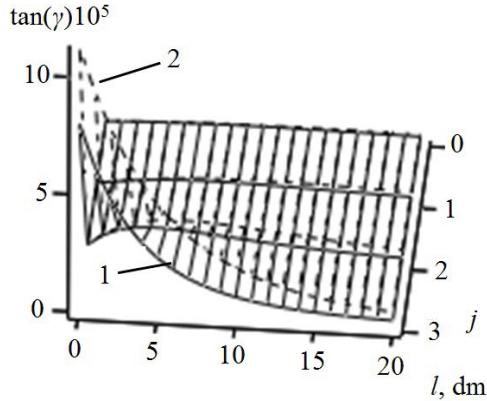


**Fig. 2.** Distribution of maximum tangents of shear angles in material located in layers with numbers  $j$  between cables along rope length  $l$

Significant rubber shear is observed only between the broken cable and the one adjacent to it along the cable length. Shear angles of rubber between other cables are much smaller compared to shears in a zone of local redistribution of forces and stresses. They change little because of rubber aging over time. Length of conveyors and hoisting heights for using rubber-cable ropes and belts exceed 100 m. This makes it possible to consider the above assumption of an infinite rope length and an infinite distance from a cable breakage to a belt (rope) end.

The second feature of influence of operating time on a rope stress-strain state is a local decrease in a value of shear modulus of elastic material in zones of increased stress. Ropes and belts operate under cyclic loads. Each cyclic load is accompanied by accumulation of residual strain. Rubber shell between cables, due to its much lower tensile strength than that of cables, practically is not loaded until the moment of cable breakage. There are no residual shear deformations in it.

### **Consideration of Cable Breakage on Stress-Strain State of Composite Flat Rubber-Cable Rope**

A change in a stress-strain state of a belt (rope) as a result of cable breakage leads to occurrence of shear in elastic shell material located between individual cables and accumulation of residual strain. Larger absolute values of total deformations that occur in rub-

ber after a cable breaks lead to larger absolute values of residual strain. According to graphical dependencies shown in Figure 2, local changes in a design of composite flat rubber-cable rope (belt) lead to local changes in their stress-strain state. Investigate the local influence of changes in properties of an elastic material that interacts with a broken cable.

### **Construction of Model of Rubber-Cable Tractive Element with a Broken Structure and Nonlinear Deformation-Dependent Rubber Shear Modulus**

Determining a stress-strain state considering the specified character of deformation changes and considering the nonlinear dependency of shear displacements on rubber shear stresses is a complex mathematical problem. Let's simplify it. Assume that the dependency of rubber shear stresses on its deformations is piecewise linear and consists of two parts. As in the studies mentioned above, we assume that the cables deform like rods. Rubber is subjected only to shear stress. The rope is infinitely long. It has  $M$  cables and is loaded with a tensile force  $P$ . The cable numbered  $j$  has a continuity breakage. The cross-section with the breakage is at a considerable distance from the rope edges. Rubber shear modulus of layers adjacent to the damaged cable at lengths  $l_0$  is different from the corresponding rubber shear modulus of the remaining layers. The linear size  $l_0$  is much smaller than the rope length, on which the stress state is changed because of a cable breaking. Direct the coordinate axis along the rope. Its origin ( $x = 0$ ) is located at the point where the cable breaks. Since the cross-section ( $x = 0$ ) is a cross-section of symmetry, the displacements of cables are symmetrical. At the same time, the cross-sections of all cables except the ends of the broken cable do not move. A gap is formed between the ends of the damaged cable. Let's denote the displacement of the end of the damaged cable  $U_0$ .

Let's single out a part of length  $l_0(0 \leq l_0)$ . Consider it the first one. Consider the part for which ( $x > l_0$ ) the second part. The first part of the rope is divided into three stripes with an unchanged number of cables in each. Include stripes that do not have a broken cable into the structure of the two extreme stripes. Give them numbers one and three. The rope part with the broken cable and the cables adjacent to it will be included in the structure of the second stripe (Fig. 3).

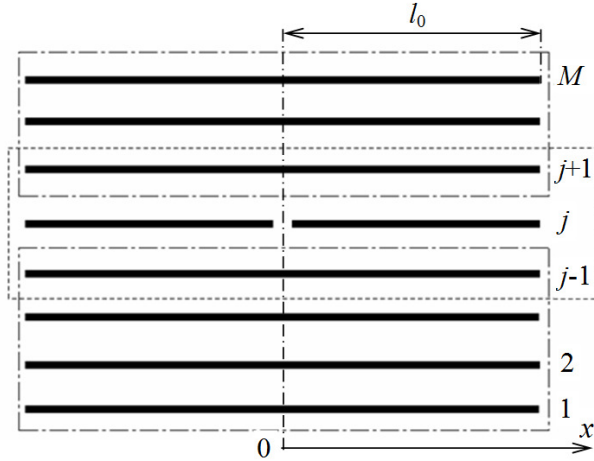


**Fig. 3.** Rope part with a broken cable

Consider the specified stripes as separate belts. A characteristic feature of such rope stripes is that the properties of elastic material between the rope stripes do not change. Shear modulus of rubber in layers between cables is not variable in our case. This allows using the conditions of their equilibrium and the form of solutions for stripes [26], considering the number of cables in stripes and properties of elastic shell. Let's make expressions that allow determining the internal forces in cables and their displacements. Write down the expressions for the extreme stripes in similar forms. In the expressions, we will use additional indices to assign the parameters to one or another rope stripe. Take into account that cross-sections of cables of the extreme stripes do not move when  $(x = 0)$ .

### Assumed Forms of Solution

For a rope stripe with cable numbers  $(1 \leq i \leq j-1)$

$$p_{1,i} = E F \sum_{m=1}^{j-2} \left[ A_m \left( e^{\beta_{1,m} x} + e^{-\beta_{1,m} x} \right) \times \right. \\ \left. \times \beta_{1,m} \cos(\mu_{1,m} (i - 0.5)) \right] + P, \quad (9)$$

$$u_{1,i} = \sum_{m=1}^{j-2} A_m \left( e^{\beta_{1,m} x} - e^{-\beta_{1,m} x} \right) \cos(\mu_{1,m} (i - 0.5)) + \frac{P x}{E F}, \quad (10)$$

where  $i$  is cable number in the first stripe;

$$\beta_{1,m} = \sqrt{\frac{2G_0 b}{(h-d)EF} [1 - \cos(\mu_{1,m})]}.$$

For the second rope stripe with cable numbers ( $j-1 \leq i \leq j+1$ )

$$p_{2,i} = EF \sum_{m=1}^2 \left[ \left( A_{m+j-2} e^{\beta_{2,m} x} - B_{m+j-2} e^{-\beta_{2,m} x} \right) \times \right. \\ \left. \times \beta_{2,m} \cos(\mu_{2,m}(i-j-1.5)) \right] + P, \quad (11)$$

$$u_{2,i} = \sum_{m=1}^2 \left[ \left( A_{m+j-2} e^{\beta_{2,m} x} + B_{m+j-2} e^{-\beta_{2,m} x} \right) \times \right. \\ \left. \times \cos(\mu_{2,m}(i-j-1.5)) \right] + \frac{Px}{EF}, \quad (12)$$

where  $\mu_{2,m} = \frac{\pi m}{3}$ ;  $\beta_{2,m} = \sqrt{\frac{2G_0 b k}{(h-d)EF} [1 - \cos(\mu_{2,m})]}$ ;  $k$  is coefficient, which considers the difference in shear modulus of rubber for the second stripe.

For a rope stripe with cable numbers ( $j+1 \leq i < M$ )

$$p_{3,i} = EF \sum_{m=1}^{M-j-1} \left[ A_{m+j} \left( e^{\beta_{3,m} x} + e^{-\beta_{3,m} x} \right) \times \right. \\ \left. \times \beta_{3,m} \cos(\mu_{3,m}(i-j-1.5)) \right] + P, \quad (13)$$

$$u_{3,i} = \sum_{m=1}^{M-j-1} \left[ A_{m+j} \left( e^{\beta_{3,m} x} - e^{-\beta_{3,m} x} \right) \times \right. \\ \left. \times \cos(\mu_{3,m}(i-j-1.5)) \right] + \frac{Px}{EF}, \quad (14)$$

where  $\mu_{3,m} = \frac{\pi m}{M-j}$ ;  $\beta_{3,m} = \sqrt{\frac{2G_0 f(t) b k_G}{(h-d)EF} [1 - \cos(\mu_{3,m})]}$ .

These solutions correspond to the conditions of influence absence of external factors on extreme cables in stripes on the interval ( $0 \leq x \leq l_0$ ). The cables adjacent to the broken one are included in two stripes – the extreme one and non-extreme one. In the extreme stripes, there are no disturbances in cables adjacent to the broken one, in accordance with solutions of (9), (10) and (13), (14). They are



loaded with only evenly distributed forces. Cables in the cross-section  $x = 0$  are immovably fixed. In a general solution, based on the principle of superposition, we add their displacements as cables, which are part of the middle stripe, to displacements of these cables without considering the force of their external load.

The end of the middle cable in the middle stripe is displaced by an unknown amount  $U_0$  under the action of an external force. Let's write the above in a form of a boundary condition for the cross-section  $x=0$

$$u_{2,i} = U_0 \begin{cases} 0, & i \neq j, \\ 1, & i = j. \end{cases} \quad (15)$$

According to (15), the law of cable displacements corresponds to the product of displacement of a middle cable and the Dirac function  $\delta$ . Let's take the Dirac function in a form of a Fourier series on a given segment of cable numbers. From expression (12), we have the following

$$\begin{aligned} & \sum_{m=1}^2 (A_{m+j-2} + B_{m+j-2}) \cos(\mu_{2,m}(i-0.5)) = \\ & = \frac{2}{3} U_0 \sum_{m=1}^2 \cos\left(\frac{3}{2} \mu_{2,m}\right) \cos(\mu_{2,m}(i-0.5)), \quad (i=1,2,3). \end{aligned} \quad (16)$$

From where

$$B_{m+j-2} = \frac{2}{3} U_0 \cos(1.5 \mu_{2,m}) - A_{m+j-2}, \quad (m=1,2). \quad (17)$$

From the condition that a load on the broken cable in the cross-section of breakage is equal to zero from expression (11) we have

$$U_0 = \frac{3P}{2\beta_{2,m} E F \cos^2(1.5 \mu_{2,m})} + 3 \frac{A_{m+j-2}}{\cos(1.5 \mu_{2,m})}. \quad (18)$$

Accordingly, expression (17) takes the form

$$B_{m+j-2} = \frac{P}{\beta_{2,m} E F \cos(1.5 \mu_{2,m})} + 2A_{m+j-2}. \quad (19)$$

Expressions of forces (11) and displacements (12) considering the general numeration of cables in the cross-section of a rope take the following forms

$$p_{2,i} = EF \sum_{m=1}^2 \left[ \left( \begin{aligned} &A_{m+j-2} \left( e^{\beta_{2,m}x} - 2e^{-\beta_{2,m}x} \right) \times \\ &\times \beta_{2,m} - \frac{Pe^{-\beta_{2,m}x}}{\cos(1.5\mu_{2,m})} \\ &\times \cos(\mu_{2,m}(i-j-1.5)) \end{aligned} \right) \times \right] + P, \quad (20)$$

$$u_{2,i} = \sum_{m=1}^2 \left[ \left( \begin{aligned} &A_{m+j-2} \left( e^{\beta_{2,m}x} + e^{-\beta_{2,m}x} + 0.5 \right) + \\ &+ \frac{P \left( e^{-\beta_{2,m}x} + 0.5 \right)}{\beta_{2,m}EF \cos(1.5\mu_{2,m})} \\ &\times \cos(\mu_{2,m}(i-j-1.5)) \end{aligned} \right) \times \right] + \frac{Px}{EF}. \quad (21)$$

Using (9), (10), (13), (14), (20), (21), we write down the values of forces and displacements as single functions on the finite axis of cable numbers

$$p_i = \frac{2EF}{M} \sum_{n=1}^{M-1} \rho_n(x) \cos(\mu_n(i-0.5)) + P, \quad (22)$$

where  $\mu_n = \frac{\pi n}{M-1}$ ;

$$\rho_n(x) = \sum_{\chi=1}^{j-1} \sum_{m=1}^{j-2} \left[ \begin{aligned} &A_m \left( e^{\beta_{1,m}x} + e^{-\beta_{1,m}x} \right) \beta_{1,m} \times \\ &\times \cos(\mu_{1,m}(\chi-0.5)) \cos(\mu_n(\chi-0.5)) \end{aligned} \right] + \\ + \sum_{\chi=1}^3 \sum_{m=1}^2 \left[ \left( \begin{aligned} &A_{m+j-2} \left( e^{\beta_{2,m}x} - 2e^{-\beta_{2,m}x} \right) \times \\ &\times \beta_{2,m} - \frac{Pe^{-\beta_{2,m}x}}{EF \cos(1.5\mu_{2,m})} \\ &\times \cos(\mu_{2,m}(\chi-0.5)) \cos(\mu_n(\chi+j-2.5)) \end{aligned} \right) \times \right] +$$

$$\begin{aligned}
& + \sum_{\chi=1}^{M-j-1} \sum_{m=1}^{M-j-1} \left[ \begin{aligned} & A_{m+2} \left( e^{\beta_3, m^x} + e^{-\beta_3, m^x} \right) \beta_{3, m} \times \\ & \times \cos(\mu_{3, m} (\chi - 0.5)) \cos(\mu_n (\chi + j - 0.5)) \end{aligned} \right] \\
u_i & = \frac{2}{M} \sum_{n=1}^M v_n(x) \cos(\mu_n (i - 0.5)) + \frac{P x}{E F}, \quad (23)
\end{aligned}$$

where

$$\begin{aligned}
v_n(x) & = \sum_{\chi=1}^{j-1} \sum_{m=1}^{j-2} \left( \begin{aligned} & A_m \left( e^{\beta_1, m^x} - e^{-\beta_1, m^x} \right) \times \\ & \times \cos(\mu_{1, m} (\chi - 0.5)) \cos(\mu_n (\chi - 0.5)) \end{aligned} \right) + \\
& + \sum_{\chi=1}^3 \sum_{m=1}^2 \left( \begin{aligned} & \left( A_{m+j-2} \left( e^{\beta_2, m^x} + e^{-\beta_2, m^x} \right) + \right. \\ & \left. + \frac{P e^{-\beta_2, m^x}}{\beta_{2, m} E F \cos(1.5 \mu_{2, m})} \right) \times \\ & \times \cos(\mu_{2, m} (\chi - 0.5)) \cos(\mu_n (\chi + j - 2.5)) \end{aligned} \right) + \\
& + \sum_{\chi=1}^{M-j-1} \sum_{m=1}^{M-j-1} \left( \begin{aligned} & A_{m+2} \left( e^{\beta_3, m^x} - e^{-\beta_3, m^x} \right) \times \\ & \times \cos(\mu_{3, m} (\chi - 0.5)) \cos(\mu_n (\chi + j - 0.5)) \end{aligned} \right).
\end{aligned}$$

Expressions (22), (23) are obtained for the first part of the rope for ( $0 \leq x \leq l_0$ ). In cross-section  $x=l_0$  the considered part of the rope interacts with its second part. Write expressions of forces ( $p_{0,i}$ ) and displacements ( $u_{0,i}$ ) for the second part in the forms [26]. At the same time, we consider that an infinite increase in the value of  $x$ -coordinate cannot lead to an infinite increase in the loading forces of cables and their displacements

$$p_{0,i} = -E F \sum_{n=1}^{M-1} B_{0,n} e^{-\beta_n^* x} \beta_n^* \cos(\mu_n (i - 0.5)) + P, \quad (24)$$

$$u_{0,i} = \sum_{n=1}^{M-1} B_{0,n} e^{-\beta_n^* x} \cos(\mu_n (i - 0.5)) + \frac{Px}{EF}; (1 \leq i \leq M), \quad (25)$$

where  $\beta_n = \sqrt{\frac{2G_0b}{(h-d)EF} [1 - \cos(\mu_n)]}$ .

At the same time, in cross-section  $x=l_0$  the conditions of joint deformation of rope parts must be fulfilled

$$p_{0,i} = p_i, \quad (26)$$

$$u_{0,i} = u_i. \quad (27)$$

From expressions (22), (23) and conditions (26), (27), we have equalities

$$B_{0,n} e^{-\beta_n^* l_0} = -\frac{2}{M \beta_n^*} \rho_n; \quad (x = l_0), \quad (28)$$

$$B_{0,n} e^{-\beta_n^* l_0} = \frac{2}{M} \nu_n; \quad (x = l_0). \quad (29)$$

Subtract (29) from (28). We get a system of  $N - 1$  equations

$$\sum_{\chi=1}^{j-1} \sum_{m=1}^{j-2} \left( A_m \left( e^{\beta_{1,m} l_0} \left( 1 + \frac{\beta_{1,m}}{\beta_n^*} \right) - e^{-\beta_{1,m} l_0} \left( 1 - \frac{\beta_{1,m}}{\beta_n^*} \right) \right) \times \right. \\ \left. \times \cos(\mu_{1,m} (\chi - 0.5)) \cos(\mu_n (\chi - 0.5)) \right) + \\ + \sum_{\chi=1}^3 \sum_{m=1}^2 \left( \left( A_{m+j-2} \left( e^{\beta_{2,m} l_0} \left( 1 + \frac{\beta_{2,m}}{\beta_n^*} \right) + \right. \right. \right. \\ \left. \left. \left. + e^{-\beta_{2,m} l_0} \left( 1 - 2 \frac{\beta_{2,m}}{\beta_n^*} \right) \right) \right) \times \right. \\ \left. \left. + \frac{Pe^{-\beta_{2,m} l_0}}{EF \cos(1.5\mu_{2,m})} \left( \frac{1}{\beta_{2,m}} - \frac{1}{\beta_n^*} \right) \right) \right) \\ \left. \times \cos(\mu_{2,m} (\chi - 0.5)) \cos(\mu_n (\chi + j - 2.5)) \right) +$$

(30)

$$\begin{aligned}
& + \sum_{\chi=1}^{M-j-1} \sum_{m=1}^{M-j-1} \left[ A_{m+2} \begin{pmatrix} e^{\beta_{3,m} l_0} \left( 1 + \frac{\beta_{3,m}}{\beta_n^*} \right) - \\ -e^{-\beta_{3,m} l_0} \left( 1 - \frac{\beta_{3,m}}{\beta_n^*} \right) \end{pmatrix} \times \right. \\
& \left. \times \cos(\mu_{3,m}(\chi - 0.5)) \cos(\mu_n(\chi + j - 0.5)) \right].
\end{aligned}$$

The solution of obtained system of equations (30) allows determining the unknown constants and internal loading forces of cables, and their displacements. The known displacements make it possible to determine tangential stresses in material of the elastic shell located between the cables, which are directly proportional to the tangent of its shear angle

$$\tan(\gamma_i) = \frac{u_i - u_{i+1}}{h}, \quad (1 \leq i < M). \quad (31)$$

## Results and Discussion

With the use of obtained dependencies, stress-strain state indicators are determined for a rope type RCR-3150 consisting of six cables. The sixth of them is broken. The area length  $l_0$  is assumed equal to 0.1 m. Coefficient of change of shear modulus is 0.5. The results of calculations are given below. Figure 4 shows the dependency of a ratio of internal loads in cables to the average load (coefficients of uneven distribution of forces among the cables) along the  $x$ -axis.

Let's pay attention to the fact that  $x = 10$  cm corresponds to the boundary of rope parts. Presence of a boundary that divides the rope into parts with different values of shear modulus practically does not affect distribution of forces among the cables. The loads on the broken cable increase as the  $x$ -coordinate increases from zero. Cable adjacent to the broken one is loaded more than the other cables. Its maximum internal load – the coefficient of uneven distribution of forces occurs in the cross-section of cable breakage. This value reaches 1.53. The value of coefficients of unevenness decreases with a cable distance from the one adjacent to the broken one and with distance from the cross-section of breakage. We compare the values

of force concentration coefficients for cases of linear and assumed nonlinear dependency of shear modulus on deformations. The analysis of results shows that an increase in the area of action of the reduced shear modulus leads to an increase in the maximum value of coefficient of uneven distribution of forces among cables. Therefore, when rope part length is 100 mm, the excess of the force concentration coefficient reaches 15 %. For a rope part length of 500 mm it reaches 5 %. For the infinite growth of the area of lower rigidity of rubber layers connecting the damaged cable with its adjacent cables, the coefficient of uneven distribution of forces infinitely approaches the corresponding coefficient obtained without considering the nonlinear law of dependency of shear modulus on the mutual shear of cables.

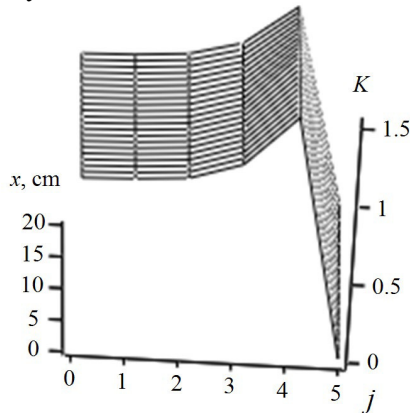


**Fig. 4.** Dependency of coefficients of uneven distribution of forces among cables with numbers  $i$  along  $x$ -axis

Butt joints have cross-sections, in which the number of cables changes, just as it changes in a rope with a broken cable. Such a change in the number of cables leads to a mutual displacement of cables in a rope cross-section. The cable with a breakage moves the most relatively to the adjacent ones. This is observed both in butt joints and in a rope with a broken cable. Accordingly, the obtained results can be extended to butt joints. Considering the nonlinearity of rubber shear deformations is expedient because the lengths of butt joint steps are smaller than the sizes of areas of stress disturbance from local change in the butt joint design.

The ratio between displacements of cables numbered  $i$  and a displacement of the broken cable in the cross-section of its breakage are shown in the Fig. 5.

The displacements of cables shown in Figure 5 in the cross-section  $x=0$  correspond to the assumed form of displacements. As the distance from the cross-section of cable breakage increases, the character of curvature of the rope cross-sections changes - the amount of curvature decreases. The established distribution of displacements made it possible to find distributions of the tangents of shear angles of elastic material between cables. Figure 6 shows the tangents of shear angles of elastic shell between cables with numbers  $i$  along the  $x$ -axis, relative to its average value.

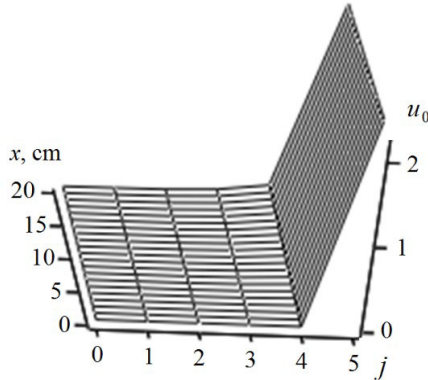


**Fig. 5.** Dependency of a product of rigidity and displacements of cables with numbers  $i$  along  $x$ -axis

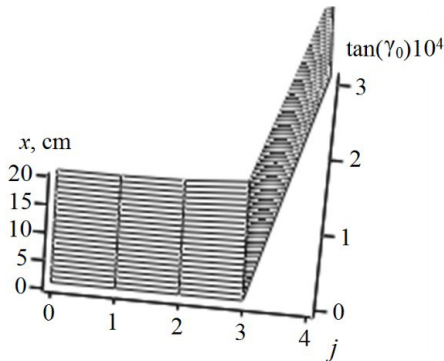


**Fig. 6.** Dependency of tangents of shear angles of elastic shell between cables with numbers  $j$  along  $x$ -axis relative to its average value

The shear of cables occurred practically only between the broken cable and the one adjacent to it. At the same time, rigidity of rubber between the specified cables in a rope part ( $0 \leq x \leq 10$  mm) is lower than the rigidity of other layers. The maximum mutual shear does not change significantly on the area ( $0 \leq x \leq l_0$ ) (Fig. 7).

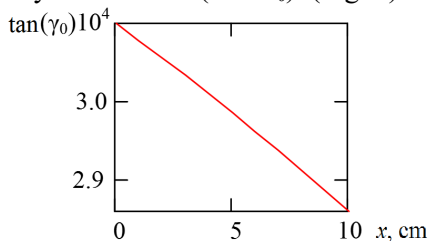


**Fig. 7.** Dependency of the larger tangents of shear angles of elastic shell between cables along  $x$ -axis related to its average value in a rope

Fig. 7 shows a slight deviation of tangents of shear angles of elastic shell from the average value.

In practice, ropes of various designs are used, including with a different number of cables. Fig. 8 shows the dependency of distribution of force distribution coefficients among cables in ropes with different numbers of cables.

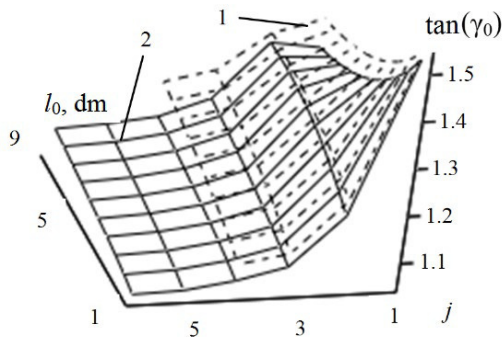


**Fig. 8.** Coefficients of force distribution among cables in ropes with a different number of cables; 1 - for a rope of five cables, 2 - for a rope of seven cables

The figure shows that an increase in a number of cables in a rope does not significantly affect the maximum values of internal loading forces of cables. The analysis of expressions (27), (28) shows that the increase in the number of cables in a rope over ten practically



does not affect the value of maximum stresses in a case of breakage of the extreme cable. In case of breakage of the middle cable, the maximum force in adjacent cables practically does not depend on their number when there are more than sixteen of them.

### **Conclusion**

By analytically solving a model of a rubber-cable tractive element with a broken structure and nonlinear deformation-dependent rubber shear modulus, the dependencies of changes in a stress state of a rubber-cable tractive element with a broken structure in a form of a cable breakage are established.

In a process of solving the model, an algorithm for determining a stress state of a rubber-cable tractive element with a broken structure is formulated. A mechanism for changing a stress state of a rubber-cable rope is established, considering the nonlinear deformation-dependent shear modulus of rubber.

It is established that an increase in area of action of the reduced shear modulus leads to an increase in the maximum value of a coefficient of uneven distribution of forces between the cables. With infinite growth of area of lower rigidity of rubber layers connecting the broken cable with the adjacent cables, the coefficient of uneven distribution of forces infinitely approaches the corresponding coefficient determined without considering the nonlinear law of the dependency of shear modulus on deformations.

The obtained results can be extended to butt joints. Considering the non-linearity of rubber shear deformations is expedient because lengths of butt joint steps are smaller than sizes of areas of stress disturbance from a local change in butt joint design.

Considering the nonlinear deformation-dependent shear modulus of rubber provides an opportunity to specify the prediction of a rope stress state with a continuity breakage of cables, increase safety and operational reliability of rubber-cable tractive elements.

The results are obtained using well-known methods of theory of composite materials of a rubber-cable rope model and its solution using analytical methods. The model considers the nonlinear law of rubber deformation. This allows considering the obtained results as sufficiently reliable and as such that they clarify the idea of a mechanism of deformation of rubber-cable ropes and belts.

## References

1. **Moldabayev, S.K., Adamchuk, A.A., Toktarov, A.A., Aben, Y., Shustov, O.O.** (2020). Approbation of the technology of efficient application of excavator-automobile complexes in the deep open mines. *Naukovyi Visnyk Natsionalnoho Hirnychoho Universytetu*, (4), pp. 30-38. DOI: 10.33271/nvngu/2020-4/030
2. **Pysmennyi, S., Fedko, M., Shvaheer, N., Chukharev, S.** (2020). Mining of rich iron ore deposits of complex structure under the conditions of rock pressure development. *E3S Web of Conferences*, 2020, 201, 01022. DOI: 10.1051/e3sconf/202020101022
3. **Tytov, O., Haddad, J., Sukhariev, V.** (2019). Modelling of mined rock thin layer disintegration taking into consideration its properties changing during compaction. *E3S Web of Conferences*, 109, 00105. DOI:10.1051/e3sconf/201910900105
4. **Shustov, O.O., Haddad, J.S., Adamchuk, A.A., Rastsvietaiev, V.O., Cherniaiev, O.V.** (2019). Improving the Construction of Mechanized Complexes for Reloading Points while Developing Deep Open Pits. *Journal of Mining Science*, 2019, 55(6), pp. 946-953. DOI: 10.1134/S1062739119066332
5. **Bondarenko, A.O., Haddad, J.S., Tytov, O.O., Alfaqs, F.** (2021). Complex for processing of rubble wastes of stone dressing. *International Review of Mechanical Engineering*, 15(1), pp. 44-50. DOI: 10.15866/ireme.v15i1.20205
6. **Peremetchyk, A., Kulikovska, O., Shvaheer, N., Chukharev, S., Fedorenko, S., Moraru, R., Panayotov, V.** (2022). Predictive geometrization of grade indices of an iron-ore deposit. *Mining of Mineral Deposits*, 16(3), pp. 67-77. DOI: 10.33271/mining16.03.067
7. **Kovalevska, I., Samusia, V., Kolosov, D., Snihur V., Pysmenkova , T.** (2020). Stability of the overworked slightly metamorphosed massif around mine working. *Mining of Mineral Deposits*, 14(2), 43-52. DOI: 10.33271/mining14.02.043
8. **Sotskov, V., Dereviahina, N., & Malanchuk, L.** (2019). Analysis of operation parameters of partial backfilling in the context of selective coal mining. *Mining of Mineral Deposits*, 13(4), 129-138. DOI: [10.33271/mining13.04.129](https://doi.org/10.33271/mining13.04.129)
9. **Shvaheer, N., Komisarenko, T., Chukharev, S., Panova, S.** (2019). Annual production enhancement at deep mining. *E3S Web of Conferences*, 123, art. no. 01043. DOI: 10.1051/e3sconf/201912301043
10. **Naumov, V., Zhambabayev, B., Agabekova, D., Zhanbirov, Z., Taran, I.** (2021). Fuzzy-logic approach to estimate the passengers' preference when choosing a bus line within the public transport system. *Communications - Scientific Letters of the University of Žilina*, 23(3), pp. A150-A157. DOI:10.26552/com.C.2021.3.A150-A157
11. **Kravets, V., Samusia, V., Kolosov, D., Bas, K., Onyshchenko, S.** (2020). Discrete mathematical model of travelling wave of conveyor transport. II International Conference Essays of Mining Science and Practic, Vol. 168. DOI: 10.1051/e3sconf/202016800030
12. **Shpachuk, V., Chuprynin, A., Daleka, V., Suprun, T.** (2020). Simulation of impact interaction of rail transport carriage in a Butt Roughness Zone. *Scientific Journal of Silesian University of Technology. Series Transport*, 106, pp. 141-152. DOI:10.20858/sjsutst.2020.106.12

13. **Sladkowski, A.V., Kyrychenko, Y.O., Kogut, P.I., Samusya, V.I., Kolosov, D.L.** (2019). Innovative designs of pumping deep-water hydrolifts based on progressive multiphase non-equilibrium models. *Naukovyi Visnyk Natsionalnoho Hirnychoho Universytetu*, (2), pp. 51-57. DOI: 10.29202/nvngu/2019-2/6
14. **Bondarenko, A.O., Maliarenko, P.O., Zapara, Ye., Bliskun, S.P.** (2020). Testing of the complex for gravitational washing of sand. *Naukovyi Visnyk Natsionalnoho Hirnychoho Universytetu*, (5), 26-32. DOI: 10.33271/nvngu/2020-5/026
15. **Shpachuk, V.P., Zasiadko, M.A., Dudko, V.V.** (2018). Investigation of stress-strain state of packet node connection in spatial vibration shakers. *Naukovyi Visnyk Natsionalnoho Hirnychoho Universytetu*, (3), 74-79. DOI: 10.29202/nvngu/2018-3/12
16. **Bazhenov, V.A., Gulyar, A.I., Piskunov, S.O., Shkryl, A.A.** (2006). Life assessment for a gas turbine blade under creep conditions based on continuum fracture mechanics. *Strength of Materials*, 38(4), pp. 392-397.
17. **Bazhenov, V.A., Gulyar, A.I., Piskunov, S.O., Shkryl, A.A.** (2008). Gas turbine blade service life assessment with account of fracture stage. *Strength of Materials*, 2008, 40(5), pp. 518-524.
18. **Vynohradov, B.V., Samusya, V.I., Kolosov, D.L.** (2019). Limitation of oscillations of vibrating machines during start-up and shutdown. *Naukovyi Visnyk Natsionalnoho Hirnychoho Universytetu*, (1), pp. 69-75. DOI: 10.29202/nvngu/2019-1/6
19. **Chigirinsky, V., Naumenko, O.** (2020). Invariant Differential Generalizations in Problems of the Elasticity Theory As Applied to Polar Coordinates. *Eastern-European Journal of Enterprise Technologies*, 5(7 (107)), 56-73. DOI: 10.15587/1729-4061.2020.213476
20. **Marasová, D., Ambriško, L., Andrejiová, M., Grinčová, A.** (2017). Examination of the process of damaging the top covering layer of a conveyor belt applying the FEM. *Journal of the International Measurement Confederation*, (112), 47-52. DOI:10.1016/j.measurement.2017.08.016
21. **Belmas, I., Kogut, P., Kolosov, D., Samusia, V., Onyshchenko, S.** (2019). Rigidity of elastic shell of rubber-cable belt during displacement of cables relatively to drum. *International Conference Essays of Mining Science and Practice*, Vol. 109, 00005. DOI: 10.1051/e3sconf/201910900005
22. **Blazej, R., Jurdziak, L., Kirjanow-Blazej, A.** et al. (2021). Identification of damage development in the core of steel cord belts with the diagnostic system. *Sci Rep* 11, 12349. DOI: 10.1038/s41598-021-91538-z
23. **Webb, C., Sikorska, J., Khan, R., & Hodkiewicz, M.** (2020). Developing and evaluating predictive conveyor belt wear models. *Data-Centric Engineering*, 1, E3. DOI: 10.1017/dce.2020.1
24. **Pang, Y., Lodewijks, G.** (2006). A Novel Embedded Conductive Detection System for Intelligent Conveyor Belt Monitoring. 2006 IEEE International Conference on Service Operations and Logistics, and Informatics, SOLI 2006. 803-808. DOI: 10.1109/SOLI.2006.328958

25. **Volohovskiy, V.Yu., Radin, V.P., & Rudyak, M.B.** (2010). Concentration of loads in cables and a bearing ability of rubber-cable conveyor belts with breakages. *MPEI Vestnik*, (5), 5-12.
26. **Bel'mas, I.V.** (1993). Stress state of rubber-rope tapes during their random damages. *Problemy Prochnosti i Nadezhnos'ti Mashin*, 1993, (6), pp. 45-48.
27. **Ropay V.A.** (2016) *Shakhtnyye uravnoveshivayushchiye kanaty: monograph [Mining balancing ropes]*. Dnipropetrovsk : National Mining University. 263 p.
28. **Levchenya, Zh.B.** (2004). Increase of reliability of butt-joint connections of conveyor belts at mining enterprises: PhD dissertation: 05.05.06.
29. **Kolosov, L.V., Bel'mas, I.V.** (1981). Use of electrical models for investigating composites. *Mechanics of Composite Materials*, 1981, 17(1), pp. 115-119.
30. **Daria Zade S.** (2013). Numerical method of determining effective characteristics of unidirectional reinforced composites. *Bulletin NTU "KhPI"*, (58), 71-77.
31. **W. Song, W. Shang and X. Li,** (2009). Finite element analysis of steel cord conveyor belt splice. *International Technology and Innovation Conference 2009 (ITIC 2009)*, Xi'an, China, pp. 1-6. DOI: 10.1049/cp.2009.1415
32. **Xianguo Li, Xinyu Long, Zhenqian Shen, Changyun Miao** (2019). Analysis of Strength Factors of Steel Cord Conveyor Belt Splices Based on the FEM. *Advances in Materials Science and Engineering*, Volume 2019, ID 6926413. DOI: 10.1155/2019/6926413
33. **Fedorko, G., Molnar, V., Michalik, P., Dovica, M., Kelemenová, T., Toth, T.** (2018). Failure analysis of conveyor belt samples under tensile load. *Journal of Industrial Textiles*. 48. 152808371876377. DOI: 10.1177/1528083718763776
34. **Andrejiova, M., Grincova, A., Marasova, D.** (2019). Failure analysis of the rubber-textile conveyor belts using classification models. *Engineering Failure Analysis*. 101. 407-417. DOI: 10.1016/j.engfailanal.2019.04.001
35. **Belmas I.V., Kolosov D.L., Kolosov A.L., Onyshchenko S.V.** (2018). Stress-strain state of rubber-cable tractive element of tubular shape. *Naukovyi Visnyk Natsionalnoho Hirnychoho Universytetu*, (2), pp. 60-69. DOI: 10.29202/nvngu/2018-2/5
36. **Kirjanów-Błażej, A., Błażej, R. Jurdziak, L., Kozłowski, T.** (2017). Core damage increase assessment in the conveyor belt with steel cords. *Diagnostyka*. 18. 93-98.
37. **Romek D., Ulbrich D., Selech J., Kowalczyk J., Wład R.** (2021). Assessment of Padding Elements Wear of Belt Conveyors Working in Combination of Rubber-Quartz-Metal Condition. *Materials (Basel)*. Aug 2;14(15):4323. DOI: 10.3390/ma14154323
38. **Yao Y., Zhang B.** (2020). Influence of the elastic modulus of a conveyor belt on the power allocation of multi-drive conveyors. *PLoS One*. Jul 7; 15(7):e0235768. DOI: 10.1371/journal.pone.0235768
39. **Zabolotny, K.S., Panchenko, E.V., Zhupiev, A.L.** (2011). *Teoriya mnog-osloynnoy namotki rezinotrosovogo kanata [Theory of multilayer rubber-cable rope winding]*. Dnipropetrovsk: NGU.
40. **Haddad, J.S., Denyshchenko, O., Kolosov, D., Bartashevskiy, S., Rastsvietaiev, V., & Cherniaiev, O.** (2021). Reducing Wear of the Mine Ropeways Components Basing Upon the Studies of Their Contact Interaction. *Archives of Mining Sciences*, 66(4), 579-594. DOI: 10.24425/ams.2021.139598

## UKRAINIAN EXPERIENCE IN IMPLEMENTING ENERGY MANAGEMENT SYSTEMS IN THE INDUSTRIAL SECTOR



**Nataliia DRESHPAK**

PhD, associate professor,  
Department of Electrical Engineering,  
Dnipro University of Technology, Ukraine

### **Abstract**

**Research objectives.** The presented research pursued the following objectives: (i) to determine the features of energy management control in technological processes at Ukrainian industrial enterprises based on the idea of sustainable development; (ii) to study the experience of Ukraine in creating a network of energy-efficient enterprises; (iii) to investigate barriers to improving the energy efficiency of industrial enterprises; (iv) to analyze the model of energy management based on ISO 50001; (v) to present the results of energy efficiency control in a coal mine at PJSC “Pavlogradvugillya”.

**Methodology.** The research was based on exploring the academic literature, international documents, and reports, and analyzing the statistical data referring to Ukrainian energy practice.

**Findings.** The existing methods of energy management at industrial enterprises are not efficient and require improvements. The main functions of such management are performed by the power engineering service, which has no indispensable ramified frame to control energy consumption directly on workstations. It is possible to improve the situation in energy consumption by applying energy management systems in enterprises. To control the efficiency of processes in manufacturing divisions, the planned indicators of energy consumption are calculated and compared with the actual indicators. Comparing the planned indicators with the actual data makes it possible to conclude the energy efficiency of the divisions.

**Conclusions and recommendations.** Implementation of continuous control is not possible without modern information technologies that allow the monitoring of the level of energy use in real-time, detect periods of high energy consumption, and take effective management decisions to optimize energy consumption.

### **Introduction**

The problem of high energy intensity of the country's gross domestic product is related not only to the use of energy-intensive equipment and outdated technologies but also to the lack of systematic understanding and management of the processes of use and consumption of energy resources [1]. The world-recognized way

of solving such problems is the implementation of energy management systems (EnMS) that meet the international standard ISO 50001. Thousands of industrial companies in Europe use energy management systems in their enterprises. In the industrial sector, from 2018 to 2019, the largest number of ISO 50001 certificates were obtained by enterprises in the metallurgical, food, and chemical industries [2]. The leaders in ISO adoption are Germany (6,243 in 2018), Great Britain (1,153), and (in recent years) China (2,364). At the same time, the following number of certificates were issued in Ukraine (according to official ISO reviews): in 2016 - 21; in 2017–189; in 2018–21; in 2019–12 [1].

Experience shows that enterprises implementing EnMS, with minimal capital investments, receive an increase in energy efficiency within the range of 10-20% [3]. This fact forms the basis of positive forecasts regarding the prospects for the development of such systems both in the world and, in particular, in Ukraine.

The law "On energy efficiency" [4] recently adopted by the Verkhovna Rada of Ukraine repeals the law "On energy saving", focusing on ensuring the "energy efficiency" of production processes with a clear definition of the meaning of this term as a quantitative indicator of the relationship between work, services, goods or energy at the output and the specified energy at the input. Based on the content of the adopted law, it is planned to strengthen control actions by the state in the field of energy resource consumption and to implement a policy of significantly reducing energy consumption.

The effectiveness of energy consumption management processes largely depends on the implementation of the idea of sustainable development in Ukraine. An analysis of the features of the implementation of this idea in the economy of Ukraine allows us to assess the effectiveness of the steps taken. Such an analysis is carried out in subsection 1. The energy efficiency of production processes is related to the perception by the company's service personnel of problems that prevent them from reducing energy consumption. Often the views existing in the enterprise do not correspond to the real state of affairs. Subsection 2 is devoted to determining the degree of significance of the existing barriers on the way to improving the energy efficiency of one of the industrial enterprises obtained through a questionnaire. Subsection 3 analyzes the structure

of the energy management system that complies with the international standard ISO 50001. The implementation of energy management systems in Ukraine had its peculiarities related to the content of consulting services provided by Western countries as part of aid and aimed at solving energy problems. Subsection 4 reveals the principles of implementation of such systems for coal mines of Ukraine and demonstrates their connection with the content of actions proposed by the ISO 50001 standard.

### **Concept of sustainable energy development in Ukraine**

It is known that the world's population is constantly growing, and the energy needs of society are increasing accordingly. Every day, humanity needs more energy to meet its needs, and this process is progressing. The development of the industrial sector using traditional sources of energy (coal, oil, gas) is accompanied by the depletion of natural resources and the emission of greenhouse gases, as a result of which the climate on the planet is gradually changing. Industrial enterprises consume about 38% (of the total volume) of the world's final energy consumption. They are the cause of 24% of total CO<sub>2</sub> emissions [5]. The environmental consequences of wasteful energy consumption make us think about how efficiently and safely we use energy resources.

The concept of sustainable development, proposed by the American economist Daly German, is the basis of the EU's strategic planning principles and is defined as "development that meets the needs of the present without jeopardizing the ability of future generations to meet their own needs" [6]. In 2012, at the UN summit (Conference, Rio+20), the Sustainable Development Goals (SDGs) were formulated, one of which (Goal 12 - Responsible consumption and production) is aimed at ensuring the transition from existing to rational models of consumption of energy resources in the production process.

To adapt the Sustainable Development Goals to the national specifics of Ukraine, national consultations were held in 2016 to discuss the relevance of the goals to the conditions of Ukraine and to determine the directions of work for their integration into strategic planning. The results of the ranking of the Sustainable Development Goals in the conditions of Ukraine confirm the significance of

introducing new energy-saving technologies and creating conditions for reducing the impact on the environment [7].

In November 2016, Ukraine signed the Memorandum on Strategic Partnership between Ukraine and the EU. As a result, our country became a full member of the European Energy Community. This agreement provides for the implementation of the third EU energy package, the purpose of which is to increase the efficiency of the use of energy resources, create competitive conditions for the functioning of the energy market, and promote the development of renewable energy sources. On April 22 of the same year, Ukraine signed the Paris Agreement and announced the goal of reducing the country's anthropogenic greenhouse gas emissions by 40% by 2030 (compared to the state of greenhouse gas emissions in 1990 [8]).

Analyzing the causes of the occurrence of greenhouse gases in Ukraine, it should be emphasized that the main consumer of primary energy resources in our country is industry [1]. Even though, according to official data, the level of energy intensity of Ukrainian enterprises is constantly decreasing, it still exceeds the indicators of developed countries. Thus, in 2015, the energy intensity of the products of the steel industry in Ukraine was 0.52 t per year. for 1 thousand dollars USA, when the average value in EU countries is 0.31 [9].

To characterize the efficiency of the use of energy resources in the world, an indicator called the Energy Trilemma Index is used. It takes into account three main criteria of energy efficiency, namely: energy security (reliability of energy supply to consumers), energy justice (fair access of consumers to energy resources), and environmental sustainability (which shows how energy resources affect the environment). According to official data, in 2019, according to the Energy Trilemma Index, Germany ranked 9th among 128 countries in terms of all indicators of energy efficiency. At the same time, Ukraine took 61st place in this rating, including the 7th place for energy security, 85th place for energy justice, and 65th place for environmental sustainability [9].

A significant part of the energy supply companies operating in the market of energy services in Ukraine belong to one owner. The monopoly on energy services limits the opportunities of other market participants to take an active part in the production or transmission of



energy, to influence the formation of fair (competitive) prices. The lack of competition causes restrictions on the free access of enterprises to energy resources, and insufficient transparency of the activities of energy companies. This creates conditions for the distortion of a clean energy supply procedure, where one enterprise has expanded access to energy resources, while another is forced to settle for unfavorable terms of energy supply or distribution.

Tariffs for energy resources for Ukrainian industry are quite high compared to EU countries [10]. So, for example, the cost of electricity for industrial enterprises is 12 euro cents per kWh. (twice as high as the price in the Czech Republic, Slovakia, and Poland). For domestic and small non-domestic consumers, the cost of 1 kWh according to Eurostat is about 5 euro cents [11]. The increase in tariffs exacerbates the issue of ensuring the energy balance of the enterprise at acceptable prices and brings the significance of its solution to the first.

### **Determining the significance of barriers to increasing the energy efficiency of production processes**

As part of the DAAD project *"Transition to Sustainable Consumption and Production in Industry: The Business Management Context"*, employees of the Dnipro University of Technology conducted research at one of the enterprises specializing in the production of hardware products (Dnipro, Ukraine). The purpose of the study was to identify barriers (negative factors) on the way to improving the sustainability of the production process and rational consumption of energy resources. The heads of the production divisions of the enterprise were asked to answer several questions formulated in the questionnaire and to quantitatively assess the significance of factors that affect the sustainability of the production process. Each factor was evaluated on a five-point scale (1 to 5 points). 13 respondents took part in the survey. Therefore, the maximum score for each factor is 65 points. Then the ratio of points in the answers and the maximum number of points that each factor could score in its category was determined. The results of factor ranking made it possible to obtain the necessary statistical data and build graphs based on them.

First of all, the general factors affecting sustainable production and energy consumption of the enterprise were subject to evaluation.

It turned out that from the point of view of the company's specialists, the lack of knowledge and lack of operational information regarding the conditions of sustainable consumption of energy resources and production of products are the most important factors that affect sustainability indicators (Fig. 1).

In particular, it turned out that the employees of the enterprise, including heads of departments, practically do not receive information about the content of new technologies and the existing experience of the production of similar products by other market participants (Fig. 2). There is a need to increase the awareness, first of all, of the company's management not only about problems related to production and energy consumption but also about conceptual issues of sustainable development. There is a high probability that such a situation is typical for the majority of production enterprises in Ukraine. If the enterprise intends to enter the international market, its activities must meet the requirements of ISO standards. The tasks of educators are obvious - they must ensure that students master the basics of current international standards in the field of sustainable production: energy, environmental, and social standards (ISO 9001, 14001, 4500, 50001) and, thus, contribute to the solution of the problem of staffing of enterprises. This also applies to business structures, which require educated specialists capable of solving problems specific to industrial production.

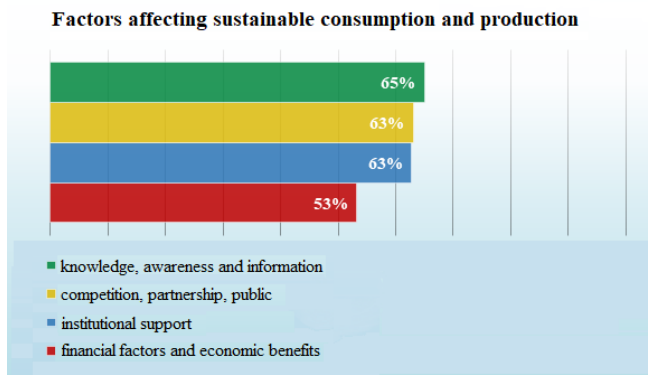


**Fig. 1. Ratio of general factors influencing the sustainability production process**

### Knowledge, awareness, information

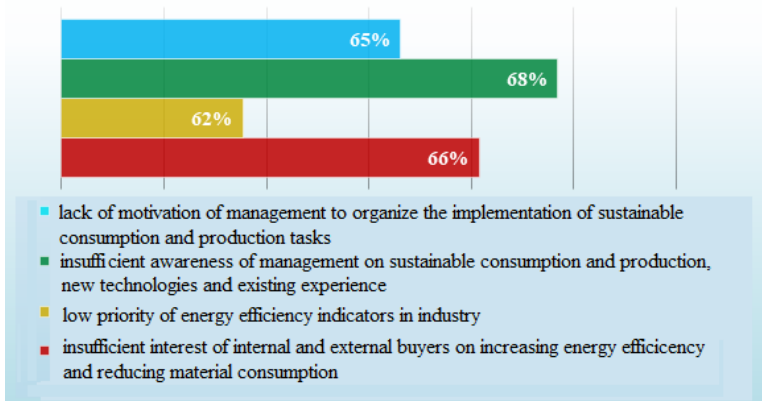
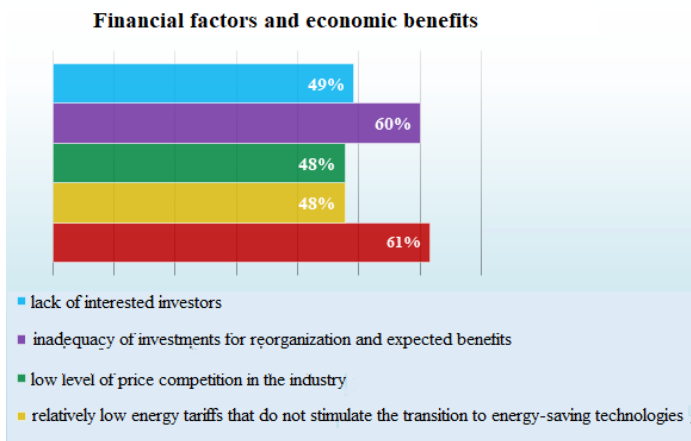


Fig. 2. Knowledge, awareness, and completeness of information as influencing factors on the stability of the production process

Another interesting result of the conducted research was that financial factors and economic benefits turned out to be the least important from the point of view of their influence on the sustainability of production (Fig. 3). This is due to limited access to cheap financial resources for the implementation of energy efficiency projects, as well as the inadequacy of investments aimed at the reorganization of the enterprise.

Despite the lack of expressed interest of enterprises in solving energy-saving tasks, we are faced with the fact that energy tariffs for industry in Ukraine are constantly increasing, and therefore the solution of these tasks is motivated by the existing tariff situation.



**Fig. 3.** Impact of financial factors and economic benefits

### **Energy management model based on the ISO 50001 standard**

The problem of high energy intensity of the country's gross domestic product is related not only to the use of energy-intensive equipment and outdated technologies but also to the lack of systematic understanding and management of the processes of use and consumption of energy resources [1]. A recognized way to solve such problems is the implementation of energy management systems (EnMS) that meet the international standard ISO 50001. The annual number of industrial enterprises certified by the International Organization for Standardization (ISO) for compliance with international energy management standards (ISO 50001) is an indicator of the prevalence of such systems, both in the country and in the world. Today, thousands of companies in Europe use energy management systems in their enterprises. In the industrial sector, from 2018 to 2019, the largest number of ISO 50001 certificates were obtained by enterprises in the metallurgical, food, and chemical industries [2].

Practical experience shows that enterprises that implement EnMS, with minimal capital investments, during the first years receive an increase in energy efficiency within the range of 10-20% [3]. The leaders of ISO implementation are Germany (6243 in 2018), Great Britain (1153), and (in recent years) China (2364) (Fig. 4). At the

same time, in Ukraine (according to official ISO reviews) the following number of certificates: in 2016 - 21; in 2017-189; in 2018-21; in 2019-12 [1], which proves the low prevalence of energy management systems in Ukraine.



**Fig. 4.** Worldwide issued ISO 50001 certificates  
(Source: IEA, 2016)

What causes this situation? The fact is that the services of the enterprise, which are usually responsible for the functioning of the EnMS, do not have experience in their implementation and operation. These services are few and their duties are mainly related to solving the current tasks of operation and repair of power equipment. Solving the tasks of increasing the level of energy efficiency is not a priority action for the management and staff of the energy service, which does not contribute to reducing energy consumption.

Another significant problem of the activity of industrial enterprises is the existing organization of the order of control and management of energy use. The main functions of managing energy use at enterprises are performed by the Chief Energy Officer, which does not have an extensive structure for monitoring energy consumption directly at workplaces. The energy service, as a rule, does not have modern information support for the management process. There are no effective mechanisms capable of timely responding to wasteful use of energy, creating conditions for optimal

energy consumption, and taking into account the specifics of production and output. Therefore, measures to increase the energy efficiency of production are often reduced to defining the content of annual energy consumption management programs without proper technical and economic substantiation of their components. Such a state of affairs with the energy management of Ukrainian enterprises is confirmed, in particular, by the results of surveys conducted in subsection 2, where the practical absence of important links in the structure of the management system, which ensures timely and meaningful information support for the processes of monitoring energy efficiency indicators, is monitored. The world practice of EnMS implementation testifies to their broad possibilities of combining reliable information about the available indicators of energy efficiency of production processes with optimal management solutions for the given conditions.

According to the requirements of ISO 50001, the cycle of operation of EnMS is based on a methodology known as the "cycle of continuous improvement" "Plan-Do-Check-Act" (PDCA) - "Plan-Do-Check-Act" or "Deming's cycle" and can be represented by the four stages [1].

Thus, the energy management implemented by the system is a complex of continuous processes and tools that are combined with the business processes of any organization, in particular, with the production of industrial products. It motivates her to constantly manage energy consumption and search for ways to improve energy performance. Processes and tools encompass not only procedures, equipment, and technologies but also the executors of planned actions. The effectiveness of any system (even a fully automated one) depends on the behavior of the people who created it, maintain its functioning, and improve its characteristics. Attention should be paid to the fact that the energy management system is a closed system, where planned indicators are formed and their implementation is ensured through the implementation of management actions. It is also important that the activity of the system extends to the totality of technological processes related to the production of products. It is obvious that when solving the tasks of increasing the energy efficiency of production processes, one should focus on the planning of the energy intensity indicators of technological processes and ensure their acceptable (from the point

of view of energy saving) values during the production process. An important operation that ensures the operation of the energy management system is the control of the efficiency of energy use by the structural divisions of the enterprise. To control the efficiency of processes in the structural divisions, the planned indicators of energy consumption are calculated and compared with the actual indicators. Comparison of planned indicators with actual data makes it possible to conclude the efficiency of energy use by this facility.

The proposed structure of EnMS within the framework of the ISO 50001 standard does not specify the content of the listed operations (planning, improvement, evaluation, etc.). Their filling can be different and correspond to specific features of the production process. The task of specifying these components rests with the developers of the system that will function in the conditions of a specific production. The justification of the decisions taken by the developers is their novelty as scientific research.

### **Principles of energy efficiency control of technological processes**

As an example, let's consider the particularities of the specification of solutions proposed in the creation of energy management systems for coal mines in Ukraine [12].

Electrical energy, as a rule, forms the basis of energy consumption in coal mines. As a rule, mines have commercial metering meters installed at the input of the substation, and, have technical metering meters installed to determine the energy consumption of powerful consumers. Usually, the existing level of energy consumption control is determined using Table 1. The above signs according to Table 1 correspond to the second or third level of control.

Table 1

Levels of energy efficiency control	
Levels	Characteristics of the control process
1	Monthly energy bills are fixed only
2	Monthly meter readings are compared with payment invoices
3	Energy consumption in separate structural divisions of the enterprise is controlled
4	Monthly meter readings are compared with the company's output and the specific energy consumption (energy efficiency) is determined
5	Operational control of energy efficiency indicators in the Centers for Energy Accounting (CEA) is carried out

The global practice of control and management of energy use provides for the allocation of separate divisions in the production structure of the enterprise with independent control of energy consumption [12]. Such links, which are allocated in the structure of the enterprise, were named the Centers for Energy Accounting (CEA). The need to separate individual links in the structure of the enterprise is connected with the general idea of solving energy efficiency tasks directly at the places of energy consumption, involving in this process a significant number of service personnel who take a direct part in the production technology. Based on the fact that the CEA is a management object, attention should be paid to its determination procedures, providing several requirements that it must meet. It:

- the energy consumption at the center must be *significant* (more than 5% in the structure of electric power consumption);
- energy meter must be installed to measure the consumption of electrical energy at the CEA;
- there must be a person responsible for energy use.

To determine the most energy-intensive consumers of energy, it is necessary to analyze the annual energy balances of an industrial enterprise, where its total costs are distributed between individual units and energy receivers. If the energy balances of the enterprise have not been drawn up, then there is a possibility of using the passport data of energy-intensive equipment for analysis. The location of the equipment on the territory of the enterprise serves as information about the possible placement of the central heating system. For example, let's analyze the energy balance (in percent) of the "Zakhidnodonbaska No. 1" coal mine. The components of this balance sheet are typical for most coal mines in Ukraine:

- mining areas	5,26
- preparatory areas	1,29
- underground transport	5,6
- air conditioning	10,88
- rise	13,32
- drainage	14,28
- ventilation	17,13
- technological surface complex	3,75
- production of compressed air	2,46
- other electrical receivers	20, 58
- lighting	0,69



As you can see, there are receivers with significant amounts of energy consumption at the mine. In the first approximation, each item of significant energy consumption should correspond to a separate CEA. The extent to which such an approach to the creation of centers is possible will be shown by the results of the fulfillment of other conditions specific to the Central Economic Center. For this, it is necessary to analyze the structure of the existing electricity distribution system at the mine.

The analysis of the scheme [12] showed that the substations of the mine have feeders that supply ventilation units, compressors, skip lifts, cage lifts, as well as other objects of the technological complex of the surface. Feeders for powering underground electrical installations are also allocated. Thus, there is a correspondence between the structure of the electricity distribution scheme and the structure of the previously mentioned components of the energy balance. Such compliance is understandable since the energy balance is compiled based on the results of energy accounting at the mine's substations. It is obvious that if the named feeder cells are provided with means of energy accounting, the created centers (CEAs) will be able to control the consumption of electricity by the components of the given energy balance.

Control of electricity consumption assumes the presence of standardized values of energy consumption. It is characteristic that not all mines have standardized indicators determined for the existing conditions of coal production. An important step in normalizing the level of energy consumption in the Central Power Plant is the determination of the parameters on which this level depends. When choosing parameters, it is necessary to ensure the fulfillment of two requirements:

- the target parameters should reflect the ultimate goal of energy use in the Central Power Plant (for example, achieving a given volume of production output);
- there should be the possibility of measuring with the necessary accuracy both target and additional parameters that also affect energy consumption.

Below, as an example, there is a table of parameters (target and additional), which are often used as those that are recommended to

be taken into account when determining the levels of energy consumed by installations (Table 2) [12].

Table 2

Select parameters that influence energy consumption at CEA

Electrical installation	Target parameter	Additional parameter
Powerful fans	Air volume	–
Low power fans	Work time	–
Powerful pumps	Fluid volume	–
Low power pumps	Work time	–
Conveyors	Work time	–
Compressors	Air volume	Ambient temperature
Air conditioning	Ambient temperature	Humidity
Lighting	Work time	Average daily temperature

Quite often, the indicator of the volume of production is used as the main (target) parameter. If a division of an industrial enterprise specializes in the production of several types of products, then it is desirable to control energy consumption on each technological line of the division, which is characterized by the production of a separate type. In conditions where it is problematic to select individual CEAs on this basis (for example, with relatively low energy consumption indicators of individual technological lines), it is possible to combine several lines into a CEA. To do this, it is necessary to determine a general indicator that will characterize the volume of energy consumption of the unit as a whole.

When implementing EnMS in production, attention should be paid to the motivation of direct executors of technological operations related to the production of products. It is necessary to determine the officials who will be personally responsible for the use of energy in the created central heating and cooling centers. Often, during the formation of the CEA, they face a problem when the structural division of the enterprise, based on which there is a possibility of creating a CEA, is subordinate to different persons. An example can be the equipment of a production facility, in which several workshops have a common energy distribution system. In this case, it is advisable to distribute the areas of responsibility of individual officials by installing additional energy meters. The optimal option for applying the proposed approach to determining the CEA is the

presence in the management structure of the unit of officials who are responsible for the work of individual production sites.

Statistical processing of experimental data with the construction of regression models is often used for the formation of no CEAs [12]. When substantiating the list of parameters on which energy consumption depends, it is also necessary to focus on the expected type of regression dependence (single or multiple regression). Fig. 5 shows a single regression in the form of a constant value of the consumed CEA energy -  $E = \text{const}$ . In this case, energy consumption  $E$  does not depend on the volume of production  $P$ . This is observed, for example, in lighting systems of industrial premises.

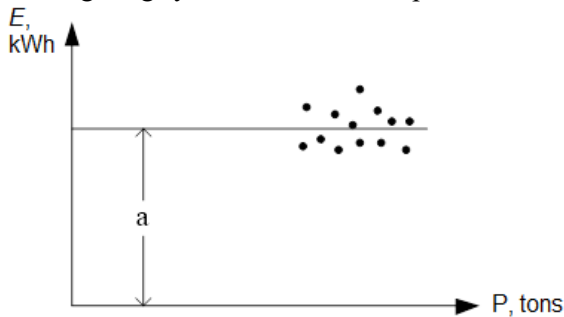


**Fig. 5.** Regression in the form of constant value  $E = \text{const}$  (Source: [12])

Nonlinear regression is usually formed in the form of a polynomial of the  $n$ th degree  $E = a + bp + cp^2 + \dots + dp^n$ . Multiregression represents the dependence of  $E$  on several parameters  $E = a + bp_1 + cp_2 + \dots + dp^n$ . Its use is advisable in the case when the influence of additional parameters on energy consumption is significant. Usually, no more than three parameters ( $p_1, p_2, p_3$ ) are used in such regression models.

Often in the practice of energy management, the regression dependence is represented as a straight line with a slope (linear regression). Fig. 6 shows the linear relationship between the parameters  $\hat{y}$  (estimated energy consumption level) and  $x$  (output volume), which is constructed based on the results of observations.

The dependence  $\hat{y} = f(x)$  is built based on the method of least squares, which ensures the minimum dispersion of  $S$  values of  $u_i$  around the function  $f(x)$

$$S = \sum_{i=1}^n [y_i - f(x_i)]^2$$

If, as a result of energy consumption control, the actual energy consumption exceeds the average value (based on the location of the regression line), then it can be considered that the energy consumption obtained is overestimated, and such a level of energy consumption is not legitimate (irrational use of energy). Conversely, values below the regression line indicate a rational level of energy consumption. Therefore, the regression line is the boundary separating the satisfactory results of the operation of the CEA from the unsatisfactory ones. In the case of unsatisfactory indicators, it is necessary to draw conclusions and take measures (management decisions) to reduce energy consumption within the capabilities of the current energy management system.

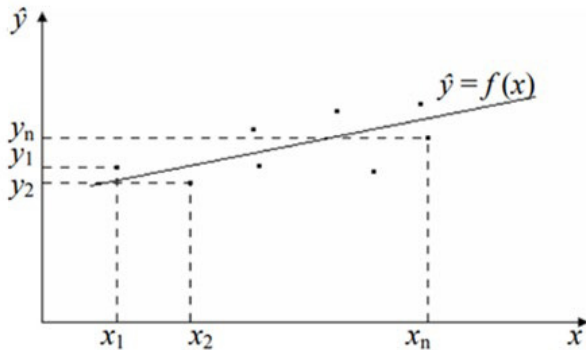
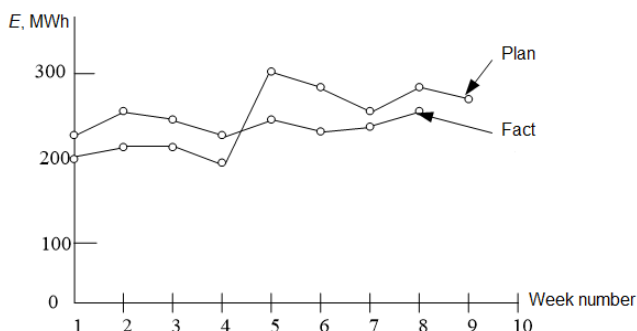


**Fig. 6.** Standard linear regression dependence  $\hat{y} = f(x)$  (Source: [12])

Based on the results of monitoring the efficiency of energy use, reports must be drawn up in the Central Power Plant. At the same time, the availability and reliability of the received information is ensured. The results of the comparison of the actual energy consumption indicators with the planned ones can be presented in the form of graphs, tables, and diagrams. Examples of control results in the form of graphs and tables are shown in Fig. 7 and Table 3 [12].

The change in the accumulated (cumulative) amount of deviations over a certain period is of interest to the energy manager, as it allows

to assess the degree of difference between the actual energy consumption indicators and the planned energy consumption during a certain period. At the same time, deviation indicators obtained during individual measurements are added. Thus, with weekly measurements, it is possible, for example, to record the result of the accumulation of energy consumption deviations for a month. This indicator can be used for the overall assessment of the efficiency of the central office during the month. The results of the control should be known to the personnel of the CEA. They are discussed by the team and analyzed to improve the situation.



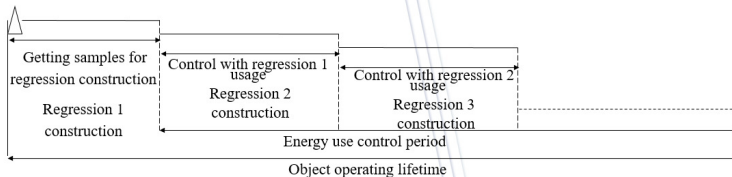
**Fig. 7.** Graphical appearance of energy consumption  
(Source: [12])

Table 3

Energy consumption control				
Week number	Actual energy consumption, kWh	Planned indicators, kWh	Deviation, kWh	Accumulated (cumulative) sum, kWh
1	170	170	0	0
2	180	210	- 30	- 30
3	200	250	- 50	- 80
4	230	180	50	- 30
5	200	170	30	0
6	150	170	- 20	- 20

Attention should be paid to the fact that the process of controlling energy consumption in the Central Power Plant is not passive. Comparing the actual energy consumption with the planned energy consumption should lead to the implementation by the center staff of actions aimed at reducing energy consumption. This means that the

location of the experimental data relative to the regression line will change, which will lead to the correction of the regression dependence (Fig. 8). Experimental data obtained in the process of controlling energy consumption can serve in the future to build the next regression dependence.



**Fig. 8.** Energy efficiency control process with plan indicators periodic changes  
(Source: [12])

The implementation of continuous control of energy efficiency is not possible without the introduction of modern information technologies that allow monitoring of the levels of energy use in real-time, identifying periods of increased energy consumption. The energy efficiency control system of production processes was developed by the employees of the Dnipro University of Technology and operated at the Heroes of Cosmos mine at PJSC “Pavlogradvugillya”. In the chief energy department of the mine, a computer program was installed that ensured the construction of regression dependencies and the processing of the results of the comparison of actual energy consumption with planned energy consumption [13]. The initial information for the work of the energy efficiency control program was the indicators of daily electricity consumption for the technological complex of the surface of the mine, underground consumers, coal lifting, as well as for the mine as a whole. These data were obtained from the Automatic energy meter reading systems (AMR) of the mine. Every day, the mine manager entered the value of the volume of coal production into this system. Thus, the input parameters of the energy efficiency control program were linked to the corresponding values of the controlled parameters of the AMR system, which allowed to ensure their joint operation. The program was implemented in the form of spreadsheets in the Excel environment [12, 13]. Fig. 9 illustrates the regression dependence of daily electricity consumption on the daily rate of coal

production. The dependence is built with confidence intervals that take into account the limited amount of statistical information obtained.

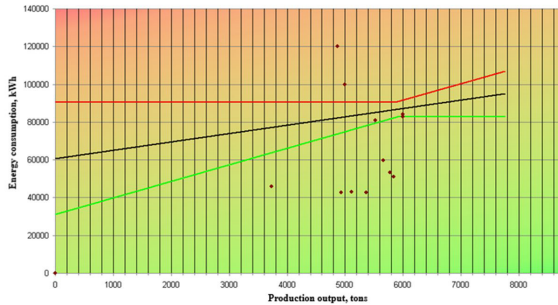


**Fig. 9.** Regression dependence of daily electricity consumption on the daily rate of coal production of the Heroes of Cosmos mine (Source: [13])

Fig. 10 illustrates the daily figures for overspending or savings of electricity. This information is subject to analysis. The causes of energy overspending should be clarified and appropriate actions should be taken to eliminate negative phenomena at workplaces.

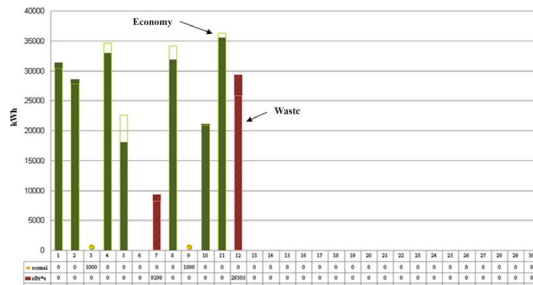


**Fig. 10.** Results of energy efficiency control of the Heroes of Cosmos mine (Source: [13])

The above-considered components of the construction and implementation of energy management systems of coal mines do not give a complete picture of the necessary actions. At the same time, when presenting the material, emphasis was placed on the presentation of fundamentally important components of the system, without which its functioning is not possible. These are positions related to the formation of planned tasks, control, and elements of energy consumption management.

## **Conclusions**

The main scientific and practical results of the work are as follows:

1. An important component of the concept of sustainable development is the application of rational models of consumption of energy resources, which ensure an increase in the energy efficiency of production processes. Ukraine is taking active steps to improve existing energy management methods.

2. The results of a questionnaire survey of the heads of production divisions of one of the industrial enterprises of Ukraine indicate a low awareness of the team regarding energy-saving tasks and methods of solving them, which indicates the expediency of implementing an energy management system at the enterprise.

3. The existing methods of controlling and managing the energy use of industrial enterprises of Ukraine, as a rule, are ineffective and require improvement. It is possible to improve their efficiency by applying energy management systems at enterprises, which are based on the principles of personal responsibility of the heads of production units for the achieved energy efficiency indicators, and involve the wide use of computer equipment.

4. The structure of energy management systems proposed by the ISO 50001 standard reveals a general approach to building such systems. These are closed-type systems with the presence of elements of energy consumption planning, assessment of its actual level, and formation of management actions that ensure an increase in the energy efficiency of processes. Specific implementation of the actions proposed by the standard should be carried out by system developers taking into account the specifics of both individual branches of industry and implementing enterprises. The justification of the decisions taken by the developers is their novelty as scientific discoveries.

5. The considered features of the construction of energy management systems of coal mines of Ukraine. Attention is focused on the process of forming planned indicators, the order of energy consumption control, and information support of the process. The content was analyzed and the specifics of the implementation of these actions were determined in the specific conditions of the operation of coal mines.



## References

1. **Chernyavskiy, A.** (2021). Guidelines for the implementation of the energy management system in accordance with the requirements of the international standard ISO 50001: 2018. Retrieved from [http://www.ukriee.org.ua/wpcontent/uploads/2021/03/EnMS-Practical-Guide-2021\\_Ukraine\\_ukr.pdf](http://www.ukriee.org.ua/wpcontent/uploads/2021/03/EnMS-Practical-Guide-2021_Ukraine_ukr.pdf).
2. Energy efficiency 2020: Fuel report (2017). Retrieved from <http://www.iea.org/digital>.
3. Ukraine has adopted national standards for energy audit and energy management in accordance with European norms (2016). Retrieved from <http://saec.gov.ua/uk/news/1184>.
4. About energy efficiency. № 1818-IX§ section I art. 5. (2021). Retrieved from <https://zakon.rada.gov.ua/laws/show/1818-20#Text>.
5. Digitalization and Energy: Technology Report 2017 (2017). Retrieved from <http://www.iea.org/digital>.
6. **Charles F. Kutscher, Jana B. Milford, Frank Kreith.** (2018) Principles of sustainable energy systems – Third edition: CRC Press Taylor & Francis, 654.
7. Sustainable Development Goals: Ukraine. National Report 2017 (2017). Retrieved from <http://surl.li/hoii>.
8. Climate agreement for Ukraine: Analytical note of the Institute of Economics and Forecasting of the National Academy of Sciences of Ukraine (2016). Retrieved from: <http://energyreform.uacrisis.org/climate> (дата звернення 26.11.2021).
9. **Palekhova, L.** (2020). Management of sustainable development: a guide to basic concepts. Tutorial. Published by Dnipro University of Technology. Retrieved from <https://mk.nmu.org.ua/ua/source>.
10. **Palekhova, L.** (2018) Positioning of industrial enterprises based on voluntary energy standards. NESEFF-NETZWERKTREFFEN Brandenburgische Technische Universität Cottbus-Senftenberg. pp. 11-19.
11. Electricity prices for household consumers, first half 2020 (Eur per kWh) (2020). Retrieved from [https://ec.europa.eu/eurostat/statisticsexplained/index.php?title=File:Electricity\\_prices\\_for\\_household\\_consumers\\_first\\_half\\_2020\\_\(EUR\\_per\\_kWh\).png](https://ec.europa.eu/eurostat/statisticsexplained/index.php?title=File:Electricity_prices_for_household_consumers_first_half_2020_(EUR_per_kWh).png).
12. **Pivnyak, G.G., Vypanasenko, S.I., Khovanska, O.I., Khatskevych, Yu.V., Dreshpak, N.S.** (2013). Energy management systems and their mathematical support. Tutorial. Published by National Mining University, 214.
13. **Dreshpak, N.S.** (2012). Measurement and control of the efficiency of electricity consumption by the enterprise's production units. Mining Electromechanics and Automatics №88, 139-143.
14. Implementation of the standard of energy management systems in the industry of Ukraine: UNIDO/GEF Project (2015). Retrieved from <http://www.ukriee.org.ua/uk/proekt/meta-proekta>.
15. Green Deal: New proposals to make sustainable products the norm and boost Europe's resource independence. (2021) Retrieved from [https://ec.europa.eu/commission/presscorner/detail/en/ip\\_22\\_2013](https://ec.europa.eu/commission/presscorner/detail/en/ip_22_2013).
16. Impacts of the EU's ecodesign and energy labelling legislation on third jurisdictions (2014) Retrieved from

[https://ec.europa.eu/energy/sites/ener/files/documents/201404\\_ieel\\_third\\_jurisdictions.pdf](https://ec.europa.eu/energy/sites/ener/files/documents/201404_ieel_third_jurisdictions.pdf).

17. Topten: Best products in Europe (2021). Retrieved from <https://www.topten.eu/private/page/energy-label>.

18. Resource bill: Which taxes will increase and by how much (2021). Retrieved from <https://www.slovoidilo.ua/2021/12/13/infografika/ekonomika/resursnyj-zakonoprojekt-yaki-podatky-zrostut-skilky>.

19. ISO 50001: Benefits for manufacturers (2019). Retrieved from <https://www.plantengineering.com/articles/iso-50001-benefits-for-manufacturers/>.

20. European platform on Life cycle assessment (2013) Retrieved from <https://eplca.jrc.ec.europa.eu/lifecycleassessment.html>.

21. **Jordaan, S.** (2021). Life cycle assessment of electricity generation: A systematic review of spatiotemporal methods. Retrieved from <https://www.sciencedirect.com/science/article/pii/S2666792421000500>.

22. **Šerešová, M.** (2020). Life cycle performance of various energy sources used in the Czech Republic. Retrieved from <https://www.mdpi.com/1996-1073/13/21/5833>.

23. **Palekhova, L., & Simon, S.** (2016). Competitive advantages through the implementation of international energy management standards. Bulletin of the Dnieper State Academy of Construction and Architecture, № 3, 42-51. Retrieved from <https://www.semanticscholar.org/paper/Competitiveadvantages-through-the-implementation-Paliekhova-Simon/9c1feb73e964bc8b5c3b9fabdbdb81d4484fb>.

24. **Dreshpak, N.S.** (2020). Energy efficiency control systems of production processes and ways of their improvement. Electrical Engineering and Power Engineering, №1, 40-48. Retrieved from <https://doi.org/10.15588/1607-6761-2020-1-5>.

25. **Dreshpak, N.S., Dreshpak, O.S. & Vypanasenko, S.I.** (2021). Certain norms of energy consumption in the task of controlling the efficiency of its use. Electrical Engineering and Power Engineering, №3, 31-39. Retrieved from <https://doi.org/10.15588/1607-6761-2021-3-3>.

26. **Shulle, Yu. A., & Rogozyanskiy, I. S.** (2016). The use of AMR to increase the efficiency of energy use at industrial enterprises. Information Technologies and Computer Engineering, № 1, 59-63. Retrieved from <http://surl.li/gptfy>.

27. Code of commercial accounting of electric energy. No311§. section I p. 1.2. (2018). Retrieved from <https://zakon.rada.gov.ua/laws/show/v0311874-18#Text>.

Scientific edition

# **MODERN FORMS OF DEVELOPMENT OF RESOURCE-SAVING TECHNOLOGIES FOR MINERALS MINING AND PROCESSING**

Multi-authored monograph

First publication

The materials of the multi-authored monograph are in the authors' edition. References are obligatory in case of full or partial reproduction of the monograph content. All rights are reserved by the monograph contributors including their scientific achievements and statements.

Co-editor **Valerii KORNIYENKO** - Professor, DSc. (Engineering), Head of  
Department of Development of Deposits and Mining, National University of  
Water and Environmental Engineering, Ukraine

Co-editor **Maria LAZAR** - Habil, Ph.D.Eng., PhD supervisor in Mines, Oil and Gas  
Environmental Engineering and Geology Department, Vice-Rector - Research and  
International Relationship, University of Petrosani, Romania

Deputy editor **Serhii CHUKHAREV**, PhD (Engineering), Associate Professor. Department  
of Development of Deposits and Mining, National University of Water and Environmental  
Engineering, Ukraine

Technical editor **Elena SAMOILUK**

Signed to print 21.01.24. Format A5.  
54 conventional printed sheets.  
The printing run is 300 copies.

UNIVERSITAS Publishing, Petroșani,  
University of Petroșani Str. Universității nr. 20, 332006,  
Petroșani, jud. Hunedoara, Romania